

100-24296

AD-A280 006



DTIC
ELECTE
JUN 03 1994

This document has been approved
for public release and sale; its
distribution is unlimited.

A Service of:

The NASA STI Program ... in Profile

Since its founding, NASA has been dedicated to ensuring U.S. leadership in aeronautics and space science. The NASA Scientific and Technical Information (STI) Program plays an important part in helping NASA maintain its leadership role.

The NASA STI Program provides access to the NASA STI Database, the largest collection of aeronautical and space science STI in the world. The Program is also NASA's institutional mechanism for disseminating the results of its research and development activities.

A number of specialized services help round out the Program's diverse offerings, including creating custom thesauri, translating material to or from 34 foreign languages, building customized databases, organizing and publishing research results.

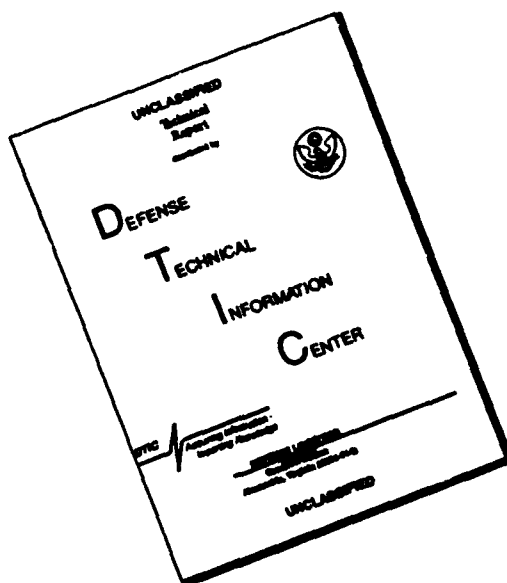
For more information about the NASA STI Program, you can:

- **Phone** the NASA Access Help Desk at (301) 621-0390
- **Fax** your question to NASA Access Help Desk at (301) 621-0134
- Send us your question via the **Internet** to help@sti.nasa.gov

- **Write to:**

NASA Access Help Desk
NASA Center for AeroSpace Information
800 Elkridge Landing Road
Linthicum Heights, MD 21090-2934

DISCLAIMER NOTICE



**THIS DOCUMENT IS BEST
QUALITY AVAILABLE. THE COPY
FURNISHED TO DTIC CONTAINED
A SIGNIFICANT NUMBER OF
PAGES WHICH DO NOT
REPRODUCE LEGIBLY.**

(NASA-RP-1046) MEASUREMENT OF AIRCRAFT
SPEED AND ALTITUDE (NASA) 311 p
BC A14/MP A01

W80-24296

CSCL 01C

H1/05 Unclass
22127

94 6 2 030

NASA Reference Publication 1046

Measurement of Aircraft Speed and Altitude

William Gracey
Langley Research Center
Hampton, Virginia

Accession For	
NTIS CRA&I	<input checked="" type="checkbox"/>
DTIC TAB	<input type="checkbox"/>
Unannounced	<input type="checkbox"/>
Justification	
By	
Distribution /	
Availability Codes	
Dist	Avail and/or Special
A-1	

NASA

National Aeronautics
and Space Administration

Scientific and Technical
Information Office

1980

PREFACE

The problem of devising instrument systems for the accurate measurement of the speed and altitude of aircraft has been the subject of a great many research investigations during the past 50 years. The greater part of this research has been performed by a variety of organizations in Great Britain, Germany, and the United States. In the United States, investigations have been conducted by government agencies (National Aeronautics and Space Administration (NASA), its predecessor, the National Advisory Committee on Aeronautics (NACA), the Federal Aviation Administration (FAA), the National Bureau of Standards (NBS), the U.S. Air Force, and the U.S. Navy), by aeronautical schools in the universities, and by aircraft manufacturers, instrument manufacturers, and air carriers. Studies relating to one area of the altitude-measuring problem (the vertical separation of aircraft) have been promoted by international organizations such as the International Civil Aviation Organization (ICAO) and the International Air Transport Association (IATA).

The results of this research have been published in several hundred reports, each of which deals with only one, or a few, of the many facets of the speed- and altitude-measuring problem. In this text, the information in these reports has been combined and is presented in a condensed, organized form. In the presentation of the material on some of the topics, only enough data have been included to define a concept or illustrate a point. For a more detailed discussion of these subjects, the reader is referred to the reference reports which are listed at the end of each chapter.

The scales of the instruments described in this text and all of the test data derived from their calibration and operational use are in U.S. Customary Units. Accordingly, it appeared inappropriate in this text to adhere to the prevailing practice of giving test values in the International System of Units (SI) as well as in the U.S. Customary system. For those readers having a need to convert any of the data to metric units, a table of conversion factors and metric equivalents is included in appendix A. Also included in appendix A are tables of airspeed and altitude in SI Units.

In writing this book, I received considerable help and support from many of my former associates at NASA Langley Research Center. I would like to acknowledge this assistance and to thank, in particular, the following:

John P. Campbell, Laurence K. Loftin, Jr., and Joseph W. Stickle who reviewed the original manuscript.

John C. Houbolt, Howard B. Edwards, Albert W. Hall, Thomas M. Moul, Virgil S. Ritchie, and Robert T. Taylor who, as members of a technical review committee, made many valuable suggestions for improving and expanding the book.

The staff of the Langley Technical Library who were most helpful in supplying reference material.

The staff of the Langley Scientific and Technical Information Programs Division who prepared the manuscript for publication.

I would also like to acknowledge the contributions of the following members of the aviation industry:

James Angus of the Kollsman Instrument Company, who provided information on servoed instruments and photographs of mechanical instruments.

O. E. E. Anderson of United Airlines, who provided information on pressure-system leak experiments and static-pressure-installation maintenance problems.

Jerome M. Paros of Paroscientific, Inc., who provided information and diagrams on digital pressure transducers.

Herbert Sandberg of Harowe Systems, Inc., who provided information on pressure-transducer systems.

William Gracey
Langley Research Center
National Aeronautics and Space Administration
Hampton, VA 23665
December 6, 1979

CONTENTS

PREFACE	iii
SYMBOLS AND ABBREVIATIONS	viii
CHAPTER I - INTRODUCTION	1
CHAPTER II - INSTRUMENT SYSTEMS AND ERRORS	3
References	6
Figures	7
CHAPTER III - STANDARD ATMOSPHERE AND EQUATIONS FOR AIRSPEED, MACH NUMBER, AND TRUE AIRSPEED	11
Standard Atmosphere	11
Airspeed Equations	14
Mach Number Equations	17
True-Airspeed Equations	18
Conversion Factors	19
References	20
Figures	22
CHAPTER IV - TOTAL-PRESSURE MEASUREMENT	25
Tubes Aligned With the Flow	25
Tubes Inclined to the Flow	26
References	30
Figures	31
CHAPTER V - STATIC-PRESSURE MEASUREMENT	47
Reference	51
Figures	52
CHAPTER VI - STATIC-PRESSURE TUBES	59
Tubes Aligned With the Flow	59
Tubes Inclined to the Flow	61
Orifice Size and Shape	62
References	63
Figures	64
CHAPTER VII - STATIC-PRESSURE INSTALLATIONS	75
Fuselage-Nose Installations	75
Wing-Tip Installations	77
Vertical-Fin Installations	78
Fuselage-Vent Installations	79
Combined Calibrations at Low and High Altitudes	80
Calibration Presentations	81
Installation Error Tolerances	81
Installation Design Considerations	82
References	83
Figures	85

CHAPTER VIII - AERODYNAMIC COMPENSATION OF POSITION ERROR	109
References	111
Figures	112
CHAPTER IX - FLIGHT CALIBRATION METHODS	121
Calibration Methods for Deriving Position Error	121
Trailing-Bomb Method	124
Trailing-Cone Method	125
Pacer-Aircraft Method	125
Tower Method	127
Tracking-Radar Method	128
Radar-Altimeter Method	128
Ground-Camera Method	129
Tracking-Radar/Pressure-Altimeter Method	130
Accelerometer Method	131
Recording-Thermometer Method	133
Trailing-Anemometer Method	134
Speed-Course Method	137
Sonic-Speed Method	137
Total-Temperature Method	138
Calibrations by Ground-Camera and Tracking-Radar Methods	139
References	144
Table 9.1	146
Figures	149
CHAPTER X - ERRORS DUE TO PRESSURE-SYSTEM LAG AND LEAKS	165
System Lag	165
System Leaks	168
References	169
Table 10.1	170
CHAPTER XI - AIRCRAFT INSTRUMENT ERRORS	171
Mechanical Instruments	171
Electrical Instrument Systems	174
Accuracy of Calibration Equipment	177
References	178
Tables	180
Figures	186
CHAPTER XII - OPERATIONAL ASPECTS OF ALTIMETRY	199
Barometric Scale Settings	199
Flight Technical Error	202
Overall Altitude Errors	203
References	206
Table 12.1	208
Figures	209

CHAPTER XIII - OTHER ALTITUDE-MEASURING METHODS	215
Radio and Radar Altimeters	215
Laser Altimeter	217
Sonic Altimeter	217
Capacitance Altimeter	217
Density Altimeter	218
Limited-Range Pressure Altimeter	218
Hypsometer	218
Cosmic-Ray Altimeter	219
Gravity Meter	219
Magnetometer	220
References	221
APPENDIX A - TABLES OF AIRSPEED, ALTITUDE, AND MACH NUMBER	223
APPENDIX B - SAMPLE CALCULATIONS	279
Part I - Static-Pressure Errors and Flight Quantities	279
Determination of Position Error Δp	279
Calculation of V_C and ΔV_C , H and ΔH , and M and ΔM	281
Calculation of C_L	282
Calculation of V	283
Part II - Pressure Increments in the International System of Units	284
Part III - Pressure-System Lag and Leaks	285
Calculation of Airspeed and Altitude Errors Due to Pressure Lag	285
Calculation of Altitude Error Due to a Leak	286
INDEX	291

SYMBOLS AND ABBREVIATIONS

a	speed of sound
a_v	vertical acceleration
a_x	longitudinal acceleration
a_z	normal acceleration
b	wing span of airplane
b'	wing span of airplane image on camera film
c	wing chord
C	total volume of instrument chambers
C_L	lift coefficient
CL	confidence level
d,D	diameter
E	elevation of airport
f	compressibility factor; focal length of camera lens
g	acceleration of gravity
h	height of aircraft above camera
H	pressure altitude, geopotential feet
H'	indicated (or measured) pressure altitude (barometric scale set to QFE)
H_i	indicated altitude (barometric scale set to QNH)
ΔH	altitude error, $H' - H$
K	recovery factor of temperature probe
l	length of aircraft
l'	length of aircraft image on camera film
L	length of pressure tubing
M	free-stream Mach number
M'	indicated (or measured) Mach number

ΔM	Mach number error, $M' - M$
N_{Re}	Reynolds number, $\rho \frac{V\ell}{\mu}$, where ℓ is a linear dimension
p	free-stream static pressure
p'	measured static pressure
Δp	static-pressure error or position error, $p' - p$; pressure drop in tubing
δp	static-pressure increment
p_a	pressure at altitude
p_c	cabin or compartment pressure
p_i	pressure inside instrument
p_l	local static pressure
Δp_l	pressure error due to leak
p_t	free-stream total pressure for subsonic flow and total pressure behind normal shock wave for supersonic flow
p'_t	measured total pressure
Δp_t	total pressure error, $p'_t - p_t$; total pressure loss through normal shock wave
p_T	test pressure
q	dynamic pressure
q_c	free-stream impact pressure
q'_c	measured impact pressure
QFE	standard altimeter setting (barometric scale set to 29.92 in. Hg)
QNE	barometric scale setting for altimeter to indicate zero at airport elevation
QNH	barometric scale setting for altimeter to indicate elevation of airport
R	gas constant for air, ft-lb/slug- $^{\circ}R$
\bar{R}	gas constant for air, ft-lb/lb-mol- $^{\circ}R$
R^*	universal gas constant

S	wing area of aircraft
t	free-air temperature, °C or °F; thickness of wing or mounting strut of pitot-static tube; time
T	free-air temperature, °K or °R
T'	indicated (or measured) total temperature, °K or °R
ΔT	temperature error, $T' - T$; temperature rise due to adiabatic heating
T_m	mean temperature of column of air, °K or °R
u	horizontal component of induced velocity
v	vertical velocity
V	free-stream velocity; true airspeed
V_c	calibrated airspeed (indicated airspeed corrected for static-pressure error)
V_e	equivalent airspeed
V_i	indicated airspeed (corrected for instrument scale error)
V_l	local velocity
ΔV_c	airspeed error, $V_i - V_c$
W	weight of aircraft
W_m	mean molecular weight of air
x	axial location of orifices (1) along static-pressure tube, (2) ahead of strut or collar of tube, (3) ahead of aircraft, or (4) to center of wave on fuselage skin
y	height of protuberance at fuselage vent
Z	height, geometric feet
ΔZ	height increment
Δz	vertical displacement of aircraft image from center line of film frame
β	angle of conical entry on total pressure tube
γ	ratio of specific heats of air, 1.4
θ	pitch attitude of airplane
λ	pressure lag constant
λ_l	pressure lag of leak

μ	coefficient of viscosity
ρ	density (mass), slugs/ft ³
$\bar{\rho}$	density (weight), lb/ft ³
σ	standard deviation
τ	acoustic lag time

ϕ radial location of orifices around static-pressure tube or fuselage

Subscripts:

i	initial
a	altitude: actual
c	critical; computed; camera
l	local; leak
m	measured; midpoint
o	sea level
s	standard

Abbreviations:

AAEE	Aeroplane and Armament Experimental Establishment (British)
AFCRC	Air Force Cambridge Research Center
AFMTC	Air Force Missile Test Center
ANA	Air Force-Navy Aeronautical
A.R.C.	Aeronautical Research Committee (British)
FAA	Federal Aviation Administration
NACA	National Advisory Committee for Aeronautics (predecessor to NASA)
NAES	Naval Air Experimental Station
NASA	National Aeronautics and Space Administration
NBS	National Bureau of Standards
NOAA	National Oceanic and Atmospheric Administration

R.A.E. Royal Aircraft Establishment (British)

WADC Wright Air Development Center (USAF)

NACA and NASA Reports:

ARR Advanced Restricted Report

RM Research Memorandum

SP Special Publication

TM Technical Memorandum

TN Technical Note

TP Technical Paper

TR or Rep. Technical Report

WR Wartime Report

CHAPTER I

INTRODUCTION

Accurate measurements of speed and altitude are essential to the safe and efficient operation of aircraft. Accurate speed measurements, for example, are needed to avoid loss of control at low speeds (stall condition) and to prevent exceedance of the aerodynamic and structural limitations of the aircraft at high speeds, whereas accurate altitude measurements are needed to insure clearance of terrain obstacles and to maintain prescribed vertical separation minima along the airways.

The instruments that are used to measure speed and altitude include the altimeter, the airspeed indicator, the true-airspeed indicator, the Machmeter, and the rate-of-climb (or vertical-speed) indicator. All these instruments are actuated by pressures, while one, the true-airspeed indicator, is actuated by air temperature as well.

Two basic pressures, static pressure and total pressure, are used to actuate the instruments. The static pressure is the atmospheric pressure at the flight level of the aircraft, while the total pressure is the sum of the static pressure and the impact pressure, which is the pressure developed by the forward speed of the aircraft. The relation of the three pressures can thus be expressed by the following equation:

$$P_t = P + q_c \quad (1.1)$$

where p_t is the total pressure, p the static pressure, and q_c the impact pressure.

The static pressure is used to actuate both the altimeter and the rate-of-climb indicator. Although this pressure varies from day to day, the decrease in static pressure with height is generally continuous at any one time and place. Accordingly, a pressure-height relation based on average atmospheric conditions has been adopted as a standard (see "standard atmosphere" in chapter III). Measurements of static pressure are then used to provide indications of height in terms of pressure altitude (chapter XII) and indications of vertical speed in terms of rate of change in the pressure altitude.

For the three forward-speed indicators, impact pressure is derived as a differential pressure from measurements of total pressure and static pressure in accordance with equation (1.1). The airspeed indicator is actuated solely by impact pressure and is calibrated to indicate true airspeed at sea-level density in the standard atmosphere; at altitude, however, the indicated airspeed is lower than the true airspeed (chapter III). The true-airspeed indicator, on the other hand, combines the measurement of impact pressure with measurements of static pressure and temperature to indicate true airspeed independent of altitude. The Machmeter (named for the Austrian physicist, Ernst Mach) combines

measurements of impact pressure and static pressure to provide indications of true airspeed as a fraction or multiple of the speed of sound (sonic speed).

The airspeed indicator, true-airspeed indicator, and Machmeter measure speed with respect to the air mass. Since the air mass can move with respect to the ground, the measurement of ground speed, the speed of basic importance to air navigation, must be derived from inputs from ground navigational aids.

The pressures and temperatures that actuate the instruments are derived from pressure and temperature sensors located at positions on the aircraft which are remote from the instruments. The problem of designing and locating the sensors for the accurate measurement of pressure and temperature is complicated by many factors. As a consequence, the pressures and temperatures registered by the sensors can be in error by amounts which, in some cases, produce sizable errors in the indications of the instruments. The indications of an instrument can also be in error because of imperfections in the instrument itself. Additional errors may be introduced because of a time lag in the transmission of the pressures to the instruments whenever the pressure at the pressure source is changing rapidly, as in the case of high-speed climbs or dives.

In the following chapter, a typical instrument system is described, and the various errors associated with the system are defined. In succeeding chapters, the errors relating to the design of the total- and static-pressure sensors and to the location of the sensors on an aircraft are discussed, and the flight calibration methods for determining the pressure errors are described. Information is then presented on ways of applying corrections for these errors and on methods of keeping the other errors within acceptable limits.

CHAPTER II

INSTRUMENT SYSTEMS AND ERRORS

The five types of instruments which are used to measure speed and altitude and the pressure and temperature sensors which actuate the instruments were described in chapter I. This chapter describes a typical instrument system (instruments and sensors) and the errors associated with the various parts of the system.

As noted in the first chapter, the two basic pressures that are employed in the measurement of speed and altitude are total pressure and static pressure. Total pressure is sensed by an opening in a forward-facing tube called a total-pressure tube or pitot tube (named for the French physicist, Henri Pitot). The static pressure is sensed by orifices in the side of another type of tube, called a static-pressure tube, or by a set of holes in the side of an aircraft fuselage, called fuselage vents or static ports. Since the pitot tube and the static-pressure tube can be combined into a single tube, two types of pressure-measuring installations are possible: a pitot-static tube installation or a pitot tube in combination with a fuselage-vent system. Diagrams of a pitot tube, a static-pressure tube, a pitot-static tube, and a pitot-tube/fuselage-vent installation are shown in figure 2.1.

The pressures that are sensed by the pitot tube and the static-pressure tube (or fuselage vents) are conveyed through tubing to pressure-sensing elements which are generally in the form of capsules, diaphragms, or bellows. All of these types of sensing elements are used in the electrical instrument systems to be described in chapter XI. The capsule-type sensing element is used in simpler, mechanical instruments described in this chapter.

The pressure capsules are formed by joining together two corrugated diaphragms which are about 2 in. in diameter. Two types of capsule are used in aircraft instruments: one for measuring absolute pressure and the other for measuring differential pressure. The absolute-pressure (or aneroid) capsule is evacuated and sealed, while the differential-pressure capsule has an opening that is connected to a pressure source. As indicated in figure 2.2, the absolute-pressure capsule reacts to the pressure inside the instrument case, while the differential-pressure capsule reacts to the difference between the pressure inside the capsule and the pressure in the instrument case. Thus, for both types of capsule, the instrument case is used as a pressure chamber to form one element of the pressure-measuring system.

Also shown in figure 2.2 are the directions of the deflection of the capsules for a given pressure change. These deflections, which are very small, are amplified through a system of gears and levers (gear train) to rotate a pointer in front of the scale on the dial of the instrument.

The routing of the pressure tubing from a total-pressure tube, static-pressure tube, and temperature probe to a set of the five types of instruments is shown in figure 2.3. The static-pressure tube is connected to all the instruments, whereas the total-pressure tube is connected only to those instru-

ments that measure forward speed. The temperature probe, which is connected to the true-airspeed indicator, is a type used with liquid-pressure thermometers. The pressure tubing from the total-pressure and static-pressure tubes is generally about 0.2 to 0.3 in. in inside diameter, whereas the capillary tubing from the temperature probe is about 0.01 to 0.02 in.

The pressure-sensing element of the altimeter (fig. 2.3) is an aneroid capsule that expands as the static pressure inside the instrument case decreases with increasing altitude. (See fig. 2.2(a).)

In the rate-of-climb indicator, the static-pressure tube is connected to a differential-pressure capsule and to a capillary tube that opens into the instrument case. With a change in static pressure, the simultaneous flow of air into, or out of, the capsule and the capillary tube is adjusted (by the size of the capillary leak) so that the capsule deflects in terms of a rate of change of pressure, which is calibrated to yield a measure of vertical speed.

The pressure-sensing element of the airspeed indicator is a differential-pressure capsule that expands as the total pressure increases. Since the pressure inside the case is the static pressure, the instrument performs a mechanical subtraction of total and static pressures to yield a measure of impact pressure in accordance with equation (1.1). (See fig. 2.2(b).)

The Machmeter contains both an aneroid capsule and a differential-pressure capsule to provide measures of static pressure and impact pressure. The deflections of the two capsules are coupled to yield, mechanically, the ratio of impact pressure to static pressure (q_c/p) which, as discussed in the next chapter, is a function of Mach number.

The true-airspeed indicator contains (1) two differential-pressure capsules to provide measures of impact pressure and air temperature and (2) an aneroid capsule to provide a measure of static pressure. Since the true airspeed is a function of dynamic pressure, derived from the measured impact pressure and static pressure as discussed in chapter V, and the air density, derived from static pressure and temperature, the deflections of the three capsules can be coupled to yield a measure of true airspeed.

Also shown in figure 2.3 are the pressures (p'_t and p') sensed by the total- and static-pressure tubes and the temperature (T') sensed by the temperature probe. For any one flight condition, the differences between p'_t and the free-stream total pressure p_t and between T' and the free-air temperature T depend primarily on the design characteristics of the pitot tube and the temperature probe. The difference between p' and the free-stream static pressure p depends on both the design of the static-pressure tube and on the location of the tube in the pressure field surrounding the aircraft (chapter V).

The difference between p'_t and p_t , called the total-pressure error Δp_t , is defined by

$$\Delta p_t = p'_t - p_t \quad (2.1)$$

Similarly, the difference between p' and p , the static-pressure error Δp , is defined by

$$\Delta p = p' - p \quad (2.2)$$

The difference between T' and T , the temperature error ΔT , is defined by

$$\Delta T = T' - T \quad (2.3)$$

As noted in the previous chapter, the indications of the instruments may be affected by errors due to the time lag in the transmission of the pressures and to imperfections in the instrument mechanism. The errors associated with the instrument mechanism depend on (1) the elastic properties of the pressure capsule (scale error, hysteresis, and drift) and (2) the effects of temperature, acceleration, and friction on the linkage mechanism. The scale error is the difference, for a given applied pressure, between the value indicated by the instrument and the correct value corresponding to the applied pressure. From the foregoing discussion, the overall error of an instrument system is a combination of

1. Total- and static-pressure errors of the pitot-static installation and the temperature error of the temperature probe
2. Errors due to time lag in the transmission of the pressures
3. Errors relating to the operation of the instrument mechanism

The magnitude and nature of the errors vary widely, so that different means are used to minimize different errors. The total-pressure, static-pressure, and temperature errors, for example, are systematic; that is, for a given flight condition, the errors are essentially repeatable and hence can be determined by calibration. The static-pressure error can be quite large, whereas the total-pressure error is generally negligible (chapters IV and VII). The magnitude of the temperature error, expressed in terms of a recovery factor, is discussed in chapter III.

The errors due to pressure lag are transitory and vary with the rate of climb or descent of the aircraft. For a given rate of change of altitude, the magnitude of the lag error depends primarily on the length and diameter of the pressure tubing and on the volume of the instruments connected to the tubing. Accordingly, the lag errors of a particular pressure system are kept within acceptable limits by proper design of the system (chapter X).

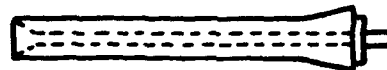
Of the various instrument errors, the scale error is systematic, while the other errors are generally random. The scale error is usually the largest of the instrument errors and can be determined by laboratory calibration. The remaining errors are kept within acceptable limits by careful design, construction, and adjustment of the instrument mechanism.

The instrument errors and the errors of the pitot-static installation are required to meet specified tolerances (allowable errors). The tolerances for the instrument errors can be combined to yield an "instrument error," and this error can be combined with the tolerance for the static-pressure error to yield an "instrument system error" (chapter XII). Mathematical procedures for combining the tolerances for the instrument errors and the static-pressure error are described in references 1 through 4.

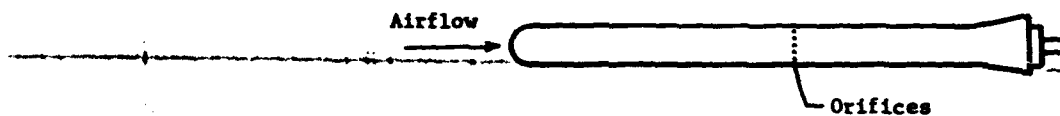
Since the scale error of the instrument and the static-pressure error of the installation can be determined by calibration, corrections for these two errors can be applied. With mechanical instrument systems, corrections for these errors are applied by means of correction charts, or cards, that are supplied to the pilot. With electrical instruments, the corrections are applied automatically by some form of computer (chapter XI). For systems in which corrections for the two errors are applied, the instrument system error is usually much lower than the error derived from a summation of the instrument and static-pressure error tolerances. The laboratory procedures for determining the scale error are described in chapter XI and the flight procedures for determining the static-pressure error are described in chapter IX. Since the procedures for determining the scale error are well established, this text emphasizes flight procedures by which static-pressure installations are calibrated.

References

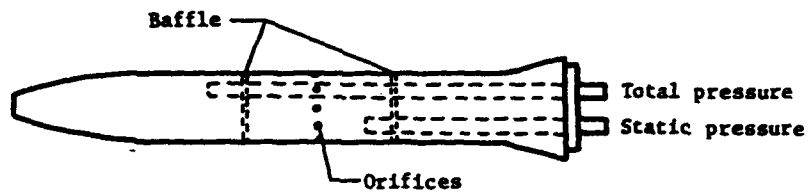
1. First Interim Report of the Panel on Vertical Separation of Aircraft. Doc. 7672-AN/860, Int. Civ. Aviat. Organ. (Montreal), Feb. 14-22, 1956.
2. Gracey, William: The Measurement of Pressure Altitude on Aircraft. NACA TN-4127, 1957.
3. Altimetry and the Vertical Separation of Aircraft. Int. Air Transp. Assoc. (Montreal), Jan. 1960.
4. Gilsinn, Judith F.; and Shier, Douglas R.: Mathematical Approaches to Evaluating Aircraft Vertical Separation Standards. Rep. No. FAA-EM-76-12, May 1976.



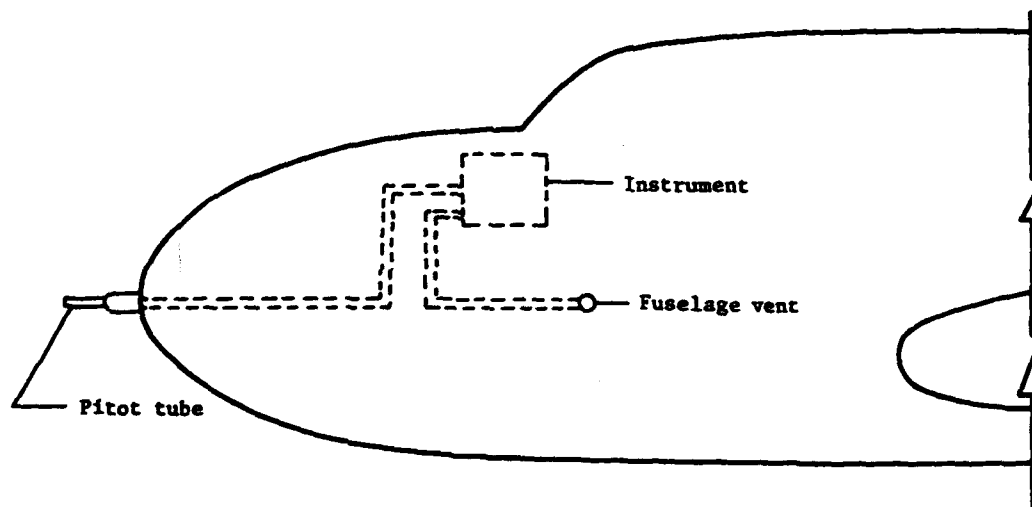
(a) Pitot tube.



(b) Static-pressure tube.

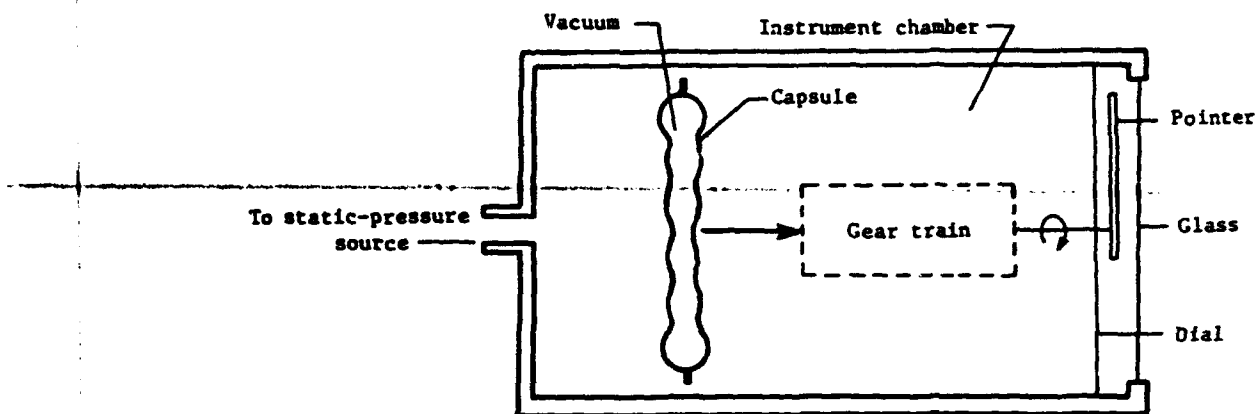


(c) Pitot-static tube.

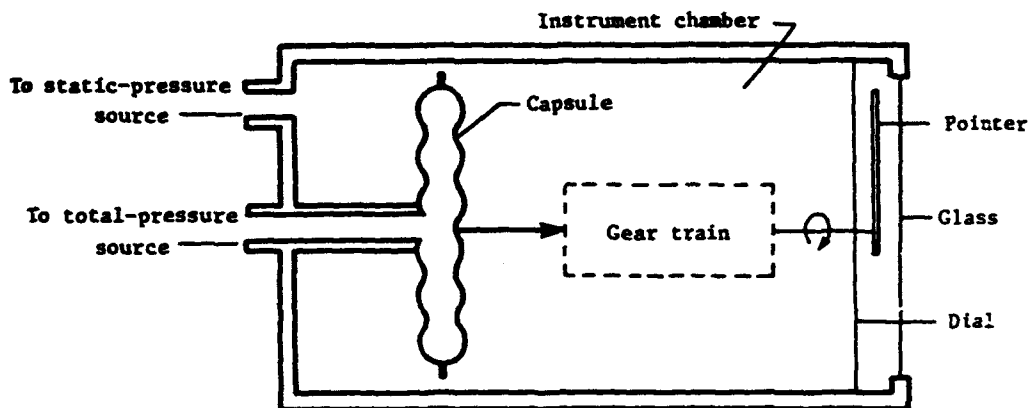


(d) Pitot-tube/fuselage-vent installation.

Figure 2.1.- Diagrams of pressure tubes and a pitot-tube/fuselage-vent installation.



(a) Aneroid capsule. For a decrease in static pressure inside the instrument case, the capsule deflects in the direction indicated by the large arrow.



(b) Differential-pressure capsule. For an increase in total pressure inside the capsule, the capsule deflects in the direction indicated by the large arrow.

Figure 2.2.- Aircraft instruments with the two types of pressure capsule.

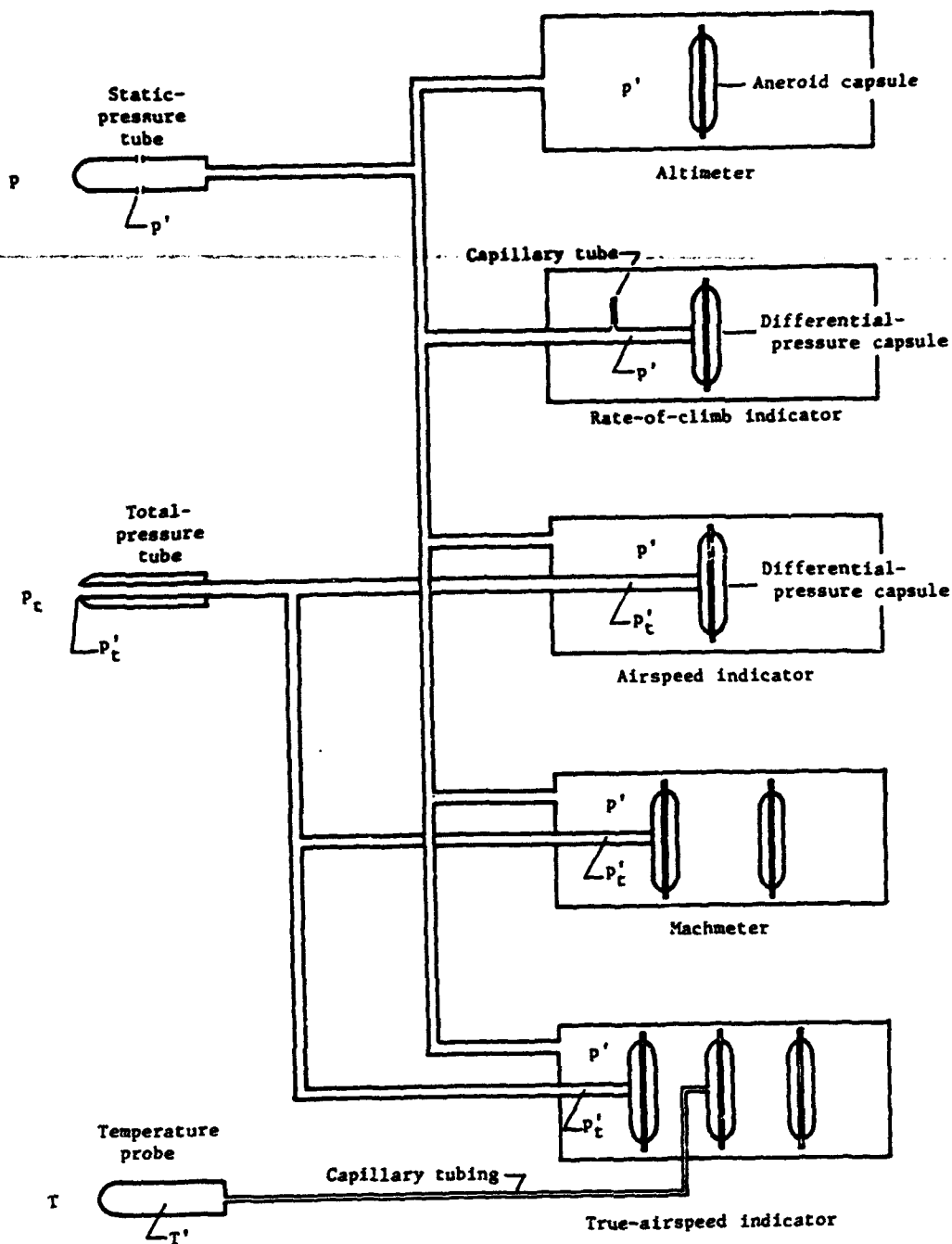


Figure 2.3.- Diagram of routing of pressure tubing from pressure and temperature sensors to five types of instruments measuring altitude and speed.

PRECEDING PAGE BLANK NOT FILLED

CHAPTER III

STANDARD ATMOSPHERE AND EQUATIONS FOR AIRSPEED, MACH NUMBER, AND TRUE AIRSPEED

As noted in chapter I, the pressure altimeter is calibrated in accordance with the pressure-height relation in the standard atmosphere. In the first section of this chapter, the equations and the atmospheric properties on which the standard atmosphere is based are presented. In succeeding sections, the equations relating (1) impact pressure to airspeed, (2) impact pressure and static pressure to Mach number, and (3) impact pressure, static pressure, and temperature to true airspeed are described. These equations are of fundamental importance to both the laboratory calibrations of the instruments and the deduction of flight parameters from measured pressures and temperature.

In the following sections, reference is made to tables of airspeed and altitude in U.S. Customary Units (appendix A). As noted in the Preface, tables of the same quantities in the International (metric) System of Units (SI) are also included in appendix A.

Standard Atmosphere

The so-called standard atmosphere is a representation of the atmosphere based on average conditions at a latitude of 45° north. A number of standard atmospheres have been developed through the years (ref. 1 through 13). Each new standard has differed from the previous standard because of the adoption of revised values of some of the physical constants on which the atmospheres are based or because of the acquisition of new information on some of the atmospheric properties (particularly at the higher altitudes). All the atmospheres are based on mean values of pressure, temperature, density, and the acceleration of gravity at sea level and on a mean value of the variation of temperature with height.

In the construction of a standard atmosphere on the basis of these mean values, assumptions are made that

1. The air is a dry, perfect gas that obeys the laws of Charles and Boyle,

$$\rho = \rho_0 \frac{p T_0}{p_0 T} \quad (3.1)$$

and thus the perfect gas law,

$$\rho = \frac{p W_m}{R^* T} = \frac{p}{R T} \quad (3.2)$$

2. The atmosphere is in hydrostatic equilibrium, so that the relation between the pressure p and the geometric height Z can be expressed by the equations,

$$dp = -g\rho \, dZ = -\bar{\rho} \, dZ \quad (3.3)$$

$$dp = -g \frac{p}{RT} \, dZ = -\frac{\bar{p}}{\bar{R}T} \, dZ \quad (3.4)$$

where ρ (or $\bar{\rho}$) is the density, p the pressure, T the temperature, g the acceleration of gravity, W_m the mean molecular weight of air, R^* the universal gas constant, and R (or \bar{R}) the gas constant for air. The two symbols given for density and the gas constant for air denote differences in units which are found in some of the reference reports. For the symbols given in this text, the unit of ρ is slugs per cubic foot and the unit of $\bar{\rho}$ is pounds per cubic foot. The value of R is 1716.5 ft-lb/slug-°R and the value of \bar{R} is 53.352 ft-lb/(lb mol)°R.

The earlier atmospheres (refs. 1 through 5) were based on the assumption that the acceleration of gravity remained constant at its sea-level value g_0 . For the later atmospheres (refs. 6 through 13), the decrease of g with height was taken into account by the formation of a new height parameter called geopotential altitude H . The relation between H and Z is given by

$$dZ = \frac{g_0}{g} \, dH \quad (3.5)$$

The value of Z/H varies uniformly from 1.0 at sea level to 1.0048 at 100 000 ft. The relation between p and H is given by the following equations:

$$dp = -g_0\rho \, dH = -\frac{g_0}{g} \bar{\rho} \, dH \quad (3.6)$$

or

$$dp = -g_0 \frac{p}{RT} \, dH = -\frac{g_0}{g} \frac{\bar{p}}{\bar{R}T} \, dH \quad (3.7)$$

Pressure-altitude tables for the calibration of altimeters in terms of geopotential feet are given in references 6 through 13. All these tables are the same for altitudes up to 65 800 ft, and the tables of references 11 through 13 are the same for altitudes up to 100 000 ft. The tables of reference 11 (the U.S. Standard Atmosphere, 1962) have been selected for presentation in this text because the pressures and altitudes are given in both U.S. Customary Units (the system of units used in this text) and SI Units. The pressure-altitude tables of references 12 and 13 are in SI Units.

The sea-level values of pressure, temperature, density, and the acceleration of gravity for the atmosphere of reference 11 are as follows:

$$P_0 = 29.9213 \text{ in. Hg or } 2116.22 \text{ lb/ft}^2$$

$$t_0 = 59.0^\circ \text{ F or } 15.0^\circ \text{ C}$$

$$T_0 = 518.67^\circ \text{ R or } 288.15^\circ \text{ K}$$

$$\rho_0 = 0.0023769 \text{ slug/ft}^3$$

$$\bar{\rho}_0 = 0.076474 \text{ lb/ft}^3$$

$$g_0 = 32.1741 \text{ ft/sec}^2$$

The temperature gradient or lapse rate dT/dH is $-0.00356616^\circ \text{ F}$ per geopotential foot from sea level to 36 090 geopotential feet. From this altitude to 65 800 ft, the temperature is constant at -69.7° F and then increases to -50.836° F at 100 000 ft.

Tables of pressure, density, temperature, coefficient of viscosity, speed of sound, and the acceleration of gravity are given in appendix A for geopotential altitudes up to 100 000 ft:

In table A1, values of pressure are given in inches of mercury (0° C) (to correspond with the scales of mercury-in-glass barometers used for calibration of altimeters); in table A2, the values are given in pounds per square foot.

In table A3, values of air density are given in pounds per cubic foot. Values in units of slugs per cubic foot can be derived by dividing the values of table A3 by the acceleration of gravity.

In tables A4 and A5, values of free-air temperature are given in degrees Fahrenheit and Celsius. Values of absolute temperature in degrees Rankine and Kelvin can be derived by means of the following equations:

$$T(^{\circ}\text{R}) = t(^{\circ}\text{F}) + 459.67 \quad (3.8)$$

$$T(^{\circ}\text{K}) = t(^{\circ}\text{C}) + 273.15 \quad (3.9)$$

In table A6, values of the coefficient of viscosity are given in pound-seconds per square foot. Values in pounds per foot-second (the unit used in ref. 11) can be derived by multiplying the values in table A6 by the acceleration of gravity.

In table A7, values of the speed of sound are given in miles per hour and knots.

In table A8, values of the acceleration of gravity are given in feet per second squared.

Airspeed Equations

In incompressible flow, the pressure developed by the forward motion of a body is called the dynamic pressure q , which is related to the true airspeed V by the equation,

$$q = \frac{1}{2} \rho V^2 \quad (3.10)$$

where ρ is the density of the air and V is the speed of the body relative to the air. Air, however, is compressible, and when airspeed is measured with a pitot-static tube, the air is compressed as it is brought to a stop in the pitot tube. As a consequence of this compression, the measured impact pressure q_c (eq. (1.1)) is higher than the dynamic pressure of equation (3.10). The effects of compressibility can be taken into account by determining the relation between the true airspeed V and the impact pressure q_c by means of the following equations:

1. The equation for the total pressure (eq. (1.1)),

$$P_t = q_c + p \quad (1.1)$$

2. The equation for the speed of sound a in air,

$$a = \sqrt{\frac{\gamma p}{\rho}} \quad (3.11)$$

where γ is the ratio of the specific heats of air.

3. Bernoulli's formula for total pressure in compressible flow,

$$P_t = p \left(1 + \frac{\gamma - 1}{2\gamma} \frac{\rho}{p} V^2 \right)^{\frac{\gamma}{\gamma - 1}} \quad (3.12)$$

4. The formula for total pressure behind a normal shock wave (for $V \geq a$),

$$P_t = \frac{1 + \gamma}{2\gamma} \rho V^2 \left[\frac{\frac{(\gamma + 1)^2}{\gamma} \frac{\rho}{p} V^2}{\frac{4\rho}{p} V^2 - 2(\gamma - 1)} \right]^{\frac{1}{\gamma - 1}} \quad (V \geq a) \quad (3.13)$$

With the substitution of equation (1.1) in equation (3.12) and equations (1.1) and (3.11) in equation (3.13), V can be expressed in terms of q_c by the following equations:

$$q_c = p \left[\left(1 + \frac{\gamma - 1}{2\gamma} \frac{\rho}{p} V^2 \right)^{\frac{\gamma}{\gamma - 1}} - 1 \right] \quad (3.14)$$

and

$$q_c = \frac{1 + \gamma}{2} \left(\frac{V}{a} \right)^2 p \left[\frac{(\gamma + 1)^2}{4\gamma - 2(\gamma - 1) \left(\frac{a}{V} \right)^2} \right]^{\frac{1}{\gamma - 1}} - p \quad (V \geq a) \quad (3.15)$$

For the calibration of airspeed indicators, the concept of calibrated airspeed V_c is introduced and, by definition, V_c is made equal to V at sea level for standard sea-level conditions. Thus, by substituting the standard sea-level values of p , ρ , and a in equations (3.14) and (3.15), V_c can be related to q_c by the following equations:

$$q_c = p_0 \left[\left(1 + \frac{\gamma - 1}{2\gamma} \frac{\rho_0}{p_0} V_c^2 \right)^{\frac{\gamma}{\gamma - 1}} - 1 \right] \quad (V_c \leq a_0) \quad (3.16)$$

and

$$q_c = \frac{1 + \gamma}{2} \left(\frac{V_c}{a_0} \right)^2 p_0 \left[\frac{(\gamma + 1)^2}{4\gamma - 2(\gamma - 1) \left(\frac{a_0}{V_c} \right)^2} \right]^{\frac{1}{\gamma - 1}} - p_0 \quad (V_c \geq a_0) \quad (3.17)$$

Airspeed indicators are calibrated in accordance with equation (3.16) for subsonic speeds ($V_c \leq a_0$) and equation (3.17) for supersonic speeds ($V_c \geq a_0$). The sea-level values of pressure, density, and speed of sound used in these equations are those given in reference 11, namely,

$$p_0 = 2116.22 \text{ lb/ft}^2$$

$$\rho_0 = 0.0023769 \text{ slug/ft}^3$$

$$a_0 = 1116.45 \text{ ft/sec}$$

The value that has been adopted for γ is 1.4. Note, however, that at high altitudes, the value of γ may vary slightly from 1.4 (refs. 11 and 14).

For subsonic speeds, the true airspeed V can be deduced from the calibrated airspeed V_C and the air density ρ by means of the following equation which is derived by dividing equation (3.14) by equation (3.16):

$$V = V_C \frac{f}{f_0} \sqrt{\frac{\rho_0}{\rho}} \quad (V \leq a) \quad (3.18)$$

where f is a compressibility factor defined by

$$f = \sqrt{\frac{\gamma}{\gamma - 1} \frac{p}{q_C} \left[\left(\frac{q_C}{p} + 1 \right)^{\frac{\gamma - 1}{\gamma}} - 1 \right]} \quad (3.19)$$

Values of f and f_0 (the compressibility factor for standard sea-level conditions) are given in figure 3.1 for values of q_C/p up to 0.893 (the ratio for $M = 1.0$ for which $V = a$). The value of ρ for use in equation (3.18) can be determined from equation (3.1) and measured values of static pressure and air temperature.

In aircraft structural design, use is made of an airspeed that equates the dynamic pressure at altitude ($q = \frac{1}{2} \rho V^2$) to the dynamic pressure at sea level for standard sea-level density ($q = \frac{1}{2} \rho_0 V_e^2$). This airspeed V_e is called the equivalent airspeed and is related to V by the following equation):

$$V_e = V \sqrt{\frac{\rho}{\rho_0}} \quad (3.20)$$

Another airspeed term, indicated airspeed, is generally defined as the indication of an airspeed indicator uncorrected for instrument error and the error of the pitot-static installation. In this text, however, the indicated airspeed V_i is defined as the airspeed indication corrected for instrument scale error (chapter II). Thus, since the calibrated airspeed V_C is the indication of an airspeed indicator corrected for both instrument scale error and static-pressure error, the difference between V_i and V_C is a measure of the static-pressure error.

To summarize the relations between V_i , V_C , and V in simple terms, V_i is the indication of an airspeed indicator corrected for instrument scale error, V_C is V_i corrected for static-pressure error, and V is the true airspeed, which is equal to V_C at sea level.

Tables relating calibrated airspeed to impact pressure are presented in references 4, 10, 12, 15, 16, and 17. The tables of reference 10 are given in this text because they are based on a revised value of the nautical mile adopted in 1959 and because the units of V_C and q_C are in U.S. Customary Units.

Values of impact pressure q_c for calibrated airspeeds V_c (or q_c' for indicated airspeeds V_i) up to 1100 mph and 1000 knots are given in tables A9 through A12 of appendix A. The values in miles per hour are based on a statute mile equal to 5280 ft, and the values in knots are based on the 1959 value of the nautical mile (6076.12 ft).

Mach Number Equations

As noted in chapter I, the Mach number M is the ratio of the true airspeed V to the speed of sound a in the ambient air; that is,

$$M = V/a \quad (3.21)$$

By substituting in this expression the equation for the speed of sound given in equation (3.11), M can be related to V by the following equation:

$$V = M \sqrt{\frac{\gamma p}{\rho}} \quad (3.22)$$

The Mach number may then be expressed in terms of p_t by substituting equation (3.22) in equations (3.12) and (3.13), which then become

$$p_t = p \left(1 + \frac{\gamma - 1}{2} M^2 \right)^{\frac{\gamma}{\gamma - 1}} \quad (3.23)$$

and

$$p_t = \frac{1 + \gamma}{2} M^2 p \left[\frac{(1 + \gamma)^2 M^2}{4\gamma M^2 - 2(\gamma - 1)} \right]^{\frac{1}{\gamma - 1}} \quad (M \geq 1) \quad (3.24)$$

With the additional substitution of equation (1.1) in equations (3.23) and (3.24), M can be expressed as a function of q_c/p as follows:

$$\frac{q_c}{p} = \left(1 + \frac{\gamma - 1}{2} M^2 \right)^{\frac{\gamma}{\gamma - 1}} - 1 \quad (M \leq 1) \quad (3.25)$$

and

$$\frac{q_c}{p} = \frac{1 + \gamma}{2} M^2 \left[\frac{(1 + \gamma)^2 M^2}{4\gamma M^2 - 2(\gamma - 1)} \right]^{\frac{1}{\gamma - 1}} - 1 \quad (M \geq 1) \quad (3.26)$$

Machmeters are calibrated in accordance with equation (3.25) for subsonic speeds ($M \leq 1$) and equation (3.26) for supersonic speeds ($M \geq 1$).

In table A26 of appendix A, values of q_c/p for given values of M (or values of q_c'/p' for given values of M') are tabulated for Mach numbers up to 5.0 (from ref. 4).

True-Airspeed Equations

As noted earlier, true airspeed can be derived from calibrated airspeed in the subsonic range by means of equation (3.18). The true airspeed can also be determined, at both subsonic and supersonic speeds, from its relation to Mach number and the speed of sound in equation (3.21). For this case, M is determined from equations (3.25) and (3.26) and a is determined by combining equations (3.1) and (3.11) which yields the following equation relating a to the temperature of the ambient air:

$$a = \sqrt{\gamma \frac{p_o}{\rho_o} \frac{T}{T_o}} \quad (3.27)$$

where T is the absolute temperature in degrees Rankine or Kelvin. For ρ_o in slugs per cubic foot and p_o in pounds per square foot, the value of a is in feet per second.

For values in terms of miles per hour or knots, the speed of sound can be calculated from any of the following equations derived from equation (3.27):

1. If a is in miles per hour and T is in degrees Rankine,

$$a = 33.424 \sqrt{T}$$

2. If a is in knots and T is in degrees Rankine,

$$a = 29.045 \sqrt{T}$$

3. If a is in miles per hour and T is in degrees Kelvin,

$$a = 44.844 \sqrt{T}$$

4. If a is in knots and T is in degrees Kelvin,

$$a = 38.968 \sqrt{T}$$

The value of T required for the calculation of a is the temperature of the free stream. While some aircraft temperature probes register free-stream temperature directly, the temperature registered by other types of probes is higher than the stream value because of the adiabatic heating effect of the air-flow on the sensor. The extent to which the probe measures the adiabatic heating effect is stated in terms of a recovery factor, which ranges from zero (no adiabatic heating) to 1.0 (full adiabatic temperature rise). The recovery factor of a temperature probe can be determined from calibration tests in a wind tunnel. An electrical-type temperature probe having a recovery factor near unity (0.99) is shown in figure 3.2 (from ref. 18).

If the recovery factor of the probe is 1.0 or if the probe is located in a region where the local velocity of the air is equal to the free-stream velocity, the free-air temperature T can be calculated from the following equation:

$$T = \frac{T'}{1 + \frac{\gamma - 1}{2} K^2} \quad (3.28)$$

where T' is the measured (or total) temperature and K is the recovery factor of the probe. For the more general case in which the recovery factor is less than 1.0 and the probe is located in a region where the local velocity differs from the free-stream value, the free-air temperature can be calculated from the following:

$$T = \left(\frac{T'}{1 + \frac{\gamma - 1}{2} K^2} \right) \left(\frac{1 + \frac{\gamma - 1}{2} M_l^2}{1 + \frac{\gamma - 1}{2} M^2} \right) \quad (3.29)$$

where M_l is the local Mach number, which can be determined from measurements of the local impact and static pressures in the region in which the probe is located.

Values of the speed of sound a in miles per hour and knots are given in table A7 of appendix A for geopotential altitudes up to 100 000 ft. The values of a are based on the values of T in the standard atmosphere of reference 11.

Values of true airspeed V for calibrated airspeeds from 0 to 1000 knots and geopotential altitudes from 0 to 100 000 ft are given in table A13 of appendix A. The values of V , V_c , and H in this table are based on the standard atmosphere of reference 11.

A chart showing the relations of calibrated airspeed, true airspeed, and Mach number for altitudes up to 60 000 ft and temperatures from -100° F to 120° F is presented in figure 3.3 (from ref. 19).

Conversion Factors

For applications requiring the conversion of the pressure units in tables A1 and A2 and A9 through A12 of appendix A to other units, conversion factors for a variety of other pressure units are given in table A27 of appendix A. For conversion of U.S. Customary Units to SI Units, conversion factors and metric equivalents are given in table A28 of appendix A (ref. 20).

References

1. Gregg, Willis Ray: Standard Atmosphere. NACA Rep. 147, 1922.
2. Diehl, Walter S.: Standard Atmosphere - Tables and Data. NACA Rep. 218, 1925. (Reprinted 1940.)
3. Brombacher, W. G.: Altitude-Pressure Tables Based on the United States Standard Atmosphere. NACA Rep. 538, 1935.
4. Tables and Data for Computing Airspeeds, Altitudes, and Mach Numbers Based on the WADC 1952 Model Atmosphere. Volume I - Altitude, Calibrated Airspeed, and Mach Number Tables. Battelle Mem. Inst. (Contract AF 33(616)82), 1953.
5. Williams, D. T.; Bell, J. C.; and Nash, W. F.: A New Standard Atmosphere: The WADC 1952 Model Atmosphere. WADC Tech. Rep. 54-215, U.S. Air Force, Mar. 1954.
6. Standard Atmosphere - Tables and Data for Altitudes to 65,800 Feet. NACA Rep. 1235, 1955. (Supersedes NACA TN 3182.)
7. Minzner, R. A.; and Ripley, W. S.: The ARDC Model Atmosphere, 1956. AFCRC TN-56-204, U.S. Air Force, Dec. 1956. (Available from DTIC as AD 110 233.)
8. Minzner, R. A.; Ripley, W. S.; and Condron, T. P.: U.S. Extension to the ICAO Standard Atmosphere - Tables and Data to 300 Standard Geopotential Kilometers. Geophys. Res. Dir. and U.S. Weather Bur., 1958.
9. Minzner, R. A.; Champion, K. S. W.; and Pond, H. L.: The ARDC Model Atmosphere, 1959. AFCRC-TR-59-267, U.S. Air Force, Aug. 1959.
10. Livingston, Sadie P.; and Gracey, William: Tables of Airspeed, Altitude, and Mach Number Based on Latest International Values for Atmospheric Properties and Physical Constants. NASA TN D-822, 1961.
11. U.S. Standard Atmosphere, 1962. NASA, U.S. Air Force, and U.S. Weather Bur., Dec. 1962.
12. Benner, Margaret S.; and Sawyer, Richard H.: Revised Tables of Airspeed, Altitude, and Mach Number Presented in the International System of Units. NASA SP-3082, 1973.
13. U.S. Standard Atmosphere, 1976. NOAA, NASA, and U.S. Air Force, Oct. 1976.
14. Deleo, Richard V.; Cannon, Peter J.; and Hagen, Floyd W.: Evaluation of New Methods for Flight Calibration of Aircraft Instrument Systems. Part I: Analysis of Altimeter, Airspeed and Free-Air-Temperature Systems. WADC TR 59-295 Pt. I, U.S. Air Force, June 1959. (Available from DTIC as AD 239 767.)

15. Zahm, A. F.: Pressure of Air on Coming to Rest From Various Speeds. NACA Rep. 247, 1926.
16. Aiken, William S., Jr.: Standard Nomenclature for Airspeeds With Tables and Charts for Use in Calculation of Airspeed. NACA Rep. 837, 1946. (Supersedes NACA TN 1120.)
17. Differential Pressures. ANA Bull. No. 418, Nov. 21, 1952.
18. Lina, Lindsay J.; and Ricker, Harry H., Jr.: Measurements of Temperature Variations in the Atmosphere Near the Tropopause With Reference to Airspeed Calibration by the Temperature Method. NACA TN 2807, 1952.
19. Baals, Donald D.; and Ritchie, Virgil S.: A Simplified Chart for Determining Mach Number and True Airspeed From Airspeed-Indicator Readings. NACA WR L-473, 1943. (Formerly NACA RB.)
20. Standard for Metric Practice. E 380-76, American Soc. Testing & Mater., 1976.

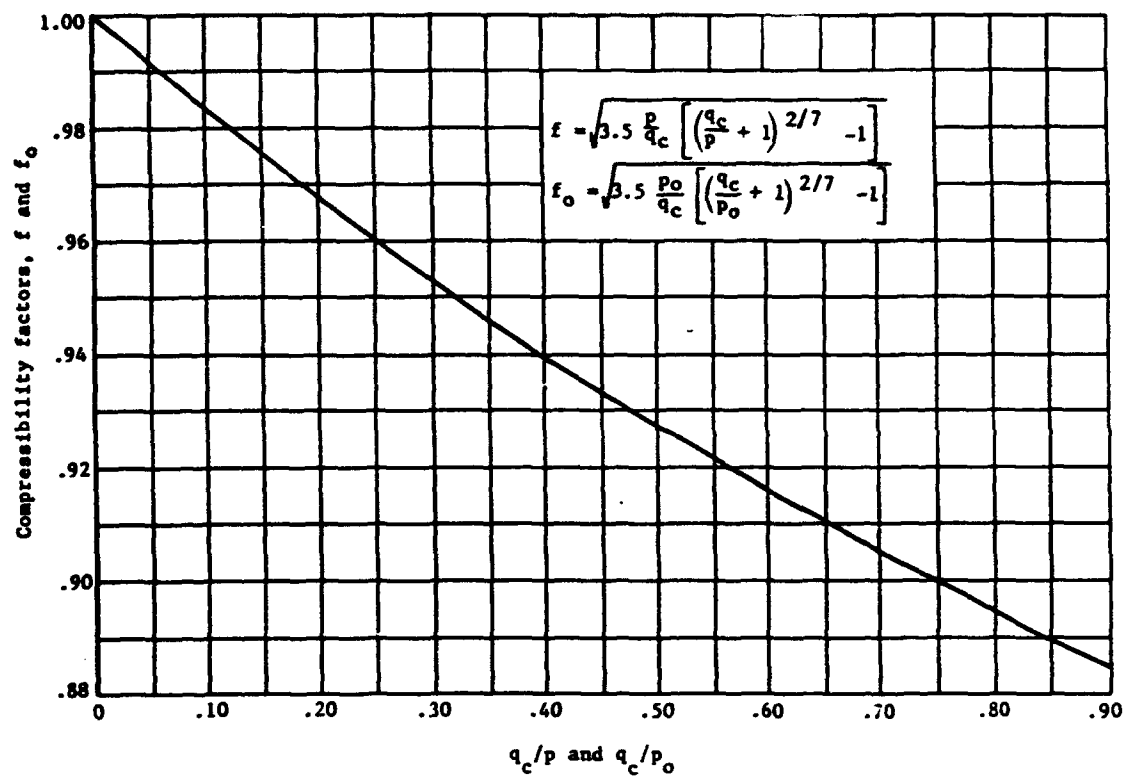


Figure 3.1.- Compressibility factors.

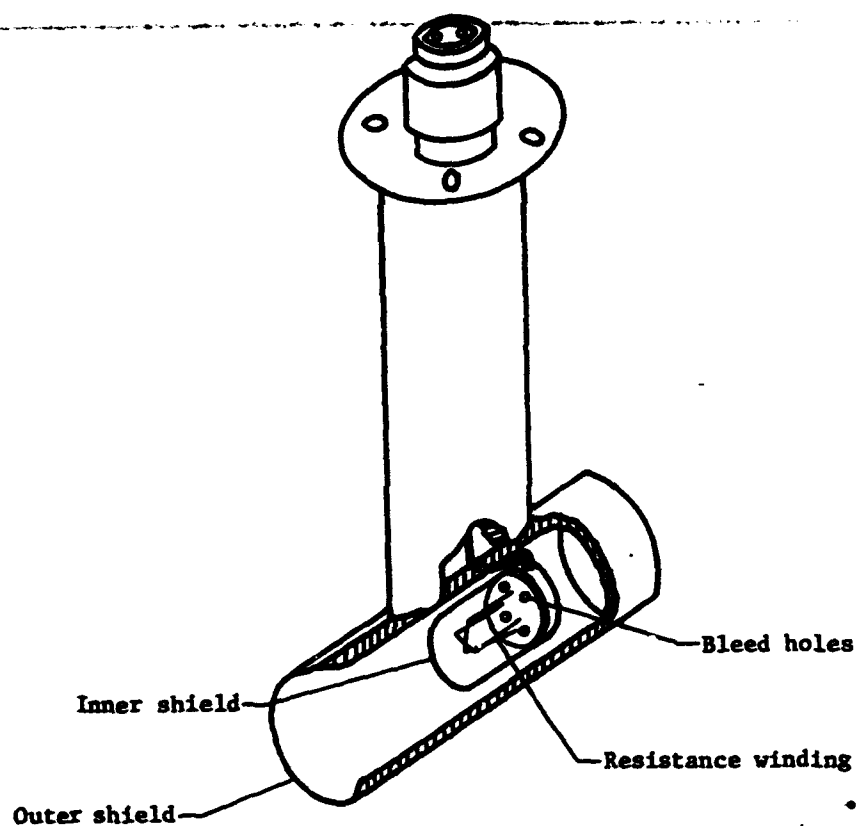


Figure 3.2.- Electrical-type temperature probe having a recovery factor of 0.99. (Adapted from ref. 18.)

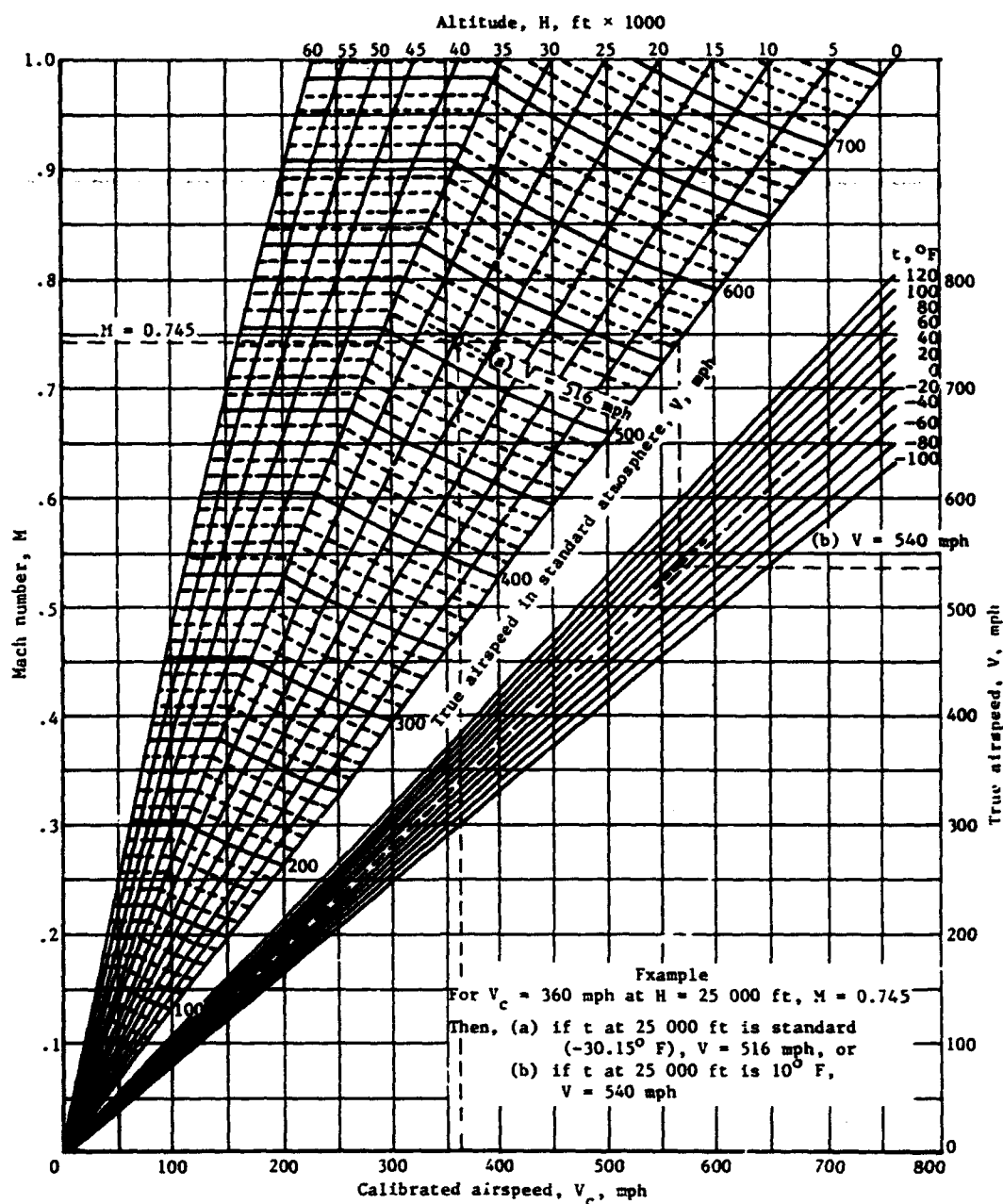


Figure 3.3.- Chart of calibrated airspeed, true airspeed, and Mach number. (Adapted from ref. 19.)

CHAPTER IV

TOTAL-PRESSURE MEASUREMENT

The equations for airspeed, Mach number, and true airspeed given in the previous chapter are all based on the measurement of impact pressure. As shown by equation (1.1), however, the impact pressure is derived from measured values of total pressure and static pressure. In this and the following chapters, therefore, the problems relating to the measurement of total pressure with pitot tubes and the measurement of static pressure with static-pressure tubes or fuselage vents are considered in some detail.

As noted in the next chapter, the static pressure at successive points along lines of airflow past a body can vary widely, whereas the total pressure along these lines of flow remains constant. For this reason, the measurement of total pressure is much less difficult than the measurement of free-stream static pressure. The measurement of total pressure is also easier because the problem of total-pressure tube design is less difficult than the design problem for static-pressure tubes.

The principal difficulty encountered in the measurement of total pressure relates to the change in the measured pressure when the pitot tube is inclined to the airflow. Since the magnitude of this change is largely dependent on the design, or configuration, of the pitot tube (which can take a wide variety of forms), the problem of measuring total pressure with tubes inclined to the flow is considered separately from the simpler case of tubes aligned with the flow.

Tubes Aligned With the Flow

When aligned with the flow in the subsonic speed range, almost any open-end tube registers total pressure correctly provided that the tube is located away from any boundary layer, wake, propeller slipstream, or engine exhaust. For operations at high subsonic speeds, the tube should be located away from any area of high curvature on the structure where shock waves form when the local speed becomes sonic. As all these locations can usually be avoided, there is generally little problem in measuring total pressure at subsonic speeds when the tube is aligned with the flow. Locations which have proved satisfactory for pitot-tube installations include positions ahead of the fuselage, wing, or vertical fin for tubes mounted on short horizontal booms or positions along the fuselage or under the wing for tubes mounted on short struts. Examples of service-type pitot tubes designed for end-mounting and strut-mounting are shown in figure 4.1.

For operations in the supersonic speed range, the tube should be located ahead of shock waves emanating from any part of the aircraft. The location that best meets this requirement is, obviously, a position ahead of the fuselage nose. When located ahead of the fuselage bow shock, however, the tube is still influenced by a shock, for a small normal shock wave forms ahead of the tube. The presence of this shock is important to the measurement of total pressure because the total pressure decreases through the shock, so that the

pressure measured by the tube is lower than the free-stream value ahead of the shock. The magnitude of the total-pressure loss through the shock Δp_t as a fraction of the free-stream total pressure p_t is given by the following expression derived by subtracting equation (3.24) from equation (3.23), dividing the resulting quantity by equation (3.23), and assigning the value of 1.4 to

$$\frac{\Delta p_t}{p_t} = 1 - \frac{1.2M^2 \left(\frac{5.76M^2}{5.6M^2 - 0.8} \right)^{2.5}}{(1 + 0.2M^2)^{3.5}} \quad (4.1)$$

where M is the free-stream Mach number. The variation of $\Delta p_t/p_t$ with Mach number for the Mach range from 1.0 to 3.0 is shown in figure 4.2. For the laboratory calibration of airspeed indicators and Machmeters in the supersonic speed range, the total-pressure loss through the shock is taken into account in the computation of the pressure tables by which the instruments are calibrated (see eqs. (3.17) and (3.26)).

Tubes Inclined to the Flow

When a pitot tube is inclined to the flow, the total pressure begins to decrease at some angle of inclination. The angular range through which the tube measures total pressure correctly is called the range of insensitivity to inclination. In this text, the range of insensitivity is defined as the angular range through which the total-pressure error remains within 1 percent of the impact pressure. For a criterion based on a smaller total-pressure error, the range of insensitivity would, of course, be smaller than that quoted for the tubes to be described in this chapter.

The configurations of the total-pressure tubes to be described are of two general types: simple pitot tubes and pitot tubes enclosed in a cylindrical shield. For the simple pitot tubes, the range of insensitivity is shown to depend for the most part on the shape of the nose section of the tube and on the size of the impact opening relative to the frontal area of the tube.

Early designers favored tubes with hemispherical nose shapes and small impact openings. An example of the use of small-bore, round-nosed tubes was the pitot-static tube designed by the German physicist, Ludwig Prandtl. The pitot part of this tube (fig. 6.5) was very sensitive to inclination, for the range of insensitivity was only $\pm 5^\circ$ (ref. 1). Of interest here is the fact that the sensitivity of the pitot tube to inclination was considered to be of little concern, because the static-pressure portion of the tube was equally sensitive to inclination in a compensating manner. As a result, the impact pressure measured by the tube remained unaffected by inclination through an angular range about $\pm 12^\circ$. As discussed in this chapter and in chapter VI, later designers have tried to reduce the sensitivity to inclination of both total- and static-pressure tubes.

In an investigation of a number of pitot-static tubes in 1935 (ref. 2), tests of pitot tubes having cylindrical nose shapes disclosed a significant design feature, namely, that the range of insensitivity could be increased by increasing the size of the pitot opening. An extrapolation of test results indicated that maximum insensitivity to inclination should be achieved with a thin-wall tube.

In another investigation in 1935, G. Kiel, a German aerodynamicist, showed in reference 3 that the range of insensitivity could be extended considerably by placing the pitot tube inside a venturi-like shield, as shown in figure 4.3. In tests of this tube at low speeds, the range of insensitivity was found to be $\pm 43^\circ$. Later tests of the tube in a NASA wind tunnel confirmed this range of insensitivity, but showed that the tube could not be used at Mach numbers greater than 0.6 because of excessive vibrations caused by the airflow around the mounting strut.

The errors of simple tubes due to inclination can be avoided by equipping the tube with a pivot and vanes to align the tube with the airstream (fig. 4.3). While swiveling tubes are satisfactory for flight-test work at subsonic speeds, they are impractical for service use on operational aircraft.

In an effort to devise fixed (as opposed to swiveling) total-pressure tubes that would be insensitive to inclination and suitable for use on both operational and flight-test aircraft, the NACA conducted a series of wind-tunnel tests on a variety of tube designs from 1951 to 1954 (refs. 4 through 9). The tests were conducted in five wind tunnels at Mach numbers ranging from 0.26 to 2.40 and at angles of inclination up to 67° . Diagrams of the tube configurations that were investigated are presented in figure 4.4. As indicated by the six series of tube designs, the configurations included shielded tubes based on the Kiel design and simple tubes with cylindrical, conical, and ogival nose shapes. For the simple tubes, the principal design variables, aside from the nose shape, were the shape of the entry to the impact opening (cylindrical, hemispherical, and conical) and the relative size of the impact opening on the face of the tube. The shielded tubes were all designed with vent holes along the aft portion of the tube to allow mounting at the end of a horizontal boom. The variables tested with the shielded tubes included (1) the shape of the entry to the throat (conical and curved), (2) the relative size of the throat (D_2/D), (3) the position of the pitot tube from the face of the shield (a/D), and (4) the area of the vents with respect to the frontal area of the shield (A_v/A_0).

The results of the tests of a few of the tubes have been selected for this text to show the effects of some of the more significant design features. An assessment of all of the design variables is given in the summary report of the investigation in reference 9.

In the presentation of the results in the figures to follow, the angle of inclination of the tube is the angle in the vertical plane (angle of attack). For symmetrical tubes, the variation of the total pressure error is the same in the horizontal plane (angle of yaw). For unsymmetrical tubes A-6, A₅-10, A₅-11, E-3, and E-4 of figure 4.4, however, the error variation at angles of attack and angles of yaw are different.

The effect of varying the size of the impact opening with respect to the frontal area of cylindrical tubes is shown by a comparison of the test results of tubes A-1 and A-2 at a Mach number of 0.26 (fig. 4.5). For the small-bore tube, the range of insensitivity is $\pm 11^\circ$, while for the thin-wall tube, it is $\pm 23^\circ$. These results confirm the data from reference 2 in showing the range of insensitivity to increase with an increase in the size of the impact opening.

The test data on figure 4.6(a) show the effect of cutting the nose of the thin-wall tube at a slant angle of 10° . The range of insensitivity is increased (from the $\pm 23^\circ$ value for the thin-wall tube) to 32° at positive angles of attack but decreased to 13° at negative angles. The effect of the 10° slant profile, therefore, is simply to shift the curve of figure 4.5(b) 10° along the angle-of-attack axis. At angles of yaw, the range of insensitivity is $\pm 23^\circ$, the same as that for the thin-wall tube. For some applications, the use of a slant-profile tube could be advantageous, since the angle-of-attack range through which an aircraft operates is greater at positive angles than at negative.

The effect of changing the shape of the internal entry of cylindrical tubes can be shown from a comparison of the test data of tubes A-2, A-5, and A-7 through A-11. Changing the entry from a cylindrical shape (tube A-2) to a hemispherical shape (tube A-5) increased the range of insensitivity by about 3° . A change to a 50° conical entry (tube A-11) showed no improvement over the value for the cylindrical entry. By decreasing the internal cone angle to 30° , however, the range of insensitivity increased to a value of $\pm 27^\circ$ (tube A-9 in fig. 4.6(b)). Decreasing the cone angle to 20° (tube A-8) and to 10° (tube A-7) produced no further extension in the range of insensitivity.

The 27° range of insensitivity for the tube with the 30° conical entry is 5° lower than that for the thin-wall, slant-profile tube at positive angles of attack. However, because of the relative fragility of the slant-profile tube and the lack of space for the installation of a deicing heating element, the tube with the 30° conical entry would be a more practical tube for service operations.

Some effects of the external nose shape on the range of insensitivity can be shown from a comparison of the data for the tubes having conical and ogival nose sections. For the tube with a 15° conical nose (tube B-1), the range of insensitivity is $\pm 21^\circ$ (fig. 4.7(a)); for the 30° nose (tube C-1), the range is $\pm 17.5^\circ$; and for the 45° nose (tube D-1), it is $\pm 14^\circ$.

The ogival-nose tube in figure 4.7(b) is a service-type tube which, in the production model, had a small wall thickness at the impact opening. To make the pitot configuration of this tube comparable with that of tubes B-1, C-1, and D-1, the impact opening was reamed to a sharp leading edge. As shown in figure 4.7(b), the range of insensitivity of this modified tube was $\pm 16^\circ$, which is about midway between that for the 30° and 45° conical-nose tubes.

The test data for a Kiel-type shielded tube having a vent area equal to the frontal area of the shield are shown on figure 4.8(a). The range of insensitivity of this tube is $\pm 41^\circ$, which is very nearly the same as that for the original Kiel design. These tests are significant, therefore, in showing that

a shielded tube can be vented along the walls of the shield, as opposed to the straight-through venting of the Kiel shield, without loss in performance.

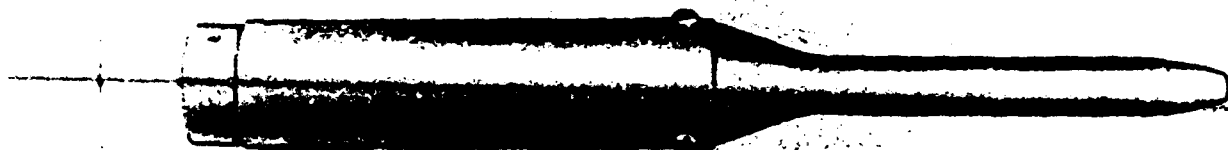
The test data presented thus far were all obtained at a Mach number of 0.26. When tubes A-2, A-6, A-9, and B-1 (figs. 4.5, 4.6, and 4.7) were tested at $M = 1.62$, the range of insensitivity was greater than that at $M = 0.26$ by as much as 4° to 10° . In contrast, the range of insensitivity of shielded tube A_S-3 (fig. 4.8(a)) was lower at $M = 1.62$ by about 3° .

In tests of the shielded tubes with the curved entries, the entry with the highest degree of curvature (tube A_S-12) provided the greatest range of insensitivity. At $M = 0.26$, for example, the range was $\pm 63^\circ$ (fig. 4.8(b)). With increasing Mach number, the range of insensitivity decreased to about 58° at $M = 1.0$ and to about 40° at $M = 1.61$ (fig. 4.9). Despite this loss in performance with increasing Mach number, however, the range of insensitivity of this shielded tube is still greater than that of any of the simple tubes at both subsonic and supersonic speeds.

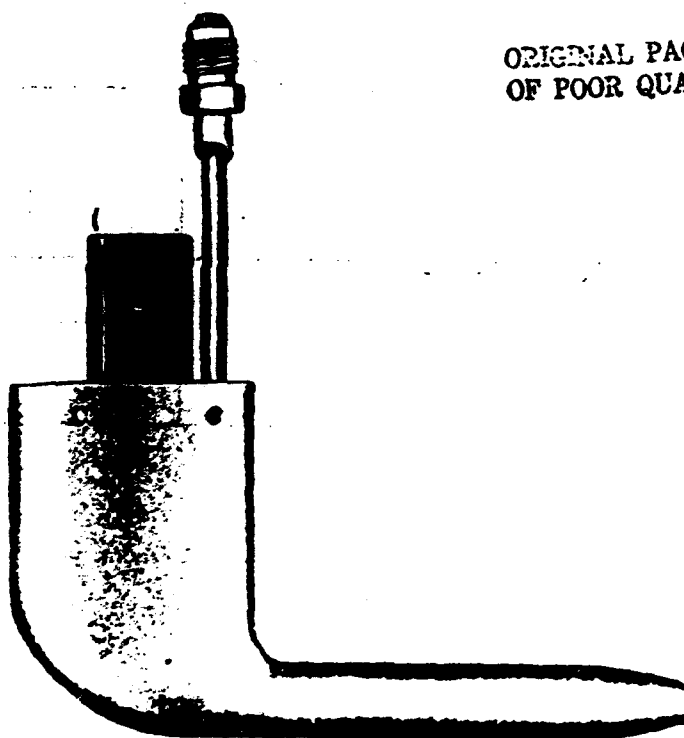
In the foregoing discussion, only the aerodynamic aspects of the design of pitot tubes have been considered. For a tube intended for operational use, the nose configuration would have to allow for the installation of an electric heating element for deicing and drain holes for the removal of any water that may be ingested. In at least two cases, pitot configurations examined in the NASA investigation have been successfully incorporated in the design of service-type pitot and pitot-static tubes; the configuration of tube A-9 is incorporated in the pitot tube shown in figure 4.10 and the configuration of tube B-4 is incorporated in the pitot-static tube described in reference 10 and shown in figure 6.14.

References

1. Eckert, B.: Experience With Flow-Direction Instruments. NACA TM 969, 1941.
2. Merriam, Kenneth G.; and Spaulding, Ellis R.: Comparative Tests of Pitot-Static Tubes. NACA TN 546, 1935.
3. Kiel, G.: Total-Head Meter With Small Sensitivity to Yaw. NACA TM 775, 1935.
4. Gracey, William; Letko, William; and Russell, Walter R.: Wind-Tunnel Investigation of a Number of Total-Pressure Tubes at High Angles of Attack - Subsonic Speeds. NACA TN 2331, 1951. (Supersedes NACA RM L50G19.)
5. Gracey, William; Coletti, Donald E.; and Russell, Walter R.: Wind-Tunnel Investigation of a Number of Total-Pressure Tubes at High Angles of Attack - Supersonic Speeds. NACA TN 2261, 1951.
6. Russell, Walter R.; Gracey, William; Letko, William; and Fournier, Paul G.: Wind-Tunnel Investigation of Six Shielded Total-Pressure Tubes at High Angles of Attack - Subsonic Speeds. NACA TN 2530, 1951.
7. Gracey, William; Pearson, Albin O.; and Russell, Walter R.: Wind-Tunnel Investigation of a Shielded Total-Pressure Tube at Transonic Speeds. NACA RM L51K19, 1952.
8. Russell, Walter R.; and Gracey, William: Wind-Tunnel Investigation of a Shielded Total-Pressure Tube at a Mach Number of 1.6. NACA RM L53L23a, 1954.
9. Gracey, William: Wind-Tunnel Investigation of a Number of Total-Pressure Tubes at High Angles of Attack - Subsonic, Transonic, and Supersonic Speeds. NACA Rep. 1303, 1957. (Supersedes NACA TN 3641.)
10. Pitot Static Tube TRU-1/A, Electrically Heated. Mil. Specif. MIL-P-25757B(ASG), Jan. 26, 1960.



(a) End mounting.



ORIGINAL PAGE IS
OF POOR QUALITY

(b) Strut mounting.

Figure 4.1.- Examples of service-type pitot tubes.

L-79-356

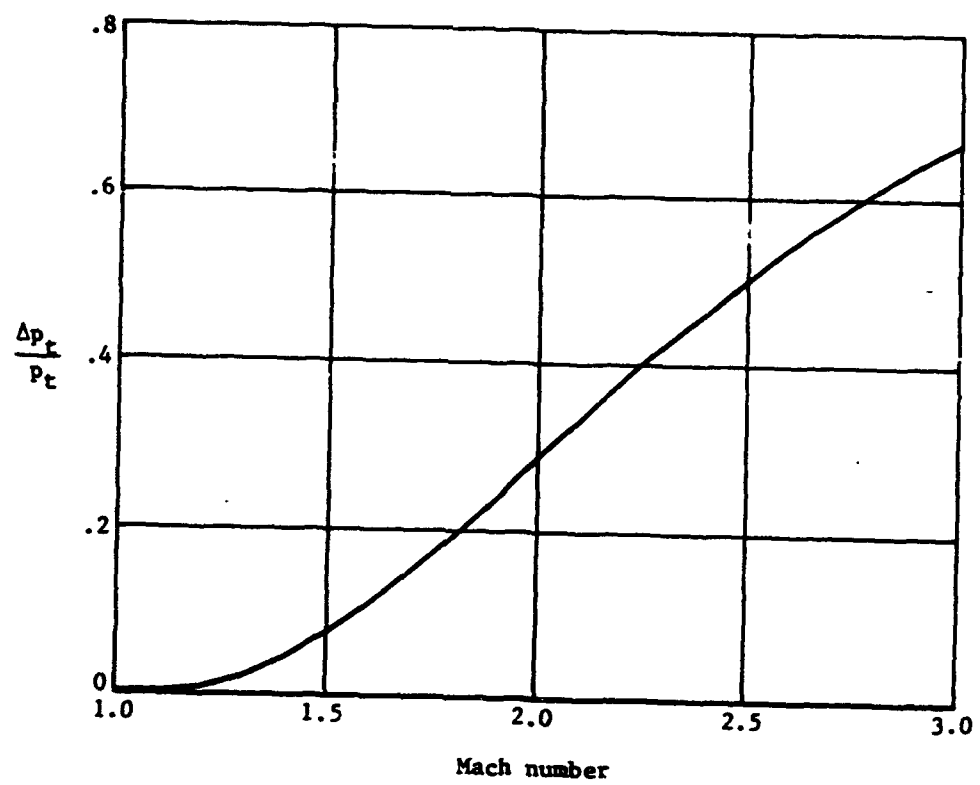
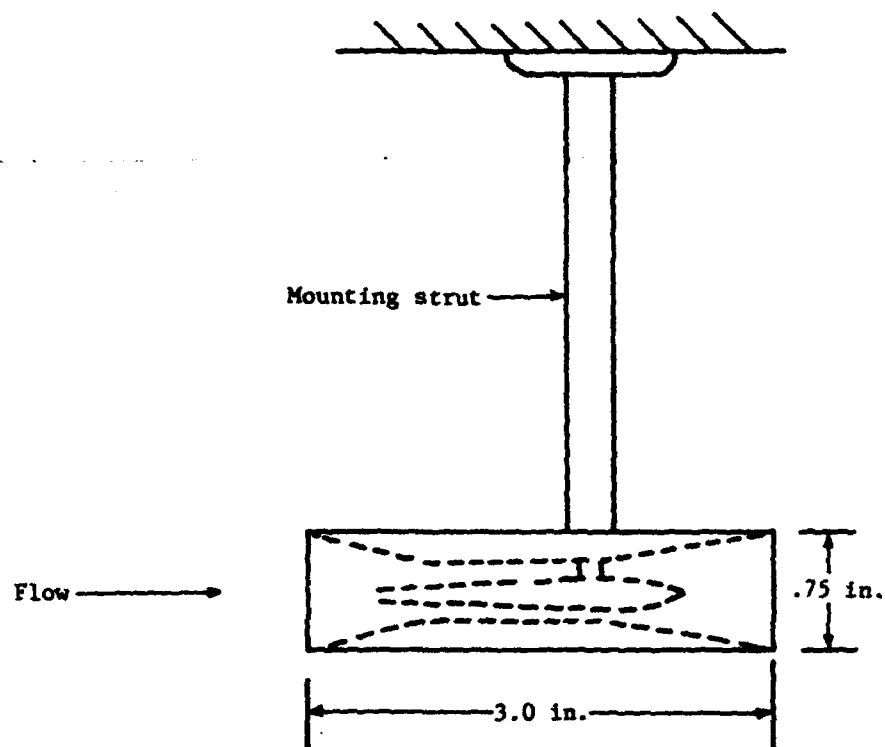
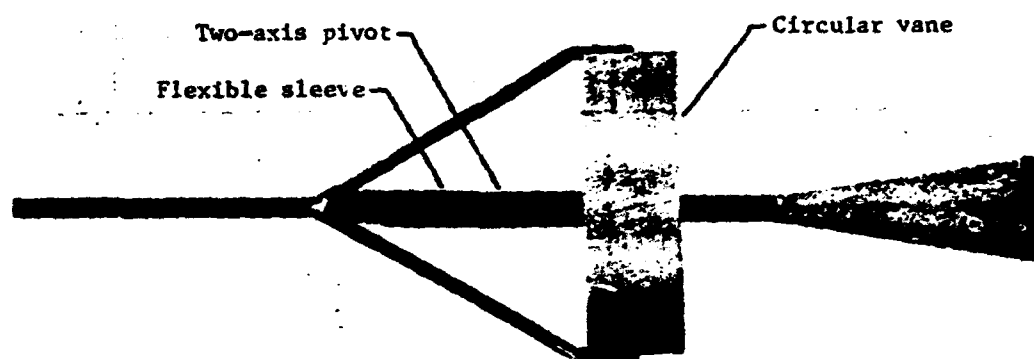


Figure 4.2.- Total-pressure loss through a normal shock wave.



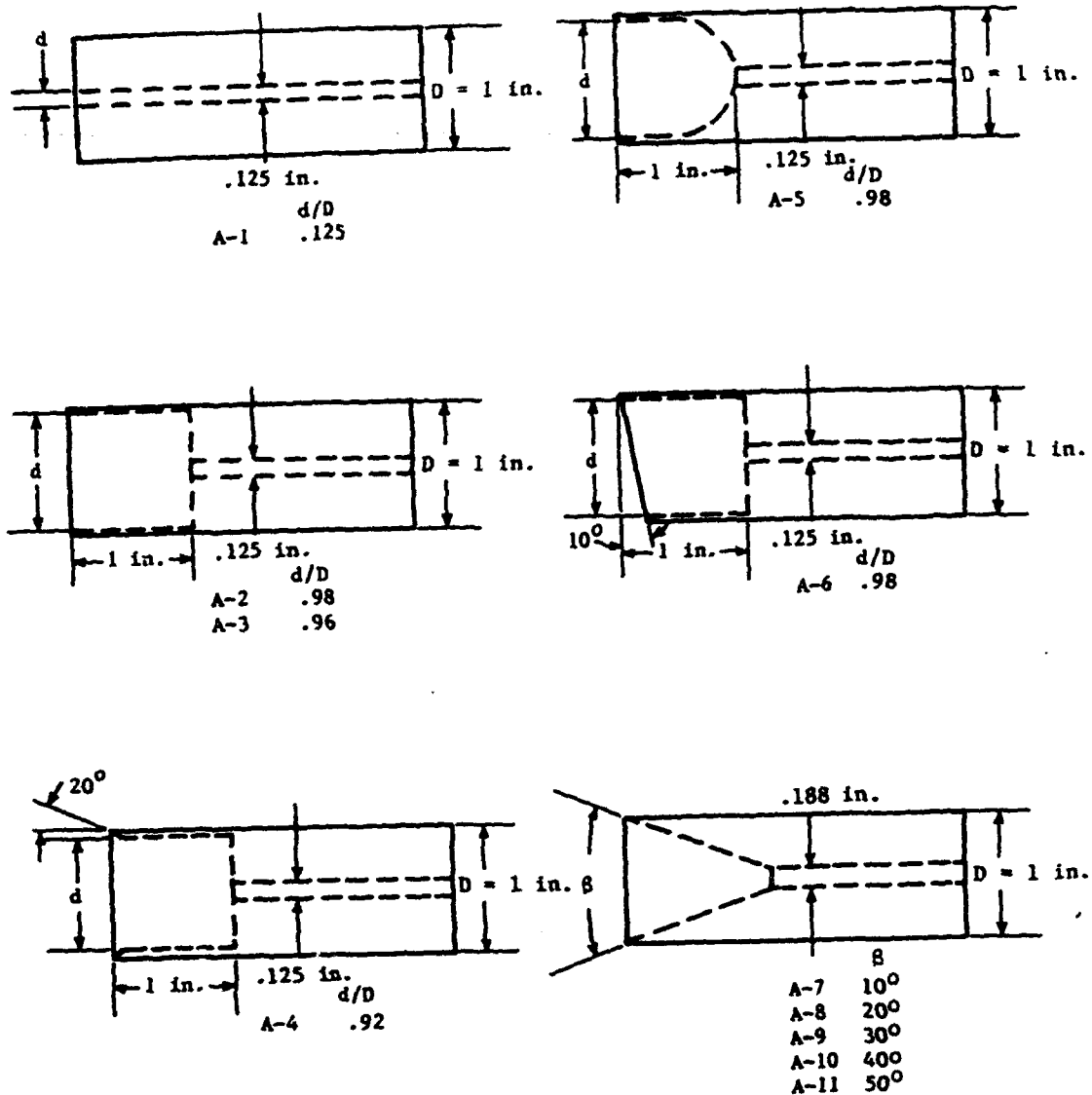
(a) Shielded total-pressure tube designed by G. Kiel.
(Adapted from ref. 3.)



(b) Swiveling total-pressure tube.

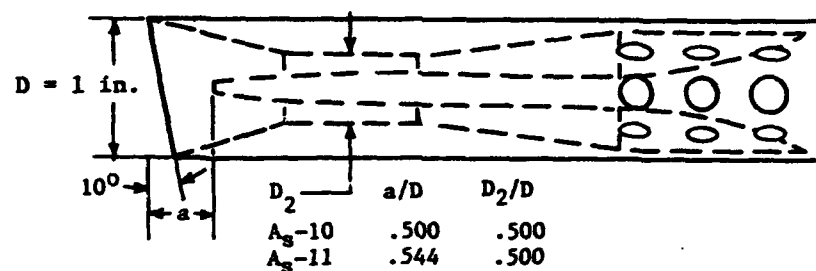
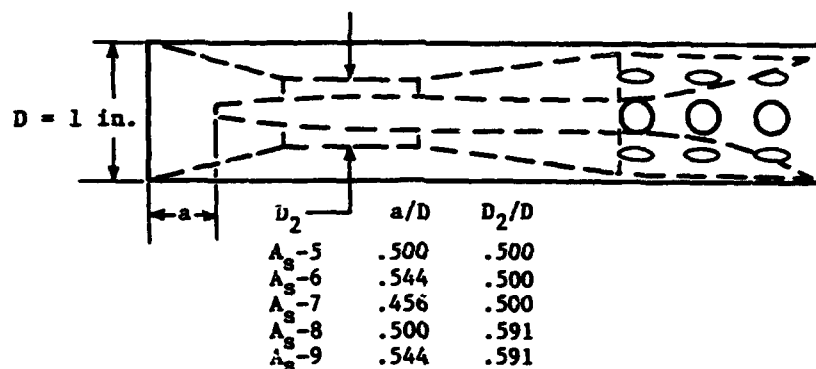
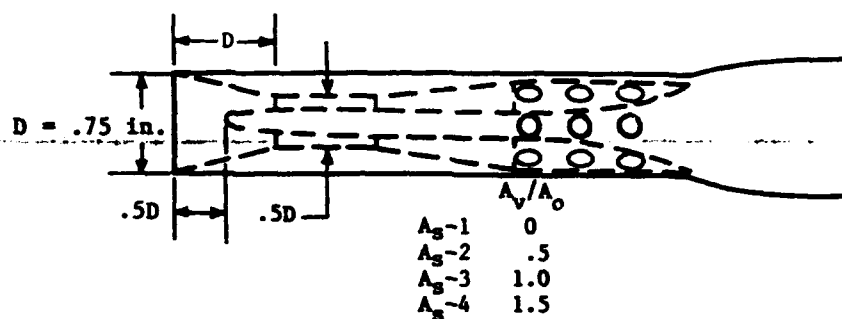
L-83-126

Figure 4.3.- Shielded and swiveling total-pressure tubes.



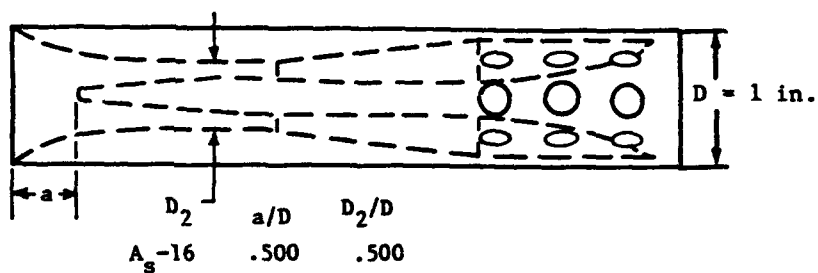
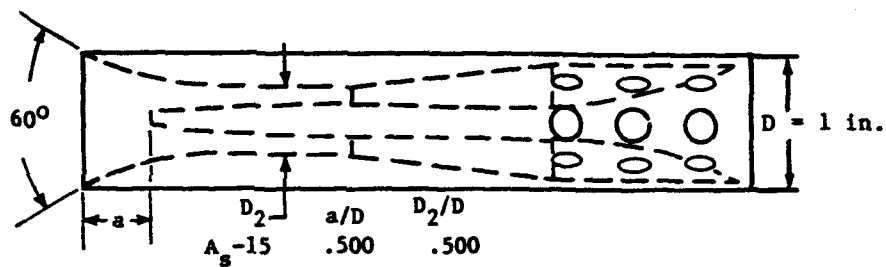
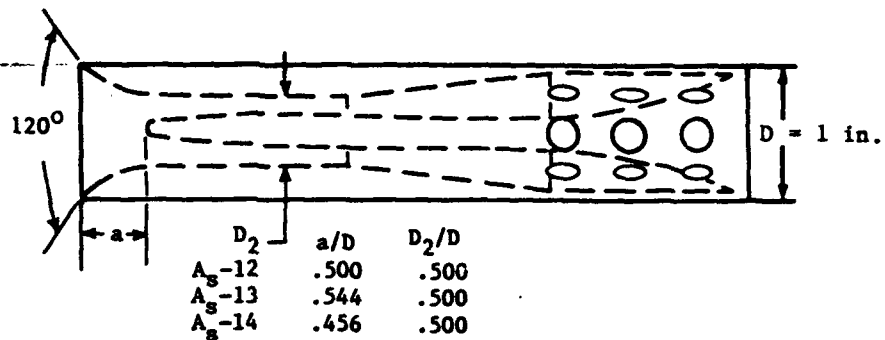
(a) Series A - cylindrical nose.

Figure 4.4.- Diagrams of total-pressure tubes examined in NACA investigations. (Adapted from ref. 9.)



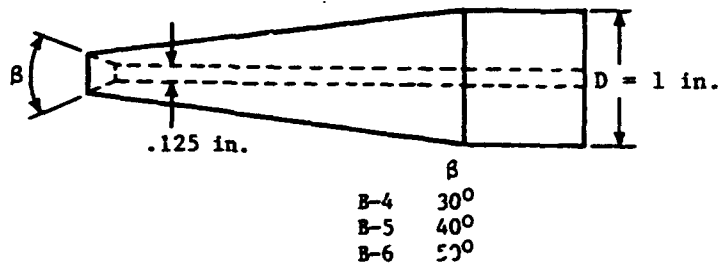
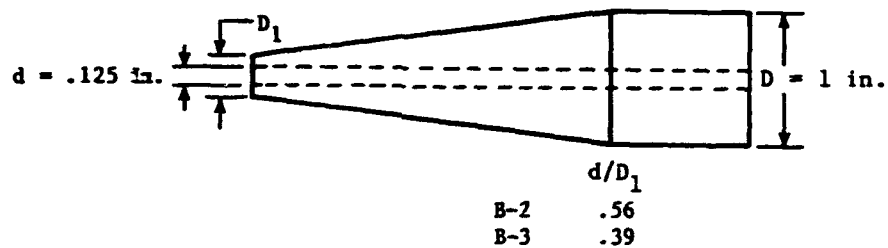
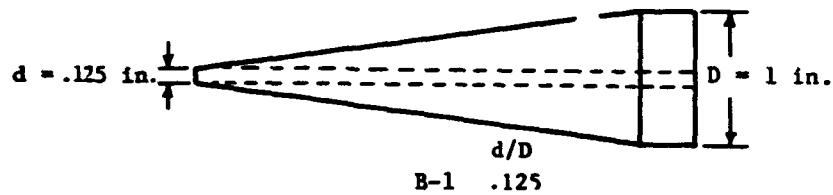
(b) Series A_s - shielded. Vent area A_v/A_o of tubes A_s-4 through A_s-16 is 1.5.

Figure 4.4.- Continued.



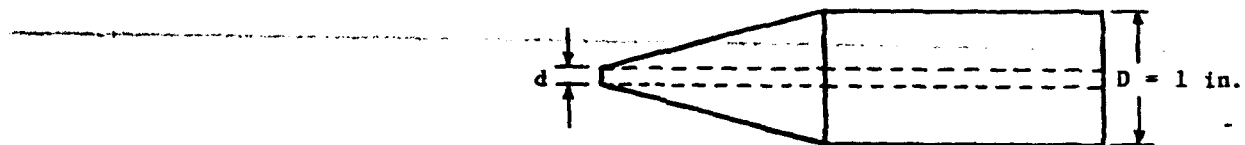
(b) Concluded.

Figure 4.4.- Continued.

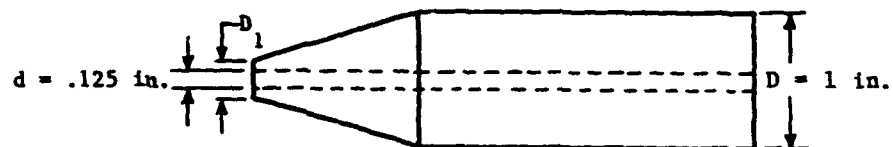


(c) Series B - 15° conical nose.

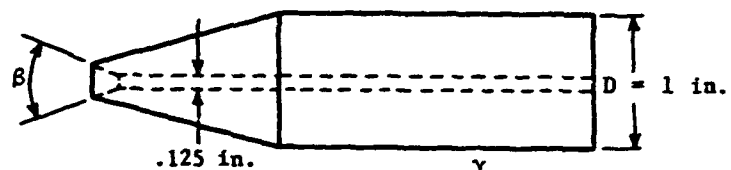
Figure 4.4.- Continued.



	d/D
C-1	.063
C-2	.125
C-3	.188



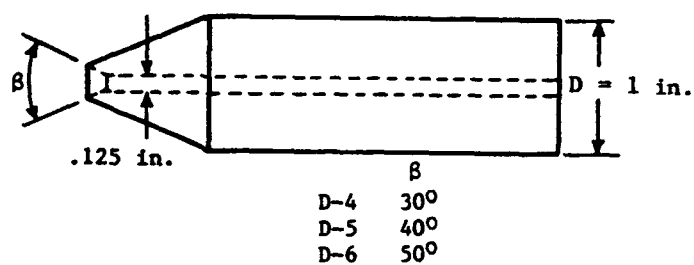
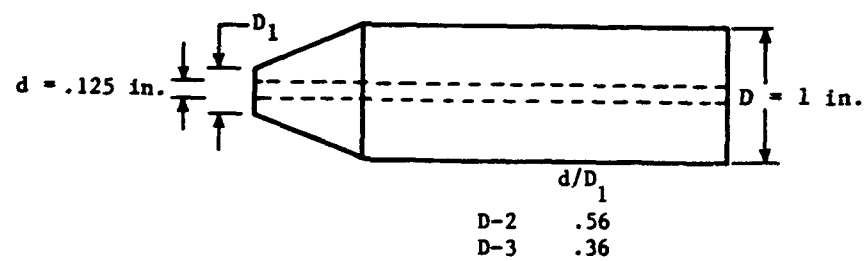
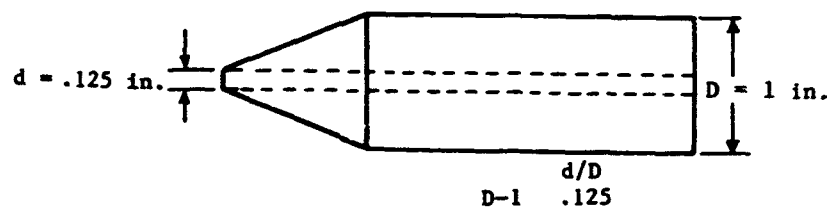
	d/D_1
C-4	.56
C-5	.39



	γ
C-6	30°
C-7	40°
C-8	50°

(d) Series C - 30° conical nose.

Figure 4.4.- Continued.

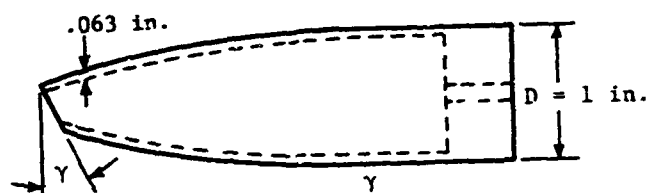


(e) Series D - 45° conical nose.

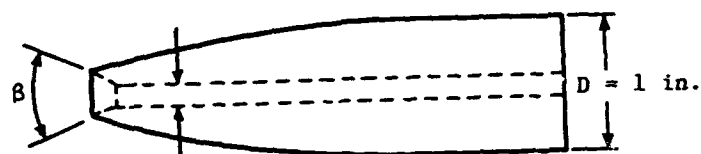
Figure 4.4.- Continued.



	d/D	D
E-1	.32	.91 in.
E-2	.43	.875 in.



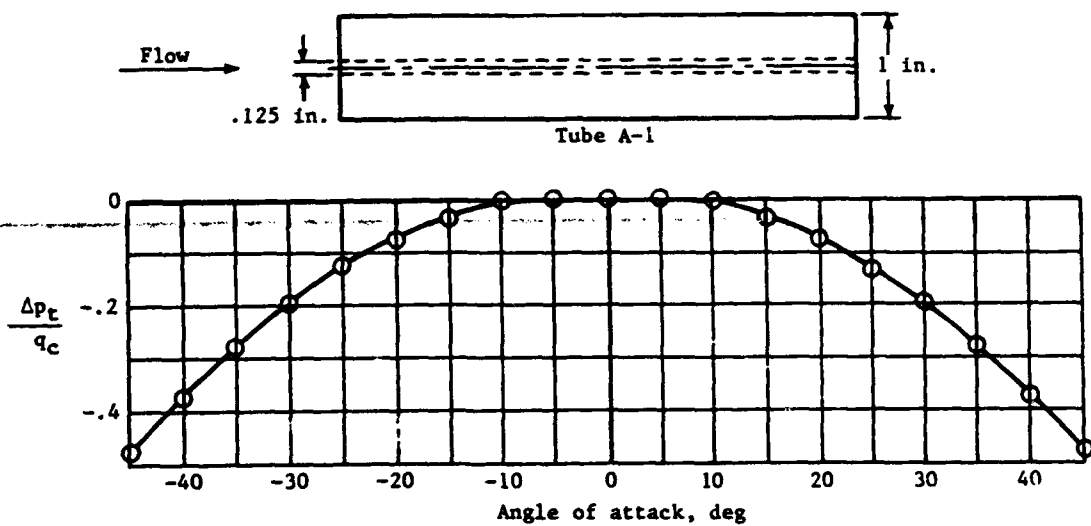
	γ
E-3	10°
E-4	20°



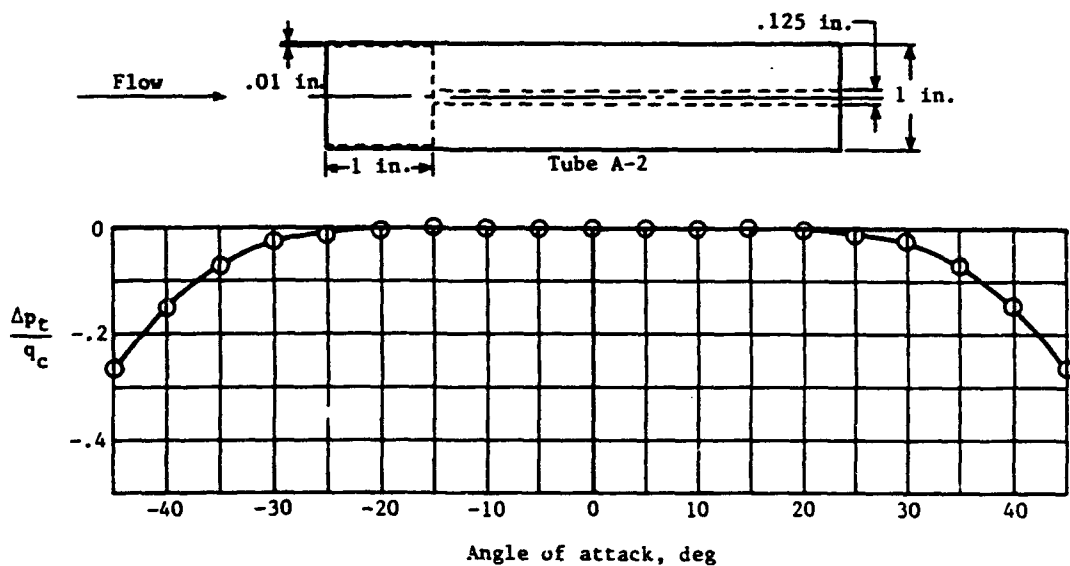
	β
E-5	30°
E-6	40°
E-7	50°

(f) Series E - ogival nose.

Figure 4.4.- Concluded.

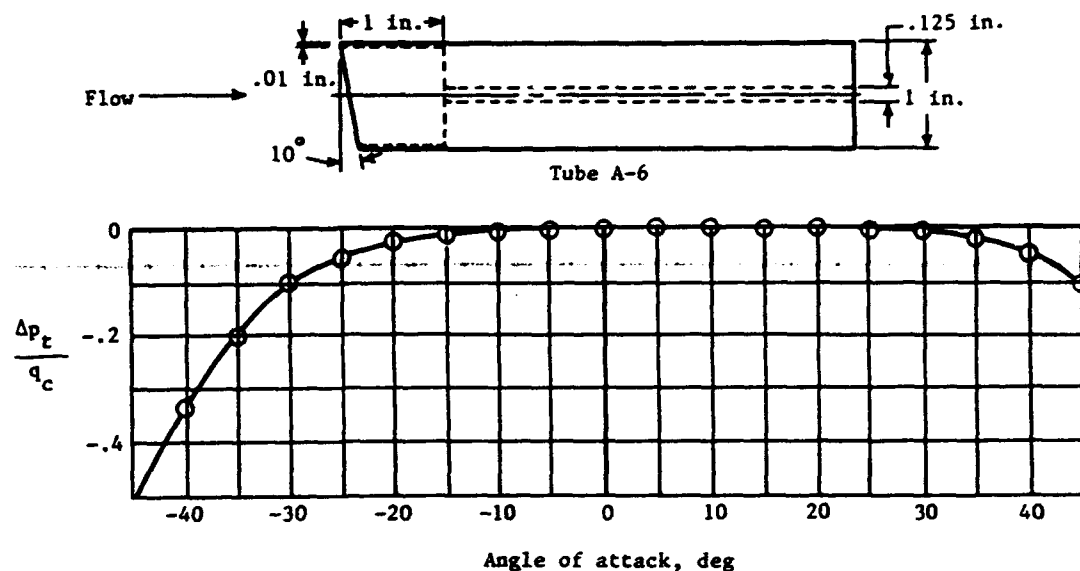


(a) Small-bore cylindrical tube.

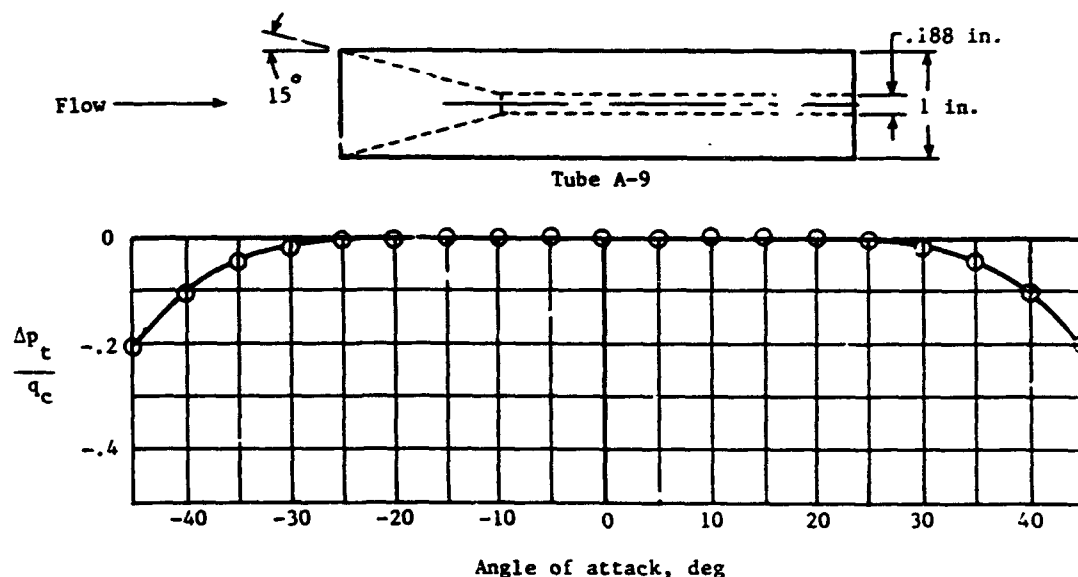


(b) Thin-wall cylindrical tube.

Figure 4.5.- Variation of total-pressure error with angle of attack for cylindrical tubes with different size impact openings. $M = 0.26$. (Adapted from ref. 4.)

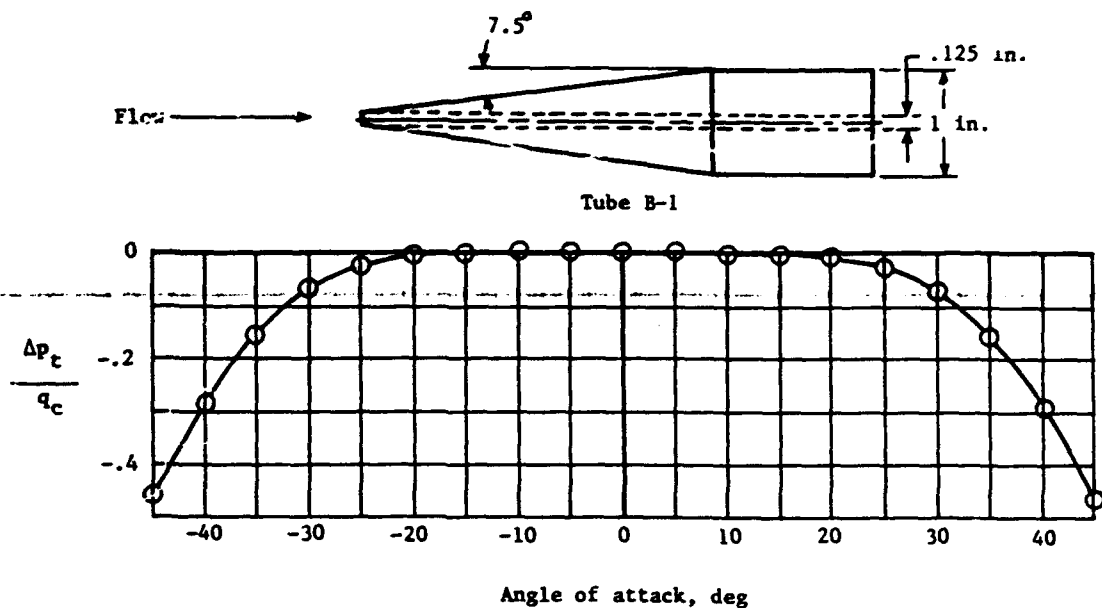


(a) Cylindrical tube with slant profile.

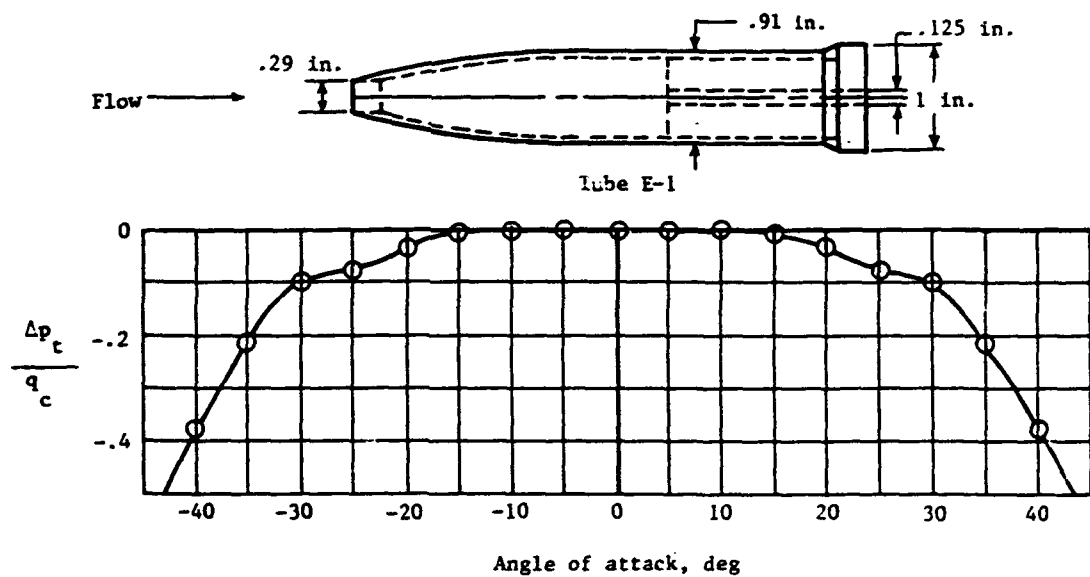


(b) Cylindrical tube with 30° conical entry.

Figure 4.6.- Variation of total-pressure error with angle of attack for cylindrical tubes with impact openings of different shapes. $M = 0.26$. (Adapted from ref. 4.)

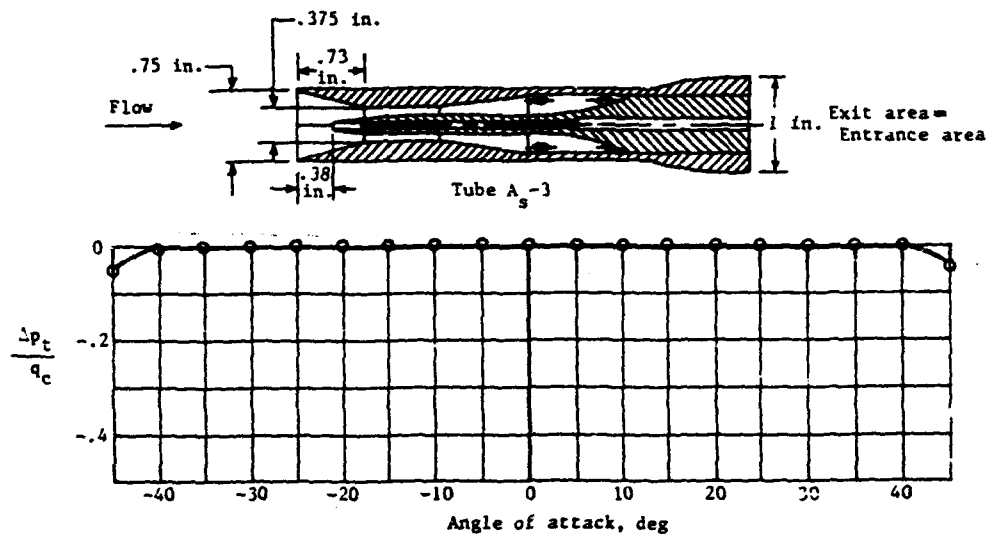


(a) 15° conical-nose tube.

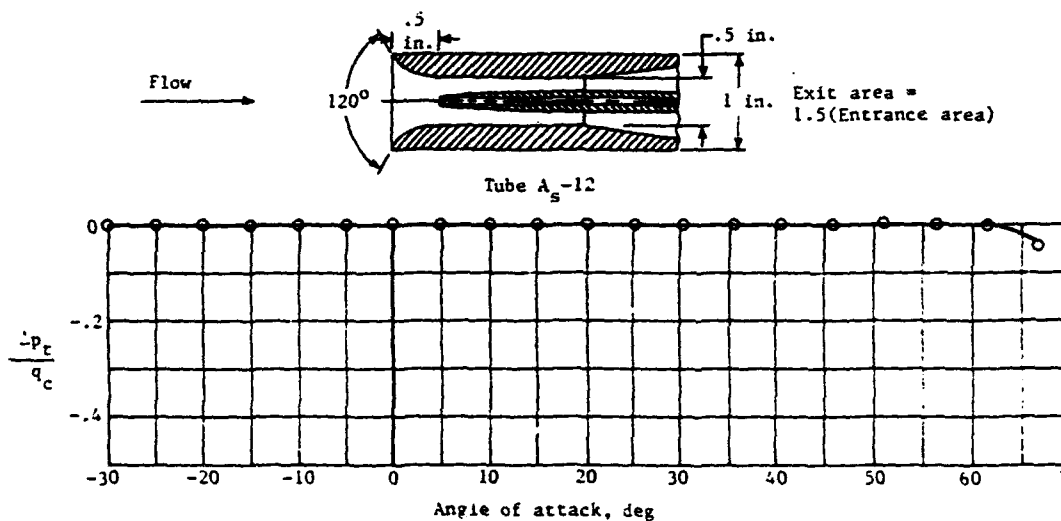


(b) Ogival-nose tube.

Figure 4.7.- Variation of total-pressure error with angle of attack for tubes having conical- and ogival-nose shapes. $M = 0.26$. (Adapted from ref. 4.)



(a) Kiel-type tube with vent holes at rear of shield.
(Adapted from ref. 4.)



(b) Shielded tube with curved entry to shield.
(Adapted from ref. 6.)

Figure 4.8.- Variation of total-pressure error with angle of attack
for two shielded tubes. $M = 0.26$.

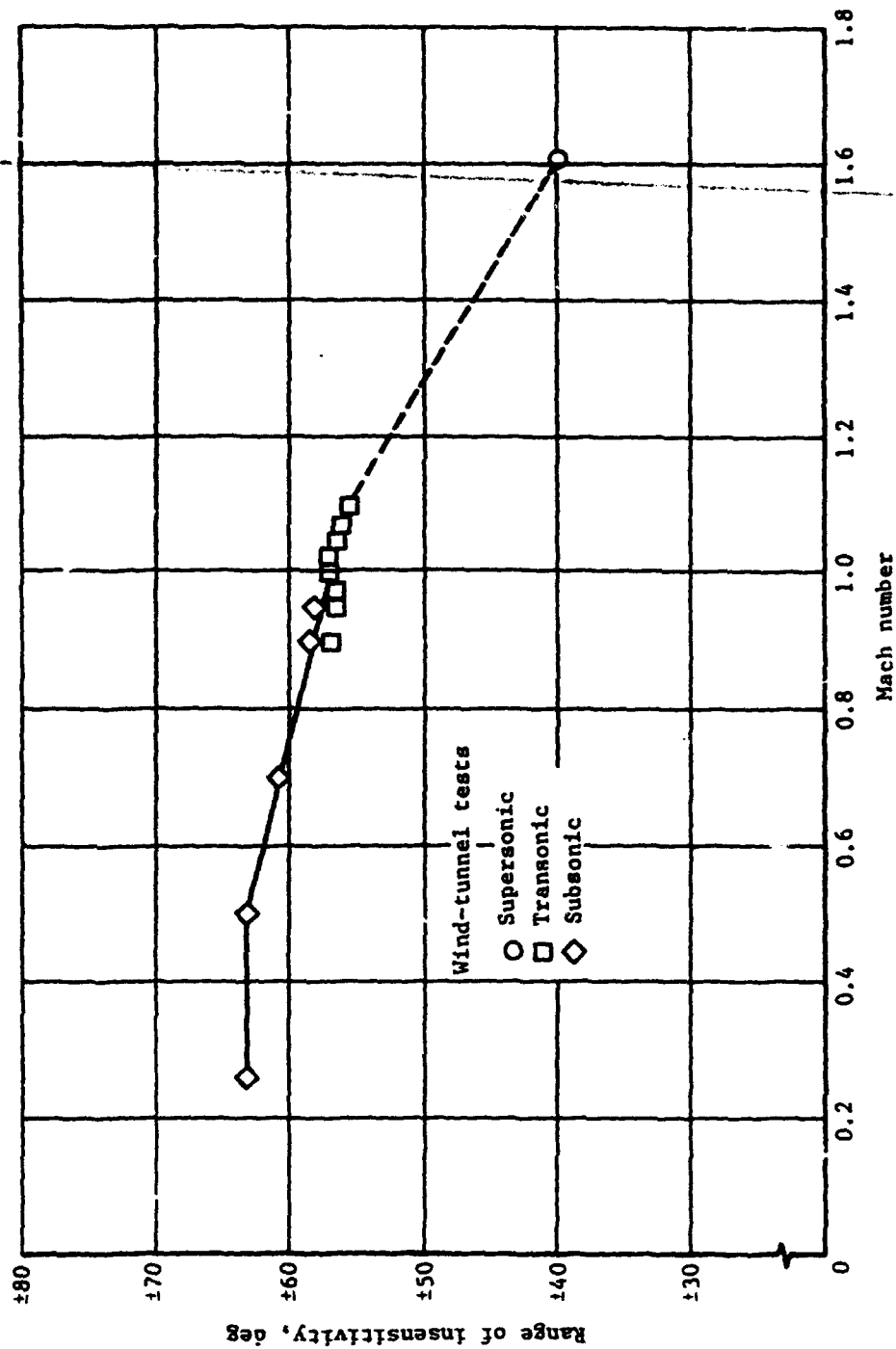


Figure 4.9.- Variation of range of insensitivity with Mach number for shielded tube A_s-12. (Adapted from ref. 8.)

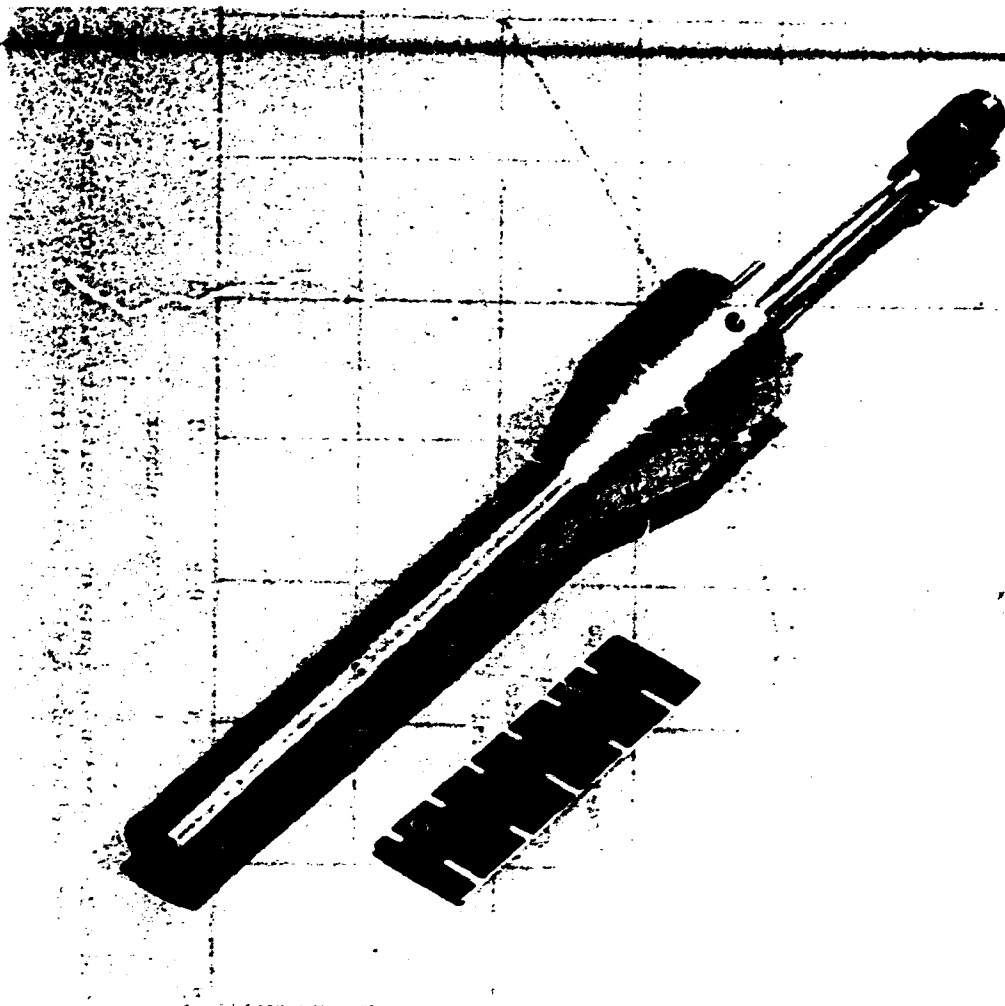


Figure 4.10.- Service-type pitot tube incorporating
pitot configuration of tube A-9.

L-79-3568

CHAPTER V

STATIC-PRESSURE MEASUREMENT

For a steady flow condition, the flow of the air over a body creates a pressure-field-in-which-the static pressures vary from point to point, while the total pressure at all points remains the same. For this reason, the measurement of free-stream static pressure on an aircraft is much more complicated than the measurement of free-stream total pressure. The pressure field created by the airflow may change with the configuration of the aircraft and with Mach number and angle of attack. For a given aircraft configuration, therefore, the problem of designing a static-pressure-measuring system is primarily one of finding a location where the static-pressure error varies by the least amount throughout the operating range of the aircraft.

The variation of the pressures in the flow field can be described by Bernoulli's equation for the total pressure p_t in incompressible flow:

$$p_t = p_l + \frac{1}{2} \rho V_l^2 = \text{Constant} \quad (5.1)$$

where p_l is the local static pressure and V_l is the local flow velocity. This equation states that the total pressure remains constant (at the free-stream value) at all points along lines of flow, whereas the local static pressure varies inversely with the square of the local velocity.

The variation of local static pressure expressed by equation (5.1) is illustrated by the diagram of the flow around a fuselagelike body in figure 5.1. The five lines of flow (streamlines) shown in this figure represent the paths of the individual particles of the air. At a great distance ahead of the body, the streamlines are parallel and the total pressure p_t , static pressure p , and velocity of the particles V on each of the streamlines are the free-stream values. As the air particles move closer to the body, the streamlines begin to diverge and the velocities of the particles begin to increase as the air flows past the body. At some considerable distance behind the body, the streamlines return to parallel flow and the pressures and velocities return to their free-stream values.

Relative magnitudes of the local pressure and the local velocity at three points near the nose of the body are also shown in figure 5.1. At a position just aft of the nose, the local velocity is higher than the free-stream velocity, and the local static pressure is lower than the free-stream static pressure. At a position directly ahead of the nose, the local velocity is lower than the stream velocity, so that the local static pressure is higher than the stream value. At a point on the leading edge of the nose, where the air particles come to a stop, the local static pressure is equal to the free-stream total pressure.

The flow pattern, or field, shown in figure 5.1 applies to incompressible flow or to compressible flow at very low speeds. For higher speeds in compressible flow, the flow field changes markedly, particularly at transonic and supersonic speeds.

In the subsonic speed range, the flow field extends in all directions from the aircraft. The difference between the local static pressure and the free-stream static pressure is greatest in the vicinity of the aircraft and decreases with distance from it. In the transonic speed range, the flow field is altered by shock waves that form along the lines of maximum curvature of the fuselage, wings, and tail surfaces. At supersonic speeds, the flow field is confined to the regions behind the shock wave that forms ahead of the nose of the fuselage (fuselage bow shock). As discussed in the next two chapters, the changes in the characteristics of the flow fields in the three speed ranges can produce large variations in the pressures measured by a static-pressure installation.

An orifice on a surface oriented parallel to the airstream has been universally used to measure static pressure on aircraft. The orifice may be located on the surface of the fuselage or on a static-pressure tube attached to some part of the aircraft. For fuselage-vent installations, the orifices are usually installed in pairs (one on each side of the fuselage) and are generally located some distance aft of the nose of the fuselage. With the static-pressure tube, the orifices are ordinarily located well aft of the nose of the tube and may either encircle the tube or be oriented in unsymmetrical arrangements described in the next chapter. On some early static-pressure tubes, the orifices were in the form of rectangular slots; on present-day tubes, the orifices are circular.

Like the total-pressure tubes described in the last chapter, the static-pressure tubes are designed with either a transverse strut for attachment to some part of the aircraft structure or with end fittings for mounting on a horizontal boom. Since the diameter of the boom is generally larger than that of the tube, the aft end of the tube is enlarged to form a collar of the same diameter as the boom. As shown in the next chapter, the mounting struts and the collars of the tubes can have a marked influence on the pressures measured by the tubes. The tubes with strut supports have generally been attached either to the underside of the wing or, in pairs, to the sides of the fuselage. The tubes designed for end-mounting on booms have been installed on the nose of the fuselage, the outboard section of the wing, and the tip of the vertical fin. Examples of service-type pitot-static tubes designed for end-mounting and strut-mounting are shown in figure 5.2.

A diagram showing four types of static-pressure-measuring installations (static-pressure tubes ahead of the fuselage nose, wing tip, and vertical fin and fuselage vents on the side of the fuselage) is presented in figure 5.3. Also shown are the local static pressures p_l and the measured static pressures p' at the four pressure sensors. For each installation, the difference between the measured pressure and the free-stream static pressure p is defined by equation (2.2):

$$\Delta p = p' - p \quad (2.2)$$

where Δp is the static-pressure error of the installation, or installation error; this error is also called the position error because the magnitude of the static-pressure error depends primarily on the position of the pressure sensor in the flow field of the aircraft.

For the fuselage-vent installation, the measured static pressure is essentially the same as the local static pressure at the vents. With the static-pressure-tube installations, on the other hand, the local static pressure is altered by the presence of the tube, because the tube creates a small flow field of its own. Since the flow of the air causes the pressures along the tube to vary in a manner similar to that described for flow about the aircraft, some part of the position error of a static-pressure-tube installation is due to the configuration of the tube (size, shape, and location of the orifices).

The errors of a static-pressure tube vary primarily with Mach number and angle of attack, while the position errors of a static-pressure installation vary primarily with Mach number and lift coefficient (a function of angle of attack). The errors of a static-pressure tube are determined by wind-tunnel tests, whereas the position errors of a static-pressure installation are determined by flight calibrations.

In steady, level flight, the lift coefficient C_L is normally a linear function of angle of attack at speeds above the stall. For this condition, C_L is defined by the following equation:

$$C_L = \frac{W}{qS} \quad (5.2)$$

where W is the weight of the aircraft, S the area of the wing, and q the dynamic pressure. Values of q can be determined from measured values of the impact pressure q_c and the static pressure p and the following equation derived from equations (3.10) and (3.22):

$$q = \frac{\gamma p M^2}{2} \quad (5.3)$$

where M is determined from the ratio q_c/p as discussed in chapter III.

In wind-tunnel calibrations of static-pressure tubes and flight calibrations of static-pressure installations, the static-pressure errors are usually presented as fractions of the static pressure, $\Delta p/p$, or as fractions of the impact pressure, $\Delta p/q_c$. For calibrations at high Mach numbers, the static-pressure error is often converted to an error in Mach number ΔM and expressed as a fraction of the Mach number, $\Delta M/M$. In this text, the static-pressure errors for all of the wind-tunnel and flight calibrations are presented in terms of $\Delta p/q_c$. For a comparison of a position error calibration in terms of $\Delta p/q_c$, $\Delta p/p$, and $\Delta M/M$, see figure 7.23.

Values of $\Delta p/q_c$ can be converted to values of $\Delta p/p$ by means of the q_c/p values given in table A26 of appendix A. A graph showing the relation of $\Delta p/p$ to $\Delta p/q_c$ for Mach numbers up to 2.0 is presented in figure 5.4.

Values of $\Delta p/q_c$ and $\Delta p/p$ can be converted to values of $\Delta M/M$ by means of the following equations from reference 1:

$$\frac{\Delta p}{p} = - \frac{1.4M^2}{1 + 0.2M^2} \frac{\Delta M}{M} \quad (5.4)$$

and

$$\frac{\Delta p}{q_c} = - \left[\frac{1}{(1 + 0.2M^2)^{3.5} - 1} \right] \frac{1.4M^2}{1 + 0.2M^2} \frac{\Delta M}{M} \quad (5.5)$$

for $M \leq 1$, and

$$\frac{\Delta p}{p} = \left(\frac{4.0}{5.6M^2 - 0.8} - 2 \right) \frac{\Delta M}{M} \quad (5.6)$$

and

$$\frac{\Delta p}{q_c} = \left(\frac{4.0}{5.6M^2 - 0.8} - 2 \right) \frac{1}{1.2M^2 \left(\frac{5.76M^2}{5.6M^2 - 0.8} \right)^{2.5} - 1} \frac{\Delta M}{M} \quad (5.7)$$

for $M \geq 1$. A graph of the relation between $\Delta p/p$ and $\Delta M/M$ and between $\Delta p/q_c$ and $\Delta M/M$ for Mach numbers up to 5.0 is presented in figure 5.5.

The altitude error ΔH , airspeed error ΔV_c , and Mach number error ΔM that are associated with the position error Δp are defined by the following equations:

$$\Delta H = H' - H \quad (5.8)$$

where H' is the indicated altitude and H is the pressure altitude,

$$\Delta V_c = V_i - V_c \quad (5.9)$$

where V_i is the indicated airspeed and V_c is the calibrated airspeed,

$$\Delta M = M' - M \quad (5.10)$$

where M' is the indicated Mach number and M is the free-stream Mach number.

To provide an indication of the errors in airspeed and altitude that result from a given static-pressure error, the altitude errors ΔH and the airspeed errors ΔV_C corresponding to a static-pressure error equal to 1 percent of the impact pressure ($\Delta p/q_C = 0.01$) are presented in figure 5.6 for Mach numbers up to 1.0 and altitudes up to 40 000 ft. The altitude errors corresponding to an error of 1 percent of the static pressure ($\Delta p/p = 0.01$) are presented in figure 5.7 for altitudes up to 50 000 ft, and the altitude errors corresponding to an error of 1 percent of the Mach number ($\Delta M/M = 0.01$) are presented in figure 5.8 for Mach numbers up to 1.0 and altitudes up to 40 000 ft. For positive static-pressure errors ($\Delta p/q_C$ or $\Delta p/p$), the signs of both ΔH and ΔV_C are negative; for positive values of $\Delta M/M$, the signs of ΔH and ΔV_C are positive.

In appendix B, sample calculations are given for the determination of ΔH , ΔV_C , and ΔM from a given value of Δp and the indicated altitude H' , the indicated airspeed V_i , and the indicated Mach number M' .

Reference

1. Zalovcik, John A.: A Radar Method of Calibrating Airspeed Installations on Airplanes in Maneuvers at High Altitudes and at Transonic and Supersonic Speeds. NACA Rep. 985, 1950. (Supersedes NACA TN 1979.)

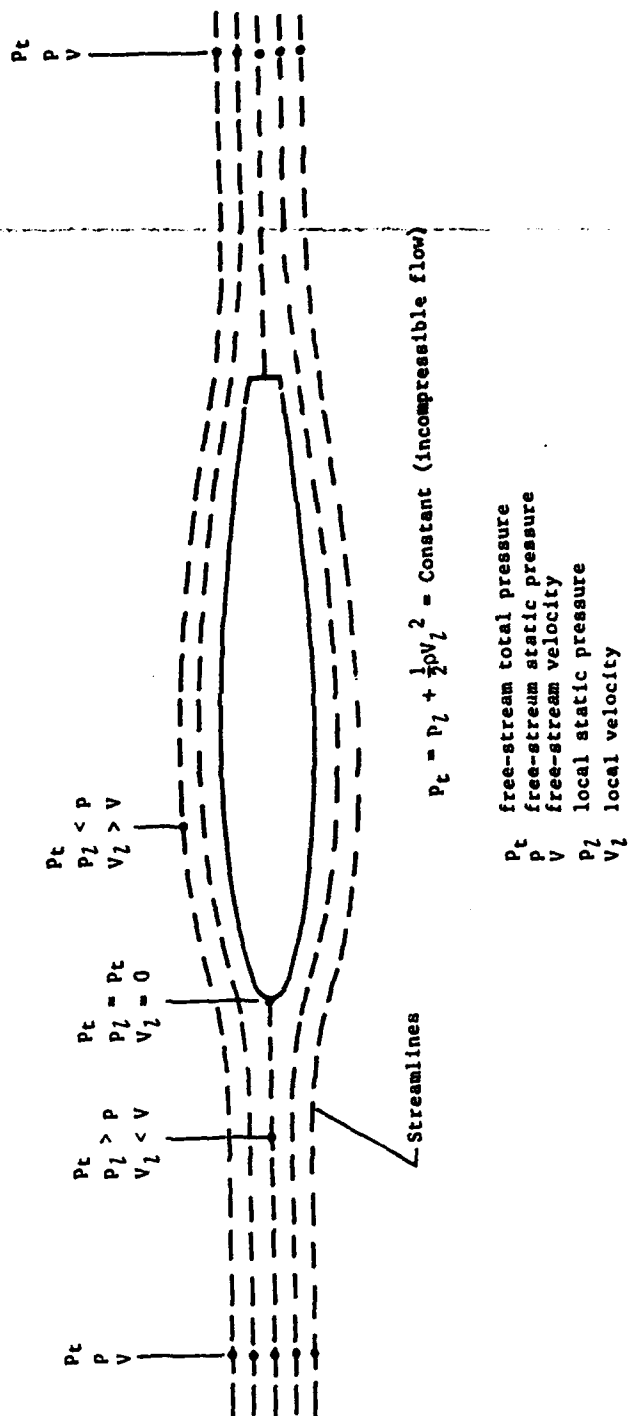
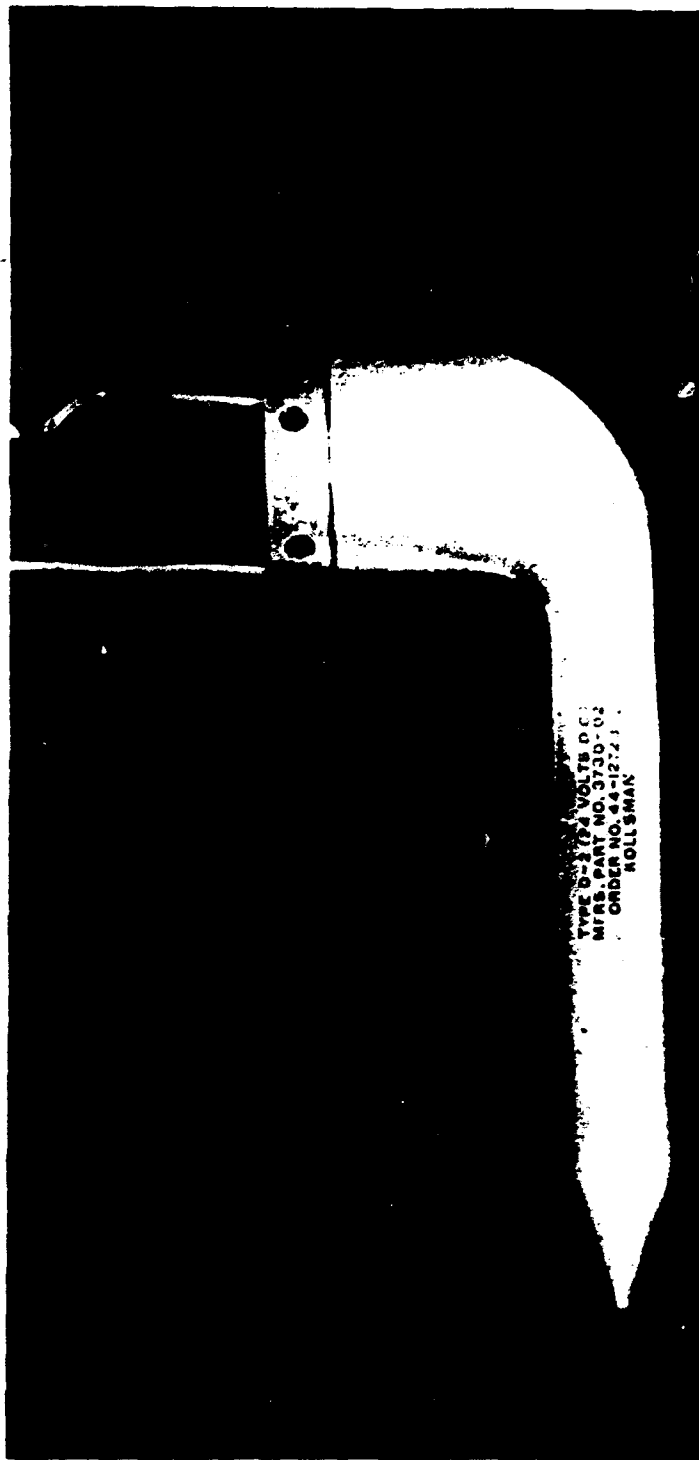


Figure 5.1.- Diagram showing local pressures and velocities in vicinity of fuselagelike body.



(a) Strut mounting.



(b) End mounting.

L-79-3847

Figure 5.2.- Examples of service-type pitot-static tubes.

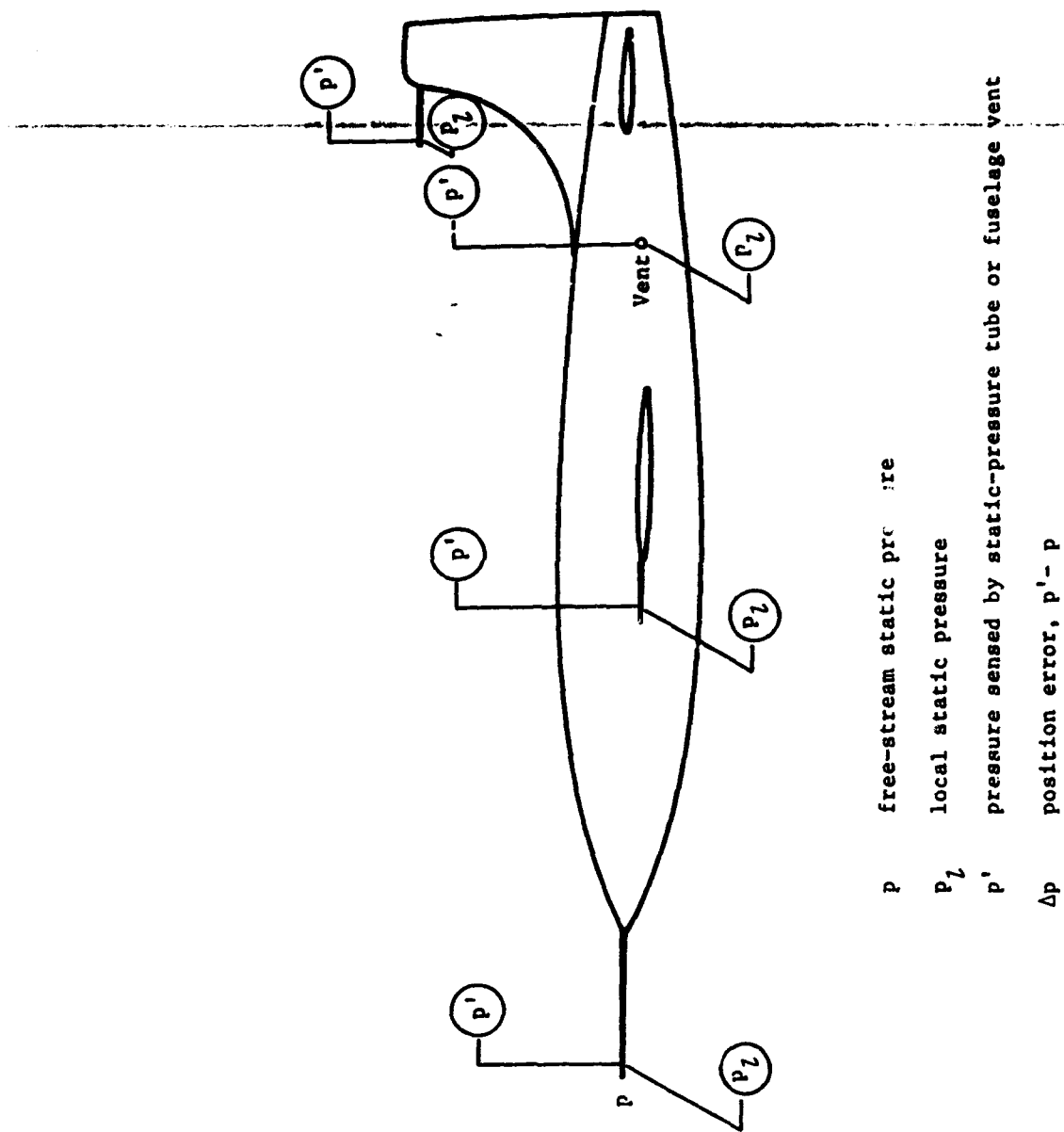


Figure 5.3.- Diagram showing various types of installations for the measurement of static pressure on an aircraft.

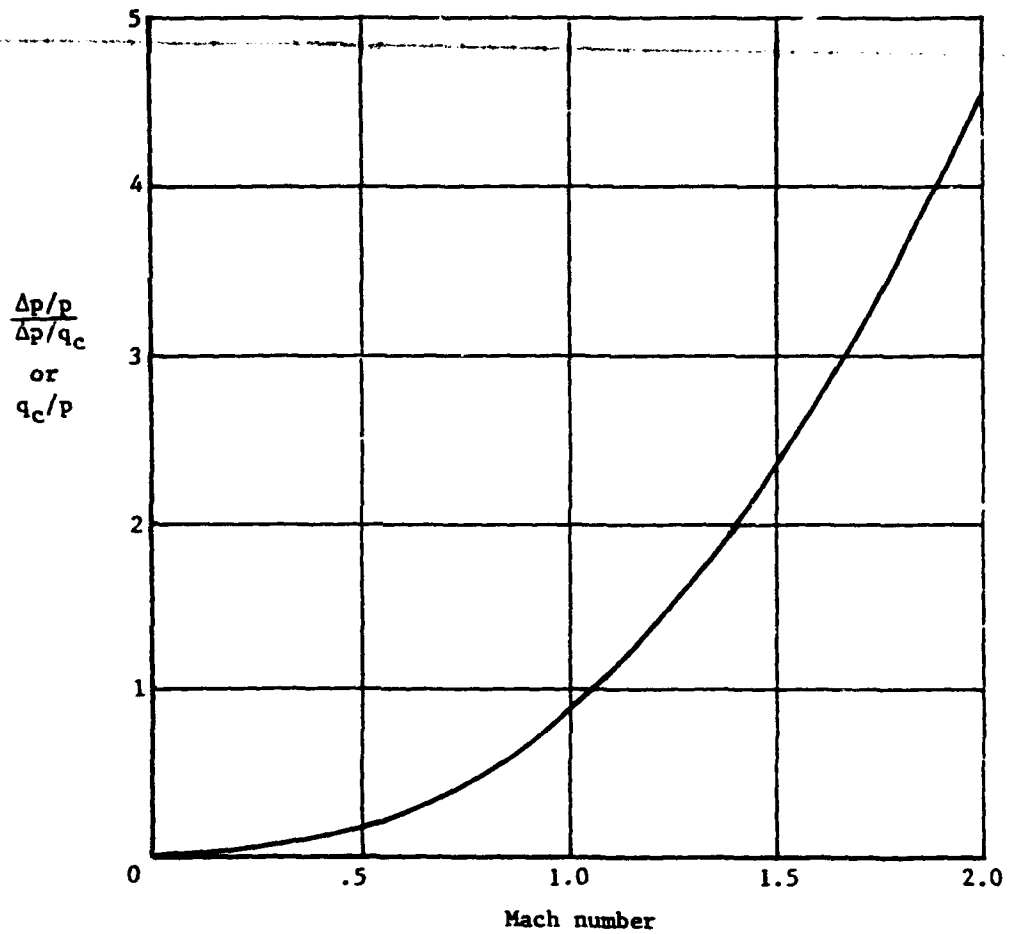


Figure 5.4.- The relation between $\Delta p/p$ and $\Delta p/q_c$.

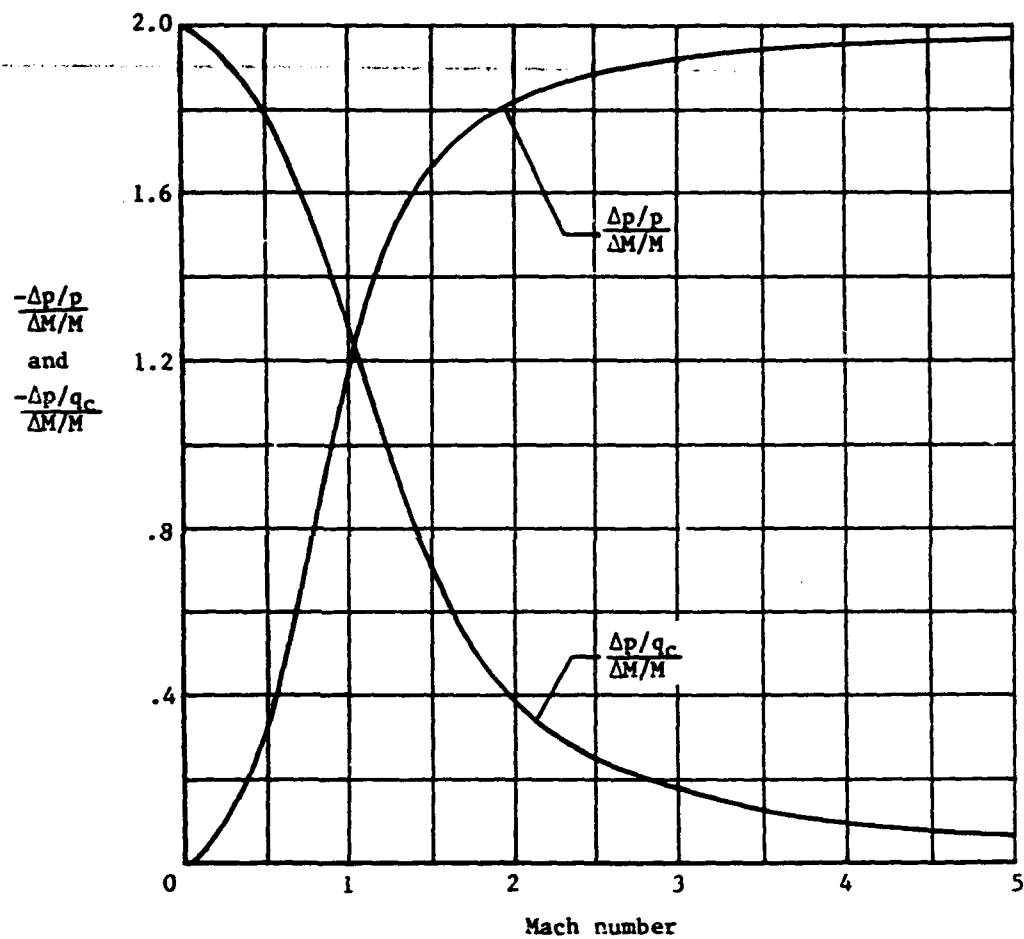
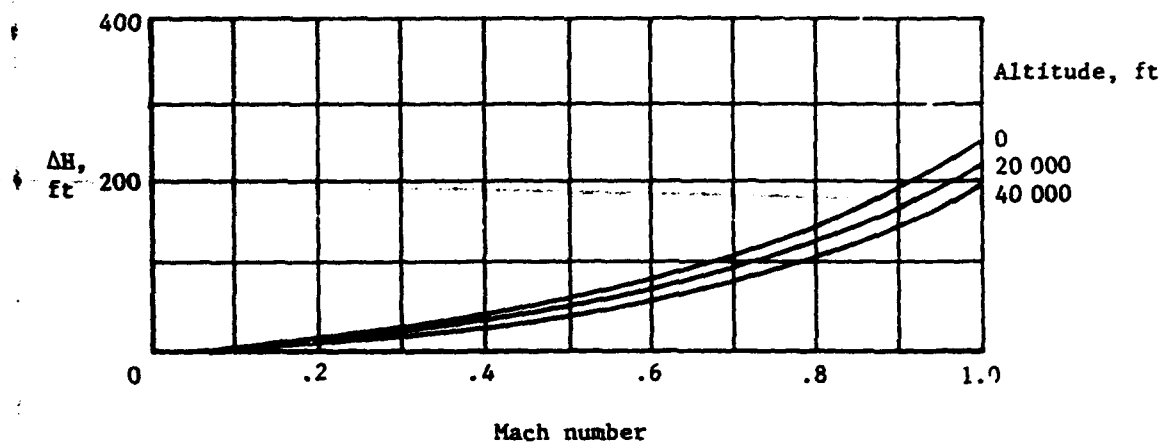
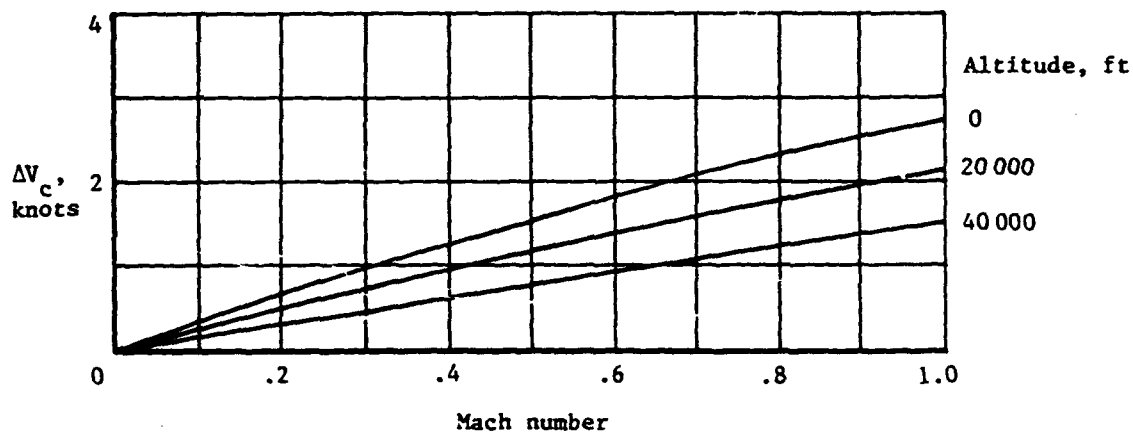


Figure 5.5.- The relation between $\Delta p/p$ and $\Delta M/M$ and between $\Delta p/q_c$ and $\Delta M/M$. (Adapted from ref. 1.)



(a) ΔH corresponding to $\Delta p/q_c = 0.01$.



(b) ΔV_c corresponding to $\Delta p/q_c = 0.01$.

Figure 5.6.- Altitude errors ΔH and airspeed errors ΔV_c corresponding to a static-pressure error of 1 percent of impact pressure ($\Delta p/q_c = 0.01$).

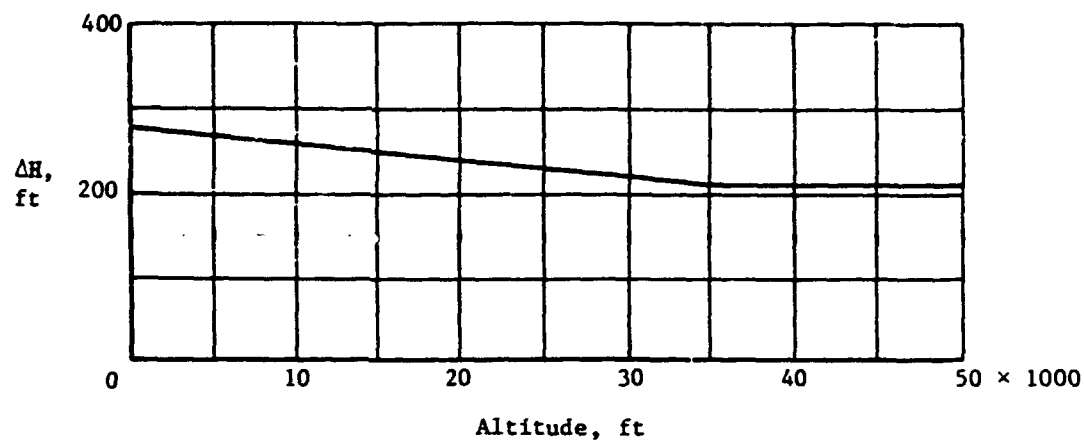


Figure 5.7.- Altitude errors ΔH corresponding to a static-pressure error of 1 percent of the static pressure ($\Delta p/p = 0.01$).

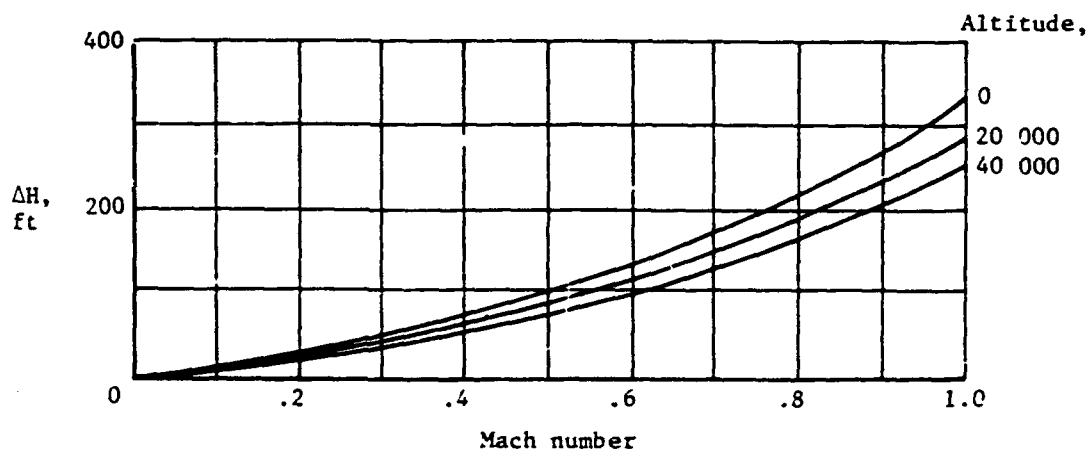


Figure 5.8.- Altitude errors ΔH corresponding to a Mach number error of 1 percent ($\Delta M/M = 0.01$).

CHAPTER VI

STATIC-PRESSURE TUBES

As discussed in the previous chapter, the flow of the air past a static-pressure tube causes the pressures along the surface of the tube to vary from one point to another. These variations in static pressure can be described in terms of pressure distributions along the tube (when the tube is aligned with the flow) and pressure distributions around the tube (when the tube is inclined to the flow).

The difference between the pressure sensed by the orifices and the free-stream static pressure is the static-pressure error of the tube, sometimes called the error of the isolated tube. In the following sections, the errors of tubes aligned with the flow are considered separately from the errors of tubes inclined to the flow. At the end of the chapter, data are presented on the effects of orifice size and shape on the pressure sensed by the tube.

Tubes Aligned With the Flow

Theoretical pressure distributions along cylindrical bodies (fig. 6.1, from ref. 1) are useful in understanding the problem of locating orifices along a static-pressure tube. For both the subsonic and supersonic flow conditions shown in the figure, the static-pressure errors are negative at a station just beyond 1 tube diameter from the nose of the tube. The pressures at this point on the tube are, therefore, below the free-stream pressure. With increasing distance from the nose, the pressures approach the free-stream pressure and should reach that value at a distance of about 5 tube diameters in subsonic flow and about 8 tube diameters in supersonic flow.

In using the theoretical data to design a tube to measure free-stream pressure, many designers place the orifices a greater distance from the nose than that indicated by the theoretical distributions. A typical example is the 10-diameter location on the tube in figure 6.2. As shown by the calibration data, the static-pressure error is near zero throughout most of the subsonic speed range.

In the subsonic speed range, the pressure at the orifices can be influenced by the presence of a strut or collar downstream from the orifices. The effect of a strut is illustrated by figure 6.3 which shows the pressure distribution for incompressible, two-dimensional flow ahead of a body of infinite length transverse to the flow. For application to pressure measurements with a static-pressure tube, this body can be considered to represent the support strut of a tube. The curve on this figure shows that the pressure errors ahead of the strut are positive (measured pressures above free-stream pressure) and that they diminish toward the free-stream value with increasing distance from the strut. This effect of a strut or other body in creating a positive pressure field upstream from the body is called the blocking effect.

Wind-tunnel tests of the blocking effect of a strut at a number of distances behind a set of static-pressure orifices were reported in reference 2. The results of the tests (fig. 6.4) confirm the theoretical variation by showing the errors to be greatest for the shortest strut position ($x/t = 3.6$) and least for the longest ($x/t = 10.5$). The rise in the errors at Mach numbers above 0.5 shows that the blocking effect increases in the upper subsonic speed range.

Early designers of static-pressure tubes favored short tubes for strut-mounting, because the blocking effect of the strut could be used to balance the negative errors incurred by locating the orifices near the nose of the tube. The outstanding example of this design concept was the Prandtl pitot-static tube (fig. 6.5) on which the orifices were located 3 tube diameters aft of the nose and 10 strut thicknesses ahead of the strut. This tube, and variations of the original design, has been the subject of many wind-tunnel investigations (refs. 3, 4, and 5, for example). In the most extensive of these tests (ref. 5), the error was essentially zero in the Mach range up to 0.5 (fig. 6.5), but increased at higher Mach numbers in the same manner as the errors of the tubes in figure 6.4.

In contrast to early tubes designed for strut-mounting, later tubes were designed for end-mounting on horizontal booms. These designs permitted the use of longer tubes on which the orifices could be located a greater distance from the nose. In addition, the collars at the rear of the tube could be so located that the blocking effect would be smaller than that of a strut. Thus, the positive and negative pressure errors at the orifices could both be made smaller than those of the strut-mounted tubes.

The blocking effect of a collar on the pressures at orifices at three locations ahead of a collar was investigated in the tests of reference 2. The results of the tests (fig. 6.6) show that even for orifices located as close to the collar as 1.8 collar diameters, the errors are relatively small (1.5 percent q_c) and essentially constant for Mach numbers up to 0.8.

A number of service-type tubes have been designed for end-mounting on booms. On one of the most widely used of these tubes (fig. 6.7), the orifices are located 5.5 tube diameters from the nose and 2.8 collar diameters ahead of the collar. As shown by figure 6.7, the static-pressure error of this tube is constant at about 0.5 percent q_c up to a Mach number of about 0.9.

Another end-mounted tube, designed for use on high-speed research aircraft, has the orifices located 9.1 tube diameters behind the nose and 5.3 collar diameters ahead of the collar. The calibration of this tube (fig. 6.8, from ref. 6) at both subsonic and supersonic speeds shows an error of 1 percent q_c at $M = 0.6$, a sharp rise in error at Mach numbers around 0.9, and an abrupt decrease to errors near zero at a Mach number just beyond 1.0. The abrupt fall of the error is due to the passage over the orifices of a shock wave that forms ahead of the collar when the flow reaches sonic speed. A similar decrease in static-pressure error at low supersonic speeds is experienced with fuselage-nose installations, as is discussed in some detail in the next section.

Tubes Inclined to the Flow

The pressures sensed by a static-pressure tube inclined to the flow depends not only on the location of the orifices along the tube but also on their spacing around the tube. When the orifices encircle the tube, the measured pressure decreases as the tube is inclined, and the static-pressure error reaches a value of -1 percent q_c at angles of attack and yaw of about 5° .

The range of insensitivity of a tube at positive angles of attack can be extended by spacing the orifices around the tube in one of two unsymmetrical arrangements. The selection of the proper spacing can be illustrated by the pressure distribution around a circular cylinder at an angle of attack of 45° and a Mach number of 0.2 (fig. 6.9, from ref. 7). This distribution shows the static-pressure error to be positive at the bottom of the tube ($\phi = 0^\circ$), negative on the top ($\phi = 180^\circ$), and zero at radial stations of about 35° . These data suggest that a tube could be made less sensitive to inclination at positive angles of attack by (1) locating two orifices approximately $\pm 35^\circ$ from the bottom of the tube or (2) locating a number of orifices on the top and bottom of the tube to achieve a balance of the positive and negative pressures in these regions. Since the pressure distribution, and thus the radial position for zero pressure error, varies with angle of attack and Mach number, null-type (dual orifice) tubes have been designed with a number of orifice stations ($\pm 30^\circ$ to $\pm 41.5^\circ$) in an attempt to produce a configuration that would be satisfactory through a range of angles of attack and Mach numbers.

In tests of a tube with orifices at the $\pm 30^\circ$ station (ref. 8), the range of insensitivity at positive angles of attack was found to be 20° at $M = 0.3$ and about 9° at $M = 0.65$ (fig. 6.10). Note that for the static-pressure tubes, the range of insensitivity is defined as the angular range through which the static-pressure error remains within 1 percent q_c of its value at an angle of attack of 0° . This definition is different from that given for the total-pressure tubes because the errors of static-pressure tubes at an angle of attack of 0° are usually not zero. However, whenever corrections are applied for the errors of static-pressure-tube installations at or near an angle of attack of 0° , the definition of the range of insensitivity for static-pressure tubes becomes the same as that for the total-pressure tubes, namely, the range through which the error remains within 1 percent q_c .

In an investigation to determine the errors at a number of orifice stations (ref. 9), a cylindrical tube was tested with orifices located at the $\pm 30^\circ$, $\pm 33^\circ$, $\pm 36^\circ$, $\pm 37.5^\circ$, and $\pm 40^\circ$ stations. The tests were conducted with the tube at an angle of attack of 12° through a Mach range from 0.4 to 1.2. The results of the tests (fig. 6.11) show the errors to be positive at the $\pm 30^\circ$, $\pm 33^\circ$, and $\pm 36^\circ$ stations and negative at the $\pm 40^\circ$ station. For the $\pm 37.5^\circ$ station, the errors were near zero through the Mach range up to 1.2.

A top-and-bottom orifice arrangement is used on the service-type tube shown in figure 6.7. With this arrangement, four orifices are spaced within a radial angle of $\pm 20^\circ$ on the top of the tube and six orifices within a radial angle of $\pm 30^\circ$ on the bottom. Tests of this tube at a Mach number of 1.2 (ref. 10) showed the range of insensitivity to be -1.5° to $+22^\circ$ (fig. 6.12). At angles of yaw, the range of insensitivity was $\pm 5^\circ$.

In an attempt to extend the range of insensitivity of this tube at positive angles of attack, the orifice configuration was altered by progressively increasing the orifice area on the bottom of the tube. For the final configuration tested (fig. 6.12(b)), the two orifices at the $\pm 30^\circ$ station on the bottom were enlarged from 0.043 in. in diameter to 0.052 in., and an additional orifice, 0.052 in. in diameter, was drilled at the 0° station just aft of the six orifices. With this configuration, the range of insensitivity was extended to $\pm 45^\circ$ at $M = 0.2$, but to only $\pm 20^\circ$ at $M = 0.68$.

The modified orifice configuration on the service tube in figure 6.12(b) was incorporated in the design of the research-type tube in figure 6.8. In tests of this tube through a Mach range from 0.6 to 2.87 (fig. 6.13), the range of insensitivity at positive angles of attack was found to be about 15° at both subsonic and supersonic speeds.

A service-type pitot-static tube exemplifying modern design trends is shown in figure 6.14 (ref. 11). For small errors at zero inclination, the orifices are located 13 tube diameters aft of the nose and 3.6 collar diameters ahead of the collar ($x/(D - d) = 7.2$). The radial position of the two orifices is $\pm 37.5^\circ$ which, as shown by the data of figure 6.11, minimizes the error at positive angles of attack up to at least 12° . The pitot configuration is the same as that of tube B-4 (chapter IV) which is insensitive to inclination (to within 1 percent q_c) at angles of attack and yaw of $\pm 21^\circ$.

Orifice Size and Shape

The influence of orifice diameter and edge shape on the pressures measured by a static-pressure tube can be seen in figure 6.15 (from ref. 12). The variation of the static-pressure error with orifice diameter for a square-edge orifice at Mach numbers of 0.4 and 0.8 is shown in figure 6.15(a). These errors can be related to the orifice size of static-pressure tubes by noting that for tubes with multiple orifices, the orifice diameter is usually on the order of 0.04 in. and for dual orifice tubes, the orifice diameter is 0.06 to 0.08 in. The effect of orifice size is, of course, included with the other effects (axial and radial location of the orifices and blocking effects of strut or collar) that contribute to the error of a static-pressure tube.

The effect of varying the edge shape of a 0.032-in.-diameter orifice for a Mach range from 0.4 to 0.8 is shown in figure 6.15(b). The errors for the rounded and angled edge shapes are referenced to the error of the square-edge orifice (which can be found from fig. 6.15(a)). The data for the various orifice configurations show the effect of edge shape to be relatively small except for the orifice with the wide curved entry. With present-day tubes, it is considered good practice to drill orifices with clean, sharp edges, free from burrs, and to make certain that the orifices are not damaged or deformed in operational use.

References

1. Kumbruch, H.: Pitot-Static Tubes for Determining the Velocity of Air. NACA TM 303, 1925.
2. Lock, C. N. H.; Knowler, A. E.; and Pearcey, H. H.: The Effect of Compressibility on Static Heads. R. & M. No. 2386, British A.R.C., Jan. 1943.
3. Walchner, O.: The Effect of Compressibility on the Pressure Reading of a Prandtl Pitot Tube at Subsonic Flow Velocity. NACA TM 917, 1939.
4. Merriam, Kenneth G.; and Spaulding, Ellis R.: Comparative Tests of Pitot-Static Tubes. NACA TN 546, 1935.
5. Hensley, Reece V.: Calibrations of Pitot-Static Tubes at High Speeds. NACA WR L-396, 1942. (Formerly NACA ACR.)
6. Richardson, Norman R.; and Pearson, Albin O.: Wind-Tunnel Calibrations of a Combined Pitot-Static Tube, Vane-Type Flow-Direction Transmitter, and Stagnation-Temperature Element at Mach Numbers From 0.60 to 2.87. NASA TN D-122, 1959.
7. Bursnall, William J.; and Loftin, Laurence K., Jr.: Experimental Investigation of the Pressure Distribution About a Yawed Circular Cylinder in the Critical Reynolds Number Range. NACA TN 2463, 1951.
8. Smith, W. E.: Wind Tunnel Calibration of Two Static-Pressure Sensing Devices. Rep. No. AF-682-A-6 (WADC Contract No. AF 33(038)-10709), Cornell Aeronaut. Lab., Inc., Dec. 1952.
9. Ritchie, Virgil S.: Several Methods for Aerodynamic Reduction of Static-Pressure Sensing Errors for Aircraft at Subsonic, Near-Sonic, and Low Supersonic Speeds. NASA TR R-18, 1959.
10. Gracey, William; and Scheithauer, Elwood F.: Flight Investigation at Large Angles of Attack of the Static-Pressure Errors of a Service Pitot-Static Tube Having a Modified Orifice Configuration. NACA TN 3159, 1954.
11. Pitot Static Tube TRU-1/A, Electrically Heated. Mil. Specif. MIL-P-25757B(ASG), Jan. 26, 1960.
12. Rayle, Roy E., Jr.: An Investigation of the Influence of Orifice Geometry on Static Pressure Measurements. M.S. Thesis, Massachusetts Inst. Technol., 1949.

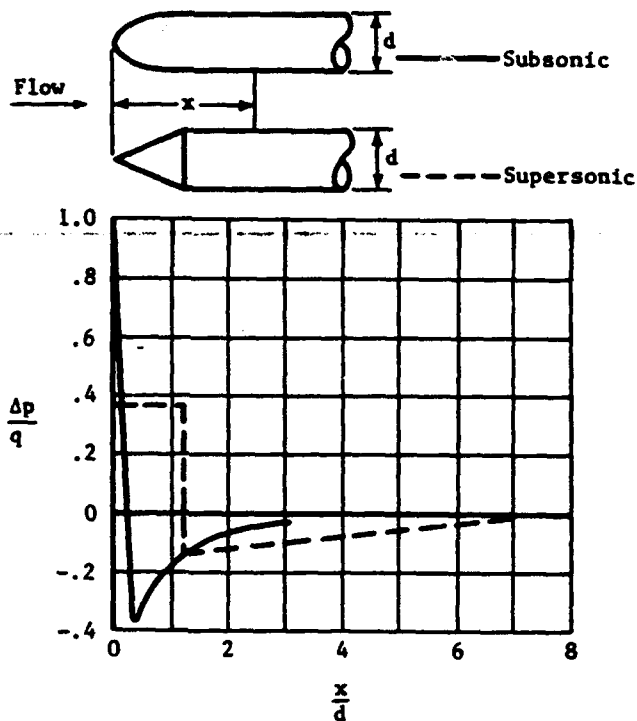


Figure 6.1.- Theoretical pressure distributions along cylindrical bodies. (Adapted from ref. 1.)

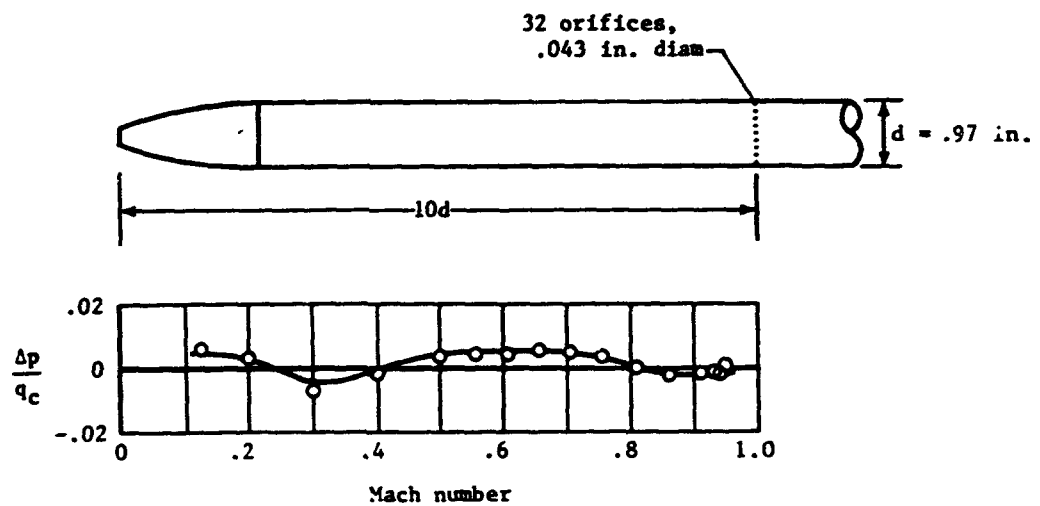


Figure 6.2.- Calibration of a static-pressure tube aligned with the flow. Support for this tube was located about 30 in. downstream from the orifices.

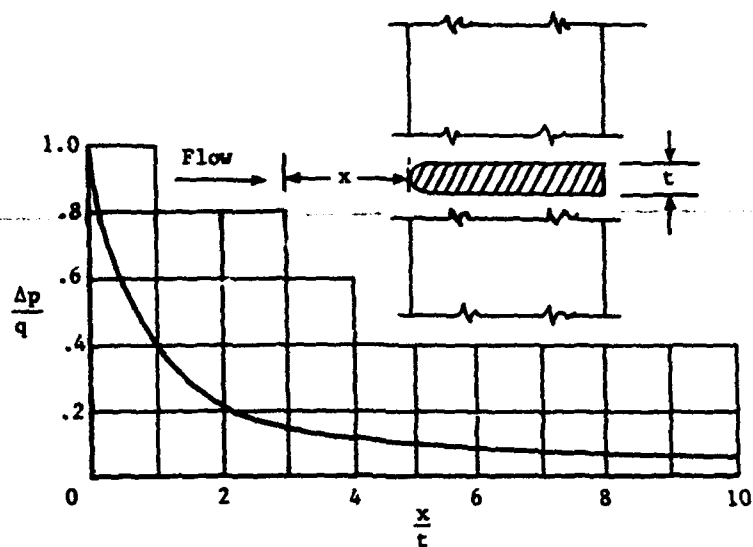


Figure 6.3.- Theoretical pressure distribution ahead of a body of infinite length transverse to the flow. (Adapted from ref. 1.)

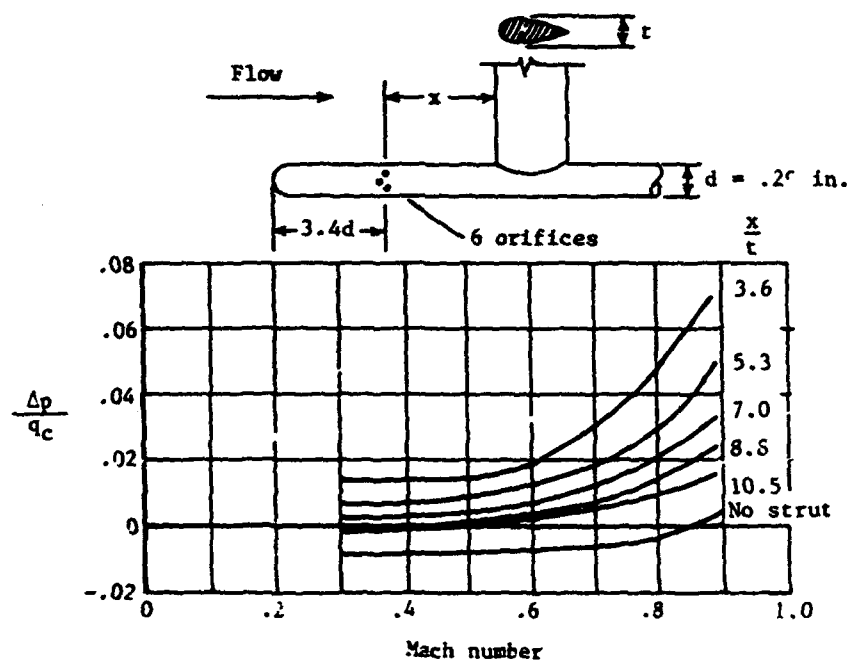


Figure 6.4.- Blocking effect of a transverse strut for a static-pressure tube aligned with the flow. (Adapted from ref. 2.)

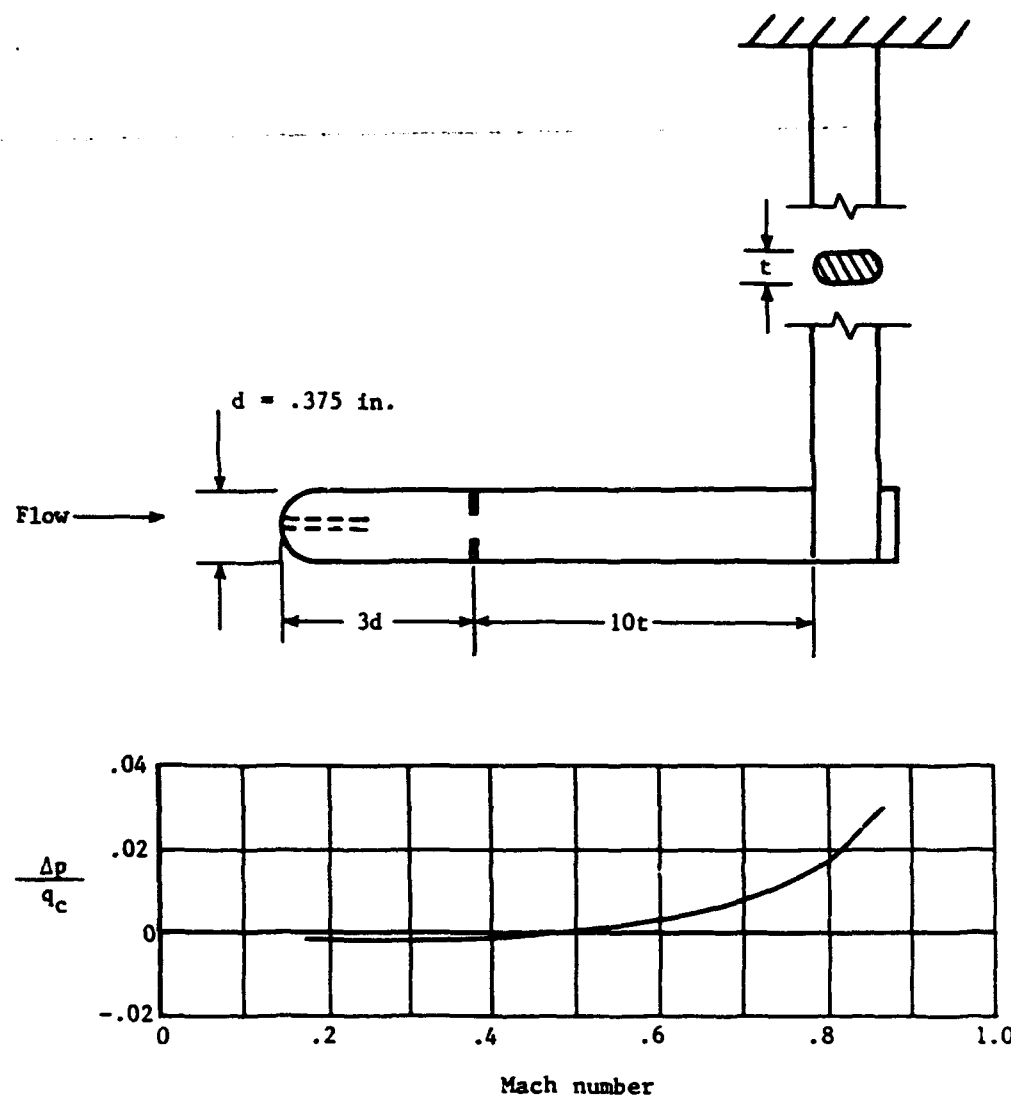


Figure 6.5.- Calibration of Prandtl pitot-static tube aligned with the flow. (Adapted from ref. 3.)

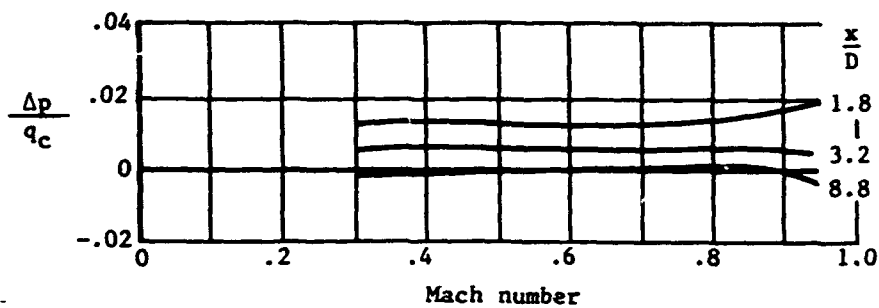
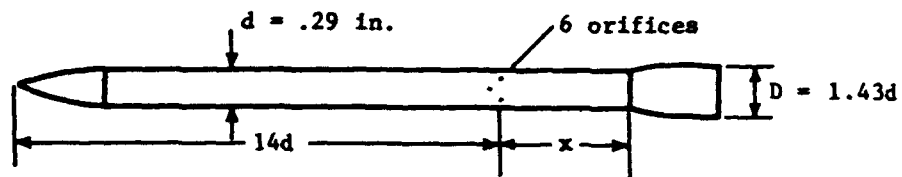


Figure 6.6.- Blocking effect of a collar for static-pressure tube aligned with the flow. (Adapted from ref. 2.)

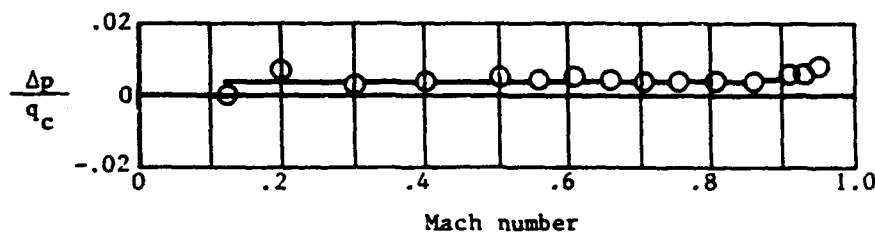
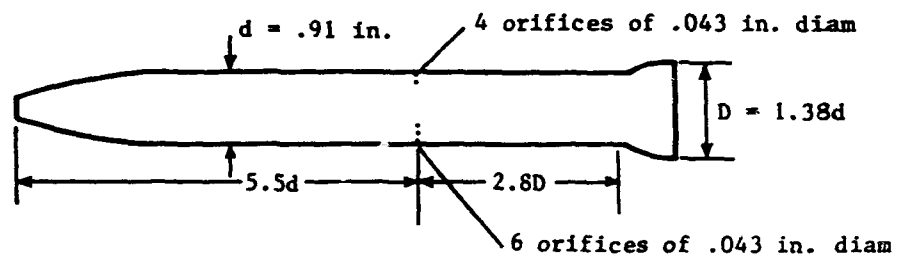


Figure 6.7.- Calibration of a service-type pitot-static tube aligned with the flow.

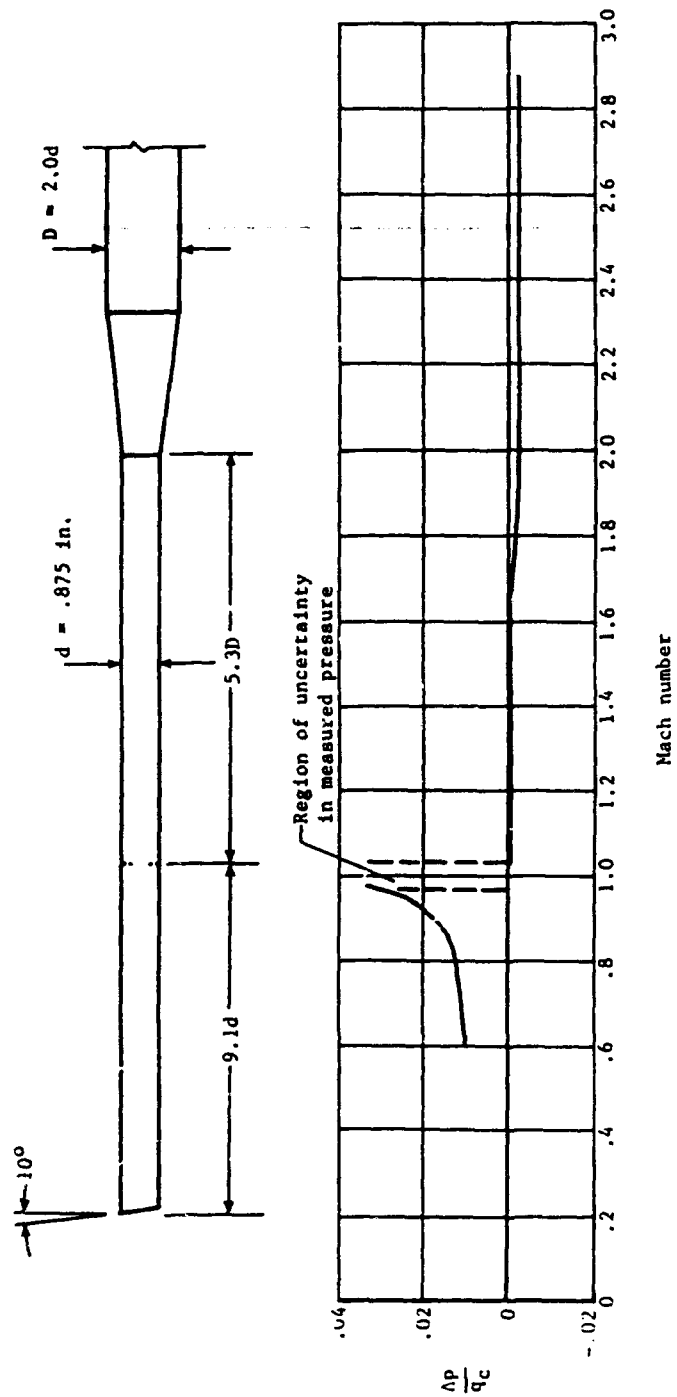


Figure 6.8.- Calibration of research-type pitot-static tube aligned with the flow.
(Adapted from ref. 6.)

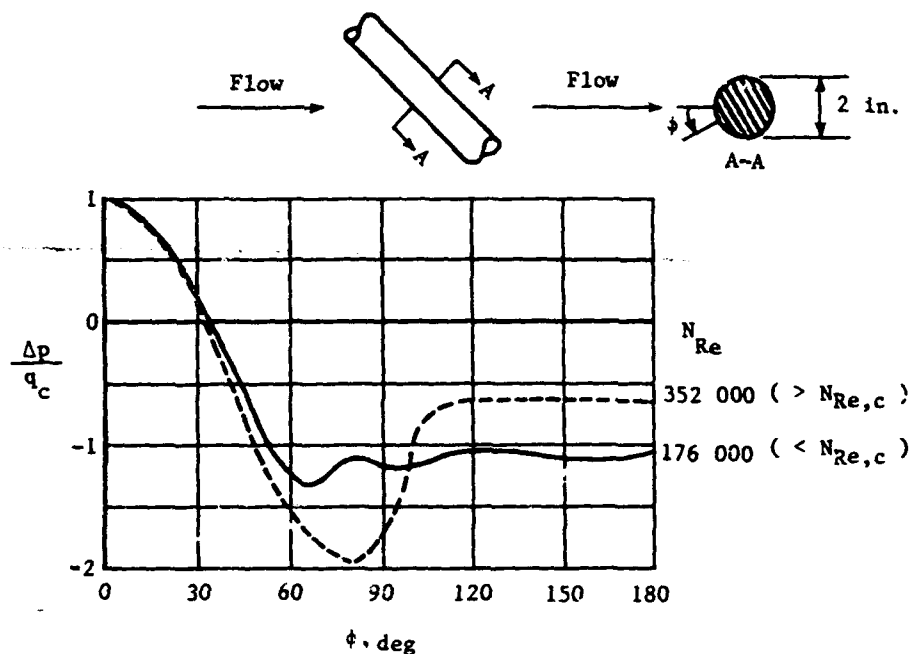


Figure 6.9.- Pressure distribution around a cylinder at an angle of attack of 45° and a Mach number of 0.2. The two pressure distributions are for flow conditions below and above the critical Reynolds number $N_{Re,c}$ at which flow separation occurs. (Adapted from ref. 7.)

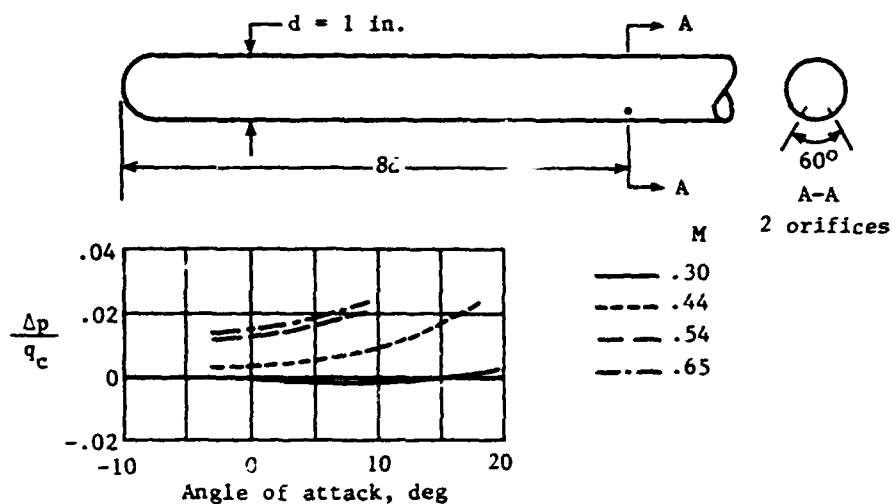


Figure 6.10.- Calibration at angles of attack of a static-pressure tube with orifices at radial stations of $\pm 30^\circ$. (Adapted from ref. 8.)

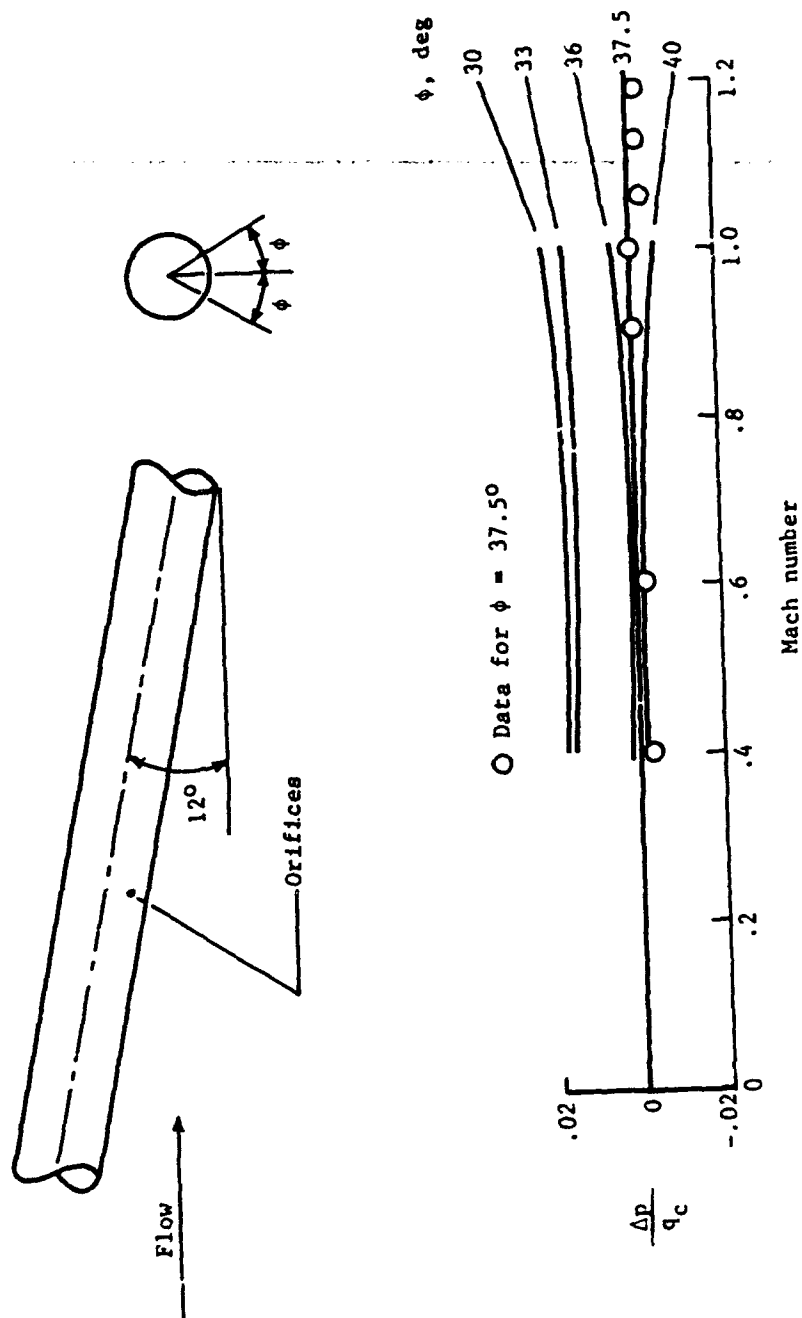
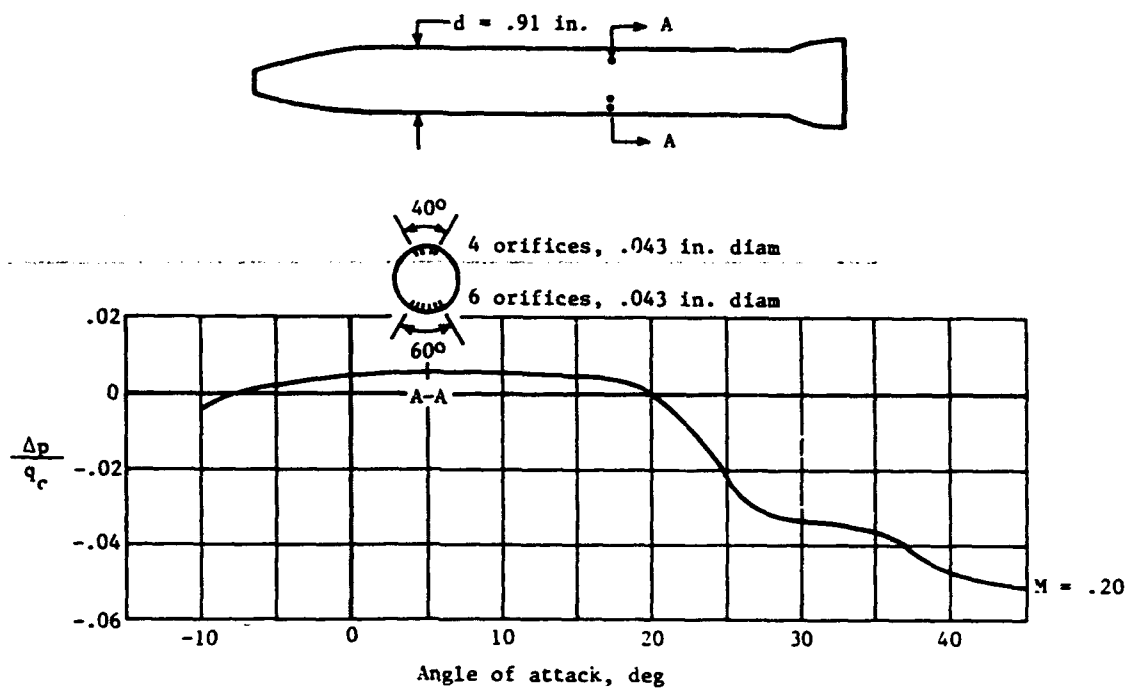
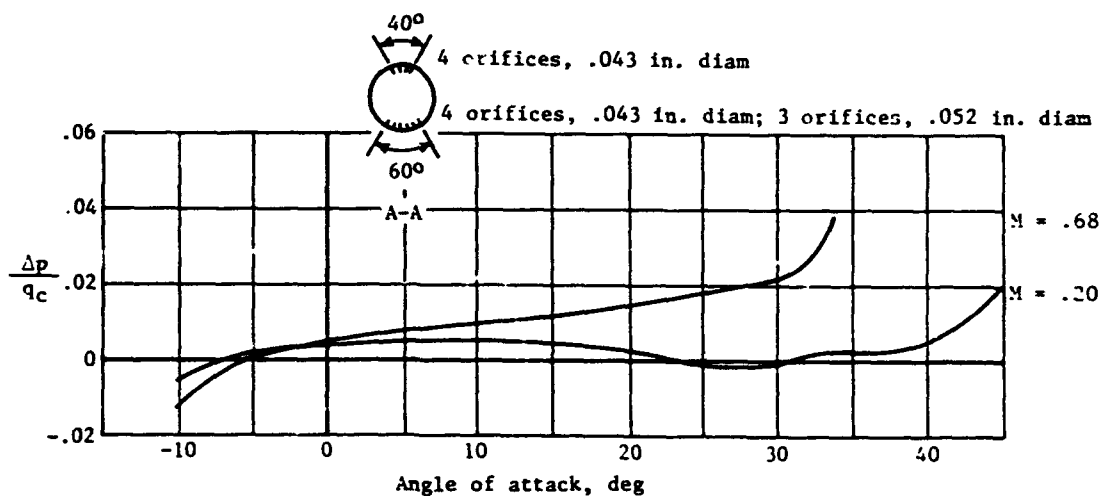


Figure 6.11.- Static-pressure errors of a tube with orifices at radial stations between $\pm 30^\circ$ and $\pm 40^\circ$. (Adapted from ref. 9.)

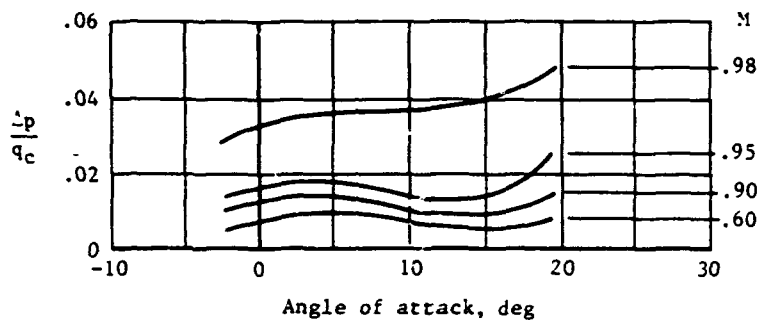
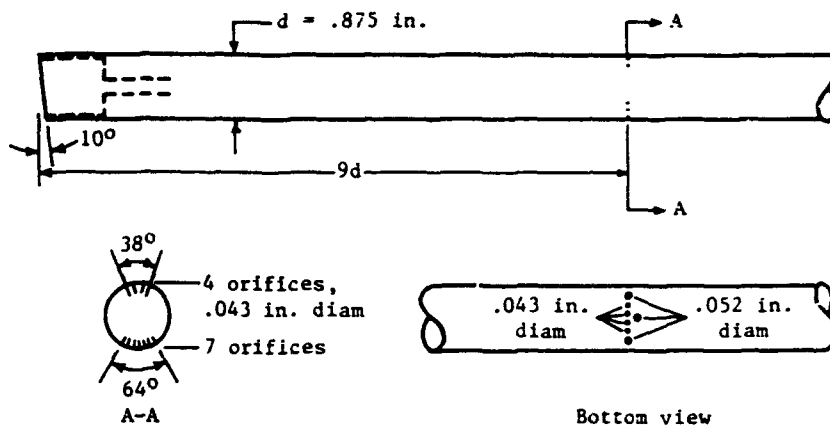


(a) Original orifice configuration.

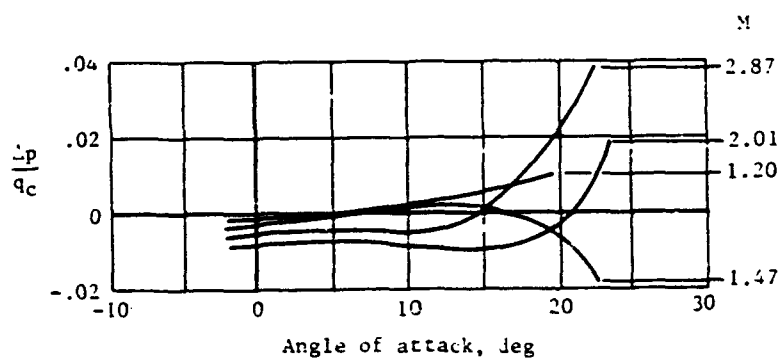


(b) Modified orifice configuration.

Figure 6.12.- Calibration of a service-type pitot-static tube at angles of attack. (Adapted from ref. 10.)



(a) Subsonic speed range.



(b) Supersonic speed range.

Figure 6.13.- Calibration of research-type pitot-static tube at angles of attack. (Adapted from ref. 6.)

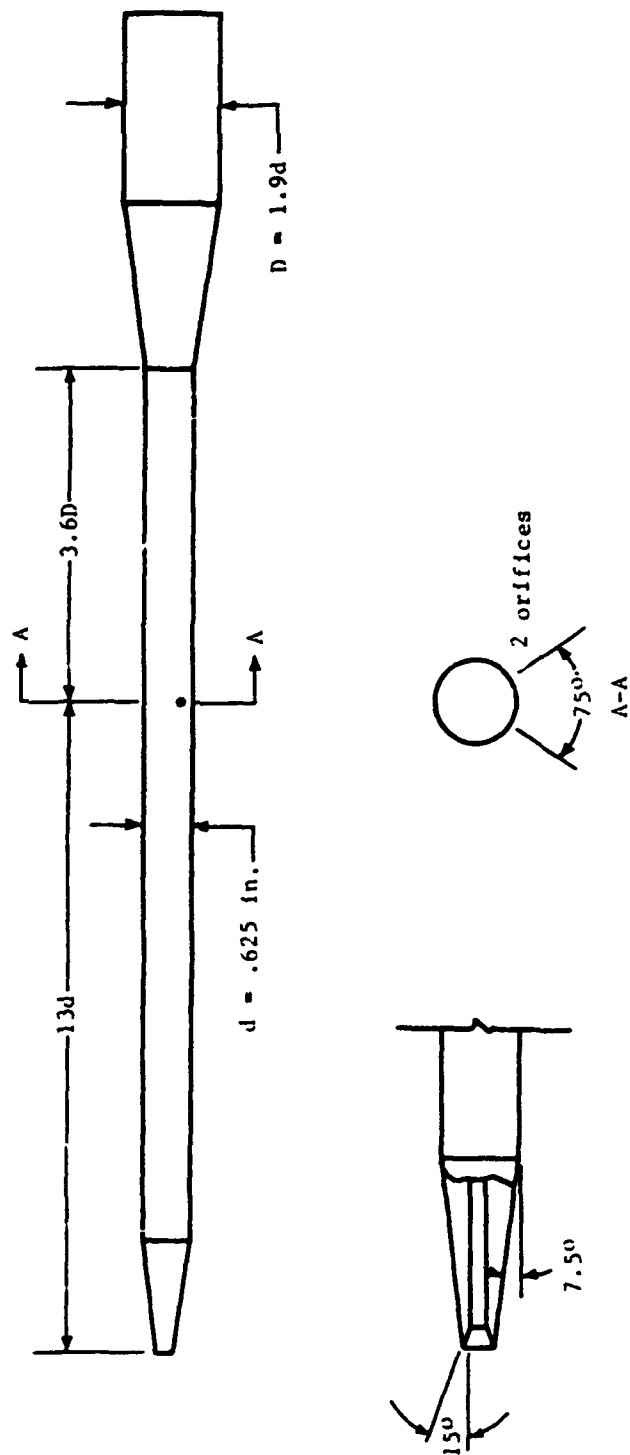
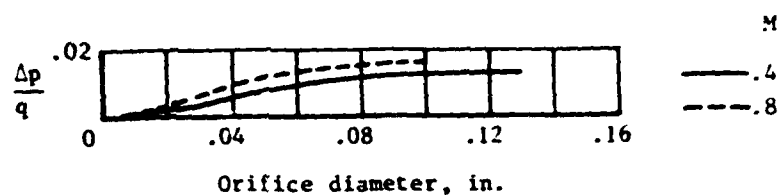
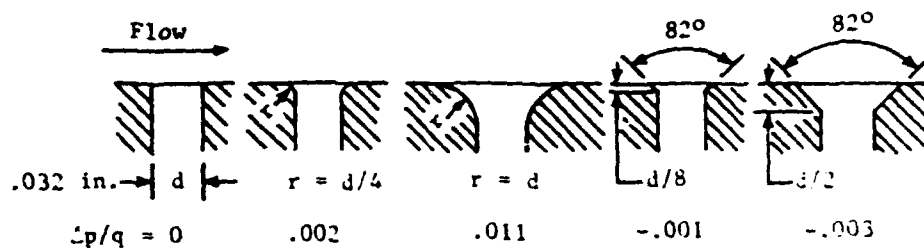


Figure 6.14.- Diagram of modern pitot-static tube. (Adapted from ref. 11.)



(a) Effect of orifice diameter.
Square-edge orifice.



(b) Effect of orifice edge shape. Error ± 0.001 and angled edge shapes referred to error of square-edge orifice.

Figure 6.15.- Effect of orifice diameter and edge shape on measured static pressure. (Adapted from ref. 10.)

CHAPTER VII

STATIC-PRESSURE INSTALLATIONS

As noted in chapter V, the position error of a static-pressure installation varies with Mach number and lift coefficient. In the low subsonic speed range, where large changes in lift coefficient can occur over a small Mach number range, the error depends largely on lift coefficient. In the high subsonic speed range, the change in lift coefficient is usually quite small, so that the error in this range depends mainly on Mach number. The errors at the low Mach numbers are determined from calibration tests at low altitudes, whereas the errors at the higher Mach numbers are determined in calibrations at high altitudes (because of the speed limitations of the aircraft at low altitudes). When the low-altitude calibration tests are conducted at heights near sea level, the curves are labeled "sea-level calibration" on the calibration charts.

As the variations of the errors with lift coefficient and Mach number differ markedly for different types of installations, the characteristics are described for four typical installations: static-pressure tubes ahead of the fuselage nose, the wing tip, and the vertical fin and fuselage-vent installations. For each installation, the variations of the errors in the low and high Mach ranges are considered separately. For one of the installations, however, the errors at low altitudes are combined with the errors at high altitudes to form a complete calibration throughout the lift coefficient and Mach number ranges.

All the calibrations to be presented apply to level-flight, cruise conditions. For the landing configuration, the calibration is generally different because of changes in the flow field that result from deflection of the flaps and extension of the landing gear.

The types of static-pressure tubes used on the fuselage-nose, wing-tip, and vertical-fin installations are shown in figure 7.1, and the type of tube used on each of the installations (tube A, B, etc.) is noted on each of the calibration charts discussed in this chapter.

Fuselage-Nose Installation

For a given position of the orifice ahead of a fuselage, the magnitude and variation of the static-pressure error depend on the shape of the fuselage and the maximum diameter of the fuselage.

The effect of nose shape can be seen from wind-tunnel tests of a cylinder of revolution having circular, elliptical, and oval nose shapes (fig. 7.2). The tests were conducted at $M = 0.2$ with the bodies at an angle of attack of 0° . The results of the tests (fig. 7.3) show that, for a given distance x/D ahead of the bodies, the blocking effect, indicated by the magnitude of the error, is greatest for the circular nose and least for the oval nose. At a distance of 1 body diameter ($x/D = 1.0$), for example, the error is 1.5 percent for the

circular nose, 4 percent q_c for the elliptical nose, and 1 percent q_c for the ogival nose.

The magnitude of the static-pressure error at three positions ahead of an airplane having an elliptical nose section is shown in figure 7.3. Also shown in the figure is the curve for the wind-tunnel model with the elliptical nose in figure 7.2. The errors for the airplane installations were determined at a low speed ($M = 0.37$) and a low angle of attack ($C_L = 0.3$), a condition comparable with that of the wind-tunnel tests. As shown by the two curves, the variation of the error with orifice position (x/D) is about the same for the two tests.

The variation of the error with Mach number at low subsonic speeds for each of the three boom lengths on the airplane in figure 7.3 is shown in figure 7.4. As this is the speed range in which the effects of lift coefficient (or angle of attack) predominate, the lift coefficients at the stall speed ($C_L = 1.2$) and at the maximum speed of the tests ($C_L = 0.3$) are noted in the figure. As shown by the three curves, the errors for nose-boom installations decrease with increasing lift coefficient.

The variation of the error of a nose-boom installation in the transonic speed range can be illustrated with calibrations of static-pressure probes ahead of a body of revolution (fig. 7.5, from ref. 2) having a profile like the X-1 research airplane (fig. 7.6). The errors were determined at three positions ahead of the body through a Mach range from 0.68 to 1.05 (fig. 7.5). For each orifice position, the errors increase rapidly in the upper subsonic range, reach peak values at Mach numbers just beyond 1.0, and then decrease abruptly to values near zero. The initial increase in the error is caused by a shock that forms around the body at its maximum diameter when the flow at that point becomes sonic. This shock isolates the negative pressure region along the rear of the body, so that the pressures at the orifices are then determined by the positive pressures along the nose section. When the free-stream flow becomes sonic, a shock wave forms ahead of the body (bow shock), and the error continues to increase as the shock moves toward the body. When the bow shock passes over the orifices, the static pressure at the orifices becomes that of the free stream, because the pressure field of the body is then confined to the region behind the shock. For all higher Mach numbers, the pressure ahead of the shock is that of the free stream, and the pressure measured by a static-pressure tube is that of the isolated tube.

In flight tests of the X-1 airplane with a type A static-pressure tube located 0.6D ahead of the nose (ref. 3), the variation of the error in the transonic speed range (fig. 7.6) was found to be similar to that of the model tests (fig. 7.5). After shock passage, the error becomes ± 0.5 percent q_c , which is the tube error of the type A tube. In later tests of the X-15 research airplane with a nose-boom installation with a type B tube, the installation error after shock passage was also found to be that of the isolated tube at Mach numbers up to 2.87 (refs. 4 and 5).

That the sharp rise in the static-pressure error in the Mach number from 0.8 to 1.0 is characteristic of fuselage-nose installations is shown by the calibrations of installations on five other airplanes (fig. 7.7, from ref. 6). The

data on this figure also show a fairly consistent decrease in the error with increasing boom length, despite the variations in the shapes of the nose sections.

The variation with Mach number of the static-pressure error ahead of fuselages with nose inlets has been determined from both model tests (ref. 2) and flight tests (ref. 7). The results of the two tests (figs. 7.8 and 7.9) show the same general variation of the error in the transonic speed range as for the X-1 model in figure 7.5 and the X-1 airplane in figure 7.6. The calibrations of nose-boom installations on five other airplanes with nose inlets (fig. 7.10, from ref. 6) show the errors in the Mach range from 0.8 to 1.0 to rise sharply in a manner similar to those for the airplanes on figure 7.7.

Wing-Tip Installations

For a given position of static-pressure orifices ahead of a wing, the magnitude and variation of the error depend on the shape of the airfoil section, the maximum thickness of the airfoil, and the spanwise location of the boom. In order to lessen the influence of the pressure field of the fuselage, the change in the flow field about the wing due to flap deflection and landing-gear extension, and the effect of propeller slipstream or jet engine exhaust, the static-pressure tube should be installed on the outboard span of the wing. For the installations to be described here, the booms were in all cases located near the wing tip.

The magnitudes of the errors ahead of a wing tip are shown in figure 7.11 for six orifice locations expressed in terms of the maximum wing thickness t . The errors were measured with the airplane at a low angle of attack ($C_L = 0.2$) at a Mach number of 0.30 (ref. 8). The test data show that the error is highest at the position closest to the wing and it decreases rapidly to a value of about 1 percent q_c at an orifice location of $x/t = 10$. Beyond this point, further reduction in the error is minimal.

The distance $x/t = 8$ for the wing in figure 7.11 is the same as the chord length of the wing at the spanwise location of the boom. For a comparison with the error at this location, the errors of 1-chord installations on nine other airplanes are included in figure 7.11. The static-pressure tube for all the installations was the same (tube A) and the errors were all measured at about the same lift coefficient. Although the airfoil sections of the various wings differed, the static-pressure errors are all in the same range. Thus the shape of the airfoil section appears to have little effect on the magnitude of the errors at a distance of 1 chord length (or greater) ahead of the wing.

The variations of the errors in the low Mach range for each of the six boom lengths on the airplane in figure 7.11 are shown in figure 7.12. In this figure, the orifice locations are given in terms of the local wing chord c . For boom lengths of 1 chord or greater, the error is very nearly constant at Mach numbers above 0.15. As speeds decrease below this Mach number, the errors for all the boom lengths become increasingly negative and reach a value of

about -6 percent q_c at the stall speed. For such large variations of the error over a small Mach range, the problem of applying corrections for the errors would be quite difficult.

In order to show the relative decrease of the error with lift coefficient for comparable boom lengths of fuselage-nose and wing-tip installations, the calibration of the 1.5D boom of the airplane in figure 7.4 is compared in figure 7.13 with that of a 1-chord wing-tip boom on the same airplane. For both of the installations, the static-pressure tube was the same (tube A) and the tests were conducted through the same lift coefficient range. As shown by the two calibrations, the magnitude of the error of the fuselage nose installation is higher than that of the wing-tip installation, but the variation of the error with lift coefficient is considerably greater for the wing-tip installation. Thus, corrections for the errors of the nose-boom installation could be applied more accurately, even though the magnitudes of the errors are higher than those of the wing-tip installation.

The variation of the errors of a wing-tip installation in the transonic speed range can be described from the calibration of a 1-chord installation on the X-1 airplane (fig. 7.14, from ref. 3). It is apparent from this calibration that the variation of the error is the same as that for the fuselage-nose installations up to the Mach number at which the discontinuity due to shock passage occurs. At this point; however, the error falls to a large negative value and then, with increasing Mach number, begins to increase to positive values. The explanation for this behavior may best be illustrated by diagrams of the shock waves ahead of the airplane (fig. 7.15). At a Mach number of 1.02, the wing bow shock has passed the orifices, and thus has effectively isolated them from the pressure field of the wing. The pressure at the orifices is then influenced by the negative pressures around the rear portion of the fuselage nose, the effect of which extends outward from the surface of the fuselage behind the Mach cone. As the Mach number increases, the cone slants backward, and the orifices come under the influence of the positive pressures around the forward portion of the fuselage nose and behind the fuselage bow shock. At some higher Mach number, the fuselage bow shock traverses the orifices, which are then isolated from the flow fields of both wing and fuselage. At this and higher Mach numbers, the static-pressure error, like that for the fuselage-nose installations, is the error of the tube itself.

Vertical-Fin Installations

The factors that affect the measurement of static pressure ahead of a vertical fin are similar to those for wing-tip installations. Calibrations of a 0.55-chord vertical-fin installation at low and high subsonic speeds are presented in figure 7.16. In the low subsonic range, the error is 1.5 percent q_c , a value that is about 1 percent lower than that for the 0.5-chord wing-tip installation in figure 7.12. In the high subsonic range, the error increases with Mach number in a manner similar to that for the wing-tip installation in figure 7.14. At some higher Mach number above 1.0, the error would be expected to decrease abruptly when the shock wave ahead of the fin passes over the orifices.

Fuselage-Vent Installations

For the purpose of selecting a location for static ports, the fuselage can, in a general way, be likened to a static-pressure tube. When the fuselage is aligned with the flow, the pressure at a vent is determined by its location along the body, and when the fuselage is inclined to the flow, the pressure is dependent on the radial position of the orifice around the body. The pressure at any given point on the body may, of course, be modified by the effects of the wing or other protuberance on the fuselage.

Because of the complex nature of the pressure distribution along the fuselage, it is difficult to predict, with any degree of certainty, those locations where the static-pressure error is a minimum. It is customary, therefore, to make pressure-distribution tests in a wind tunnel with a detailed replica of the aircraft and to choose from the results a number of vent locations that appear promising. These locations are then calibrated on the full-scale aircraft and the best location is chosen for the operational installation.

In the midsubsonic speed range, the errors of the three static-pressure-tube installations (fuselage nose, wing tip, and vertical fin) are in all cases positive. In contrast, the errors of fuselage-vent installations can be either positive or negative. This fact is illustrated by the calibrations of the fuselage-vent systems on three transport airplanes (fig. 7.17, from ref. 9).

In the high subsonic speed range, the errors of fuselage-vent installations can vary with Mach number in the same general way as the errors of the static-pressure-tube installations. For the installation on the turbojet transport shown in figure 7.18 (ref. 10), for example, the error rises in the Mach range above 0.8 (due to the blocking effect of the wing) in a manner similar to that for each of the static-pressure-tube installations.

With another vent installation, for which the vents were located just aft of the fuselage nose (fig. 7.19, from ref. 11), the error exhibits a discontinuity similar to that of the wing-tip installation of figure 7.14. With the fuselage-vent system, however, the discontinuity in the calibration occurs at a Mach number below 1.0 and through a range of Mach numbers (as opposed to the abrupt discontinuity of the wing-tip installation at Mach 1.02). The discontinuity occurs below Mach 1.0 because of passage of local shocks over the vents, and the measured pressures fluctuate because of instability of the shock.

To minimize the errors due to angle of attack, the fuselage vents on most turbojet transports are installed in pairs at radial positions of $\pm 35^\circ$ to $\pm 45^\circ$ from the bottom of the fuselage. This vent arrangement also reduces to some extent the effects of angle of yaw or sideslip. In unpublished tests of a vent system on a transport aircraft, for example, the error remained within 1 percent q_∞ at angles of sideslip up to $\pm 7^\circ$ at a Mach number of 0.8.

The static ports on present-day aircraft are in the form of either a single large hole (on the order of $3/8$ in. in diameter) or a number of small orifices arranged in a salt-shaker pattern. With the single large port, the measured pressures can be altered by deformations of the edge of the vent.

With the salt-shaker pattern, the measured pressures can be affected by deformations of the orifices as discussed in chapter VI. For both types of ports, the measured pressures can also be altered by changes in the contour of the fuselage skin in the vicinity of the port; such changes can result from damage caused by ground handling, repairs to the skin, or aging of the aircraft.

The effects of simulated damage to the ports (in the form of protuberances and changes in edge shape) and of skin waviness in the vicinity of the ports were determined in tests reported in reference 12. The results of the tests (fig. 7.20(a)) show that even relatively small deformations at the edge of the vent can produce sizable changes in the measured pressure. For a vent located close to a wave in the fuselage skin, the effects can also be appreciable (fig. 7.20(b)). To avoid the possibility of the kind of skin waviness that can occur with thin skins and to provide a uniform vent configuration, some manufacturers install a thick plate having a machined surface that extends some distance around the vents. Such plates also provide a higher degree of consistency in the calibrations of a given type aircraft (ref. 10).

Combined Calibrations at Low and High Altitudes

As mentioned earlier, the calibrations of installations at low and high altitudes usually are not joined (e.g., fig. 7.16), because the low-altitude calibration is not carried to sufficiently high Mach numbers and the high-altitude calibration is not carried to sufficiently low Mach numbers. In one case, however, the calibration of a wing-tip installation was extended down to the stall at a series of altitudes by means of a high-speed trailing bomb to be described in chapter IX.

The calibrations at five altitudes are shown in figure 7.21 (from ref. 10). For the sea-level calibration, the variation of the error with lift coefficient in the low Mach range is the characteristic variation expected of wing-tip installations. Of interest with this set of calibrations, however, is the fact that the error variation at each of the altitudes above sea level is essentially the same. Of further interest is the fact that the calibrations all converge at a Mach number of about 0.75. At Mach numbers beyond this point, where the errors are basically a function of Mach number, the error variation for all the altitudes can be represented by a single curve.

In the lower Mach range where the error is primarily a function of lift coefficient (below $M = 0.75$ for this installation), the lift coefficient for a given value of the error should be the same at each altitude. For an error of -0.075, for example, the lift coefficient at $M = 1.9$ at sea level should be the same as that at $M = 2.3$ at 10 000 ft, $M = 2.7$ at 20 000 ft, etc. Computations of the lift coefficients at each altitude show that they are, in fact, approximately the same.

The primary dependence of the static-pressure error on lift coefficient in the lower Mach range has led a number of investigators to devise analytical methods for predicting the errors at altitude from the errors measured in a sea-level calibration. In two methods proposed by British investigators (refs. 14 and 15), the errors at altitude are computed from a consideration of the Mach

number as well as the lift coefficient at which the sea-level value was determined. Other investigators have extrapolated the sea-level values on the simple assumption that the errors are dependent solely on lift coefficient. Each of these methods is limited, of course, to the Mach range below that at which shocks form on the body.

An example of the application of the extrapolation method based only on the lift coefficient dependence is shown in figure 7.22 (from ref. 16). In this example, the extrapolation of a sea-level calibration to 25 000 ft is compared with the flight-test calibration at 25 000 ft. The test data from which the sea-level and 25 000-foot calibrations were derived are discussed in chapter IX. As indicated by the agreement between the measured and computed errors at altitude, the simpler computational method would appear to be adequate for the prediction of the errors at altitude.

Calibration Presentations

The errors of the static-pressure installations described in this chapter have in all cases been expressed as fractions of the impact pressure, as $\Delta p/q_c$. As noted in chapter V, however, the static-pressure errors are sometimes presented as fractions of the static pressure, $\Delta p/p$, or the Mach number, $\Delta M/M$.

Comparable values of $\Delta p/q_c$, $\Delta p/p$, and $\Delta M/M$ for a hypothetical Δp variation based on calibrations of fuselage nose installations are shown in figure 7.23 for a Mach number range from 0.2 (the stall speed) to 2.0. For this example, the variations in terms of $\Delta p/p$ and $\Delta M/M$ were derived from the $\Delta p/q_c$ variation by using figures 5.4 and 5.5.

In the high subsonic range (above $M = 0.8$), the variation of the errors with Mach number for each of the three calibrations is roughly the same and the peak values of the errors are generally of the same magnitude. In the low subsonic range, however, the variation of the error with lift coefficient, as shown by the decrease in the magnitude of the error from $M = 0.4$ to 0.2, is greatest for the $\Delta p/q_c$ calibration and least for the $\Delta p/p$ calibration. In the supersonic range, where $\Delta p/q_c$ is constant, the magnitudes of $\Delta p/p$ and $\Delta M/M$ both increase with increasing Mach number.

Even though the position error of an installation in terms of $\Delta p/q_c$ in the supersonic range may be small, the altitude error corresponding to the static-pressure error can be quite large. For a value of $\Delta p/q_c$ of 1 percent, for example, the altitude error at $M = 2.0$ and an altitude of 40 000 ft is 965 ft.

Installation-Error Tolerances

The errors of static-pressure installations on civil and military aircraft are required to conform to specified tolerances (refs. 17 and 18). For civil transport aircraft, the allowable static-pressure error is stated in terms of an altitude error of 30 ft per 100 knots indicated airspeed, corrected to standard conditions. For military aircraft, the static-pressure error is stated in the same terms, except that the allowable altitude error is 25 ft per 100 knots.

The altitude errors corresponding to the civil and military requirements for a Mach range up to 1.0 and for altitudes up to 40 000 ft are presented in figure 7.24.

Installation Design Considerations

From a consideration of the variations of the errors of the four types static-pressure installations with lift coefficient and Mach number, it should be evident that a primary consideration in the selection of an installation for a new aircraft is the Mach range through which it is designed to operate.

If the operating range extends to supersonic speeds, the fuselage-nose installation is obviously the best choice, because the installation error at supersonic speeds will be that of the tube itself. The error of the tube at supersonic speeds can be determined from wind-tunnel tests, so that the final calibration of the installation could be limited to the subsonic speed range. The errors in the subsonic range might be relatively large, but the variation of the errors with Mach number and lift coefficient follows a consistent pattern for which corrections for the errors can be applied by means of air data computers to be described in chapter XI. The errors of fuselage-nose installation at subsonic speeds can also be minimized by use of specially designed contour tubes to be discussed in the next chapter.

Aircraft designed for operations in the subsonic speed range ordinarily cruise at Mach numbers below 0.9. For this Mach range, any of the other three installations - wing tip, vertical fin, and fuselage vent - should prove satisfactory. If the shape of the fuselage approximates that of a circular cylinder, satisfactory locations can usually be found in areas where the static-pressure errors will be small and where the measured pressures will not be adversely affected by local shocks in the upper subsonic range. With the wing-tip and vertical-fin installations, very small (and consistent) errors can be realized when the boom length is about 0.5 chord length at the vertical fin or 1 chord length at the wing tip.

With all the installations, the pressure sensor should be designed and located to prevent obstruction of the static-pressure orifices or fuselage by debris, water ingestion, or ice. The distance of the pressure source from the cockpit should also be considered because long lengths of pressure tubing can introduce pressure lag errors, a subject to be discussed in chapter X. These considerations, together with the many other factors that must be taken into account in the design of pitot-static systems, are discussed in considerable detail in reference 19.

References

1. Letko, William: Investigation of the Fuselage Interference on a Pitot-Static Tube Extending Forward From the Nose of the Fuselage. NACA TN 1496, 1947.
2. O'Bryan, Thomas C.; Danforth, Edward C. B.; and Johnston, J. Ford.: Error in Airspeed Measurement Due to the Static-Pressure Field Ahead of an Airplane at Transonic Speeds. NACA Rep. 1239, 1955. (Supersedes NACA RM's L9C25 by Danforth and Johnston, L50L28 by Danforth and O'Bryan, and L52A17 by O'Bryan.)
3. Goodman, Harold R.; and Yancey, Roxanah B.: The Static-Pressure Error of Wing and Fuselage Airspeed Installations of the X-1 Airplanes in Transonic Flight. NACA RM L9G22, 1949.
4. Larson, Terry J.; and Webb, Lannie D.: Calibration and Comparisons of Pressure-Type Airspeed-Altitude Systems of the X-15 Airplane From Subsonic to High Supersonic Speeds. NASA TN D-1724, 1963.
5. Richardson, Norman R.; and Pearson, Albin O.: Wind-Tunnel Calibrations of a Combined Pitot-Static Tube, Vane-Type Flow-Direction Transmitter, and Stagnation-Temperature Element at Mach Numbers From 0.60 to 2.87. NASA TN D-122, 1959.
6. Larson, Terry J.; Stillwell, Wendell H.; and Armistead, Katherine H.: Static-Pressure Error Calibrations for Nose-Boom Airspeed Installations of 17 Airplanes. NACA RM H57A02, 1957.
7. Roe, M.: Position Error Calibration of Three Airspeed Systems on the F-86A Airplane Through the Transonic Speed Range and in Maneuvering Flight. Rep. No. NA-51-864, North American Aviation, Inc., Oct. 5, 1951.
8. Gracey, William; and Scheithauer, Elwood F.: Flight Investigation of the Variation of Static-Pressure Error of a Static-Pressure Tube With Distance Ahead of a Wing and a Fuselage. NACA TN 2311, 1951.
9. Silsby, Norman S.; and Stickle, Joseph W.: Flight Calibrations of Fuselage Static-Pressure-Vent Installations for Three Types of Transports. NASA TN D-1356, 1962.
10. Brumby, Ralph E.: The Influence of Aerodynamic Cleanness of Aircraft Static Port Installations on Static Position Error Repeatability. Rep. No. DAC-67485, Douglas Aircraft Co., Nov. 1968.
11. Thompson, Jim Rogers; Bray, Richard S.; and Cooper, George E.: Flight Calibration of Four Airspeed Systems on a Swept-Wing Airplane at Mach Numbers up to 1.04 by the NACA Radar-Phototeodolite Method. NACA TN 3526, 1955. (Supersedes NACA RM A50H24.)

12. Somerville, T. V.; and Jefferies, R. L.: Note on Model Tests of Static Vents. Effect of Degrees of Flushness, Waviness of Skin and Proximity of Rivets. B. A. Dep. Note - Wind Tunnels No. 531, British R.A.E., Sept. 1941.
13. Smith, K. W.: The Measurement of Position Error at High Speeds and Altitude by Means of a Trailing Static Head. C. P. No. 160, British A.R.C., 1954.
14. Weaver, A. K.: The Calibration of Air Speed and Altimeter Systems. Rep. No. AAEE/Res/244, British Min. Supply, Aug. 18, 1949.
15. Charnley, W. J.; and Fleming, I.: Corrections Applied to Air-Speed Indicator and Altimeter Readings for Position Error and Compressibility Effects. Rep. No. Aero. 2299, British R.A.E., Feb. 1949.
16. Gracey, William; and Stickle, Joseph W.: Calibrations of Aircraft Static-Pressure Systems by Ground-Camera and Ground-Radar Methods. NASA TN D-2012, 1963.
17. Static Pressure Systems. Airworthiness Standards: Transport Category Airplanes, FAR Pt. 25, Sec. 1325, FAA, June 1974, pp. 104-105.
18. Instrument Systems, Pitot Tube and Flush Static Port Operated, Installation of. Mil. Specif. MIL-I-6155A, Dec. 31, 1960.
19. Design and Installation of Pitot-Static Systems for Transport Aircraft. ARP 920, Soc. Automot. Eng., Oct. 15, 1968.

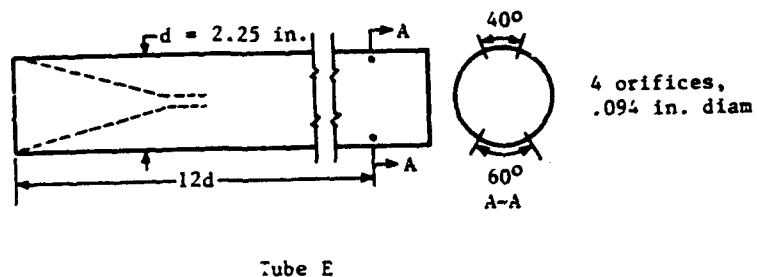
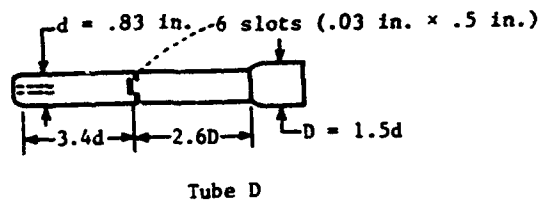
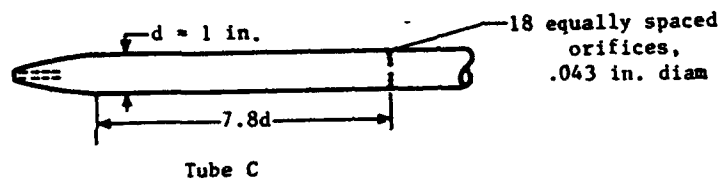
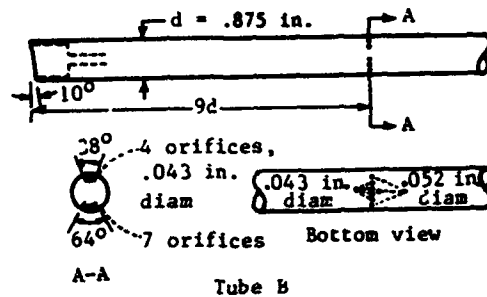
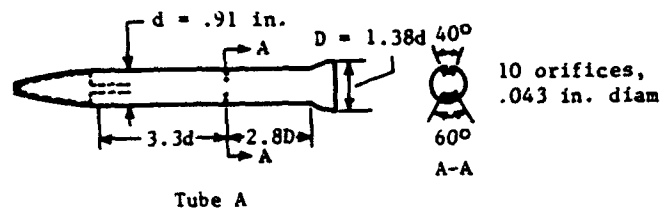


Figure 7.1.- Diagrams of static-pressure tubes used on aircraft installations.

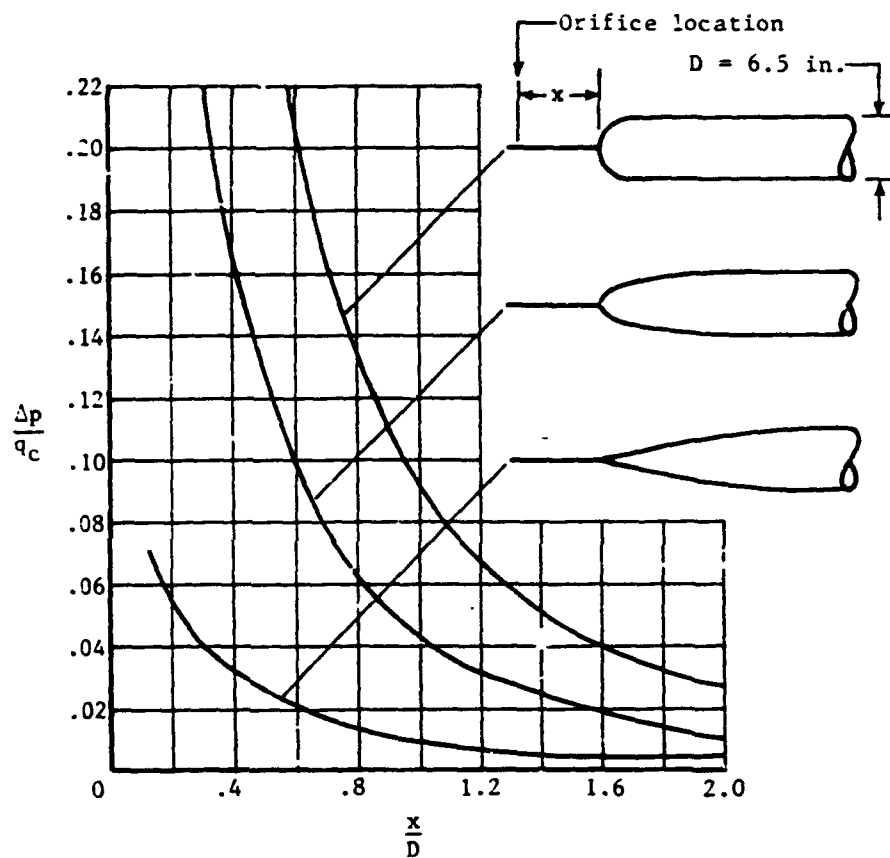


Figure 7.2.- Static-pressure errors at various distances ahead of three bodies of revolution aligned with the flow at $\alpha = 0.21$. (Adapted from ref. 1.)

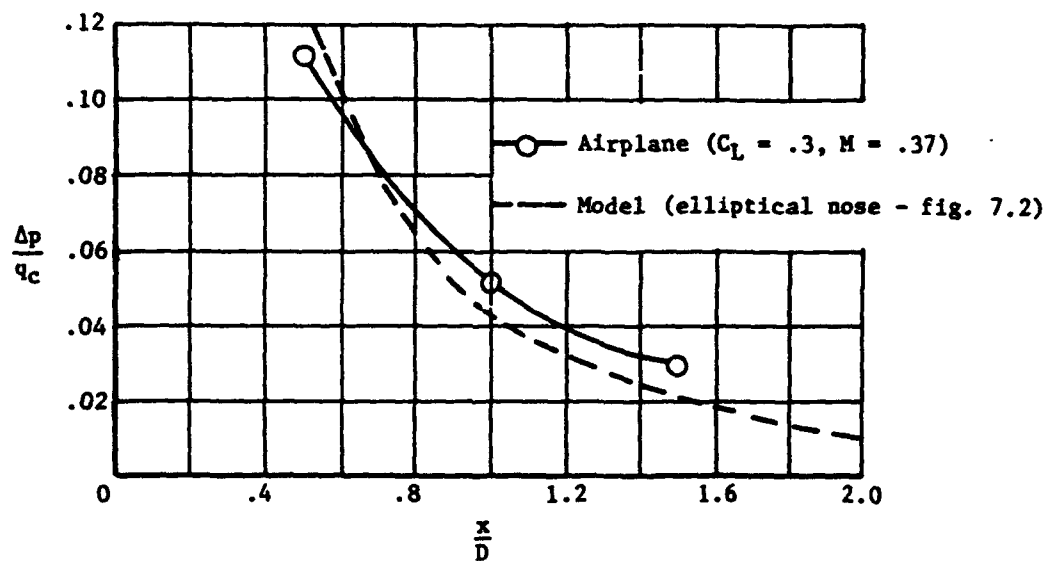
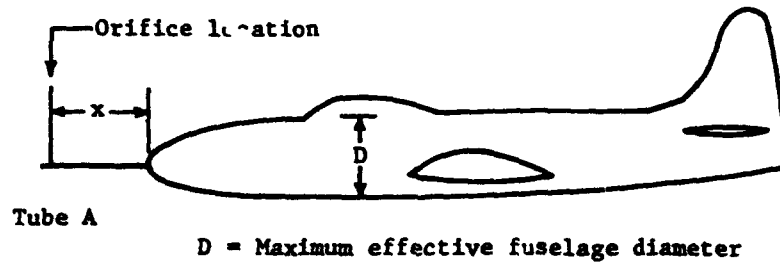


Figure 7.3.- Static-pressure errors at three positions ahead of the fuselage nose of an airplane. (Adapted from ref. 8.)

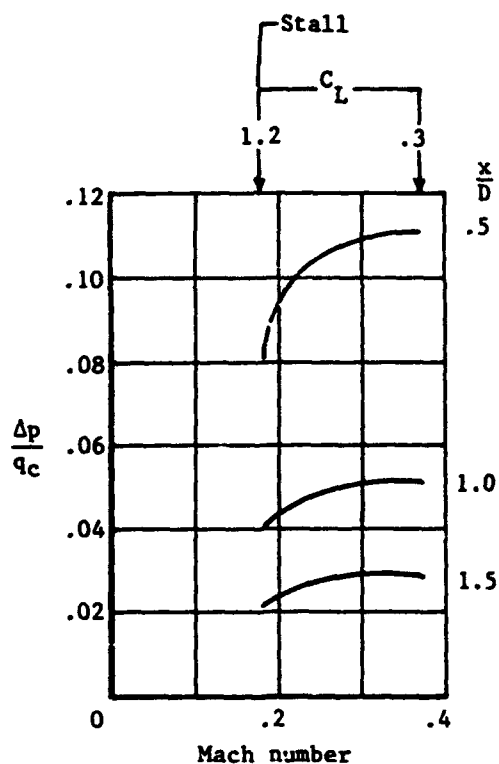
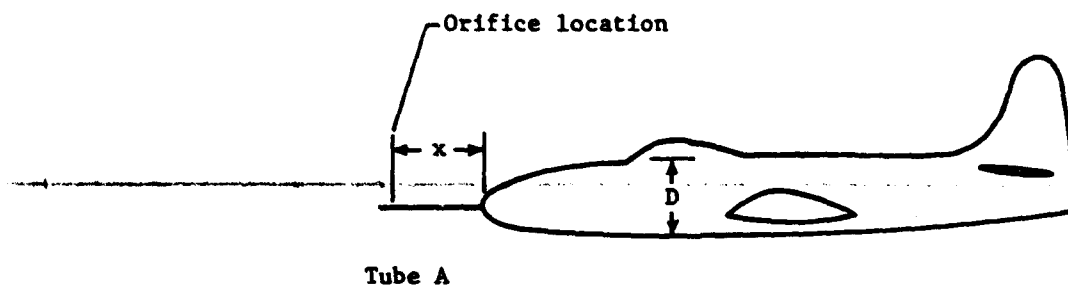


Figure 7.4.- Variation of static-pressure errors of fuselage-nose installations in low subsonic speed range. (Adapted from ref. 8.)

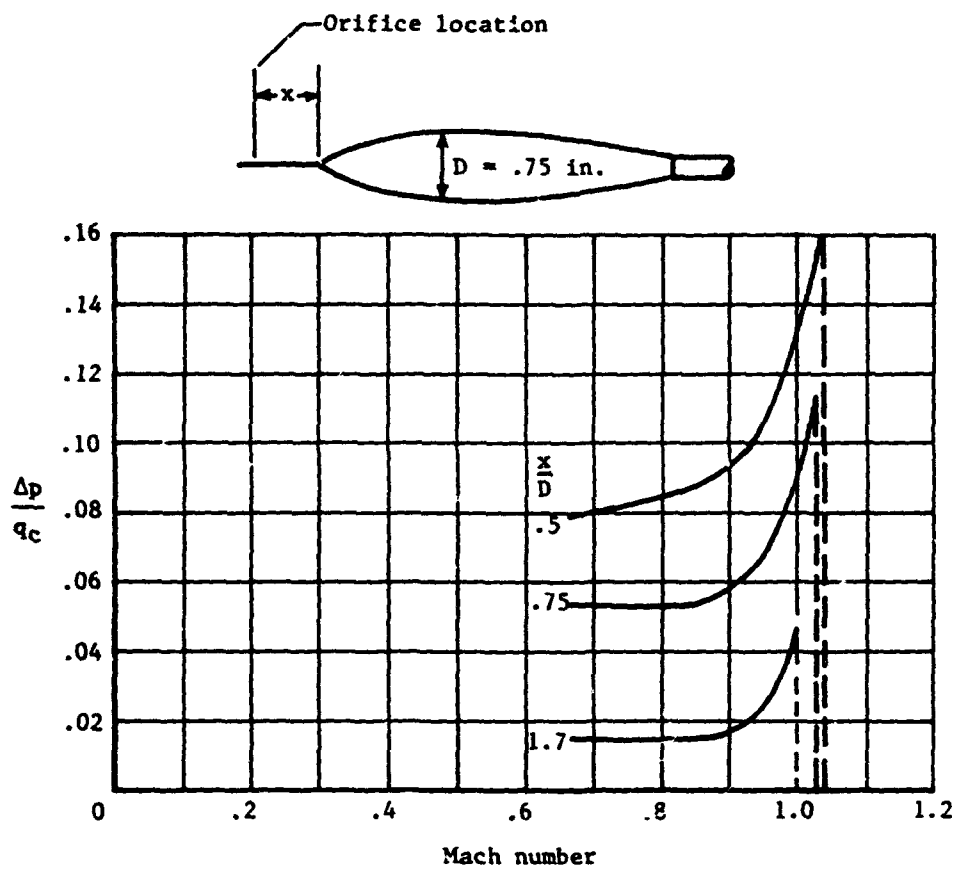


Figure 7.5.- Variation of static-pressure error ahead of a model of an airplane fuselage in the transonic speed range. (Adapted from ref. 2.)

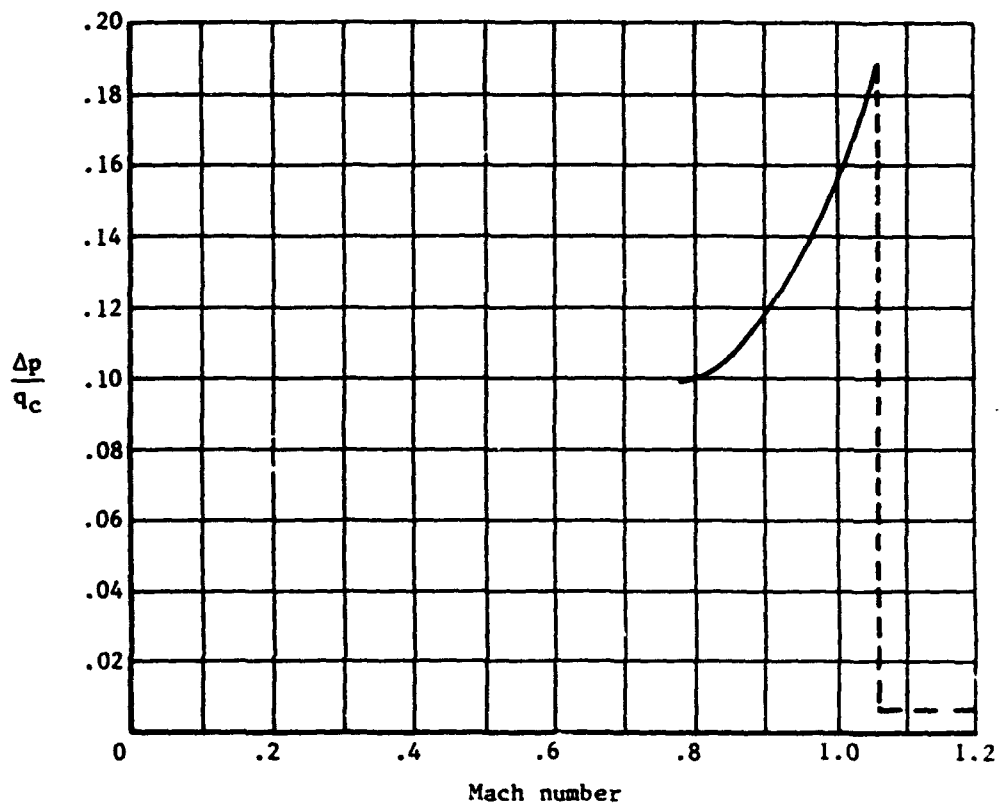
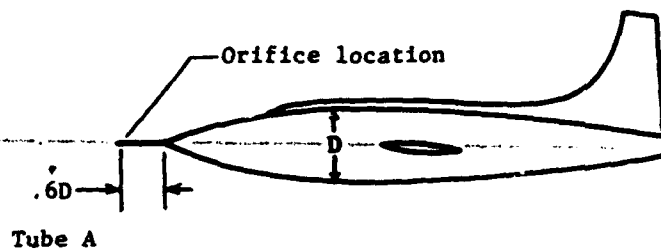


Figure 7.6.- Variation of static-pressure error of fuselage-nose installation in transonic speed range. (Adapted from ref. 3.)

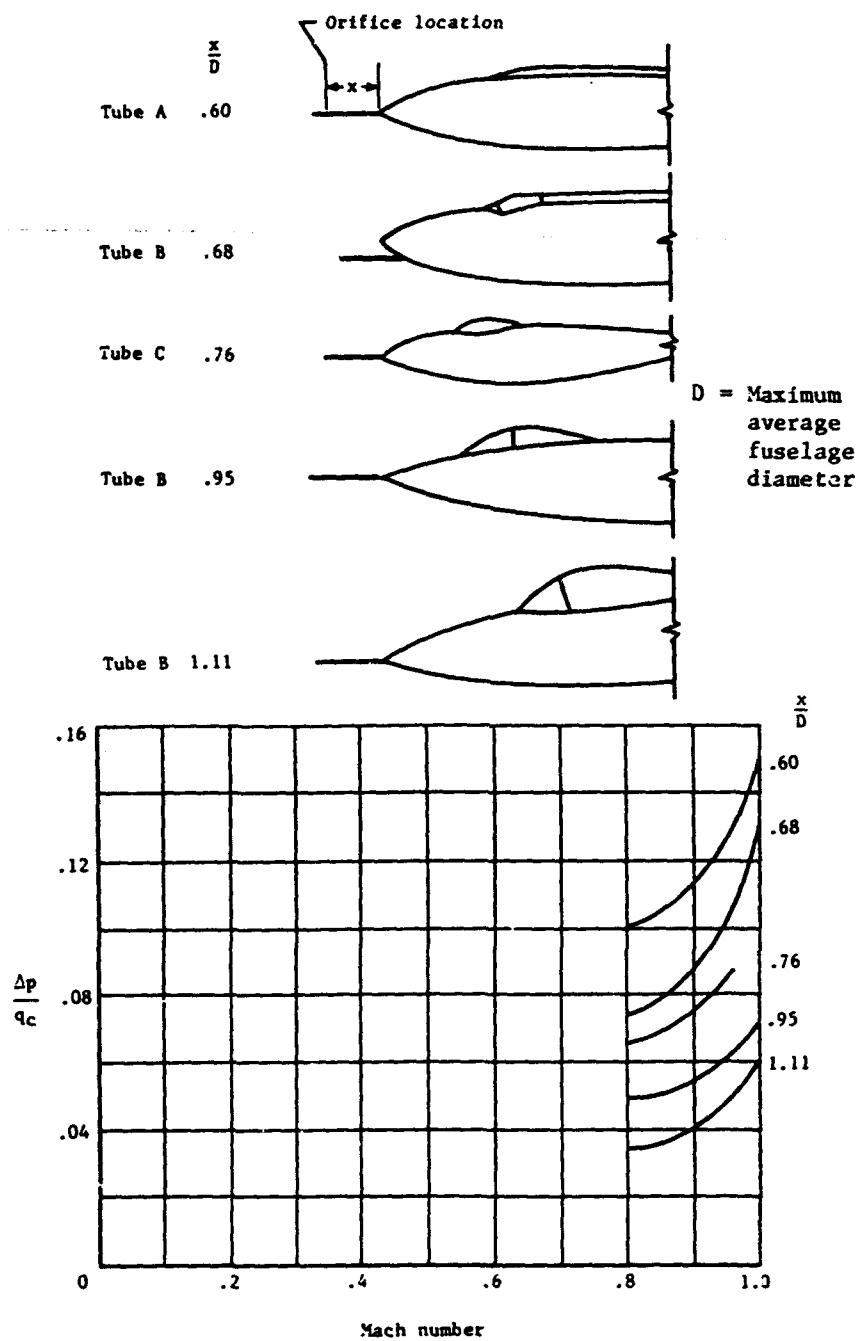


Figure 7.7.- Calibrations of fuselage-nose installations on five airplanes. (Adapted from ref. 6.)

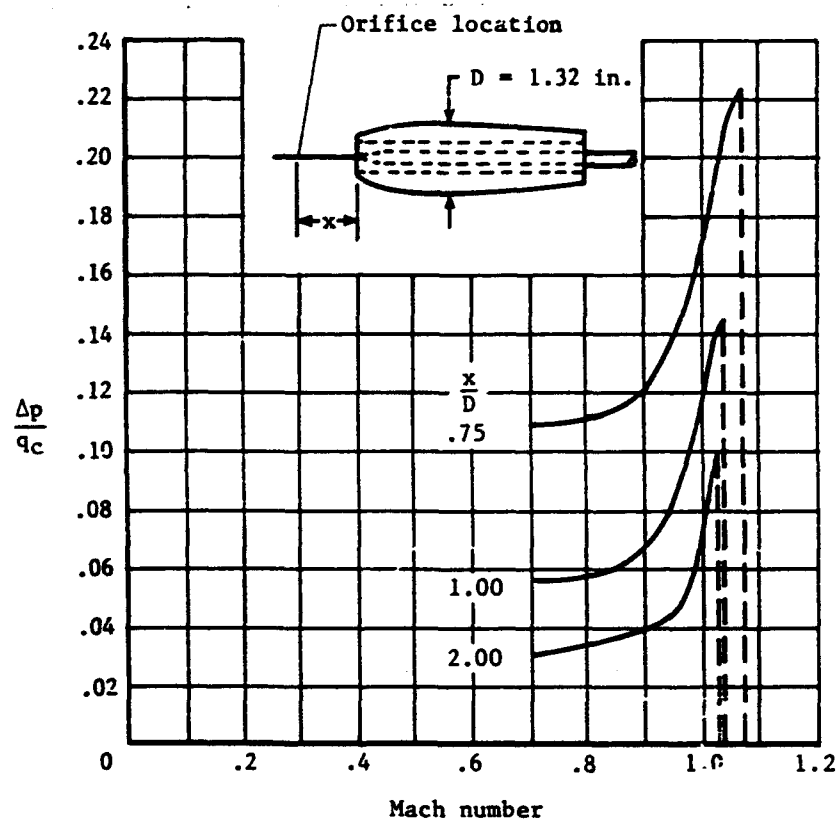


Figure 7.8.- Variation of static-pressure error ahead of model with nose inlet in transonic speed range. (Adapted from ref. 7.)

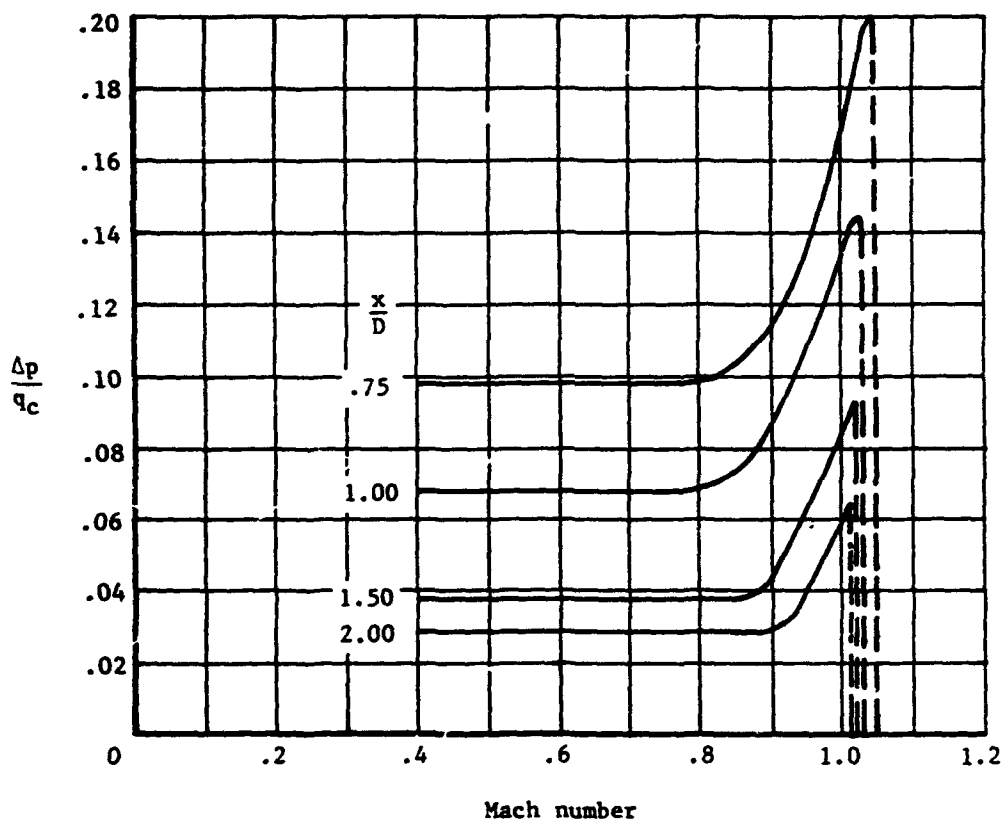
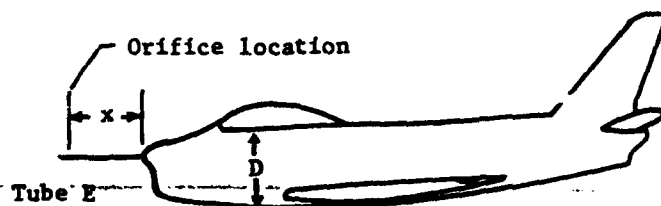


Figure 7.9.- Variation of static-pressure errors in transonic speed range of fuselage-nose installations on airplane with nose inlet. (Adapted from ref. 7.)

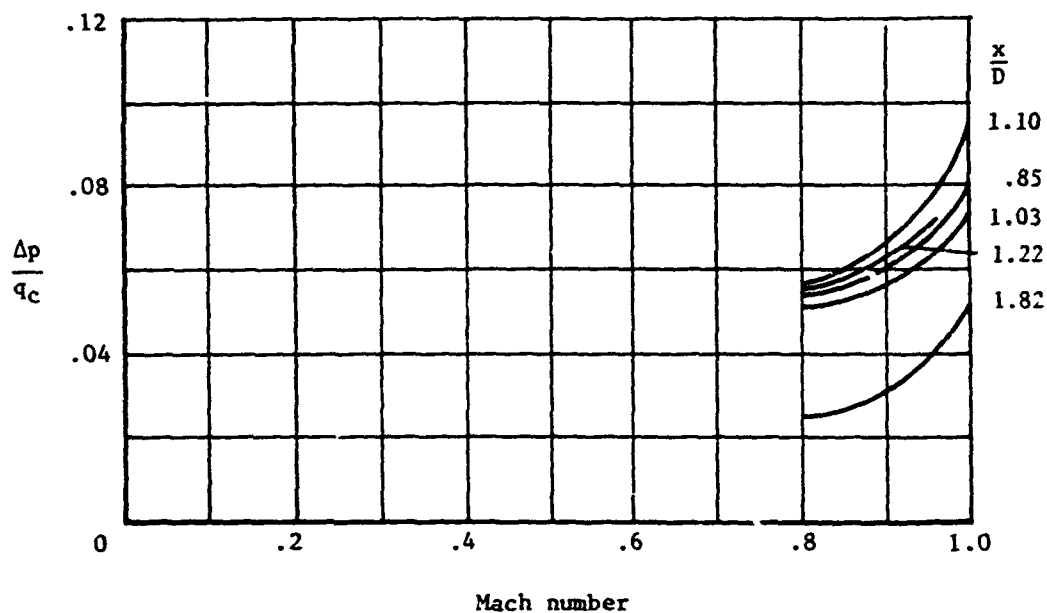
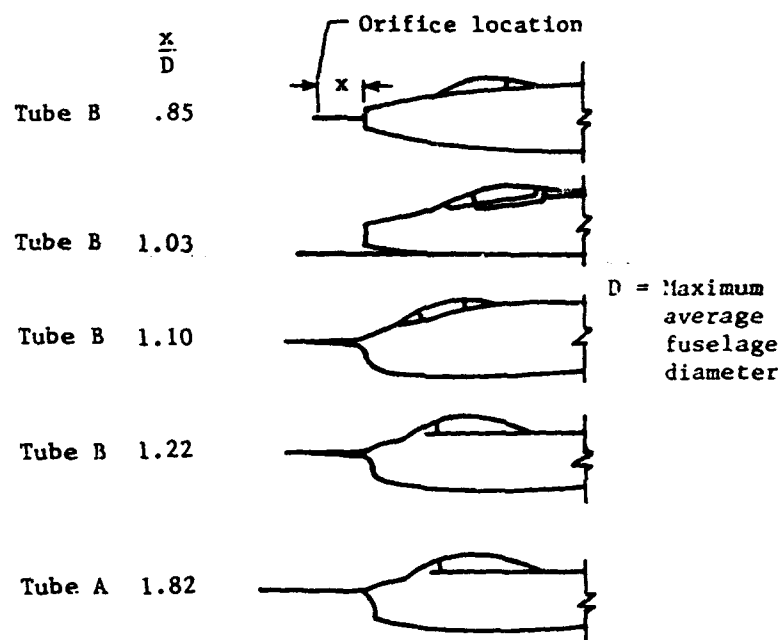


Figure 7.10.- Calibrations of fuselage-nose installations on five airplanes with nose inlets. (Adapted from ref. 6.)

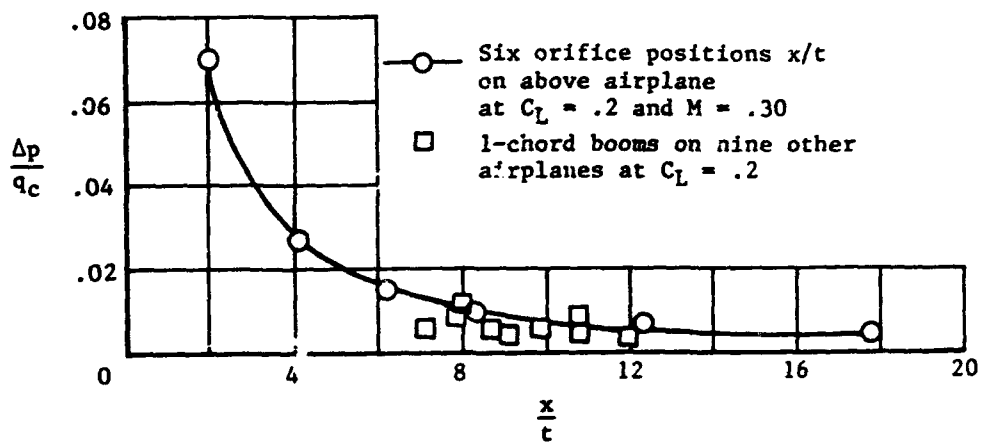
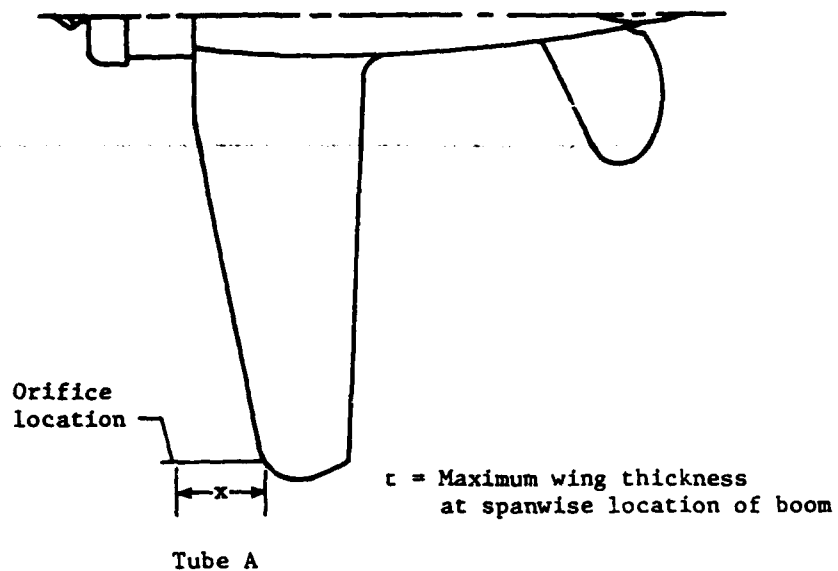


Figure 7.11.- Static-pressure errors at various positions ahead of wing tips of ten airplanes. (Adapted from ref. 8.)

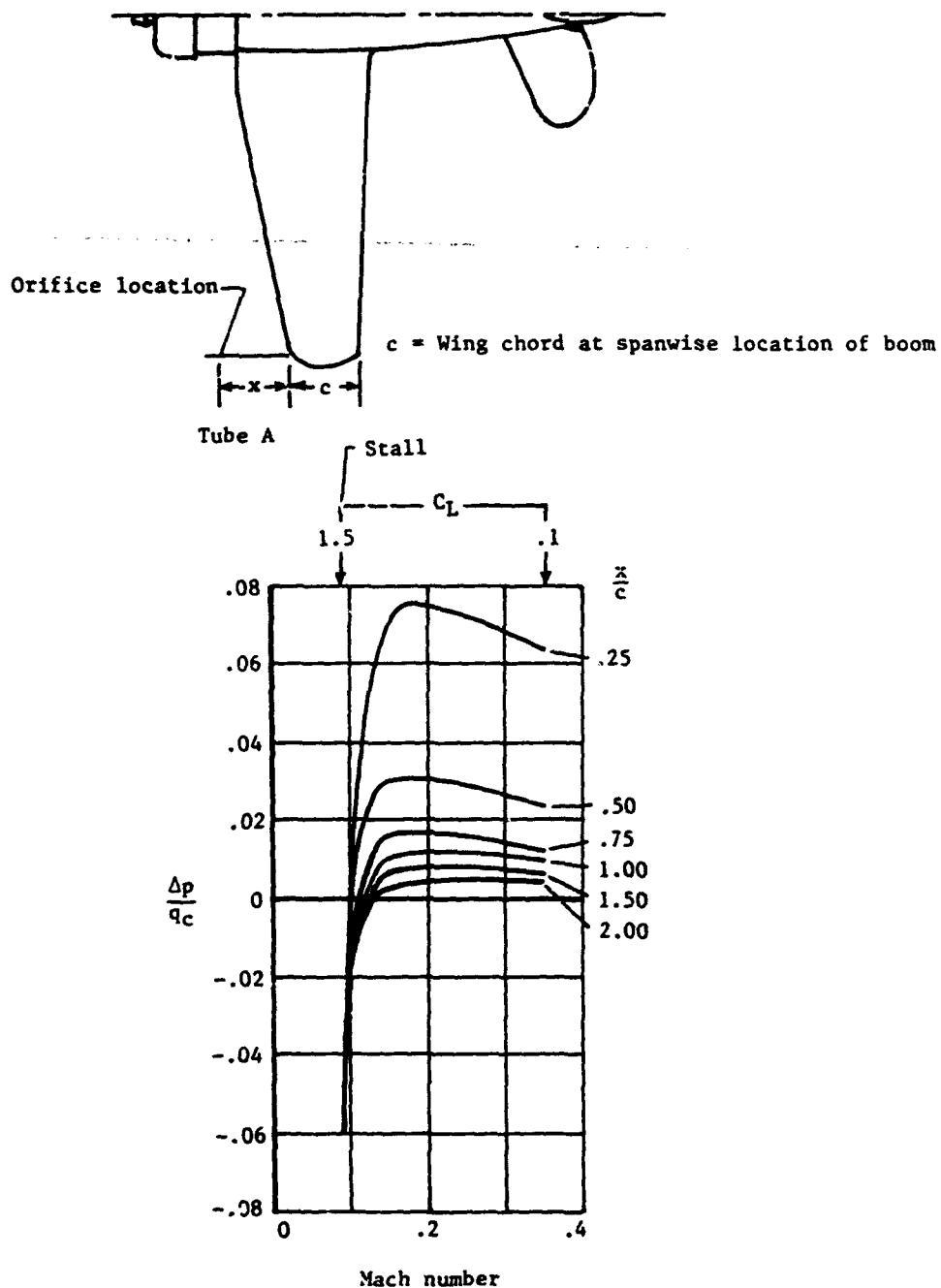


Figure 7.12.- Variation of static-pressure errors of wing-tip installations in low subsonic speed range. (Adapted from ref. 8.)

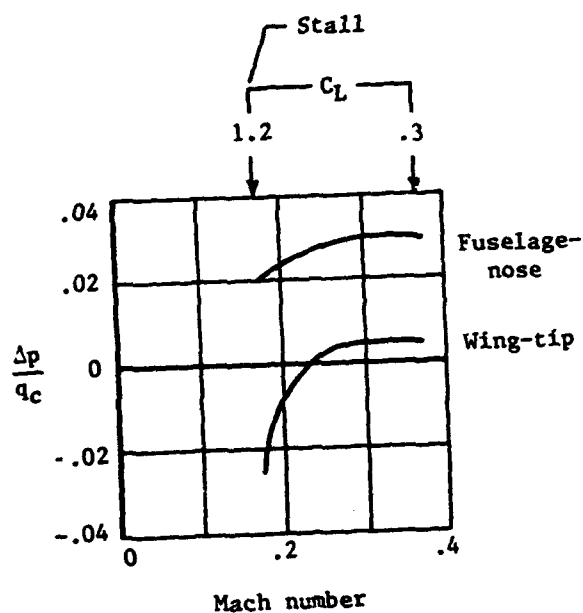
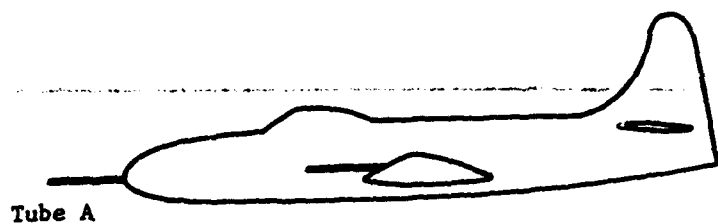


Figure 7.13.- Variation of static-pressure errors of wing-tip and fuselage-nose installations of same boom length. (Adapted from ref. 8.)

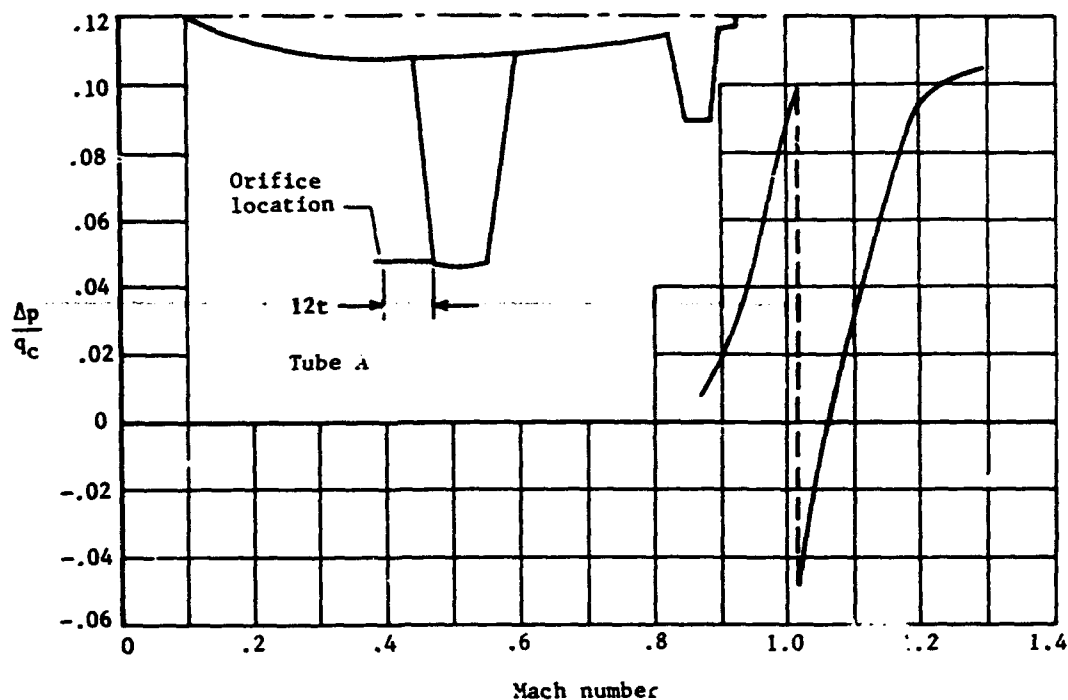


Figure 7.14.- Variation of static-pressure error of wing-tip installation in transonic speed range. (Adapted from ref. 3.)

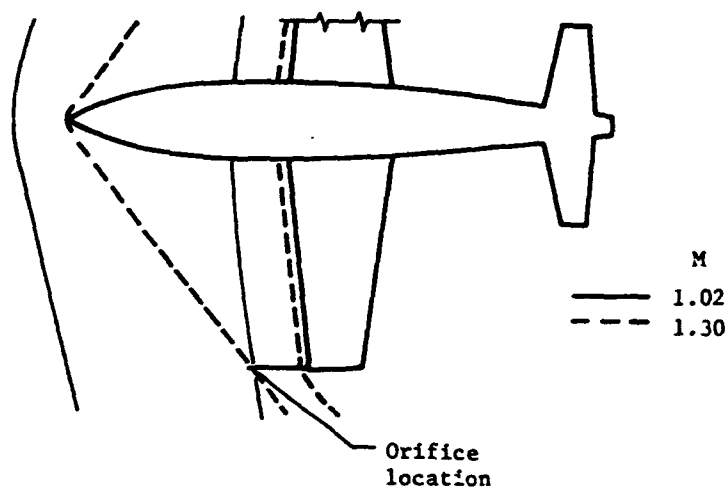


Figure 7.15.- Diagram showing position of shock waves with respect to a wing-tip installation in transonic speed range.

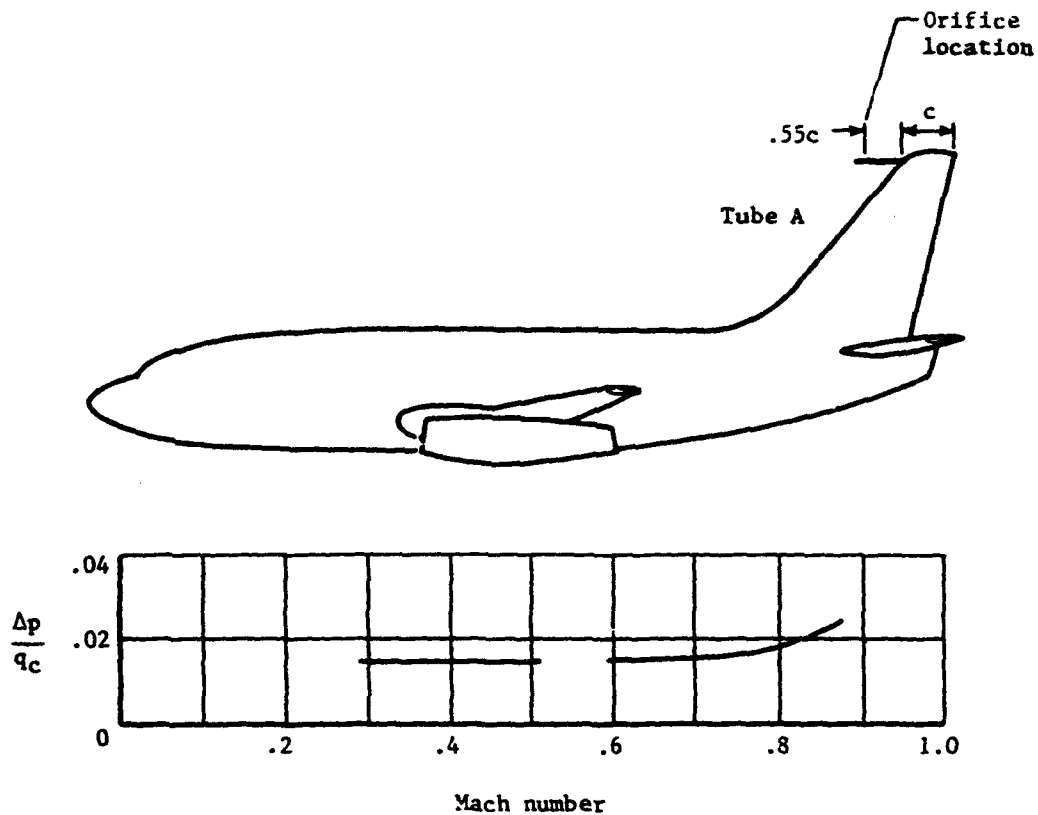


Figure 7.16.- Variation of static-pressure error of vertical-fin installation in low and high subsonic speed range.

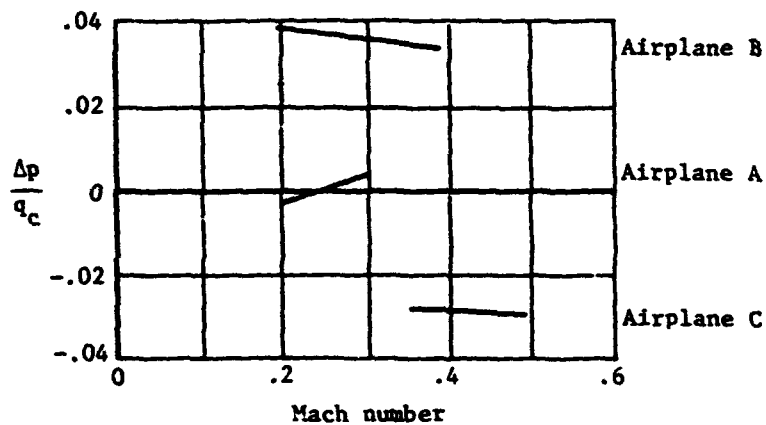
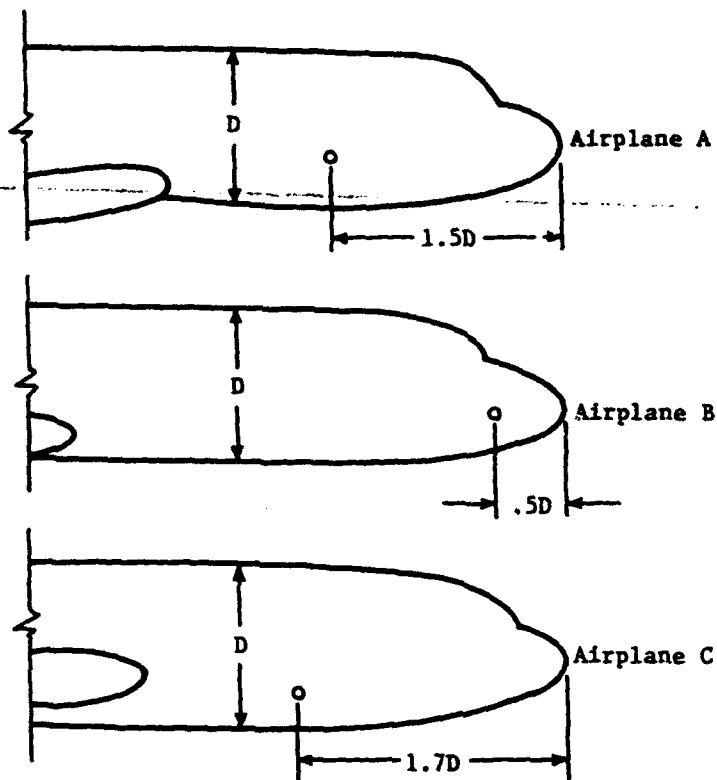


Figure 7.17.- Variation of static-pressure errors of fuselage-vent installations of three airplanes. (Adapted from ref. 9.)

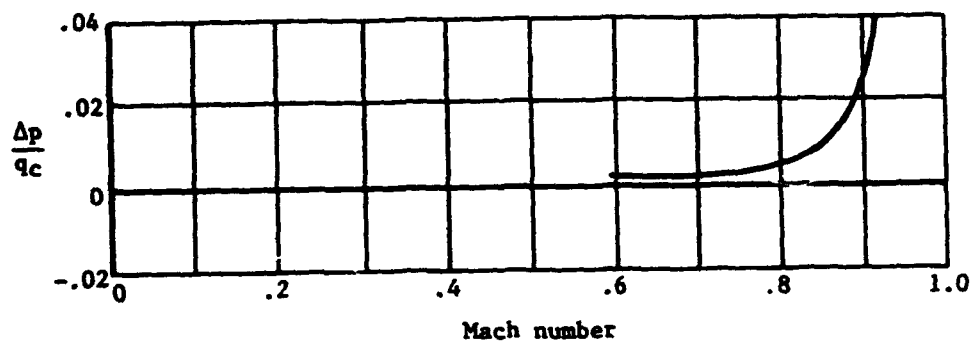
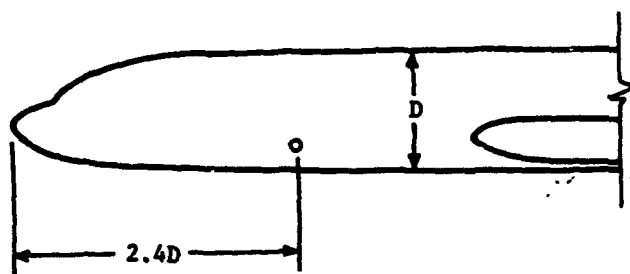


Figure 7.18.- Variation of static-pressure error of a fuselage-vent installation in high subsonic speed range. (Adapted from ref. 10.)

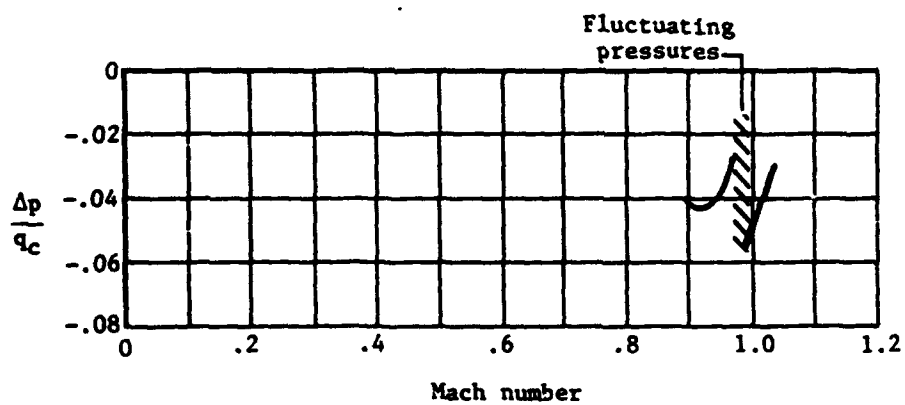
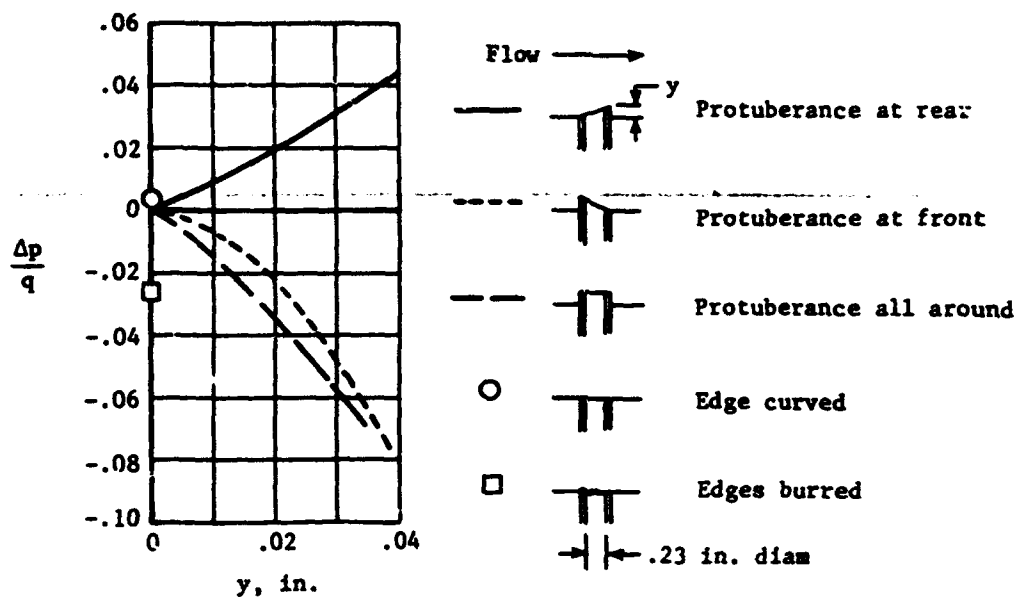
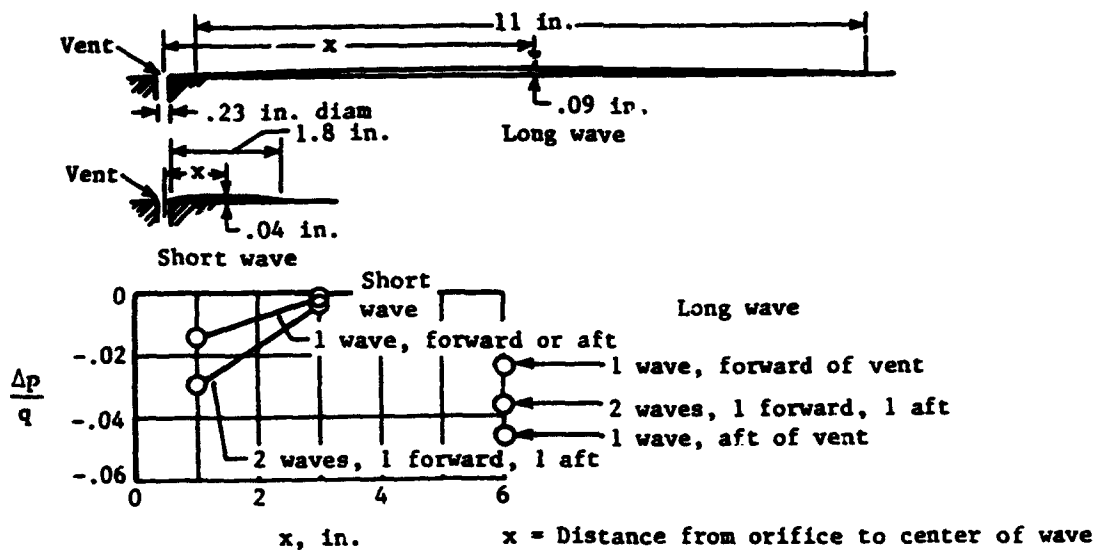


Figure 7.19.- Variation of static-pressure error of a fuselage-vent installation in transonic speed range. (Adapted from ref. 11.)



(a) Effect of protuberances and indentations.



(b) Effect of waviness of skin in vicinity of vent.

Figure 7.20.- Effect of protuberances and skin waviness on static pressures measured by a fuselage vent. (Adapted from ref. 12.)

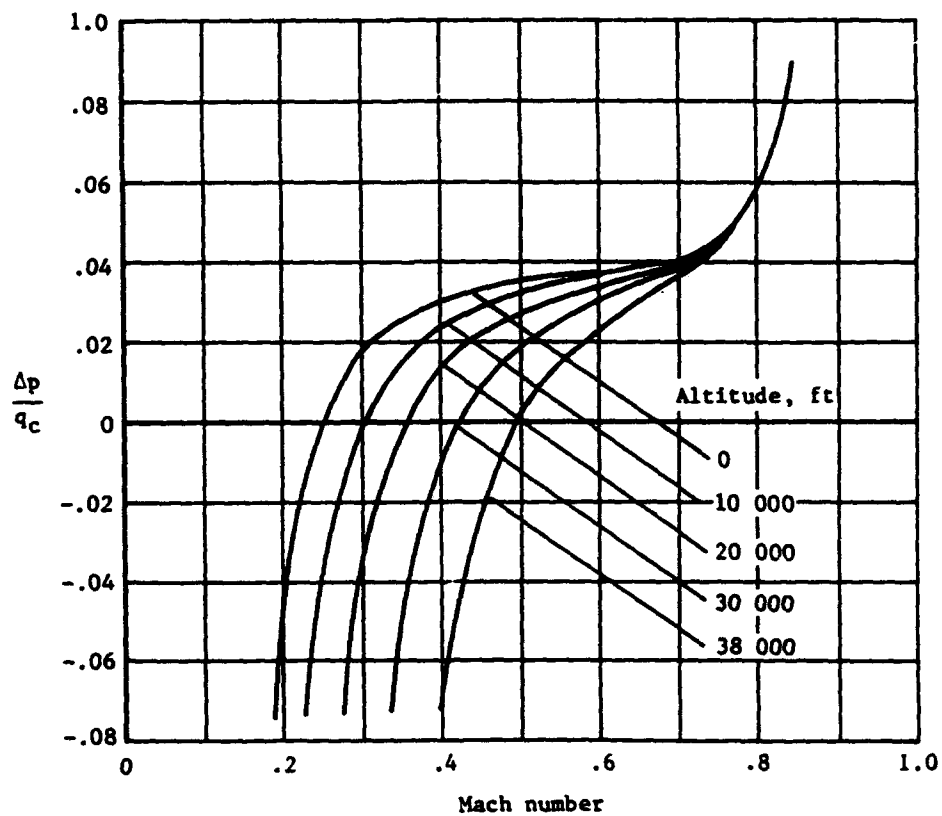
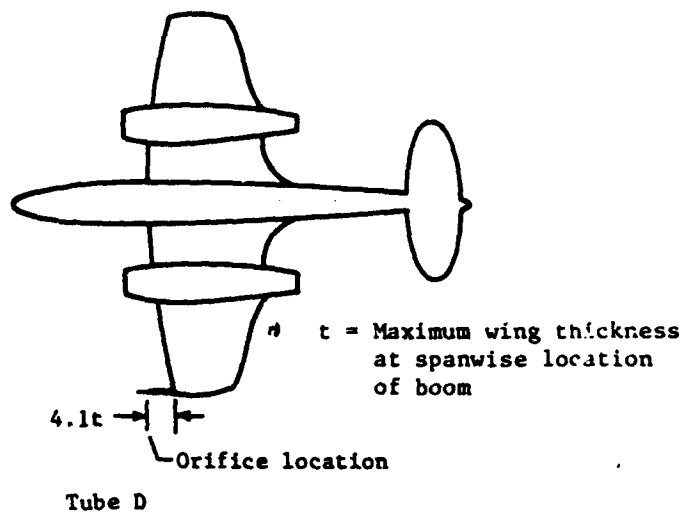


Figure 7.21.- Variation of static-pressure error of a wing-tip installation at five altitudes. (Adapted from ref. 13.)

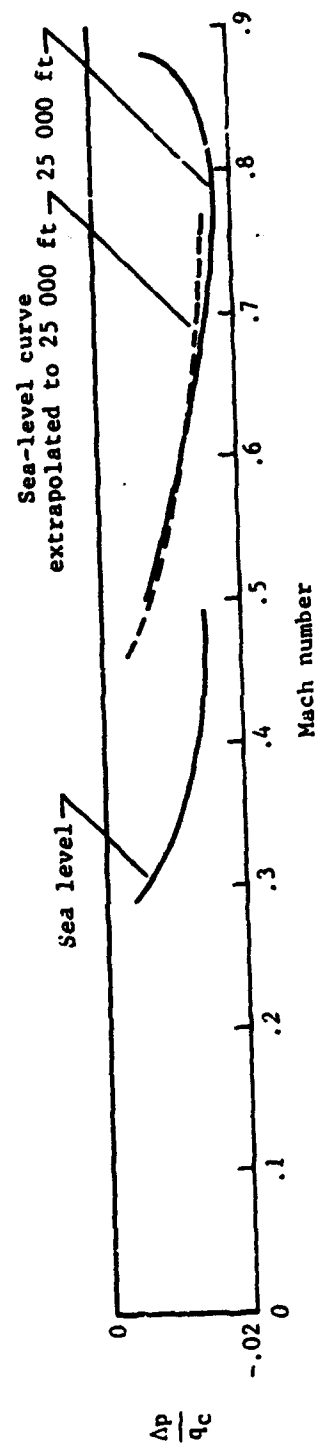


Figure 7.22.- Comparison of calibration of a static-pressure installation at altitude with extrapolation of sea-level calibration to that altitude. (Adapted from ref. 16.)

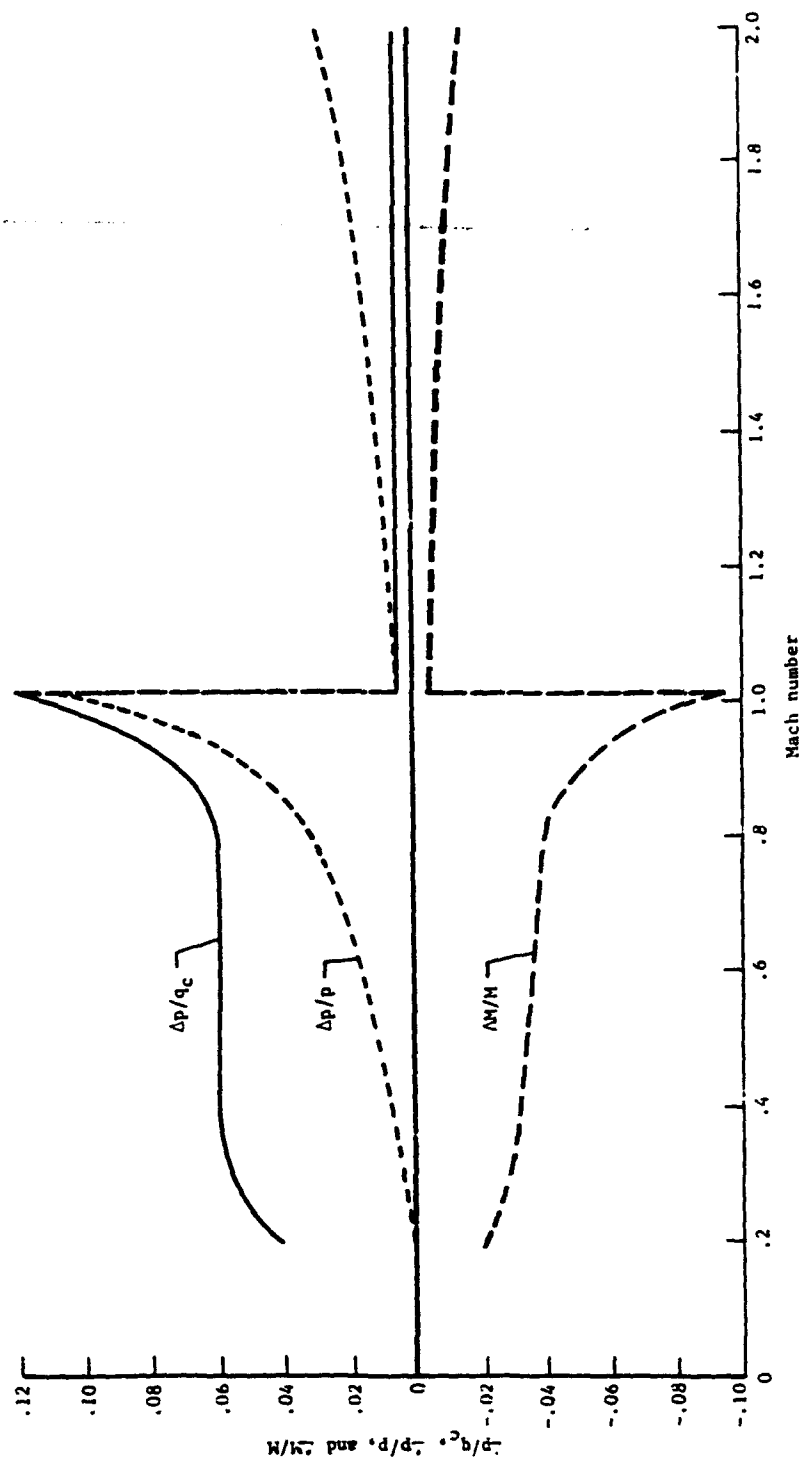


Figure 7.23.- Hypothetical calibration of a nose-boom installation expressed in terms of $\Delta p/q_c$, $\Delta p/p$, and $\Delta M/M$.

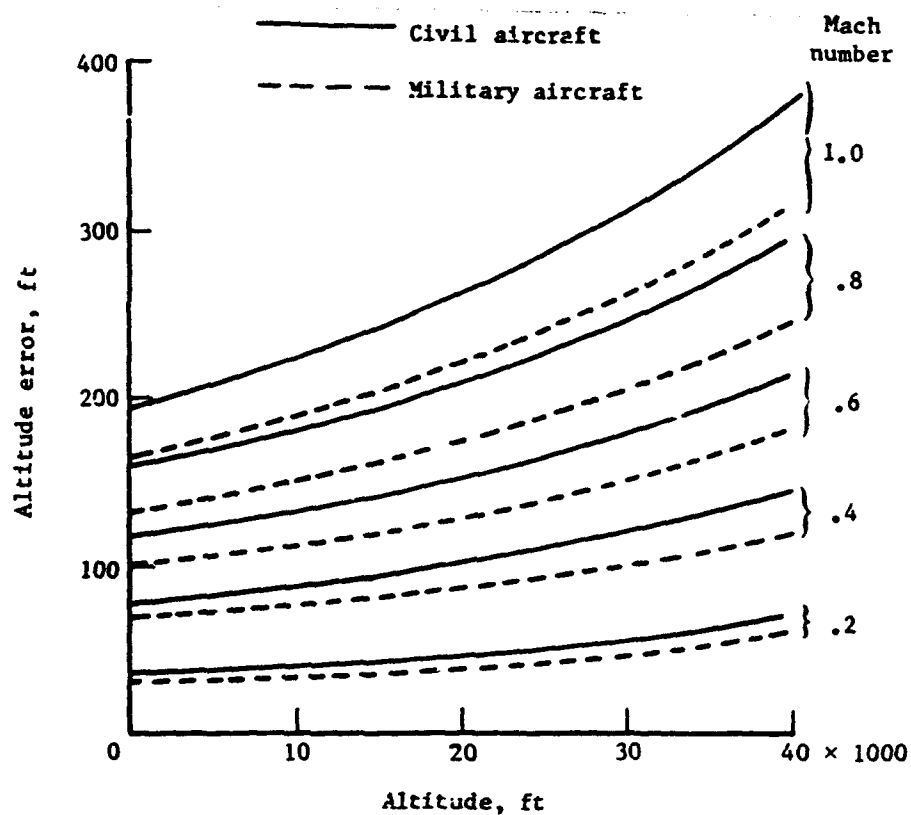


Figure 7.24.- Altitude errors corresponding to allowable static-pressure errors of installations on civil and military aircraft. (Adapted from refs. 17 and 18.)

CHAPTER VIII

AERODYNAMIC COMPENSATION OF POSITION ERROR

For research-type static-pressure installations, corrections for the position errors are normally applied during the reduction of the test data after the flight. For service-type installations, corrections for the position errors are applied during the flight by means of correction cards or automatic computing systems (chapter II). With some service installations, however, the position errors are effectively canceled at the static-pressure source, so that the need for manual or automatic corrections is eliminated. This cancellation or reduction of the position errors at the static-pressure source is accomplished by applying the concept of aerodynamic compensation to be discussed in this chapter.

With fuselage-vent installations, the position errors of the original vent configuration are compensated by installing small ramps or projecting plates in the vicinity of the vents (ref. 1). These devices are designed to alter the local flow in such a way that the local static pressure at the vents is changed to a value more nearly equal to the static pressure of the free stream.

With static-pressure-tube installations, the conventional tube is replaced with a specially contoured tube, called a compensated tube, that is designed to nullify the position errors of the conventional tube installation. The shape of the compensated tube and the location of the orifices along the tube are so designed that the static-pressure errors of the tube are equal and opposite to the position errors of the conventional tube installation.

The concept of compensation of position error is illustrated in figure 8.1 by hypothetical calibrations of a fuselage-nose installation. The curve labeled "position error" represents the calibration of a conventional tube at a given position ahead of the fuselage nose, the curve labeled "compensated tube error" represents the variation of the static-pressure error of the isolated compensated tube, and the dashed line along the zero axis represents the calibration of the compensated tube when installed at the same position as the conventional tube.

In an investigation of compensated tubes designed to reduce the position errors of fuselage-nose installations in the subsonic speed range (ref. 2), the negative tube errors required to balance the positive position errors were created with a tube having a collar with a conical afterbody and orifices at the base of the afterbody. In a more extensive investigation (ref. 3), the negative tube errors were developed with two types of tubes having ogival nose shapes. In one type, the orifices were located along the ogive near the nose, while in the other type they were located on a contoured contraction of the tube some distance behind the nose. With both types of tubes, the shape of the tube and the location of the orifices along the tube can be designed to compensate the position errors at a given position ahead of a fuselage having a given nose shape.

In the investigation of reference 3, three compensated tubes (a long ogival tube, a short ogival tube, and a contoured contraction tube (fig. 8.2)) were tested on a body of revolution having an ogival nose shape. The calibration of the long ogival tube with its orifices 0.95 of the body diameter (D) ahead of the body is shown in figure 8.3. The data for the curve labeled "position error" were obtained with a conventional (i.e., cylindrical) tube with orifices 10 tube diameters aft of the nose of the tube. The data obtained with the compensated tube (circular test points) show the position error to be effectively compensated throughout the subsonic speed range. To determine how well the larger position errors at a shorter distance ahead of the body could be compensated, tests were conducted with the short ogival tube with the orifices at a distance of 0.27 D ahead of the body. As indicated by the data from these tests (fig. 8.4), the position error for this location was also compensated throughout the subsonic speed range. In tests of the contoured contraction tube with orifices at a distance ahead of the body, comparable with that of the tube with the long ogival nose (fig. 8.5), the position error was compensated to the same extent throughout the subsonic speed range.

Since the tube errors of the compensated tubes are negative in the subsonic speed range, the position errors of the nose-boom installations in figures 8.3, 8.4, and 8.5 would be expected to become negative at the low supersonic speed at which the body bow shock traverses the orifices. In tests of the installations of figures 8.3 and 8.5 at low supersonic speeds, the position errors at a Mach number just beyond 1 were found to be -3 percent q_c for the installation in figure 8.3 and -4 percent q_c for the installation of figure 8.5.

However, for a tube having a shape similar to that of the long ogival tube but with orifices nearer the nose (fig. 8.6 from ref. 4), the error is only -0.5 percent q_c at the Mach number following shock passage ($M \approx 1.01$). At $M = 1.2$ the error is still small, but at $M = 1.65$ the error is about 1 percent q_c , a sizable error in terms of altitude error (550 ft, for example, at 40 000 ft).

In other tests in reference 3, the nose of the long ogival tube was cut to form a pitot opening having a conical entry of 82° . Cutting the tip of the tube was found to change the error compensation by less than 0.3 percent q_c at Mach numbers up to 1.2.

In further tests of the long ogival tube, orifices were located at a radial station of $\pm 37.5^\circ$ to reduce the errors at positive angles of attack. The results of the tests of this tube (fig. 8.7) show the error to be essentially zero at angles of attack up to 15° at a Mach number of 0.6. Note that the errors on this figure are incremental errors from the error of the tube at an angle of attack of 0° .

Compensated static-pressure tubes similar to those tested in the investigation of reference 3 have been used on the fuselage-nose installations of at least three airplanes (refs. 4, 5, and 6). The calibration of an installation on an F-104 fighter is shown in figure 8.8(a), on a B-70 bomber in figure 8.8(b), and on a British Harrier VTOL airplane in figure 8.8(c). For each of the installations, the static-pressure errors with the compensated tubes are within about

1 percent q_c throughout the subsonic speed range. The tubes used on these installations were pitot-static tubes with pitot openings similar to that of the tube in figure 8.6.

Although compensated tubes have been designed to minimize the errors of fuselage-nose installations at Mach numbers as high as 1.2, the errors of these tubes would be expected to be larger than those of conventional tubes at higher supersonic speeds. As a means of achieving small errors at both subsonic and supersonic speeds, it was suggested in reference 3 that a tube could be designed that would combine the features of the compensated tube for subsonic operation and the conventional tube for supersonic operations. With this type tube, one set of orifices would be located on the ogival nose of a cylindrical tube and a second set of orifices at least 10 tube diameters aft of the nose. A tube of this type would, of course, require an automatic pressure switch which would be activated at the speed at which the shock passes over the rear set of orifices.

References

1. Howard, J. R.: Wind Tunnel Tests of Alternate Static Source Protuberances for the F-86A Airplane. Rep. No. NA-49-449, North American Aviation, Inc., June 16, 1949.
2. Smetana, Frederick O.; Stuart, Jay Wm.; and Wilber, Paul C.: Investigation of Free-Stream Pressure and Stagnation Pressure Measurement From Transonic and Supersonic Aircraft. Interim Phase Report III - Development and Flight Test of Aerodynamic Static Pressure Compensation for a Service Type Aircraft. WADC Tech. Rep. 55-238, U.S. Air Force, July 1957.
3. Ritchie, Virgil S.: Several Methods for Aerodynamic Reduction of Static-Pressure Sensing Errors for Aircraft at Subsonic, Near-Sonic, and Low Supersonic Speeds. NASA TR R-18, 1959.
4. Carrillo, J. G.: Flight Calibration of the F-104 Compensating Airspeed Head. Rep. No. LR-16959, Lockheed California Co., June 18, 1963.
5. Webb, Lannie D.; and Washington, Harold P.: Flight Calibration of Compensated and Uncompensated Pitot-Static Airspeed Probes and Application of the Probes to Supersonic Cruise Vehicles. NASA TN D-6827, 1972.
6. Du Feu, A. N.: Altimeters - The Way Ahead? Proceedings of the 8th International Aerospace Instrumentation Symposium (Cranfield, England), Mar. 1975.

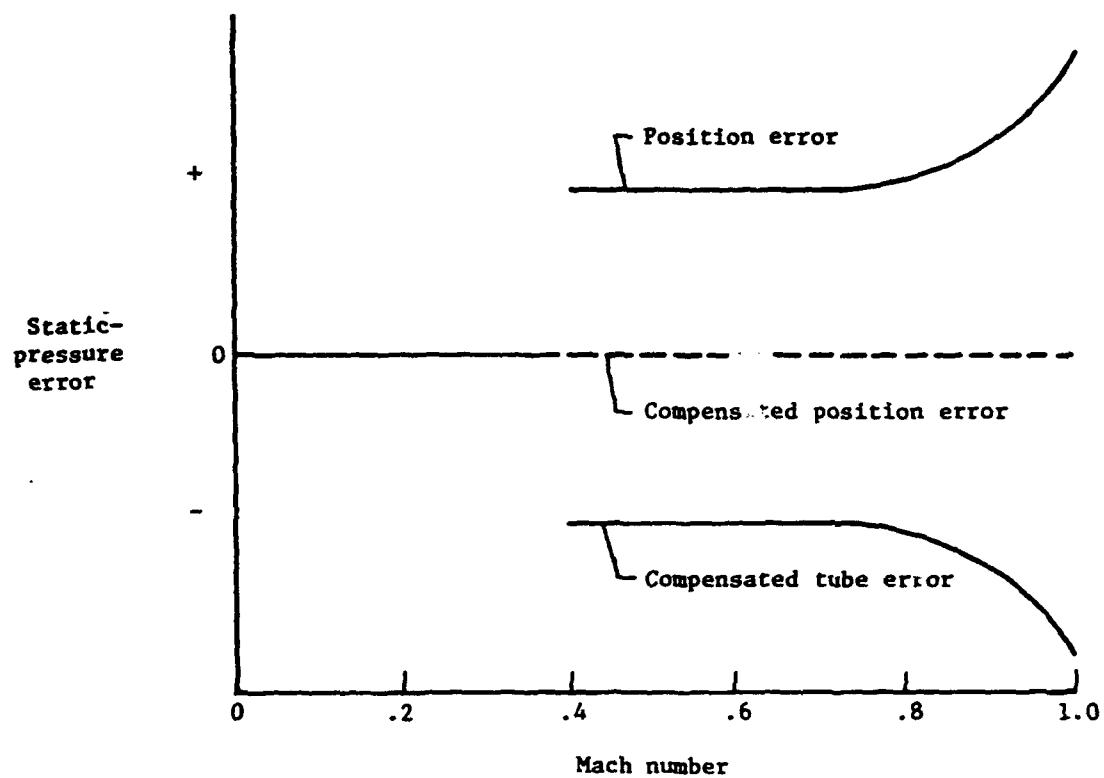
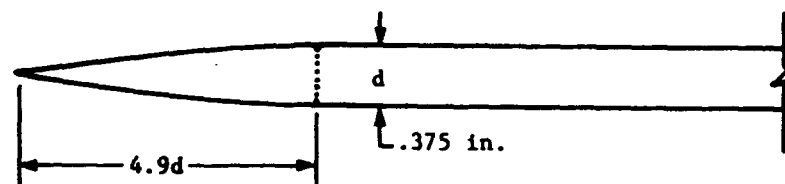
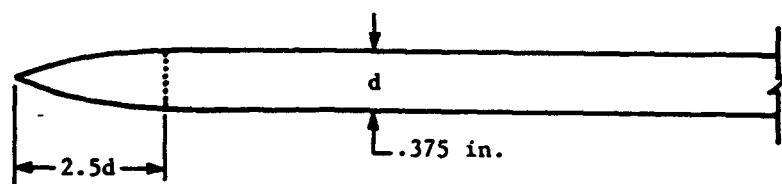


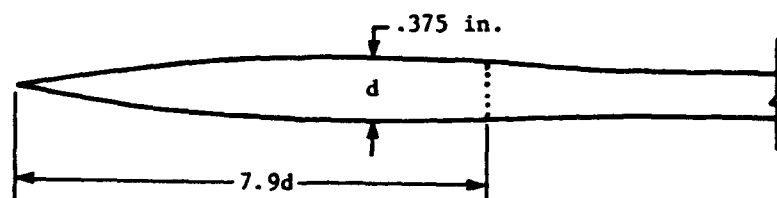
Figure 8.1.- Illustration of concept of aerodynamic compensation of position error.



(a) Long ogival tube.



(b) Short ogival tube.



(c) Contoured contraction tube.

Figure 8.2.- Diagrams of compensated static-pressure tubes.
(Adapted from ref. 3.)

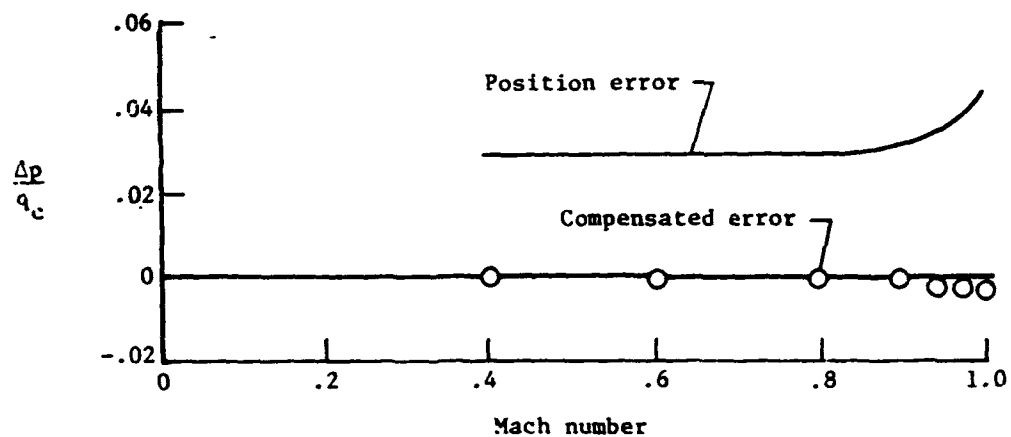
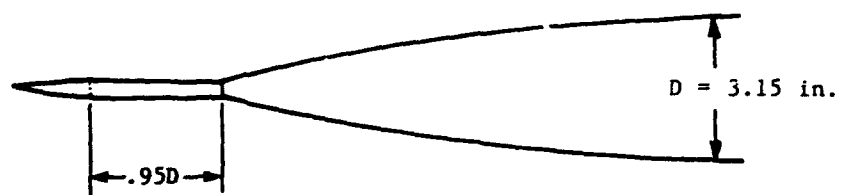


Figure 8.3.- Calibration of long ogival tube with orifices 0.95D ahead of body. (Adapted from ref. 3.)

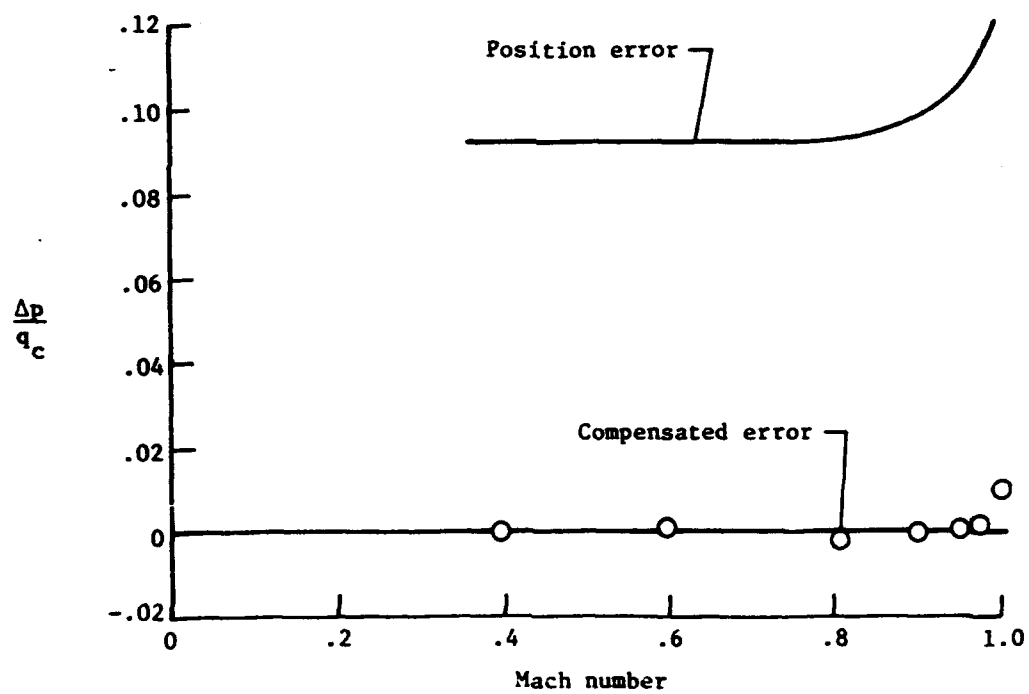


Figure 9.4.- Calibration of short ogival tube with orifices 0.27D ahead of body. (Adapted from ref. 3.)

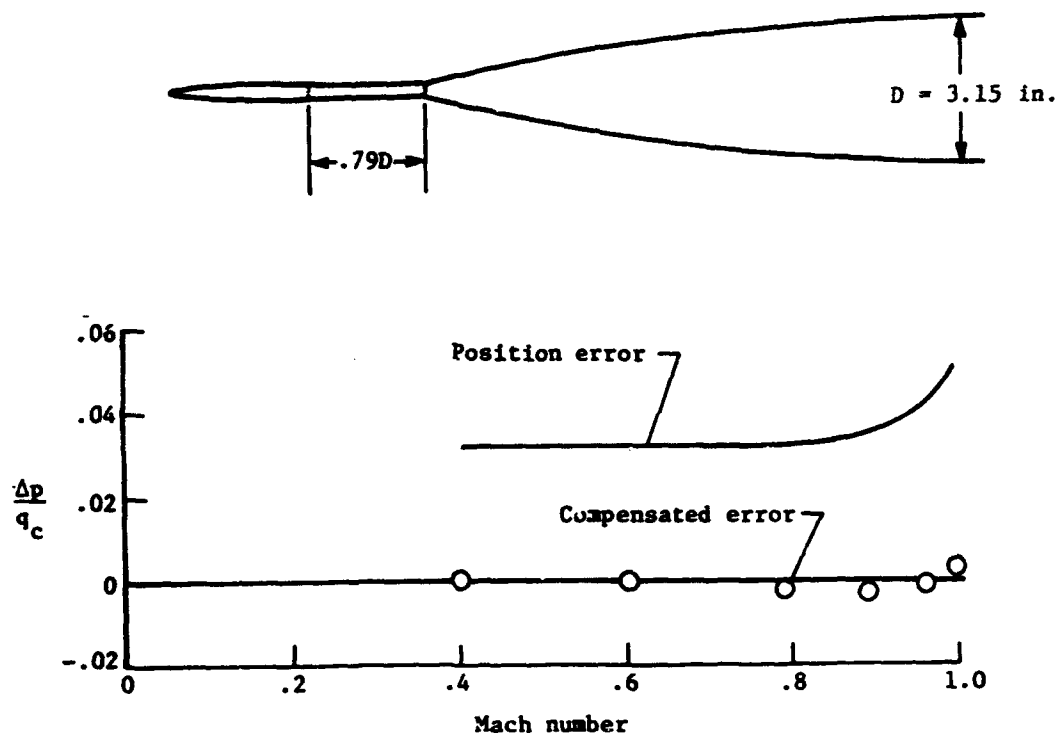


Figure 8.5.- Calibration of contoured contraction tube with orifices 0.79D ahead of body. (Adapted from ref. 3.)

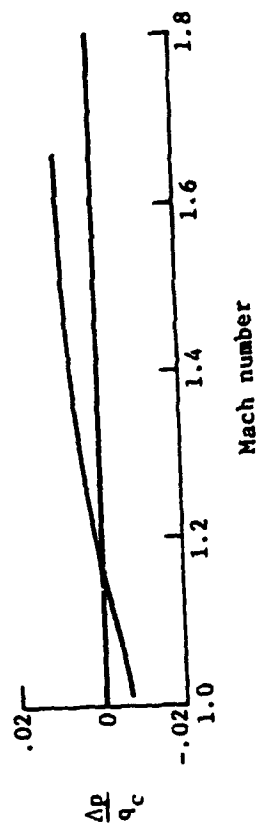
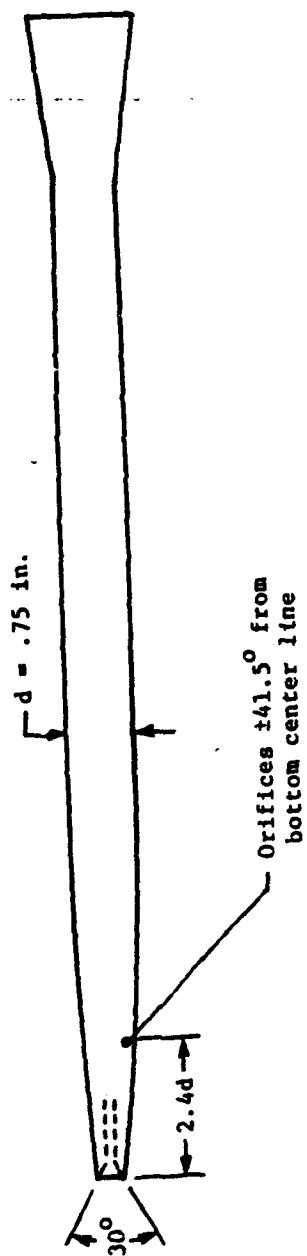


Figure 8.6.- Calibration of service-type compensated tube at supersonic speeds.
(Adapted from ref. 4.)

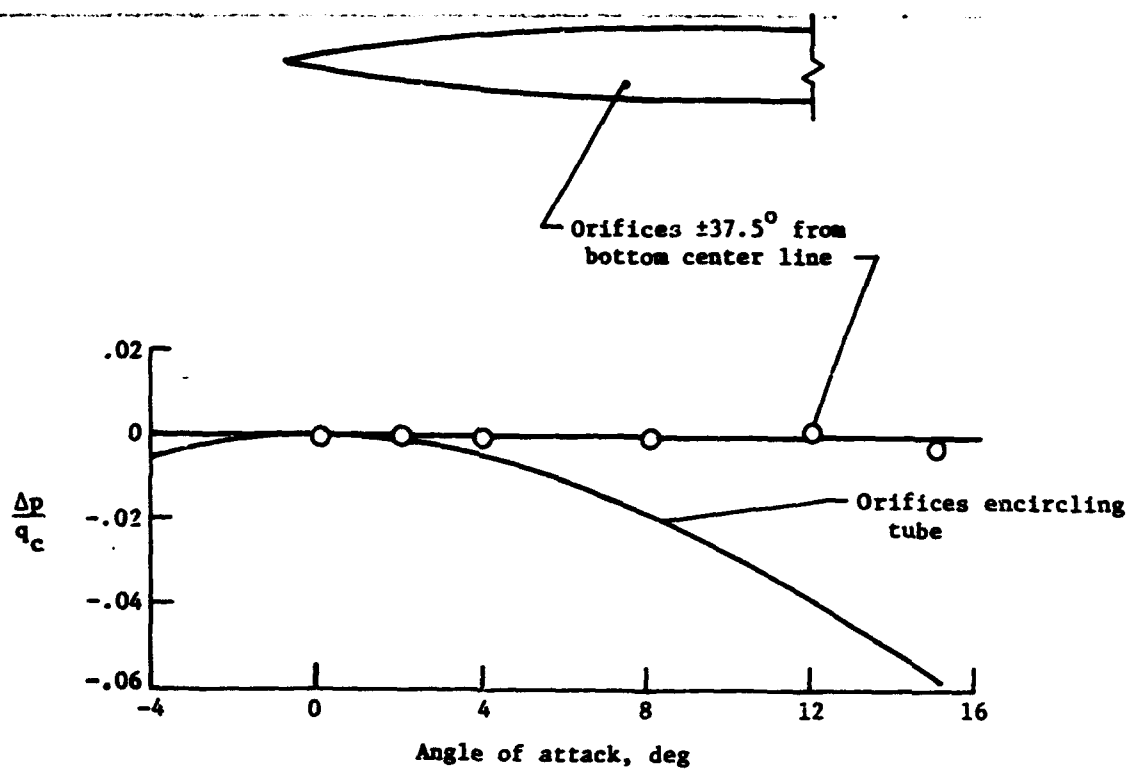
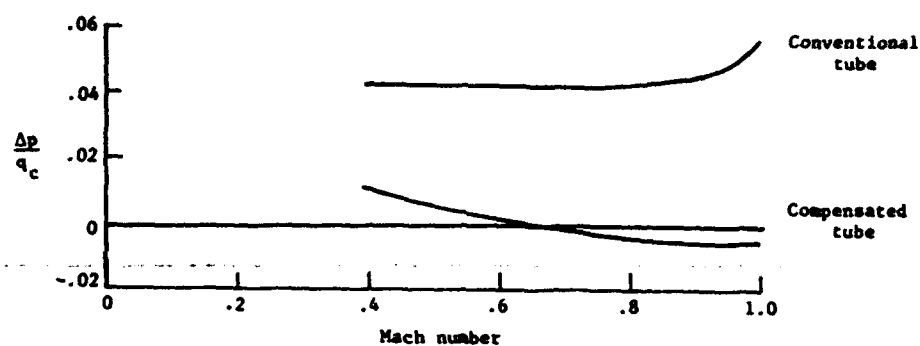
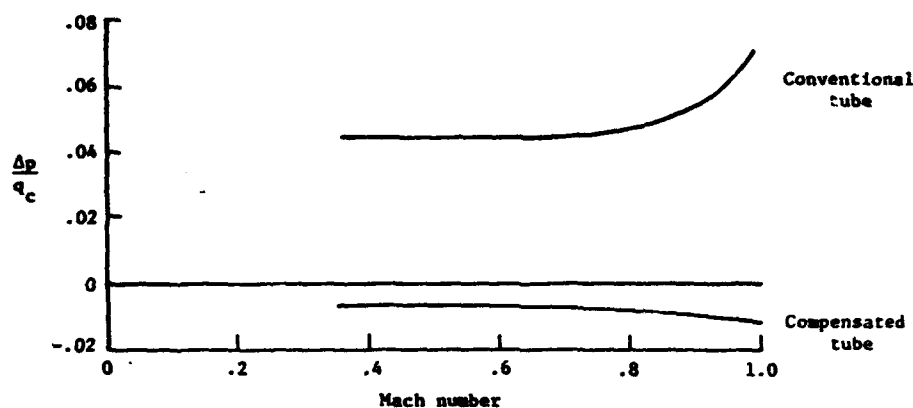


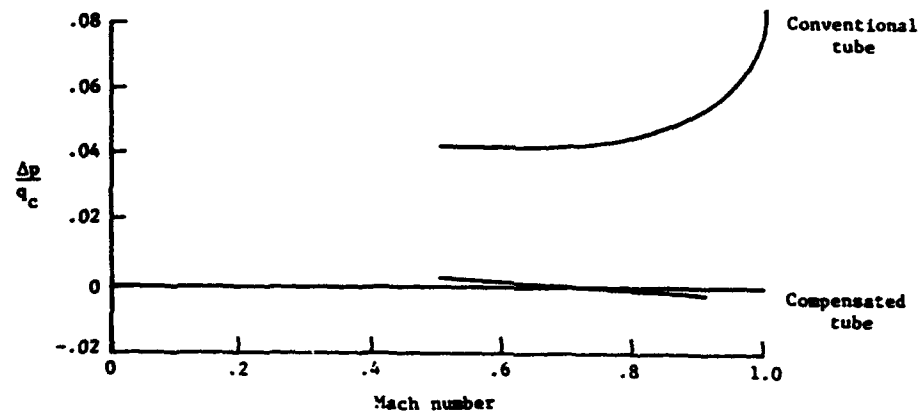
Figure 8.7.- Variation of errors with angle of attack of compensated tubes with orifices encircling the tube and at a radial station of $\pm 37.5^\circ$. $M = 0.6$. Errors on this figure are incremental errors from the error at zero angle of attack. (Adapted from ref. 3.)



(a) F-104 airplane. (Adapted from ref. 4.)



(b) B-70 airplane. (Adapted from ref. 5.)



(c) Harrier airplane. (Adapted from ref. 6.)

Figure 8.8.- Calibrations of compensated static-pressure-tube installations on three airplanes.

CHAPTER IX

FLIGHT CALIBRATION METHODS

The accuracy with which altitude, airspeed, and Mach number are determined from pitot-static measurements depends for the most part on the accuracy with which the position error of the static-pressure installation is established by a flight calibration of the installation. The accuracy of airspeed and Mach number also depends on the accuracy of the total-pressure measurement, but as noted in chapter IV, the total-pressure error at low angles of attack is generally negligible. For flight tests in which accurate measurements of total pressure at high angles of attack are required, the total-pressure installation can be calibrated against a test installation (swiveling or shielded total-pressure tube) which is insensitive to angle of attack. Since the difference between the pressures of the two installations can be measured with a sensitive differential-pressure instrument, the errors of the aircraft total-pressure installation can be determined with a high degree of accuracy.

In contrast to the ease with which the total-pressure error can be determined, the position error of the static-pressure installation can be quite difficult to determine. This difficulty is reflected in the wide variety of calibration methods that have been devised for the determination of this error. These methods are first discussed in terms of the measuring principles that form the basis of the calibration techniques. Application of each of the methods is then described in terms of accuracies, operational limitations, and instrumentation requirements. In a final section, the calibration of an airplane installation by two of the methods is described in some detail.

Calibration Methods for Deriving Position Error

As an introduction to the description of the various methods for determining the position error Δp , the calibration techniques are classified in terms of four parameters from which position error is derived: (1) free-stream static pressure p , (2) free-air temperature T , (3) true airspeed V , and (4) Mach number M . A listing of the calibration methods in accordance with this classification is as follows:

1. Free-stream static-pressure methods (Δp derived from measurements of p' and p)

- (a) p measured at reference pressure source

- Trailing-bomb method
 - Trailing-cone method
 - Pacer-aircraft method

PRECEDING PAGE BLANK NOT FILMED

(b) p derived from height of aircraft and measured pressure gradient

Tower method

Tracking-radar method

Radar-altimeter method

(c) p at height of aircraft calculated from p and T at ground

Ground-camera method

(d) p derived from change in height of airplane from initial height

Tracking-radar/pressure-altimeter method

Accelerometer method

2. Temperature method (Δp derived from T' and pressure-temperature survey)

Recording-thermometer method

3. True-airspeed methods (Δp derived from values of V)

Trailing-anemometer method

Speed-course method

4. Mach number methods (Δp derived from values of M' and M)

Sonic-speed method

Total-temperature method

Note that although the names given to most of the methods are based on specific measuring equipment, the measuring principles of some of the methods can be applied with other types of equipment.

For the free-stream static-pressure methods, Δp is determined as the difference between the static pressure p' measured by the aircraft installation and the free-stream static pressure p at the flight level of the aircraft. The four basic techniques for determining the value of p at the flight level are illustrated by the diagrams in figure 9.1.

With the first of these techniques, p is measured from a reference pressure source moving with the aircraft, but located where the effect of the pressure field of the aircraft is negligible. As shown in figure 9.1(a), the reference pressure source is either (1) a pressure sensor trailed below the aircraft (trailing bomb) or behind it (trailing cone) or (2) a calibrated static-pressure installation on another aircraft (pacer aircraft) flying alongside the test aircraft.

In the second technique (fig. 9.1(b)), the value of p at the flight level 2 is obtained from an interpolation of the measured pressure gradient through the test altitude range. For the tower method, the pressure gradient is measured through a small height range near the ground, while for the

tracking-radar and radar-altimeter methods, the gradient is determined through a wide height range at high altitudes.

In the third technique (fig. 9.1(c)), p at the height Z of the aircraft is calculated from measurements of p and T at the ground and an assumed standard temperature gradient up to the flight level. To minimize the errors that might be introduced by the assumption of the standard temperature gradient, the height of the aircraft should be less than about 500 ft.

With the fourth technique (fig. 9.1(d)), p at the height Z of the aircraft is derived from (1) measurements of the change in height from an initial height, (2) measurements of p' and T' at the initial height and at an air-speed for which Δp is known, and (3) either an assumption of a standard temperature gradient or an integration of equation (3.4). For the tracking-radar/pressure-altimeter method, the height increment is determined from a tracking radar, whereas with the accelerometer method, the height increment is derived from measurements of the aircraft accelerations and attitude.

In the temperature method (recording thermometer), values of Δp are determined from measurements of p' and values of p derived from (1) measurements of T' and (2) a pressure-temperature survey of the test altitude range.

For the true-airspeed methods, values of Δp are derived from measured values of V , p' , q'_c , and T' . The values of V are determined by two techniques: from measurements with a wind-driven anemometer suspended below the aircraft or by timed runs over a prescribed ground course.

With the Mach number methods, Δp is derived from values of ΔM , which are determined from measurements of M' and M . In the sonic-speed method, the values of M are derived from measurements of V and the speed of sound a , while in the total-temperature method, the values of M are determined from measurements of T' and T (derived from a temperature-height survey of the test altitude range).

Of the various methods outlined in the foregoing paragraphs, some can be applied only at low altitudes, while others can be applied only at high altitudes. For the low-altitude calibration methods, the maximum speed at which the tests can be conducted is restricted by the speed capability of the aircraft at the test altitude or by some limitation in the calibration method. For the high-altitude methods, the speed range of the calibration is determined by the minimum and maximum Mach numbers at which the aircraft can be flown at the test altitude. Thus, for some airplanes, a complete calibration throughout the Mach range may require tests at a number of altitudes using more than one calibration method.

With some of the methods, the tests must be conducted in steady, level flight, whereas with others, the tests can be conducted in dives and accelerated maneuvers as well as in level flight. In the first case, indicating instruments can be used for the measurement of the flight quantities, whereas in the second, recording instruments must be employed. Recording instruments provide measurements of the flight quantities against a time scale and, in addition, generally provide greater accuracy than indicating instruments.

In the following sections, the operational limitations (speed and altitude), instrumentations requirements, and accuracy (or precision) of each method are discussed in detail. As an aid in comparing the various calibration techniques, the characteristics of each method are summarized in table 9.1. From an examination of this table, it is evident that the selection of a method for the calibration of an installation on a particular airplane requires consideration of a variety of factors, such as (1) the desired accuracy in the determination of Δp , (2) the speed and altitude range for which calibration data are required, and (3) the available instrumentation. In general, greater accuracy, and thus more complex instrumentation, is required for the calibrations of flight research installations than for the installations on service aircraft.

Trailing-Bomb Method

With the trailing-bomb method, the static pressure measured by the aircraft installation is compared directly with the static pressure measured by orifices on a bomb-shaped body suspended on a long length of pressure tubing below the aircraft (refs. 1 and 2). With one type of bomb (fig. 9.2), the orifices are on the body of the bomb, while with another type (fig. 9.3), they are on a static-pressure tube ahead of the bomb. The type of bomb shown in figure 9.2 is a weighted body (15 lb), whereas the type shown in figure 9.3 has small wings set at a negative angle of incidence to keep the bomb below the aircraft. Both types are equipped with vanes on the afterbody to keep the orifices aligned with the airflow.

Since a trailing bomb, like static-pressure tube, may have static-pressure error, this error should be determined (by calibration in a wind tunnel) so that corrections for the error can be applied. For both of the bombs in figures 9.2 and 9.3, the static-pressure error is 0.5 percent q_c .

The length of tubing required to place the bomb in a region where the local static pressure approximates free-stream static pressure was shown in reference 1 to be about 2 times the wing span of the aircraft (fig. 9.1(a)). Since the bomb is below the aircraft, the static pressure at the bomb is higher than the static pressure at the flight level of the aircraft. However, as the decrease in pressure with height inside the suspension tubing is the same as that of the outside air, the pressure measured by the instrument in the aircraft is the pressure at the flight level.

The accuracy with which Δp is determined with the trailing-bomb method depends on (1) the accuracy of the measurement of the difference between p' and the local pressure p_l at the bomb and (2) how closely the value of p_l approximates p . Since Δp is very small compared with p' and p_l , the difference between the two pressures is measured most precisely with a sensitive differential-pressure indicator or recorder.

With trailing bombs, calibrations can be conducted through a wide range of altitudes and through a speed range from the stall speed to the maximum speed at which the bomb can be towed. This limiting speed is determined by the speed at which the suspension tubing develops unstable oscillations (ref. 3). For the

bomb in figure 9.2, instability of the suspension tubing is encountered at a Mach number of about 0.4. The bomb in figure 9.3, on the other hand, has been towed successfully at Mach numbers as high as 0.85 (at an altitude of 38 000 ft).

The accuracy of the trailing-bomb method with the equipment used in the tests of reference 4 varied from about ± 2.0 percent q_c at 60 knots ($M = 0.1$) to about ± 0.2 percent q_c at 220 knots ($M = 0.35$).

Trailing-Cone method

With the trailing-cone method (ref. 5), the static pressure measured by the aircraft installation is compared with the pressure measured by a set of orifices near the end of a long length of pressure tubing trailed behind the aircraft (figs. 9.1(a) and 9.4). A lightweight drag cone is attached to the end of the tube to keep the tubing taut.

The accuracy with which free-stream static pressure is measured with a trailing-cone system depends on the configuration of the cone system (size and shape of the cone and position of the orifices ahead of the cone (ref. 6)), on the distance of the cone behind the aircraft, and on the type of the aircraft (size, configuration, and propulsion system). Because of the uncertainties associated with each of these variables, trailing-cone systems have not been considered suitable for the basic calibration of an aircraft static-pressure installation. However, since the difference between the pressures of the cone system and the aircraft installation can be measured with good precision (i.e., repeatability), a calibrated cone system is useful as a secondary standard for production line testing. In practice, a cone system at a given trail length behind a particular airplane is calibrated by methods such as the tower or tracking-radar methods for which values of the free-stream static pressure are determined with a higher degree of certainty. The calibrated cone system is then used for the periodic recalibration of the installation on that airplane or for the original calibrations on airplanes of the same model (ref. 7).

With trailing-cone systems, calibrations can be conducted through a wide range of altitude and from relatively low speeds (defined by the minimum speed at which the pressure tubing trails straight back) to speeds as high as $M = 1.5$ (ref. 8).

In unpublished tests of a variety of cone systems, conducted by NASA Langley Research Center, the precision of the measurement of Δp was found to be ± 0.2 percent q_c at $M = 0.7$ to 0.88.

Pacer-Aircraft Method

With the pacer-aircraft method, a measure of the free-stream static pressure is derived from the calibrated static-pressure installation of a pacer aircraft flying alongside the test aircraft being calibrated (refs. 9 and 10).

The difference ΔH between the altimeter indication H' in the test aircraft and the corrected altimeter indication H in the pacer aircraft is found from equation (5.8):

$$\Delta H = H' - H \quad (5.8)$$

where ΔH is the altitude error. The pressures p' and p corresponding to the values of H' and H can be found in table A2 of appendix A. The difference between p' and p is then the position error Δp for the test aircraft. The value of Δp can also be found from the value of ΔH and equation (3.6). An example of the determination of Δp by the two procedures is given in part II of appendix B.

Since the value of Δp (a small quantity) is determined as the difference between two large quantities (p' and p), the altimeters in the two aircraft should be precision instruments which, to minimize hysteresis errors, should be calibrated only to the altitudes at which the tests are to be conducted. The precision with which Δp is determined, however, depends not only on the accuracy of the two altimeters, but also on the degree to which the two aircraft maintain formation flight. At very low speeds, the precision of the measurements generally deteriorates because of an inability to maintain formation flight. At high speeds, on the other hand, where speed and position control are more precise, the value of Δp can be determined with good precision (± 0.2 percent M for M up to 1.0 and altitudes up to 35 000 ft (ref. 10)). The corresponding precision in terms of $\Delta p/q_c$ is about ± 0.7 percent at $M = 0.5$ and about ± 0.2 percent at $M = 1.0$.

For best results with the pacer-aircraft method, the speed capability of the pacer aircraft should be very nearly that of the test aircraft. The speed range of the calibration tests is limited to speeds well above the stall of either aircraft and to the maximum level-flight speed of either aircraft.

In a variation of the pacer-aircraft method, a reference aircraft is flown at constant altitude at a low airspeed for which the position error is known (refs. 11 and 12). The test aircraft is then flown past the reference aircraft in a series of level-flight, constant-speed runs. The indications of the altimeters in the two aircraft are noted at the instant the test aircraft flies past, and the position error of the test aircraft is determined from the difference between the indications of the two altimeters.

The reference-aircraft method differs from the pacer-aircraft method in that the installation in the reference aircraft requires a calibration at only one airspeed, and the speed range of the calibration of the test aircraft is not limited to the speed capability of the reference aircraft.

The accuracy of this method is generally lower than that of the pacer-aircraft method because of the difficulty in synchronizing the altimeter indications in the two aircraft and because the height of the test aircraft at the time of the fly-by may differ from that of the reference aircraft.

Tower Method

For calibrations with the tower method, the aircraft is flown at constant speed and constant altitude past the top of a tall tower (ref. 11). For each test run, the position error Δp is determined as the difference between (1) the static pressure p' as measured by the cockpit altimeter at the instant the aircraft passes the tower and (2) the free-stream static pressure p at the height of the aircraft determined by interpolation of measured values of p at a number of points along the tower height (fig. 9.1(b)).

A movie camera mounted with the axis of the lens aligned with the horizontal is often used to determine the airplane height. With this technique, the height increment ΔZ of the airplane with respect to the lens axis is computed from the equation:

$$\Delta Z = \frac{l}{l'} \Delta z \quad (9.1)$$

where l is the length of the aircraft, l' is the length of its image, and Δz is the displacement of the image from the center line of the film frame. The aircraft height Z is then determined from the elevation of the camera and the height increment ΔZ .

It may be noted that precise measures of ΔZ are more important in determining Δp in terms of $\Delta p/q_c$ than in terms of $\Delta p/p$. For an error of 1 ft in ΔZ , for example, the error in $\Delta p/p$ would be only 0.004 percent, whereas the error in $\Delta p/q_c$ would be 1 percent at 50 knots, 0.2 percent at 100 knots, and 0.1 percent at 150 knots. The reference point on the aircraft for the ΔZ measurements should be the vertical position of the altimeter in the aircraft.

For accurate measurements of p' , the cockpit altimeter should be a precision instrument, and to minimize hysteresis errors, the laboratory calibration of the instrument should be limited to an altitude range only slightly greater than the tower height. Since the altimeter is used to measure pressure rather than altitude, it is convenient to calibrate the instrument as a pressure gage, that is, in terms of pressure versus altimeter indication.

The accuracy of the tower method depends primarily on the accuracy of the pressure measurements p' and p , since the height measurements (aircraft and pressure gradient) can be measured with good accuracy. To retain the advantage of the limited-range calibration of the altimeter in the laboratory, the height of the aircraft during the calibration tests should at all times be restricted to the same limited altitude range.

The speed range for calibrations by the tower method is limited to airspeeds well above the stall speed and up to the maximum level-flight speed of the aircraft at the tower height.

In tests (unpublished) of the tower method at the NASA Langley Research Center, the accuracy of the measurement of Δp was found to range from ± 1.0 percent q_c at 90 knots ($M = 0.15$) to ± 0.2 percent q_c at 190 knots ($M = 0.3$).

Tracking-Radar Method

With this high-altitude calibration method, the position error Δp is determined as the difference between the measured static pressure p' and the free-stream static pressure p which is determined from measurements of the height of the aircraft by the tracking radar and from a pressure-height survey of the test altitude range (ref. 13).

The pressure-height survey is conducted prior to the calibration tests in one of two ways: (1) by tracking a radiosonde (transmitting pressure measurements) as it ascends through the test altitude range or (2) tracking the aircraft through the test altitude range while flying at a low indicated airspeed for which the position error Δp is known from a calibration by a low-altitude method (fig. 9.1(b)). With the aircraft tracking procedure, the value of p at each height is determined from equation (2.2) expressed here as

$$p = p' - \Delta p \quad (9.2)$$

where p' is the static pressure measured by the aircraft installation and Δp is the position error of the installation at the airspeed of the ascent.

For the higher speeds of the calibration test runs, the height of the aircraft is measured continuously by the tracking radar. The position error Δp at the test airspeed is then determined from equation (2.2) here restated as

$$\Delta p = p' - p \quad (2.2)$$

where p' is the pressure of the aircraft installation during the test run and p is the free-stream static pressure at the height of the aircraft determined from the pressure-height survey. Because the pressure-height relation may change during the period of the tests, it is advisable to repeat the survey at the conclusion of the test runs.

With the tracking-radar method, calibrations can be conducted in dives as well as in level flight. The accuracy of the method, as determined by calibration tests to be described later in the chapter, is about ± 0.2 percent q_c at $M = 0.5$ and ± 0.1 percent q_c at $M = 0.88$.

It may be noted that this calibration method has also been used with other types of ground-tracking equipment such as the radar-phototheodolite of references 14 and 15 and the phototheodolite of reference 16.

Radar-Altimeter Method

With this high-altitude method, the position error of the aircraft installation is derived from the height of the aircraft measured with an onboard radar altimeter and from a pressure-height survey of the test altitude range (ref. 17). The pressure-height survey is conducted by flying the aircraft at a low, constant

airspeed for which the position error is known from a calibration by one of the low-altitude methods.

Because of the height-measuring characteristics of the radar altimeter, the calibration tests are restricted to level-flight runs and to test areas over a level ground reference plane, such as a large body of water.

The accuracy of the method at a Mach number of 0.8 and an altitude of 30 000 ft is about ± 1 percent q_c (ref. 17).

Ground-Camera Method

For calibrations with this method, the aircraft is flown in a series of constant-speed, level-flight runs over a camera located on the ground (ref. 13). For each test run, the position error Δp is determined as the difference between (1) the static pressure p' measured by the aircraft installation when the aircraft is directly above the camera and (2) the free-stream static pressure p computed from the measured height of the aircraft, measured values of p and T at the camera station, and the assumption of a standard temperature gradient. The height of the aircraft above the camera is calculated on the basis of the dimensions of the aircraft and its film image and the focal length of the camera lens (fig. 9.1(c)).

The calibration tests with the camera method are limited to speeds well above the stall and up to the maximum level-flight airspeed of the aircraft at the height of the tests. Since the application of the method requires the assumption of a standard temperature gradient, accurate measurements of the free-stream static pressure can be realized at heights no greater than about 500 ft.

The accuracy of the method, as determined in calibration tests to be described later in the chapter, is about ± 0.2 percent q_c at 200 knots ($M = 0.3$) and ± 0.1 percent q_c at 320 knots ($M = 0.5$).

In another method for determining the height of an aircraft with a camera, a movie camera is installed in the aircraft with the camera lens facing downward (ref. 18). The camera photographs reference marks on a runway as the aircraft flies at a constant speed and altitude along the runway. Its height above the runway is then determined from the geometry of the camera lens system as in the ground-camera method.

With another calibration technique for measuring aircraft heights near the ground, the height is determined from measurements of elevation angles with a theodolite (ref. 19). With two theodolites located an equal distance on each side of a ground course, the height of an aircraft flying at constant altitude along the ground course is determined from the intersection of the two lines of sight to the aircraft. The theodolite used in the tests of reference 14 was a simple angle-measuring device called a sighting stand.

Tracking-Radar/Pressure-Altimeter Method

For calibration tests with this high-altitude method, the aircraft is first stabilized at a selected height and at a low airspeed for which the position error Δp is known from a calibration by one of the low-altitude methods. The aircraft is then accelerated at a constant altitude (constant p') indicated by the cockpit altimeter (ref. 10). During the calibration test run, the variation of Δp with airspeed causes the pilot to vary the height of the aircraft in order to maintain constant p' . At any given airspeed, therefore, the change in height corresponds to a change in free-stream static pressure from which the position error Δp can be determined from the following equation:

$$\Delta p = p_1' - (p_1 - \delta p) \quad (9.3)$$

where p_1' is the initial (and constant) value of the static pressure measured by aircraft installation, p_1 is the free-stream static pressure at the initial height, and δp is the change in free-stream static pressure corresponding to the change in height (fig. 9.1(d)).

The initial height Z_1 of the aircraft and the change in height ΔZ from the initial height are determined from continuous measurements with a tracking radar. The free-stream values of p , q_c , and T at the initial height are determined from the initial indicated values p' , q_c' , and T' corrected for the known position error Δp_1 at the initial airspeed. The pressure increment δp corresponding to a height increment ΔZ is computed from equation (3.3), expressed here as

$$\delta p = -g\rho_1 \Delta Z \quad (9.4)$$

where ρ_1 is the density at the initial height and is calculated from equation (3.1), expressed here as

$$\rho_1 = \rho_0 \frac{p_1 T_0}{p_0 T_1} \quad (9.5)$$

where p_0 and T_0 are the standard sea-level values.

Since $p_1' = p_1 + \Delta p_1$, p_1' can be substituted in equation (9.3) to yield

$$\Delta p = \Delta p_1 + \delta p \quad (9.6)$$

Since the values of p during the calibration test run are based on a constant value of ρ determined at the initial height, the accuracy in the determination of δp varies with ΔZ . Whenever ΔZ is too great for accurate determinations of δp from a single initial height, successive sets of initial conditions can be established at various points during the flight.

The accuracy of this method, as determined in the tests reported in reference 10, varies from about $\pm 0.01M$ at $M = 0.5$ to about $\pm 0.02M$ at $M = 3.0$. The corresponding errors in terms of $\Delta p/q_c$ are ± 3.5 percent and ± 0.1 percent.

Accelerometer Method

In the accelerometer method (ref. 20), the value of Δp is determined from the measured static pressure p' and the free-stream static pressure p calculated from the value of p at an initial reference height. The value of p at the reference height is established by flying the aircraft at a constant, low airspeed for which the position error Δp is known from a calibration by a low-altitude method. The change in p from its initial value is derived from the change in height from the initial height which is calculated from measurements of the accelerations and pitch attitude of the aircraft (fig. 9.1(d)).

The application of the method is restricted to vertical-plane maneuvers from the initial stabilized condition. During the maneuver, the variation of p with height Z is obtained from equation (3.4):

$$dp = - \frac{p}{RT} dz \quad (3.4)$$

The value of T can be derived approximately from the measured temperature T' and equation (3.28). Since the value of M in this equation is not known, the value of T at any given airspeed in the test run can be stated in terms of M' as follows:

$$T \approx \frac{T'}{1 + 0.2KM'^2} \quad (9.7)$$

where K is the recovery factor of the temperature probe and γ in equation (3.28) is 1.4. Since the use of M' in equation (3.28) results in a small error in the value of p in equation (3.4); two or more approximations may be necessary.

The integration of equation (3.4) results in the following equation:

$$\left(\frac{p}{p_1}\right)^n = 1 - n \int_{Z_1}^Z \left(\frac{p}{p_1}\right)^n \frac{dz}{RT} \quad (9.8)$$

where the subscript 1 refers to initial conditions.

Substitution of p' for p in the right side of equation (9.8) and further substitution of equation (9.7) for T results in

$$\left(\frac{p}{p_1}\right)^n = 1 - n \int_{Z_1}^Z \left(\frac{p'}{p_1}\right) \left(\frac{1 + 0.2KM'^2}{RT'}\right) dz \quad (9.9)$$

The values of n may be selected so that only one approximation is required for the determination of p (appendix A of ref. 20). For a value of K near unity and for subsonic and low supersonic speeds, a value of n of $\frac{\gamma-1}{\gamma}$ or 0.286 gives satisfactory results.

The change in height dZ in equation (9.9) may be determined from the vertical velocity computed from (1) values of p' and T' for an initial condition where Δp is known and (2) the vertical acceleration computed from measurements of normal and longitudinal accelerations and pitch attitude angles:

$$dZ = \left(v_1 + \int_{t_1}^t a_v dt \right) dt \quad (9.10)$$

where t is time and the initial vertical velocity v_1 is

$$v_1 = \frac{-\bar{R}T_1}{P_1} \left(\frac{dp}{dt} \right)_1 \quad (9.11)$$

and

$$a_v = a_z \cos \theta - a_x \sin \theta - g \quad (9.12)$$

where a_v is the vertical acceleration, a_z is the normal acceleration, a_x is the longitudinal acceleration, and θ is the pitch attitude angle of the aircraft.

For any given instant during the calibration test run, the difference between the value of p determined from equation (9.9) and the measured value of p' is the position error Δp of the aircraft installation at that instant.

The application of the accelerometer method requires the continuous measurement of p' , q'_c , T' , a_z , a_x , and θ against a time scale. The pressures, temperatures, and accelerations should be measured with research-type recording instruments. For the measurement of T' , the recovery factor K of the temperature probe should be very nearly 1.0. The attitude angle θ can be measured with a horizon camera, a Sun camera, or an attitude gyroscope. A detailed discussion of the problems associated with the use of each of the three attitude-angle measuring instruments is given in reference 20.

The accuracy of the method depends primarily on the accuracy in the determination of θ and the accuracy of the acceleration measurements. In a flight evaluation of the accuracy of the method (ref. 20), the position error Δp of an aircraft installation was determined with an accuracy of about ± 0.5 percent q_c in shallow dives from an altitude of 31 000 ft at Mach numbers from 0.6 to 0.8.

With the restriction that maneuvers during the test runs be conducted in a vertical plane, calibration data can be obtained with the aircraft in level flight, climbs, dives, push-downs, pull-outs, or any combination of these maneuvers. The test maneuver should cover as short a time interval as practical (less than 2 minutes) in order to avoid an accumulation of errors in the measurements.

Recording-Thermometer Method

With this high-altitude method, values of Δp are determined from values of p' measured by the aircraft installation and values of the free-stream static pressure p derived from a pressure-temperature survey of the test altitude range (ref. 21).

The p/T relation is determined by flying the aircraft at a low airspeed for which the value of Δp of the static-pressure installation is known from a calibration by a low-altitude calibration method. The value of T at the survey airspeed is determined from measurements of T' and equation (3.28) with $\gamma = 1.4$:

$$T = \frac{T'}{1 + 0.2KM^2} \quad (9.13)$$

where K is the recovery factor of the temperature probe and M is derived from values of q'_c and p' (both corrected for the value of Δp at the survey speed). As noted in chapter III, the use of equation (3.28) requires that K be near unity.

For the calibration test runs, continuous recordings are made of p' , q'_c , and T' . Then, at any given instant during the test run, the value of p can be obtained as a function of T from the measured value of T' , equation (9.13), and equations (3.23) and (3.24), expressed here (with $\gamma = 1.4$) as

$$\left. \begin{aligned} \frac{p_t}{p} &= (1 + 0.2M^2)^{3.5} & (M \leq 1) \\ \text{and} & \\ \frac{p_t}{p} &= 1.2M^2 \left(\frac{5.76M^2}{5.6M^2 - 0.8} \right)^{2.5} & (M \geq 1) \end{aligned} \right\} \quad (9.14)$$

where p_t is derived from measured values of p' and q'_c . Combining equations (9.13) and (9.14) and eliminating M yields the following equations:

$$\begin{aligned}
 p &= \frac{P_t}{\left[1 + \frac{1}{K} \left(\frac{T'}{T} - 1\right)\right]^{3.5}} & (M \leq 1) \\
 \text{and} & \\
 p &= \frac{P_t}{\frac{6}{K} \left(\frac{T'}{T} - 1\right)} \left[\frac{\frac{28}{K} \left(\frac{T'}{T} - 1\right) - 0.8}{\frac{28.8}{K} \left(\frac{T'}{T} - 1\right)} \right]^{2.5} & (M \geq 1)
 \end{aligned}
 \tag{9.15}$$

Equation (9.15) is an expression of another p/T curve which, when compared with the p/T survey plot, yields an intersection that defines the values of p and T for the test condition.

The accuracy of the recording thermometer method depends, for the most part, on the variation of the free-air temperature T with time and distance (both vertical and horizontal), on the value of the recovery factor K , and on the accuracy with which K is known.

The effects of atmospheric temperature variations can be minimized by conducting the calibration tests on days when the thermal currents at the test altitudes are very small or at altitudes where the thermal currents are negligible (generally above 35 000 ft). The effects of air temperature variations can also be reduced by repeating the p/T surveys at various times during the calibration tests. Since there is no temperature gradient at altitudes above 35 000 ft, the accuracy of this calibration method improves appreciably at these altitudes. At altitudes below 35 000 ft, for example, an error of 1°F in the measurement of T' at $M = 0.8$ corresponds to an error in M of about 0.02. Above 35 000 ft, the error in M for a temperature error of 1°F would be $1/3$ of this value.

For altitudes below 35 000 ft, an error of 0.01 in the value of K (for K of unity) corresponds to an error in M of about 0.01 at $M = 0.8$. For higher altitudes, the error in M is appreciably lower.

With pressure recorders having an accuracy of 0.25 percent of full scale, the combined error in the measurement of p' and q_c' produces an error in M of about 0.004 at $M = 0.8$ and 30 000 ft (ref. 21).

The accuracy of the method at $M = 0.8$ and an altitude of 30 000 ft based on the errors given for T' , K , p' , and q_c' is estimated to be about ± 2.3 percent M . The corresponding error in $\Delta p/q_c$ is about ± 4.5 percent.

Trailing-Anemometer Method

With this calibration method, the position error Δp of the aircraft installation is derived from measured values of true airspeed V , impact

pressure q'_C , static pressure p' , and air temperature T' . The true airspeed is measured with a wind-driven anemometer suspended on a long cable below the aircraft (ref. 22).

For speeds below $M = 0.2$, the effects of compressibility are sufficiently small that q_C can be approximated (within 1 percent) by q . Therefore, from equation (3.10),

$$q_C \approx q = \frac{1}{2} \rho v^2 \quad (M \leq 0.2) \quad (9.16)$$

In equation (1.1), p_t can usually be considered correct, so that

$$q'_C = p_t - p' \quad (9.17)$$

From equation (2.2),

$$p' = p + \Delta p \quad (9.18)$$

By combining equations (9.17) and (9.18),

$$q'_C = p_t - (p + \Delta p) \quad (9.19)$$

Then, since $q_C = p_t - p$,

$$q_C = q'_C + \Delta p \quad (9.20)$$

Equation (9.16) can then be written as

$$q'_C + \Delta p \approx \frac{1}{2} \rho v^2 \quad (M \leq 0.2) \quad (9.21)$$

With the substitution of equation (3.2),

$$\rho = \frac{p}{RT} \quad (3.2)$$

for ρ in equation (9.21),

$$q'_C + \Delta p \approx \frac{p v^2}{2RT} \quad (M \leq 0.2) \quad (9.22)$$

With the further substitution of $p' - \Delta p$ for p (eq. (9.2)) and T' for T (since, for $M \leq 0.2$, $T' \approx T$), equation (9.22) becomes

$$q_c' + \Delta p \approx \frac{(p' - \Delta p)v^2}{2RT'} \quad (M \leq 0.2) \quad (9.23)$$

The position error Δp can then be found from the following equation:

$$\Delta p = \frac{\frac{p'v^2}{2RT'} - q_c'}{1 + \frac{v^2}{2RT'}} \quad (M \leq 0.2) \quad (9.24)$$

The anemometer assembly of reference 22 consists of (1) a small six-bladed, low-inertia propeller that activates a self-generating tachometer, (2) a low-drag housing with tail fins to keep the body aligned with the airstream, and (3) a support cable that transmits the tachometer signals to a magnetic tape recorder in the aircraft (fig. 9.5).

The rotational speed of the anemometer propeller is proportional to true airspeed. Accurate measurements of true airspeed are realized, however, only when the anemometer is trailed in a region where the local velocity is that of the free stream, that is, where the velocity induced by the flow around the aircraft is zero (or nearly so). An example of an induced velocity field below an airplane is presented in figure 9.6 as contours of constant velocity ratios u/V , where u is the horizontal component of induced velocity. The vertical and horizontal distances below the airplane are given in terms of the fractions z/b and x/b , where b is the wing span. Also shown in the figure are anemometer positions (with a 100-ft cable length) for the airplane at a low speed with flaps down and at a high speed with flaps up. For both anemometer positions, the induced velocity is essentially zero and, since $V_l = V - u$, the local velocity, is very nearly the free-stream velocity.

The usable speed range of the anemometer system of figure 9.5 is from 7 knots to about 165 knots (the speed at which the suspension cable develops unstable oscillations). Because of the $M = 0.2$ limitation of this method, however, the maximum speed of the calibration tests is restricted to airspeeds of about 130 knots at altitudes near sea level.

In tests of the anemometer of figure 9.5 with impact pressure recorders of widely differing sensitivities, the accuracy of the calibration tests with the most sensitive recorder was ± 0.5 knot at 40 knots, while that with the least sensitive recorder was ± 3.0 knots at 50 knots. The effect of this single element of the instrumentation on the accuracy of the test results illustrates the fact that the stated accuracy of a calibration method is dependent not only on the inherent accuracy of the calibration technique, but also on the accuracies of each of the component instruments. For an insight into the contribution of the various component errors for the anemometer tests of reference 22, the reader is referred to table I of that report.

For the anemometer system having an accuracy of ± 0.5 knot at 40 knots ($M = 0.08$), the accuracy at 100 knots ($M = 0.16$) was also ± 0.5 knot. The corresponding accuracies in terms of $\Delta p/q_c$ are ± 2.5 percent and ± 1 percent.

Speed-Course Method

The measured quantities and equations for the measurement of Δp by the speed-course method are the same as those for the trailing-anemometer method. With the speed-course method, however, the true airspeed is derived from measurements of the ground speed of the aircraft and the wind speed at the flight level (ref. 23).

The ground speed is determined by measuring the time for the aircraft to fly, in a constant indicated airspeed and altitude, between landmarks a known distance apart. The wind speed at the flight level can be measured by a wind-speed indicator or the effects of the winds can be effectively canceled by flying a triangular course or by flying in opposite directions along a straight-line course. For best results, the tests should be conducted when the wind speed is near zero, such as the period just after sunrise or before sunset.

The values of q'_c , p' , and T' needed for the solution of equation (9.24) can be derived from measurements with an airspeed indicator, pressure altimeter, and indicating thermometer. From values of the indicated airspeed V_i , the value of q'_c can be calculated from the equation,

$$q'_c = \frac{1}{2} \rho_0 V_i^2 \quad (9.25)$$

where the unit of ρ_0 is slugs per cubic foot and the unit of V_i is feet per second.

The application of the speed-course method is limited to airspeeds well above the stall speed and up to maximum speeds defined by the $M = 0.2$ limitation referred to in the preceding discussion, namely, about 130 knots at altitudes near sea level.

The accuracy of the method is largely dependent on the accuracy of the time measurements of the speed run, the constancy of the wind speed, and the constancy of the airspeed throughout the speed run.

Sonic-Speed Method

With the sonic-speed method (ref. 15), the position error Δp is derived from the Mach number error ΔM which is defined as

$$\Delta M = M' - M \quad (5.10)$$

where M is the free-stream Mach number and M' is the indicated Mach number which is derived from measurements of q'_c and p' .

ORIGINAL
OF POOR QUALITY

The value of M is derived from equation (3.21):

$$M = V/a \quad (3.21)$$

where V is the true airspeed of the aircraft and a is the speed of sound at the level of the test runs. The true airspeed V is determined from the ground speed of the aircraft and the wind speed at the flight level, and the speed of sound a is derived from the free-air temperature T at the flight level and equation (3.27).

For the calibration tests, the aircraft is flown in a series of constant-speed, level-flight runs during which the ground speed and the height of the aircraft are measured with a tracking radar. Prior to the test runs, the variations of wind speed and free-air temperature with height are determined by tracking a rawinsonde through the test altitude range.

The values of ΔM determined by this method can be converted to values of $\Delta p/p$ or $\Delta p/q_c$ by means of equations (5.4) through (5.7).

The accuracy of the method depends on the accuracy of the rawinsonde thermometer and the accuracy of the ground-tracking equipment in measuring the speed and height of the aircraft and the rawinsonde.

In calibration tests with the sonic-speed method using a radar-phototheodolite for ground tracking (ref. 15), the accuracy in the measurement of the ground speed of the airplane was found to be 50 to 75 ft/sec. The accuracy of the measurement of wind speed was found to depend on the height and elevation angle of the rawinsonde from the tracking station; at a height of 50 000 ft and an elevation angle of 20° , the accuracy of the wind-speed measurement was 1.8 knots. The accuracy of the measurements of the height of the airplane and the rawinsonde was about 100 ft, and the accuracy of the temperature measured by the rawinsonde thermometer was about 1°C .

In an analysis based on the foregoing accuracies, the accuracy in the measurement of Mach number was estimated, in reference 15, to be about $0.06M$ at $M = 1.0$ and altitudes between 50 000 and 80 000 ft. The corresponding error in $\Delta p/q_c$ at $M = 1.0$ is about 8 percent.

Total-Temperature Method

With the total-temperature method (ref. 24), the position error Δp is derived from $\Delta M = M' - M$, where M' is determined from q'_c and p' and M is calculated from equation (3.28) with $\gamma = 1.4$, here expressed as

$$M = \sqrt{\frac{1}{0.2K} \left(\frac{T'}{T} - 1 \right)} \quad (9.26)$$

where T is the free-air temperature, T' the measured (or total) temperature, and K the recovery factor of the temperature probe. As noted in chapter III,

equation (3.28) is valid only when $K = 1$ or when the probe is located in a region where the local velocity V_l is equal to the free-stream velocity V . Since V_l in the regions near the aircraft where a probe might be located is usually different from V , the application of this method requires, essentially, that the recovery factor of the probe be 1.

The calibration tests are conducted by flying the aircraft in a series of speed runs during which the height of the aircraft is measured with ground-tracking equipment and T' , q_c' , and p' are measured with recording instruments. The value of T at the height of the test run is derived from a temperature-height survey which is made prior to the calibration tests by tracking a radiosonde (transmitting temperature measurements) through the test altitude range.

As in the case of the sonic-speed method, the values of ΔM derived from M' and M can be converted to values of $\Delta p/p$ or $\Delta p/q_c$ by use of equations (5.4) through (5.7).

The accuracy of the calibration method depends, for the most part, on the accuracies in the measurement of T' and T .

In one series of calibration tests using the total-temperature method (ref. 24), the overall accuracy in the measurement of T (including accuracies of radiosonde thermometer and ground-tracking equipment) was estimated to be $\pm 2.5^\circ \text{F}$. The accuracy of the measurement of T' by the recording thermometer was about $\pm 1^\circ \text{F}$. For these two accuracies in the temperature measurements, the accuracy of the value of M was estimated to be about $\pm 0.02M$.

In a later series of tests (ref. 10), the accuracy of the determination of M was found to range from $\pm 0.01M$ at $M = 1.5$ (30 000 ft) to $\pm 0.04M$ at $M = 3.0$ (60 000 to 70 000 ft). The corresponding errors in terms of $\Delta p/q_c$ are ± 0.5 percent and ± 2.0 percent.

Calibrations by Ground-Camera and Tracking-Radar Methods

In this section, a series of tests designed to determine the accuracies that can be realized with the ground-camera and tracking-radar methods is described. These two methods were selected for accuracy tests (ref. 13) because (1) the ground-camera method like the tower method provides accurate determinations of the free-stream static pressure at heights near the ground, while at the same time allowing greater flexibility in the choice of test heights and locations, and (2) the tracking-radar method, using the aircraft tracking procedure for measuring static pressure in the pressure-height survey, provides the most direct means of deriving precise measures of free-stream static pressure at high altitudes.

The tests of the two calibration methods were conducted using a large turbojet transport as the test vehicle. The calibration tests with the ground-camera method were conducted at heights of about 500 ft and those with the tracking-radar method at altitudes of about 25 000 ft.

Test instrumentation.- The pressure-measuring instruments used for both calibration methods consisted of an airspeed-altitude recorder and a recording statoscope (fig. 9.7). The airspeed-altitude recorder was connected to the service pitot-static installation of the airplane and the recording statoscope to the static-pressure source (fuselage vents) of that installation.

The recording statoscope is a sensitive differential-pressure instrument which, for these tests, measured the difference between the pressures from the fuselage-vent system and a constant reference pressure in a thermostatically controlled chamber. Since the reference pressure in the chamber could be fixed at any selected height, the difference between the static pressure at that height and the static pressure at other heights could be measured more precisely with the statoscope than with the recording altimeter.

The pressures measured by both the recording statoscope and the airspeed-altitude recorder were recorded as traces along a moving photographic film. Each of the recorders was equipped with an event-marking device for synchronizing the measured pressures with the heights of the airplane measured with the ground camera or tracking radar.

The instrumentation for the ground-camera method consisted of a 5 by 5 in. single-exposure camera having a 7-in. focal length, a mercury-in-glass thermometer, a precision altimeter, and a radio transmitter (fig. 9.8). The camera was mounted with its optical axis aligned with the vertical and was equipped with a sighting device to aid in photographing the airplane when it was directly overhead. By transmitting a radio signal the instant he actuated the camera, the photographer synchronized the records of the instruments in the airplane with the photograph of the airplane. At the time of each test run, the atmospheric pressure and temperature at the camera station were measured with the altimeter and the thermometer.

The precision-tracking radar was used for the ground-radar method (fig. 9.9). This radar provided measurements of elevation angle and slant range from which the geometric height of the airplane could be computed. The elevation angle and slant range were recorded on a magnetic tape which was synchronized with the records of the airborne instruments by radio signals.

Ground-camera tests.- With the airplane at rest on the ground prior to the test runs, the statoscope chamber was sealed and the pressure in the chamber recorded. The airplane was then flown over the camera at an altitude of about 500 ft at a succession of test airspeeds. When the airplane returned to the ground, the pressure in the statoscope was recorded again to measure any difference from the initial recording.

The pressure recorded by the statoscope when the airplane is above the camera is the sum of (1) the difference between the static pressure at the ground level where the statoscope was sealed and the static pressure at the flight level of the airplane and (2) the position error of the static-pressure installation.

As shown in figure 9.10, the flight level Z of the airplane is determined from the elevation E_C of the camera station, the height h_C of the camera lens above E_C , and the height h of the airplane above the camera lens, measured at the level of the wing tips. For airplanes with wings that flex upward in flight, the value of h is adjusted by an amount Δh to account for the deflection of the wing tips. The height h is calculated from

$$h = \frac{bf}{b'} \quad (9.27)$$

where b is the wing span of the airplane, b' the span of the airplane image on the photographic film, and f the focal length of the camera lens.

Since the reference height at which the statoscope is sealed is Z_r , the difference between this height and the flight level is $Z - Z_r = \Delta Z$. The decrease in the static pressure δp_C through this height increment is computed from equation (3.3) expressed here as

$$\delta p_C = -\bar{\rho}_m \Delta Z \quad (9.28)$$

where $\bar{\rho}_m$ is the density at the midpoint between Z_r and Z . The density at the midpoint is computed from the following equation:

$$\bar{\rho}_m = \bar{\rho} - (\bar{\rho}_s - \bar{\rho}_{s,m}) \quad (9.29)$$

where $\bar{\rho}$ is the density at the camera (determined from measurements of p and T at that elevation), $\bar{\rho}_s$ is the standard density at the camera elevation, and $\bar{\rho}_{s,m}$ is the standard density at the midpoint.

The position error Δp of the aircraft installation is then determined from

$$\Delta p = \delta p - \delta p_C \quad (9.30)$$

where δp is the pressure increment measured by the statoscope and δp_C is the pressure increment computed from equation (9.28).

A sample calculation of the determination of Δp by the ground-camera method is given in part I of appendix B.

In the tests to determine the accuracy of the ground-camera method, four test runs were made at each of four airspeeds (150, 200, 260, and 320 knots) during one flight and at two airspeeds during a second flight. Since the weight of the airplane varied by as much as 15 percent during a flight, the weight for each test run was computed (from indications of the fuel consumed) so that the static-pressure errors at each test speed could be compared directly on the basis of lift coefficient.

The results of the tests are presented in figure 9.11 in terms of the variation of the position error of the aircraft installation with lift coefficient. The standard deviation σ of these data, determined from measurements of the displacement of the data points from the faired curve, is about 0.3 lb/ft^2 , which corresponds to an altitude error of about 4 ft at sea level. For this value of σ , the maximum probable error (defined as 3 times the standard deviation and having a probability of 99.7 percent) is about 1 lb/ft^2 , or about 12 ft at sea level. The corresponding error (1σ) in terms of $\Delta p/q_c$ is ± 0.2 percent at 200 knots ($M = 0.3$) and ± 0.1 percent at 320 knots ($M = 0.5$).

The confidence with which the mean value of the data was determined is given by the following equation for a confidence level CL of 99 percent:

$$CL_{99} = 5.84 \frac{\sigma}{\sqrt{n - 1}} \quad (9.31)$$

where n is the number of measurements for a given test condition. For the value of σ of 4 ft and for four measurements at each of the test airspeeds, the confidence level of the data is 10 ft. Thus, for a given position error in terms of an altitude error, the accuracy of the value of the altitude error, for a confidence level of 99 percent, is ± 10 ft.

Tracking-radar tests.— For the pressure-height survey required of the tracking-radar method, the airplane was flown in a series of level-flight runs at each of three altitudes (24 000, 25 000, and 26 000 ft) through an area about 10 miles in diameter. For each survey run, the geometric height of the airplane was measured by the radar. Prior to the first survey run, the statoscope was sealed at an altitude of 24 000 ft with the airplane at an indicated airspeed 200 knots. With the airplane remaining at 200 knots, survey runs were then made at six locations at each of the three test altitudes. For each survey run, the value of the pressure measured by the statoscope was corrected for the position error at the 200-knot speed determined by the ground-camera tests. These corrected pressures thus provided a measure of free-stream static pressure at each measured geometric height.

After the initial pressure-height survey, four calibration test runs were made at each of three airspeeds (235, 320, and 370 knots) at an altitude of about 25 000 ft. Immediately after the last test run, a second pressure-height survey was made at the same airspeed and altitudes as in the initial survey.

Figure 9.12 is a plot of the initial pressure-height survey and of the second survey 72 min later. For each calibration test run, the free-stream static pressure was determined from the geometric height of the airplane, the time of the run after the initial survey, and an interpolation of the two surveys for the pressure at that time. Note that the pressure and height scales the figure are broken to provide expanded scales for the two measurements. For the evaluation of the data of the tests, the surveys were plotted on a much larger chart to form continuous curves throughout the height range.

The results of the high-altitude calibration tests are presented in figure 9.13 in terms of the variation of the position error of the aircraft installation with lift coefficient. For these data, the standard deviation is about 0.34 lb/ft^2 with a corresponding altitude error of about 10 ft at an altitude of 25 000 ft. The maximum probable error, therefore, is about 1 lb/ft^2 or about 30 ft at 25 000 ft. The corresponding error (1 σ) in terms of $\Delta p/q_c$ is ± 0.2 percent at 235 knots ($M = 0.5$) and ± 0.1 percent at 370 knots ($M = 0.88$). The confidence level of the mean of the data (for $CL = 99$ percent) is ± 34 ft.

The variation of the static-pressure errors of figures 9.11 and 9.13 as a function of M rather than C_L was shown previously in figure 7.22.

Since the flight manual for the test airplane gives the position errors of the fuselage-vent system in terms of altitude errors, the position errors in figures 9.11 and 9.13 have been converted to altitude errors and plotted in figure 9.14. For sea-level calibrations, the flight-manual values and the calibration with the ground-camera method are essentially the same. At an altitude of 25 000 ft, the flight-manual values and the tracking-radar calibration differ by less than 50 ft for airspeeds up to 350 knots.

In the description of the tracking-radar method given in this chapter, some details relating to the experimental procedure and the test data evaluation have been omitted. For a complete discussion of the application of this method, the reader is referred to reference 13.

References

1. Thompson, F. L.: The Measurement of Air Speed of Airplanes. NACA TN 616, 1937.
2. Smith, K. W.: The Measurement of Position Error at High Speeds and Altitude by Means of a Trailing Static Head. C.P. No. 160, British A.R.C., 1954.
3. Phillips, William H.: Theoretical Analysis of Oscillations of a Towed Cable. NACA TN 1796, 1949.
4. Gracey, William; and Scheithauer, Elwood F.: Flight Investigation of the Variation of Static-Pressure Error of a Static-Pressure Tube With Distance Ahead of a Wing and a Fuselage. NACA TN 2311, 1951.
5. Ikhtari, Paul A.; and Marth, Verlyn G.: Trailing Cone Static Pressure Measurement Device. J. Aircraft, vol. 1, no. 2, Mar.-Apr. 1964, pp. 93-94.
6. Jordan, Frank L., Jr.; and Ritchie, Virgil S.: Subsonic Wind-Tunnel Tests of a Trailing-Cone Device for Calibrating Aircraft Static-Pressure Systems. NASA TN D-7217, 1973.
7. Brumby, Ralph E.: The Influence of Aerodynamic Cleanness of Aircraft Static Port Installations on Static Position Error Repeatability. Rep. No. DAC-67485, Douglas Aircraft Co., Nov. 1968.
8. Trailing Cone Method of Measuring Static Source Position Error (F-4B Airplanes); Second Interim Report. Rep. No. FT2122-27R-65, Naval Air Test Center, Apr. 26, 1965. (Available from DTIC as AD 462 821.)
9. Levon, K. C.: Pressure Error Measurement Using the Formation Method. C.P. No. 126, British A.R.C., 1953.
10. Webb, Lannie D.; and Washington, Harold P.: Flight Calibration of Compensated and Uncompensated Pitot-Static Airspeed Probes and Application of the Probes to Supersonic Cruise Vehicles. NASA TN D-6827, 1972.
11. Thompson, F. L.; and Zalovcik, John A.: Airspeed Measurements in Flight at High Speeds. NACA ARR, 1942.
12. Fuhrman, R. A.; Wheatley, J. P.; Lytle, W. J.; and Doyle, G. B.: Preliminary Report on Airspeed-Altimeter System Calibration at High Mach Numbers. Phase A - The Altimeter Depression Method Using a Base Airplane at Altitude. Test Pilot Training Div., U.S. Naval Air Test Center, Mar. 3, 1952.
13. Gracey, William; and Stickle, Joseph W.: Calibrations of Aircraft Static-Pressure Systems by Ground-Camera and Ground-Radar Methods. NASA TN D-2012, 1963.

14. Zalovcik, John A.: A Radar Method of Calibrating Airspeed Installations on Airplanes in Maneuvers at High Altitudes and at Transonic and Supersonic Speeds. NACA Rep. 985, 1950. (Supersedes NACA TN 1979.)
15. Larson, Terry J.; and Webb, Lannie D.: Calibrations and Comparisons of Pressure-Type Airspeed-Altitude Systems of the X-15 Airplane From Subsonic to High Supersonic Speeds. NASA TN D-1724, 1963.
16. Smith, Eugene S.: Askania Cine-Theodolite Data Reduction Manual. AFMTC-TR-60-1, U.S. Air Force, Jan. 1960.
17. Thompson, Jim Rogers; and Kurbjun, Max C.: Evaluation of the Accuracy of an Aircraft Radio Altimeter for Use in a Method of Airspeed Calibration. NACA TN 3186, 1954.
18. Hesse, W. J.: Position Error Determination by Stadiametric Ranging With a 35 mm Movie Camera. Tech. Rep. No. 2-55, Test Pilot Training Div., U.S. Naval Air Test Center, June 24, 1955.
19. Schoenfeld, L. I.; and Harding, G. A.: Report on the Dual Sighting Stand and Other Methods of Calibrating Altimeter and Airspeed Installations. Rep. No. NAES-INSTR-16-44 (Project No. TED NAM 3335), NAES, Philadelphia Navy Yard, Eur. Aeronaut., Aug. 15, 1944.
20. Zalovcik, John A.; Lina, Lindsay J.; and Trant, James P., Jr.: A Method of Calibrating Airspeed Installations on Airplanes at Transonic and Supersonic Speeds by the Use of Accelerometer and Attitude-Angle Measurements. NACA Rep. 1145, 1953. (Supersedes NACA TN 2099 by Zalovcik and NACA TN 2570 by Lina and Trant.)
21. Zalovcik, John A.: A Method of Calibrating Airspeed Installations on Airplanes at Transonic and Supersonic Speeds by Use of Temperature Measurements. NACA TN 2046, 1950.
22. Fisher, Bruce D.; Holmes, Bruce J.; and Stough, H. Paul, III: A Flight Evaluation of Trailing Anemometer for Low-Speed Calibrations of Airspeed Systems on Research Aircraft. NASA TP-1135, 1978.
23. Thompson, F. L.: Procedure for Determining Speed and Climbing Performance of Airships. NACA TN 564, 1936.
24. Brunn, Cyril D.; and Stillwell, Wendell H.: Mach Number Measurements and Calibrations During Flight at High Speeds and at High Altitudes Including Data for the D-558-II Research Airplane. NACA RM H55J18, 1956.

TABLE 9.1.- FLIGHT CALIBRATION METHODS FOR DETERMINING

Calibration method	Operational limits			Method accuracy or precision ^a (approximate 1G values)	
	Test altitude range	Speed restrictions		Accuracy, percent q_c	Precision, percent q_c
		Minimum	Maximum		
Trailing bomb	Low/high	Stall speed	$C_M = 0.4$ to 0.85	± 2.0 (M = 0.1) ± 0.2 (M = 0.35)	
Trailing cone	Low/high	Min. LFS ³	$M = 1.5$		± 0.2 (M = 0.7 to 0.88)
Pacer and aft	Low/high	Min. LFS	Max. LFS		± 0.7 (M = 0.5) ± 0.2 (M = 1.0)
Tower	Very low	Min. LFS	Max. LFS	± 1.0 (M = 0.15) ± 0.2 (M = 0.30)	
Tracking radar	High	Min. LFS	Max. dive speed	± 0.2 (M = 0.5) ± 0.1 (M = 0.88)	
Radar altimeter	High	Min. LFS	Max. LFS	± 1.0 (M = 0.8)	
Ground camera	Very low	Min. LFS	Max. LFS	± 0.2 (M = 0.3) ± 0.1 (M = 0.5)	
Tracking-radar/ pressure- altimeter	High	Min. LFS	Max. LFS	± 3.5 (M = 0.5) ± 0.1 (M = 3.0)	
Accelerometer	High	Min. LFS	Max. dive speed ⁹	± 0.5 (M = 0.6 to 0.8)	
Recording thermometer	High	Min. LFS	Max. dive speed	± 4.5 (M = 0.8)	
Trailing anemometer	Low	Stall speed	$M = 0.2$	± 2.5 (M = 0.08) ± 1.0 (M = 0.16)	
Speed course	Low	Min. LFS	$M = 0.2$		
Sonic speed	High	Min. LFS	Max. LFS	± 8.0 (M = 1.0)	
Total temperature	High	Min. LFS	Max. dive speed	± 0.5 (M = 1.5) ± 2.0 (M = 3.0)	

See page 148 for footnotes.

POSITION ERROR OF STATIC-PRESSURE INSTALLATION

Calibration method requirements						Refs.
Initial reference pressure, p , obtained from -	Survey of atmosphere	Measurements		Instruments (b)		
		Aircraft	Ground	Aircraft	Ground	
---	---	q_c', p', p	---	ASI, Alt, DPI	---	1,2,3,4
---	---	q_c', p', p	---	ASI, Alt, DPI	---	5,6,7,8
---	---	q_c', p'	---	ASI, Alt	---	9,10
---	Pressure-height	q_c', p'	$Z_c, \Delta Z$	ASI, Alt	Camera in tower	11
Low-speed calibration ^f	Pressure-height	q_c', p'	Z	IPR, APR	Tracking radar	13
Low-speed calibration	Pressure-height	q_c', p', Z	---	ASI, Alt, Radar alt.	---	17
---	---	q_c', p'	p, T, Z	ASI, Alt	Camera, Alt or barograph, IT	13
Low-speed calibration	---	q_c', p', T'	Z	Alt, IPR, APR, RT	Tracking radar	10
Low-speed calibration	---	$q_c', p', T', a_x, a_z, \theta$	---	IPR, APR, RT, RA, AAR	---	20
Low-speed calibration	Pressure-temperature	q_c', p', T'	---	IPR, APR, RT	---	21
---	---	q_c', p', T', V	---	IPR, APR, RT, Trailing anemometer	---	22
---	---	q_c', p', T'	$^i v_q, T$	ASI, Alt, IT	Stop watch	23
---	Temperature-height, Wind speed	q_c', p'	V_q, Z	IPR, APR	Tracking radar, Rawinsonde	15
---	Temperature-height	q_c', p', T'	Z	IPR, APR, RT	Tracking radar, Radiosonde	10,24

FOOTNOTES FOR TABLE 9.1

^aValues quoted have been achieved. With different instrumentation and experimental techniques, the accuracy or precision obtained may vary from these values.

^bThe following abbreviations are used in this column:

AAR	attitude-angle recorder
Alt	altimeter
APR	absolute-pressure recorder
ASI	airspeed indicator
DPI	differential-pressure instrument
IPR	impact-pressure recorder
IT	indicating thermometer
RA	recording accelerometer
RT	recording thermometer

^cMaximum speed at which bomb can be trailed without unstable oscillations in suspension cable.

^dLFS level flight speed

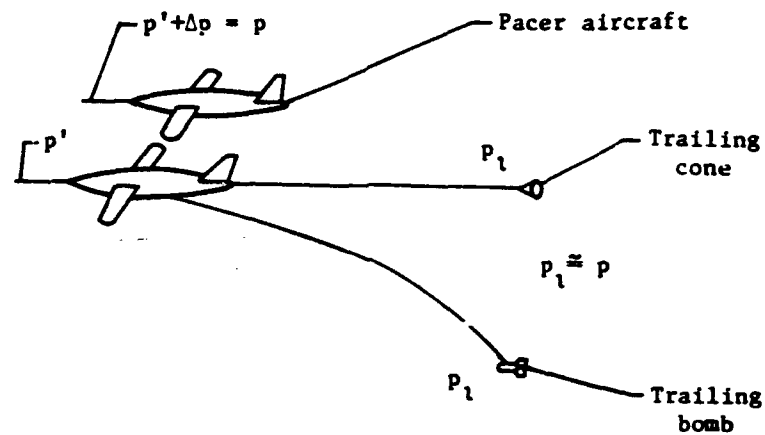
^e $M = 1.5$ is the highest speed at which tests have been conducted (ref. 8).

^fLow-speed calibration is necessary if radiosonde is not used to make pressure-height survey.

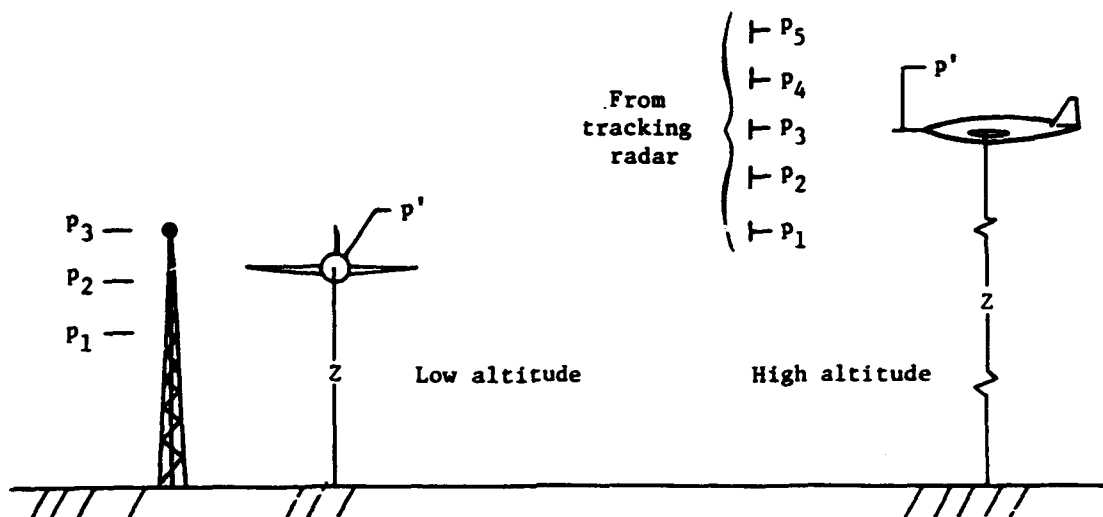
^gManeuvers must be conducted in vertical plane.

^h $M = 2.0$ limitation determined by a requirement that $q_c \approx q$.

ⁱ v_g ground speed of aircraft

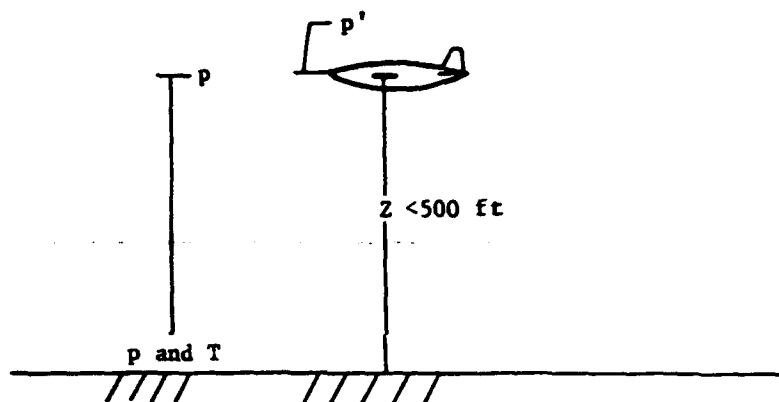


(a) p measured at reference pressure source below, behind, or alongside aircraft.

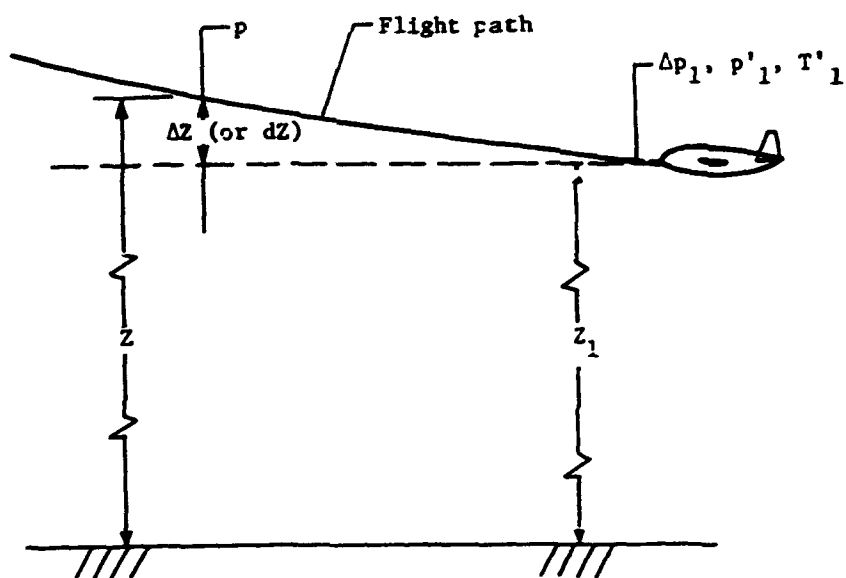


(b) p derived from measurement of height of aircraft and pressure gradient at test altitude range.

Figure 9.1.- Four techniques for determining free-stream static pressure p at flight level of aircraft.

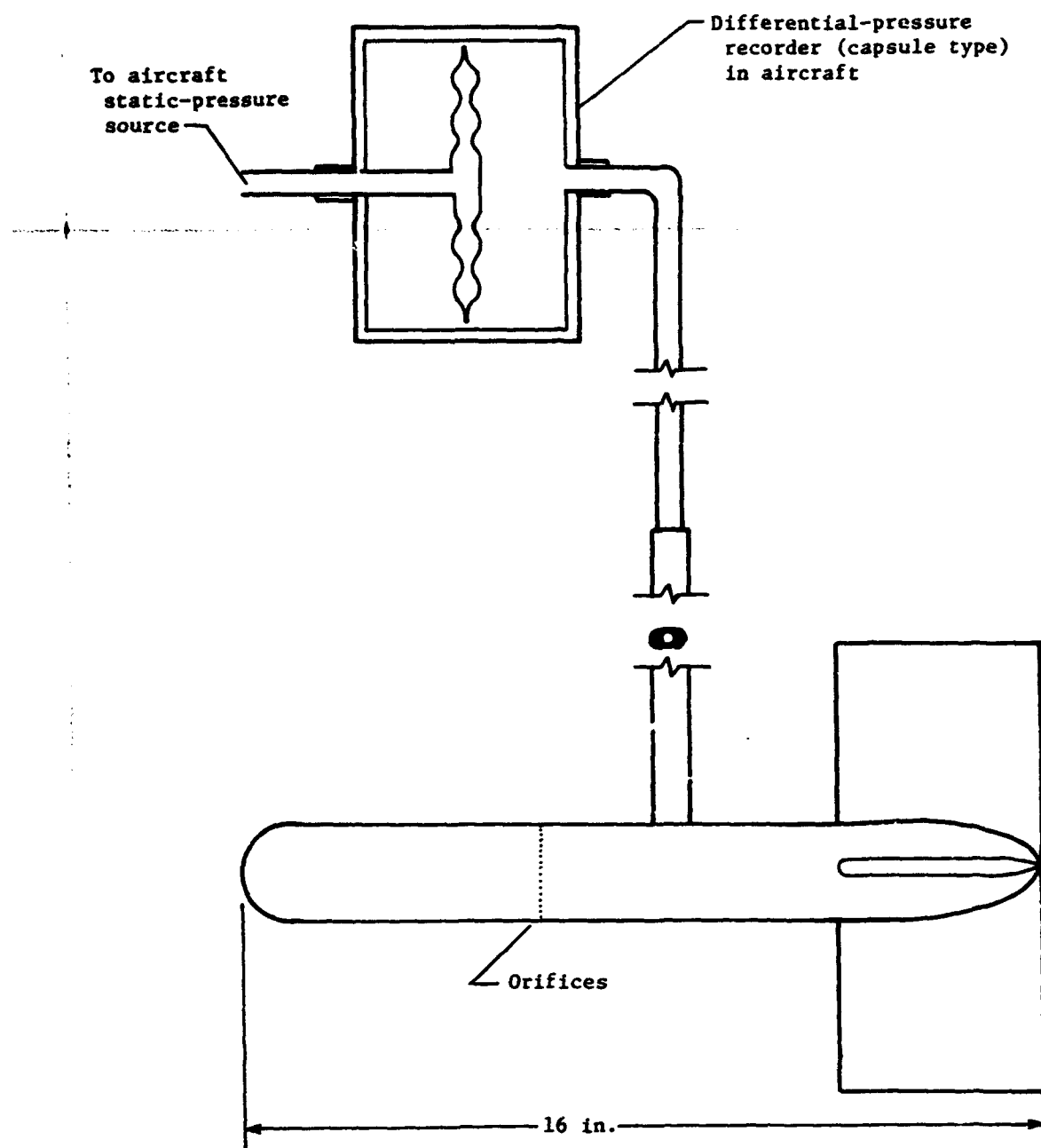


(c) p at height of aircraft calculated from p and T at ground and assumption of standard temperature gradient.



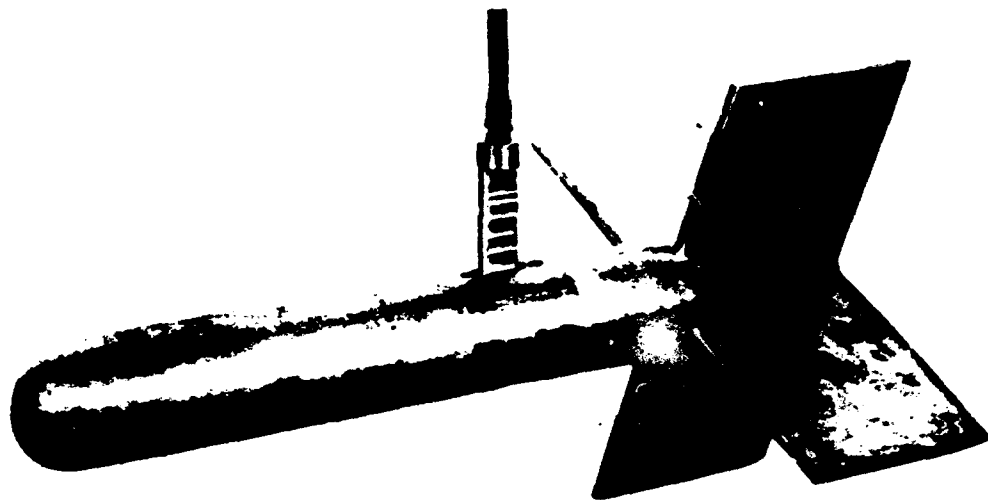
(d) p at height of aircraft derived from change in height from an initial height.

Figure 9.1.- Concluded.



(a) Diagram.

Figure 9.2.- Trailing bomb. Weight = 15 lb. (Adapted from ref. 1.)



L-79-357

(b) Photograph.

Figure 9.2.- Concluded.

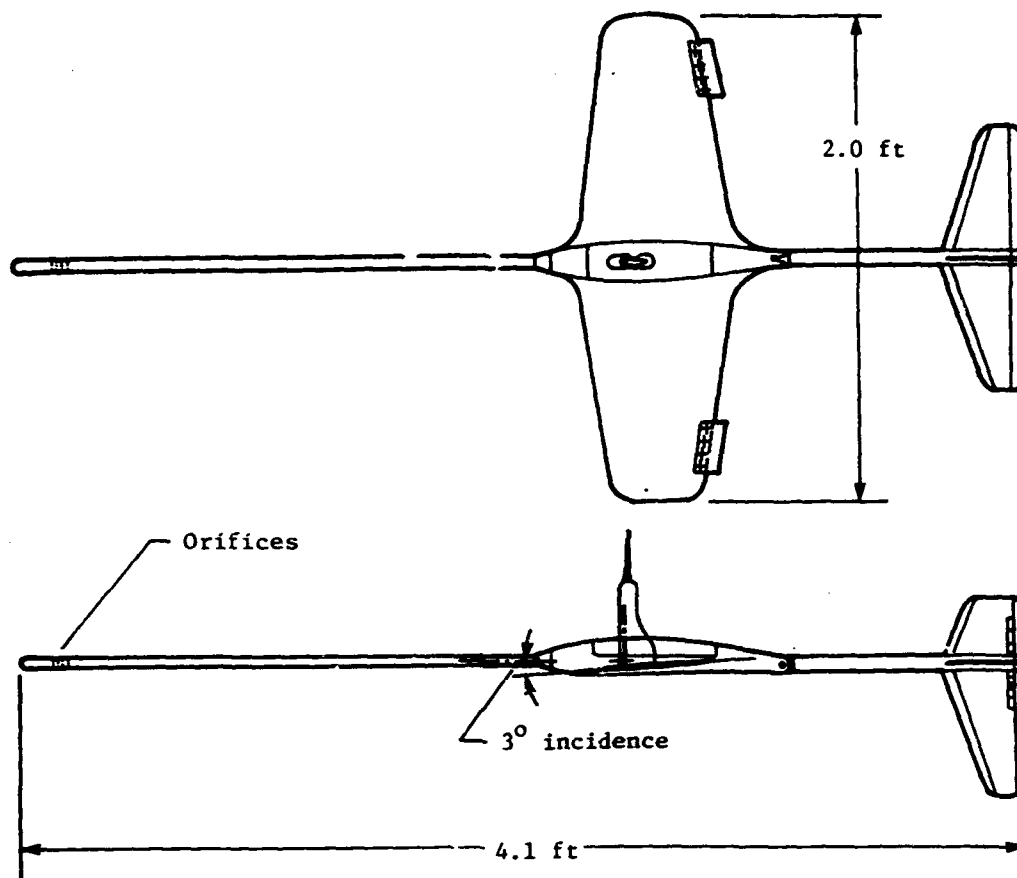


Figure 9.3.- Trailing bomb with wings at negative angle of incidence. (Adapted from ref. 2.)

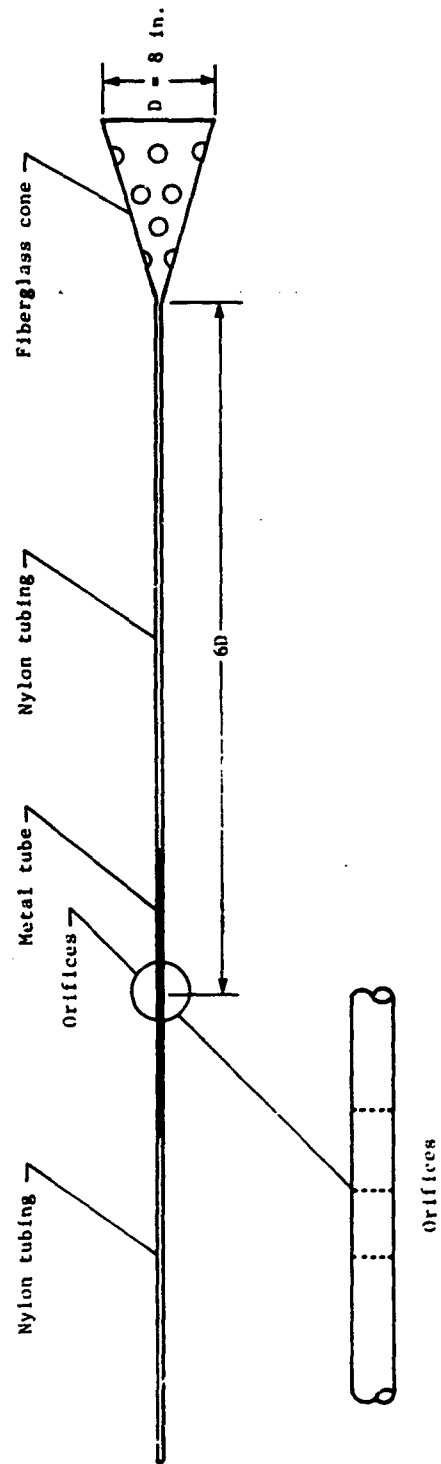
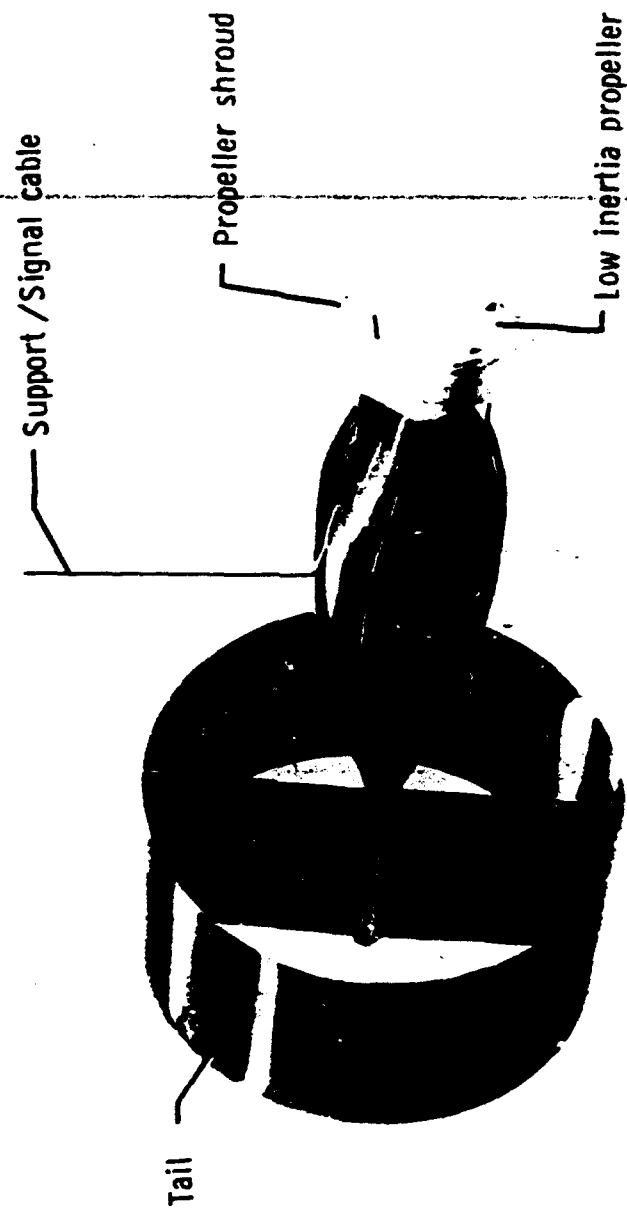


Figure 9.4.- Trailing static-pressure cone system.



L-77-398

Figure 9.5.- Trailing anemometer.

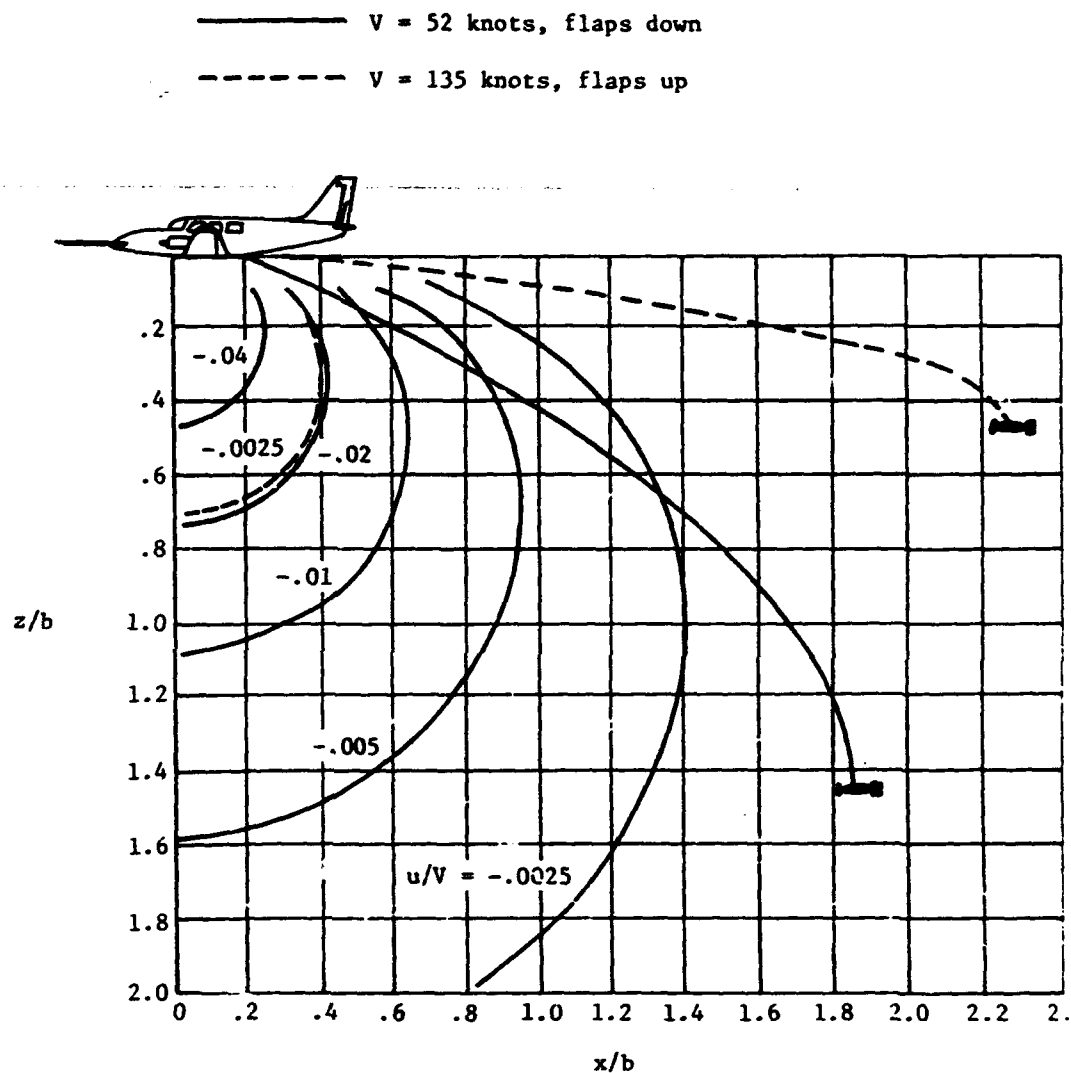
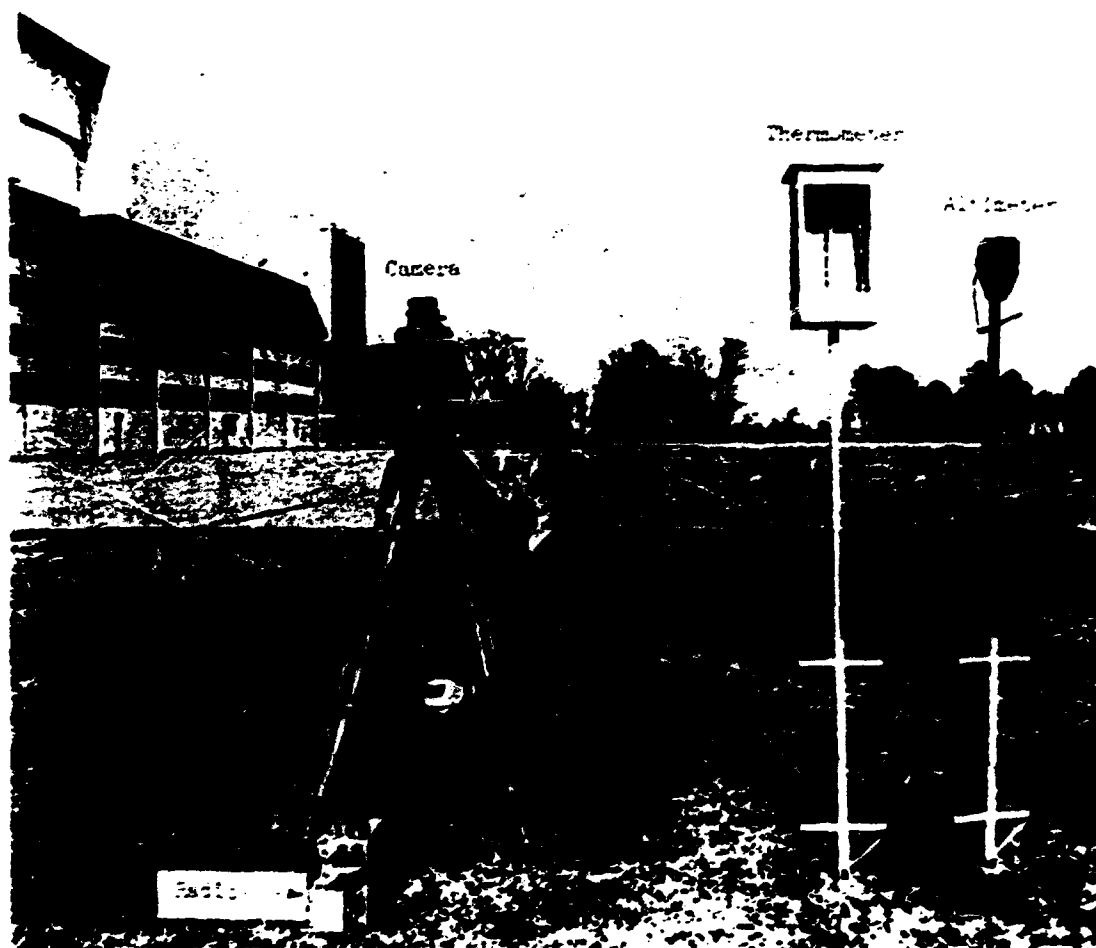


Figure 9.6.- Anemometer trail positions for two flight conditions superimposed on induced velocity field below airplane. z is vertical distance, x is horizontal distance, and b is wing span. (Adapted from ref. 22.)



1-63-509.1

Figure 9.7.- Instruments installed in airplane for calibrations of the aircraft static-pressure installation. (Adapted from ref. 13.)



L-62-1489.1

Figure 9.8.- Ground-based equipment used for calibrations at low altitudes. (Adapted from ref. 13.)

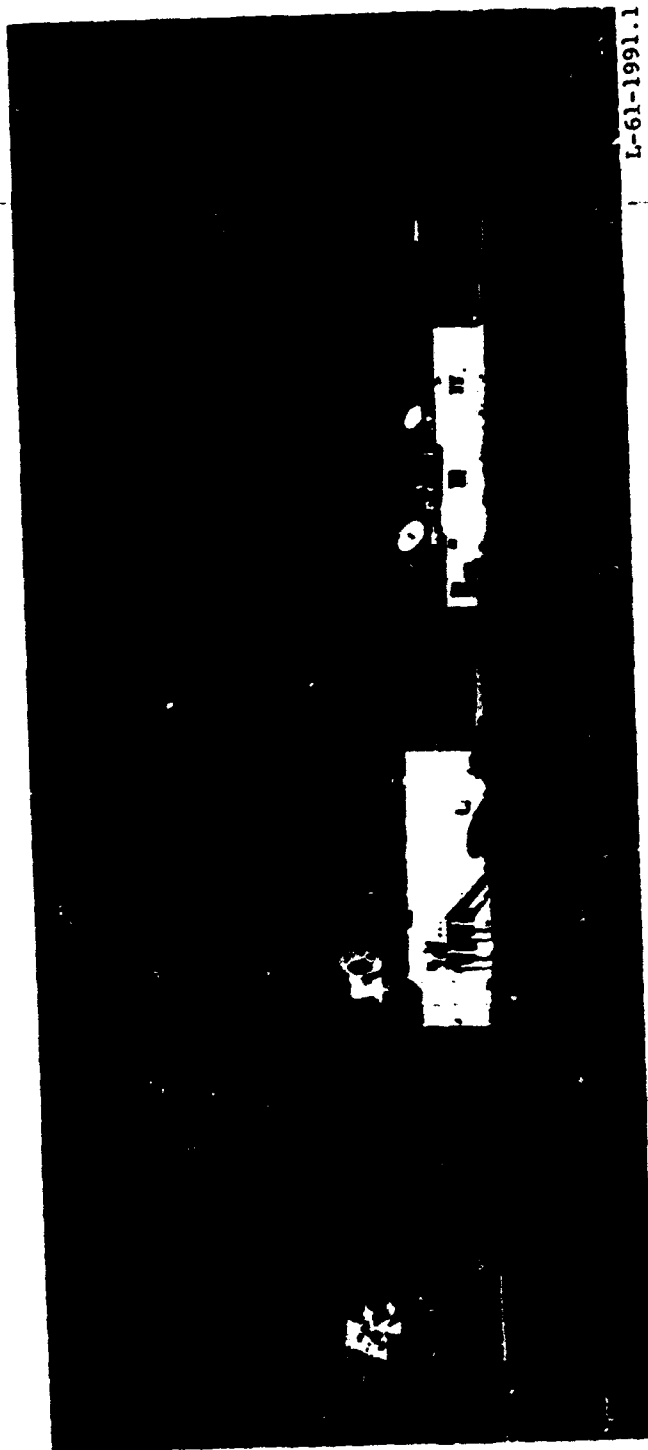


Figure 9.9.- Tracking radar used for calibrations at high altitudes. (Adapted from ref. 13.)

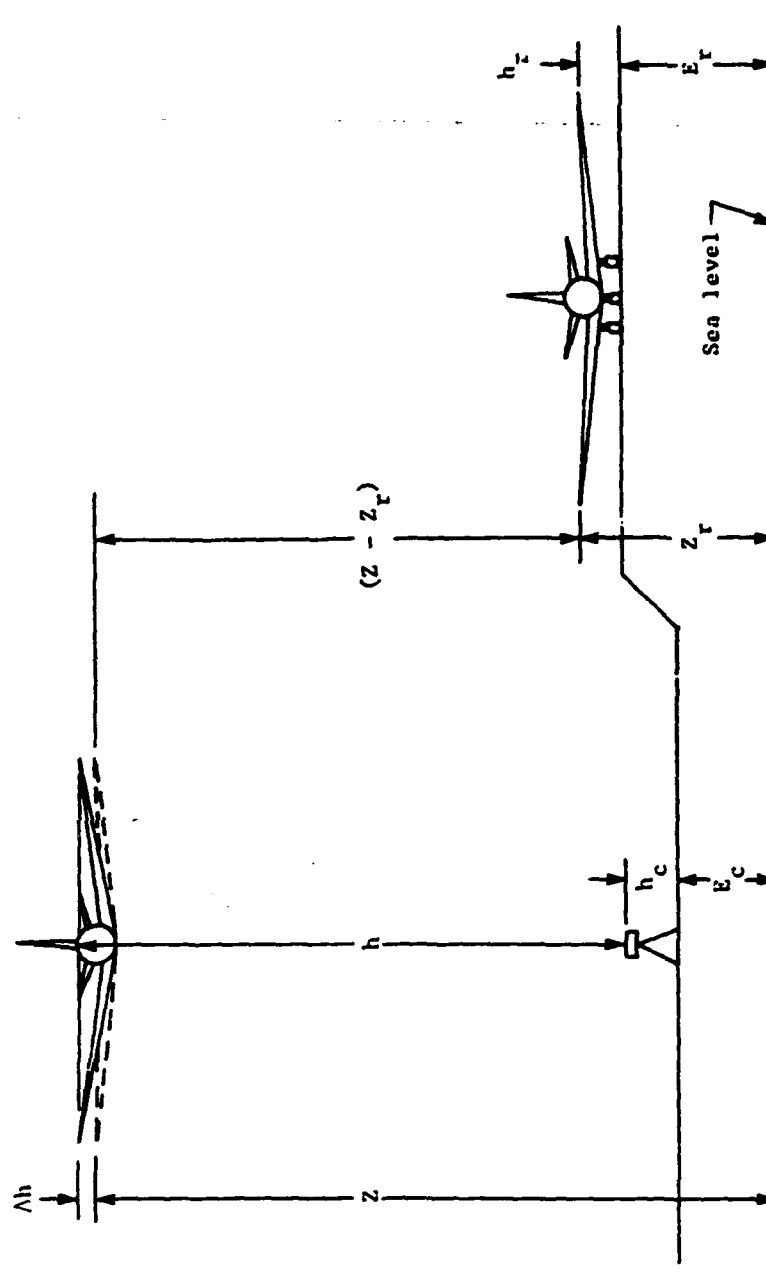


Figure 9.10.- Diagram showing dimensions required for determining flight level of airplane with ground-camera method. (Adapted from ref. 13.)

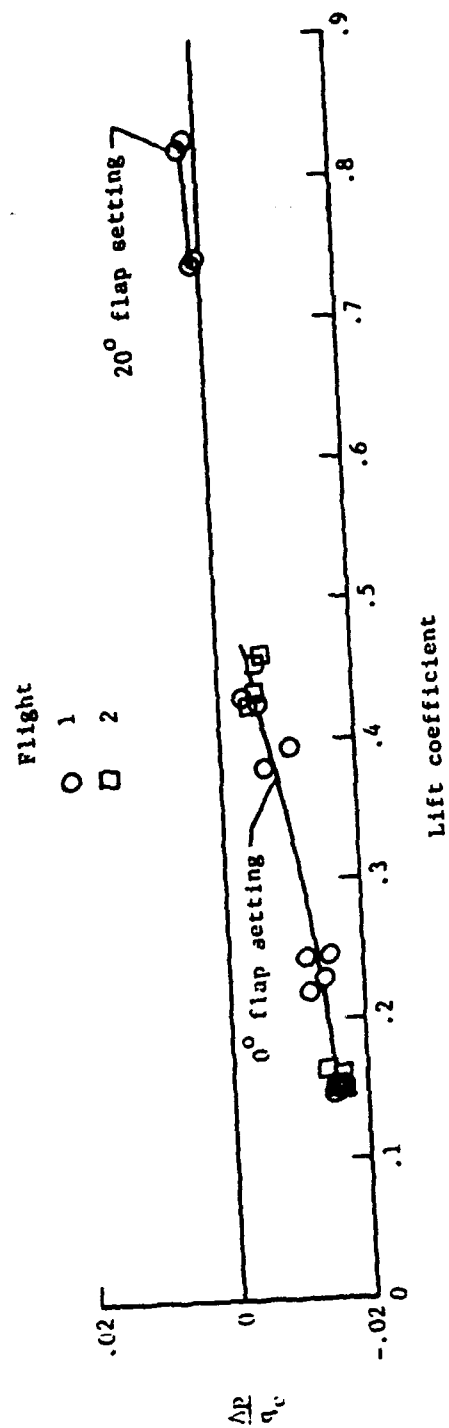


Figure 9.11.- Calibration of fuselage-vent system at an altitude of 500 ft.
(Adapted from ref. 13.)

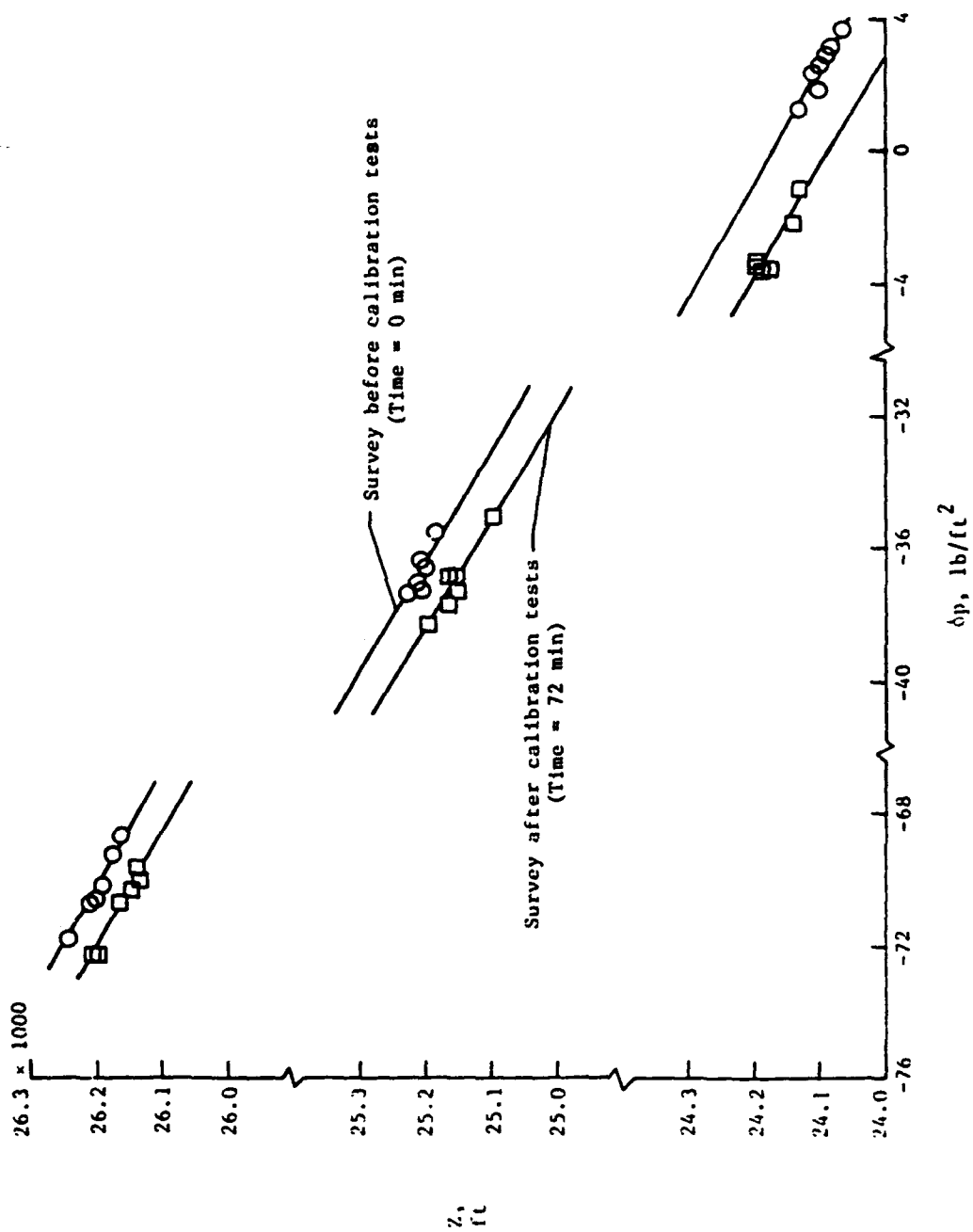


Figure 9.12.- Pressure-height survey at altitudes from 24 000 to 26 000 ft.
(Adapted from ref. 13.)

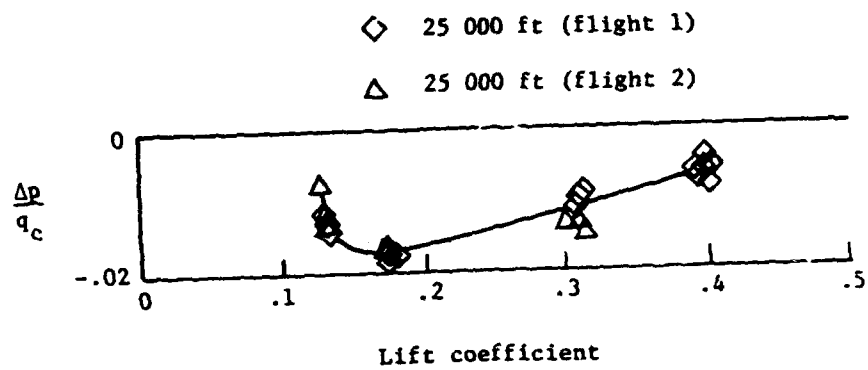


Figure 9.13.- Calibration of fuselage-vent system at an altitude of 25 000 ft. (Adapted from ref. 13.)

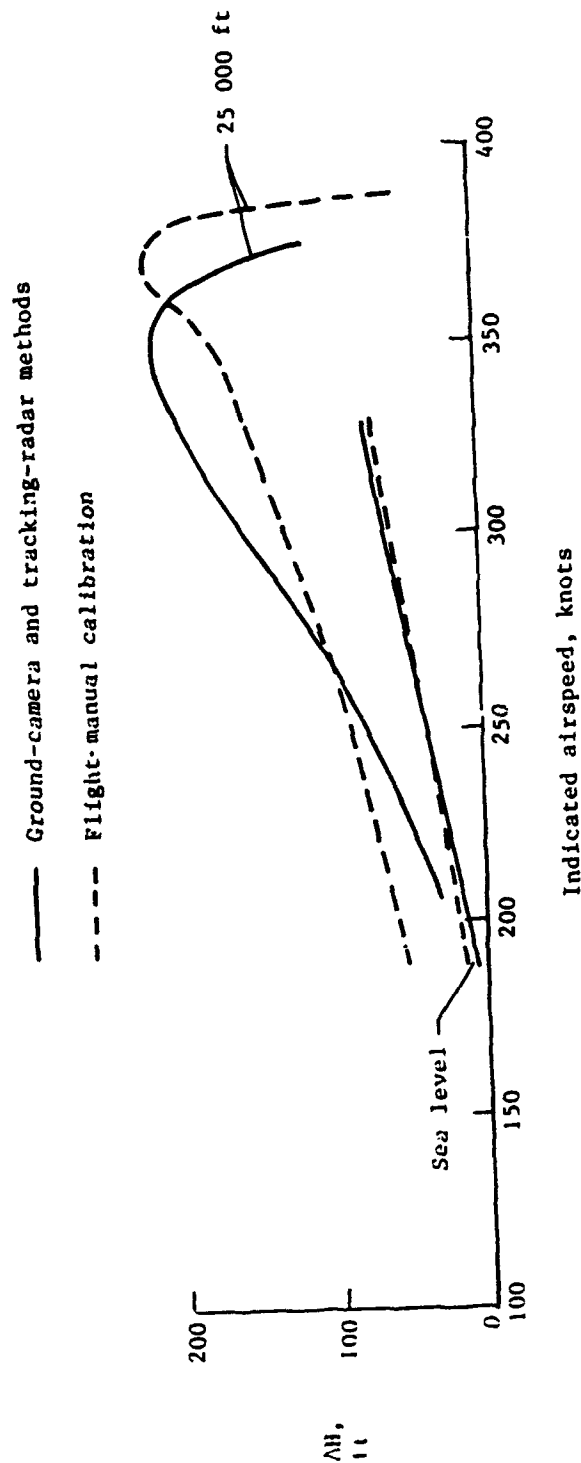


Figure 9.14.- Comparison of flight-manual calibration with calibrations determined by ground-camera and tracking-radar methods. (Adapted from ref. 13.)

CHAPTER X

ERRORS DUE TO PRESSURE-SYSTEM LAG AND LEAKS

As noted in chapter II, the pressure at an instrument can be different from the pressure at the pressure source because of a time lag in the transmission of pressures. The pressure at the instrument can also differ from that at the pressure source when there is a leak in the pressure system. For both cases, the instrument indications will be in error by an amount corresponding to the pressure drop in the system. In this chapter, analytical and experimental methods for determining the errors due to pressure-system lag and leaks are discussed. Sample calculations of an estimation of the lag and leak errors of a given pressure system are given in part II of appendix B.

System Lag

When the pressure at the pressure source is changing rapidly, as in the case of high-speed dives or climbs, air flows into, or out of, the pressure source (pitot tube, static-pressure tube, or fuselage vents). Under these conditions, the pressure at the instruments lags behind the pressure at the source because of (1) the time for the pressure change to propagate along the tubing (acoustic lag) and (2) the pressure drop associated with the flow through the tubing (pressure lag). In the following sections, mathematical expressions for both forms of lag are described.

Acoustic lag.- As noted in reference 1, the speed of the pressure propagation along the pressure tubing is the speed of sound. The magnitude of the acoustic lag thus depends only on the speed of sound a and the length of the tubing L as expressed in the following equation:

$$\tau = L/a \quad (10.1)$$

where τ is the acoustic lag time. Since the speed of sound at the lower altitudes is on the order of 1000 ft/sec, errors due to acoustic lag are of concern only for pressure systems having very long lengths of pressure tubing. For the tubing lengths of the instrument systems in service aircraft, errors associated with acoustic lag are of no significance.

Pressure lag.- When air in tubing between a pressure source and an instrument is flowing, the pressure at the instrument is different from the pressure at the source, and the indication of the instrument is in error by an amount equivalent to the pressure drop between the two ends of the tubing. For a rate of pressure change dp/dt at the pressure source, the pressure drop Δp and the lag of the pressure system are related by the following equation:

$$\Delta p = L \frac{dp}{dt} \quad (10.2)$$

where λ is the lag constant of the system defined by the following equation from reference 2:

$$\lambda = \frac{128\mu LC}{\pi d^4 p} \quad (10.3)$$

where L and d are the length and internal diameter of the tubing, C is the total volume of the instrument chambers, p is the pressure, and μ is the coefficient of viscosity of air. This equation assumes laminar flow in the tubing and applies rigorously only to straight tubing of constant diameter.

Once the value of λ of an instrument system is known, the errors in air-speed and altitude associated with any given rate of climb or descent of the aircraft can be determined from equation (10.2) and the appropriate pressure table in appendix A.

The condition of laminar flow required by equation (10.2) is met when the pressure drop Δp along the tubing remains lower than that given by the following equation from reference 2:

$$\Delta p = - \frac{32\mu^2 L N_{Re}}{\rho d^3} \quad (10.4)$$

where N_{Re} is the Reynolds number. Since airflow in a straight tube remains laminar for N_{Re} no greater than about 2000, the limiting pressure drop for laminar flow at sea level can be expressed as

$$\frac{\Delta p}{L} = \frac{6.5 \times 10^{-3}}{d^3} \quad (10.5)$$

where $\Delta p/L$ is in pounds per square ft per ft and d is the internal diameter of the tubing in inches. At altitude, the limiting pressure drop for laminar flow is given by

$$\frac{\Delta p}{L} = \frac{P_o(\mu_a)^2}{P_a(\mu_o)^2} \left(\frac{6.5 \times 10^{-3}}{d^3} \right) \quad (10.6)$$

where the subscripts o and a refer to sea level and altitude. In table 10. the limiting pressure drops for laminar flow at sea level and 30 000 ft are given for four tubing diameters.

For relatively simple pressure systems with few bends and tees in the tubing, the lag constant can usually be calculated with satisfactory accuracy from equation (10.2) and a knowledge of the geometry of the system. For more complex pressure systems, and especially for those research installations in which lag is an important factor, the lag constant of the system can be determined experimentally by one of the three test procedures described in refer-

ence 1. The computational procedures for correcting measured pressures for pressure-lag errors are also given in reference 1.

For pitot-static pressure systems, the lag characteristics of mechanical instrument systems differ markedly from those of systems incorporating electrical pressure transducers. With the mechanical instruments, for example, the lag of the pitot system is very much smaller than that of the static-pressure system because of the great difference in the volumes at the ends of the two pressure lines. The volume at the end of the pitot line is very small (the volume of the differential-pressure capsule), whereas the volume at the end of the static-pressure line is the combined volume of all instrument chambers connected to the line (fig. 2.3). Thus, for those instruments connected to both the pitot and static-pressure lines, the errors in the indications due to lag are determined primarily by the lag in the static-pressure system.

For the measurement of airspeed (or impact pressure) in research investigations, the lags of the pitot and static-pressure systems are sometimes "balanced" in an attempt to eliminate the airspeed error due to the difference in the lag of the two systems. This balancing of the lag of the two systems is accomplished by adding tubing to the pitot system until the lag of that system equals the lag of the static-pressure system. However, while balancing the pressure lines can often eliminate airspeed errors in rate-of-climb testing, airspeed errors in dive testing can be larger than those that were present before balancing (ref. 1).

With systems employing electrical pressure transducers (figs. 11.13 and 11.14), the lag in the pitot and static-pressure lines is essentially the same because the volumes at the ends of the two lines are very nearly equal. Since the volumes of the transducers are also very small and since the length of tubing between the transducer and the pressure source is generally short, the lag of this type system is usually so small that it is of no concern.

Means of reducing lag.- In the design of a pressure system incorporating mechanical instruments, the principal means of reducing the acoustic lag and pressure lag are related to the size of the tubing and the instrument volume. For example, the acoustic lag (eq. (10.1)) can be minimized by simply keeping the pressure tubing line reasonably short, while the pressure lag (eq. (10.2)) can be reduced by reducing tubing length, increasing tubing diameter, or reducing instrument volume. For installations requiring more than one set of instruments, the volume at the end of each pressure line can be reduced by installing a separate pressure source for each set of instruments. For a system with a given instrument volume, the lag can generally be reduced by increasing the diameter of the tubing. However, if the tubing is connected to a static-pressure tube, any increase in the tubing diameter should be related to the number and size of the orifices, because usually the total area of the orifices should be about the same as the cross-sectional area of the tubing. Finally, for any pressure system, the pressure lag can be reduced by minimizing the number of bends and connections in the tubing system. For a more extensive discussion of the influence of the various design parameters on the lag of pressure-measuring systems, the reader is referred to reference 3.

With systems employing electrical pressure transducers, both forms of errors are small because of the small volume of the pressure chambers and the short lengths of tubing ordinarily used with this type system.

System Leaks

The pressure at the instrument can be different from that at the pressure source if there is a leak in the system and if the pressure outside the system is different from that inside. A leak within the cockpit of a pressurized cabin, for example, can alter the pressure inside the instrument when the aircraft is at a high altitude. On the other hand, a leak in a part of the system in an unpressurized area might have little effect. The magnitude of the pressure error due to a leak, therefore, depends not only on the size of the leak but also on the pressure drop across the leak.

To minimize pressure errors resulting from leaks, the civil and military agencies require leak tests of individual instruments (for case leaks) and of the complete instrument system installed in the aircraft. The tests of the static-pressure system are conducted by applying suction to the static-pressure source until the pressure in the system reaches a specified pressure altitude. With the pressure held constant, the effects of any leaks appear as rates of change in airspeed and altitude indicated by the cockpit instruments. Tests of the pitot system are conducted in the same manner, except that pressure is applied to the pitot tube.

A number of different leak tolerances for the systems have been specified from time to time, by the civil and military agencies. The most stringent of these tolerances requires the leak rate for the static-pressure system to be more than 100 ft/min (indicated by the altimeter) when the system pressure corresponds to the maximum pressure altitude for which the aircraft is certified. For the pitot system, the tolerance is 1 knot/min (indicated by the airspeed indicator) when the system pressure equals the impact pressure corresponding to the maximum speed of the aircraft.

The errors in airspeed and altitude that result from a leak of a given size and a given pressure differential across the leak can be determined from (1) the leak rate (i.e., the rate of pressure change dp/dt) determined from a ground test of the system, (2) the lag constant λ computed from equation (10.3), and (3) the lag constant λ_l of the leak. The value of λ_l can be calculated from the following equation:

$$\lambda_l = \left(\frac{P_{T,o} - P_{T,a}}{dp/dt} \right) \left(\frac{P_{T,o} + P_{T,a}}{P_c + P_a} \right)$$

where

$P_{T,o}$ ambient pressure during ground test

$P_{T,a}$ test pressure in system during ground test

dp/dt rate of pressure change due to leak measured in ground test
 P_a pressure at pitot or static-pressure source at flight altitude
 P_c compartment or cabin pressure at flight altitude

The pressure error Δp_l due to the leak can then be computed from

$$\Delta p_l = p_i - p_a = \frac{\lambda}{\lambda_l + \lambda} (P_c - P_a) \quad (10.8)$$

where p_i is the pressure inside the instrument. From the value of Δp_l , the corresponding errors in airspeed and altitude can be determined from the tables in appendix A.

The errors in the instrument indications that result from a leak in the pressure system can also be determined experimentally in flight. In tests reported in reference 4, for example, a calibrated leak device, capable of introducing five different size leaks into a pressure system, was connected to the static-pressure line in the cockpit of a transport airplane. The altitude error produced by each leak was then determined at a number of altitudes and for different cabin pressures. After the flight tests, ground tests were conducted to measure the leak rate of each leak in terms of altitude change per minute. The ground and flight tests thus provided a means of directly relating the altitude error and leak rate of a given size leak. The results of these tests showed that for leaks producing altitude errors as small as 10 ft, the leak rate was much larger than the 100 ft/min rate specified for the leak tolerance discussed earlier. In other words, the altimeter errors of systems complying with this leak tolerance would be essentially negligible.

References

1. Huston, Wilber B.: Accuracy of Airspeed Measurements and Flight Calibration Procedures. NACA Rep. 919, 1948. (Supersedes NACA TN 1605.)
2. Wildhack, W. A.: Pressure Drop in Tubing in Aircraft Instrument Installations. NACA TN 593, 1937.
3. Lamb, J. P., Jr.: The Influence of Geometry Parameters Upon Lag Error in Airborne Pressure Measuring Systems. WADC Tech. Rep. 57-351, U.S. Air Force, July 1957. (Available from DTIC as AD 130 790.)
4. Wheatley, J. L.: Relation of Static System Leakage to Altitude Error. Rep. No. F 1096 A, Eng. Dep., United Air Lines, Inc., June 20, 1967.

TABLE 10.1.- LIMITING PRESSURE DROP PER FOOT FOR
LAMINAR FLOW IN TUBING

Tubing diameter, in.		Limiting $\Delta p/L$, (lb/ft ²)/ft, at -	
Outside	Inside	Sea level	30 000 ft
1/8	0.060	30.1	69.4
3/16	.114	4.4	10.0
1/4	.188	1.0	2.3
5/16	.250	.4	1.0

CHAPTER XI

AIRCRAFT INSTRUMENT ERRORS

Aircraft instruments are required to meet specified standards of accuracy. These accuracies are expressed in terms of error tolerances (allowable errors) which may be stated as a percent of the measured quantity, as a percent of the full-scale range of the instrument, or as a series of individual tolerances for given values of the measured quantities.

The specified accuracies of the instruments vary depending on the type of instrument and on the state of the art at the time the instrument was developed. The accuracy of the "precision" mechanical altimeter, for example, is greater than that of the older "sensitive" altimeter. Similarly, the accuracies of electrical instruments are greater than those of the mechanical types, and of the two electrical instrument systems, the electronic pressure-transducer system is somewhat more accurate than the servoed instrument systems.

Until recent years, mechanical instruments were used in all types of aircraft; they are still widely used in general aviation aircraft and in older civil transport and military aircraft. Servoed instrument systems, a later development, have been used for some years in turbojet transport and military jet aircraft, while electronic pressure-transducer systems, an even later development, are now being used in some turbojet transport and military jet aircraft.

The Federal Aviation Administration specifies the accuracy of instruments used in civil aircraft, while the U.S. Air Force, Army, and Navy specify the accuracy of instruments used in military aircraft. For the instruments discussed in this chapter, the accuracies have, for the most part, been extracted from instrument standards specified by the Air Force.

Mechanical Instruments

As noted in chapter II, the scale error (i.e., the difference between an instrument indication and the correct value) is generally the largest of the various instrument errors. Thus, the determination of this error is the primary concern of the laboratory testing of the instruments.

When it has been determined that the scale errors of a particular instrument conform to the specified tolerances, the instrument is considered acceptable for operational use. However, since the scale error is systematic (repeatable), many aircraft operators require that corrections for the error be applied in order to achieve an accuracy greater than the specified accuracy.

In this section, the specified tolerances for the errors of each type of instrument are presented and the laboratory test procedures for the calibration of the instruments are outlined.

Altimeter.— The altitude display of the mechanical altimeter is a circular scale with one or more rotating pointers. Examples of dial-type altitude displays are the three-pointer display of figure 11.1(a) and the drum-pointer (or similar counter-pointer) display of figure 11.1(b). With the three-pointer display, the long pointer rotates one revolution per 1000 ft, the short pointer one revolution per 10 000 ft, and the pointer with the triangular index one revolution per 100 000 ft. With the drum-pointer (or counter-pointer) display, the pointer rotates one revolution per 1000 ft and the drum (or counter) rotates to indicate 1000-ft or 10 000-ft increments. Thus, for altimeters with an 80 000-ft range, the long pointer on both types of displays rotates 80 times.

Since the scale of the altimeter is uniform, whereas the decrease in pressure with height is exponential, the pressure increment corresponding to a given height increment decreases with altitude (for example, the increment is 76 lb/ft² per 1000 ft at sea level, 19 lb/ft² per 1000 ft at 40 000 ft, and 3 lb/ft² per 1000 ft at 80 000 ft). As a result, measurement of pressure altitude becomes increasingly difficult at higher altitudes. As is shown later, this measurement difficulty is reflected in the much larger scale errors that are allowed at higher altitudes.

As a consequence of the great scale sensitivity of the altimeter, errors due to hysteresis and drift can be of significance. These errors, together with the errors due to aftereffect (hysteresis at sea-level pressure) and recovery (drift at sea-level pressure), are illustrated in a description of a scale-error calibration (fig. 11.2).

For the scale-error calibration of an altimeter, the instrument is connected to a mercury barometer and a suction pump. The barometric subdial of the altimeter is set to 29.92 (fig. 11.1(a)), and the system pressure is adjusted to 29.92 in. Hg. The altimeter indication at this initial test point is noted, and then the pressure is reduced, at a rate corresponding to about 3000 ft/min, to the next test point (fig. 11.2). At each test point, the pressure is held constant for about 2 min and the instrument is vibrated before the altimeter indication is noted. When the test point at the maximum test altitude has been reached, the pressure is increased to two hysteresis test points, and thereafter to the initial test pressure. The altimeter indication at this point is higher than the initial indication (because of aftereffect) and decreases slowly toward the initial indication (because of recovery effect). After a sufficient time lapse, the indication returns to the initial indication (called the rest point). The recovery error is the extent of this return during a specified time period.

As indicated in figure 11.2, the hysteresis is the difference, at a given test pressure, between the instrument indications determined when the pressure is decreasing and when it is increasing. If the pressure is held constant at a given value during the pressure cycle (as at point A in fig. 11.2), the instrument indication drifts toward point B. This drift is always in a direction to "close" the hysteresis loop.

For the certification of an altimeter for operational use, the scale errors determined at decreasing pressures are required to fall within the scale-error tolerance band (fig. 11.2) defined by the specified error tolerance. These

scale errors (circular test points in fig. 11.2) are the values used in the preparation of correction charts or for the scale-error corrections in air data computers.

The scale-error tolerances for two types of sensitive altimeters (refs. 1 and 2) and two types of precision altimeters (refs. 3, 4, and 5) are presented in table 11.1. Also tabulated are the hysteresis tolerances at two test altitudes and the aftereffect tolerance at sea-level pressure. Note that the calibration standards for these instruments do not require tests for the drift and recovery errors. A comparison of the scale-error tolerances for the four altimeters provides an indication of the improved accuracy that has been achieved through the years.

Determination of the hysteresis at two test points, specified by standard test procedures, defines only a part of the hysteresis cycle. In tests to determine the complete hysteresis cycles of three types of altimeter (ref. 6), a number of type C-12, C-13, and MA-1 altimeters were calibrated throughout the hysteresis cycle. The calibrations of representative instruments of each altimeter type are presented in figure 11.3. In table 11.2, values of hysteresis errors (at the standard test points) for all the instruments are compared with the hysteresis tolerances. Also tabulated are the aftereffect errors and tolerances. These results are of interest in showing the hysteresis and aftereffect errors of the precision-type altimeter to be very much lower than the specified tolerances.

In further tests of the three types of altimeter, the drift errors were determined through 1-hour and 6-hour test periods. The drift errors of a representative instrument of each altimeter type are shown in figure 11.4. These data show the major part of the 6-hour drift occurs within a short period after the start of the test.

Airspeed indicator.- An example of a mechanical-type airspeed indicator is the disk-pointer instrument shown in figure 11.5. The range of this indicator is 50 to 650 knots and the scale-error tolerances through this speed range are given in table 11.3 (from ref. 7).

The airspeed indicator is calibrated by applying pressures to the pitot port of the instrument and measuring the difference between these pressures and the existing atmospheric pressure with a mercury manometer. The differential pressures corresponding to given values of calibrated airspeed are listed in tables A9 and A11 of appendix A.

True-airspeed indicator.- Since the true-airspeed indicator requires input of impact pressure, static pressure, and temperature, an instrument having a given range of true airspeed must be designed for specific ranges of altitude and temperature. With the indicator of reference 8, for example, the true-airspeed range is 450 knots, the altitude range is 0 to 35,000 ft, and the temperature range is -60°C to 40°C . A photograph of this instrument is shown in figure 11.6.

For the laboratory calibration of the instrument, the temperature probe is immersed in a temperature-controlled bath, and the pressure inside the instrument case is adjusted to a specified value of pressure altitude (measured with a barometer). Pressures corresponding to given values of calibrated airspeed, measured with a manometer, are then applied to the pitot port of the instrument.

As the tables of the scale-error tolerances for the true-airspeed indicator are too extensive to be included in this text, only a few of the extreme values are listed in table 11.4 to indicate the specified accuracy of the instrument.

Machmeter.— An example of a mechanical-type Machmeter, having a range from 0.5 to 1.5, is shown in figure 11.7. Of the 43 test points required for calibration of this Machmeter, the differences between the indicated and test Mach numbers are required to meet the following tolerances (ref. 9):

- ±0.008M for 32 test points
- ±0.010M for 7 test points
- ±0.015M for 4 test points

Since the Machmeter is actuated by impact pressure and static pressure, the instrument is calibrated with the static pressure in the instrument case held constant while pressures corresponding to given values of calibrated airspeed are applied to the pitot port. An abbreviated list of the test Mach numbers specified for the scale-error calibration is given in table 11.5 (from ref. 9).

Rate-of-climb indicator.— As noted in chapter II, the rate-of-climb indicator is designed with a capillary tube that controls the rate of flow of air from the static-pressure source into the instrument chamber. This device provides correct measures of vertical speed when the aircraft is in a steady climb or descent. For the rapid changes in vertical speed that can occur at the start and finish of a climb or descent, however, the indicated vertical speed lags the correct value. To overcome this lag, a vertical acceleration element has been incorporated in later models called instantaneous (or inertial) vertical-speed indicators.

An example of a simple rate-of-climb indicator is shown in figure 11.8 and described in reference 10. For the calibration of this instrument, the indicator is placed in a vacuum chamber together with a precision altimeter. Suction is applied to the chamber to establish a given rate of change of altitude, indicated by the altimeter and timed with a stop watch. The scale error of the indicator is then determined as the difference between the measured rate of change of altitude and the rate indicated by the rate-of-climb indicator. The tolerances for an indicator having a range of 0-6000 ft/min are listed in table 11.6 (from ref. 10).

Electrical Instrument Systems

To illustrate the differences between mechanical and electrical instrument systems, diagrams of a mechanical system and of the two types of electrical systems are presented in figure 11.9.

With the mechanical instrument system, the pressure-sensing element (capsule) is located in the instrument, the instrument indications are not corrected for scale error or the position error of the static-pressure installation, and the flight information is presented on dial-pointer displays (single or multiple pointer, drum-pointer, or counter-pointer).

With the servoed instrument system, the pressure-sensing element (capsule) is located in a computer (central air data computer (ref. 11)) which can correct for both the scale error of the capsule and the position error of the static-pressure installation. The output signals of the computer thus represent corrected flight quantities (pressure altitude, calibrated airspeed, etc.). These computer-corrected signals are transmitted to the instrument where the flight information is presented on dial-pointer displays (including the counter-drum-pointer display in fig. 11.10) or on vertically moving scale displays such as those in figure 11.11.

With electronic pressure-transducer systems, the pressure-sensing element (diaphragm or bellows) is located in the electrical pressure transducer. The signals generated in the transducer are linearized in a microprocessor (computer) which can also apply corrections for the position error of the static-pressure installation. These corrected signals can then be presented on dial-pointer displays, vertical scale displays, LED (light emitting diode) displays, or CRT (cathode ray tube) displays.

As noted previously, the accuracy of servoed instrument systems is greater than that of mechanical instruments and the accuracy of electronic pressure-transducer systems is generally greater than that of servoed instrument systems. In the following sections, the accuracies of a servoed instrument system and of two types of electronic pressure-transducer systems are discussed.

Servoed instrument system.- The servoed instrument system is a form of servomechanism incorporating feedback between the computer and the instrument (fig. 11.12). In the computer, a synchrotel is actuated by the deflections of a capsule, while in the instrument, the pointer or other type display is actuated (through a gear train) by a servomotor that is controlled by signals generated by the differences in the electrical fields of the synchrotel in the computer and another synchrotel in the instrument. Additional synchrotels in the computer are controlled by two-dimensional cams to generate the correctional signals for the scale error of the capsule and the position error of the static-pressure installation.

The accuracy of a servoed instrument system is determined by (1) the basic accuracy of the computer (which includes the accuracy of the scale-error correction), (2) the accuracy of the position-error correction, and (3) the accuracy with which the corrected signals from the computer are transmitted and displayed in the instrument.

The basic accuracy of an air data computer stated in terms of the error tolerances for each of the flight quantities is as follows:

Altitude	± 15 ft at sea level to ± 80 ft at 50 000 ft
Airspeed	± 2 knots at 100 knots to ± 4 knots at 500 knots
True airspeed	± 4 knots throughout the range of the instrument
Mach number	± 0.01 at Mach 0.2 to ± 0.005 at Mach 0.95
Vertical speed	± 2 percent of the indicated value

The accuracy with which the position error is corrected in the air data computer varies depending on the slope of the calibration curve. For position-error calibrations with low slopes, the accuracy of the position-error correction is greater than for calibrations with steep slopes.

The accuracy with which the computer-generated signals are transmitted and displayed on the various servoed instruments (refs. 12 through 15) is given by the following specified error tolerances:

Altimeter	± 15 ft
Airspeed indicator	± 1 knot
True-airspeed indicator	± 1 knot
Machmeter	$\pm 0.001M$
Vertical-speed indicator	± 2 percent of indicated value

For installations incorporating servoed systems, a mechanical counterpart of each servoed instrument is installed on the instrument panel for emergency use whenever the servoed system becomes inoperative because of electrical power failure. With one type of altimeter (a servopneumatic type in which the capsule is located in the instrument), the mechanical transmission is activated by a monitoring circuit whenever the servoed system becomes inoperative.

Electronic pressure-transducer systems.- An electrical pressure transducer is a small pressure-sensing device that produces electrical signals proportional to the deflection of a capsule, diaphragm, bellows, or other pressure-sensing element (ref. 16). Depending on the characteristics of the transducer element, the output signal can be either digital (variable frequency) or analog (variable voltage).

In the digital transducer described in reference 17, the pressure-sensing element is a single bellows in the absolute-pressure transducer and two opposing bellows in the differential-pressure transducer (fig. 11.13). The transducer element in these units is a quartz crystal oscillating beam which is driven at its resonant frequency through piezoelectric excitation. The variation in this resonant frequency with load applied by the bellows provides a digital output signal that is proportional to the applied pressure. When these output signals are linearized in a microprocessor as noted earlier, they can be transmitted to

either a cockpit display or a magnetic tape recorder (in flight-test applications). The repeatability of the transducer is ± 0.005 percent of the full-scale pressure range, while the accuracy of the transducer system is about ± 0.05 percent of full scale. If corrections for the position error of the static-pressure installation are applied, the additional error for this correction depends on the slope of the position-error calibration curve, as in the case of served systems.

For analog transducers, the pressure-sensing element is a flat, circular diaphragm that divides the transducer assembly into two chambers (fig. 11.14). The transducer element most commonly used in this type of transducer is either a variable-capacitance or a variable-reluctance device. These and other transducer elements (strain gage, variable-resistance device, etc.) are described in reference 16.

Analog transducers are used primarily in flight-test recording systems, for which the output signals of the transducers are recorded on magnetic tape either in analog form (frequency modulation) or in digital form (analog-to-digital conversion). For analog recording, the output signal is processed in a signal control unit and a voltage-controlled oscillator, whereas for digital recording the signal is processed in a signal control unit and a pulse code modulator. The accuracy of analog recording systems is about ± 1 percent of the full-scale pressure range, while the accuracy of analog-to-digital recording systems is about ± 0.4 percent of full scale.

Accuracy of Calibration Equipment

The accuracy with which instrument errors are determined depends fundamentally on the accuracy of the calibration test apparatus and the calibration test technique. With high-grade barometers and manometers and skilled operators, it is possible to duplicate pressure measurements with a precision of 0.001 in. Hg (ref. 18). For routine calibrations, however, the accuracy is probably no better than 0.005 in. Hg at sea-level pressure and 0.003 in. Hg at pressures corresponding to altitudes on the order of 70 000 ft. The altitude errors corresponding to these pressure accuracies are 5 ft at sea level and 50 ft at 70 000 ft.

For the tests of reference 6, two different types of barometers were used to measure scale errors and drift errors. The barometer for the scale-error tests was equipped with an automatic system for measuring the height of the mercury column, whereas the barometer for the drift tests had an automatic mechanism for maintaining the pressure in the system at a selected value. With the first barometer, the pressures were indicated by a digital counter in pounds per square foot, and the repeatability of the readings was found to be ± 1.1 lb/ft². With the second barometer, the scale was graduated in inches of mercury, and the accuracy of the pressure controller was found to be 0.001 in. Hg. Altitude increments corresponding to pressure accuracies of ± 1.1 lb/ft² and 0.001 in. Hg are given in figure 11.15.

References

1. Technical Manual Overhaul - Sensitive Altimeters. T.O. 5F3-4-2-3 (Formerly 05-30-17), U.S. Air Force, Mar. 15, 1946; Change 10, Mar. 25, 1977.
2. Altimeter, Pressure Actuated, Sensitive Type. TSO-C10a, CAA, Mar. 1, 1949.
3. Technical Manual Overhaul - Sensitive Altimeter, AF Type MA-1.
T.O. 5F3-2-4-3, U.S. Air Force, May 1, 1955; Change 9, Oct. 1, 1977.
4. Technical Manual Overhaul - Pressure Altimeter, AF Type No. AAU-3/A.
T.O. 5F3-3-9-3, U.S. Air Force, Mar. 31, 1960; Change 6, Sept. 30, 1976.
5. Altimeter, Pressure Actuated, Sensitive Type. TSO-C10b, FAA, Sept. 1, 1959.
6. Gracey, William; and Stell, Richard E.: Repeatability, Drift, and After-effect of Three Types of Aircraft Altimeters. NASA TM D-922, 1961.
7. Technical Order Overhaul Instructions - Sensitive Airspeed Indicator.
T.O. 5F8-2-8-3 (Formerly 05-10-10), U.S. Air Force, Aug. 1, 1953; Changed Dec. 15, 1967.
8. Technical Manual Overhaul - True Airspeed Indicators, AF Type M-1A.
T.O. 5F8-2-7-3, U.S. Air Force, June 26, 1959; Change 3, Dec. 1, 1977.
9. Technical Manual Overhaul - Transonic Machmeter, AF Type A-1B.
T.O. 5F8-8-3-3 (T.O. No. 05-20CA-2), U.S. Air Force, Sept. 15, 1962; Change 7, Dec. 30, 1977.
10. Technical Manual Overhaul - Rate of Climb Indicator. T.O. 5F8-9-2-13, U.S. Air Force, July 15, 1956; Change 6, Nov. 25, 1976.
11. Dickman, Thomas J.: A Standard Digital Air Data Computer. 1976. Data Symposium Proceedings, S. Kalatiska, D. M. Layton, L. V. Schmidt, and L. Thomas, eds., U.S. Naval Postgraduate School, Sept. 1976, pp. 111-136.
12. Technical Manual Overhaul Instructions - Counter-Drum-Pointer Servoed Altimeter, Type No. AAU-19/A. T.O. 5F3-3-15-13 and NAVAIR 05-10-2, U.S. Air Force and Naval Air Systems Command, Jan. 15, 1971; Change 11, July 5, 1978.
13. Technical Manual Field Maintenance Instructions - Altitude-Vertical Speed Indicating System A/A24G-11. T.O. 5F4-18-2, U.S. Air Force, Sept. 15, 1968; Change 5, Nov. 15, 1978.
14. Technical Manual Overhaul - Sensitive Servoed Mach Number Indicator, A.F. Type ME-5. T.O. 5F8-2-4-03, U.S. Air Force, Apr. 28, 1961; Change 5, May 31, 1978.

15. Amplifier-Indicator Group, Indicated Airspeed A/A24G-10. Mil. Specif. MIL-A-27670C(USAF), Aug. 16, 1965.
16. Norton, Harry N.: Handbook of Transducers for Electronic Measuring Systems. Prentice-Hall, Inc., c.1969.
17. Paros, Jerome M.: Digital Pressure Transducers. Meas. & Data, vol. 10, no. 2, Mar.-Apr. 1976, pp. 74-79.
- * 18. Brombacher, W. G.; Johnson, D. P.; and Cross, J. L.: Mercury Barometers and Manometers. NBS Monogr. 8, U.S. Dep. Commer., May 20, 1960.

TABLE 11.1.- ERROR TOLERANCES FOR FOUR TYPES OF ALTIMETERS^a

[From refs. 1 to 5]

Test-point altitude, ft	Sensitive altimeters		Precision altimeters	
	^b Type C-12	^b Type C-13	^b Type MA-1	^b Type MA-8/A
Scale-error tolerance, ft				
0	±50	±50	±30	±30
5 000	±150	±100	±55	±55
10 000	±175	±150	±80	±80
15 000	±235	±200	±105	±105
20 000	±300	±200	±130	±130
25 000	±375	±300	±155	±155
30 000	±450	±300	±180	±180
35 000	±525	±300	±205	±205
40 000	±600		±300	±230
45 000	±675		±400	±255
50 000	±750		±500	±280
60 000			±800	±800
70 000			±1200	±1200
80 000			±1500	±1500
Hysteresis tolerance, ft				
16 000	----	±70	-----	-----
18 000	----	±70	-----	-----
20 000	±150	----	±100	±100
25 000	±150	----	±100	±100
Aftereffect tolerance, ft				
0	±60	±50	±50	±30

^aAbbreviated list of test points.^bU.S. Air Force types.

TABLE 11.2.- HYSTERESIS AND AFTEREFFECT OF

THREE TYPES OF ALTIMETERS

[From ref. 6]

Altimeter type	Minimum	Maximum	Average	Tolerance
Hysteresis, ft				
C-12	80	160	112	150
C-13	60	110	87	70
MA-1	10	45	25	100
Aftereffect, ft				
C-12	25	60	41	60
C-13	25	55	33	50
MA-1	5	20	10	50

TABLE 11.3.- SCALE-ERROR TOLERANCES OF

AIRSPPEED INDICATOR^a

[From ref. 7]

Calibrated airspeed, knots	Tolerance, knots
50	±4.0
80	±2.0
150	±2.5
250	±3.0
300	±4.0
550	±5.0
650	±5.0

^aAbbreviated list of test points.

TABLE 11.4.- SCALE-ERROR TOLERANCES OF TRUE-AIRSPEED INDICATOR^a

[From ref. 8]

Altitude, ft	Calibrated airspeed, knots	True airspeed, knots, for bulb temperature of -			
		-60° C	-40° C	0° C	40° C
0	100	---	---	---	104 ± 7
	450	373 ± 8	390 ± 8	423 ± 9	---
5 000	100	---	---	160 ± 7	114 ± 7
	450	403 ± 8	421 ± 8	---	---
10 000	100	103 ± 7	108 ± 7	117 ± 7	---
	450	434 ± 9	---	---	---
15 000	100	114 ± 7	119 ± 7	129 ± 7	---
	400	424 ± 9	444 ± 7	---	---
20 000	100	126 ± 7	132 ± 7	---	---
	350	410 ± 8	429 ± 7	---	---
35 000	100	174 ± 6	182 ± 6	---	---
	250	---	423 ± 9	---	---

^aAbbreviated list of test points.

TABLE 11.5.- SCALE-ERROR TOLERANCES FOR THE MACHMETER

[From ref. 9]

(a) Tolerances

Tolerance	No. of test Mach numbers
$\pm 0.008M$	32
$\pm 0.010M$	7
$\pm 0.015M$	4
Total	43

(b) Test Mach numbers for scale-error calibration^a

Altitude, ft	Calibrated airspeed, mph	Test Mach number
0	400	0.526
	1100	1.445
5 000	400	.573
	1000	1.418
10 000	400	.625
	900	1.378
15 000	300	.518
	900	1.498
20 000	300	.570
	800	1.443
35 000	200	.528
	600	1.430
50 000	200	.732
	450	1.476

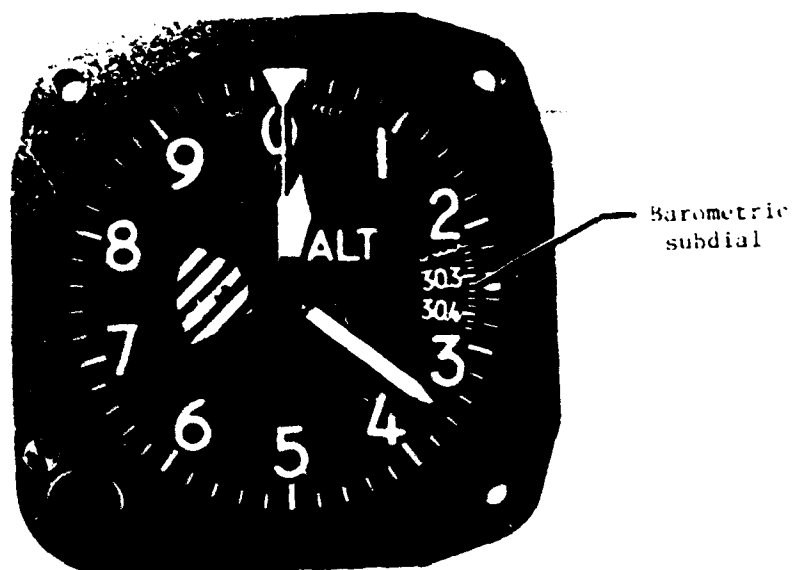
^aAbbreviated list of test points.

TABLE 11.6.- SCALE-ERROR TOLERANCES FOR THE

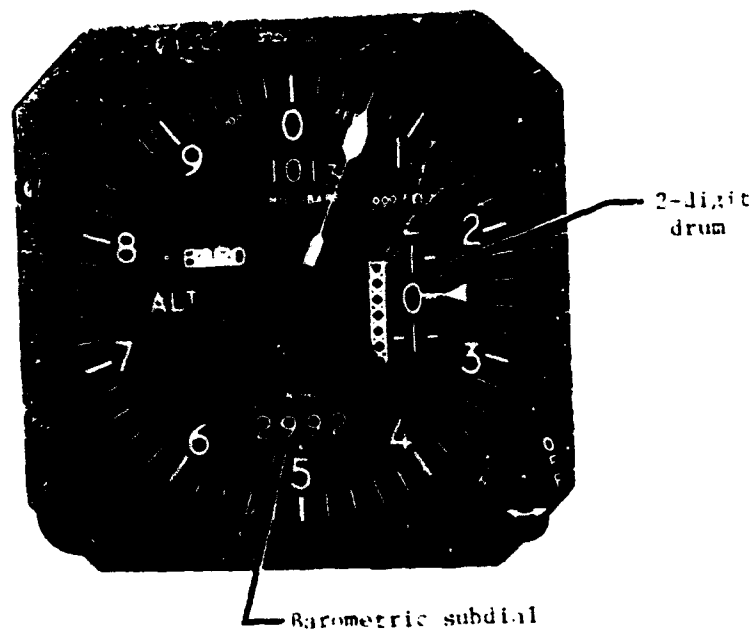
RATE-OF-CLIMB INDICATOR

[From ref. 10]

Altitude, ft	Test altitude rate of change, ft/min	Tolerance, ft/min
1 000 to 1 500	500	±100
1 000 to 2 000	1000	±200
2 000 to 4 000	2000	±300
2 000 to 4 000	3000	±300
2 000 to 4 000	4000	±400
2 000 to 4 000	5000	±500
15 000 to 17 000	2000	±300
15 000 to 17 000	4000	±400
28 000 to 30 000	2000	±300
28 000 to 30 000	4000	±400



(a) Three-pointer display ORIGINAL PAGE 1:
OF POOR QUALITY



(b) Drum-pointer display.

L-79-358

Figure 11.1.- Pressure altimeters with different altitude
displays. (Courtesy of Kollsman Instrument Co.)

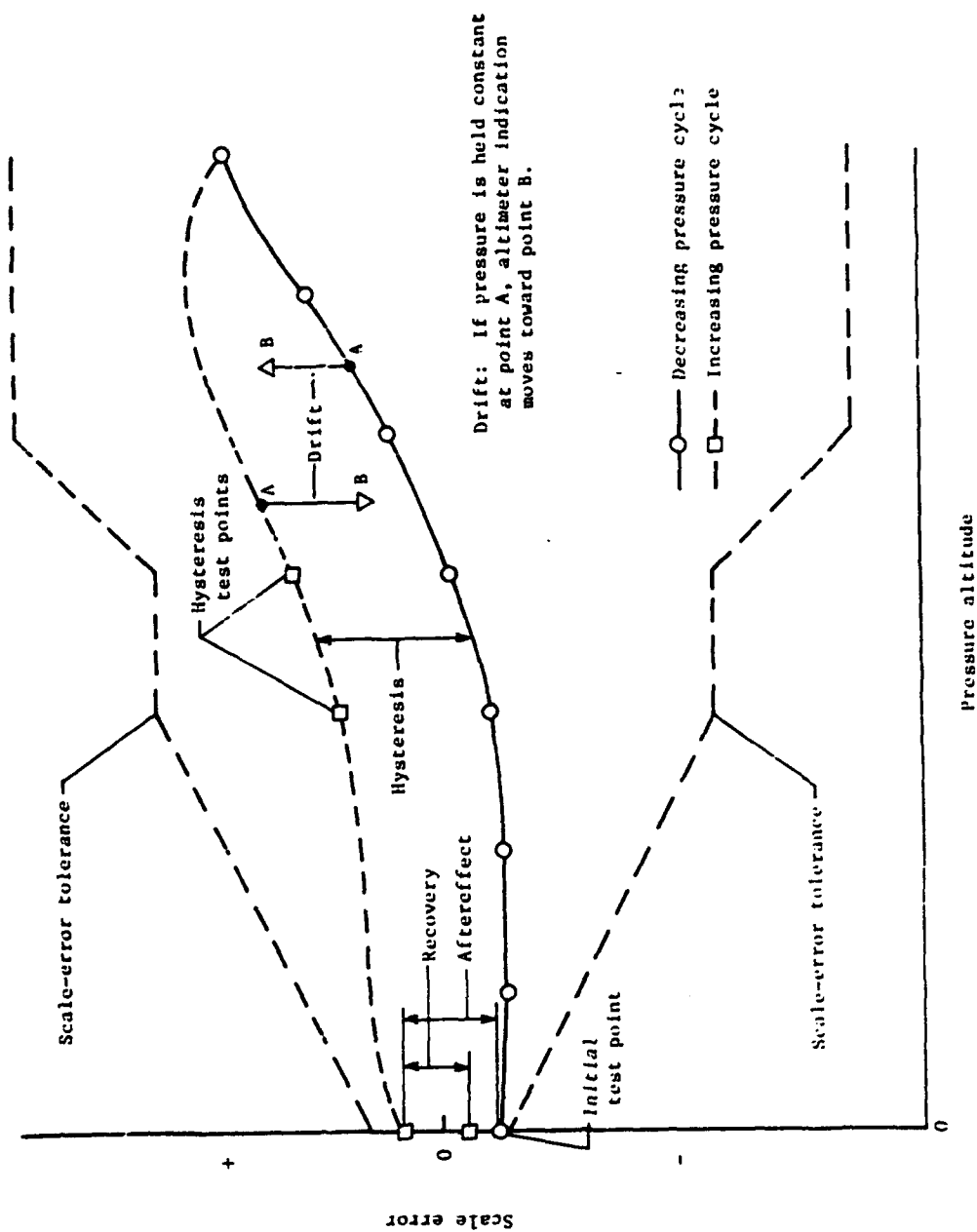
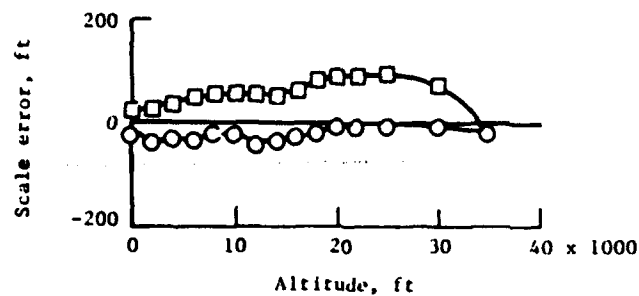
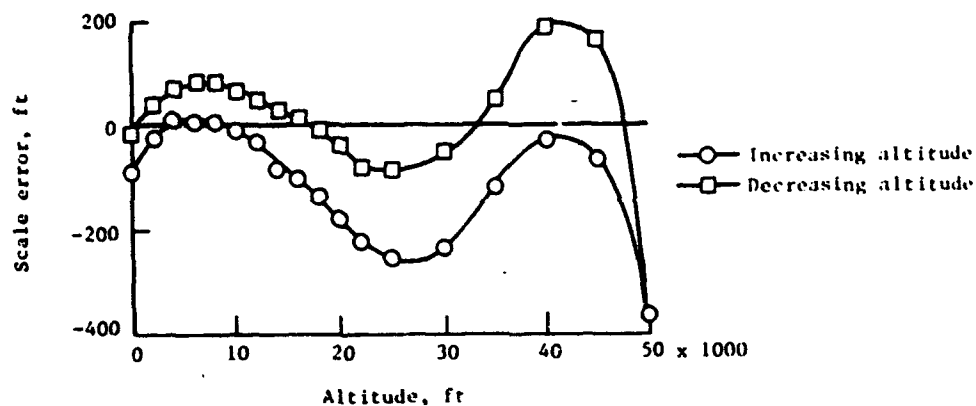


Figure 11.2.- Illustration of scale-error calibration of a pressure altimeter. Also shown are the errors due to hysteresis, drift, aftereffect, and recovery.



(a) Type C-13.

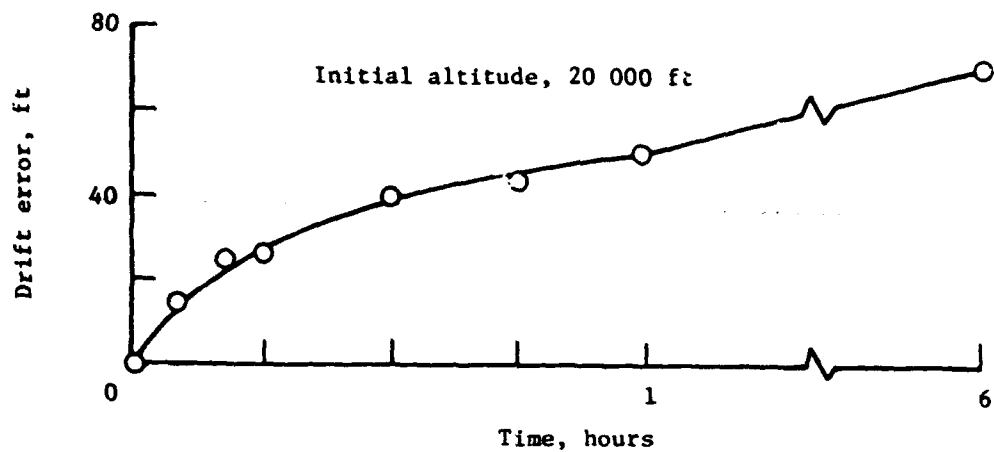


(b) Type C-12.

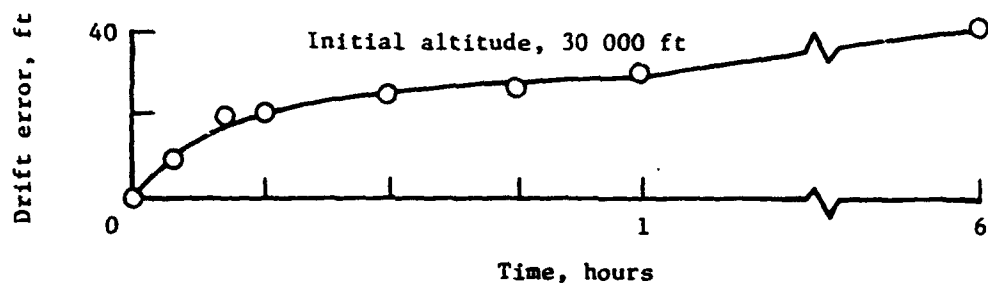


(c) Type MA-1.

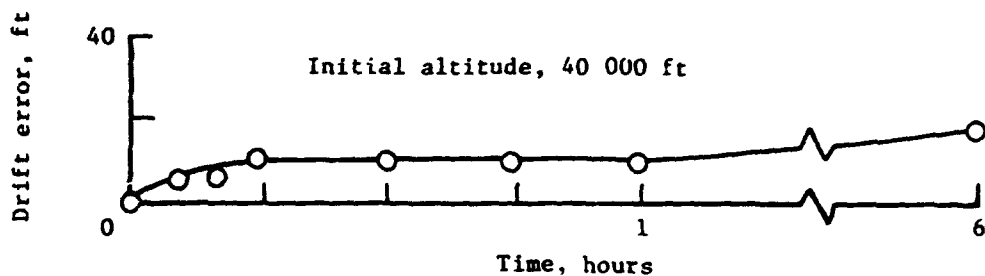
Figure 11.3.- Scale errors and hysteresis of three types of altimeters. (Adapted from ref. 6.)



(a) Type C-13.

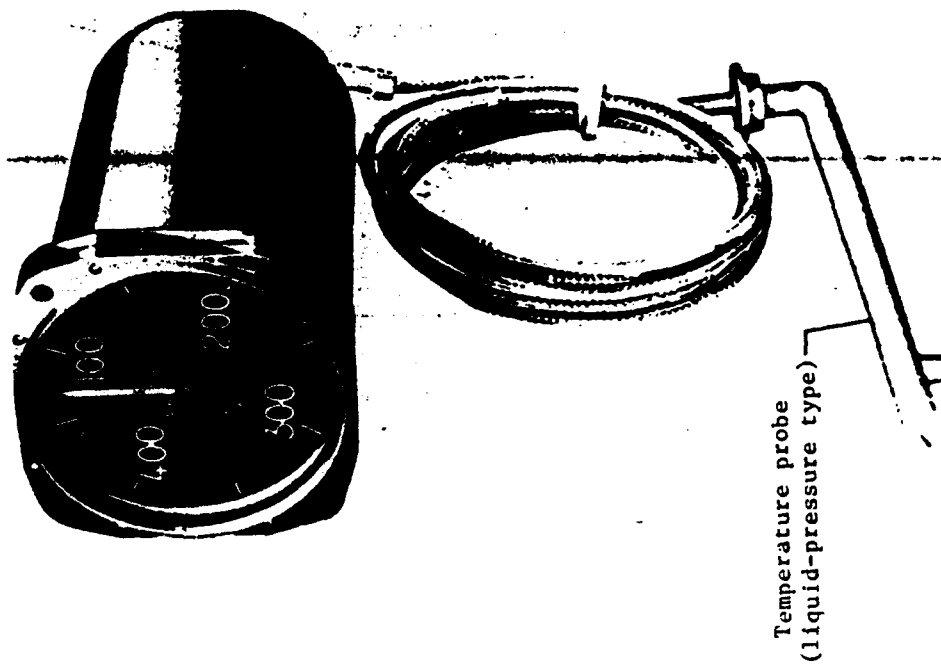


(b) Type C-12.



(c) Type MA-1.

Figure 11.4.- Drift errors of three types of altimeters.
(Adapted from ref. 3.)



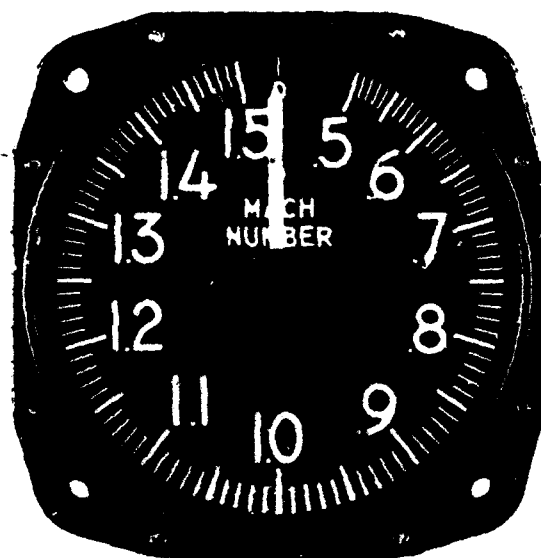
L-79-360
(Courtesy
of Kollman Instrument Co.)

Figure 11.6.- True-airspeed indicator.



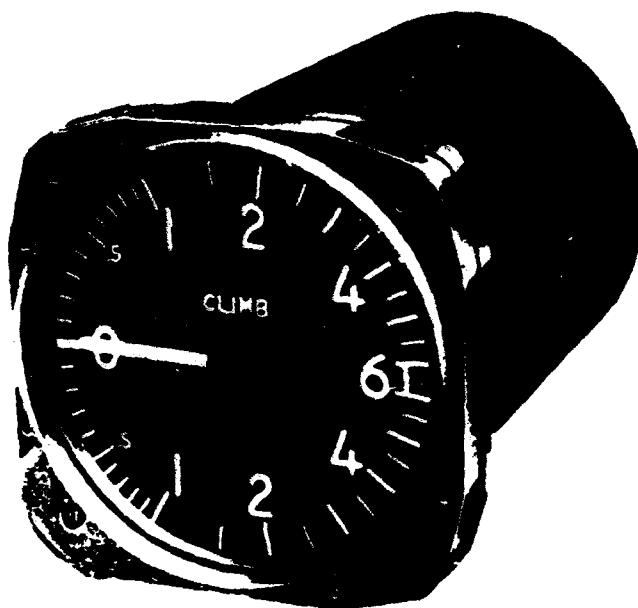
L-79-359
(Courtesy of
Kollman Instrument Co.)

Figure 11.5.- Airspeed indicator.



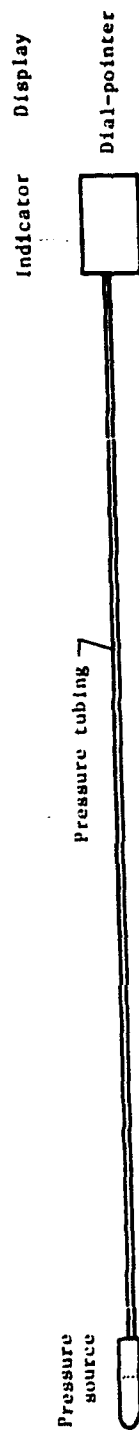
L-79-361

Figure 11.7.- Machmeter. (Courtesy of Kollsman Instrument Co.)

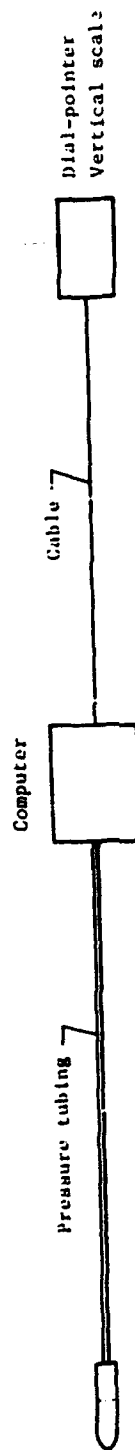


L-79-362

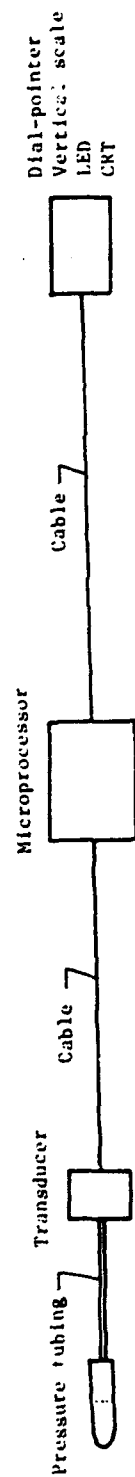
Figure 11.8.- Rate-of-climb indicator. (Courtesy of Kollsman Instrument Co.)



(a) Mechanical instrument system.

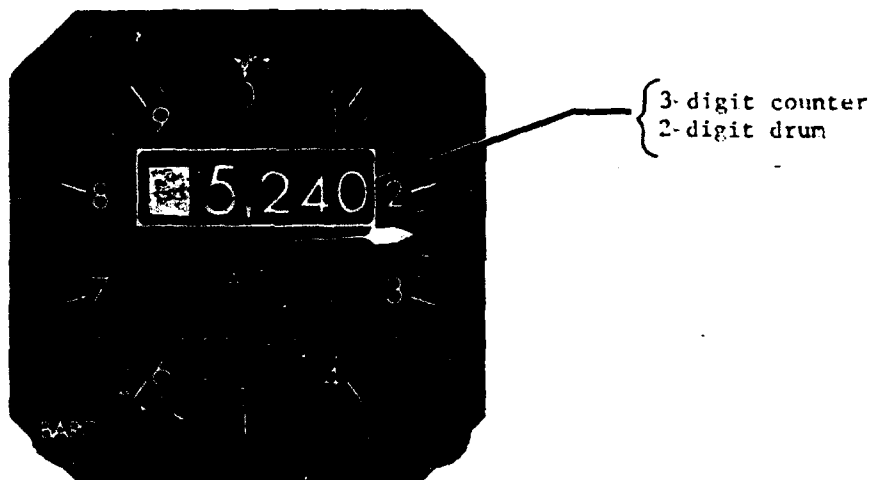


(b) Servoed instrument system.

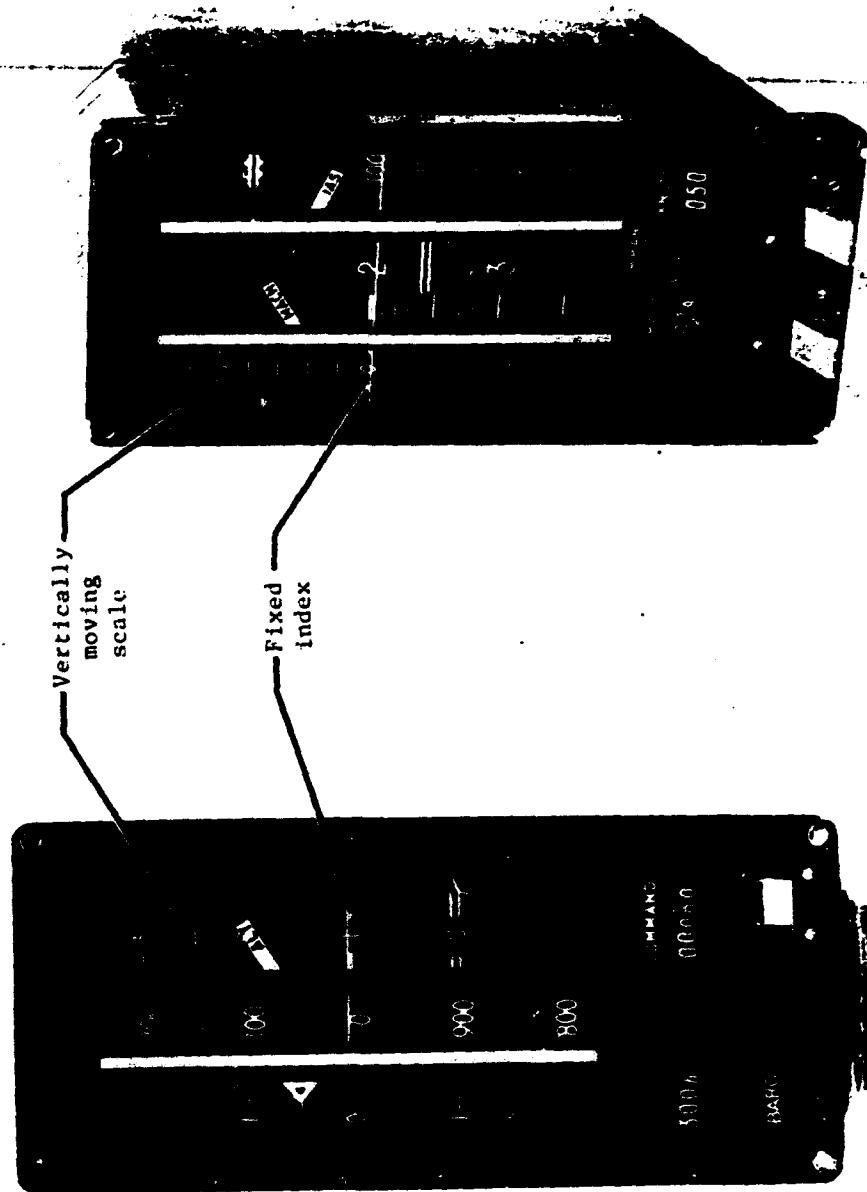


(c) Electronic pressure-transducer system.

Figure 11.9.- Diagram of mechanical and electrical instrument systems.



L-79-363
Figure 11.10.- Counter-drum-pointer servoed altimeter.
(Courtesy of Harowe Systems, Inc.)



(a) Altitude/vertical-speed indicator. (b) Airspeed/Mach-number indicator.
L-79-364

Figure 11.11.- Servoed instruments with vertical-scale displays.
(Courtesy of Kollsman Instrument Co.)

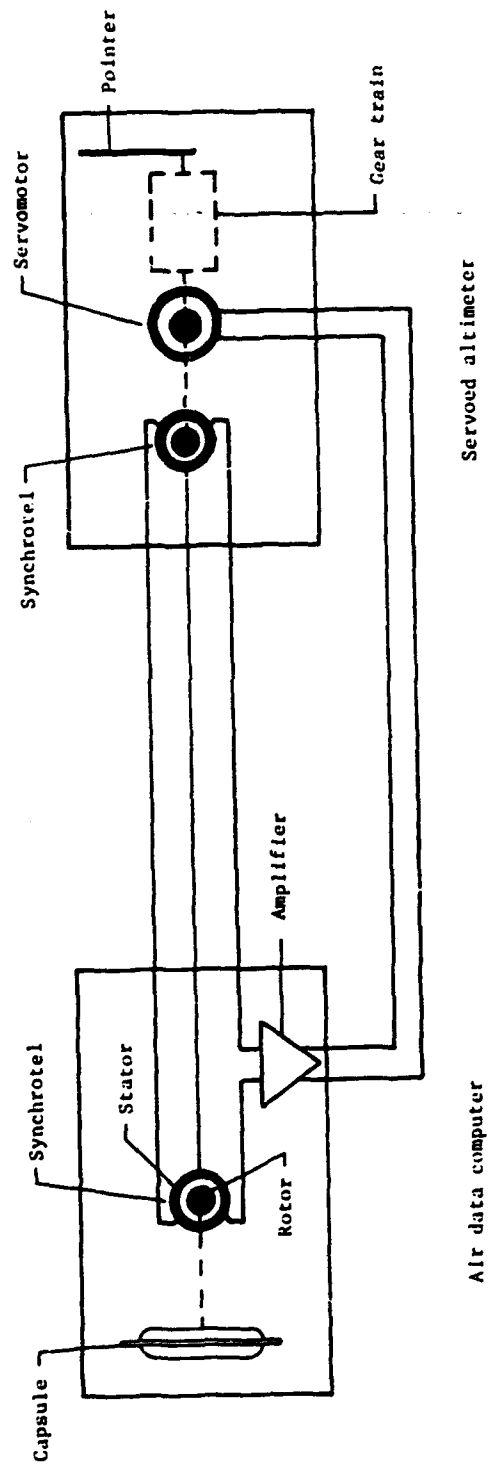
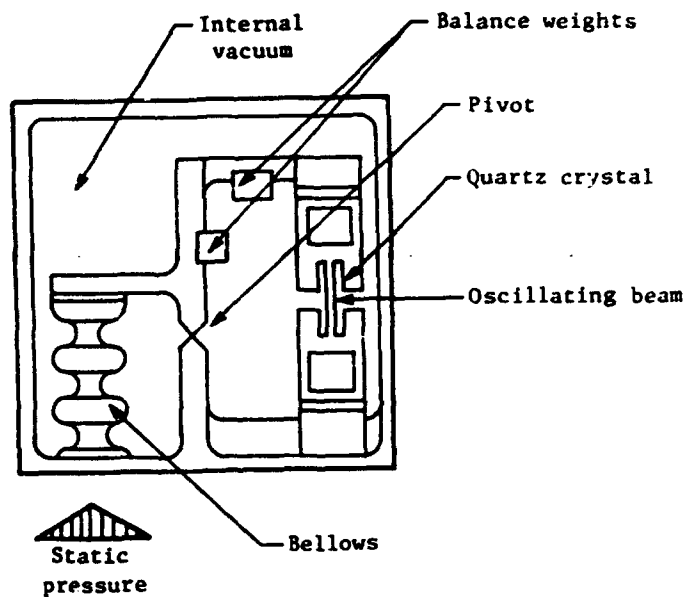
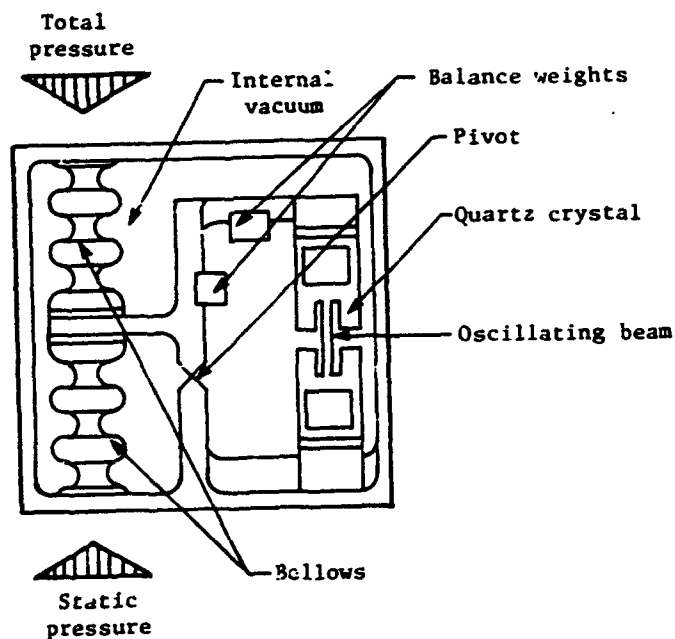


Figure 11.12.- Simplified diagram of a servoed altimeter system.

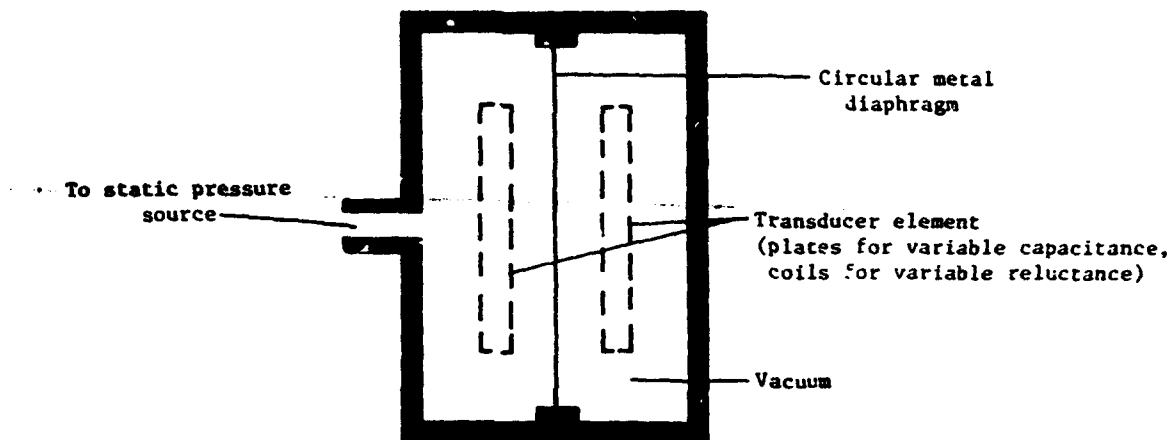


(a) Absolute-pressure transducer.

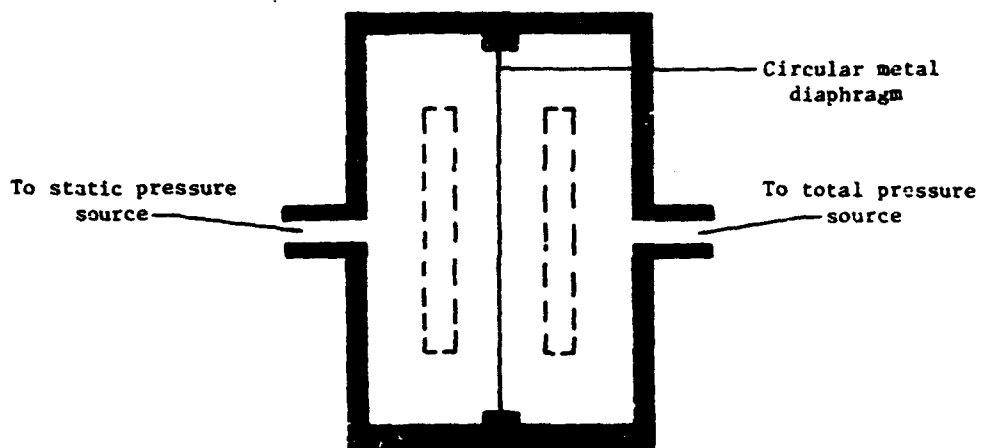


(b) Differential-pressure transducer.

Figure 11.13.- Quartz crystal digital pressure transducer.
(Courtesy of Paroscientific, Inc.)



(a) Absolute-pressure transducer.



(b) Differential-pressure transducer.

Figure 11.14.- Analog pressure transducers.

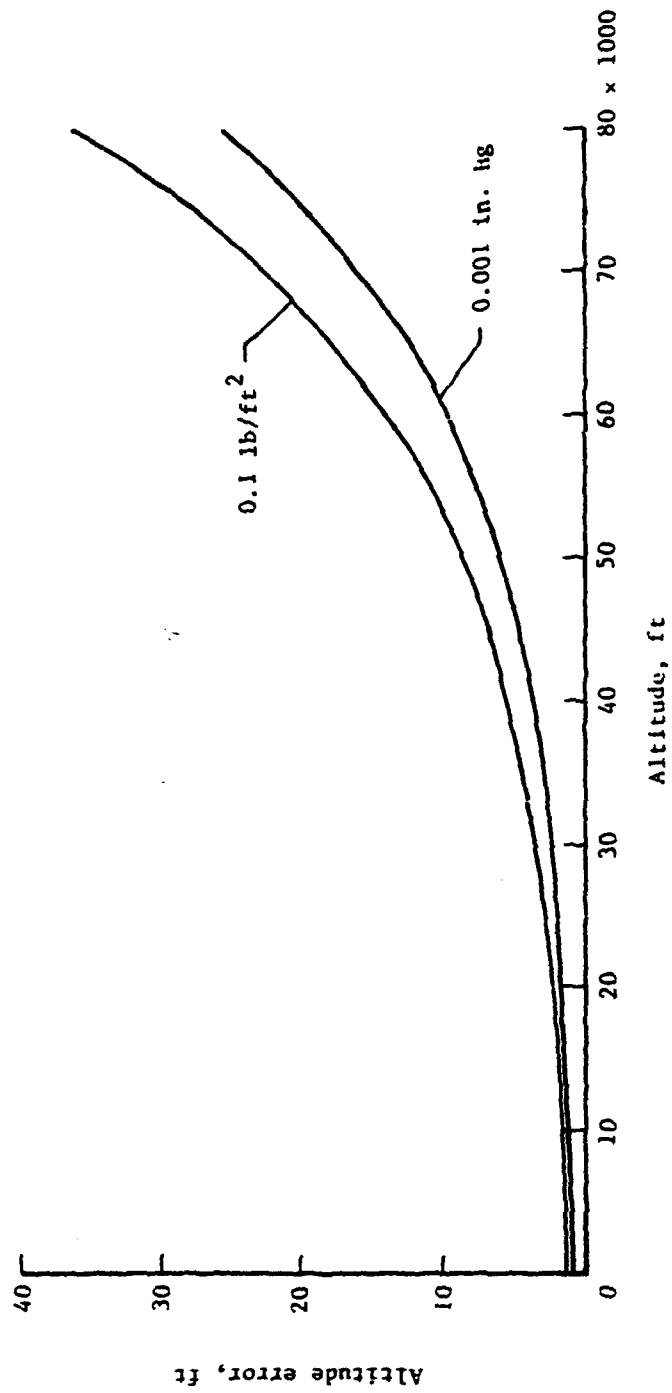


Figure 11.15.- Altitude errors corresponding to two pressure accuracies.
(Adapted from ref. 6.)

ORIGINAL PAGE IS
OF POOR QUALITY

CHAPTER XII

OPERATIONAL ASPECTS OF ALTIMETRY

In the description of the altimeter test procedures in chapter XI, it was noted that altimeters are calibrated with the barometric subdial scale set at 29.92 in. Hg, the sea-level pressure in the standard atmosphere. If the barometric subdial is also set at 29.92 in. Hg for operational use, the altimeter indicates pressure altitude above sea level. This pressure altitude differs from the geometric height whenever the sea-level pressure or temperature gradient of the atmosphere differs from the standard value. To account for these variations in pressure and temperature, the barometric subdial can be adjusted so that the altimeter indicates either the elevation of the airport or zero height at the airport elevation. Thus, in service operations, the barometric subdial may be set at one of three settings, which are assigned the following Q signals in the Aeronautical Code:

- QFE barometric subdial set at 29.92 in. Hg
- QNH barometric subdial setting for altimeter to indicate elevation of airport
- QNE barometric subdial setting for altimeter to indicate zero at the airport

The QNH settings are used by all aircraft for take-off and landing and for the vertical separation of aircraft at altitudes below 18 000 ft (ref. 1). The QNE settings are used by some airline operators during landing approaches to provide a cross-check with another altimeter set to QNH. The QFE settings are used by all aircraft for vertical separation at altitudes above 18 000 ft.

In practice, the pilot adjusts the barometric scale prior to take-off until the altimeter indicates the elevation of the airport (QNH value). Before landing at his destination, he resets the barometric scale to the existing QNH value for that area so that the altimeter indicates the elevation of that airport when the aircraft lands. The current QNH settings are measured at the airport weather stations and are reported to the pilots by radio.

Barometric Scale Settings

The mechanisms that rotate the barometric scale and the pointers of the altimeter are linked together so that adjusting the barometric scale rotates the pointer. The correspondence between the two scales is the same as the pressure-height relation in the standard atmosphere.

The interaction between the barometric scale and the altimeter pointer can be illustrated with the two hypothetical atmospheric conditions shown in figure 12.1. The curve to the right in both charts represents the pressure-height relation in the standard atmosphere. Since the barometric scale and the altitude scale of the altimeter have the same relation, an identical curve,

representing the two altimeter scales, can be thought to lie on top of the atmospheric curve. Thus the abscissa of the charts can be labeled barometric subdial scale as well as atmospheric pressure, and the ordinate can be labeled altimeter scale as well as geometric height.

The curve to the left in figure 12.1(a) represents an atmospheric condition in which the temperature gradient is standard and the sea-level pressure is 28.75 in. Hg. For this condition, the altimeter indicates 1100 ft if the barometric scale is set at 29.92 in. Hg. When the scale is adjusted to 28.75 in. Hg, the altimeter scale curve is moved down until it intersects 28.75 in. Hg on the zero-height axis. The altimeter pointer will then indicate zero, and the altimeter will indicate geometric height throughout the altitude range.

The curve to the left in figure 12.1(b) depicts an atmospheric condition in which the sea-level pressure is standard and the temperature gradient is below standard. For this condition, the altimeter indicates zero height at sea level when the barometric scale is set at 29.92 in. Hg (the existing sea-level pressure). At heights above sea level, however, the altimeter indications are higher than the geometric heights. For example, if the altimeter is taken to a height of 15 000 ft where the existing pressure is 14.82 in. Hg, the altimeter will indicate 18 200 ft (as shown by the intersection of this pressure with the altimeter scale curve).

When the airport elevation is at sea level, the QNH value is the same as the existing sea-level pressure. When the airport elevation is an appreciable height above sea level, however, the QNH value differs from the sea-level pressure whenever the temperature gradient differs from that in the standard atmosphere. This difference can be illustrated by the example shown in figure 12.2. For the case shown, the airport elevation is 5000 ft, the sea-level pressure is 29.92 in. Hg, and the temperature gradient is below standard. When an altimeter at the airport is adjusted to indicate 5000 ft, the barometric scale indicates 28.30 in. Hg (as shown by the intersection of the altimeter scale curve with the zero-height axis). For this case, therefore, the barometric subdial indicates a QNH value that is different from the actual pressure at sea level.

When the barometric scale is set to the QNH value at an airport, the altimeter should provide approximate measures of geometric height through the relatively small height range required to clear ground obstacles during take-off and landing. In an investigation to determine how accurately the altimeters in service aircraft measure geometric height in routine operations (ref. 2), the geometric heights of a wide variety of aircraft (civil transport, military, and general aviation) were measured by a ground camera at a point 3500 ft from the end of the runway of a commercial airport. The altitudes indicated by the cockpit altimeters over this point were observed by the pilots and reported to the ground station.

The results of the tests showed that for an average geometric height of 280 ft in the landing approach, the distribution of the altimeter system errors of all of the aircraft had a bias of +10 ft and a maximum probable error (99.7 percent probability) of +150 ft about the bias. For an average geometric height of 440 ft during take-off, the bias of the error distribution was +33 ft

and the maximum probable error was ± 207 ft. The signs of the bias values of the two error distributions were in directions that could be accounted for by pressure-system lag and instrument friction lag.

The QNH setting is also used on cross-country flights where altitude information is needed for terrain clearance in mountainous areas and for the vertical separation of aircraft below 18 000 ft. On such flights, the pilots are required to continually reset the barometric scales to the QNH values reported by stations along the route.

Even with altimeters set to the latest reported QNH settings, however, the vertical separation between two aircraft may be less than the prescribed minimum. The separation may be reduced, for example, when two aircraft approach each other from airports reporting different QNH settings. The separation may also be reduced if there is a change in the atmospheric conditions after an altimeter has been set to a QNH value. The effects of atmospheric changes depend on the distance between the QNH reporting stations and on the variation of the atmospheric pressure with time. In an analysis of these effects in reference 3, the following conditions were assumed: a distance of 130 miles between stations, a pressure variation of 4 millibars per hour, and a time lapse of 1/2 hour from the time of the QNH report. At the midpoint between the stations, the altitude error under these conditions was estimated to be 200 ft. As noted in the study, however, even this value might be too conservative, for errors of as much as 500 ft have been reported at the boundaries of QNH reporting stations in some areas of Europe.

To avoid the uncertainties in the indications of altimeters set to QNH for high-altitude and transoceanic flights, the altimeters of all aircraft operating above 18 000 ft are set to the QFE value (29.92 in. Hg). With this setting, the altimeters in the aircraft above any given point on the Earth are referenced to the same pressure. If the reference pressure changes, the flight level of each of the aircraft moves up or down by the same amount, so that the relative separation remains the same (assuming that the temperature gradient of the air is standard). If the temperature gradient varies from the standard, the distance between the flight levels decreases when the gradient is below standard and increases when the gradient is above standard.

During flights over mountains, the difference between the indicated altitude and the geometric height presents the greatest hazard when the atmospheric temperature is extremely low, for then the altimeter indication is higher than the geometric height. To determine the altimeter errors that might be encountered at extremely low temperatures, the geometric heights at given flight levels were computed for the coldest day in the winter of 1961-62 at three airports in the northwestern United States. The temperature-height profiles for this day at the three airports are shown in figure 12.3 together with the temperature variation in the standard atmosphere.

For each of the airport locations, the aircraft was considered to be flying at the minimum en route altitude specified by the civil regulations (2000 ft above the highest peak in the region). The barometric scale was assumed to be set to the existing QNH value, so that the indicated altitudes were measures of

the pressure altitude above the airport. The geometric height Z of the aircraft was computed from

$$Z = E + (H_i - E) \frac{T_{m,a}}{T_{m,s}} \quad (12.1)$$

where E is the elevation of the airport, H_i the indicated altitude, and $T_{m,a}$ and $T_{m,s}$ the actual and standard mean temperatures of the air between the airport and the flight level. The results of these computations, listed in table 12.1, show the difference between the indicated altitude and the geometric height, $H_i - Z$, to be as much as 950 ft.

The preceding discussion has considered only the effects of atmospheric variations on the indications of altimeters set to QNH. The accuracy of the altitude indications, however, also depends on the accuracy with which the QNH value is measured at the ground station and on how closely the pilot adjusts the barometric scale to the reported value. The altitude perceived by the pilot in turn depends on his interpretation of the altitude displayed on the instrument dial. With the three-pointer altitude display (chapter XI), pilots sometimes misread the displayed altitude by one or more thousands of feet. The drum-pointer and counter-pointer displays, with digital readouts in 1000-ft increments, were developed to overcome this kind of reading error.

Flight Technical Error

The actual flight level of an aircraft during cruising flight usually differs from its assigned flight level by an amount equal to the instrument system error (defined in chapter II). Because of difficulties in constantly maintaining level flight (either because of the characteristics of the elevator control system or deficiencies in the autopilot and its altitude-hold, or height-lock, system), the aircraft may occasionally deviate from the flight level the pilot is attempting to maintain. These occasional deviations from level flight are called flight technical error (ref. 3).

Efforts to collect statistical information on the magnitude and frequency of the flight technical error were initiated by the International Civil Aviation Organization (ICAO) in 1956. Additional investigations were conducted by the British Ministry of Transport and Civil Aviation (MTCA) in 1957, the U.S. Civil Aeronautics Administration (CAA) in 1958, the National Aeronautics and Space Administration (NASA) in 1961-63, and the International Air Transport Association (IATA) in 1962, 1963, and 1965 (refs. 4 through 9).

In the initial ICAO study, and in the later CAA and MTCA studies, the pilot of civil aircraft were asked to keep records of all excursions of the aircraft from level flight as indicated by the cockpit altimeters. In these three studies, pilot observations of altitude deviations were collected from a wide variety of aircraft in cruising flight at altitudes up to 28 000 ft.

The pilots' reports were correlated in terms of the magnitudes of the deviations and the frequency of their occurrence. The deviations were randomly

distributed about the flight level and had values that would conform, approximately, to a normal distribution curve. The probability of the occurrence of a deviation of a given magnitude could, therefore, be calculated. The magnitude selected by ICAO was the maximum probable error, defined as the value equal to three times the standard deviation (σ) of the data. This maximum probable error represents the altitude deviation that would be equaled or exceeded for 0.3 percent of the deviations. The data collected in the ICAO, CAA, and MTCA studies showed the flight technical error to increase with altitude and to have a 3σ value of about 500 ft at an altitude of 40 000 ft (ref. 3).

In the IATA investigations (refs. 5 and 6), pilot reports of altitude deviations were obtained in routine flights of commercial transports flying across the North Atlantic Ocean at altitudes above 29 000 ft. The data from these flights were analyzed, as in the ICAO study, to yield a 3σ value which was found to be 190 ft for these particular operations. The much lower value from these tests (compared with 500 ft found in the earlier studies) can be accounted for by the fact that the transports in the IATA tests were equipped with autopilots with altitude-hold systems, whereas the aircraft in the earlier tests were operated, for the most part, under manual control.

In the NASA investigations (refs. 8 and 9), the flight technical errors were determined from an evaluation of the altitude traces obtained from NASA recording altimeters. These recorders were installed in a variety of civil transports flying both domestic and transoceanic routes at altitudes up to 40 000 ft. The altitude recordings were analyzed in terms of the altitude deviation beyond which the airplane would be expected to operate for 0.3 percent of the cruise time. Since this criterion provides an indication of the length of time the airplane was away from its flight level, it represents a more meaningful measure of collision exposure than that provided by the 3σ errors.

The results of the NASA analysis are presented in figure 12.4. The values of the altitude deviations are plotted at the middle of each 5000-ft altitude bracket within which the values were recorded. The deviations were all experienced when the airplanes were under autopilot altitude-hold control. With the exception of one airplane, the deviations in the altitude range below 25 000 ft were within 160 ft. The deviations in the altitude range above 25 000 ft were within 225 ft.

Overall Altitude Errors

The overall altitude error is the deviation of an aircraft from its assigned altitude, that is, the sum of the altimeter-system error and the flight technical error (fig. 12.5). A number of attempts have been made to estimate the overall altitude errors of aircraft (refs. 3, 4, 6, and 10 to 13) to see whether these overall errors provide adequate clearance within the prescribed vertical separation minima (1000 ft for altitudes up to 29 000 ft and 2000 ft for altitudes above 29 000 ft (ref. 1)). For the altitude range from 29 000 to 40 000 ft, assessments have also been made to see whether the overall altitude errors would permit a reduction in the separation minimum from 2000 to 1000 ft. As shown in the following discussion, the validity of these

assessments depends on the accuracy of the values assigned to the altimeter-system and flight technical errors and on the procedure by which these errors are combined.

In an early assessment of the errors of aircraft operating in the 29 000-ft to 40 000-ft range (ref. 10), the overall altitude error was determined by combining the altimeter-system and flight technical errors by statistical summation. With this procedure for combining the errors, the maximum probable value (3 σ) of the overall altitude error was determined as three times the square root of the sum of the squares of the standard deviations of the individual errors. The value of the altimeter-system error was derived from a survey of the available data on the instrument and static-pressure errors of the aircraft in service at the time of the study. An analysis of these data showed the two errors to be normally distributed, to increase with altitude, and to have maximum probable values at an altitude of 40 000 ft of 250 ft for the instrument error and 265 ft for the static-pressure error. The maximum probable value for the flight technical error was the 500-ft value determined in the studies discussed in the previous section. From these three values, the maximum probable overall alti-

tude error was calculated to be $3 \sqrt{\left(\frac{250}{3}\right)^2 + \left(\frac{265}{3}\right)^2 + \left(\frac{500}{3}\right)^2}$ or 618 ft. This

618-ft value was considered to represent the deviation that would be equaled or exceeded by 0.3 percent of the aircraft assigned to a flight level of 40 000 ft. For aircraft flying adjacent flight levels, the overall altitude errors of the aircraft on the two levels were calculated by combining two of the 618-ft values

by statistical summation. This calculation, $3 \sqrt{\left(\frac{618}{3}\right)^2 + \left(\frac{618}{3}\right)^2}$, which can also

be expressed as $618\sqrt{2}$, yields a value of 874 ft, which was then considered to represent the loss in vertical separation that would be experienced by 0.3 percent of the aircraft assigned to the two flight levels. When this separation-loss figure was increased by 50 ft to account for the vertical dimensions of the aircraft, the actual separation for an assigned separation of 1000 ft was 76 ft.

A more conservative approach to the vertical separation problem would require that the maximum probable overall altitude errors of the aircraft on adjacent flight levels be less than one-half of the vertical separation minimum, or 500 ft for an assigned separation of 1000 ft. This approach was taken by IATA in its assessment of the altimeter and flight technical errors in reference 6. The altimeter-system errors for this study were determined experimentally during the same tests, discussed in the previous section, that the flight technical errors of commercial transports were measured over the North Atlantic in the altitude range above 29 000 ft. In these tests, the combined altimeter-system errors of two aircraft were determined from a comparison of the geometric and indicated altitudes of aircraft on adjacent flight levels. The indicated altitudes were measured with the cockpit altimeters, while the geometric altitudes were measured with radar altimeters. The results of the tests showed the combined altimeter-system errors to have a normal distribution with a maximum probable value (3 σ) of 510 ft. From this value for two aircraft, the maximum probable value for one aircraft was calculated to be $510/\sqrt{2}$, or 360 ft. The overall altitude error for one aircraft was then determined as the statistical sum of this 360-ft value and the maximum probable value of the flight technical

error (190 ft) which had also been measured in the IATA tests. The resulting error, $3 \sqrt{\left(\frac{360}{3}\right)^2 + \left(\frac{190}{3}\right)^2}$ or 408 ft, is thus 92 ft less than one-half the 1000-ft separation minimum.

While the vertical separation problem is a major part of the collision avoidance problem for aircraft flying at adjacent flight levels, the longitudinal and lateral separations of the aircraft must also be taken into account in any assessment of collision risk. A mathematical model for estimating collision probabilities is described in references 14 and 15. An assessment of this model and of other methods of evaluating collision risk is contained in reference 16.

ORIGINAL PAGE IS
OF POOR QUALITY

References

1. Aeronaut. Staff: Airman's Information Manual. Part 1 - Basic Flight Manual and ATC Procedures. Aero Publishers, Inc., 1977.
2. Gracey, William; Jewel, Joseph W., Jr.; and Carpenter, Gene T.: Measurement of the Errors of Service Altimeter Installations During Landing-Approach and Take-Off Operations. NASA TN D-463, 1960.
3. First Interim Report of the Panel on Vertical Separation of Aircraft. Doc. 7672-AN/860, Int. Civ. Aviat. Organ. (Montreal), Feb. 14-22, 1956.
4. Panel on Vertical Separation of Aircraft: Summary of the Work of the Vertical Separation Panel. VS P-WP/57, Int. Civ. Aviat. Organ. (Montreal), Feb. 15, 1961.
5. Report on Pressure Altimeter System Accuracy Study - North Atlantic Region. DOC. GEN. 1922, Int. Air Trans. Assoc. (Montreal), July-Aug. 1962.
6. Report on Vertical Separation Study - NAT Region. DOC. GEN. 1951, Int. Air Trans. Assoc. (Montreal), Mar. 1964.
7. Anderson, R. G.: Results of the 1965 Flight-Deck Data Collection on Height Keeping Over the North Atlantic. Tech Rep. No. 65268, British R.A.E., Nov. 1965.
8. Gracey, William; and Shipp, Jo Ann: Random Deviations From Cruise Altitudes of a Turbojet Transport at Altitudes Between 20,000 and 41,000 Feet. NASA TN D-820, 1961.
9. Kolnick, Joseph J.; and Bentley, Barbara S.: Random Deviations From Stabilized Cruise Altitudes of Commercial Transports at Altitudes up to 40,000 Feet With Autopilot in Altitude Hold. NASA TN D-1950, 1963.
10. Altimetry and the Vertical Separation of Aircraft. Int. Air Trans. Assoc. (Montreal), Jan. 1960.
11. Gracey, William: The Measurement of Pressure Altitude on Aircraft. NACA TN 4127, 1957.
12. Altimetry. Paper 215-58/DO-88, Radio Technical Commission for Aeronautics, Nov. 1, 1958.
13. Gracey, William: Recent Developments in Pressure Altimetry. J. Aircraft, vol. 2, no. 3, May-June 1965, pp. 161-165.
14. Reich, P. G.: A Theory of Safe Separation Standards for Air Traffic Control. Tech Rep. No. 64041, British R.A.E., Nov. 1964.

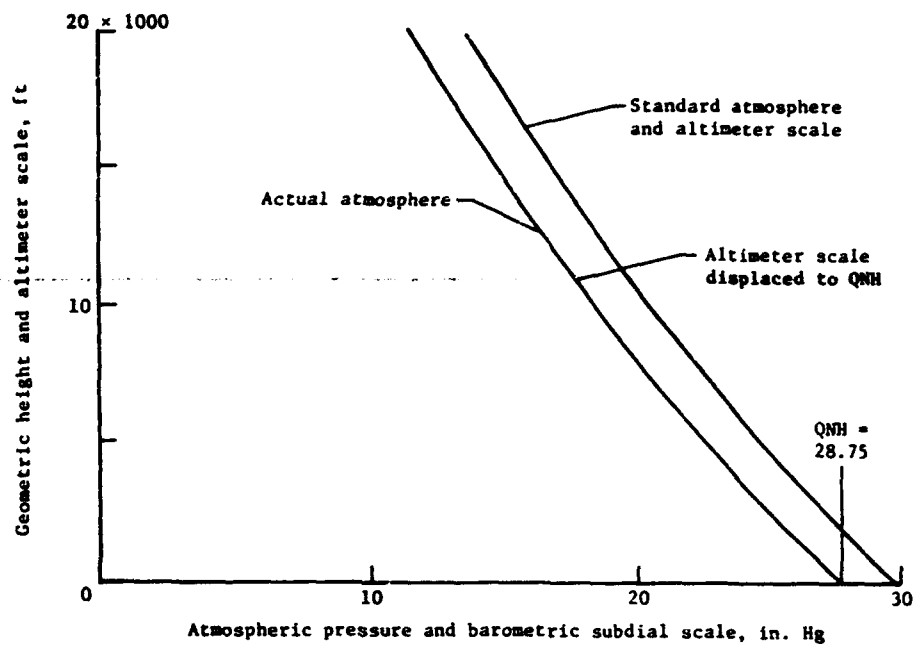
15. Reich, P. G.; and Anderson, R. G.: Separation Standards in the Long Range Air Traffic Control Region, With Special Reference to Vertical Separation. Tech. Memo. Math 68, British R.A.E., Oct. 1965.
16. Gilsinn, Judith F.; and Shier, Douglas R.: Mathematical Approaches to Evaluating Aircraft Vertical Separation Standards. Rep. No. FAA-EM-76-12, May 1976.

TABLE 12.1.- INDICATED ALTITUDES AND GEOMETRIC HEIGHTS FOR
LOW-TEMPERATURE ATMOSPHERES AT THREE AIRPORTS

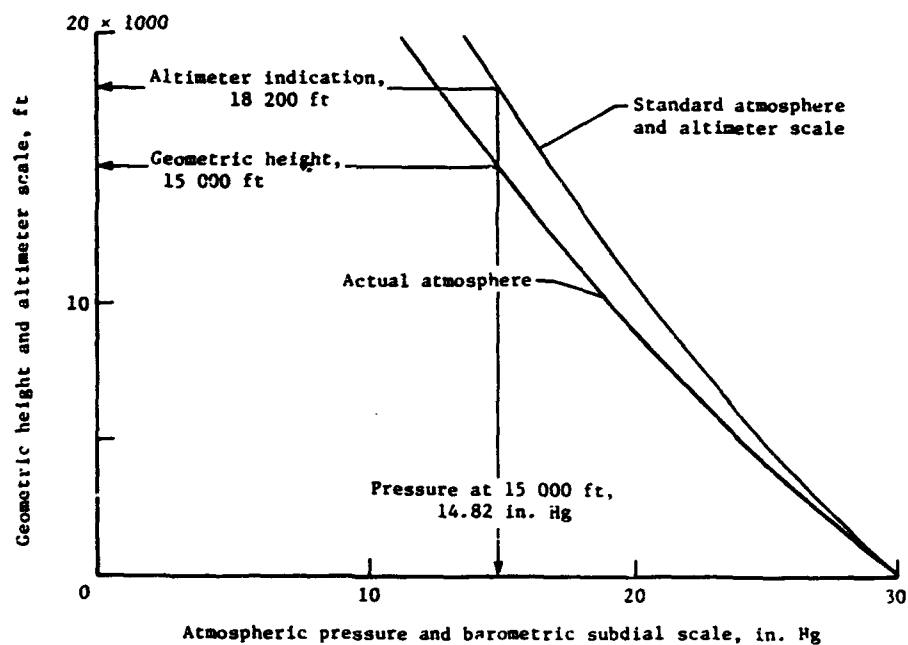
QNH station	^a H_i , ft	^b Z , ft	$H_i - Z$, ft
Seattle, Washington	12 000	11 225	775
Great Falls, Montana	13 000	12 150	850
Spokane, Washington	14 000	13 050	950

^aAltitude indicated by altimeter with barometric subdial set to QNH.

^bGeometric height computed from equation (12.1).

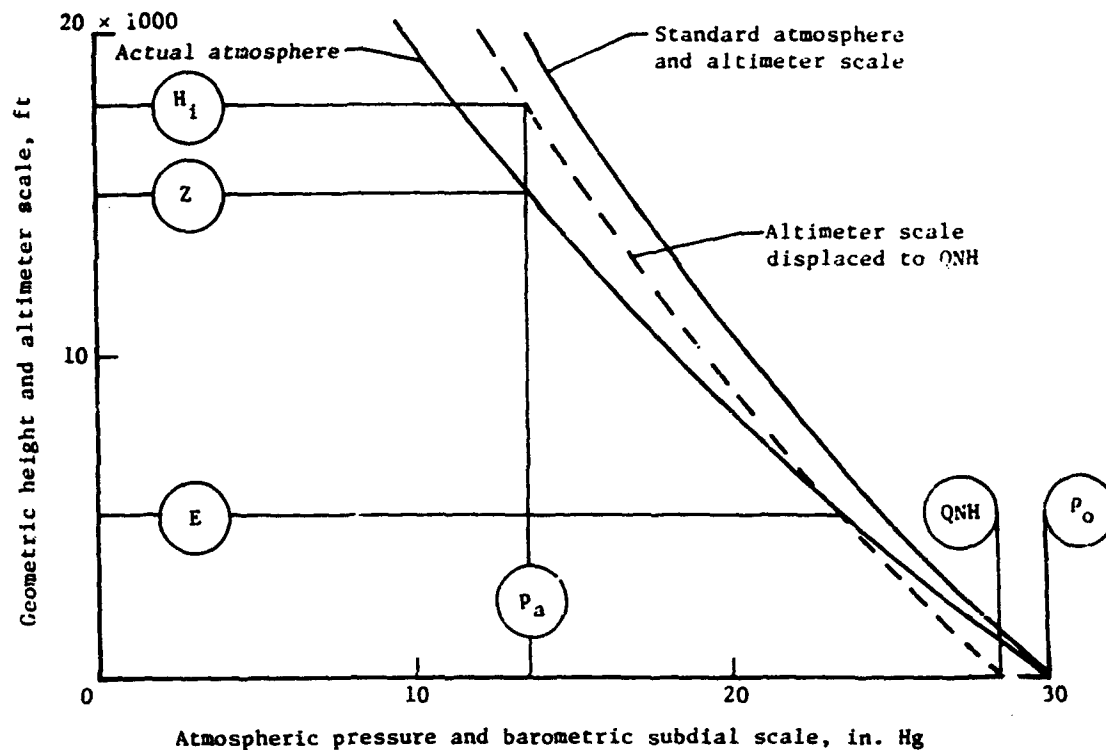


(a) Sea-level pressure below standard and temperature gradient standard.



(b) Sea-level pressure standard and temperature gradient below standard.

Figure 12.1.- Two hypothetical pressure-height variations in the atmosphere.



- E elevation of airport
- QNH barometric scale setting at elevation E
- P_o pressure at sea level
- Z geometric height of airplane
- P_a pressure at height Z
- H_i height indicated by altimeter at Z

Figure 12.2.- Pressure-height variation in an atmosphere in which the sea-level pressure is standard and the temperature gradient is below standard. Altimeter at elevation E is set to the QNH value at that elevation.

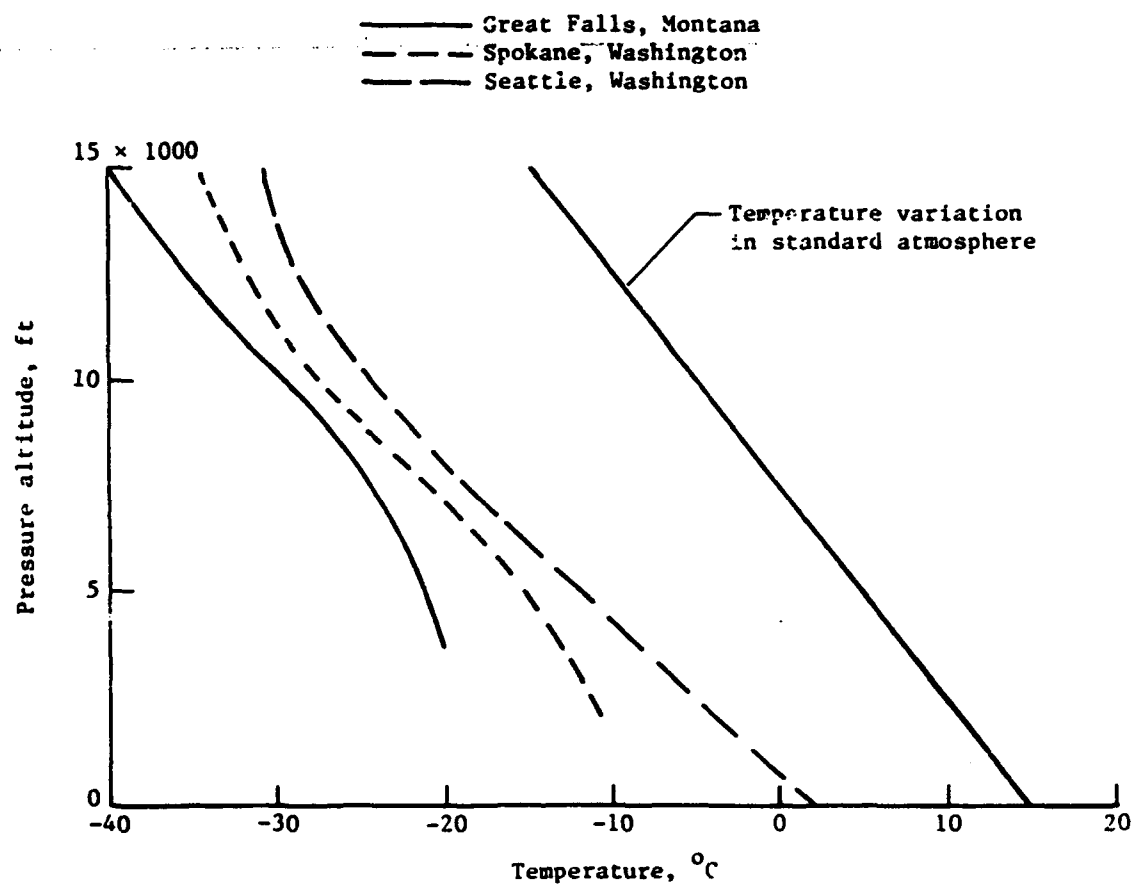


Figure 12.3.- Low-temperature atmospheres at three airports in the northwestern United States.

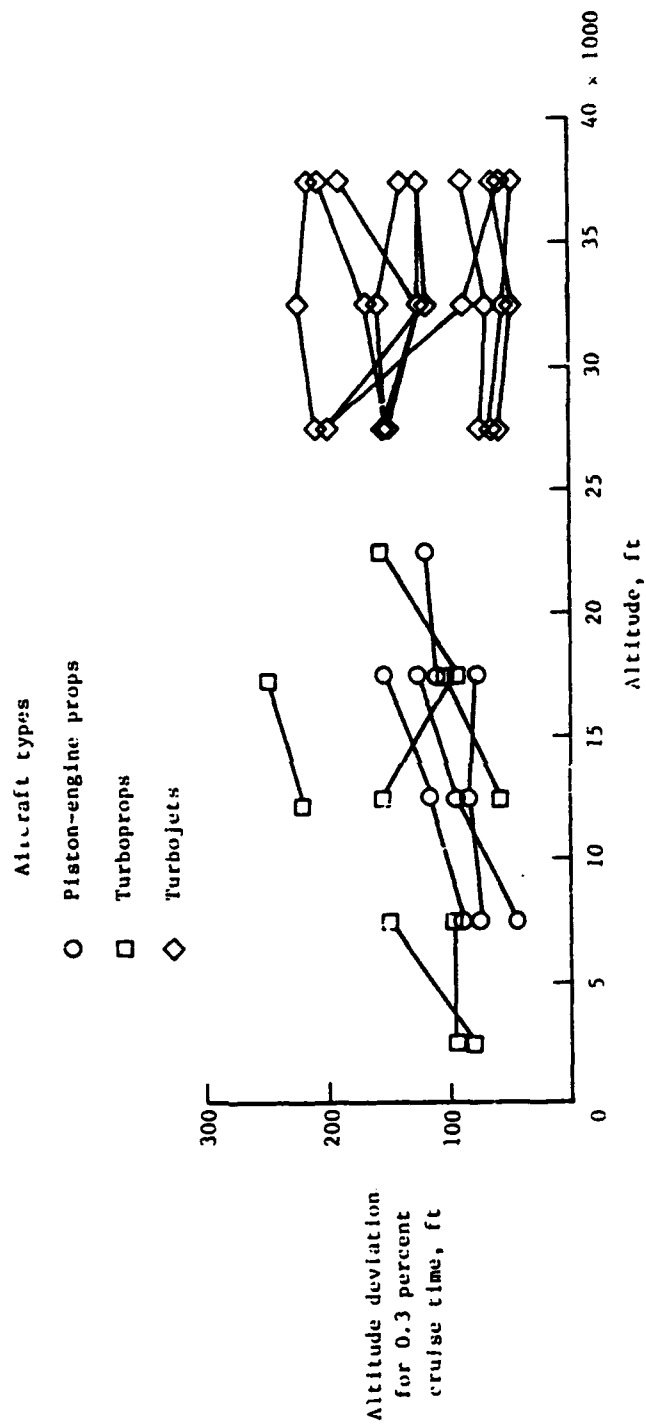


Figure 12.4.- Flight technical errors of 19 civil transports. Altitude deviations for each airplane are plotted at the midpoint of each 5000-ft altitude bracket within which the data were recorded. (Adapted from ref. 9.)

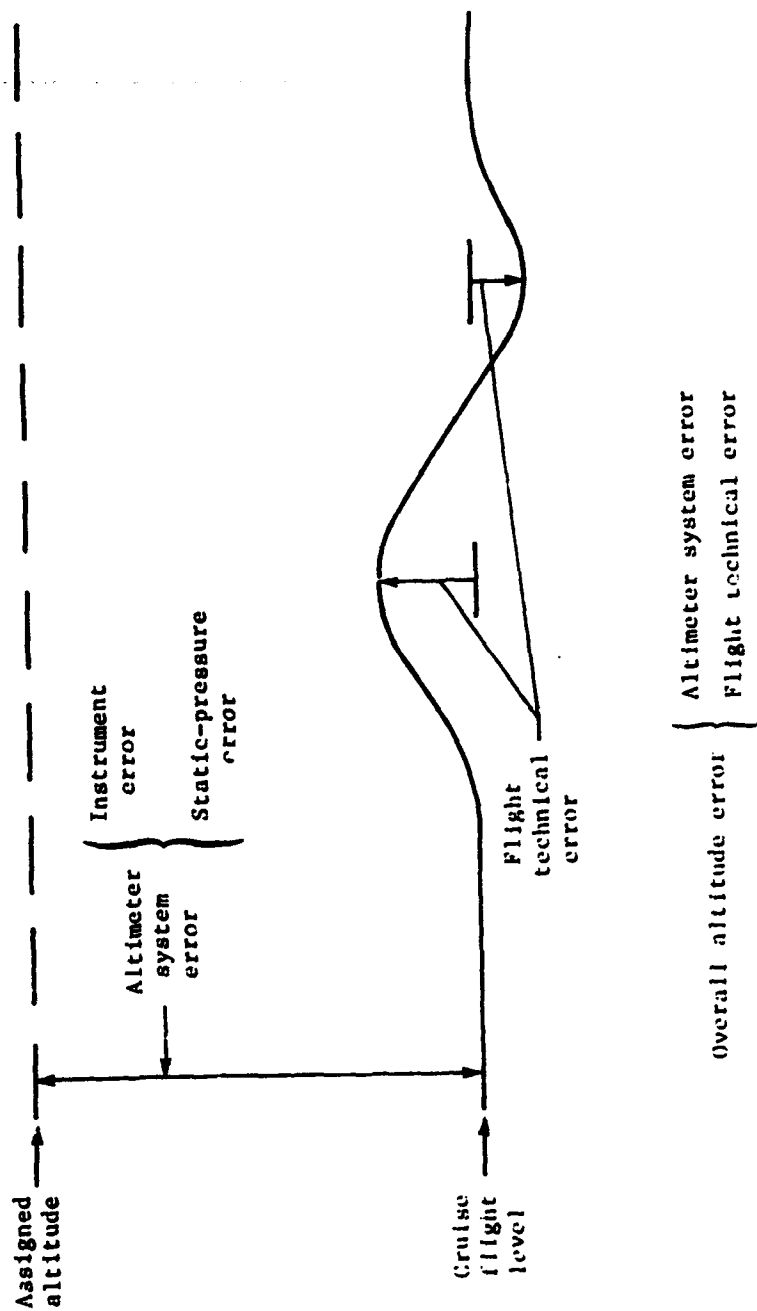


Figure 12.5.- Overall altitude error. (Adapted from ref. 13.)

PRECEDING PAGE BLANK NOT FILMED

CHAPTER XIII

OTHER ALTITUDE-MEASURING METHODS

Thus far, the only altitude-measuring method that has been discussed is based on the measurement of atmospheric pressure and the pressure-height variation in the standard atmosphere. Because of the exponential decrease of pressure with height in this atmosphere and the decreased accuracy of the pressure altimeter at altitudes above 50 000 ft, a variety of other methods have been investigated for measuring altitude at high altitudes (refs. 1 and 2). A number of low-range altimeters have also been investigated for measuring height above the terrain during landing approaches. For a discussion of both the high-range and low-range methods, the various altimeters are grouped according to the following classification:

Measurement of height above the terrain

- Radio and radar altimeters
- Laser altimeter
- Sonic altimeter
- Capacitance altimeter

Measurement of altitude (pressure or density) above sea level

- Density altimeter
- Limited-range pressure altimeter
- Hypsometer

Measurement of height above sea level

- Cosmic-ray altimeter
- Gravity meter
- Magnetometer

Of all the altimeters in the foregoing list, only the radio and radar altimeters have been developed for operational use in service aircraft. The limited-range pressure altimeter has been used in flight tests of an experimental airplane, while the hypsometer has been used in radiosondes, rocketsondes, and balloons. The remaining altimeters have been developed as experimental models to test the feasibility of the altitude-measuring principles.

Radio and Radar Altimeters

Measurement of height by radio and radar altimeters is accomplished by transmitting a radio-frequency wave from the aircraft to the ground and measuring some characteristic of the reflected wave.

With radio altimeters, a continuous wave, modulated in either frequency or amplitude, is transmitted from the aircraft, and the return signal is compared with a sample of the instantaneous signal being transmitted. In the frequency-

modulated type, the difference between the frequencies of the transmitted and received signals, which is a function of the modulation rate and time, provides a measure of the height. In the phase-comparison-type altimeter, the phase relation between the transmitted signal (which may be either frequency or amplitude modulated) and the received signal provides a measure of the signal transit time and, thus, of height.

The accuracy of radio altimeters is generally ± 2 ft for heights up to 40 ft and ± 2.5 percent of the height for heights above 40 ft. The height range is usually limited to 3000 ft because the errors become excessive at greater heights.

With the radar altimeter, the radiation is transmitted as a series of discrete pulses, and the distance between the aircraft and the ground is determined by measuring the time for the reflected wave to be received at the aircraft. Since the accuracy of the instrument depends on the width of the transmitted pulse and on the accuracy of the time measurement, measurements at low heights require ultrashort pulses and extremely precise time measurements. For this reason, the lower limit of the range of radar altimeters is generally at least 500 ft above the ground.

The accuracy of radar altimeters is $\pm (25 \text{ ft} + 0.225 \text{ percent of the height})$ and the height range is 500 ft to 60 000 ft. To provide height measurements below 500 ft, some manufacturers have developed radio-radar altimeters in which the radio altimeter operates from 0 to 3000 ft and the radar altimeter from 3000 ft to 60 000 ft.

The accuracy and the maximum range of radar and radio altimeters depend not only on the characteristics of the instrument but also on the nature of the terrain below the aircraft. With the exception of very smooth and dense surfaces (such as calm lakes and paved runway surfaces), the reflection of the transmitted wave from the terrain is diffuse rather than specular (mirror reflection). This diffused scattering of the wave results in a loss in power of the reflected wave which, in combination with the power lost by the absorption of wave energy by the terrain, limits the maximum altitude capability of the altimeter.

The accuracy of the height indications can also be affected when the transmitted signal is captured and reflected by the terrain nearest the aircraft. Thus, when the aircraft is flying in the vicinity of mountains, the altimeter may measure the distance to some part of the nearest hill.

Radar and radio altimeters have a high order of accuracy and are valuable instruments for indications of terrain clearance. They would be unsuitable for the vertical separation of aircraft at high altitudes, however, because they measure height above the terrain rather than above sea level. Furthermore, the accuracy of the radar at an altitude of 50 000 ft is not significantly better than that of the best of the present-day computer-corrected pressure altimeters.

Laser Altimeter

A laser-type altimeter has recently been developed for measuring height above the terrain at altitudes up to 3000 ft (ref. 3). The laser system consists of a pulsed laser transmitter and receiver and a timing device to measure the transit time of the pulse to the ground and back to the receiver.

The experimental model described in reference 3 has been flight-tested over various types of terrain (farmland, wooded areas, and open bodies of water) at altitudes up to 2000 ft. Recordings of the ground profiles indicated good signal return over well-defined terrain, but some uncertainty in the height measurements over wooded areas where the laser pulses did not always penetrate the foliage to the ground level. In addition, discontinuities in the recorded data occurred over surfaces with low diffuse reflectivity, such as asphalt paving.

Sonic Altimeter

Sonic altimeters measure height above the terrain by transmitting a sound wave from the aircraft and measuring either (1) the time for the ground-reflected signal to be received at the aircraft or (2) the phase shift of the reflected signal. Because of the relatively low speed of sound, altimeters utilizing sound transmission are limited to low altitudes and low speeds. For one pulse-type altimeter, the altitude limitation is 300 ft and the aircraft-speed limitation is 150 knots.

The reliability of sonic altimeters is very dependent on the character of the terrain below the aircraft. In flight tests of a pulse-type altimeter over a soft terrain such as grassland, for example, the pointer of the indicator fluctuated through a wide amplitude. Even over hard surfaces such as a concrete runway, pointer fluctuations occurred at altitudes above 100 ft because of the weak signal return at those heights.

Capacitance Altimeter

Since an aircraft and the Earth can act as the two plates of a condenser, the capacitance, which varies with the distance between the two plates, can be used as a means of measuring the height of the aircraft above the ground. In one application of this method (ref. 4), use was made of the principle that the capacitance between two insulated conductors is altered by the proximity of a third conductor. Thus, two insulated electrodes can be mounted some distance apart on an aircraft, so that the capacitance between the electrodes provides a measure of the distance between the aircraft and the ground. The change in capacitance with height is greatest when the aircraft is close to the ground and decreases rapidly as the height of the aircraft increases.

In the development of the capacitance altimeter reported in reference 4, flight tests were conducted with various types of electrodes installed on the wing tips or on the underside of the fuselage of a variety of aircraft. The results of the tests showed that the altitude range over which reliable height indications could be obtained was generally less than 200 ft.

Density Altimeter

A number of devices have been investigated for the measurement of air density on radiosondes, aircraft, and missiles. In one system, air from an air-sampling sensor is brought into a chamber where the density of that air is determined by (1) measuring the breakdown potential between two electrodes, (2) measuring the change in resistance of a heated wire resulting from the cooling action of the air, or (3) ionizing the air by means of a heated or radioactive cathode and then measuring the resulting ionic current. In another system, a beta- or ultraviolet-ray emitter on the forward part of the aircraft ionizes a portion of the air immediately ahead of the aircraft; the backscatter produced by the ionization of the air is then measured by a detector located near the emitter.

The altitude range of density-type altimeters begins at an altitude of about 50 000 ft, because at lower altitudes, the measurements are adversely affected by the presence of water vapor in the air. The use of a density altimeter as an operational instrument, therefore, would require an auxiliary pressure altimeter below 50 000 ft. Furthermore, since the accuracy of the density altimeters that have been developed is no greater than that of the pressure altimeter, the density altimeter offers no advantage over present-day operational systems.

Limited-Range Pressure Altimeter

With the limited-range pressure altimeter, the aneroid is a so-called collapsed, or nesting, capsule that is designed to start its deflection at some high altitude. In one design of this type of instrument, the lower limit of the operating range was 50 000 ft. Thus, like the density altimeter, the use of a limited-range pressure altimeter would require an auxiliary pressure altimeter at the lower altitudes. The accuracy that can be achieved with the limited-range pressure altimeter is greater than that of the pressure altimeter in the range from 50 000 to 80 000 ft, but is no greater than the accuracy of the digital-type transducer system described in chapter XI.

Hypsometer

The operation of the hypsometer is based on the principle that the boiling point of a pure liquid is a function of the atmospheric pressure acting on the surface of the liquid (refs. 5, 6, and 7). The atmospheric pressure can thus be derived from measurements of the temperature just above the surface of a boiling liquid. The attractive feature of this instrument is that the boiling point of most liquids is approximately a logarithmic function of pressure and, thus, varies in an approximately linear manner with altitude.

In its simplest form, the hypsometer consists of an insulated container which is open to the atmosphere, an evaporative liquid which boils at some reduced pressure, and a temperature-measuring element located in the vapor above the surface of the liquid. In a more advanced form, a condenser, surrounded with a coolant, is attached to the liquid container in order to reflux the vapor back to the container. This type has the advantage that the level of the

evaporative fluid remains approximately constant and thereby insures more consistent measurements of the vapor temperature. It has the additional advantage of having a longer operating time for a given quantity of fluid because vapor is not lost as rapidly as with the simplified type.

The accuracy that can be achieved with a hypsometer depends on the degree to which the vapor-liquid equilibrium is maintained, on the stability of the temperature-measuring element, and on the accuracy of the thermometer. Since the best accuracy that can be achieved is no greater than about 0.5 percent of the indicated altitude, the accuracy of hypsometer systems is considerably lower than that of the pressure altimeter.

Cosmic-Ray Altimeter

Measurement of altitude by means of cosmic rays is possible because the intensity of the cosmic rays in the atmosphere increases in an approximately linear manner with height through an altitude range from about 15 000 ft to 100 000 ft. Measurements below 15 000 ft are unreliable because of the marked decrease in the variation of cosmic-ray intensity with height near the Earth.

A cosmic-ray altimeter utilizing two groups of five Geiger counters to detect the concentration of the cosmic radiation is described in reference 8. The outputs of the Geiger counters, which provide a statistical measure of the radiation, are registered on a galvanometer which is calibrated in terms of altitude. In flight tests of a model of this instrument through an altitude range up to 30 000 ft, the altitude indications agreed with those of a pressure altimeter to within ± 500 ft at altitudes above 15 000 ft.

The use of cosmic rays for the measurement of altitude would be limited by the fact that the cosmic-ray intensity at a given height varies markedly with latitude. A cosmic-ray altimeter would also be affected by the large variations in cosmic radiation that accompany solar flares and magnetic storms.

Gravity Meter

Measurement of gravity can be used as a means of deriving altitude because the acceleration of gravity decreases with height in a linear manner (for altitudes up to 100 000 ft) and because the gravitational-height relation is essentially invariant (along a line above any given point on the Earth).

The change in the acceleration of gravity from sea level to 100 000 ft in the middle latitudes, however, is only about $0.01g$. With one airborne gravity meter (ref. 9), the best accuracy that could be attained was about $10^{-3}g$, which is equivalent to a height error of about 100 ft.

Also, the accuracy of the height measurements would be determined to a large extent by horizontal gravity gradients. The gradient between the equator and the poles, for example, is about $0.005g$, or an equivalent height increment of about 50 000 ft. Horizontal gradients also occur because of gravitational anomalies due to local variations in the density of the Earth. Over some

regions of the Earth the gradients can be as much as $10^{-5}g$, or 100 ft, per mile (ref. 10). Although the gradients due to anomalies are attenuated with height, the effects remain severe even at appreciable altitudes. The tests of reference 9, for example, showed that, in a level flight run at 12 500 ft over a mountainous area, a gravimeter recorded a change of $10^{-4}g$, or 1000 ft, over a distance of about 30 miles.

The measurements of a gravity meter are also affected by accelerations resulting from (1) changes in the aircraft attitude, (2) aircraft response to air turbulence, (3) maneuvers, and (4) airspeed with respect to the Earth's rotation. The accelerations resulting from flight through turbulent air and from vertical-plane maneuvers can, of course, be very large with respect to the $0.01g$ increment corresponding to the 100 000-ft altitude range. The accelerations which result from the speed of the aircraft with respect to the Earth's rotation are in the form of centrifugal and Coriolis accelerations which, for some flight conditions, can be quite large (ref. 2).

Magnetometer

The magnetometer measures the total field intensity at any given point within the Earth's magnetic field. Since the magnetic field strength decreases with distance above the Earth, the magnetometer has been investigated as a possible means of measuring height (ref. 11).

The measurements of a magnetometer, however, would be affected by the variation of the vertical rate of change of intensity with latitude (due to the convergence of the lines of force at the poles). This change in intensity with height varies from about 6 gammas per 1000 ft at the equator to about 10 gammas per 1000 ft at the poles. Thus, for the 3-gamma accuracy of the magnetometer described in reference 11, the error in the height measurement would vary from about 500 ft at the equator to about 300 ft at the poles.

The measurements of a magnetometer would also be affected by erratic variations of the field intensity over certain portions of the Earth. Periodic variations, which occur with the solar cycle, can be as much as 80 gammas at the equator while being negligible at the poles. Aperiodic variations, associated with aurora and magnetic storm activity, can be quite severe. The effect of the aurora can cause changes of as much as 100 gammas at the poles while being negligible at the equator, whereas magnetic storm activity can account for fluctuations of as much as 200 gammas.

References

1. RTCA Special Committee 70: Altimetry. Paper 215-58/DO-88, Radio Tech. Comm. Aeronaut., Nov. 1, 1958.
2. Gracey, William: Survey of Altitude-Measuring Methods for the Vertical Separation of Aircraft. NASA TN D-738, 1961.
3. Youmans, D. G.: Flight Testing of an Airborne Laser Terrain Profiler. Rep. R-1106 (Contract No. 14-08-001-14548), Charles Stark Draper Lab., Inc., Aug. 1977.
4. Watton, W. L.; and Pemberton, M. E.: A Direct-Capacitance Aircraft Altimeter. Proc. Inst. Electr. Eng. (London), vol. 96, pt. 3, 1949, pp. 203-213.
5. Conover, Walter C.; and Stroud, W. G.: A High-Altitude Radiosonde Hypsometer. J. Meteorol., vol. 15, no. 1, Feb. 1958, pp. 63-68.
6. Wagner, Walter C.: Hypsometer for Constant Level Balloon. Instrumentation for Geophysics and Astrophysics No. 14, AFCRC-TR-60-262, U.S. Air Force, June 1960.
7. Expendable Pressure Sensor Rocketsonde - Phase I. Rep. No. 1329 (Contract AF 33(600)-37984), Bendix Aviation Corp., Oct. 15, 1959.
8. Barghausen, John W. B.; and Van Allen, James A.: Altimeter Actuated by Cosmic Rays. U.S. Patent 2,573,823, Apr. 20, 1948.
9. Nettleton, L. L.; LaCoste, Lucien; and Harrison, J. C.: Tests of an Airborne Gravity Meter. Geophysics, vol. 25, no. 1, Feb. 1960, pp. 181-202.
10. Luskin, Bernard; and Davidson, Maurice J.: Geophysical Techniques for Precision Navigation at Sea. Tech Rep. No. 14, CU-40-57-NObsr 64547-Geol., Lamont Geological Observatory, Feb. 1957. (Available from DTIC as AD 139 263.)
11. Cahill, Laurence J., Jr.; and Van Allen, James A.: High Altitude Measurements of the Earth's Magnetic Field With a Proton Precession Magnetometer. J. Geophys. Res., vol. 61, no. 3, Sept. 1956, pp. 547-558.

PRECEDING PAGE BLANK NOT FILMED
APPENDIX A

TABLES OF AIRSPEED, ALTITUDE, AND MACH NUMBER

Some of the tables in this appendix present the independent variable in two parts: large increments in the left column and smaller increments along the top row. In table A1, for example, the pressure at 1100 ft is 28.7508 in. Hg.

The following tables are presented:

	Page
TABLE A1.- STATIC PRESSURE - in. Hg for H in geopotential ft	225
TABLE A2.- STATIC PRESSURE - lb/ft ² for H in geopotential ft	227
TABLE A3.- DENSITY - lb/ft ³ for H in geopotential ft	229
TABLE A4.- TEMPERATURE - °F for H in geopotential ft	231
TABLE A5.- TEMPERATURE - °C for H in geopotential ft	233
TABLE A6.- COEFFICIENT OF VISCOSITY - lb-sec/ft ² for H in geopotential ft	235
TABLE A7.- SPEED OF SOUND - mph and knots for H in geopotential ft . . .	236
TABLE A8.- ACCELERATION DUE TO GRAVITY - ft/sec ² for H in geopotential ft	237
TABLE A9.- IMPACT PRESSURE - in. Hg for V _C in mph	238
TABLE A10.- IMPACT PRESSURE - lb/ft ² for V _C in mph	240
TABLE A11.- IMPACT PRESSURE - in. Hg for V _C in knots	242
TABLE A12.- IMPACT PRESSURE - lb/ft ² for V _C in knots	244
TABLE A13.- TRUE AIRSPEED - knots for H in geopotential ft	246
TABLE A14.- STATIC PRESSURE - mm Hg for H in geopotential m	247
TABLE A15.- STATIC PRESSURE - Pa for H in geopotential m	248
TABLE A16.- DENSITY - kg/m ³ for H in geopotential m	249
TABLE A17.- TEMPERATURE - °C for H in geopotential m	250
TABLE A18.- COEFFICIENT OF VISCOSITY - Pa-sec for H in geopotential m	251

APPENDIX A

	Page
TABLE A19.- SPEED OF SOUND - km/hr and knots for H in geopotential m	252
TABLE A20.- ACCELERATION DUE TO GRAVITY - m/sec ² for H in geopotential m	253
TABLE A21.- IMPACT PRESSURE - mm Hg for V _C in km/hr	254
TABLE A22.- IMPACT PRESSURE - Pa for V _C in km/hr	257
TABLE A23.- IMPACT PRESSURE - mm Hg for V _C in knots	260
TABLE A24.- IMPACT PRESSURE - Pa for V _C in knots	262
TABLE A25.- TRUE AIRSPEED - knots for H in geopotential m	264
TABLE A26.- MACH NUMBER	265
TABLE A27.- CONVERSION FACTORS FOR VARIOUS PRESSURE UNITS	275
TABLE A28.- CONVERSION FACTORS, EQUIVALENTS, AND FORMULAS FOR U.S. CUSTOMARY UNITS AND THE INTERNATIONAL SYSTEM OF UNITS (SI).	276

REFERENCES

- A1. U.S. Standard Atmosphere, 1962. NASA, U.S. Air Force, and U.S. Weather Bur., Dec. 1962.
- A2. Livingston, Sadie P.; and Gracey, William: Tables of Airspeed, Altitude, and Mach Number Based on Latest International Values for Atmospheric Properties and Physical Constants. NASA TN D-822, 1961.
- A3. Tables and Data for Computing Airspeeds, Altitudes, and Mach Numbers Based on the WADC 1952 Model Atmosphere. Volume I - Altitude, Calibrated Airspeed, and Mach Number Tables. Battelle Mem. Inst. Contract AF 33(616)82, 1952.
- A4. Brombacher, W. G.; Johnson, D. P.; and Cross, J. L.: Mercury Barometers and Manometers. NBS Monogr. 8, U.S. Dep. Commer., May 20, 1960.
- A5. Standard for Metric Practice. E 380-76, American Soc. Testing & Mater., 1976.

APPENDIX A

TABLE A1.- STATIC PRESSURE p (OR p') IN INCHES OF MERCURY ($^{\circ}$ C) FOR VALUES OF
PRESSURE ALTITUDE H (OR INDICATED ALTITUDE H') IN GEOPOTENTIAL FEET

[From ref. A1]

ORIGINAL PAGE 1
OF POOR QUALITY

H, ft	0	100	200	300	400	500	600	700	800	900
-1 000	31.0185									
0		30.0295	30.1381	30.2471	30.3563	30.4659	30.5757	30.6859	30.7965	30.9073
1 000	29.9213	29.8133	29.7056	29.5983	29.4913	29.3846	29.2782	29.1721	29.0663	28.9608
2 000	28.8557	28.7508	28.6463	28.5421	28.4382	28.3345	28.2312	28.1282	28.0255	27.9231
3 000	27.8210	27.7193	27.6178	27.5166	27.4157	27.3151	27.2146	27.1148	27.0152	26.9158
4 000	26.8167	26.7179	26.6194	26.5211	26.4232	26.3256	26.2283	26.1312	26.0345	25.9380
5 000	25.8418	25.7460	25.6504	25.5551	25.4600	25.3653	25.2709	25.1767	25.0828	24.9892
6 000	24.8959	24.8029	24.7107	24.6177	24.5255	24.4336	24.3420	24.2506	24.1595	24.0687
7 000	23.9782	23.8880	23.7980	23.7083	23.6189	23.5298	23.4409	23.3523	23.2640	23.1759
8 000	23.0881	23.0006	22.9133	22.8264	22.7397	22.6532	22.5670	22.4811	22.3955	22.3101
9 000	22.2250	22.1401	22.0555	21.9712	21.8871	21.8033	21.7197	21.6364	21.5534	21.4706
10 000	21.3381	21.3059	21.2238	21.1421	21.0606	20.9794	20.8984	20.8177	20.7372	20.6569
11 000	20.5770	20.4972	20.4178	20.3385	20.2596	20.1808	20.1024	20.0241	19.9461	19.8684
12 000	19.7909	19.7137	19.6367	19.5599	19.4834	19.4071	19.3311	19.2553	19.1797	19.1044
13 000	19.0294	18.9545	18.8799	18.8056	18.7315	18.6576	18.5839	18.5105	18.4374	18.3644
14 000	18.2917	18.2192	18.1470	18.0750	18.0032	17.9317	17.8603	17.7893	17.7184	17.6478
15 000	17.5774	17.5072	17.4373	17.3675	17.2981	17.2288	17.1597	17.0909	17.0223	16.9540
16 000	16.8858	16.8179	16.7502	16.6827	16.6154	16.5484	16.4816	16.4150	16.3486	16.2824
17 000	16.2164	16.1507	16.0852	16.0199	15.9548	15.8899	15.8252	15.7608	15.6966	15.6325
18 000	15.5687	15.5051	15.4417	15.3785	15.3156	15.2528	15.1903	15.1279	15.0658	15.0038
19 000	14.9421	14.8806	14.8193	14.7582	14.6973	14.6366	14.5761	14.5158	14.4557	14.3958
20 000	14.3361	14.2766	14.2173	14.1582	14.0993	14.0406	13.9821	13.9238	13.8657	13.8078
21 000	13.7501	13.6926	13.6353	13.5782	13.5212	13.4645	13.4079	13.3516	13.2954	13.2395
22 000	13.1837	13.1281	13.0727	13.0175	12.9625	12.9076	12.8530	12.7985	12.7443	12.6902
23 000	12.6363	12.5826	12.5291	12.4757	12.4226	12.3696	12.3168	12.2642	12.2118	12.1595
24 000	12.1075	12.0556	12.0039	11.9524	11.9010	11.8499	11.7989	11.7481	11.6974	11.6470
25 000	11.5967	11.5466	11.4967	11.4469	11.3974	11.3480	11.2987	11.2497	11.2008	11.1521
26 000	11.1035	11.0552	11.0070	10.9589	10.9111	10.8634	10.8159	10.7685	10.7213	10.6743
27 000	10.6275	10.5808	10.5343	10.4879	10.4417	10.3957	10.3499	10.3042	10.2587	10.2133
28 000	10.1681	10.1230	10.0782	10.0335	9.98889	9.94450	9.90026	9.85619	9.81227	9.76851
29 000	9.72491	9.68147	9.63818	9.59505	9.55208	9.50926	9.46660	9.42410	9.38174	9.33955
30 000	9.29750	9.25561	9.21388	9.17229	9.13086	9.08958	9.04845	9.00747	8.96665	8.92597
31 000	8.88544	8.84506	8.80483	8.76475	8.72481	8.68502	8.64539	8.60589	8.56654	8.52734
32 000	8.48829	8.44938	8.41060	8.37199	8.33351	8.29517	8.25698	8.21893	8.18102	8.14326
33 000	8.10563	8.06815	8.03081	7.99360	7.95654	7.91961	7.88283	7.84618	7.80967	7.77330
34 000	7.73707	7.70097	7.66501	7.62919	7.59350	7.55794	7.52253	7.48724	7.45209	7.41708
35 000	7.38219	7.34744	7.31283	7.27834	7.24399	7.20977	7.17568	7.14172	7.10789	7.07419
36 000	7.04062		6.97386		6.90762		6.84189		6.77667	
37 000	6.71195		6.64775		6.58415		6.52116		6.45878	
38 000	6.39699		6.33579		6.27518		6.21515		6.15569	
39 000	6.09680		6.03847		5.98071		5.92349		5.86682	
40 000	5.81070		5.75511		5.70005		5.64552		5.59151	
41 000	5.53802		5.48504		5.43257		5.38060		5.32912	
42 000	5.27814		5.22765		5.17763		5.12810		5.07904	
43 000	5.03045		4.98233		4.93466		4.88746		4.84070	
44 000	4.79439		4.74852		4.70310		4.65810		4.61354	
45 000	4.56941		4.52569		4.48240		4.43951		4.39704	
46 000	4.35498		4.31332		4.27205		4.23118		4.19070	
47 000	4.15061		4.11091		4.07158		4.03263		3.99405	
48 000	3.95584		3.91800		3.88051		3.84339		3.80662	
49 000	3.77020		3.73414		3.69841		3.66303		3.62799	
50 000	3.59328		3.55891		3.52486		3.49114		3.45774	

APPENDIX A

TABLE A1.- Concluded

H, ft	0	200	400	600	800
50 000	3.42466	3.39190	3.35945	3.32731	3.29548
51 000	3.26395	3.23273	3.20180	3.17117	3.14083
52 000	3.11079	3.08103	3.05155	3.02236	2.99344
53 000	2.96481	2.93644	2.90835	2.88053	2.85297
54 000	2.82568	2.79865	2.77187	2.74535	2.71909
55 000	2.69308	2.66731	2.64180	2.61652	2.59149
56 000	2.56670	2.54215	2.51783	2.49374	2.46988
57 000	2.44625	2.42285	2.39967	2.37672	2.35398
58 000	2.33146	2.30916	2.28706	2.26519	2.24351
59 000	2.22205	2.20079	2.17974	2.15889	2.13823
60 000	2.11778	2.09752	2.07745	2.05758	2.03789
61 000	2.01840	1.99909	1.97996	1.96102	1.94226
62 000	1.92368	1.90528	1.88705	1.86900	1.85112
63 000	1.83341	1.81587	1.79850	1.78129	1.76425
64 000	1.74737	1.73066	1.71410	1.69770	1.68146
65 000	1.66538	1.64944	1.63366	1.61803	1.60256
66 000	1.58723	1.57206	1.55703	1.54216	1.52742
67 000	1.51284	1.49840	1.48410	1.46994	1.45591
68 000	1.44203	1.42828	1.41467	1.40119	1.38784
69 000	1.37463	1.36154	1.34858	1.33575	1.32304
70 000	1.31046	1.29800	1.28567	1.27345	1.26135
71 000	1.24938	1.23751	1.22577	1.21414	1.20262
72 000	1.19122	1.17992	1.16874	1.15767	1.14670
73 000	1.13584	1.12509	1.11444	1.10389	1.09345
74 000	1.08311	1.07287	1.06273	1.05269	1.04274
75 000	1.03290	1.02314	1.01349	1.00392	.994453
76 000	.985074	.975787	.966589	.957481	.948461
77 000	.939529	.930682	.921922	.913248	.904656
78 000	.896148	.887722	.879377	.871114	.862931
79 000	.854826	.846799	.838851	.830979	.823183
80 000	.815462	.807816	.800243	.792744	.785317
81 000	.777962	.770677	.763463	.756317	.749241
82 000	.742233	.735293	.728419	.721612	.714870
83 000	.708192	.701579	.695029	.688543	.682119
84 000	.675756	.669454	.663213	.657031	.650910
85 000	.644846	.638841	.632893	.627003	.621169
86 000	.615390	.609667	.603999	.598385	.592824
87 000	.587317	.581862	.576460	.571106	.565809
88 000	.560560	.555361	.550212	.545111	.540060
89 000	.535056	.530101	.525192	.520330	.515515
90 000	.510745	.506021	.501342	.496707	.492117
91 000	.487570	.483066	.478605	.474187	.469810
92 000	.465475	.461182	.456928	.452716	.448543
93 000	.444410	.440316	.436261	.432244	.428265
94 000	.424324	.420421	.416554	.412724	.408930
95 000	.405172	.401449	.397762	.394110	.390492
96 000	.386908	.383358	.379842	.376358	.372906
97 000	.369490	.366105	.362751	.359429	.356138
98 000	.352879	.349650	.346451	.343283	.340144
99 000	.337035	.333955	.330904	.327882	.324888
100 000	.321922				

APPENDIX A

OF FOUR QUANTITIES

TABLE A2.- STATIC PRESSURE p (OR p') IN POUNDS PER SQUARE FOOT FOR VALUES OF
PRESSURE ALTITUDE H (OR INDICATED ALTITUDE H') IN GEOPOTENTIAL FEET

[Derived from ref. A1]

H, ft	0	100	200	300	400	500	600	700	800	900
-1 000 -C	2193.82	2123.87	2131.55	2139.26	2146.99	2154.74	2162.50	2170.29	2178.12	2185.96
0	2116.22	2108.58	2100.96	2093.38	2085.81	2078.26	2070.74	2063.23	2055.75	2048.29
1 000	2040.85	2033.43	2026.04	2018.67	2011.33	2003.99	1996.69	1989.40	1982.14	1974.89
2 000	1967.67	1960.48	1953.30	1946.14	1939.01	1931.29	1924.80	1917.73	1910.68	1903.65
3 000	1896.64	1889.66	1882.69	1875.74	1868.81	1861.91	1855.03	1848.16	1841.32	1834.50
4 000	1827.69	1820.92	1814.16	1807.42	1800.69	1793.99	1787.31	1780.65	1774.01	1767.39
5 000	1760.79	1754.21	1747.65	1741.12	1734.60	1728.10	1721.62	1715.15	1708.71	1702.29
6 000	1695.89	1689.51	1683.14	1676.80	1670.48	1664.17	1657.89	1651.62	1645.37	1639.14
7 000	1632.93	1626.75	1620.57	1614.42	1608.29	1602.17	1596.08	1590.00	1583.95	1577.91
8 000	1571.90	1565.89	1559.90	1553.94	1547.99	1542.06	1536.15	1530.26	1524.39	1518.53
9 000	1512.70	1506.89	1501.08	1495.30	1489.54	1483.79	1478.06	1472.36	1466.66	1460.98
10 000	1455.33	1449.69	1444.07	1438.46	1432.88	1427.31	1421.77	1416.23	1410.71	1405.22
11 000	1399.74	1394.28	1388.83	1383.40	1377.99	1372.59	1367.22	1361.85	1356.51	1351.18
12 000	1345.88	1340.58	1335.30	1330.05	1324.81	1319.58	1314.37	1309.18	1304.01	1298.84
13 000	1293.70	1288.57	1283.47	1278.38	1273.30	1268.24	1263.19	1258.17	1253.16	1248.16
14 000	1243.18	1238.22	1233.27	1228.34	1223.43	1218.53	1213.64	1208.77	1203.92	1199.09
15 000	1194.27	1189.47	1184.68	1179.90	1175.14	1170.41	1165.68	1160.97	1156.27	1151.59
16 000	1146.92	1142.28	1137.65	1133.03	1128.42	1123.83	1119.26	1114.70	1110.16	1105.63
17 000	1101.11	1096.62	1092.13	1087.66	1083.21	1078.77	1074.35	1069.94	1065.55	1061.16
18 000	1056.80	1052.45	1048.11	1043.79	1039.48	1035.19	1030.91	1026.65	1022.40	1018.16
19 000	1013.94	1009.73	1005.54	1001.36	997.190	993.038	988.901	984.777	980.666	976.573
20 000	972.492	968.426	964.373	960.334	956.303	952.293	948.290	944.308	940.333	936.380
21 000	932.433	928.501	924.582	920.678	916.788	912.905	909.044	905.189	901.356	897.530
22 000	893.717	889.919	886.136	882.359	878.603	874.855	871.120	867.400	863.694	859.995
23 000	856.317	852.647	848.990	845.348	841.713	838.098	834.491	830.898	827.313	823.748
24 000	820.191	816.647	813.118	809.596	806.095	802.601	799.114	795.649	792.190	788.746
25 000	785.308	781.892	778.483	775.081	771.701	768.327	764.968	761.615	758.277	754.953
26 000	751.643	748.340	745.051	741.769	738.502	735.248	732.009	728.777	725.559	722.348
27 000	719.151	715.951	712.793	709.631	706.476	703.337	700.206	697.091	693.985	690.890
28 000	687.806	684.734	681.672	678.621	675.582	672.554	669.537	666.531	663.535	660.551
29 000	657.577	654.614	651.663	648.721	645.791	642.871	639.962	637.064	634.177	631.300
30 000	628.433	625.577	622.732	619.897	617.073	614.258	611.456	608.662	605.879	603.106
31 000	600.344	597.593	594.850	592.119	589.397	586.686	583.985	581.294	578.612	575.942
32 000	573.280	570.630	567.989	565.357	562.736	560.124	557.523	554.930	552.348	549.776
33 000	547.214	544.660	542.117	539.584	537.059	534.544	532.040	529.544	527.058	524.582
34 000	522.114	519.657	517.209	514.769	512.340	509.920	507.509	505.107	502.714	500.331
35 000	497.956		493.235		488.550		483.901		479.288	
36 000	474.711		470.170		465.672		461.217		456.805	
37 000	452.435		448.106		443.820		439.574		435.369	
38 000	431.203		427.078		422.993		418.946		414.938	
39 000	410.969		407.037		403.143		399.286		395.466	
40 000	391.683		387.936		384.225		380.549		376.908	
41 000	373.303		369.732		366.194		362.691		359.221	
42 000	355.785		352.381		349.010		345.671		342.364	
43 000	339.089		335.845		332.632		329.450		326.298	
44 000	323.177		320.084		317.023		313.990		310.986	
45 000	308.011		305.065		302.146		299.255		296.392	
46 000	293.527		290.749		287.967		285.213		282.484	
47 000	279.781		277.105		274.454		271.828		269.229	
48 000	266.652		264.102		261.574		259.072		256.594	
49 000	254.139		251.708		249.300		246.915		244.553	

APPENDIX A

TABLE A2.- Concluded

H, ft	0	200	400	600	800
50 000	242.213	239.896	237.601	235.328	233.177
51 000	230.847	228.639	226.451	224.285	222.139
52 000	220.014	217.910	215.825	213.760	211.715
53 000	209.690	207.683	205.697	203.729	201.780
54 000	199.850	197.938	196.044	194.168	192.311
55 000	190.471	188.649	186.844	185.057	183.286
56 000	181.533	179.797	178.077	176.373	174.685
57 000	173.014	171.359	169.720	168.096	166.488
58 000	164.895	163.318	161.755	160.208	158.675
59 000	157.157	155.654	154.165	152.690	151.229
60 000	149.783	148.350	146.930	145.525	144.132
61 000	142.754	141.388	140.035	138.696	137.369
62 000	136.055	134.753	133.464	132.187	130.923
63 000	129.670	128.430	127.201	125.984	124.779
64 000	123.585	122.403	121.187	120.072	118.923
65 000	117.785	116.659	115.543	114.437	113.343
66 000	112.259	111.186	110.123	109.071	108.029
67 000	106.997	105.976	104.965	103.963	102.971
68 000	101.989	101.017	100.054	99.1008	98.1566
69 000	97.2224	96.2966	95.3800	94.4725	93.5736
70 000	92.6839	91.8026	90.9306	90.0663	89.2105
71 000	88.3639	87.5244	86.6941	85.8715	85.0567
72 000	84.2505	83.4513	82.6605	81.8776	81.1017
73 000	80.3336	79.5733	78.8211	78.0739	77.3356
74 000	76.6043	75.8800	75.1623	74.4528	73.7490
75 000	73.0531	72.3626	71.6803	71.0034	70.3339
76 000	69.6705	69.0137	68.3632	67.7190	67.0810
77 000	66.4493	65.8236	65.2040	64.5906	63.9829
78 000	63.3811	62.7852	62.1950	61.6106	61.0318
79 000	60.4586	59.8909	59.3287	58.7720	58.2206
80 000	57.6745	57.1338	56.5981	56.0678	55.5425
81 000	55.0223	54.5071	53.9969	53.4914	52.9910
82 000	52.4953	52.0045	51.5183	51.0369	50.5601
83 000	50.0877	49.6200	49.1568	48.6980	48.2437
84 000	47.7937	47.3479	46.9065	46.4693	46.0364
85 000	45.6075	45.1828	44.7621	44.3455	43.9329
86 000	43.5242	43.1194	42.7186	42.3215	41.9282
87 000	41.5387	41.1529	40.7738	40.3924	40.0175
88 000	39.6463	39.2786	38.9144	38.5537	38.1964
89 000	37.8425	37.4920	37.1448	36.8009	36.4604
90 000	36.1231	35.7889	35.4580	35.1302	34.8056
91 000	34.4840	34.1654	33.8499	33.5374	33.2279
92 000	32.9213	32.6176	32.3168	32.0189	31.7237
93 000	31.4314	31.1419	30.8551	30.5710	30.2896
94 000	30.0108	29.7348	29.4613	29.1904	28.9221
95 000	28.6563	28.3930	28.1322	27.8739	27.6180
96 000	27.3645	27.1135	26.8648	26.6184	26.3744
97 000	26.1326	25.8932	25.6560	25.4210	25.1883
98 000	24.9578	24.7294	24.5032	24.2791	24.0571
99 000	23.8372	23.6194	23.4036	23.1898	22.9781
100 000	22.7683				

APPENDIX A

ORIGINAL PAGE IS
OF POOR QUALITY

TABLE A1.- DENSITY ρ IN POUNDS PER CUBIC FOOT FOR VALUES OF

PRESSURE ALTITUDE H IN GEOPOTENTIAL FEET

[From ref. A1]

H, ft	0	100	200	300	400	500	600	700	800	900
0	.076474	.076251	.076028	.075805	.075583	.075362	.075141	.074920	.074700	.074480
1 000	.074261	.074013	.073825	.073607	.073390	.073174	.072957	.072742	.072527	.072312
2 000	.072098	.071884	.071671	.071458	.071246	.071034	.070823	.070612	.070402	.070192
3 000	.069983	.069774	.069566	.069358	.069150	.068943	.068737	.068531	.068325	.068120
4 000	.067916	.067712	.067508	.067305	.067102	.066900	.066698	.066497	.066296	.066096
5 000	.065896	.065696	.065497	.065299	.065101	.064903	.064706	.064509	.064313	.064117
6 000	.063922	.063727	.063532	.063339	.063145	.062952	.062759	.062567	.062376	.062184
7 000	.061993	.061803	.061613	.061424	.061235	.061046	.060858	.060670	.060483	.060296
8 000	.060110	.059924	.059739	.059554	.059369	.059185	.059001	.058818	.058635	.058453
9 000	.058271	.058089	.057908	.057727	.057547	.057367	.057188	.057009	.056830	.056652
10 000	.056475	.056297	.056121	.055944	.055768	.055593	.055418	.055243	.055069	.054895
11 000	.054721	.054548	.054376	.054203	.054032	.053860	.053689	.053519	.053349	.053179
12 000	.053010	.052841	.052673	.052505	.052337	.052170	.052003	.051837	.051671	.051505
13 000	.051340	.051175	.051011	.050847	.050683	.050520	.050357	.050195	.050033	.049871
14 000	.049710	.049549	.049389	.049229	.049071	.048910	.048752	.048593	.048435	.048279
15 000	.048120	.047964	.047807	.047651	.047496	.047340	.047185	.047031	.046877	.046723
16 000	.046570	.046417	.046264	.046112	.045961	.045809	.045658	.045508	.045357	.045207
17 000	.045058	.044909	.044760	.044612	.044464	.044316	.044169	.044022	.043876	.043729
18 000	.043584	.043438	.043293	.043149	.043005	.042861	.042717	.042574	.042431	.042289
19 000	.042147	.042005	.041864	.041723	.041582	.041442	.041302	.041163	.041024	.040885
20 000	.040746	.040608	.040471	.040333	.040196	.040060	.039923	.039787	.039652	.039517
21 000	.039382	.039247	.039113	.038979	.038846	.038713	.038580	.038448	.038316	.038184
22 000	.038052	.037921	.037791	.037660	.037530	.037401	.037271	.037143	.037014	.036886
23 000	.036758	.036630	.036503	.036376	.036249	.036123	.035997	.035872	.035746	.035621
24 000	.035497	.035373	.035249	.035125	.035002	.034879	.034757	.034634	.034511	.034389
25 000	.034270	.034149	.034028	.033908	.033788	.033668	.033549	.033430	.033311	.033193
26 000	.033075	.032957	.032840	.032723	.032606	.032490	.032374	.032258	.032142	.032027
27 000	.031912	.031798	.031684	.031570	.031456	.031343	.031230	.031117	.031005	.030893
28 000	.030781	.030670	.030559	.030448	.030338	.030227	.030118	.030008	.029899	.029790
29 000	.029681	.029573	.029465	.029357	.029250	.029143	.029036	.028929	.028823	.028717
30 000	.028611	.028506	.028401	.028296	.028192	.028088	.027984	.027880	.027777	.027674
31 000	.027571	.027469	.027367	.027265	.027164	.027062	.026961	.026861	.026760	.026660
32 000	.026561	.026461	.026362	.026263	.026164	.026066	.025968	.025870	.025773	.025675
33 000	.025578	.025482	.025385	.025289	.025193	.025098	.025003	.024908	.024813	.024719
34 000	.024624	.024530	.024437	.024343	.024250	.024157	.024064	.023973	.023881	.023789
35 000	.023697		.023515		.023334		.023154		.022973	
36 000	.022798		.022598		.022382		.022166		.021951	
37 000	.021746		.021538		.021332		.021127		.020923	
38 000	.020725		.020527		.020330		.020136		.019943	
39 000	.019753		.019564		.019376		.019191		.019007	
40 000	.018826		.018646		.018467		.018291		.018116	
41 000	.017942		.017771		.017601		.017432		.017264	
42 000	.017100		.016937		.016775		.016614		.016455	
43 000	.016298		.016142		.015987		.015835		.015684	
44 000	.015533		.015384		.015237		.015091		.014947	
45 000	.014804		.014662		.014522		.014383		.014244	
46 000	.014139		.013994		.013841		.013691		.013542	
47 000	.013447		.013319		.013191		.013065		.012940	
48 000	.012916		.012794		.012672		.012552		.012433	
49 000	.012215		.012096		.011982		.011868		.011754	

APPENDIX A

TABLE A3.- Concluded

H, ft	0	200	400	600	800
50 000	0.011642	0.011530	0.011420	0.011311	0.011202
51 000	.011095	.010989	.010884	.010780	.010677
52 000	.010575	.010473	.010373	.010274	.010176
53 000	.010078	.0099820	.0098865	.0097919	.0096982
54 000	.0096055	.0095136	.0094226	.0093324	.0092431
55 000	.0091547	.0090671	.0089804	.0088945	.0088094
56 000	.0087251	.0086416	.0085590	.0084771	.0083960
57 000	.0083157	.0082361	.0081573	.0080793	.0079020
58 000	.0079254	.0078496	.0077745	.0077001	.0076265
59 000	.0075535	.0074813	.0074097	.0073388	.0072686
60 000	.0071991	.0071302	.0070620	.0069944	.0069275
61 000	.0068612	.0067956	.0067306	.0066662	.0066024
62 000	.0065393	.0064767	.0064147	.0063534	.0062926
63 000	.0062324	.0061728	.0061137	.0060552	.0059973
64 000	.0059399	.0058831	.0058268	.0057711	.0057159
65 000	.0056612	.0056070	.0055534	.0055003	.0054462
66 000	.0053926	.0053396	.0052871	.0052351	.0051836
67 000	.0051327	.0050823	.0050323	.0049829	.0049340
68 000	.0048856	.0048376	.0047902	.0047432	.0046967
69 000	.0046507	.0046051	.0045600	.0045154	.0044712
70 000	.0044274	.0043841	.0043412	.0042988	.0042567
71 000	.0042151	.0041740	.0041332	.0040928	.0040529
72 000	.0040133	.0039742	.0039354	.0038970	.0038590
73 000	.0038214	.0037842	.0037473	.0037108	.0036747
74 000	.0036385	.0036035	.0035685	.0035338	.0034994
75 000	.0034654	.0034318	.0033984	.0033654	.0033327
76 000	.0033004	.0032684	.0032367	.0032053	.0031742
77 000	.0031434	.0031130	.0030828	.0030530	.0030234
78 000	.0029942	.0029652	.0029365	.0029081	.0028800
79 000	.0028521	.0028246	.0027973	.0027703	.0027435
80 000	.0027171	.0026908	.0026649	.0026392	.0026137
81 000	.0025885	.0025636	.0025389	.0025144	.0024902
82 000	.0024663	.0024425	.0024190	.0023956	.0023727
83 000	.0023499	.0023273	.0023050	.0022828	.0022609
84 000	.0022392	.0022177	.0021964	.0021754	.0021546
85 000	.0021339	.0021134	.0020932	.0020731	.0020533
86 000	.0020336	.0020141	.0019949	.0019758	.0019569
87 000	.0019382	.0019197	.0019013	.0018831	.0018651
88 000	.0018474	.0018297	.0018123	.0017950	.0017779
89 000	.0017609	.0017441	.0017275	.0017110	.0016946
90 000	.0016786	.0016626	.0016468	.0016311	.0016156
91 000	.0016003	.0015851	.0015700	.0015551	.0015403
92 000	.0015257	.0015112	.0014969	.0014827	.0014687
93 000	.0014547	.0014409	.0014272	.0014137	.0014003
94 000	.0013873	.0013739	.0013609	.0013480	.0013353
95 000	.0013226	.0013091	.0012957	.0012825	.0012693
96 000	.0012613	.0012484	.0012357	.0012231	.0012104
97 000	.0012029	.0011906	.0011783	.0011662	.0011541
98 000	.0011473	.0011355	.0011235	.0011115	.0011000
99 000	.0010943	.0010829	.0010713	.0010597	.0010483
100 000	.0010434				

APPENDIX A

TABLE A4.- TEMPERATURE t IN DEGREES FAHRENHEIT FOR VALUES OF
PRESSURE ALTITUDE H IN GEOPOTENTIAL FEET

[From ref. A1]

H, ft	0	100	200	300	400	500	600	700	800	900
0	59.000	58.643	58.287	57.930	57.574	57.217	56.860	56.504	56.147	55.790
1 000	55.434	55.077	54.721	54.364	54.007	53.651	53.294	52.938	52.581	52.224
2 000	51.868	51.511	51.154	50.798	50.441	50.085	49.728	49.371	49.015	48.658
3 000	48.302	47.945	47.588	47.232	46.875	46.518	46.162	45.805	45.449	45.092
4 000	44.735	44.379	44.022	43.666	43.309	42.952	42.596	42.239	41.882	41.526
5 000	41.169	40.813	40.456	40.099	39.743	39.386	39.029	38.673	38.316	37.960
6 000	37.603	37.246	36.890	36.533	36.177	35.820	35.463	35.107	34.750	34.393
7 000	34.037	33.680	33.324	32.967	32.610	32.254	31.897	31.541	31.184	30.827
8 000	30.471	30.114	29.757	29.401	29.044	28.688	28.331	27.974	27.618	27.261
9 000	26.905	26.548	26.191	25.835	25.478	25.121	24.765	24.408	24.052	23.695
10 000	23.338	22.982	22.625	22.269	21.912	21.555	21.199	20.842	20.485	20.129
11 000	19.772	19.416	19.059	18.702	18.346	17.989	17.633	17.276	16.919	16.563
12 000	16.206	15.849	15.493	15.136	14.780	14.423	14.066	13.710	13.353	12.997
13 000	12.640	12.283	11.927	11.570	11.213	10.857	10.500	10.144	9.787	9.430
14 000	9.074	8.717	8.361	8.004	7.647	7.291	6.934	6.577	6.221	5.864
15 000	5.508	5.151	4.794	4.438	4.081	3.725	3.368	3.011	2.655	2.298
16 000	1.941	1.585	1.228	.872	.515	.158	-.198	-.555	-.911	-1.268
17 000	-1.265	-1.981	-2.338	-2.695	-3.051	-3.408	-3.764	-4.121	-4.478	-4.834
18 000	-5.191	-5.547	-5.904	-6.261	-6.617	-6.974	-7.331	-7.687	-8.044	-8.400
19 000	-8.757	-9.114	-9.470	-9.827	-10.184	-10.540	-10.897	-11.253	-11.610	-11.967
20 000	-12.323	-12.680	-13.036	-13.393	-13.750	-14.106	-14.463	-14.820	-15.176	-15.533
21 000	-15.889	-16.246	-16.603	-16.959	-17.316	-17.672	-18.029	-18.386	-18.742	-19.099
22 000	-19.456	-19.812	-20.169	-20.525	-20.882	-21.239	-21.595	-21.952	-22.308	-22.665
23 000	-23.022	-23.378	-23.735	-24.092	-24.448	-24.805	-25.161	-25.518	-25.875	-26.231
24 000	-26.588	-26.944	-27.301	-27.658	-28.014	-28.371	-28.728	-29.084	-29.441	-29.797
25 000	-30.154	-30.511	-30.867	-31.224	-31.580	-31.937	-32.294	-32.650	-33.007	-33.364
26 000	-33.720	-34.077	-34.433	-34.790	-35.147	-35.503	-35.860	-36.216	-36.573	-36.930
27 000	-37.286	-37.643	-38.000	-38.356	-38.713	-39.069	-39.426	-39.783	-40.139	-40.496
28 000	-40.852	-41.209	-41.566	-41.922	-42.279	-42.636	-42.992	-43.349	-43.705	-44.062
29 000	-44.419	-44.775	-45.132	-45.488	-45.845	-46.202	-46.558	-46.915	-47.272	-47.628
30 000	-47.985	-48.341	-48.698	-49.055	-49.411	-49.768	-50.124	-50.481	-50.838	-51.194
31 000	-51.551	-51.908	-52.264	-52.621	-52.977	-53.334	-53.691	-54.047	-54.404	-54.761
32 000	-55.117	-55.474	-55.830	-56.187	-56.544	-56.900	-57.257	-57.613	-57.970	-58.327
33 000	-58.683	-59.040	-59.397	-59.753	-60.110	-60.466	-60.823	-61.180	-61.536	-61.893
34 000	-62.249	-62.606	-62.963	-63.319	-63.676	-64.033	-64.389	-64.746	-65.102	-65.459
35 000	-65.816		-66.529		-67.242		-67.955		-68.669	
36 000	-69.382									
36 000										
to	-69.700									
65 000										

APPENDIX A

TABLE A4.- Concluded

H, ft	0	200	400	600	800
65 000					-69.599
66 000	-69.490	-69.380	-69.270	-69.161	-69.051
67 000	-68.941	-68.831	-68.722	-68.612	-68.520
68 000	-68.392	-68.283	-68.173	-68.063	-67.954
69 000	-67.844	-67.734	-67.624	-67.515	-67.405
70 000	-67.295	-67.185	-67.076	-66.966	-66.856
71 000	-66.747	-66.637	-66.527	-66.417	-66.308
72 000	-66.198	-66.088	-65.978	-65.869	-65.759
73 000	-65.649	-65.540	-65.430	-65.320	-65.210
74 000	-65.101	-64.991	-64.881	-64.771	-64.662
75 000	-64.552	-64.442	-64.333	-64.223	-64.113
76 000	-64.003	-63.894	-63.784	-63.674	-63.564
77 000	-63.455	-63.345	-63.235	-63.126	-63.016
78 000	-62.906	-62.796	-62.687	-62.577	-62.467
79 000	-62.357	-62.248	-62.138	-62.028	-61.919
80 000	-61.809	-61.699	-61.589	-61.480	-61.370
81 000	-61.260	-61.150	-61.041	-60.931	-60.821
82 000	-60.712	-60.602	-60.492	-60.382	-60.273
83 000	-60.163	-60.053	-59.943	-59.834	-59.724
84 000	-59.614	-59.505	-59.395	-59.285	-59.175
85 000	-59.066	-58.956	-58.846	-58.736	-58.627
86 000	-58.517	-58.407	-58.298	-58.188	-58.078
87 000	-57.968	-57.859	-57.749	-57.639	-57.529
88 000	-57.420	-57.310	-57.200	-57.090	-56.981
89 000	-56.871	-56.761	-56.652	-56.542	-56.432
90 000	-56.322	-56.213	-56.103	-55.993	-55.883
91 000	-55.774	-55.664	-55.554	-55.445	-55.335
92 000	-55.225	-55.115	-55.006	-54.896	-54.786
93 000	-54.676	-54.567	-54.457	-54.347	-54.238
94 000	-54.128	-54.018	-53.908	-53.799	-53.689
95 000	-53.579	-53.469	-53.360	-53.250	-53.140
96 000	-53.031	-52.921	-52.811	-52.701	-52.592
97 000	-52.482	-52.372	-52.262	-52.153	-52.043
98 000	-51.933	-51.824	-51.714	-51.604	-51.494
99 000	-51.385	-51.275	-51.165	-51.055	-50.946
100 000	-50.836				

APPENDIX A

ORIGINAL PAGE IS
OF POOR QUALITYTABLE A5.- TEMPERATURE t IN DEGREES CENTIGRADE FOR VALUES OF
PRESSURE ALTITUDE H IN GEOPOTENTIAL FEET

[From ref. A1]

H, ft	0	100	200	300	400	500	600	700	800	900
0	15.000	14.802	14.604	14.406	14.208	14.009	13.811	13.613	13.415	13.217
1 000	13.019	12.821	12.623	12.424	12.226	12.028	11.830	11.632	11.434	11.236
2 000	11.038	10.839	10.641	10.443	10.245	10.047	9.849	9.651	9.453	9.255
3 000	9.056	8.858	8.660	8.462	8.264	8.066	7.868	7.670	7.471	7.273
4 000	7.075	6.877	6.679	6.481	6.283	6.085	5.886	5.688	5.490	5.292
5 000	5.094	4.896	4.698	4.500	4.302	4.103	3.905	3.707	3.509	3.311
6 000	3.113	2.915	2.717	2.518	2.320	2.122	1.924	1.726	1.528	1.330
7 000	1.132	.933	.735	.537	.339	.141	-.057	-.255	-.453	-.651
8 000	-.850	-1.048	-1.246	-1.444	-1.642	-1.840	-2.038	-2.236	-2.435	-2.633
9 000	-2.831	-3.029	-3.227	-3.425	-3.623	-3.821	-4.020	-4.218	-4.416	-4.614
10 000	-4.812	-5.010	-5.208	-5.406	-5.604	-5.803	-6.001	-6.199	-6.397	-6.595
11 000	-6.793	-6.991	-7.189	-7.388	-7.586	-7.784	-7.982	-8.180	-8.378	-8.576
12 000	-8.774	-8.973	-9.171	-9.369	-9.567	-9.765	-9.963	-10.161	-10.359	-10.557
13 000	-10.756	-10.954	-11.152	-11.350	-11.548	-11.746	-11.944	-12.142	-12.341	-12.539
14 000	-12.737	-12.935	-13.133	-13.331	-13.529	-13.727	-13.926	-14.124	-14.322	-14.520
15 000	-14.718	-14.916	-15.114	-15.312	-15.510	-15.709	-15.907	-16.105	-16.303	-16.501
16 000	-16.699	-16.897	-17.095	-17.294	-17.492	-17.690	-17.888	-18.086	-18.284	-18.482
17 000	-18.680	-18.879	-19.077	-19.275	-19.473	-19.671	-19.869	-20.067	-20.265	-20.463
18 000	-20.662	-20.860	-21.058	-21.256	-21.454	-21.652	-21.850	-22.048	-22.247	-22.445
19 000	-22.643	-22.841	-23.039	-23.237	-23.435	-23.633	-23.832	-24.030	-24.228	-24.426
20 000	-24.624	-24.822	-25.020	-25.218	-25.416	-25.615	-25.813	-26.011	-26.209	-26.407
21 000	-26.605	-26.803	-27.001	-27.200	-27.398	-27.596	-27.794	-27.992	-28.190	-28.388
22 000	-28.586	-28.785	-28.983	-29.181	-29.379	-29.577	-29.775	-29.973	-30.171	-30.369
23 000	-30.568	-30.766	-30.964	-31.162	-31.360	-31.558	-31.756	-31.954	-32.153	-32.351
24 000	-32.549	-32.747	-32.945	-33.143	-33.341	-33.539	-33.738	-33.936	-34.134	-34.332
25 000	-34.530	-34.728	-34.926	-35.124	-35.322	-35.521	-35.719	-35.917	-36.115	-36.313
26 000	-36.511	-36.709	-36.907	-37.106	-37.304	-37.502	-37.700	-37.898	-38.096	-38.294
27 000	-38.492	-38.691	-38.889	-39.087	-39.285	-39.483	-39.681	-39.879	-40.077	-40.275
28 000	-40.474	-40.672	-40.870	-41.068	-41.266	-41.464	-41.662	-41.860	-42.059	-42.257
29 000	-42.455	-42.653	-42.851	-43.049	-43.247	-43.445	-43.644	-43.842	-44.040	-44.238
30 000	-44.436	-44.634	-44.832	-45.030	-45.228	-45.427	-45.625	-45.823	-46.021	-46.219
31 000	-46.417	-46.615	-46.813	-47.012	-47.210	-47.408	-47.606	-47.804	-48.002	-48.200
32 000	-48.398	-48.597	-48.795	-48.993	-49.191	-49.389	-49.587	-49.785	-49.983	-50.181
33 000	-50.380	-50.578	-50.776	-50.974	-51.172	-51.370	-51.568	-51.766	-51.965	-52.163
34 000	-52.361	-52.559	-52.757	-52.955	-53.153	-53.351	-53.550	-53.748	-53.946	-54.144
35 000	-54.342		-54.738		-55.134		-55.531		-55.927	
36 000	-56.323									
36 090 to 65 800	-56.500									

APPENDIX A

TABLE A5.- Concluded

H, ft	0	200	400	600	800
65 000					-56.444
66 000	-56.383	-56.322	-56.261	-56.200	-56.139
67 000	-56.078	-56.017	-55.956	-55.896	-55.835
68 000	-55.774	-55.713	-55.652	-55.591	-55.530
69 000	-55.469	-55.408	-55.347	-55.286	-55.225
70 000	-55.164	-55.103	-55.042	-54.981	-54.920
71 000	-54.859	-54.798	-54.737	-54.676	-54.615
72 000	-54.554	-54.493	-54.432	-54.372	-54.311
73 000	-54.250	-54.189	-54.128	-54.067	-54.006
74 000	-53.945	-53.884	-53.823	-53.762	-53.701
75 000	-53.640	-53.579	-53.518	-53.457	-53.396
76 000	-53.335	-53.274	-53.213	-53.152	-53.091
77 000	-53.030	-52.969	-52.908	-52.848	-52.787
78 000	-52.726	-52.665	-52.604	-52.543	-52.482
79 000	-52.421	-52.360	-52.299	-52.238	-52.177
80 000	-52.116	-52.055	-51.994	-51.933	-51.872
81 000	-51.811	-51.750	-51.689	-51.628	-51.567
82 000	-51.506	-51.445	-51.384	-51.324	-51.263
83 000	-51.202	-51.141	-51.080	-51.019	-50.958
84 000	-50.897	-50.836	-50.775	-50.714	-50.653
85 000	-50.592	-50.531	-50.470	-50.409	-50.348
86 000	-50.287	-50.226	-50.165	-50.104	-50.043
87 000	-49.982	-49.921	-49.860	-49.800	-49.739
88 000	-49.678	-49.617	-49.556	-49.495	-49.434
89 000	-49.373	-49.312	-49.251	-49.190	-49.129
90 000	-49.068	-49.007	-48.946	-48.885	-48.824
91 000	-48.763	-48.702	-48.641	-48.580	-48.519
92 000	-48.458	-48.397	-48.336	-48.276	-48.215
93 000	-48.154	-48.093	-48.032	-47.971	-47.910
94 000	-47.849	-47.788	-47.727	-47.666	-47.605
95 000	-47.544	-47.483	-47.422	-47.361	-47.300
96 000	-47.239	-47.178	-47.117	-47.056	-46.995
97 000	-46.934	-46.873	-46.812	-46.752	-46.691
98 000	-46.630	-46.569	-46.508	-46.447	-46.386
99 000	-46.325	-46.264	-46.203	-46.142	-46.081
100 000	-46.020				

APPENDIX A

ORIGINAL PAGE IS
OF POOR QUALITY

TABLE A6.- COEFFICIENT OF VISCOSITY μ in POUND-SECONDS PER SQUARE FOOT

FOR VALUES OF PRESSURE ALTITUDE H IN GEOPOTENTIAL FEET

[From ref. A1]

H, ft	μ , lb-sec/ft ²	H, ft	μ , lb-sec/ft ²
0	3.7372×10^{-7}	36 090	
1 000	3.7173	to	2.9691×10^{-7}
2 000	3.6971	65 800	
3 000	3.6769	66 000	2.9704
4 000	3.6567	67 000	2.9740
5 000	3.6365	68 000	2.9774
6 000	3.6163	69 000	2.9809
7 000	3.5958		
8 000	3.5752	70 000	2.9844
9 000	3.5547	71 000	2.9879
		72 000	2.9914
10 000	3.5342	73 000	2.9949
11 000	3.5134	74 000	2.9984
12 000	3.4926	75 000	3.0018
13 000	3.4717	76 000	3.0053
14 000	3.4509	77 000	3.0088
15 000	3.4301	78 000	3.0123
16 000	3.4090	79 000	3.0157
17 000	3.3878		
18 000	3.3667	80 000	3.0192
19 000	3.3452	81 000	3.0227
		82 000	3.0261
20 000	3.3238	83 000	3.0296
21 000	3.3027	84 000	3.0331
22 000	3.2809	85 000	3.0365
23 000	3.2595	86 000	3.0400
24 000	3.2377	87 000	3.0435
25 000	3.2160	88 000	3.0469
26 000	3.1942	89 000	3.0504
27 000	3.1721		
28 000	3.1501	90 000	3.0538
29 000	3.1280	91 000	3.0573
		92 000	3.0607
30 000	3.1060	93 000	3.0641
31 000	3.0837	94 000	3.0676
32 000	3.0614	95 000	3.0710
33 000	3.0389	96 000	3.0744
34 000	3.0164	97 000	3.0779
35 000	2.9938	98 000	3.0813
36 000	2.9711	99 000	3.0847
		100 000	3.0882

APPENDIX A

TABLE A7.- SPEED OF SOUND *a* IN MILES PER HOUR AND KNOTS FOR VALUES
OF PRESSURE ALTITUDE *H* IN GEOPOTENTIAL FEET

[From ref. A1]

H, ft	a, mph	a, knots	H, ft	a, mph	a, knots
0	761.22	661.48	36 090		
1 000	758.60	659.20	to	660.05	573.57
2 000	755.97	656.92	65 800		
3 000	753.33	654.62	66 000	660.23	573.73
4 000	750.67	652.32	67 000	660.70	574.13
5 000	748.01	650.01	68 000	661.16	574.53
6 000	745.35	647.69	69 000	661.62	574.93
7 000	742.67	645.35			
8 000	739.98	643.03	70 000	662.09	575.34
9 000	737.29	640.68	71 000	662.54	575.73
			72 000	663.01	576.14
10 000	734.58	638.33	73 000	663.47	576.54
11 000	731.86	635.97	74 000	663.93	576.94
12 000	729.13	633.60	75 000	664.39	577.34
13 000	726.40	631.22	76 000	664.85	577.74
14 000	723.65	628.84	77 000	665.32	578.15
15 000	720.89	626.44	78 000	665.77	578.54
16 000	718.12	624.03	79 000	666.24	578.95
17 000	715.34	621.62			
18 000	712.55	619.19	80 000	666.70	579.34
19 000	709.75	616.76	81 000	667.16	579.75
			82 000	667.62	580.14
20 000	706.94	614.32	83 000	668.07	580.54
21 000	704.12	611.86	84 000	668.53	580.94
22 000	701.28	609.40	85 000	668.99	581.34
23 000	698.44	606.93	86 000	669.45	581.74
24 000	695.58	604.44	87 000	669.91	582.13
25 000	692.71	601.95	88 000	670.36	582.53
26 000	689.83	599.44	89 000	670.82	582.93
27 000	686.93	596.93			
28 000	684.03	594.41	90 000	671.28	583.32
29 000	681.11	591.87	91 000	671.73	583.72
			92 000	672.19	584.12
30 000	678.18	589.32	93 000	672.65	584.51
31 000	675.24	586.76	94 000	673.10	584.91
32 000	672.28	584.20	95 000	673.55	585.30
33 000	669.31	581.61	96 000	674.01	585.70
34 000	666.33	579.02	97 000	674.47	586.10
35 000	663.33	576.42	98 000	674.92	586.49
36 000	660.32	573.80	99 000	675.37	586.88
			100 000	675.82	587.28

APPENDIX A

ORIGINAL PAGE IS
OF POOR QUALITY

TABLE A8.- ACCELERATION DUE TO GRAVITY g IN FEET PER SECOND SQUARED

FOR VALUES OF PRESSURE ALTITUDE H IN GEOPOTENTIAL FEET

[From ref. A1]

H , ft	g , ft/sec ²	H , ft	g , ft/sec ²
0	32.174	50 000	32.020
1 000	32.171	51 000	32.017
2 000	32.168	52 000	32.014
3 000	32.165	53 000	32.011
4 000	32.162	54 000	32.008
5 000	32.159	55 000	32.005
6 000	32.156	56 000	32.001
7 000	32.152	57 000	31.998
8 000	32.149	58 000	31.995
9 000	32.145	59 000	31.992
10 000	32.143	60 000	31.989
11 000	32.140	61 000	31.986
12 000	32.137	62 000	31.983
13 000	32.134	63 000	31.980
14 000	32.131	64 000	31.977
15 000	32.128	65 000	31.974
16 000	32.125	66 000	31.971
17 000	32.122	67 000	31.968
18 000	32.119	68 000	31.965
19 000	32.115	69 000	31.961
20 000	32.112	70 000	31.958
21 000	32.109	71 000	31.955
22 000	32.106	72 000	31.952
23 000	32.103	73 000	31.949
24 000	32.100	74 000	31.946
25 000	32.097	75 000	31.943
26 000	32.094	76 000	31.940
27 000	32.091	77 000	31.937
28 000	32.088	78 000	31.934
29 000	32.085	79 000	31.931
30 000	32.082	80 000	31.928
31 000	32.078	81 000	31.925
32 000	32.075	82 000	31.922
33 000	32.072	83 000	31.918
34 000	32.069	84 000	31.915
35 000	32.066	85 000	31.912
36 000	32.063	86 000	31.909
37 000	32.060	87 000	31.906
38 000	32.057	88 000	31.903
39 000	32.054	89 000	31.900
40 000	32.051	90 000	31.897
41 000	32.048	91 000	31.894
42 000	32.045	92 000	31.891
43 000	32.041	93 000	31.888
44 000	32.038	94 000	31.885
45 000	32.035	95 000	31.882
46 000	32.032	96 000	31.878
47 000	32.029	97 000	31.875
48 000	32.026	98 000	31.872
49 000	32.023	99 000	31.869
		100 000	31.866

APPENDIX A

TABLE A9.- IMPACT PRESSURE q_c (OR q_c') IN INCHES OF MERCURY (10^3 C) FOR VALUES OF
CALIBRATED AIRSPEED V_c (OR INDICATED AIRSPEED V_i) IN MILES PER HOUR
[From ref. A2]

V_c mph	0	1	2	3	4	5	6	7	8	9
0	0.000000	0.000030	0.000147	0.000323	0.000574	0.000901	0.001299	0.001768	0.002313	0.002932
10	.003611	.004377	.005203	.006104	.007088	.008136	.009258	.010451	.011708	.013049
20	.014461	.015939	.017501	.019129	.020825	.022594	.024440	.026358	.028347	.030412
30	.032539	.034751	.037025	.039382	.041806	.044304	.046869	.049508	.052228	.055119
40	.057871	.060866	.063816	.066806	.070034	.073256	.076551	.079920	.083358	.086876
50	.090464	.094126	.097851	.101652	.105535	.109485	.113509	.117603	.121771	.126016
60	.130231	.134712	.139179	.143709	.148323	.152999	.157751	.162574	.167472	.172448
70	.177496	.182606	.187804	.193064	.198411	.203818	.209302	.214859	.220437	.226136
80	.231977	.237832	.243751	.249756	.255824	.261976	.268196	.274489	.280853	.287298
90	.293812	.300397	.307058	.313802	.320606	.327488	.334454	.341485	.348592	.355770
100	.363029	.370347	.377756	.385239	.392785	.400406	.408111	.415888	.423736	.431659
110	.439657	.447733	.455874	.464097	.472391	.480772	.489213	.497731	.506328	.515008
120	.523742	.532566	.541464	.550443	.559480	.568606	.577777	.587070	.596414	.605837
130	.615334	.624912	.634564	.644292	.654085	.663965	.673914	.683940	.694039	.704227
140	.714481	.724804	.735210	.745698	.756263	.766894	.777600	.788395	.799257	.810199
150	.821216	.832311	.843483	.854734	.866050	.877456	.888931	.900480	.912117	.923825
160	.935611	.947472	.959413	.971424	.983524	.995699	1.00795	1.02028	1.03268	1.04516
170	1.05772	1.07036	1.08307	1.09586	1.10873	1.12168	1.13470	1.14782	1.16103	1.17426
180	1.18760	1.20103	1.21451	1.22809	1.24175	1.25548	1.26929	1.28319	1.29716	1.31120
190	1.32533	1.33953	1.35382	1.36819	1.38263	1.39716	1.41176	1.42645	1.44121	1.45605
200	1.47097	1.48597	1.50106	1.51622	1.53146	1.54679	1.56219	1.57768	1.59324	1.60889
210	1.62461	1.64042	1.65630	1.67228	1.68833	1.70445	1.72066	1.73695	1.75333	1.76978
220	1.78631	1.80294	1.81964	1.83642	1.85328	1.87022	1.88725	1.90435	1.92155	1.93882
230	1.95617	1.97362	1.99114	2.00874	2.02643	2.04419	2.06204	2.07998	2.09800	2.11610
240	2.13429	2.15255	2.17090	2.18933	2.20785	2.22645	2.24514	2.26390	2.28276	2.30170
250	2.32071	2.33983	2.35902	2.37829	2.39765	2.41710	2.43662	2.45624	2.47594	2.49572
260	2.51558	2.53555	2.55558	2.57571	2.59592	2.61622	2.63659	2.65706	2.67762	2.69826
270	2.71899	2.73980	2.76070	2.78168	2.80276	2.82392	2.84516	2.86650	2.88792	2.90943
280	2.93102	2.95271	2.97448	2.99634	3.01828	3.04032	3.06244	3.08464	3.10695	3.12933
290	3.15181	3.17436	3.19703	3.21976	3.24260	3.26552	3.28853	3.31163	3.33481	3.35809
300	3.38145	3.40491	3.42845	3.45209	3.47582	3.49963	3.52354	3.54754	3.57163	3.59581
310	3.62008	3.64444	3.66890	3.69343	3.71807	3.74279	3.76761	3.79253	3.81752	3.84262
320	3.86781	3.89308	3.91845	3.94392	3.96947	3.99512	4.02087	4.04670	4.07262	4.09865
330	4.12477	4.15097	4.17728	4.20367	4.23016	4.25674	4.28343	4.31020	4.33707	4.36403
340	4.39109	4.41824	4.44549	4.47282	4.50027	4.52780	4.55544	4.58316	4.61098	4.63880
350	4.66691	4.69502	4.72323	4.75153	4.77993	4.80843	4.83703	4.86572	4.89452	4.92343
360	4.95238	4.98147	5.01064	5.03992	5.06931	5.09878	5.12835	5.15803	5.18780	5.21768
370	5.24764	5.27772	5.30788	5.33816	5.36853	5.39899	5.42957	5.46024	5.49100	5.52187
380	5.55285	5.58392	5.61510	5.64638	5.67775	5.70923	5.74080	5.77249	5.80428	5.83617
390	5.86816	5.90025	5.93244	5.96475	5.99715	6.02965	6.06227	6.09498	6.12780	6.16071
400	6.19373	6.22686	6.26012	6.29343	6.32688	6.36043	6.39407	6.42783	6.46169	6.49566
410	6.52974	6.56393	6.59820	6.63260	6.66710	6.70171	6.73642	6.77124	6.80617	6.84121
420	6.87635	6.91161	6.94696	6.98243	7.01800	7.05369	7.08949	7.12539	7.16140	7.19752
430	7.23375	7.27009	7.30655	7.34310	7.37978	7.41656	7.45344	7.49046	7.52757	7.56479
440	7.60213	7.63958	7.67713	7.71480	7.75258	7.79048	7.82849	7.86660	7.90485	7.94319
450	7.98166	8.02022	8.05891	8.09772	8.13663	8.17566	8.21481	8.25407	8.29345	8.33294
460	8.37254	8.41226	8.45209	8.49205	8.53212	8.57229	8.61261	8.65302	8.69356	8.73421
470	8.77498	8.81587	8.85688	8.89800	8.93924	8.98060	9.02208	9.06368	9.10540	9.14723
480	9.18919	9.23127	9.27346	9.31578	9.35821	9.40077	9.44345	9.48625	9.52917	9.57221
490	9.61537	9.65866	9.70227	9.74560	9.78926	9.83313	9.87729	9.92165	9.96620	10.01094
500	10.05536	10.10043	10.14529	10.19077	10.23626	10.28276	10.32927	10.37600	10.42294	10.47009
510	10.51746	10.56503	10.61262	10.66033	10.70844	10.75677	10.80521	10.85386	10.90261	10.95147
520	11.00044	11.04927	11.09823	11.14730	11.19648	11.24577	11.29527	11.34497	11.39477	11.44467
530	11.49467	11.54477	11.59497	11.64527	11.69567	11.74617	11.79677	11.84747	11.89827	11.94917
540	12.00017	12.05127	12.10247	12.15367	12.20487	12.25607	12.30727	12.35847	12.40967	12.46087
550	12.51207	12.56327	12.61447	12.66567	12.71687	12.76807	12.81927	12.87047	12.92167	12.97287
560	13.02407	13.07527	13.12647	13.17767	13.22887	13.27997	13.33117	13.38237	13.43357	13.48477
570	13.53597	13.58717	13.63837	13.68957	13.74077	13.79197	13.84317	13.89437	13.94557	14.00000
580	14.04997	14.10117	14.15237	14.20357	14.25477	14.30597	14.35717	14.40837	14.45957	14.51077
590	14.56197	14.61317	14.66437	14.71557	14.76677	14.81797	14.86917	14.92037	14.97157	15.02277

APPENDIX A

TABLE A9.- Concluded

ORIGINAL PAGE IS
OF POOR QUALITY

V _c mph	0	1	2	3	4	5	6	7	8	9
600	15.1613	15.2195	15.2778	15.3361	15.3950	15.4538	15.5128	15.5719	15.6312	15.6906
610	15.7502	15.8099	15.8698	15.9298	15.9900	16.0503	16.1108	16.1715	16.2323	16.2933
620	16.3544	16.4156	16.4771	16.5387	16.6004	16.6623	16.7244	16.7866	16.8490	16.9116
630	16.9743	17.0371	17.1001	17.1633	17.2267	17.2902	17.3538	17.4176	17.4816	17.5458
640	17.6101	17.6746	17.7392	17.8040	17.8690	17.9341	17.9994	18.0649	18.1305	18.1963
650	18.2622	18.3284	18.3946	18.4611	18.5277	18.5945	18.6615	18.7286	18.7959	18.8634
660	18.9310	18.9988	19.0668	19.1349	19.2032	19.2717	19.3404	19.4092	19.4782	19.5474
670	19.6167	19.6863	19.7560	19.8258	19.8959	19.9661	20.0365	20.1070	20.1778	20.2487
680	20.3198	20.3911	20.4625	20.5341	20.6059	20.6779	20.7501	20.8224	20.8949	20.9676
690	21.0405	21.1136	21.1868	21.2602	21.3338	21.4076	21.4816	21.5557	21.6300	21.7046
700	21.7793	21.8541	21.9292	22.0045	22.0799	22.1555	22.2313	22.3073	22.3835	22.4599
710	22.5364	22.6132	22.6901	22.7672	22.8446	22.9220	22.9997	23.0776	23.1557	23.2339
720	23.3124	23.3911	23.4699	23.5489	23.6281	23.7076	23.7872	23.8670	23.9470	24.0272
730	24.1076	24.1881	24.2689	24.3499	24.4311	24.5125	24.5940	24.6758	24.7578	24.8399
740	24.9223	25.0049	25.0877	25.1706	25.2538	25.3372	25.4207	25.5045	25.5885	25.6727
750	25.7571	25.8417	25.9265	26.0115	26.0967	26.1821	26.2677	26.3535	26.4396	26.5258
760	26.6122	26.6989	26.7861	26.8731	26.9604	27.0479	27.1356	27.2235	27.3116	27.4000
770	27.4885	27.5772	27.6661	27.7553	27.8446	27.9341	28.0239	28.1138	28.2040	28.2943
780	28.3848	28.4756	28.5665	28.6577	28.7490	28.8405	28.9323	29.0242	29.1163	29.2086
790	29.3011	29.3939	29.4868	29.5799	29.6732	29.7667	29.8603	29.9542	30.0483	30.1425
800	30.2370	30.3316	30.4264	30.5214	30.6166	30.7120	30.8076	30.9034	30.9994	31.0955
810	31.1918	31.2884	31.3851	31.4820	31.5791	31.6763	31.7738	31.8714	31.9692	32.0672
820	32.1654	32.2638	32.3624	32.4611	32.5600	32.6591	32.7584	32.8579	32.9575	33.0574
830	33.1574	33.2576	33.3579	33.4585	33.5592	33.6601	33.7612	33.8625	33.9639	34.0655
840	34.1674	34.2693	34.3715	34.4738	34.5763	34.6790	34.7819	34.8849	34.9881	35.0915
850	35.1951	35.2988	35.4027	35.5068	35.6111	35.7155	35.8201	35.9249	36.0299	36.1350
860	36.2403	36.3458	36.4514	36.5572	36.6632	36.7694	36.8757	36.9822	37.0889	37.1957
870	37.3027	37.4099	37.5173	37.6248	37.7325	37.8404	37.9484	38.0566	38.1649	38.2735
880	38.3822	38.4910	38.6001	38.7093	38.8187	38.9282	39.0379	39.1478	39.2578	39.3680
890	39.4784	39.5889	39.6996	39.8105	39.9215	40.0327	40.1441	40.2556	40.3673	40.4792
900	40.5912	40.7034	40.8157	40.9283	41.0409	41.1538	41.2668	41.3799	41.4933	41.6068
910	41.7204	41.8342	41.9482	42.0624	42.1767	42.2911	42.4057	42.5205	42.6355	42.7506
920	42.8659	42.9813	43.0969	43.2126	43.3286	43.4446	43.5609	43.6772	43.7938	43.9105
930	44.0274	44.1444	44.2616	44.3790	44.4965	44.6141	44.7320	44.8499	44.9681	45.0864
940	45.2049	45.3235	45.4422	45.5612	45.6803	45.7995	45.9189	46.0385	46.1581	46.2781
950	46.3981	46.5183	46.6386	46.7591	46.8798	47.0006	47.1216	47.2427	47.3640	47.4854
960	47.6070	47.7288	47.8506	47.9727	48.0949	48.2173	48.3398	48.4625	48.5853	48.7083
970	48.8315	48.9547	49.0782	49.2018	49.3256	49.4495	49.5735	49.6977	49.8221	49.9467
980	50.0713	50.1962	50.3211	50.4463	50.5716	50.6970	50.8226	50.9484	51.0743	51.2003
990	51.3265	51.4529	51.5794	51.7061	51.8329	51.9598	52.0870	52.2142	52.3417	52.4692
1000	52.5970	52.7248	52.8529	52.9810	53.1094	53.2379	53.3665	53.4953	53.6242	53.7533
1010	53.8825	54.0119	54.1414	54.2711	54.4010	54.5309	54.6611	54.7914	54.9218	55.0524
1020	55.1831	55.3140	55.4450	55.5762	55.7076	55.8390	55.9707	56.1024	56.2344	56.3665
1030	56.4987	56.6311	56.7636	56.8963	57.0291	57.1621	57.2952	57.4285	57.5619	57.6954
1040	57.8292	57.9630	58.0970	58.2312	58.3655	58.4999	58.6345	58.7693	58.9042	59.0392
1050	59.1744	59.3098	59.4452	59.5809	59.7167	59.8526	59.9887	60.1249	60.2613	60.3978
1060	60.5344	60.6712	60.8082	60.9453	61.0826	61.2200	61.3575	61.4952	61.6330	61.7711
1070	61.9091	62.0474	62.1858	62.3244	62.4631	62.6020	62.7410	62.8801	63.0194	63.1589
1080	63.2985	63.4382	63.5781	63.7181	63.8583	63.9986	64.1391	64.2797	64.4204	64.5613
1090	64.7023	64.8435	64.9849	65.1263	65.2680	65.4097	65.5517	65.6937	65.8359	65.9783
1100	66.1208									

APPENDIX A

TABLE A10.- IMPACT PRESSURE q_c FOR q_0 IN POUNDS PER SQUARE FOOT FOR VALUES V_0 CALIBRATED AIRSPEED V_0 OR INDICATED AIRSPEED V_i IN MILES PER HOUR
[From ref. A.]

V_0 mph	0	1	2	3	4	5	6	7	8	9
0	0	0.002116	0.010369	0.022855	0.040631	0.063698	0.091844	0.125068	0.163384	0.20779
10	.255427	.109603	.368010	.431708	.501332	.575393	.654758	.739195	.828076	.92249
20	1.02277	1.12731	1.23778	1.35290	1.47289	1.59796	1.72853	1.86418	2.00490	2.1515
30	2.30139	2.45777	2.61861	2.78516	2.95678	3.13348	3.31484	3.50149	3.69386	3.891
40	4.03298	4.30058	4.51347	4.73059	4.95322	5.18113	5.41413	5.65242	5.89557	6.1444
50	6.39817	6.65720	6.92066	7.18942	7.46411	7.74345	8.02804	8.31758	8.61237	8.9127
60	9.21782	9.52763	9.84358	10.1640	10.4903	10.8211	11.1571	11.4983	11.8447	12.196
70	12.5536	12.9151	13.2826	13.6547	14.0328	14.4152	14.8032	15.1961	15.5942	15.998
80	16.4068	16.8210	17.2366	17.6643	18.0934	18.5285	18.9685	19.4135	19.8637	20.319
90	20.7802	21.2460	21.7170	22.1940	22.6753	23.1620	23.6547	24.1520	24.6546	25.162
100	25.6756	26.1933	26.7172	27.2465	27.7802	28.3192	28.8641	29.4141	29.9692	30.5296
110	31.0953	31.6664	32.2423	32.8238	33.4104	34.0032	34.6001	35.2026	35.8106	36.4245
120	37.0423	37.6663	38.2957	38.9308	39.5699	40.2153	40.8654	41.5212	42.1821	42.8485
130	43.5202	44.1976	44.8803	45.5683	46.2609	46.9597	47.6633	48.3725	49.0867	49.8073
140	50.5325	51.2626	51.9986	52.7434	53.4876	54.2395	54.9967	55.7602	56.5284	57.3021
150	58.0815	58.8662	59.6564	60.4521	61.2524	62.0591	62.8707	63.6876	64.5105	65.3386
160	66.1722	67.0111	67.8557	68.7051	69.5609	70.4220	71.2882	72.1603	73.0372	73.919
170	74.8063	75.7224	76.6016	77.5062	78.4162	79.3321	80.2531	81.1806	82.1133	83.0517
180	83.9943	84.9441	85.8973	86.8582	87.8241	88.7956	89.7723	90.7550	91.7425	92.734
190	93.7355	94.7401	95.7508	96.7666	97.7885	98.8161	99.8486	100.887	101.931	102.981
200	104.936	105.997	107.064	107.236	108.315	109.399	110.488	111.583	112.683	113.792
210	114.903	116.021	117.144	118.274	119.409	120.549	121.696	122.848	124.006	125.175
220	126.339	127.515	128.696	129.883	131.075	132.274	133.478	134.688	135.904	137.125
230	138.353	139.587	140.826	142.071	143.322	144.578	145.841	147.109	148.383	149.663
240	150.950	152.242	153.539	154.843	156.153	157.469	158.790	160.117	161.451	162.792
250	164.135	165.487	166.84	168.208	169.577	170.952	172.333	173.720	175.114	176.514
260	177.918	179.333	180.747	182.170	183.599	185.035	186.476	187.924	189.378	190.837
270	192.304	193.776	195.254	196.738	198.228	199.725	201.229	202.737	204.251	205.773
280	207.300	208.834	210.374	211.919	213.472	215.030	216.595	218.165	219.742	221.326
290	222.915	224.511	226.114	227.722	229.337	230.954	232.585	234.219	235.856	237.505
300	239.157	240.817	242.481	244.153	245.831	247.516	249.207	250.904	252.608	254.319
310	256.035	257.757	259.487	261.222	262.965	264.714	266.469	268.231	269.999	271.774
320	273.556	275.343	277.137	278.939	280.746	282.560	284.381	286.208	288.041	289.882
330	291.729	293.582	295.443	297.310	299.183	301.063	302.950	304.844	306.745	308.652
340	310.565	312.485	314.412	316.346	318.287	320.234	322.189	324.149	326.117	328.092
350	330.373	332.361	334.356	336.358	338.366	340.382	342.402	344.424	346.448	348.473
360	350.263	352.320	354.384	356.455	358.533	360.618	362.709	364.808	366.914	369.026
370	371.146	373.273	375.406	377.548	379.695	381.852	384.013	386.182	388.356	390.541
380	392.732	394.937	397.134	399.347	401.566	403.792	406.025	408.266	410.514	412.777
390	415.332	417.572	419.819	421.864	424.155	426.454	428.761	431.074	433.396	435.724
400	438.759	440.932	442.753	445.110	447.476	449.849	452.228	454.616	457.011	459.414
410	461.824	464.242	466.666	469.099	471.533	473.977	476.442	478.924	481.425	483.945
420	486.336	488.837	491.332	493.841	496.357	498.881	501.413	503.952	506.499	509.053
430	511.616	514.266	516.764	519.350	521.944	524.545	527.153	529.771	532.396	535.029
440	537.670	540.318	542.974	545.619	548.311	550.991	553.679	556.375	559.075	561.781
450	564.513	567.240	569.976	572.721	575.473	578.233	581.002	583.779	586.564	589.357
460	592.158	594.957	597.764	600.610	603.445	606.286	609.137	611.996	614.862	617.737
470	620.621	623.519	626.413	629.322	632.236	635.164	638.097	641.040	643.991	646.949
480	649.916	652.892	655.877	658.870	661.871	664.881	667.899	670.926	673.962	677.005
490	680.959	683.120	686.191	689.269	692.357	695.453	698.558	701.671	704.793	707.925
500	711.765	714.933	717.369	720.536	723.711	726.895	730.088	733.290	736.501	739.714
510	742.448	746.295	749.431	752.687	755.951	759.125	762.507	765.794	769.094	772.404
520	775.726	779.354	782.391	785.737	789.193	792.457	795.830	799.213	802.604	806.004
530	809.418	812.837	816.267	819.735	823.153	826.611	830.077	833.552	837.034	840.525
540	844.37	847.951	851.575	854.677	858.249	861.791	865.443	869.034	872.644	876.264
550	879.654	883.224	886.833	890.462	894.110	897.744	901.416	905.074	908.751	912.444
560	916.136	919.843	923.560	927.247	931.024	934.774	938.524	942.299	946.074	949.875
570	953.612	957.441	961.271	965.112	968.944	972.774	976.611	980.454	984.304	988.175
580	992.171	996.040	999.928	1003.81	1007.66	1011.51	1015.37	1019.24	1023.11	1027.01
590	1031.11	1035.02	1038.95	1042.89	1046.81	1050.74	1054.64	1058.51	1062.41	1066.34

APPENDIX A

ORIGINAL PAGE IS
OF POOR QUALITY

TABLE A10.- Concluded

V _c mph	0	1	2	3	4	5	6	7	8	9
600	1072.30	1076.42	1080.54	1084.68	1088.83	1092.99	1097.16	1101.34	1105.53	1109.73
610	1113.95	1118.17	1122.41	1126.65	1130.91	1135.18	1139.46	1143.75	1148.05	1152.36
620	1156.68	1161.02	1165.36	1169.72	1174.09	1178.46	1182.85	1187.25	1191.67	1196.09
630	1200.53	1204.97	1209.43	1213.90	1218.38	1222.87	1227.37	1231.88	1236.41	1240.95
640	1245.49	1250.06	1254.63	1259.21	1263.81	1268.41	1273.03	1277.66	1282.30	1286.95
650	1291.62	1296.30	1300.98	1305.68	1310.40	1315.12	1319.86	1324.60	1329.36	1334.13
660	1338.92	1343.71	1348.52	1353.34	1358.17	1363.02	1367.87	1372.74	1377.62	1382.51
670	1387.42	1392.33	1397.26	1402.21	1407.16	1412.12	1417.10	1422.09	1427.10	1432.11
680	1437.14	1442.18	1447.24	1452.30	1457.38	1462.47	1467.57	1472.69	1477.82	1482.96
690	1488.12	1493.28	1498.46	1503.66	1508.86	1514.08	1519.31	1524.55	1529.81	1535.08
700	1540.37	1545.66	1550.97	1556.29	1561.63	1566.98	1572.34	1577.71	1583.10	1588.50
710	1593.92	1599.34	1604.79	1610.24	1615.71	1621.19	1626.68	1632.19	1637.71	1643.25
720	1648.80	1654.36	1659.94	1665.53	1671.13	1676.75	1682.38	1688.02	1693.68	1699.35
730	1705.04	1710.74	1716.45	1722.18	1727.92	1733.67	1739.44	1745.23	1751.02	1756.83
740	1762.66	1768.50	1774.35	1780.22	1786.10	1792.00	1797.91	1803.84	1809.78	1815.73
750	1821.70	1827.68	1833.68	1839.69	1845.72	1851.76	1857.81	1863.88	1869.97	1876.07
760	1882.18	1888.31	1894.48	1900.64	1906.81	1913.00	1919.20	1925.42	1931.65	1937.89
770	1944.16	1950.43	1956.72	1963.02	1969.34	1975.68	1980.02	1988.38	1994.76	2001.15
780	2007.55	2013.97	2020.40	2026.85	2033.31	2039.78	2046.27	2052.77	2059.29	2065.82
790	2072.36	2078.92	2085.49	2092.07	2098.67	2105.28	2111.91	2118.55	2125.20	2131.86
800	2138.54	2145.24	2151.94	2158.67	2165.40	2172.15	2178.91	2185.68	2192.47	2199.27
810	2206.08	2212.91	2219.75	2226.60	2233.47	2240.35	2247.24	2254.14	2261.06	2267.99
820	2274.94	2281.90	2288.87	2295.85	2302.85	2309.86	2316.88	2323.91	2330.96	2338.02
830	2345.09	2352.16	2359.28	2366.39	2373.52	2380.65	2387.80	2394.97	2402.14	2409.33
840	2416.53	2423.74	2430.96	2438.20	2445.45	2452.71	2459.99	2467.28	2474.58	2481.89
850	2489.22	2496.55	2503.90	2511.26	2518.64	2526.02	2533.42	2540.83	2548.26	2555.69
860	2563.14	2570.60	2578.07	2585.55	2593.05	2600.56	2608.08	2615.61	2623.16	2630.71
870	2638.28	2645.86	2653.45	2661.06	2668.68	2676.30	2683.94	2691.60	2699.26	2706.94
880	2714.62	2722.32	2730.04	2737.76	2745.50	2753.24	2761.00	2768.77	2776.56	2784.35
890	2792.16	2799.98	2807.80	2815.65	2823.50	2831.36	2839.24	2847.13	2855.03	2862.94
900	2870.87	2878.80	2886.74	2894.70	2902.67	2910.65	2918.64	2926.65	2934.66	2942.69
910	2950.73	2958.78	2966.84	2974.91	2982.99	2991.09	2999.20	3007.32	3015.45	3023.59
920	3031.74	3039.90	3048.08	3056.27	3064.46	3072.67	3080.89	3089.13	3097.37	3105.62
930	3113.89	3122.17	3130.46	3138.76	3147.07	3155.39	3163.72	3172.07	3180.42	3188.79
940	3197.17	3205.56	3213.96	3222.37	3230.79	3239.22	3247.67	3256.13	3264.59	3273.07
950	3281.56	3290.06	3298.57	3307.09	3315.63	3324.17	3332.73	3341.30	3349.87	3358.46
960	3367.06	3375.67	3384.29	3392.93	3401.57	3410.23	3418.89	3427.57	3436.25	3444.95
970	3453.66	3462.38	3471.11	3479.86	3488.61	3497.37	3506.15	3514.93	3523.73	3532.54
980	3541.36	3550.18	3559.02	3567.87	3576.73	3585.61	3594.49	3603.38	3612.29	3621.20
990	3630.13	3639.07	3648.02	3656.97	3665.94	3674.92	3683.91	3692.92	3701.93	3710.95
1000	3719.98	3729.03	3738.08	3747.15	3756.22	3765.31	3774.41	3783.52	3792.64	3801.77
1010	3810.91	3820.06	3829.22	3838.39	3847.57	3856.77	3865.97	3875.19	3884.41	3893.65
1020	3902.89	3912.15	3921.42	3930.70	3939.98	3949.28	3958.59	3967.91	3977.24	3986.59
1030	3995.94	4005.33	4014.67	4024.06	4033.45	4042.86	4052.27	4061.70	4071.13	4080.58
1040	4090.04	4099.53	4108.98	4118.47	4127.97	4137.48	4147.00	4156.53	4166.07	4175.62
1050	4185.18	4194.75	4204.34	4213.93	4223.53	4233.15	4242.77	4252.41	4262.05	4271.71
1060	4281.37	4291.05	4300.73	4310.43	4320.14	4329.85	4339.58	4349.32	4359.07	4368.83
1070	4378.60	4388.38	4398.17	4407.97	4417.78	4427.60	4437.43	4447.27	4457.13	4466.99
1080	4476.86	4486.74	4496.64	4506.54	4516.45	4526.38	4536.31	4546.26	4556.21	4566.16
1090	4576.15	4586.14	4596.13	4606.14	4616.16	4626.18	4636.22	4646.27	4656.32	4666.39
1100	4676.47									

APPENDIX A

TABLE A11.- IMPACT PRESSURE q_c (OR q_c') IN INCHES OF MERCURY FOR VALUES OF
CALIBRATED AIRSPEED V_c (OR INDICATED AIRSPEED V_i) IN KNOTS
[From ref. A2]

V_c knots	0	1	2	3	4	5	6	7	8	9
0	0	0.000051	0.000189	0.000428	0.000763	0.001194	0.001726	0.002346	0.003067	0.003885
10	.004784	.005790	.006891	.008085	.009381	.010776	.012255	.013833	.015508	.017283
20	.019153	.021118	.023171	.025331	.027581	.029930	.032372	.034909	.037551	.040297
30	.043108	.046031	.049047	.052165	.055375	.058676	.062067	.065550	.069125	.072796
40	.076655	.080548	.084528	.088606	.092777	.097047	.101412	.105879	.110443	.115110
50	.119841	.124691	.129640	.134682	.139822	.145052	.150381	.155815	.161347	.166975
60	.172679	.178492	.184417	.190422	.196526	.202732	.209039	.215433	.221929	.228521
70	.235205	.242000	.248888	.255866	.262945	.270120	.277409	.284773	.292241	.299811
80	.307483	.315247	.323108	.331067	.339119	.347281	.355539	.363887	.372334	.380886
90	.389532	.398282	.407121	.416067	.425109	.434250	.443490	.452825	.462257	.471786
100	.481424	.491160	.500993	.510923	.520953	.531073	.541317	.551637	.562068	.572597
110	.583225	.593949	.604783	.615708	.626740	.637855	.649085	.660413	.671840	.683375
120	.694996	.706731	.718562	.730483	.742511	.754653	.766882	.779212	.791651	.804191
130	.816826	.829561	.842403	.855344	.868384	.881528	.894767	.908125	.921579	.935129
140	.948779	.962531	.976394	.990364	1.004442	1.018633	1.032866	1.047233	1.061720	1.076328
150	1.09097	1.10575	1.12063	1.13563	1.15072	1.16591	1.18122	1.19663	1.21213	1.22774
160	1.24347	1.25929	1.27521	1.29125	1.30738	1.32352	1.33996	1.35641	1.37298	1.38963
170	1.40640	1.42327	1.44025	1.45733	1.47452	1.49181	1.50921	1.52671	1.54432	1.56205
180	1.57987	1.59780	1.61584	1.63398	1.65223	1.67059	1.68906	1.70763	1.72632	1.74513
190	1.76400	1.78300	1.80211	1.82133	1.84066	1.86010	1.87964	1.89930	1.91905	1.93893
200	1.95891	1.97900	1.99920	2.01951	2.03992	2.06045	2.08108	2.10183	2.12269	2.14366
210	2.16473	2.18593	2.20722	2.22864	2.25016	2.27179	2.29354	2.31539	2.33735	2.35944
220	2.38162	2.40392	2.42634	2.44887	2.47151	2.49426	2.51713	2.54011	2.56320	2.58641
230	2.60972	2.63315	2.65670	2.68036	2.70412	2.72799	2.75202	2.77614	2.80037	2.82471
240	2.84918	2.87375	2.89845	2.92325	2.94818	2.97321	2.99838	3.02365	3.04904	3.07455
250	3.10015	3.12590	3.15176	3.17773	3.20381	3.23003	3.25636	3.28281	3.30937	3.33605
260	3.36284	3.38977	3.41680	3.44396	3.47124	3.49864	3.52615	3.55378	3.58154	3.60941
270	3.63741	3.66553	3.69377	3.72212	3.75060	3.77921	3.80792	3.83678	3.86574	3.89483
280	3.92404	3.95337	3.98283	4.01241	4.04212	4.07194	4.10189	4.13197	4.16216	4.19250
290	4.22293	4.25351	4.28421	4.31503	4.34597	4.37704	4.40825	4.43957	4.47102	4.50260
300	4.53433	4.56613	4.59809	4.63017	4.66238	4.69473	4.72721	4.75983	4.79252	4.82537
310	4.85834	4.89146	4.92469	4.95806	4.99156	5.02519	5.05896	5.09284	5.12687	5.16101
320	5.19529	5.22971	5.26425	5.29892	5.33374	5.36869	5.40375	5.43896	5.47430	5.50977
330	5.54538	5.58111	5.61699	5.65300	5.68914	5.72542	5.76183	5.79838	5.83506	5.87187
340	5.90883	5.94592	5.98315	6.02051	6.05801	6.09565	6.13344	6.17135	6.20939	6.24755
350	6.28593	6.32438	6.36298	6.40173	6.44061	6.47963	6.51880	6.55811	6.59755	6.63713
360	6.67687	6.71674	6.75674	6.79690	6.83719	6.87764	6.91822	6.95894	6.99981	7.04082
370	7.08199	7.12328	7.16472	7.20631	7.24804	7.28991	7.33194	7.37412	7.41643	7.45887
380	7.50151	7.54427	7.58717	7.63021	7.67342	7.71677	7.76027	7.80391	7.84770	7.89165
390	7.93575	7.97997	8.02434	8.06889	8.11363	8.15847	8.20341	8.24853	8.29383	8.33931
400	8.38499	8.43075	8.47668	8.52274	8.56897	8.61535	8.66186	8.70856	8.75540	8.80241
410	8.84955	8.89687	8.94434	8.99196	9.03974	9.08768	9.13579	9.18404	9.23244	9.28099
420	9.32975	9.37864	9.42769	9.47691	9.52628	9.57581	9.62551	9.67536	9.72538	9.77556
430	9.82591	9.87640	9.92708	9.97791	10.0289	10.0801	10.1314	10.1829	10.2345	10.2864
440	10.3384	10.3900	10.4428	10.4953	10.5487	10.6023	10.6560	10.7100	10.7643	10.8188
450	10.8675	10.9221	10.9753	11.0295	11.0836	11.1380	11.1925	11.2472	11.3020	11.3569
460	11.4115	11.4661	11.5208	11.5757	11.6306	11.6857	11.7409	11.7963	11.8518	11.9074
470	11.9627	12.0183	12.0741	12.1300	12.1860	12.2422	12.2985	12.3550	12.4116	12.4683
480	12.5253	12.5817	12.6383	12.6950	12.7518	12.8087	12.8657	12.9228	12.9800	13.0373
490	13.0947	13.1526	13.2106	13.2687	13.3269	13.3852	13.4436	13.5021	13.5607	13.6194

APPENDIX A

TABLE AII.- Concluded

V _c knots	0	1	2	3	4	5	6	7	8	9
500	12.7756	13.8385	13.9015	13.9647	14.0281	14.0917	14.1555	14.2195	14.2836	14.3480
510	14.4126	14.4773	14.5423	14.6074	14.6727	14.7383	14.8040	14.8699	14.9361	15.0024
520	15.0689	15.1356	15.2026	15.2697	15.3370	15.4045	15.4722	15.5402	15.6083	15.6766
530	15.7451	15.8139	15.8828	15.9519	16.0213	16.0908	16.1606	16.2305	16.3007	16.3711
540	16.4417	16.5125	16.5835	16.6547	16.7261	16.7977	16.8695	16.9416	17.0138	17.0863
550	17.1590	17.2319	17.3050	17.3783	17.4518	17.5256	17.5996	17.6737	17.7481	17.8228
560	17.8976	17.9726	18.0479	18.1234	18.1991	18.2750	18.3512	18.4275	18.5041	18.5809
570	18.6580	18.7352	18.8127	18.8904	18.9683	19.0465	19.1248	19.2034	19.2823	19.3613
580	19.4406	19.5201	19.5999	19.6798	19.7600	19.8405	19.9211	20.0020	20.0831	20.1645
590	20.2461	20.3279	20.4099	20.4922	20.5748	20.6575	20.7405	20.8238	20.9072	20.9909
600	21.0749	21.1591	21.2435	21.3282	21.4131	21.4982	21.5836	21.6693	21.7551	21.8413
610	21.9276	22.0142	22.1011	22.1882	22.2755	22.3631	22.4510	22.5391	22.6274	22.7160
620	22.8048	22.8939	22.9833	23.0729	23.1627	23.2528	23.3432	23.4338	23.5246	23.6156
630	23.7071	23.7987	23.8906	23.9828	24.0752	24.1679	24.2608	24.3540	24.4474	24.5411
640	24.6351	24.7293	24.8238	24.9186	25.0136	25.1089	25.2044	25.3003	25.3964	25.4927
650	25.5893	25.6862	25.7834	25.8809	25.9786	26.0765	26.1748	26.2733	26.3721	26.4712
660	26.5705	26.6702	26.7701	26.8703	26.9707	27.0714	27.1724	27.2737	27.3753	27.4771
670	27.5792	27.6815	27.7842	27.8871	27.9902	28.0937	28.1974	28.3013	28.4056	28.5101
680	28.6148	28.7198	28.8251	28.9306	29.0364	29.1425	29.2489	29.3554	29.4622	29.5693
690	29.6767	29.7843	29.8922	30.0003	30.1086	30.2173	30.3261	30.4353	30.5447	30.6543
700	30.7642	30.8743	30.9847	31.0953	31.2062	31.3173	31.4287	31.5403	31.6522	31.7643
710	31.8766	31.9892	32.1021	32.2151	32.3285	32.4421	32.5559	32.6699	32.7842	32.8988
720	33.0135	33.1285	33.2438	33.3593	33.4750	33.5910	33.7072	33.8236	33.9403	34.0571
730	34.1744	34.2918	34.4094	34.5272	34.6453	34.7636	34.8822	35.0010	35.1200	35.2393
740	35.3587	35.4785	35.5984	35.7186	35.8390	35.9596	36.0805	36.2016	36.3229	36.4444
750	36.5662	36.6882	36.8104	36.9329	37.0555	37.1785	37.3016	37.4249	37.5485	37.6723
760	37.7954	37.9206	38.0451	38.1698	38.2947	38.4198	38.5452	38.6708	38.7966	38.9226
770	39.0489	39.1741	39.3021	39.4295	39.5561	39.6835	39.8111	39.9388	40.0668	40.1949
780	40.3235	40.4522	40.5811	40.7102	40.8395	40.9690	41.0988	41.2287	41.3589	41.4893
790	41.6199	41.7507	41.8818	42.0130	42.1445	42.2762	42.4081	42.5402	42.6725	42.8051
800	42.9378	43.0708	43.2040	43.3377	43.4719	43.6064	43.7413	43.8765	44.0119	44.1476
810	44.2837	44.4191	44.5547	44.6906	44.8266	44.9629	45.0995	45.2363	45.3733	45.5105
820	45.6473	45.7844	45.9218	46.0594	46.1972	46.3352	46.4734	46.6119	46.7505	46.8893
830	47.0284	47.1676	47.3071	47.4467	47.5866	47.7267	47.8670	48.0074	48.1481	48.2890
840	48.4211	48.5614	48.7029	48.8446	48.9866	49.1287	49.2710	49.4135	49.5562	49.6991
850	49.8423	49.9857	50.1292	50.2730	50.4169	50.5611	50.7055	50.8501	50.9948	51.1397
860	51.2849	51.4303	51.5758	51.7216	51.8676	52.0138	52.1601	52.3067	52.4534	52.6003
870	52.7476	52.8950	53.0426	53.1904	53.3383	53.4865	53.6349	53.7834	53.9321	54.0810
880	54.2294	54.3798	54.5293	54.6791	54.8291	54.9792	55.1295	55.2799	55.4305	55.5812
890	55.7320	55.8844	56.0369	56.1897	56.3426	56.4956	56.6488	56.8021	56.9556	57.1092
900	57.2624	57.4164	57.5705	57.7248	57.8793	58.0340	58.1888	58.3438	58.4989	58.6542
910	58.8097	58.9654	59.1213	59.2774	59.4336	59.5900	59.7465	59.9032	60.0601	60.2171
920	60.3743	60.5316	60.6891	60.8468	61.0047	61.1628	61.3210	61.4793	61.6378	61.7964
930	61.9551	62.1139	62.2729	62.4321	62.5914	62.7509	62.9105	63.0703	63.2302	63.3903
940	63.5505	63.7109	63.8715	64.0323	64.1932	64.3543	64.5155	64.6768	64.8383	65.0000
950	65.1618	65.3234	65.4852	65.6471	65.8092	65.9714	66.1338	66.2963	66.4589	66.6217
960	66.7846	66.9474	67.1104	67.2735	67.4368	67.5999	67.7633	67.9268	68.0905	68.2543
970	68.4183	68.5824	68.7467	68.9112	69.0758	69.2405	69.4054	69.5704	69.7355	69.9007
980	70.0660	70.2313	70.3968	70.5624	70.7281	70.8940	71.0599	71.2260	71.3922	71.5585
990	71.7250	71.8917	72.0586	72.2256	72.3927	72.5600	72.7274	72.8950	73.0627	73.2305

APPENDIX A

TABLE A12.- IMPACT PRESSURE q_c (OR q_c^*) IN POUNDS PER SQUARE FOOT FOR VALUES OF

CALIBRATED AIRSPEED V_c (OR INDICATED AIRSPEED V_i) IN KNOTS

[From ref. A2]

V_c Knots	0	1	2	3	4	5	6	7	8	9
0	0	3.003598	9.013332	9.030262	9.053964	9.084437	9.122106	9.165911	9.214912	9.269174
10	3.338381	4.094886	4.87365	5.67802	6.50646	7.36415	8.246591	9.158327	10.1044	11.08991
20	1.35438	1.49363	1.63880	1.79159	1.95073	2.11685	2.290954	2.473999	2.666996	2.870944
30	3.04883	3.25559	3.46890	3.68941	3.91648	4.14990	4.38915	4.63496	4.88798	5.14792
40	5.42154	5.69686	5.97831	6.26675	6.56175	6.86374	7.17249	7.48781	7.80951	8.13749
50	8.47587	8.81891	9.16893	9.52552	9.88908	10.25990	10.63859	11.02492	11.41891	11.82044
60	12.2129	12.6241	13.0431	13.4678	13.8995	14.3384	14.7845	15.2368	15.6952	16.1594
70	16.6352	17.1158	17.6029	18.0964	18.5971	19.1046	19.6189	20.1399	20.6669	21.1994
80	21.7471	22.2963	22.8522	23.4151	23.9846	24.5619	25.1469	25.7394	26.3398	26.9476
90	27.5520	28.1690	28.7941	29.4266	30.0664	30.7129	31.3664	32.0266	32.6936	33.3666
100	34.0493	34.7379	35.4333	36.1357	36.8450	37.5612	38.2853	39.0152	39.7529	40.4976
110	41.2433	42.0078	42.7740	43.5467	44.3269	45.1111	45.9023	46.7005	47.5067	48.3213
120	49.1544	49.9844	50.8212	51.6643	52.5150	53.3737	54.2404	55.1157	56.0004	56.8934
130	57.7710	58.6717	59.5800	60.4952	61.4175	62.3477	63.2844	64.2282	65.1799	66.1391
140	67.1235	68.0762	69.0366	69.9947	70.9601	71.9321	72.9101	73.8944	74.8854	75.8834
150	77.1538	78.2056	79.2576	80.3107	81.3661	82.4237	83.4834	84.5434	85.6034	86.6634
160	87.9462	89.0650	90.1811	91.2953	92.4068	93.5147	94.6191	95.7294	96.8454	97.9564
170	99.4636	100.662	101.863	103.071	104.287	105.510	106.741	107.979	109.224	110.476
180	111.738	113.006	114.282	115.565	116.856	118.155	119.460	120.774	122.096	123.424
190	124.761	126.105	127.456	128.816	130.183	131.557	132.939	134.330	135.727	137.133
200	140.546	141.967	143.396	144.832	146.276	147.728	149.187	150.655	152.130	153.614
210	153.103	154.602	156.108	157.623	159.145	160.675	162.213	163.759	165.312	166.874
220	168.443	170.020	171.606	173.199	174.800	176.410	178.027	179.651	181.285	182.927
230	184.576	186.233	187.898	189.572	191.252	192.942	194.640	196.346	198.059	199.781
240	201.511	203.250	204.996	206.750	208.511	210.284	212.064	213.851	215.647	217.451
250	217.662	219.483	221.312	223.149	224.994	226.846	228.613	230.384	232.169	233.964
260	237.841	239.746	241.657	243.575	245.507	247.445	249.391	251.345	253.309	255.281
270	257.260	259.249	261.246	263.252	265.266	267.289	269.320	271.361	273.419	275.487
280	277.533	279.607	281.691	283.782	285.884	287.993	290.111	292.236	294.374	296.519
290	298.672	300.835	302.996	305.186	307.374	309.572	311.779	313.994	316.216	318.444
300	320.694	322.945	325.205	327.474	329.753	332.047	334.356	336.671	338.994	341.324
310	343.612	345.954	348.304	350.665	353.034	355.413	357.801	360.197	362.602	365.014
320	367.443	369.877	372.310	374.753	377.205	379.674	382.157	384.647	387.147	389.654
330	392.270	394.721	397.169	399.635	402.107	404.597	407.091	409.597	412.114	414.644
340	417.909	420.433	422.964	425.503	428.040	431.100	433.674	436.254	438.844	441.444
350	444.576	447.180	449.780	452.380	455.000	457.624	460.254	462.894	465.544	468.204
360	472.230	474.849	477.479	480.119	482.764	485.414	488.074	490.744	493.424	496.104
370	497.881	500.521	503.161	505.811	508.464	511.124	513.794	516.464	519.144	521.824
380	530.593	533.277	535.962	538.656	541.354	544.054	546.764	549.474	552.184	554.894
390	561.265	564.005	566.745	569.495	572.245	575.004	577.764	580.524	583.284	586.044
400	593.339	596.125	598.910	601.695	604.480	607.264	610.054	612.844	615.634	618.424
410	625.895	628.702	631.509	634.316	637.124	640.000	642.874	645.744	648.614	651.484
420	659.656	662.530	665.404	668.279	671.154	674.024	676.894	679.764	682.634	685.504
430	694.949	697.834	700.719	703.604	706.484	709.364	712.244	715.119	717.994	720.864
440	731.193	734.084	736.974	739.864	742.754	745.644	748.529	751.414	754.294	757.174
450	766.613	769.504	772.394	775.284	778.174	781.059	783.944	786.824	789.704	792.584
460	802.237	805.124	808.014	810.904	813.794	816.679	819.564	822.444	825.324	828.204
470	847.190	850.084	852.974	855.864	858.749	861.634	864.514	867.394	870.274	873.149
480	889.199	892.084	894.969	897.854	900.734	903.614	906.489	909.364	912.239	915.114
490	931.591	934.474	937.354	940.234	943.114	945.989	948.864	951.739	954.614	957.489

APPENDIX A

ORIGINAL PAGE IS
OF POOR QUALITY

TABLE A12.- Concluded

V _c knots	0	1	2	3	4	5	6	7	8	9
500	974.298	978.741	983.199	987.669	992.154	996.651	1001.16	1005.69	1010.23	1014.78
510	1019.35	1023.93	1028.52	1033.13	1037.75	1042.38	1047.03	1051.69	1056.37	1061.06
520	1065.77	1070.49	1075.22	1079.97	1084.73	1089.50	1094.29	1099.10	1103.91	1108.75
530	1113.59	1118.46	1123.33	1128.22	1133.12	1138.04	1142.98	1147.92	1152.89	1157.87
540	1162.86	1167.86	1172.88	1177.92	1182.97	1188.04	1193.12	1198.21	1203.32	1208.45
550	1213.59	1218.75	1223.92	1229.10	1234.30	1239.52	1244.75	1250.00	1255.26	1260.54
560	1265.83	1271.14	1276.46	1281.80	1287.15	1292.52	1297.91	1303.31	1308.73	1314.16
570	1319.61	1325.07	1330.55	1336.05	1341.56	1347.08	1352.63	1358.19	1363.76	1369.35
580	1374.96	1380.58	1386.22	1391.88	1397.55	1403.24	1408.94	1414.67	1420.40	1426.16
590	1431.93	1437.71	1443.52	1449.34	1455.17	1461.03	1466.90	1472.78	1478.69	1484.61
600	1490.55	1496.50	1502.47	1508.46	1514.47	1520.49	1526.53	1532.58	1538.66	1544.75
610	1550.86	1556.98	1563.13	1569.29	1575.46	1581.66	1587.87	1594.10	1600.35	1606.62
620	1612.90	1619.20	1625.52	1631.86	1638.21	1644.58	1650.97	1657.38	1663.81	1670.25
630	1676.71	1683.19	1689.69	1696.21	1702.75	1709.30	1715.87	1722.46	1729.07	1735.70
640	1742.35	1749.01	1755.69	1762.40	1769.12	1775.86	1782.61	1789.39	1796.19	1803.00
650	1809.84	1816.69	1823.56	1830.45	1837.36	1844.29	1851.24	1858.21	1865.20	1872.21
660	1879.23	1886.28	1893.35	1900.43	1907.54	1914.66	1921.80	1928.97	1936.15	1943.35
670	1950.57	1957.81	1965.07	1972.35	1979.64	1986.96	1994.29	2001.65	2009.02	2016.41
680	2023.82	2031.24	2038.69	2046.15	2053.64	2061.14	2068.66	2076.20	2083.75	2091.33
690	2098.92	2106.53	2114.16	2121.81	2129.47	2137.15	2144.85	2152.57	2160.31	2168.06
700	2175.83	2183.62	2191.43	2199.25	2207.09	2214.95	2222.83	2230.73	2238.64	2246.57
710	2254.51	2262.48	2270.46	2278.45	2286.47	2294.50	2302.55	2310.62	2318.70	2326.80
720	2334.92	2343.06	2351.21	2359.38	2367.56	2375.76	2382.98	2392.22	2400.47	2408.74
730	2417.03	2425.33	2433.65	2441.98	2450.33	2458.70	2467.09	2475.49	2483.91	2492.34
740	2500.79	2509.26	2517.74	2526.24	2534.75	2543.29	2551.83	2560.40	2568.98	2577.57
750	2586.19	2594.82	2603.46	2612.12	2620.80	2629.49	2638.20	2646.92	2655.66	2664.42
760	2673.19	2681.98	2690.78	2699.60	2708.44	2717.29	2726.16	2735.04	2743.94	2752.85
770	2761.78	2770.72	2779.69	2788.66	2797.65	2806.66	2815.68	2824.72	2833.78	2842.84
780	2851.93	2861.03	2870.14	2879.27	2888.42	2897.58	2906.76	2915.95	2925.16	2934.39
790	2943.62	2952.87	2962.14	2971.42	2980.72	2990.04	2999.36	3008.71	3018.07	3027.44
800	3036.83	3046.23	3055.65	3065.09	3074.54	3084.00	3093.48	3102.97	3112.48	3122.01
810	3131.54	3141.10	3150.67	3160.25	3169.85	3179.46	3189.09	3198.73	3208.39	3218.06
820	3227.75	3237.45	3247.17	3256.90	3266.65	3276.41	3286.18	3295.97	3305.78	3315.60
830	3325.43	3335.28	3345.14	3355.02	3364.91	3374.82	3384.74	3394.68	3404.63	3414.59
840	3424.57	3434.56	3444.57	3454.60	3464.63	3474.69	3484.75	3494.83	3504.93	3515.04
850	3525.16	3535.30	3545.45	3555.62	3565.80	3575.99	3586.20	3596.43	3606.67	3616.92
860	3627.19	3637.47	3647.76	3658.07	3668.40	3678.73	3689.09	3699.45	3709.84	3720.23
870	3730.64	3741.06	3751.50	3761.95	3772.42	3782.90	3793.39	3803.90	3814.42	3824.96
880	3835.51	3846.07	3856.65	3867.24	3877.85	3888.47	3899.11	3909.75	3920.42	3931.19
890	3941.78	3952.49	3963.21	3973.94	3984.69	3995.45	4006.22	4017.01	4027.81	4038.63
900	4049.46	4060.30	4071.16	4082.03	4092.92	4103.82	4114.73	4125.66	4136.60	4147.55
910	4158.52	4169.51	4180.50	4191.51	4202.54	4213.58	4224.63	4235.69	4246.77	4257.86
920	4268.97	4280.09	4291.23	4302.37	4313.54	4324.71	4335.90	4347.11	4358.32	4369.55
930	4380.80	4392.06	4403.33	4414.61	4425.91	4437.22	4448.55	4459.89	4471.24	4482.61
940	4493.99	4505.39	4516.79	4528.21	4539.65	4551.10	4562.56	4574.04	4585.53	4597.03
950	4608.55	4620.08	4631.62	4643.18	4654.75	4666.33	4677.93	4689.54	4701.17	4712.81
960	4724.46	4736.13	4747.81	4759.50	4771.21	4782.93	4794.66	4806.41	4818.17	4829.94
970	4841.73	4853.53	4865.34	4877.17	4889.01	4900.87	4912.73	4924.62	4936.51	4948.42
980	4960.34	4972.28	4984.22	4996.19	5008.16	5020.15	5032.15	5044.17	5056.20	5068.24
990	5080.30	5092.36	5104.45	5116.54	5128.65	5140.78	5152.91	5165.06	5177.22	5189.40
1000	5201.59									

APPENDIX A

TABLE A13.- TRUE AIRSPEED V IN KNOTS FOR VALUES OF CALIBRATED
AIRSPEED V_C IN KNOTS AND VALUES OF PRESSURE ALTITUDE H
IN GEOPOTENTIAL FEET

[Computation of V based on standard temperature at each altitude]

V_C , knots H , ft	100	200	300	400	500	600	700	800	900	1000
0	100.0	200.0	300.0	400.0	500.0	600.0	700.0	800.0	900.0	1000
5 000	107.7	215.0	321.6	427.4	532.2	635.8	740.3	847.3	955.2	1064
10 000	116.2	231.6	345.4	457.2	566.8	674.5	785.0	900.5	1018	1136
15 000	125.8	250.0	371.5	489.4	603.8	716.3	835.2	960.9	1089	1218
20 000	137.2	270.5	400.1	524.4	643.4	763.0	892.4	1030	1170	1310
25 000	148.7	293.4	431.5	562.0	686.6	816.2	958.0	1109	1263	1418
30 000	162.4	318.9	465.9	602.6	735.4	877.5	1034	1201	1370	1541
35 000	178.0	347.4	503.5	646.9	791.6	948.7	1122	1307	1494	1682
40 000	199.1	385.6	553.7	708.9	871.5	1049	1245	1454	1666	1878
45 000	223.7	429.1	610.0	782.4	967.0	1169	1392	1629	1869	
50 000	251.0	476.4	671.6	865.7	1076	1306	1559	1827		
55 000	281.3	527.3	740.3	960.3	1199	1460	1747			
60 000	314.9	581.8	817.9	1068	1340	1636	1961			
65 000	351.8	640.4	906.0	1191	1499	1835				
70 000	394.8	709.9	1013	1338	1690	2073				
75 000	440.3	785.3	1130	1501	1901					
80 000	489.4	870.3	1263	1684	2139					
85 000	540.2	962.9	1408	1885						
90 000	596.2	1071	1576	2111						
95 000	656.2	1193	1766							
100 000	722.2	1330	1979							

APPENDIX A

ORIGINAL PAGE 1
OF POOR QUALITYTABLE A14.- STATIC PRESSURE p (OR p') IN MILLIMETERS OF MERCURY ($Q^2 C$) FOR VALUES OFPRESSURE ALTITUDE H (OR INDICATED ALTITUDE H') IN GEOPOTENTIAL METERS

[From ref. A1]

H , m	0	100	200	300	400	500	600	700	800	900
-1 000	854.538									
-0		769.054	778.195	787.424	796.741	806.147	815.644	825.230	834.908	844.677
0	760.000	751.032	742.151	733.354	724.643	716.015	707.470	699.009	690.629	682.331
1 000	674.114	665.978	657.921	649.943	642.043	634.222	626.478	618.810	611.219	603.703
2 000	596.263	588.997	581.604	574.385	567.239	560.165	553.162	546.231	539.370	532.579
3 000	525.857	519.204	512.620	506.103	499.654	493.271	486.954	480.703	474.518	468.396
4 000	462.339	456.346	450.416	444.548	438.742	432.998	427.314	421.692	416.129	410.626
5 000	405.182	399.797	394.470	389.200	383.988	378.832	373.732	368.688	363.700	358.766
6 000	353.886	349.061	344.289	339.569	334.903	330.288	325.725	321.213	316.752	312.341
7 000	307.981	303.669	299.407	295.193	291.027	286.909	282.838	278.814	274.837	270.906
8 000	267.020	263.180	259.384	255.633	251.926	248.263	244.643	241.066	237.531	234.038
9 000	230.587	227.177	223.809	220.481	217.193	213.944	210.736	207.566	204.435	201.343
10 000	198.288	195.271	192.291	189.349	186.442	183.573	180.738	177.940	175.177	172.448
11 000	169.754	167.098	164.484	161.911	159.377	156.884	154.430	152.013	149.635	147.294
12 000	144.990	142.721	140.488	138.290	136.127	133.997	131.901	129.837	127.806	125.806
13 000	123.838	121.900	119.993	118.116	116.268	114.449	112.658	110.896	109.161	107.453
14 000	105.772	104.117	102.488	100.885	99.3064	97.7527	96.2234	94.7179	93.2361	91.7774
15 000	90.3415	88.9281	87.5368	86.1672	84.8191	83.4921	82.1859	80.9001	79.6344	78.3885
16 000	77.1621	75.9549	74.7665	73.5968	72.4454	71.3119	70.1963	69.0980	68.0170	66.9528
17 000	65.9053	64.8742	63.8593	62.8602	61.8767	60.9087	59.9557	59.0177	58.0944	57.1855
18 000	56.2908	55.4101	54.5432	53.6899	52.8499	52.0230	51.2091	50.4080	49.6193	48.8430
19 000	48.0788	47.3267	46.5862	45.8574	45.1399	44.4337	43.7385	43.0542	42.3806	41.7176
20 000	41.0649	40.4226	39.7906	39.1688	38.5570	37.9550	37.3627	36.7799	36.2064	35.6421
21 000	35.0865	34.5406	34.0031	33.4741	32.9536	32.4414	31.9375	31.4415	30.9536	30.4733
22 000	30.0008	29.5358	29.0782	28.6279	28.1848	27.7487	27.3196	26.8973	26.4817	26.0727
23 000	25.6703	25.2742	24.8844	24.5008	24.1232	23.7517	23.3861	23.0262	22.6720	22.3235
24 000	21.9804	21.6428	21.3105	20.9835	20.6616	20.3448	20.0330	19.7261	19.4240	19.1268
25 000	18.8341	18.5461	18.2627	17.9837	17.7090	17.4387	17.1726	16.9107	16.6530	16.3992
26 000	16.1495	15.9036	15.6616	15.4234	15.1889	14.9581	14.7309	14.5072	14.2871	14.0704
27 000	13.8575	13.6470	13.4403	13.2367	13.0364	12.8392	12.6450	12.4539	12.2657	12.0805
28 000	11.8981	11.7186	11.5418	11.3678	11.1965	11.0279	10.8618	10.6984	10.5375	10.3790
29 000	10.2237	10.0694	9.91825	9.76939	9.62281	9.47851	9.33643	9.19654	9.05881	8.92321
30 000	8.78943									

APPENDIX A

TABLE A15.- STATIC PRESSURE p (OR p') IN PASCALS FOR VALUES OF PRESSURE ALTITUDE H
(OR INDICATED ALTITUDE H') IN GEOPOTENTIAL METERS
[From ref. A1]

H , m	0	100	200	300	400	500	600	700	800	900
-1 000	113 929.									
0		102 532.	103 751.	104 981.	106 223.	107 477.	108 744.	110 022.	111 312.	112 614.
1 000	101 325.	100 129.	98 945.3	97 772.5	96 611.1	95 460.8	94 321.6	93 193.5	92 076.3	90 970.0
2 000	89 874.5	88 789.7	87 715.5	86 651.9	85 598.7	84 556.0	83 523.5	82 501.3	81 489.2	80 487.2
3 000	79 495.2	78 513.1	77 540.9	76 578.4	75 625.6	74 682.5	73 748.9	72 824.8	71 910.0	71 004.6
4 000	70 108.5	69 221.5	68 343.7	67 474.8	66 615.0	65 764.0	64 921.9	64 088.5	63 263.8	62 447.7
5 000	61 640.2	60 841.1	60 050.5	59 268.1	58 494.1	57 728.3	56 970.6	56 220.9	55 479.3	54 745.7
6 000	54 019.9	53 301.9	52 591.6	51 889.1	51 194.1	50 506.8	49 826.9	49 154.4	48 489.3	47 831.5
7 000	47 181.0	46 537.6	45 901.4	45 272.2	44 650.0	44 034.8	43 425.4	42 821.9	42 224.2	41 632.1
8 000	41 060.7	40 485.9	39 917.6	39 355.8	38 800.4	38 251.4	37 708.7	37 172.2	36 641.9	36 117.6
9 000	35 599.8	35 087.8	34 581.7	34 081.6	33 587.4	33 099.0	32 616.4	32 139.4	31 667.2	31 200.5
10 000	30 742.4	30 287.8	29 838.7	29 395.0	28 956.6	28 523.6	28 095.8	27 673.2	27 255.8	26 843.5
11 000	26 436.2	26 034.0	25 636.7	25 244.4	24 857.0	24 474.3	24 096.5	23 723.4	23 355.0	22 991.2
12 000	22 672.0	22 277.9	21 892.4	21 506.3	21 124.6	20 746.1	20 371.9	20 001.8	19 635.7	19 273.6
13 000	19 230.4	18 877.9	18 529.2	18 184.2	17 842.8	17 504.8	17 171.3	16 842.2	16 517.4	16 196.8
14 000	15 910.4	15 582.1	15 257.8	14 937.5	14 621.1	14 308.6	13 999.9	13 695.9	13 396.5	13 101.6
15 000	14 101.8	13 881.1	13 664.0	13 450.2	13 239.8	13 032.6	12 828.7	12 628.0	12 430.5	12 236.1
16 000	12 044.5	11 856.1	11 670.6	11 488.0	11 308.3	11 131.4	10 957.2	10 785.9	10 617.0	10 450.4
17 000	10 287.4	10 126.5	9 968.05	9 812.10	9 658.59	9 507.48	9 358.73	9 212.31	9 068.18	8 926.31
18 000	8 786.66	8 649.19	8 513.87	8 380.67	8 249.55	8 120.49	7 993.44	7 868.38	7 745.28	7 624.11
19 000	7 504.82	7 387.41	7 271.83	7 158.06	7 046.07	6 935.83	6 827.32	6 720.51	6 615.36	6 511.87
20 000	6 409.99	6 309.70	6 210.98	6 113.81	6 018.16	5 924.01	5 831.32	5 740.09	5 650.29	5 561.89
21 000	5 474.87	5 389.24	5 304.98	5 222.08	5 140.51	5 060.25	4 981.28	4 903.58	4 827.12	4 751.89
22 000	4 677.87	4 605.04	4 533.37	4 462.85	4 393.45	4 325.17	4 257.98	4 191.86	4 126.80	4 062.78
23 000	3 999.73	3 937.78	3 876.78	3 816.74	3 757.66	3 699.53	3 642.31	3 586.11	3 530.91	3 476.79
24 000	3 422.42	3 369.61	3 317.65	3 266.50	3 216.17	3 166.57	3 117.68	3 069.41	3 021.75	2 974.69
25 000	2 930.48	2 885.47	2 841.17	2 797.56	2 754.65	2 712.41	2 670.84	2 629.93	2 589.66	2 550.02
26 000	2 511.31	2 472.62	2 434.82	2 397.62	2 361.01	2 324.97	2 289.50	2 254.59	2 220.21	2 186.35
27 000	2 153.38	2 120.31	2 088.04	2 056.28	2 025.02	1 994.25	1 963.96	1 934.14	1 904.79	1 875.89
28 000	1 847.45	1 819.45	1 791.89	1 764.75	1 738.04	1 711.75	1 685.86	1 660.36	1 635.23	1 610.46
29 000	1 586.28	1 562.35	1 538.78	1 515.59	1 492.75	1 470.26	1 448.13	1 426.33	1 404.84	1 383.65
30 000	1 362.36	1 342.48	1 322.32	1 302.48	1 282.94	1 263.70	1 244.76	1 226.11	1 207.74	1 189.65
31 000	1 171.96									

APPENDIX A

ORIGINAL PAGE IS
OF POOR QUALITY

TABLE A16.- DENSITY ρ IN KILOGRAMS PER CUBIC METER FOR VALUES OF

PRESSURE ALTITUDE H IN GEOPOTENTIAL METERS

[From ref. A1]

H, m	0	100	200	300	400	500	600	700	800	900
0	1.2250	1.2133	1.2017	1.1901	1.1786	1.1673	1.1560	1.1448	1.1336	1.1226
1 000	1.1116	1.1008	1.0900	1.0793	1.0686	1.0581	1.0476	1.0372	1.0269	1.0166
2 000	1.0065	.99641	.98641	.97648	.96663	.95886	.94716	.93754	.92799	.91852
3 000	.90912	.89980	.89055	.88137	.87226	.86323	.85427	.84538	.83656	.82781
4 000	.81913	.81052	.80198	.79351	.78511	.77677	.76851	.76031	.75218	.74411
5 000	.73612	.72818	.72032	.71251	.70478	.69711	.68950	.68195	.67447	.66705
6 000	.65970	.65240	.64517	.63800	.63089	.62384	.61686	.60993	.60306	.59625
7 000	.58950	.58261	.57618	.56960	.56308	.55662	.55022	.54387	.53758	.53135
8 000	.52517	.51904	.51297	.50696	.50100	.49509	.48924	.48343	.47769	.47199
9 000	.46635	.46076	.45522	.44973	.44429	.43890	.43356	.42827	.42304	.41785
10 000	.41271	.40761	.40257	.39757	.39263	.38772	.38287	.37806	.37330	.36859
11 000	.36392	.35822	.35262	.34710	.34167	.33633	.33106	.32589	.32079	.31577
12 000	.31083	.30596	.30118	.29647	.29183	.28726	.28277	.27834	.27399	.26970
13 000	.26548	.26133	.25724	.25322	.24925	.24535	.24152	.23774	.23402	.23036
14 000	.22675	.22331	.21971	.21628	.21289	.20956	.20628	.20306	.19988	.19675
15 000	.19367	.19064	.18766	.18472	.18183	.17899	.17619	.17343	.17072	.16805
16 000	.16542	.16283	.16028	.15778	.15531	.15288	.15049	.14813	.14581	.14353
17 000	.14129	.13908	.13690	.13476	.13265	.13058	.12853	.12652	.12454	.12259
18 000	.12068	.11879	.11693	.11510	.11330	.11153	.10978	.10806	.10637	.10471
19 000	.10307	.10146	.099871	.098309	.096771	.095257	.093766	.092292	.090855	.089434
20 000	.088035	.086618	.085224	.083854	.082506	.081180	.079877	.078594	.077333	.076093
21 000	.074873	.073674	.072494	.071333	.070192	.069069	.067965	.066872	.065791	.064761
22 000	.063727	.062711	.061711	.060728	.059760	.058809	.057873	.056952	.056047	.055156
23 000	.054280	.053418	.052570	.051737	.050916	.050109	.049315	.048534	.047766	.047011
24 000	.046267	.045536	.044816	.044109	.043412	.042727	.042054	.041392	.040739	.040097
25 000	.039466	.038845	.038234	.037633	.037041	.036459	.035887	.035324	.034770	.034224
26 000	.033688	.033160	.032641	.032130	.031628	.031133	.030646	.030168	.029696	.029233
27 000	.028777	.028328	.027886	.027452	.027024	.026604	.026190	.025781	.025376	.024977
28 000	.024599	.024217	.023841	.023471	.023107	.022749	.022396	.022048	.021704	.021372
29 000	.021042	.020717	.020397	.020082	.019771	.019466	.019166	.018871	.018580	.018294
30 000	.018012	.017735	.017462	.017193	.016929	.016669	.016413	.016161	.015913	.015669

APPENDIX A

TABLE A17.- TEMPERATURE t IN DEGREES CENTIGRADE FOR VALUES OF
PRESSURE ALTITUDE H IN GEOPOTENTIAL METERS

[From ref. A1]

H, m	0	100	200	300	400	500	600	700	800	900
0	15.000	14.350	13.700	13.050	12.400	11.750	11.100	10.450	9.800	9.150
1 000	8.500	7.850	7.200	6.550	5.900	5.250	4.600	3.950	3.300	2.650
2 000	2.000	1.350	.700	.050	-.600	-1.250	-1.900	-2.550	-3.200	-3.850
3 000	-4.500	-5.150	-5.800	-6.450	-7.100	-7.750	-8.400	-9.050	-9.700	-10.350
4 000	-11.000	-11.650	-12.300	-12.950	-13.600	-14.250	-14.900	-15.550	-16.200	-16.850
5 000	-17.500	-18.150	-18.800	-19.450	-20.100	-20.750	-21.400	-22.050	-22.700	-23.350
6 000	-24.000	-24.650	-25.300	-25.950	-26.600	-27.250	-27.900	-28.550	-29.200	-29.850
7 000	-30.500	-31.150	-31.800	-32.450	-33.100	-33.750	-34.400	-35.050	-35.700	-36.350
8 000	-37.000	-37.650	-38.300	-38.950	-39.600	-40.250	-40.900	-41.550	-42.200	-42.850
9 000	-43.500	-44.150	-44.800	-45.450	-46.100	-46.750	-47.400	-48.050	-48.700	-49.350
10 000	-50.000	-50.650	-51.300	-51.950	-52.600	-53.250	-53.900	-54.550	-55.200	-55.850
11 000	-56.500	-56.500	-56.500	-56.500	-56.500	-56.500	-56.500	-56.500	-56.500	-56.500
12 000	-56.500	-56.500	-56.500	-56.500	-56.500	-56.500	-56.500	-56.500	-56.500	-56.500
13 000	-56.500	-56.500	-56.500	-56.500	-56.500	-56.500	-56.500	-56.500	-56.500	-56.500
14 000	-56.500	-56.500	-56.500	-56.500	-56.500	-56.500	-56.500	-56.500	-56.500	-56.500
15 000	-56.500	-56.500	-56.500	-56.500	-56.500	-56.500	-56.500	-56.500	-56.500	-56.500
16 000	-56.500	-56.500	-56.500	-56.500	-56.500	-56.500	-56.500	-56.500	-56.500	-56.500
17 000	-56.500	-56.500	-56.500	-56.500	-56.500	-56.500	-56.500	-56.500	-56.500	-56.500
18 000	-56.500	-56.500	-56.500	-56.500	-56.500	-56.500	-56.500	-56.500	-56.500	-56.500
19 000	-56.500	-56.500	-56.500	-56.500	-56.500	-56.500	-56.500	-56.500	-56.500	-56.500
20 000	-56.500	-56.400	-56.300	-56.200	-56.100	-56.000	-55.900	-55.800	-55.700	-55.600
21 000	-55.500	-55.400	-55.300	-55.200	-55.100	-55.000	-54.900	-54.800	-54.700	-54.600
22 000	-54.500	-54.400	-54.300	-54.200	-54.100	-54.000	-53.900	-53.800	-53.700	-53.600
23 000	-53.500	-53.400	-53.300	-53.200	-53.100	-53.000	-52.900	-52.800	-52.700	-52.600
24 000	-52.500	-52.400	-52.300	-52.200	-52.100	-52.000	-51.900	-51.800	-51.700	-51.600
25 000	-51.500	-51.400	-51.300	-51.200	-51.100	-51.000	-50.900	-50.800	-50.700	-50.600
26 000	-50.500	-50.400	-50.300	-50.200	-50.100	-50.000	-49.900	-49.800	-49.700	-49.600
27 000	-49.500	-49.400	-49.300	-49.200	-49.100	-49.000	-48.900	-48.800	-48.700	-48.600
28 000	-48.500	-48.400	-48.300	-48.200	-48.100	-48.000	-47.900	-47.800	-47.700	-47.600
29 000	-47.500	-47.400	-47.300	-47.200	-47.100	-47.000	-46.900	-46.800	-46.700	-46.600
30 000	-46.500	-46.400	-46.300	-46.200	-46.100	-46.000	-45.900	-45.800	-45.700	-45.600

APPENDIX A

ORIGINAL PAGE IS
OF POOR QUALITYTABLE A18.- COEFFICIENT OF VISCOSITY μ IN PASCAL-SECONDS FORVALUES OF PRESSURE ALTITUDE H IN GEOPOTENTIAL METERS

[From ref. A1]

H, m	μ , Pa-sec	H, m	μ , Pa-sec
0	1.7894×10^{-5}	15 000	1.4216×10^{-5}
500	1.7737	15 500	1.4216
1 000	1.7578	16 000	1.4216
1 500	1.7419	16 500	1.4216
2 000	1.7260	17 000	1.4216
2 500	1.7099	17 500	1.4216
3 000	1.6937	18 000	1.4216
3 500	1.6775	18 500	1.4216
4 000	1.6611	19 000	1.4216
4 500	1.6447	19 500	1.4216
5 000	1.6281	20 000	1.4216
5 500	1.6115	20 500	1.4244
6 000	1.5947	21 000	1.4271
6 500	1.5779	21 500	1.4298
7 000	1.5610	22 000	1.4326
7 500	1.5439	22 500	1.4353
8 000	1.5268	23 000	1.4381
8 500	1.5095	23 500	1.4408
9 000	1.4922	24 000	1.4435
9 500	1.4747	24 500	1.4462
10 000	1.4571	25 000	1.4490
10 500	1.4394	25 500	1.4517
11 000	1.4216	26 000	1.4544
11 500	1.4216	26 500	1.4571
12 000	1.4216	27 000	1.4598
12 500	1.4216	27 500	1.4625
13 000	1.4216	28 000	1.4652
13 500	1.4216	28 500	1.4679
14 000	1.4216	29 000	1.4706
14 500	1.4216	29 500	1.4733
		30 000	1.4760

APPENDIX A

TABLE A19.- SPEED OF SOUND a IN KILOMETERS PER HOUR AND KNOTS
FOR VALUES OF PRESSURE ALTITUDE H IN GEOPOTENTIAL METERS

[From ref. A1]

H, m	a, km/hr	a, knots	H, m	a, km/hr	a, knots
0	1225.06	661.48	15 000	1062.25	573.57
500	1218.13	657.74	15 500	1062.25	573.57
1 000	1211.14	653.98	16 000	1062.25	573.57
1 500	1204.15	650.19	16 500	1062.25	573.57
2 000	1197.10	646.38	17 000	1062.25	573.57
2 500	1190.01	642.56	17 500	1062.25	573.57
3 000	1182.88	638.70	18 000	1062.25	573.57
3 500	1175.70	634.83	18 500	1062.25	573.57
4 000	1168.48	630.93	19 000	1062.25	573.57
4 500	1161.22	627.01	19 500	1062.25	573.57
5 000	1153.90	623.06	20 000	1062.25	573.57
5 500	1146.55	619.09	20 500	1063.48	574.23
6 000	1139.14	615.09	21 000	1064.94	575.02
6 500	1131.69	611.06	21 500	1065.92	575.55
7 000	1124.18	607.01	22 000	1067.14	576.21
7 500	1116.63	602.93	22 500	1068.36	576.87
8 000	1109.03	598.83	23 000	1069.58	577.53
8 500	1101.37	594.69	23 500	1070.79	578.18
9 000	1093.65	590.53	24 000	1072.01	578.84
9 500	1085.89	586.33	24 500	1073.22	579.50
10 000	1078.07	582.11	25 000	1074.44	580.15
10 500	1070.19	577.85	25 500	1075.65	580.80
11 000	1062.25	573.57	26 000	1076.86	581.46
11 500	1062.25	573.57	26 500	1078.07	582.11
12 000	1062.25	573.57	27 000	1079.27	582.76
12 500	1062.25	573.57	27 500	1080.48	583.41
13 000	1062.25	573.57	28 000	1081.68	584.06
13 500	1062.25	573.57	28 500	1082.89	584.71
14 000	1062.25	573.57	29 000	1084.09	585.36
14 500	1062.25	573.57	29 500	1085.29	586.01
			30 000	1086.49	586.66

ORIGINAL PAGE IS
OF POOR QUALITY

APPENDIX A

TABLE A20.- ACCELERATION DUE TO GRAVITY g IN METERS PER SECOND SQUARED
FOR VALUES OF PRESSURE ALTITUDE H IN GEOPOTENTIAL METERS
[From ref. A1]

H, m	g , m/sec ²	H, m	g , m/sec ²
0	9.8066	15 000	9.7604
500	9.8051	15 500	9.7589
1 000	9.8036	16 000	9.7573
1 500	9.8020	16 500	9.7558
2 000	9.8005	17 000	9.7543
2 500	9.7989	17 500	9.7525
3 000	9.7974	18 000	9.7512
3 500	9.7959	18 500	9.7496
4 000	9.7943	19 000	9.7481
4 500	9.7928	19 500	9.7466
5 000	9.7912	20 000	9.7450
5 500	9.7897	20 500	9.7435
6 000	9.7881	21 000	9.7420
6 500	9.7866	21 500	9.7404
7 000	9.7851	22 000	9.7389
7 500	9.7835	22 500	9.7373
8 000	9.7820	23 000	9.7358
8 500	9.7804	23 500	9.7343
9 000	9.7789	24 000	9.7327
9 500	9.7774	24 500	9.7312
10 000	9.7758	25 000	9.7297
10 500	9.7743	25 500	9.7281
11 000	9.7727	26 000	9.7266
11 500	9.7712	26 500	9.7250
12 000	9.7697	27 000	9.7235
12 500	9.7681	27 500	9.7220
13 000	9.7666	28 000	9.7204
13 500	9.7650	28 500	9.7189
14 000	9.7635	29 000	9.7174
14 500	9.7620	29 500	9.7158
		30 000	9.7143

APPENDIX A

TABLE A21.- IMPACT PRESSURE q_c (OR q_c') IN MILLIMETERS OF MERCURY (10^3 C) FOR VALUES OF CALIBRATED AIRSPEED V_c (OR INDICATED AIRSPEED V_i) IN KILOMETERS PER HOUR

[Derived from ref. A2]

V_c km/hr	0	1	2	3	4	5	6	7	8	9
0	0	0	0.001	0.003	0.006	0.009	0.013	0.017	0.023	0.029
10	.035	.043	.051	.060	.069	.080	.091	.102	.115	.128
20	.142	.156	.172	.188	.204	.222	.240	.258	.278	.298
30	.319	.341	.363	.386	.410	.434	.460	.485	.512	.539
40	.567	.596	.625	.656	.687	.718	.750	.783	.817	.851
50	.887	.922	.959	.996	1.034	1.073	1.112	1.152	1.193	1.235
60	1.277	1.320	1.364	1.408	1.453	1.499	1.545	1.592	1.640	1.689
70	1.738	1.788	1.839	1.891	1.943	1.996	2.049	2.104	2.159	2.215
80	2.271	2.328	2.386	2.445	2.504	2.564	2.625	2.686	2.749	2.812
90	2.875	2.940	3.005	3.070	3.137	3.204	3.272	3.341	3.410	3.480
100	3.551	3.622	3.694	3.767	3.841	3.915	3.990	4.066	4.143	4.220
110	4.298	4.377	4.456	4.536	4.617	4.698	4.781	4.864	4.947	5.032
120	5.117	5.203	5.289	5.377	5.465	5.553	5.643	5.733	5.824	5.915
130	6.008	6.101	6.194	6.289	6.384	6.480	6.577	6.674	6.772	6.871
140	6.971	7.071	7.172	7.274	7.376	7.479	7.583	7.688	7.793	7.899
150	8.006	8.113	8.222	8.331	8.440	8.551	8.662	8.774	8.886	9.000
160	9.114	9.228	9.344	9.460	9.577	9.695	9.813	9.932	10.052	10.173
170	10.294	10.416	10.539	10.662	10.787	10.912	11.037	11.164	11.291	11.419
180	11.547	11.677	11.807	11.938	12.069	12.202	12.335	12.468	12.603	12.738
190	12.874	13.011	13.148	13.286	13.425	13.565	13.705	13.846	13.988	14.131
200	14.274	14.418	14.563	14.709	14.855	15.002	15.150	15.298	15.447	15.597
210	15.748	15.899	16.052	16.205	16.358	16.513	16.668	16.824	16.980	17.138
220	17.296	17.455	17.614	17.775	17.936	18.098	18.260	18.424	18.588	18.753
230	18.918	19.084	19.251	19.419	19.588	19.757	19.927	20.098	20.270	20.442
240	20.615	20.789	20.963	21.139	21.315	21.492	21.669	21.847	22.027	22.206
250	22.387	22.568	22.750	22.933	23.117	23.301	23.486	23.672	23.859	24.046
260	24.234	24.423	24.613	24.803	24.994	25.186	25.379	25.572	25.767	25.962
270	26.157	26.354	26.551	26.749	26.948	27.147	27.348	27.549	27.751	27.953
280	28.156	28.361	28.565	28.771	28.978	29.185	29.393	29.601	29.811	30.021
290	30.232	30.444	30.657	30.870	31.084	31.299	31.515	31.731	31.948	32.166
300	32.385	32.604	32.825	33.046	33.268	33.490	33.714	33.938	34.163	34.388
310	34.615	34.842	35.070	35.299	35.529	35.759	35.990	36.222	36.455	36.688
320	36.923	37.158	37.394	37.630	37.868	38.106	38.345	38.585	38.825	39.067
330	39.309	39.552	39.795	40.040	40.285	40.531	40.778	41.026	41.274	41.524
340	41.774	42.025	42.276	42.529	42.782	43.036	43.291	43.546	43.803	44.060
350	44.318	44.577	44.836	45.097	45.358	45.620	45.883	46.146	46.411	46.676
360	46.942	47.208	47.476	47.744	48.014	48.284	48.555	48.826	49.099	49.372
370	49.646	49.921	50.196	50.473	50.750	51.028	51.307	51.587	51.867	52.149
380	52.431	52.714	52.998	53.282	53.568	53.854	54.141	54.429	54.717	55.007
390	55.297	55.588	55.880	56.173	56.467	56.761	57.056	57.352	57.649	57.947
400	58.245	58.545	58.845	59.146	59.448	59.751	60.054	60.358	60.664	60.971
410	61.277	61.585	61.893	62.203	62.513	62.824	63.136	63.448	63.762	64.076
420	64.391	64.707	65.024	65.342	65.660	65.980	66.300	66.621	66.943	67.266
430	67.589	67.913	68.239	68.565	68.892	69.220	69.548	69.878	70.208	70.539
440	70.671	71.004	71.338	71.672	72.008	72.344	72.681	73.019	73.358	73.698
450	74.238	74.580	74.922	75.265	75.609	75.954	76.300	76.647	76.994	77.342
460	77.691	78.041	78.392	78.744	79.097	79.450	79.805	80.160	80.516	80.872
470	81.231	81.590	81.949	82.310	82.671	83.033	83.396	83.760	84.125	84.491
480	84.957	85.325	85.693	86.062	86.432	86.804	87.175	87.548	87.922	88.296
490	89.572	89.948	90.325	90.703	91.082	91.462	91.843	92.224	92.607	92.990
500	93.375	93.760	94.146	94.533	94.921	95.310	95.699	96.090	96.481	96.874
510	96.267	96.661	97.056	97.452	97.849	98.247	98.647	99.046	99.447	99.848
520	100.25	100.65	101.06	101.46	101.87	102.27	102.68	103.09	103.50	103.91
530	104.31	104.72	105.13	105.54	105.95	106.36	106.77	107.18	107.59	108.00
540	108.41	108.82	109.23	109.64	110.05	110.46	110.87	111.28	111.69	112.10
550	112.51	112.92	113.33	113.74	114.15	114.56	114.97	115.38	115.79	116.20
560	116.61	117.02	117.43	117.84	118.25	118.66	119.07	119.48	119.89	120.30
570	120.71	121.12	121.53	121.94	122.35	122.76	123.17	123.58	123.99	124.40
580	124.81	125.22	125.63	126.04	126.45	126.86	127.27	127.68	128.09	128.50
590	128.91	129.32	129.73	130.14	130.55	130.96	131.37	131.78	132.19	132.60
600	133.01	133.42	133.83	134.24	134.65	135.06	135.47	135.88	136.29	136.70

APPENDIX A

TABLE A21.- Continued

ORIGINAL PAGE IS
OF POOR QUALITY

V _c km/hr	0	1	2	3	4	5	6	7	8	9
600	135.45	135.93	136.41	136.89	137.37	137.86	138.34	138.83	139.31	139.80
610	140.29	140.77	141.26	141.75	142.24	142.74	143.23	143.73	144.22	144.72
620	145.22	145.72	146.22	146.72	147.22	147.72	148.22	148.73	149.23	149.74
630	150.25	150.76	151.26	151.78	152.29	152.80	153.31	153.83	154.34	154.86
640	155.38	155.90	156.42	156.94	157.46	157.98	158.51	159.03	159.56	160.08
650	160.61	161.14	161.67	162.20	162.73	163.27	163.80	164.34	164.87	165.41
660	165.95	166.49	167.03	167.57	168.11	168.66	169.20	169.75	170.29	170.84
670	171.39	171.94	172.49	173.04	173.59	174.15	174.70	175.26	175.82	176.37
680	176.93	177.49	178.06	178.62	179.18	179.75	180.31	180.88	181.45	182.02
690	182.59	183.16	183.73	184.30	184.88	185.45	186.03	186.61	187.18	187.76
700	188.35	188.93	189.51	190.09	190.68	191.27	191.85	192.44	193.03	193.62
710	194.21	194.81	195.40	196.00	196.59	197.19	197.79	198.39	198.99	199.59
720	200.19	200.79	201.40	202.01	202.61	203.22	203.83	204.44	205.05	205.66
730	206.28	206.89	207.51	208.13	208.75	209.36	209.99	210.61	211.23	211.85
740	212.48	213.11	213.73	214.36	214.99	215.62	216.25	216.89	217.52	218.16
750	218.79	219.43	220.07	220.71	221.35	221.99	222.64	223.28	223.93	224.57
760	225.22	225.87	226.52	227.17	227.82	228.48	229.13	229.79	230.45	231.10
770	231.76	232.48	233.09	233.75	234.41	235.08	235.75	236.42	237.08	237.75
780	238.43	239.10	239.77	240.45	241.12	241.80	242.48	243.16	243.84	244.52
790	245.21	245.89	246.58	247.26	247.95	248.64	249.33	250.02	250.72	251.41
800	252.10	252.80	253.50	254.20	254.90	255.60	256.30	257.01	257.71	258.42
810	259.12	259.83	260.54	261.25	261.97	262.68	263.40	264.11	264.83	265.55
820	266.27	266.99	267.71	268.43	269.16	269.89	270.61	271.34	272.07	272.80
830	273.53	274.27	275.00	275.74	276.48	277.22	277.96	278.70	279.44	280.18
840	280.93	281.67	282.42	283.17	283.92	284.67	285.42	286.17	286.93	287.69
850	288.45	289.21	289.97	290.73	291.49	292.26	293.02	293.79	294.56	295.32
860	296.10	296.87	297.64	298.41	299.19	299.97	300.75	301.53	302.31	303.01
870	303.87	304.66	305.44	306.23	307.02	307.81	308.60	309.40	310.19	310.98
880	311.78	312.58	313.38	314.18	314.98	315.79	316.59	317.40	318.20	319.01
890	319.82	320.64	321.45	322.26	323.08	323.90	324.71	325.53	326.35	327.18
900	328.00	328.83	329.65	330.48	331.31	332.14	332.97	333.81	334.64	335.48
910	336.31	337.15	337.99	338.84	339.68	340.52	341.37	342.22	343.06	343.91
920	344.77	345.62	346.47	347.33	348.18	349.04	349.90	350.76	351.63	352.49
930	353.36	354.22	355.09	355.96	356.83	357.70	358.58	359.45	360.33	361.21
940	362.09	362.97	363.85	364.73	365.62	366.51	367.39	368.28	369.18	370.07
950	370.96	371.86	372.76	373.65	374.55	375.45	376.36	377.26	378.17	379.07
960	379.98	380.89	381.80	382.72	383.63	384.55	385.46	386.38	387.30	388.22
970	389.15	390.07	391.00	391.93	392.85	393.79	394.72	395.65	396.59	397.52
980	398.46	399.40	400.34	401.29	402.23	403.18	404.12	405.07	406.02	406.97
990	407.93	408.88	409.84	410.80	411.75	412.72	413.68	414.64	415.61	416.57
1000	417.54	418.51	419.48	420.46	421.43	422.41	423.39	424.37	425.35	426.33
1010	427.31	428.30	429.29	430.27	431.26	432.26	433.25	434.24	435.24	436.24
1020	437.24	438.24	439.24	440.25	441.25	442.26	443.27	444.28	445.29	446.31
1030	447.32	448.34	449.36	450.38	451.40	452.42	453.45	454.48	455.51	456.54
1040	457.57	458.60	459.64	460.67	461.71	462.75	463.79	464.83	465.88	466.93
1050	467.97	469.02	470.07	471.13	472.18	473.24	474.29	475.35	476.42	477.48
1060	478.54	479.61	480.68	481.75	482.82	483.89	484.96	486.04	487.12	488.20
1070	489.28	490.36	491.44	492.53	493.62	494.71	495.80	496.89	497.99	499.08
1080	500.18	501.28	502.37	503.49	504.59	505.68	506.80	507.91	509.03	510.14
1090	511.25	512.37	513.49	514.61	515.73	516.86	517.98	519.11	520.24	521.37
1100	522.50	523.64	524.77	525.91	527.05	528.19	529.33	530.48	531.62	532.77
1110	533.92	535.07	536.23	537.38	538.54	539.70	540.86	542.02	543.19	544.35
1120	545.52	546.69	547.86	549.03	550.21	551.38	552.56	553.74	554.93	556.11
1130	557.30	558.48	559.67	560.86	562.06	563.25	564.45	565.65	566.85	568.05
1140	569.25	570.46	571.67	572.88	574.09	575.30	576.52	577.73	578.95	580.17
1150	581.39	582.62	583.84	585.07	586.30	587.53	588.77	590.00	591.24	592.48
1160	593.72	594.96	596.21	597.46	598.71	599.95	601.21	602.46	603.72	604.96
1170	606.24	607.50	608.76	610.03	611.30	612.57	613.84	615.11	616.39	617.67
1180	618.95	620.22	621.51	622.80	624.08	625.37	626.66	627.96	629.25	630.55
1190	631.85	633.15	634.45	635.75	637.06	638.37	639.68	640.99	642.31	643.62

APPENDIX A

TABLE A21.- Concluded

V _c km/hr	0	1	2	3	4	5	6	7	8	9
1200	644.94	646.26	647.59	648.91	650.24	651.56	652.89	654.23	655.56	656.90
1210	658.24	659.58	660.92	662.26	663.61	664.96	666.31	667.66	669.02	670.37
1220	671.73	673.09	674.46	675.82	677.19	678.56	679.93	681.30	682.68	684.05
1230	685.43	686.81	688.20	689.58	690.97	692.36	693.75	695.14	696.54	697.94
1240	699.33	700.74	702.14	703.54	704.95	706.36	707.77	709.19	710.60	712.02
1250	713.44	714.86	716.28	717.71	719.13	720.56	721.99	723.43	724.86	726.30
1260	727.73	729.18	730.62	732.07	733.51	734.96	736.41	737.86	739.32	740.77
1270	742.21	743.69	745.15	746.62	748.08	749.55	751.02	752.49	753.97	755.44
1280	756.92	758.40	759.88	761.36	762.85	764.33	765.82	767.31	768.80	770.30
1290	771.79	773.29	774.79	776.29	777.79	779.30	780.81	782.32	783.83	785.34
1300	786.85	788.37	789.89	791.41	792.93	794.45	795.98	797.51	799.04	800.57
1310	802.10	803.63	805.17	806.71	808.25	809.79	811.33	812.88	814.43	815.98
1320	817.53	819.08	820.63	822.19	823.75	825.31	826.87	828.43	830.00	831.57
1330	833.13	834.71	836.28	837.85	839.43	841.01	842.59	844.17	845.75	847.33
1340	848.92	850.51	852.10	853.69	855.28	856.88	858.48	860.07	861.68	863.28
1350	864.88	866.49	868.09	869.70	871.31	872.93	874.54	876.16	877.78	879.40
1360	881.02	882.64	884.26	885.89	887.52	889.15	890.78	892.42	894.05	895.69
1370	897.33	898.97	900.61	902.25	903.90	905.54	907.19	908.84	910.50	912.15
1380	913.80	915.46	917.12	918.78	920.45	922.11	923.77	925.44	927.11	928.78
1390	930.45	932.13	933.80	935.48	937.16	938.84	940.52	942.21	943.89	945.58
1400	947.27	948.96	950.66	952.35	954.05	955.74	957.44	959.14	960.85	962.55
1410	964.26	965.96	967.67	969.38	971.10	972.81	974.53	976.24	977.96	979.68
1420	981.41	983.13	984.86	986.58	988.31	990.04	991.76	993.51	995.24	996.98
1430	998.72	1000.46	1002.20	1003.94	1005.69	1007.42	1009.16	1010.94	1012.69	1014.44
1440	1016.20	1017.95	1019.71	1021.47	1023.23	1025.05	1026.75	1028.53	1030.29	1032.06
1450	1033.83	1035.61	1037.38	1039.16	1040.93	1042.71	1044.49	1046.28	1048.06	1049.85
1460	1051.63	1052.42	1055.21	1057.00	1058.80	1060.59	1062.39	1064.19	1065.99	1067.79
1470	1069.59	1071.40	1073.20	1075.01	1076.82	1078.63	1080.44	1082.26	1084.07	1085.89
1480	1087.71	1089.53	1091.35	1093.17	1095.00	1096.83	1098.66	1100.48	1102.32	1104.15
1490	1105.98	1107.82	1109.66	1111.50	1113.34	1115.18	1117.02	1118.87	1120.72	1122.57
1500	1124.42	1126.27	1128.12	1129.98	1131.83	1133.69	1135.55	1137.41	1139.27	1141.14
1510	1143.00	1144.87	1146.74	1148.61	1150.48	1152.35	1154.23	1156.11	1157.98	1159.88
1520	1161.75	1163.63	1165.51	1167.40	1169.29	1171.18	1173.07	1174.96	1176.85	1178.75
1530	1180.64	1182.54	1184.44	1186.34	1188.24	1190.15	1192.05	1193.96	1195.87	1197.78
1540	1199.69	1201.61	1203.52	1205.44	1207.36	1209.28	1211.20	1213.12	1215.04	1216.97
1550	1218.90	1220.83	1222.76	1224.69	1226.62	1228.56	1230.49	1232.43	1234.37	1236.31
1560	1238.25	1240.20	1242.14	1244.09	1246.04	1247.99	1249.94	1251.89	1253.85	1255.80
1570	1257.76	1259.72	1261.68	1263.64	1265.60	1267.57	1269.54	1271.50	1273.47	1275.44
1580	1277.42	1279.39	1281.37	1283.34	1285.32	1287.30	1289.28	1291.27	1293.25	1295.24
1590	1297.22	1299.21	1301.20	1303.20	1305.19	1307.18	1309.18	1311.18	1313.16	1315.18
1600	1317.18	1319.19	1321.19	1323.20	1325.21	1327.22	1329.23	1331.24	1333.25	1335.27
1610	1337.29	1339.31	1341.33	1343.35	1345.37	1347.40	1349.42	1351.45	1353.46	1355.51
1620	1357.54	1359.57	1361.61	1363.65	1365.68	1367.72	1369.76	1371.81	1373.85	1375.90
1630	1377.94	1379.99	1382.04	1384.09	1386.15	1388.20	1390.25	1392.30	1394.37	1396.43
1640	1398.49	1400.56	1402.62	1404.69	1406.75	1408.82	1410.89	1412.97	1415.04	1417.11
1650	1419.19	1421.27	1423.35	1425.43	1427.51	1429.59	1431.68	1433.76	1435.85	1437.94
1660	1440.03	1442.12	1444.22	1446.31	1448.41	1450.51	1452.61	1454.71	1456.81	1458.92
1670	1461.02	1463.13	1465.23	1467.35	1469.46	1471.57	1473.68	1475.80	1477.92	1480.03
1680	1482.15	1484.28	1486.40	1488.52	1490.65	1492.78	1494.91	1497.04	1499.17	1501.30
1690	1503.42	1505.57	1507.71	1509.85	1511.99	1514.13	1516.27	1518.42	1520.56	1522.71
1700	1524.86									

APPENDIX A

TABLE A2.1 - IMPACT PRESSURE q (OR q_z) IN PASCALS FOR VALUES OF CALIBRATED AIRSPEED V_c (OR INDICATED AIRSPEED V_i) IN KILOMETERS PER HOUR

[Derived from ref. A2]

V_c , km/hr	0	1	2	3	4	5	6	7	8	9
0	0	0.05	0.19	0.43	0.76	1.18	1.75	2.42	3.19	4.05
10	4.73	5.72	6.81	7.99	9.26	10.63	12.10	13.66	15.31	17.04
20	18.91	20.84	22.88	25.00	27.23	29.54	31.95	34.46	37.06	39.75
30	42.54	45.43	48.40	51.48	54.64	57.91	61.26	64.72	68.26	71.89
40	75.64	79.47	83.39	87.41	91.53	95.74	100.04	104.44	108.93	113.51
50	118.20	122.98	127.85	132.82	137.88	143.04	148.29	153.63	159.06	164.58
60	170.24	175.97	181.79	187.70	193.71	199.82	206.02	212.31	218.69	225.17
70	231.77	238.44	245.21	252.08	259.04	266.09	273.24	280.49	287.83	295.24
80	302.79	310.42	318.14	325.95	333.86	341.87	349.97	358.17	366.45	374.80
90	383.33	391.91	400.58	409.35	418.21	427.17	436.23	445.37	454.59	463.89
100	473.40	482.93	492.55	502.26	512.09	522.01	532.02	542.12	552.31	562.58
110	573.01	583.50	594.08	604.76	615.53	626.40	637.37	648.44	659.60	670.84
120	682.19	693.64	705.19	716.81	728.55	740.37	752.31	764.34	776.44	788.61
130	800.96	813.36	825.87	838.46	851.14	863.95	876.83	889.82	902.89	916.03
140	929.34	942.71	956.17	969.73	983.39	997.14	1011.00	1024.94	1038.97	1053.07
150	1067.4	1081.7	1096.1	1110.6	1125.3	1140.0	1154.8	1169.7	1184.7	1199.7
160	1215.0	1230.3	1245.7	1261.1	1276.8	1292.5	1308.3	1324.1	1340.0	1355.9
170	1372.4	1388.7	1405.1	1421.5	1438.1	1454.8	1471.5	1488.4	1505.2	1522.1
180	1539.5	1556.8	1574.1	1591.6	1609.1	1626.7	1644.3	1662.0	1679.7	1697.5
190	1716.4	1734.6	1752.9	1771.4	1789.9	1808.5	1827.1	1845.8	1864.5	1883.3
200	1903.1	1922.3	1941.6	1961.0	1980.5	1999.1	2017.8	2036.6	2055.4	2074.3
210	2099.6	2119.8	2140.0	2160.3	2180.9	2201.5	2222.2	2242.9	2263.7	2284.4
220	2305.9	2327.1	2348.4	2369.8	2391.2	2412.8	2434.5	2456.2	2478.0	2499.7
230	2522.2	2544.4	2566.7	2589.0	2611.5	2634.1	2656.8	2679.5	2702.3	2725.1
240	2748.4	2771.6	2794.9	2818.3	2841.7	2865.3	2888.9	2912.6	2936.3	2960.0
250	2984.7	3008.9	3033.1	3057.5	3082.0	3106.6	3131.2	3155.9	3180.6	3205.3
260	3231.0	3256.2	3281.4	3306.8	3332.3	3357.9	3383.5	3409.2	3434.9	3460.6
270	3487.4	3513.6	3539.9	3566.2	3592.7	3619.2	3645.8	3672.4	3699.0	3725.6
280	3753.9	3781.1	3808.4	3835.8	3863.4	3891.0	3918.6	3946.3	3974.0	4001.7
290	4030.6	4058.9	4087.2	4115.6	4144.1	4172.7	4201.3	4229.9	4258.5	4287.1
300	4317.6	4346.3	4375.0	4403.7	4432.5	4461.3	4490.1	4518.9	4547.7	4576.5
310	4614.9	4644.2	4673.6	4703.0	4732.5	4762.0	4791.5	4821.0	4850.5	4880.0
320	4922.6	4952.0	4981.5	5011.0	5040.5	5070.0	5100.0	5130.0	5160.0	5190.0
330	5240.7	5270.1	5300.0	5330.0	5360.0	5390.0	5420.0	5450.0	5480.0	5510.0
340	5569.4	5600.0	5630.0	5660.0	5690.0	5720.0	5750.0	5780.0	5810.0	5840.0
350	5908.6	5940.0	5970.0	6000.0	6030.0	6060.0	6090.0	6120.0	6150.0	6180.0
360	6258.4	6290.0	6320.0	6350.0	6380.0	6410.0	6440.0	6470.0	6500.0	6530.0
370	6618.9	6650.0	6680.0	6710.0	6740.0	6770.0	6800.0	6830.0	6860.0	6890.0
380	6990.2	7020.0	7050.0	7080.0	7110.0	7140.0	7170.0	7200.0	7230.0	7260.0
390	7372.4	7400.0	7430.0	7460.0	7490.0	7520.0	7550.0	7580.0	7610.0	7640.0
400	7765.4	7790.0	7820.0	7850.0	7880.0	7910.0	7940.0	7970.0	8000.0	8030.0
410	8169.6	8190.0	8220.0	8250.0	8280.0	8310.0	8340.0	8370.0	8400.0	8430.0
420	8584.8	8610.0	8640.0	8670.0	8700.0	8730.0	8760.0	8790.0	8820.0	8850.0
430	8911.1	8940.0	8970.0	9000.0	9030.0	9060.0	9090.0	9120.0	9150.0	9180.0
440	9249.7	9280.0	9310.0	9340.0	9370.0	9400.0	9430.0	9460.0	9490.0	9520.0
450	9677.6	9710.0	9740.0	9770.0	9800.0	9830.0	9860.0	9890.0	9920.0	9950.0
460	10005.8	10040.0	10070.0	10100.0	10130.0	10160.0	10190.0	10220.0	10250.0	10280.0
470	10411.1	10440.0	10470.0	10500.0	10530.0	10560.0	10590.0	10620.0	10650.0	10680.0
480	10816.4	10840.0	10870.0	10900.0	10930.0	10960.0	10990.0	11020.0	11050.0	11080.0
490	11221.6	11240.0	11270.0	11300.0	11330.0	11360.0	11390.0	11420.0	11450.0	11480.0
500	11626.8	11640.0	11670.0	11700.0	11730.0	11760.0	11790.0	11820.0	11850.0	11880.0
510	12031.9	12040.0	12070.0	12100.0	12130.0	12160.0	12190.0	12220.0	12250.0	12280.0
520	12436.9	12440.0	12470.0	12500.0	12530.0	12560.0	12590.0	12620.0	12650.0	12680.0
530	12841.8	12840.0	12870.0	12900.0	12930.0	12960.0	12990.0	13020.0	13050.0	13080.0
540	13246.6	13240.0	13270.0	13300.0	13330.0	13360.0	13390.0	13420.0	13450.0	13480.0
550	13651.3	13640.0	13670.0	13700.0	13730.0	13760.0	13790.0	13820.0	13850.0	13880.0
560	14055.8	14040.0	14070.0	14100.0	14130.0	14160.0	14190.0	14220.0	14250.0	14280.0
570	14460.1	14440.0	14470.0	14500.0	14530.0	14560.0	14590.0	14620.0	14650.0	14680.0
580	14864.2	14840.0	14870.0	14900.0	14930.0	14960.0	14990.0	15020.0	15050.0	15080.0
590	15268.1	15240.0	15270.0	15300.0	15330.0	15360.0	15390.0	15420.0	15450.0	15480.0
600	15671.8	15640.0	15670.0	15700.0	15730.0	15760.0	15790.0	15820.0	15850.0	15880.0
610	16075.3	16040.0	16070.0	16100.0	16130.0	16160.0	16190.0	16220.0	16250.0	16280.0
620	16478.5	16440.0	16470.0	16500.0	16530.0	16560.0	16590.0	16620.0	16650.0	16680.0
630	16881.5	16840.0	16870.0	16900.0	16930.0	16960.0	16990.0	17020.0	17050.0	17080.0
640	17284.3	17240.0	17270.0	17300.0	17330.0	17360.0	17390.0	17420.0	17450.0	17480.0
650	17686.8	17640.0	17670.0	17700.0	17730.0	17760.0	17790.0	17820.0	17850.0	17880.0
660	18089.0	18040.0	18070.0	18100.0	18130.0	18160.0	18190.0	18220.0	18250.0	18280.0
670	18490.9	18440.0	18470.0	18500.0	18530.0	18560.0	18590.0	18620.0	18650.0	18680.0
680	18892.5	18840.0	18870.0	18900.0	18930.0	18960.0	18990.0	19020.0	19050.0	19080.0
690	19293.8	19240.0	19270.0	19300.0	19330.0	19360.0	19390.0	19420.0	19450.0	19480.0
700	19694.7	19640.0	19670.0	19700.0	19730.0	19760.0	19790.0	19820.0	19850.0	19880.0
710	20095.3	20040.0	20070.0	20100.0	20130.0	20160.0	20190.0	20220.0	20250.0	20280.0
720	20495.5	20440.0	20470.0	20500.0	20530.0	20560.0	20590.0	20620.0	20650.0	20680.0
730	20895.3	20840.0	20870.0	20900.0	20930.0	20960.0	20990.0	21020.0	21050.0	21080.0
740	21294.7	21240.0	21270.0	21300.0	21330.0	21360.0	21390.0	21420.0	21450.0	21480.0
750	21693.7	21640.0	21670.0	21700.0	21730.0	21760.0	21790.0	21820.0	21850.0	21880.0
760	22092.3	22040.0	22070.0	22100.0	22130.0	22160.0	22190.0	22220.0	22250.0	22280.0
770	22490.5	22440.0	22470.0	22500.0	22530.0	22560.0	22590.0	22620.0	22650.0	22680.0
780	22888.3	22840.0	22870.0	22900.0	22930.0	22960.0	22990.0	23020.0	23050.0	23080.0
790	23285.7	23240.0	23270.0	23300.0	23330.0	23360.0	23390.0	23420.0	23450.0	23480.0
800	23682.7	23640.0	23670.0	23700.0	23730.0	23760.0	23790.0	23820.0	23850.0	23880.0
810	24079.3	24040.0	24070.0	24100.0	24130.0	24160.0	24190.0	24220.0	24250.0	24280.0
820	24475.5	24440.0	24470.0	24500.0	24530.0	24560.0	24590.0	24620.0	24650.0	24680.0
830	24871.3	24840.0	24870.0	24900.0	24930.0	24960.0	24990.0	25020.0	25050.0	25080.0
840	25266.7	25240.0	25270.0	25300.0	25330.0	25360.0	25390.0	25420.0	25450.0	25480.0
850	25661.7	25640.0	25670.0	25700.0	25730.0	25760.0	25790.0	25820.0	25850.0	25880.0
860	26056.3	26040.0	26070.0	26100.0	26130.0	26160.0	26190.0	26220.0	26250.0	26280.0
870	26450.9	26440.0	26470.0	26500.0	26530.0	26560.0	26590.0	26620.0	26650.0	26680.0
880	26845.5	26840.0	26870.0	26900.0	26930.0	26960.0	26990.0	27020.0	27050.0	27080.0
890	27240.1	27240.0	27270.0	27300.0	27330.0	27360.0	27390.0	27420.0	27450.0	27480.0
900	27634.7	27640.0	27670.0	27700.0	27730.0	27760.0	27790.0	27820.0	27850.0	27880.0
910	28029.3	28040.0	28070.0	28100.0	28130.0	28160.0	28190.0	28220.0	28250.0	28280.0
920	28423.9	28440.0	28470.0	28500.0	28530.0	28560.0	28590.0	28620.0	28650.0	28680.0
930	28818.5	28840.0	28870.0	28900.0	28930.0	28960.0	28990.0	29020.0	29050.0	29080.0
940	29213.1	29240.0	29270.0	29300.0	29330.0	29360.0	29390.0	29420.0		

APPENDIX A

TABLE A22.- Continued

V _c , km/hr	0	1	2	3	4	5	6	7	8	9
600	18 059	18 123	18 197	18 251	18 315	18 379	18 444	18 509	18 573	18 634
610	18 703	18 768	18 834	18 899	18 965	19 030	19 096	19 162	19 228	19 294
620	19 361	19 427	19 494	19 560	19 627	19 694	19 761	19 828	19 895	19 964
630	20 031	20 099	20 167	20 235	20 303	20 372	20 440	20 509	20 577	20 646
640	20 715	20 785	20 854	20 923	20 993	21 063	21 132	21 202	21 273	21 343
650	21 413	21 484	21 554	21 625	21 696	21 767	21 838	21 909	21 981	22 052
660	22 125	22 197	22 269	22 341	22 413	22 486	22 558	22 631	22 704	22 777
670	22 850	22 923	22 997	23 070	23 144	23 218	23 292	23 366	23 441	23 515
680	23 589	23 664	23 739	23 814	23 889	23 964	24 040	24 115	24 191	24 267
690	24 342	24 419	24 495	24 572	24 648	24 725	24 802	24 879	24 956	25 033
700	25 111	25 188	25 266	25 344	25 422	25 500	25 578	25 657	25 735	25 814
710	25 893	25 972	26 051	26 131	26 210	26 290	26 369	26 449	26 529	26 609
720	26 690	26 770	26 851	26 932	27 013	27 094	27 175	27 256	27 337	27 418
730	27 501	27 585	27 666	27 748	27 830	27 913	27 996	28 079	28 162	28 246
740	28 328	28 412	28 495	28 579	28 663	28 747	28 831	28 916	29 000	29 085
750	29 170	29 255	29 340	29 425	29 511	29 597	29 682	29 768	29 854	29 941
760	30 027	30 113	30 200	30 287	30 374	30 461	30 549	30 636	30 724	30 812
770	30 899	30 988	31 076	31 164	31 253	31 341	31 431	31 519	31 609	31 699
780	31 787	31 877	31 967	32 057	32 147	32 237	32 328	32 418	32 509	32 600
790	32 691	32 783	32 874	32 966	33 057	33 149	33 241	33 333	33 425	33 517
800	33 611	33 704	33 797	33 890	33 984	34 077	34 171	34 265	34 359	34 453
810	34 547	34 642	34 736	34 831	34 926	35 021	35 116	35 211	35 306	35 401
820	35 499	35 596	35 692	35 788	35 885	35 981	36 078	36 175	36 272	36 369
830	36 468	36 566	36 664	36 762	36 860	36 959	37 058	37 157	37 256	37 355
840	37 454	37 553	37 653	37 753	37 853	37 953	38 053	38 154	38 255	38 356
850	38 456	38 558	38 659	38 761	38 862	38 964	39 066	39 168	39 271	39 373
860	39 476	39 579	39 682	39 785	39 889	39 992	40 096	40 199	40 304	40 408
870	40 513	40 618	40 722	40 826	40 931	41 036	41 141	41 246	41 351	41 456
880	41 560	41 664	41 769	41 874	41 979	42 084	42 189	42 294	42 400	42 505
890	42 611	42 718	42 824	42 930	43 036	43 143	43 249	43 356	43 463	43 569
900	43 677	43 784	43 891	44 000	44 107	44 215	44 323	44 431	44 540	44 648
910	44 758	44 866	44 975	45 084	45 193	45 302	45 411	45 521	45 630	45 740
920	45 849	45 959	46 068	46 178	46 288	46 398	46 508	46 618	46 728	46 838
930	46 948	47 058	47 168	47 278	47 388	47 498	47 608	47 718	47 828	47 938
940	48 048	48 158	48 268	48 378	48 488	48 598	48 708	48 818	48 928	49 038
950	49 148	49 258	49 368	49 478	49 588	49 698	49 808	49 918	50 028	50 138
960	50 248	50 358	50 468	50 578	50 688	50 798	50 908	51 018	51 128	51 238
970	51 348	51 458	51 568	51 678	51 788	51 898	52 008	52 118	52 228	52 338
980	52 448	52 558	52 668	52 778	52 888	52 998	53 108	53 218	53 328	53 438
990	53 548	53 658	53 768	53 878	53 988	54 098	54 208	54 318	54 428	54 538
1000	54 648	54 758	54 868	54 978	55 088	55 198	55 308	55 418	55 528	55 638
1010	55 748	55 858	55 968	56 078	56 188	56 298	56 408	56 518	56 628	56 738
1020	56 848	56 958	57 068	57 178	57 288	57 398	57 508	57 618	57 728	57 838
1030	57 948	58 058	58 168	58 278	58 388	58 498	58 608	58 718	58 828	58 938
1040	59 048	59 158	59 268	59 378	59 488	59 598	59 708	59 818	59 928	60 038
1050	60 148	60 258	60 368	60 478	60 588	60 698	60 808	60 918	61 028	61 138
1060	61 248	61 358	61 468	61 578	61 688	61 798	61 908	62 018	62 128	62 238
1070	62 348	62 458	62 568	62 678	62 788	62 898	63 008	63 118	63 228	63 338
1080	63 448	63 558	63 668	63 778	63 888	63 998	64 108	64 218	64 328	64 438
1090	64 548	64 658	64 768	64 878	64 988	65 098	65 208	65 318	65 428	65 538
1100	65 648	65 758	65 868	65 978	66 088	66 198	66 308	66 418	66 528	66 638
1110	66 748	66 858	66 968	67 078	67 188	67 298	67 408	67 518	67 628	67 738
1120	67 848	67 958	68 068	68 178	68 288	68 398	68 508	68 618	68 728	68 838
1130	68 948	69 058	69 168	69 278	69 388	69 498	69 608	69 718	69 828	69 938
1140	70 048	70 158	70 268	70 378	70 488	70 598	70 708	70 818	70 928	71 038
1150	71 148	71 258	71 368	71 478	71 588	71 698	71 808	71 918	72 028	72 138
1160	72 248	72 358	72 468	72 578	72 688	72 798	72 908	73 018	73 128	73 238
1170	73 348	73 458	73 568	73 678	73 788	73 898	74 008	74 118	74 228	74 338
1180	74 448	74 558	74 668	74 778	74 888	74 998	75 108	75 218	75 328	75 438
1190	75 548	75 658	75 768	75 878	75 988	76 098	76 208	76 318	76 428	76 538
1200	76 648	76 758	76 868	76 978	77 088	77 198	77 308	77 418	77 528	77 638

APPENDIX A

ORIGINAL PAGE IS
OF POOR QUALITY

TABLE A22.- Concluded

V _C km/hr	0	1	2	3	4	5	6	7	8	9
1200	85 965	86 161	86 338	86 514	86 691	86 868	87 046	87 223	87 401	87 578
1210	87 758	87 936	88 115	88 295	88 474	88 654	88 834	89 014	89 195	89 376
1220	89 557	89 738	89 920	90 102	90 284	90 467	90 650	90 833	91 016	91 200
1230	91 383	91 568	91 752	91 937	92 122	92 307	92 492	92 678	92 864	93 051
1240	93 237	93 424	93 611	93 798	93 986	94 174	94 362	94 550	94 739	94 928
1250	95 117	95 307	95 496	95 686	95 877	96 067	96 258	96 449	96 640	96 832
1260	97 024	97 216	97 408	97 601	97 793	97 987	98 180	98 374	98 567	98 761
1270	98 956	99 151	99 346	99 541	99 736	99 932	100 127	100 324	100 520	100 717
1280	100 914	101 111	101 309	101 506	101 704	101 903	102 101	102 299	102 498	102 698
1290	102 897	103 097	103 297	103 497	103 697	103 898	104 099	104 300	104 502	104 703
1300	104 905	105 107	105 310	105 513	105 715	105 919	106 122	106 326	106 529	106 734
1310	106 938	107 142	107 347	107 552	107 758	107 958	108 169	108 375	108 581	108 788
1320	108 995	109 202	109 409	109 616	109 824	110 032	110 240	110 449	110 657	110 866
1330	111 075	111 285	111 494	111 704	111 914	112 125	112 335	112 546	112 757	112 969
1340	113 180	113 392	113 604	113 816	114 028	114 241	114 454	114 667	114 881	115 094
1350	115 308	115 522	115 736	115 951	116 166	116 381	116 596	116 811	117 027	117 243
1360	117 459	117 676	117 892	118 109	118 326	118 544	118 761	118 979	119 197	119 415
1370	119 634	119 852	120 071	120 290	120 509	120 729	120 949	121 169	121 389	121 607
1380	121 831	122 052	122 273	122 494	122 716	122 938	123 160	123 382	123 605	123 827
1390	124 050	124 274	124 497	124 721	124 945	125 169	125 393	125 618	125 842	126 067
1400	126 293	126 518	126 744	126 970	127 196	127 422	127 648	127 875	128 102	128 329
1410	128 557	128 785	129 012	129 240	129 469	129 697	129 926	130 155	130 384	130 614
1420	130 843	131 073	131 303	131 534	131 764	131 995	132 226	132 457	132 688	132 919
1430	133 152	133 384	133 616	133 848	134 081	134 314	134 547	134 780	135 014	135 246
1440	135 482	135 716	135 950	136 185	136 420	136 655	136 890	137 125	137 361	137 597
1450	137 833	138 070	138 306	138 543	138 780	139 017	139 254	139 491	139 729	139 966
1460	140 206	140 445	140 683	140 922	141 161	141 401	141 641	141 881	142 121	142 361
1470	142 600	142 841	143 082	143 323	143 563	143 805	144 047	144 289	144 531	144 773
1480	145 117	145 359	145 602	145 845	146 088	146 332	146 575	146 819	147 062	147 306
1490	147 452	147 697	147 942	148 187	148 433	148 678	148 924	149 169	149 415	149 661
1500	149 907	150 157	150 404	150 651	150 899	151 146	151 394	151 642	151 891	152 139
1510	152 388	152 637	152 886	153 135	153 385	153 635	153 885	154 135	154 385	154 635
1520	154 885	155 136	155 389	155 640	155 892	156 144	156 396	156 648	156 901	157 153
1530	157 406	157 659	157 913	158 166	158 420	158 674	158 928	159 182	159 436	159 690
1540	159 946	160 201	160 456	160 711	160 966	161 221	161 476	161 731	161 986	162 241
1550	162 496	162 753	163 010	163 267	163 524	163 781	164 038	164 295	164 552	164 809
1560	165 067	165 326	165 585	165 844	166 103	166 362	166 621	166 880	167 139	167 398
1570	167 657	167 917	168 176	168 436	168 695	168 955	169 214	169 474	169 733	170 000
1580	170 259	170 519	170 779	171 039	171 298	171 558	171 818	172 077	172 337	172 597
1590	172 857	173 117	173 377	173 637	173 897	174 157	174 417	174 677	174 937	175 197
1600	175 457	175 717	175 977	176 237	176 497	176 757	177 017	177 277	177 537	177 797
1610	178 057	178 317	178 577	178 837	179 097	179 357	179 617	179 877	180 137	180 397
1620	180 657	180 917	181 177	181 437	181 697	181 957	182 217	182 477	182 737	182 997
1630	183 257	183 517	183 777	184 037	184 297	184 557	184 817	185 077	185 337	185 597
1640	185 857	186 117	186 377	186 637	186 897	187 157	187 417	187 677	187 937	188 197
1650	188 457	188 717	188 977	189 237	189 497	189 757	190 017	190 277	190 537	190 797
1660	191 057	191 317	191 577	191 837	192 097	192 357	192 617	192 877	193 137	193 397
1670	193 657	193 917	194 177	194 437	194 697	194 957	195 217	195 477	195 737	195 997
1680	196 257	196 517	196 777	197 037	197 297	197 557	197 817	198 077	198 337	198 597
1690	198 857	199 117	199 377	199 637	199 897	200 157	200 417	200 677	200 937	201 197

APPENDIX A

TABLE A23.- IMPACT PRESSURE q_c (OR q_c') IN MILLIMETERS OF MERCURY (10^3) FOR
VALUES OF CALIBRATED AIRSPEED V_c (OR INDICATED AIRSPEED V_i) IN KNOTS

[Derived from ref. A2]

V_c , knots	0	1	2	3	4	5	6	7	8	9
0	0	0.001	0.005	0.011	0.019	0.030	0.044	0.060	0.078	0.098
10	.122	.147	.175	.205	.238	.274	.311	.351	.394	.439
20	.486	.536	.589	.643	.701	.760	.822	.887	.954	1.023
30	1.095	1.169	1.246	1.325	1.406	1.490	1.577	1.666	1.757	1.851
40	1.947	2.046	2.147	2.250	2.356	2.465	2.576	2.689	2.805	2.923
50	3.044	3.167	3.293	3.421	3.551	3.684	3.820	3.958	4.099	4.241
60	4.386	4.534	4.684	4.837	4.992	5.149	5.309	5.472	5.637	5.804
70	5.974	6.147	6.322	6.499	6.679	6.861	7.046	7.233	7.423	7.615
80	7.810	8.007	8.207	8.409	8.614	8.821	9.030	9.241	9.455	9.674
90	9.894	10.116	10.341	10.568	10.796	11.026	11.264	11.502	11.741	11.983
100	12.228	12.475	12.725	12.977	13.232	13.489	13.749	14.011	14.275	14.544
110	14.814	15.086	15.361	15.639	15.919	16.201	16.487	16.774	17.065	17.357
120	17.653	17.951	18.251	18.554	18.860	19.168	19.479	19.792	20.108	20.426
130	20.747	21.071	21.397	21.725	22.057	22.391	22.727	23.066	23.406	23.752
140	24.099	24.448	24.800	25.155	25.512	25.872	26.234	26.599	26.967	27.337
150	27.710	28.086	28.464	28.845	29.228	29.614	30.003	30.394	30.788	31.184
160	31.584	31.986	32.390	32.797	33.207	33.620	34.035	34.453	34.873	35.296
170	35.722	36.151	36.582	37.016	37.452	37.892	38.333	38.778	39.225	39.675
180	40.128	40.584	41.042	41.503	41.966	42.433	42.902	43.373	43.846	44.325
190	44.805	45.288	45.773	46.261	46.752	47.246	47.742	48.242	48.743	49.248
200	49.756	50.266	50.779	51.295	51.813	52.335	52.859	53.386	53.916	54.448
210	54.984	55.522	56.063	56.607	57.153	57.703	58.255	58.810	59.368	59.929
220	60.493	61.060	61.629	62.202	62.777	63.354	63.935	64.519	65.105	65.696
230	66.287	66.882	67.480	68.081	68.685	69.292	69.901	70.514	71.129	71.748
240	72.369	72.993	73.621	74.251	74.884	75.520	76.159	76.801	77.446	78.093
250	78.744	79.398	80.055	80.714	81.377	82.043	82.711	83.381	84.054	84.730
260	85.416	86.100	86.787	87.476	88.169	88.865	89.564	90.265	90.970	91.678
270	92.390	93.104	93.821	94.542	95.265	95.992	96.721	97.454	98.190	98.929
280	99.671	100.41	101.16	101.91	102.67	103.43	104.19	104.96	105.73	106.50
290	107.26	108.04	108.82	109.60	110.39	111.18	111.97	112.76	113.56	114.37
300	115.17	115.98	116.78	117.59	118.41	119.23	120.05	120.88	121.71	122.54
310	123.40	124.24	125.08	125.93	126.78	127.64	128.50	129.36	130.23	131.10
320	131.96	132.83	133.71	134.59	135.48	136.37	137.27	138.17	139.08	140.00
330	140.85	141.76	142.67	143.58	144.50	145.42	146.35	147.28	148.21	149.15
340	150.09	151.03	151.97	152.92	153.87	154.83	155.79	156.75	157.71	158.68
350	159.66	160.64	161.62	162.61	163.60	164.60	165.60	166.60	167.61	168.62
360	169.63	170.63	171.63	172.64	173.65	174.66	175.67	176.68	177.69	178.70
370	179.68	180.71	181.73	182.75	183.78	184.81	185.84	186.87	187.90	188.93
380	189.94	191.00	192.05	193.11	194.17	195.23	196.29	197.35	198.41	199.48
390	200.52	201.60	202.67	203.75	204.83	205.91	206.99	208.07	209.15	210.24
400	211.32	212.42	213.51	214.61	215.71	216.81	217.91	219.01	220.11	221.22
410	222.33	223.45	224.56	225.68	226.79	227.91	229.03	230.15	231.27	232.39
420	233.51	234.64	235.77	236.90	238.03	239.16	240.29	241.42	242.55	243.68
430	244.81	245.95	247.09	248.23	249.37	250.51	251.65	252.79	253.93	255.07
440	256.21	257.36	258.51	259.66	260.81	261.96	263.11	264.26	265.41	266.56
450	267.71	268.87	269.99	271.11	272.23	273.35	274.47	275.59	276.71	277.83
460	278.95	280.08	281.21	282.34	283.47	284.60	285.73	286.86	287.99	289.12
470	290.25	291.39	292.53	293.67	294.81	295.95	297.09	298.23	299.37	300.51
480	301.65	302.80	303.94	305.08	306.23	307.37	308.51	309.65	310.79	311.93
490	313.07	314.22	315.37	316.51	317.66	318.80	319.94	321.08	322.22	323.36
500	324.50	325.65	326.79	327.93	329.07	330.21	331.35	332.49	333.63	334.77

APPENDIX A

TABLE A23.- Concluded

V _c , knots	0	1	2	3	4	5	6	7	8	9
500	349.90	351.50	353.10	354.70	356.32	357.93	359.55	361.18	362.81	364.44
510	366.08	367.73	369.38	371.03	372.69	374.35	376.02	377.70	379.38	381.06
520	382.75	384.45	386.15	387.85	389.56	391.28	393.00	394.72	396.45	398.19
530	399.93	401.67	403.42	405.18	406.94	408.71	410.48	412.26	414.04	415.83
540	417.62	419.42	421.22	423.03	424.84	426.66	428.49	430.32	432.15	433.99
550	435.84	437.69	439.55	441.41	443.28	445.15	447.03	448.91	450.80	452.70
560	454.60	456.51	458.42	460.34	462.26	464.19	466.12	468.06	470.01	471.96
570	473.91	475.88	477.84	479.82	481.80	483.78	485.77	487.77	489.77	491.78
580	493.79	495.81	497.84	499.87	501.90	503.95	506.00	508.05	510.11	512.18
590	514.25	516.33	518.41	520.50	522.60	524.70	526.81	528.92	531.04	533.17
600	535.30	537.44	539.59	541.74	543.89	546.06	548.22	550.40	552.58	554.77
610	556.96	559.16	561.37	563.58	565.80	568.02	570.25	572.49	574.74	576.99
620	579.24	581.51	583.78	586.05	588.33	590.62	592.92	595.22	597.53	599.84
630	602.16	604.49	606.82	609.16	611.51	613.86	616.22	618.59	620.96	623.34
640	625.73	628.12	630.53	632.93	635.35	637.77	640.19	642.63	645.07	647.52
650	649.97	652.43	654.90	657.37	659.86	662.34	664.84	667.34	669.85	672.37
660	674.90	677.42	679.97	682.51	685.06	687.62	690.18	692.75	695.33	697.92
670	700.51	703.11	705.72	708.33	710.95	713.58	716.21	718.85	721.50	724.16
680	726.82	729.48	732.16	734.84	737.53	740.22	742.92	745.63	748.34	751.06
690	753.79	756.52	759.26	762.01	764.76	767.52	770.28	773.05	775.83	778.62
700	781.41	784.21	787.01	789.82	792.64	795.46	798.29	801.12	803.97	806.81
710	809.67	812.53	815.39	818.26	821.14	824.03	826.92	829.82	832.72	835.63
720	838.54	841.47	844.39	847.33	850.27	853.21	856.16	859.12	862.08	865.05
730	868.11	871.01	874.00	876.99	879.99	883.00	886.01	889.02	892.05	895.08
740	898.11	901.15	904.20	907.25	910.31	913.37	916.44	919.52	922.60	925.69
750	928.78	931.88	934.99	938.10	941.21	944.33	947.46	950.59	953.73	956.88
760	960.03	963.18	966.35	969.51	972.69	975.86	979.05	982.24	985.43	988.64
770	991.84	995.06	998.27	1001.50	1004.72	1007.96	1011.20	1014.46	1017.73	1020.96
780	1024.22	1027.49	1030.76	1034.04	1037.32	1040.61	1043.91	1047.21	1050.52	1053.83
790	1057.15	1060.47	1063.80	1067.13	1070.47	1073.82	1077.17	1080.52	1083.88	1087.25
800	1090.62	1094.00	1097.38	1100.77	1104.16	1107.56	1110.97	1114.38	1117.79	1121.21
810	1124.64	1128.07	1131.50	1134.95	1138.39	1141.85	1145.30	1148.77	1152.23	1155.71
820	1159.19	1162.67	1166.16	1169.66	1173.16	1176.66	1180.17	1183.69	1187.21	1190.73
830	1194.27	1197.80	1201.35	1204.89	1208.45	1212.00	1215.57	1219.13	1222.71	1226.29
840	1229.87	1233.46	1237.06	1240.68	1244.26	1247.87	1251.48	1255.10	1258.73	1262.36
850	1266.00	1269.64	1273.28	1276.93	1280.59	1284.25	1287.92	1291.59	1295.27	1298.95
860	1302.64	1306.33	1310.03	1313.73	1317.44	1321.15	1324.87	1328.59	1332.32	1336.05
870	1339.79	1343.53	1347.28	1351.04	1354.79	1358.56	1362.33	1366.10	1369.88	1373.66
880	1377.45	1381.24	1385.05	1388.85	1392.66	1396.47	1400.29	1404.11	1407.94	1411.78
890	1415.62	1419.46	1423.31	1427.17	1431.03	1434.89	1438.76	1442.63	1446.51	1450.40
900	1454.29	1458.18	1462.08	1465.99	1469.90	1473.81	1477.73	1481.65	1485.58	1489.51
910	1493.46	1497.41	1501.36	1505.32	1509.28	1513.25	1517.23	1521.21	1525.20	1529.19
920	1533.18	1537.18	1541.19	1545.20	1549.22	1553.24	1557.27	1561.30	1565.34	1569.38
930	1573.25	1577.32	1581.39	1585.48	1589.58	1593.68	1597.79	1601.90	1606.01	1610.13
940	1613.93	1618.08	1622.12	1626.18	1630.25	1634.33	1638.42	1642.51	1646.61	1650.72
950	1655.87	1659.91	1663.96	1668.01	1672.07	1676.14	1680.22	1684.30	1688.39	1692.48
960	1696.73	1700.84	1704.95	1709.07	1713.19	1717.32	1721.45	1725.59	1729.73	1733.88
970	1738.43	1742.58	1746.73	1750.89	1755.05	1759.22	1763.39	1767.57	1771.75	1775.93
980	1781.41	1785.60	1789.79	1793.99	1798.19	1802.40	1806.61	1810.83	1815.05	1819.28
990	1824.49	1828.73	1832.97	1837.22	1841.47	1845.73	1850.00	1854.27	1858.54	1862.82

APPENDIX A

TABLE A24.- IMPACT PRESSURE q_c (OR q_c') IN PASCALS FOR VALUES OF
CALIBRATED AIRSPEED V_c (OR INDICATED AIRSPEED V_i) IN KNOTS
[Derived from ref. A2]

V_c knots	0	1	2	3	4	5	6	7	8	9
0	0	0.16	0.65	1.45	2.59	4.05	5.84	7.94	10.37	13.12
10	16.21	19.62	23.34	27.40	31.78	36.48	41.50	46.86	52.53	58.53
20	64.86	71.50	78.45	85.78	93.40	101.35	109.62	118.22	127.14	136.39
30	145.97	155.86	166.09	176.64	187.51	198.71	210.24	222.09	234.27	246.77
40	259.60	272.75	286.23	300.04	314.17	328.63	343.42	358.53	373.97	389.74
50	405.83	422.25	439.00	456.07	473.47	491.20	509.26	527.64	546.35	565.39
60	584.76	604.46	624.48	644.84	665.52	686.53	707.87	729.54	751.53	773.86
70	796.52	819.50	842.82	866.46	890.44	914.75	939.38	964.35	989.65	1 015.3
80	1 041.2	1 067.5	1 094.2	1 121.1	1 148.4	1 176.0	1 204.0	1 232.3	1 260.9	1 289.4
90	1 319.1	1 348.7	1 378.7	1 408.9	1 439.6	1 470.5	1 501.8	1 533.4	1 565.4	1 597.7
100	1 630.3	1 663.2	1 696.5	1 730.2	1 764.1	1 798.4	1 833.1	1 868.1	1 903.4	1 939.0
110	1 975.0	2 011.3	2 048.0	2 085.0	2 122.3	2 160.0	2 198.0	2 236.4	2 275.1	2 314.1
120	2 353.5	2 393.2	2 433.3	2 473.7	2 514.4	2 555.5	2 596.9	2 638.7	2 680.8	2 723.3
130	2 766.0	2 809.2	2 852.7	2 896.5	2 940.6	2 985.2	3 030.0	3 075.1	3 120.5	3 166.2
140	3 122.9	3 259.5	3 306.4	3 353.7	3 401.3	3 449.3	3 497.6	3 546.1	3 595.1	3 644.7
150	3 694.4	3 744.4	3 794.9	3 845.6	3 896.7	3 948.2	4 000.0	4 052.1	4 104.7	4 157.6
160	4 210.8	4 264.4	4 318.3	4 372.6	4 427.3	4 482.2	4 537.3	4 592.6	4 648.4	4 704.4
170	4 762.6	4 819.7	4 877.2	4 935.0	4 993.2	5 051.8	5 110.7	5 170.0	5 229.6	5 289.5
180	5 350.0	5 410.7	5 471.8	5 533.2	5 595.0	5 657.2	5 719.7	5 782.6	5 845.7	5 909.1
190	5 973.5	6 037.9	6 102.6	6 167.7	6 233.1	6 298.9	6 365.1	6 431.7	6 498.6	6 565.8
200	6 633.5	6 701.6	6 770.0	6 838.7	6 907.9	6 977.4	7 047.3	7 117.5	7 188.2	7 259.2
210	7 330.6	7 402.3	7 474.4	7 546.9	7 619.8	7 693.1	7 766.7	7 840.7	7 915.1	7 989.9
220	8 065.0	8 140.6	8 216.5	8 292.8	8 369.5	8 446.5	8 524.0	8 601.9	8 680.2	8 758.9
230	8 837.5	8 915.9	8 996.6	9 076.7	9 157.2	9 238.1	9 319.1	9 401.1	9 483.1	9 565.6
240	9 648.4	9 731.6	9 815.2	9 899.3	9 983.7	10 068	10 154	10 239	10 325	10 411
250	10 498	10 585	10 673	10 761	10 849	10 938	11 027	11 117	11 207	11 297
260	11 388	11 479	11 570	11 662	11 755	11 848	11 941	12 034	12 128	12 222
270	12 318	12 413	12 508	12 604	12 701	12 798	12 895	12 993	13 091	13 189
280	13 288	13 387	13 487	13 587	13 688	13 789	13 890	13 992	14 095	14 197
290	14 300	14 404	14 509	14 612	14 717	14 822	14 928	15 034	15 141	15 247
300	15 355	15 463	15 571	15 680	15 789	15 898	16 008	16 118	16 229	16 340
310	16 452	16 564	16 677	16 790	16 903	17 017	17 132	17 246	17 361	17 477
320	17 593	17 710	17 827	17 944	18 062	18 180	18 299	18 418	18 537	18 656
330	18 779	18 900	19 021	19 143	19 266	19 388	19 512	19 635	19 759	19 884
340	20 009	20 135	20 261	20 388	20 515	20 642	20 770	20 898	21 027	21 157
350	21 286	21 417	21 547	21 679	21 810	21 942	22 075	22 208	22 341	22 475
360	22 610	22 745	22 881	23 017	23 153	23 290	23 428	23 566	23 704	23 844
370	23 982	24 122	24 263	24 403	24 545	24 686	24 829	24 971	25 115	25 259
380	25 430	25 548	25 693	25 839	25 985	26 132	26 279	26 427	26 575	26 724
390	26 873	27 023	27 174	27 325	27 476	27 628	27 780	27 933	28 086	28 240
400	28 395	28 550	28 705	28 861	29 016	29 175	29 332	29 490	29 648	29 807
410	29 968	30 128	30 289	30 450	30 612	30 774	30 937	31 101	31 264	31 428
420	31 594	31 761	31 926	32 092	32 257	32 423	32 596	32 768	32 941	33 114
430	33 274	33 445	33 617	33 789	33 961	34 135	34 309	34 483	34 657	34 832
440	35 110	35 286	35 464	35 641	35 817	35 994	36 174	36 354	36 534	36 715
450	36 891	37 074	37 257	37 440	37 623	37 807	37 991	38 176	38 361	38 546
460	38 731	38 919	39 108	39 297	39 487	39 677	39 868	40 059	40 250	40 441
470	40 636	40 831	41 026	41 221	41 417	41 613	41 809	42 006	42 203	42 400
480	42 597	42 797	42 996	43 195	43 395	43 594	43 794	43 994	44 194	44 394
490	44 597	44 799	44 999	45 199	45 399	45 599	45 799	45 999	46 199	46 399

APPENDIX A

TABLE A24.- Concluded

ORIGINAL PAGE IS
OF POOR QUALITY

V _C knots	0	1	2	3	4	5	6	7	8	9
500	46 650	46 862	47 076	47 290	47 505	47 720	47 936	48 153	48 370	48 588
510	48 807	49 026	49 246	49 466	49 688	49 910	50 132	50 355	50 579	50 804
520	51 029	51 255	51 482	51 709	51 937	52 166	52 395	52 625	52 856	53 087
530	53 319	53 552	53 785	54 020	54 254	54 490	54 726	54 963	55 201	55 439
540	55 678	55 918	56 158	56 399	56 641	56 884	57 127	57 371	57 616	57 861
550	58 107	58 354	58 601	58 850	59 099	59 349	59 599	59 850	60 102	60 355
560	60 608	60 862	61 117	61 373	61 629	61 886	62 144	62 403	62 662	62 922
570	63 183	63 445	63 707	63 970	64 234	64 499	64 764	65 030	65 297	65 565
580	65 833	66 103	66 373	66 644	66 915	67 187	67 461	67 735	68 009	68 285
590	68 561	68 838	69 116	69 395	69 674	69 954	70 235	70 517	70 800	71 083
600	71 368	71 653	71 939	72 225	72 513	72 801	73 091	73 381	73 671	73 963
610	74 255	74 549	74 843	75 138	75 434	75 730	76 028	76 326	76 625	76 925
620	77 226	77 528	77 830	78 134	78 438	78 743	79 049	79 356	79 662	79 972
630	80 281	80 592	80 903	81 215	81 528	81 842	82 156	82 472	82 788	83 106
640	83 424	83 743	84 063	84 384	84 706	85 028	85 352	85 676	86 002	86 328
650	86 655	86 983	87 312	87 642	87 973	88 305	88 638	88 972	89 306	89 642
660	89 978	90 316	90 654	90 993	91 333	91 674	92 016	92 359	92 703	93 048
670	93 394	93 740	94 088	94 436	94 786	95 136	95 487	95 839	96 192	96 546
680	96 900	97 256	97 613	97 970	98 328	98 688	99 048	99 409	99 770	100 133
690	100 497	100 861	101 226	101 592	101 960	102 327	102 696	103 065	103 436	103 807
700	104 179	104 552	104 926	105 301	105 676	106 053	106 430	106 808	107 187	107 566
710	107 947	108 328	108 710	109 093	109 477	109 861	110 247	110 633	111 020	111 408
720	111 797	112 186	112 576	112 968	113 359	113 752	114 146	114 540	114 935	115 331
730	115 728	116 125	116 524	116 923	117 323	117 723	118 124	118 527	118 930	119 334
740	119 738	120 144	120 550	120 957	121 365	121 773	122 182	122 592	123 003	123 415
750	123 827	124 240	124 654	125 069	125 484	125 900	126 317	126 735	127 154	127 573
760	127 993	128 414	128 835	129 257	129 681	130 105	130 529	130 954	131 380	131 807
770	132 235	132 663	133 092	133 522	133 952	134 384	134 816	135 248	135 682	136 116
780	136 551	136 987	137 423	137 860	138 298	138 737	139 176	139 616	140 057	140 499
790	140 941	141 384	141 828	142 272	142 717	143 164	143 610	144 058	144 506	144 954
800	145 404	145 854	146 305	146 757	147 209	147 662	148 117	148 571	149 026	149 482
810	149 939	150 397	150 855	151 314	151 773	152 233	152 694	153 156	153 618	154 082
820	154 545	155 010	155 475	155 941	156 408	156 875	157 343	157 811	158 281	158 751
830	159 222	159 694	160 166	160 639	161 113	161 587	162 062	162 539	163 014	163 491
840	163 969	164 448	164 927	165 407	165 887	166 369	166 851	167 333	167 817	168 301
850	168 785	169 271	169 757	170 244	170 731	171 219	171 708	172 198	172 688	173 179
860	173 670	174 163	174 656	175 149	175 644	176 139	176 634	177 131	177 628	178 125
870	178 624	179 123	179 623	180 123	180 624	181 126	181 628	182 131	182 635	183 140
880	183 645	184 151	184 657	185 164	185 672	186 181	186 690	187 200	187 710	188 221
890	188 733	189 246	189 759	190 273	190 788	191 303	191 819	192 335	192 852	193 370
900	193 889	194 408	194 928	195 449	195 970	196 492	197 014	197 537	198 061	198 586
910	199 111	199 637	200 163	200 691	201 218	201 747	202 276	202 806	203 336	203 867
920	204 399	204 932	205 465	205 999	206 533	207 068	207 603	208 140	208 677	209 216
930	209 753	210 292	210 832	211 372	211 913	212 455	212 997	213 540	214 084	214 629
940	215 173	215 719	216 265	216 812	217 359	217 908	218 456	219 006	219 556	220 107
950	220 658	221 210	221 763	222 316	222 870	223 425	223 980	224 536	225 093	225 650
960	226 208	226 767	227 326	227 886	228 446	229 008	229 569	230 132	230 695	231 259
970	231 823	232 388	232 954	233 519	234 087	234 654	235 223	235 792	236 361	236 931
980	237 502	238 074	238 646	239 218	239 792	240 366	240 941	241 516	242 092	242 668
990	243 246	243 823	244 402	244 981	245 561	246 141	246 722	247 304	247 886	248 469
1000	249 053									

APPENDIX A

TABLE A25.- TRUE AIRSPEED V IN KNOTS FOR VALUES OF CALIBRATED
AIRSPEED V_c IN KNOTS AND VALUES OF PRESSURE ALTITUDE H
IN GEOPOTENTIAL METERS

[Computation of V based on standard temperature at each altitude]

V_c , knots H , m	100	200	300	400	500	600	700	800	900	1000
0	100.0	200.0	300.0	400.0	500.0	600.0	700.0	800.0	900.0	1000
2 000	110.2	220.0	328.8	436.4	542.8	647.8	753.7	863.2	973.3	1085
4 000	122.1	243.0	361.4	477.0	589.6	700.1	815.4	933.2	1061	1186
6 000	135.8	269.2	398.2	522.1	640.8	759.9	888.6	1025	1165	1305
8 000	152.0	299.5	439.8	571.9	698.2	830.7	975.9	1131	1288	1447
10 000	170.9	334.5	486.6	626.9	765.9	916.1	1082	1258	1436	1618
12 000	196.2	380.4	546.8	700.3	860.4	1035	1228	1434	1642	1851
14 000	228.5	437.6	621.1	797.1	986.2	1193	1422	1664	1911	
16 000	265.7	501.3	704.8	911.3	1135	1380	1650	1936		
18 000	308.3	571.2	802.4	1047	1312	1601	1919			
20 000	356.6	648.1	917.7	1207	1520	1862				
22 000	412.7	739.1	1058	1402	1773					
24 000	475.1	845.0	1224	1630	2069					
26 000	543.5	969.1	1418	1896						
28 000	618.0	1115	1644							
30 000	700.7	1285	1909							

APPENDIX A

TABLE A26.- RATIO OF IMPACT PRESSURE TO STATIC PRESSURE q_c/p (OR q'_c/p') FOR
VALUES OF MACH NUMBER M (OR INDICATED MACH NUMBER M')

[From ref. A3]

ORIGINAL PAGE 15
OF POOR QUALITY

M	0	0.001	0.002	0.003	0.004	0.005	0.006	0.007	0.008	0.009
0.100	0.00702	0.00716	0.00730	0.00745	0.00759	0.00774	0.00789	0.00804	0.00819	0.00834
.110	.00850	.00865	.00881	.00897	.00913	.00929	.00945	.00962	.00987	.00995
.120	.01012	.01029	.01046	.01063	.01080	.01098	.01116	.01134	.01152	.01170
.130	.01188	.01206	.01225	.01244	.01263	.01282	.01301	.01320	.01339	.01359
.140	.01379	.01399	.01419	.01439	.01459	.01480	.01500	.01521	.01542	.01563
.150	.01584	.01605	.01627	.01648	.01670	.01692	.01714	.01736	.01758	.01781
.160	.01804	.01826	.01849	.01872	.01895	.01919	.01942	.01966	.01990	.02014
.170	.02038	.02062	.02086	.02111	.02135	.02160	.02185	.02210	.02236	.02261
.180	.02286	.02312	.02338	.02364	.02390	.02416	.02443	.02469	.02496	.02523
.190	.02550	.02577	.02604	.02632	.02659	.02687	.02715	.02743	.02771	.02800
.200	.02828	.02857	.02886	.02914	.02944	.02973	.03002	.03032	.03061	.03091
.210	.03121	.03151	.03182	.03212	.03243	.03273	.03304	.03335	.03366	.03398
.220	.03429	.03461	.03493	.03525	.03557	.03589	.03621	.03654	.03686	.03719
.230	.03752	.03785	.03819	.03852	.03886	.03919	.03953	.03987	.04022	.04056
.240	.04090	.04125	.04160	.04195	.04230	.04265	.04301	.04336	.04372	.04408
.250	.04444	.04480	.04516	.04553	.04589	.04626	.04663	.04700	.04738	.04775
.260	.04813	.04850	.04888	.04926	.04964	.05003	.05041	.05080	.05119	.05158
.270	.05197	.05236	.05275	.05315	.05355	.05395	.05435	.05475	.05515	.05556
.280	.05596	.05637	.05678	.05719	.05761	.05802	.05844	.05886	.05927	.05970
.290	.06012	.06054	.06097	.06140	.06182	.06225	.06269	.06312	.06356	.06400
.300	.06443	.06487	.06531	.06575	.06620	.06665	.06709	.06754	.06799	.06845
.310	.06890	.06936	.06982	.07027	.07074	.07120	.07166	.07213	.07259	.07306
.320	.07353	.07401	.07448	.07496	.07543	.07591	.07639	.07687	.07736	.07784
.330	.07833	.07882	.07931	.07980	.08029	.08079	.08128	.08178	.08228	.08278
.340	.08329	.08379	.08430	.08481	.08531	.08583	.08634	.08685	.08737	.08789
.350	.08841	.08893	.08945	.08998	.09050	.09103	.09156	.09209	.09263	.09316
.360	.09370	.09424	.09478	.09532	.09586	.09641	.09695	.09750	.09805	.09860
.370	.09916	.09971	.10027	.10083	.10139	.10195	.10251	.10308	.10364	.10421
.380	.10478	.10535	.10593	.10650	.10708	.10766	.10824	.10882	.10941	.11000
.390	.11058	.11117	.11176	.11235	.11295	.11354	.11414	.11474	.11534	.11595
.400	.11655	.11716	.11777	.11838	.11899	.11960	.12022	.12084	.12146	.12208
.410	.12270	.12332	.12395	.12458	.12521	.12584	.12647	.12711	.12774	.12838
.420	.12902	.12966	.13031	.13095	.13160	.13225	.13290	.13355	.13421	.13487
.430	.13552	.13618	.13685	.13751	.13818	.13884	.13951	.14018	.14086	.14154
.440	.14221	.14289	.14357	.14425	.14493	.14562	.14630	.14699	.14768	.14838
.450	.14907	.14977	.15047	.15117	.15187	.15257	.15328	.15399	.15470	.15541
.460	.15612	.15684	.15755	.15827	.15899	.15971	.16044	.16117	.16190	.16263
.470	.16336	.16409	.16483	.16557	.16631	.16705	.16779	.16854	.16928	.17003
.480	.17077	.17154	.17229	.17305	.17381	.17457	.17533	.1761	.17686	.17763
.490	.17840	.17917	.17995	.18072	.18150	.18228	.18307	.18385	.18463	.18542
.500	.18621	.18700	.18780	.18859	.18939	.19019	.19099	.19179	.19259	.19341
.510	.19422	.19503	.19584	.19666	.19748	.19830	.19912	.19994	.20077	.20160
.520	.20242	.20326	.20409	.20492	.20576	.20660	.20744	.20829	.20913	.21000
.530	.21083	.21168	.21253	.21339	.21425	.21511	.21597	.21683	.21770	.21857
.540	.21944	.22031	.22118	.22205	.22294	.22382	.22471	.22560	.22649	.22739
.550	.22828	.22918	.23009	.23099	.23190	.23281	.23372	.23463	.23555	.23647
.560	.23727	.23819	.23911	.24002	.24094	.24186	.24279	.24372	.24465	.24558
.570	.24651	.24744	.24838	.24932	.25026	.25121	.25216	.25311	.25406	.25501
.580	.25596	.25691	.25787	.25883	.25979	.26075	.26171	.26267	.26363	.26459
.590	.26556	.26652	.26749	.26846	.26943	.27040	.27137	.27234	.27331	.27429

APPENDIX A

TABLE A26.- Continued

M	0	0.001	0.002	0.003	0.004	0.005	0.006	0.007	0.008	0.009
0.600	0.27550	0.27650	0.27751	0.27851	0.27952	0.28053	0.28154	0.28255	0.28357	0.28458
.610	.28561	.28663	.28766	.28869	.28972	.29075	.29178	.29282	.29386	.29489
.620	.29594	.29699	.29804	.29909	.30014	.30119	.30225	.30331	.30437	.30544
.630	.30650	.30757	.30864	.30972	.31079	.31187	.31295	.31403	.31512	.31621
.640	.31729	.31839	.31948	.32058	.32168	.32278	.32388	.32499	.32610	.32721
.650	.32832	.32944	.33056	.33168	.33280	.33393	.33505	.33618	.33732	.33845
.660	.33959	.34073	.34187	.34301	.34416	.34531	.34646	.34762	.34877	.34991
.670	.35110	.35226	.35343	.35460	.35577	.35694	.35812	.35930	.36048	.36166
.680	.36285	.36404	.36523	.36642	.36762	.36882	.37002	.37122	.37243	.37364
.690	.37485	.37606	.37728	.37850	.37972	.38094	.38217	.38340	.38463	.38586
.700	.38710	.38834	.38958	.39083	.39207	.39332	.39458	.39583	.39709	.39834
.710	.39961	.40088	.40214	.40341	.40469	.40596	.40724	.40852	.40980	.41108
.720	.41238	.41367	.41496	.41626	.41756	.41886	.42017	.42147	.42278	.42409
.730	.42541	.42673	.42805	.42937	.43070	.43203	.43336	.43469	.43603	.43737
.740	.43871	.44005	.44140	.44275	.44410	.44546	.44682	.44818	.44954	.45091
.750	.45228	.45365	.45503	.45640	.45778	.45917	.46055	.46194	.46333	.46472
.760	.46612	.46752	.46893	.47033	.47174	.47315	.47457	.47598	.47740	.47881
.770	.48025	.48168	.48311	.48454	.48598	.48742	.48886	.49030	.49175	.49319
.780	.49466	.49611	.49757	.49903	.50050	.50197	.50344	.50491	.50639	.50787
.790	.50935	.51084	.51233	.51382	.51531	.51681	.51831	.51981	.52132	.52282
.800	.52434	.52586	.52737	.52889	.53042	.53195	.53347	.53501	.53654	.53808
.810	.53962	.54117	.54272	.54427	.54582	.54738	.54894	.55050	.55207	.55364
.820	.55521	.55679	.55836	.55994	.56153	.56312	.56471	.56630	.56790	.56950
.830	.57110	.57271	.57432	.57593	.57754	.57916	.58078	.58241	.58404	.58567
.840	.58730	.58894	.59058	.59222	.59387	.59552	.59717	.59883	.60049	.60215
.850	.60382	.60549	.60716	.60884	.61051	.61220	.61388	.61557	.61726	.61895
.860	.62066	.62236	.62406	.62577	.62748	.62920	.63091	.63263	.63436	.63608
.870	.63782	.63955	.64129	.64303	.64477	.64652	.64827	.65003	.65178	.65354
.880	.65531	.65708	.65885	.66062	.66240	.66418	.66596	.66775	.66954	.67133
.890	.67314	.67494	.67674	.67855	.68036	.68218	.68399	.68582	.68764	.68947
.900	.69130	.69314	.69498	.69682	.69867	.70052	.70237	.70423	.70609	.70794
.910	.70982	.71169	.71356	.71544	.71732	.71920	.72109	.72298	.72488	.72677
.920	.72868	.73059	.73250	.73441	.73633	.73825	.74017	.74210	.74403	.74596
.930	.74790	.74984	.75179	.75374	.75569	.75765	.75961	.76157	.76354	.76551
.940	.76749	.76946	.77145	.77343	.77542	.77741	.77941	.78141	.78342	.78544
.950	.78744	.78945	.79147	.79350	.79552	.79755	.79959	.80163	.80367	.80572
.960	.80776	.80982	.81187	.81394	.81600	.81807	.82014	.82222	.82430	.82638
.970	.82847	.83056	.83266	.83476	.83686	.83897	.84108	.84319	.84531	.84743
.980	.84956	.85169	.85383	.85597	.85811	.86025	.86241	.86456	.86672	.86887
.990	.87105	.87322	.87539	.87757	.87975	.88194	.88413	.88632	.88852	.89071
1.000	.89293	.89514	.89735	.89957	.90180	.90402	.90625	.90849	.91073	.91297
1.010	.91521	.91746	.91972	.92198	.92424	.92651	.92878	.93105	.93333	.93561
1.020	.93790	.94019	.94248	.94478	.94708	.94938	.95169	.95401	.95632	.95864
1.030	.96097	.96330	.96563	.96796	.97030	.97265	.97500	.97735	.97970	.98205
1.040	.98442	.98679	.98916	.99153	.99391	.99629	.99868	1.00106	1.00346	1.00585
1.050	1.00825	1.01066	1.01306	1.01547	1.01789	1.02031	1.02273	1.02515	1.02758	1.03000
1.060	1.03245	1.03489	1.03734	1.03978	1.04224	1.04469	1.04715	1.04961	1.05208	1.05454
1.070	1.05702	1.05949	1.06197	1.06446	1.06694	1.06944	1.07193	1.07443	1.07693	1.07943
1.080	1.08194	1.08445	1.08697	1.08949	1.09201	1.09454	1.09707	1.09960	1.10214	1.10467
1.090	1.10722	1.10977	1.11232	1.11487	1.11743	1.11999	1.12255	1.12511	1.12767	1.13023

APPENDIX A

ORIGINAL PAGE 1
OF POOR QUALITY

TABLE A26.- Continued

M	0	0.001	0.002	0.003	0.004	0.005	0.006	0.007	0.008	0.009
1.100	1.13285	1.13543	1.13801	1.14060	1.14320	1.14579	1.14839	1.15099	1.15360	1.15621
1.110	1.15882	1.16144	1.16406	1.16668	1.16930	1.17193	1.17457	1.17720	1.17984	1.18249
1.120	1.18513	1.18778	1.19044	1.19309	1.19575	1.19842	1.20108	1.20375	1.20643	1.20910
1.130	1.21178	1.21447	1.21715	1.21985	1.22254	1.22524	1.22794	1.23064	1.23335	1.23606
1.140	1.23877	1.24149	1.24421	1.24693	1.24966	1.25239	1.25512	1.25785	1.26059	1.26334
1.150	1.26608	1.26883	1.27159	1.27434	1.27710	1.27986	1.28263	1.28540	1.28817	1.29095
1.160	1.29372	1.29651	1.29929	1.30208	1.30487	1.30767	1.31047	1.31327	1.31607	1.31888
1.170	1.32169	1.32450	1.32732	1.33014	1.33297	1.33579	1.33862	1.34146	1.34429	1.34713
1.180	1.34998	1.35282	1.35567	1.35852	1.36138	1.36424	1.36710	1.36997	1.37284	1.37571
1.190	1.37858	1.38146	1.38434	1.38722	1.39011	1.39300	1.39590	1.39879	1.40169	1.40460
1.200	1.40750	1.41041	1.41332	1.41624	1.41916	1.42208	1.42500	1.42793	1.43086	1.43380
1.210	1.43674	1.43968	1.44262	1.44557	1.44852	1.45147	1.45442	1.45738	1.46035	1.46331
1.220	1.46628	1.46925	1.47223	1.47520	1.47818	1.48117	1.48416	1.48715	1.49014	1.49313
1.230	1.49613	1.49914	1.50214	1.50515	1.50816	1.51118	1.51419	1.51721	1.52024	1.52326
1.240	1.52629	1.52933	1.53236	1.53540	1.53844	1.54149	1.54454	1.54759	1.55064	1.55370
1.250	1.55676	1.55982	1.56289	1.56596	1.56903	1.57210	1.57518	1.57826	1.58135	1.58444
1.260	1.58753	1.59062	1.59372	1.59682	1.59992	1.60302	1.60613	1.60924	1.61236	1.61548
1.270	1.61860	1.62172	1.62485	1.62797	1.63111	1.63424	1.63738	1.64052	1.64367	1.64681
1.280	1.64996	1.65321	1.65627	1.65943	1.66260	1.66576	1.66893	1.67210	1.67527	1.67845
1.290	1.68163	1.68481	1.68800	1.69119	1.69438	1.69753	1.70077	1.70397	1.70718	1.71038
1.300	1.71359	1.71681	1.72002	1.72324	1.72646	1.72969	1.73291	1.73614	1.73938	1.74261
1.310	1.74585	1.74909	1.75234	1.75559	1.75884	1.76209	1.76535	1.76861	1.77187	1.77513
1.320	1.77840	1.78167	1.78495	1.78823	1.79151	1.79479	1.79807	1.80136	1.80465	1.80795
1.330	1.81125	1.81455	1.81785	1.82116	1.82447	1.82778	1.83109	1.83441	1.83773	1.84105
1.340	1.84438	1.84771	1.85104	1.85438	1.85772	1.86106	1.86440	1.86775	1.87110	1.87445
1.350	1.87781	1.88116	1.88452	1.88789	1.89126	1.89463	1.89800	1.90137	1.90475	1.90813
1.360	1.91152	1.91491	1.91830	1.92169	1.92508	1.92848	1.93188	1.93529	1.93870	1.94211
1.370	1.94552	1.94893	1.95235	1.95577	1.95920	1.96263	1.96606	1.96949	1.97293	1.97636
1.380	1.97981	1.98325	1.98670	1.99015	1.99360	1.99706	2.00052	2.00398	2.00744	2.01091
1.390	2.01438	2.01785	2.02133	2.02481	2.02829	2.03177	2.03526	2.03875	2.04224	2.04574
1.400	2.04924	2.05274	2.05624	2.05975	2.06326	2.06677	2.07029	2.07380	2.07733	2.08085
1.410	2.08438	2.08791	2.09144	2.09497	2.09851	2.10205	2.10560	2.10914	2.11269	2.11624
1.420	2.11980	2.12336	2.12692	2.13048	2.13405	2.13762	2.14119	2.14476	2.14834	2.15192
1.430	2.15551	2.15909	2.16268	2.16627	2.16987	2.17346	2.17706	2.18067	2.18427	2.18788
1.440	2.19149	2.19511	2.19872	2.20234	2.20597	2.20959	2.21322	2.21685	2.22048	2.22412
1.450	2.22776	2.23140	2.23505	2.23869	2.24234	2.24600	2.24965	2.25331	2.25697	2.26064
1.460	2.26431	2.26798	2.27165	2.27532	2.27900	2.28268	2.28637	2.29005	2.29374	2.29744
1.470	2.30113	2.30483	2.30853	2.31223	2.31594	2.31965	2.32336	2.32707	2.33079	2.33451
1.480	2.33823	2.34196	2.34569	2.34942	2.35315	2.35689	2.36063	2.36437	2.36812	2.37187
1.490	2.37562	2.37937	2.38313	2.38688	2.39065	2.39441	2.39818	2.40195	2.40572	2.40950
1.500	2.41327	2.41706	2.42084	2.42463	2.42842	2.43221	2.43600	2.43980	2.44360	2.44740
1.510	2.45121	2.45502	2.45883	2.46264	2.46646	2.47028	2.47410	2.47793	2.48176	2.48559
1.520	2.48942	2.49326	2.49710	2.50094	2.50478	2.50863	2.51248	2.51633	2.52019	2.52405
1.530	2.52791	2.53177	2.53564	2.53951	2.54338	2.54725	2.55113	2.55501	2.55889	2.56278
1.540	2.56667	2.57056	2.57445	2.57835	2.58225	2.58615	2.59005	2.59396	2.59787	2.60179
1.550	2.60570	2.60962	2.61354	2.61747	2.62139	2.62532	2.62925	2.63319	2.63713	2.64107
1.560	2.64501	2.64896	2.65290	2.65686	2.66081	2.66477	2.66873	2.67269	2.67665	2.68062
1.570	2.68459	2.68856	2.69254	2.69652	2.70050	2.70449	2.70847	2.71246	2.71645	2.72045
1.580	2.72445	2.72845	2.73245	2.73645	2.74046	2.74448	2.74849	2.75251	2.75653	2.76055
1.590	2.76457	2.76860	2.77263	2.77666	2.78070	2.78474	2.78878	2.79282	2.79687	2.80091

APPENDIX A

TABLE A26.- Continued

M	0	0.001	0.002	0.003	0.004	0.005	0.006	0.007	0.008	0.009
1.600	2.80497	2.80903	2.81308	2.81714	2.82121	2.82527	2.82934	2.83341	2.83749	2.84156
1.610	2.84564	2.84972	2.85381	2.85790	2.86199	2.86608	2.87017	2.87427	2.87837	2.88246
1.620	2.88658	2.89069	2.89480	2.89892	2.90304	2.90716	2.91128	2.91540	2.91953	2.92365
1.630	2.92780	2.93193	2.93607	2.94021	2.94436	2.94850	2.95265	2.95681	2.96096	2.96511
1.640	2.96928	2.97344	2.97761	2.98178	2.98595	2.99012	2.99430	2.99848	3.00266	3.00684
1.650	3.01103	3.01522	3.01941	3.02361	3.02781	3.03201	3.03621	3.04042	3.04463	3.04884
1.660	3.05305	3.05727	3.06149	3.06571	3.06994	3.07417	3.07840	3.08263	3.08687	3.09111
1.670	3.09535	3.09959	3.10384	3.10809	3.11234	3.11659	3.12085	3.12511	3.12937	3.13363
1.680	3.13791	3.14218	3.14645	3.15073	3.15501	3.15929	3.16357	3.16786	3.17215	3.17644
1.690	3.18074	3.18503	3.18933	3.19364	3.19794	3.20225	3.20656	3.21088	3.21519	3.21950
1.700	3.22383	3.22816	3.23248	3.23681	3.24115	3.24548	3.24982	3.25416	3.25850	3.26284
1.710	3.26720	3.27155	3.27590	3.28026	3.28462	3.28898	3.29335	3.29771	3.30208	3.30644
1.720	3.31083	3.31521	3.31959	3.32397	3.32836	3.33275	3.33714	3.34154	3.34593	3.35033
1.730	3.35473	3.35914	3.36355	3.36796	3.37237	3.37679	3.38120	3.38562	3.39005	3.39447
1.740	3.39890	3.40333	3.40777	3.41221	3.41665	3.42109	3.42553	3.42998	3.43443	3.43887
1.750	3.44334	3.44780	3.45226	3.45672	3.46119	3.46566	3.47013	3.47460	3.47908	3.48355
1.760	3.48804	3.49253	3.49701	3.50150	3.50600	3.51049	3.51499	3.51949	3.52400	3.52850
1.770	3.53301	3.53752	3.54204	3.54655	3.55107	3.55560	3.56012	3.56465	3.56918	3.57371
1.780	3.57825	3.58278	3.58732	3.59187	3.59642	3.60096	3.60552	3.61007	3.61463	3.61919
1.790	3.62375	3.62831	3.63288	3.63745	3.64202	3.64660	3.65118	3.65576	3.66034	3.66492
1.800	3.66952	3.67411	3.67870	3.68330	3.68790	3.69250	3.69710	3.70171	3.70632	3.71093
1.810	3.71555	3.72017	3.72479	3.72941	3.73404	3.73867	3.74330	3.74793	3.75257	3.75720
1.820	3.76185	3.76649	3.77114	3.77579	3.78044	3.78510	3.78975	3.79442	3.79908	3.80375
1.830	3.80841	3.81308	3.81776	3.82243	3.82711	3.83179	3.83648	3.84117	3.84585	3.85054
1.840	3.85524	3.85994	3.86464	3.86934	3.87405	3.87876	3.88347	3.88818	3.89290	3.89761
1.850	3.90234	3.90706	3.91179	3.91652	3.92125	3.92598	3.93072	3.93546	3.94020	3.94494
1.860	3.94970	3.95445	3.95920	3.96396	3.96871	3.97347	3.97822	3.98300	3.98777	3.99255
1.870	3.99732	4.00210	4.00688	4.01166	4.01644	4.02123	4.02602	4.03081	4.03561	4.04040
1.880	4.04521	4.05001	4.05482	4.05963	4.06444	4.06925	4.07407	4.07889	4.08371	4.08853
1.890	4.09336	4.09819	4.10302	4.10786	4.11270	4.11754	4.12238	4.12722	4.13207	4.13691
1.900	4.14178	4.14663	4.15149	4.15635	4.16122	4.16608	4.17095	4.17583	4.18070	4.18558
1.910	4.19046	4.19534	4.20023	4.20511	4.21000	4.21490	4.21979	4.22469	4.22959	4.23448
1.920	4.23940	4.24431	4.24922	4.25414	4.25905	4.26397	4.26890	4.27382	4.27875	4.28367
1.930	4.28861	4.29355	4.29848	4.30342	4.30837	4.31331	4.31826	4.32321	4.32817	4.33311
1.940	4.33808	4.34304	4.34801	4.35298	4.35795	4.36292	4.36789	4.37287	4.37785	4.38282
1.950	4.38782	4.39281	4.39780	4.40279	4.40779	4.41278	4.41777	4.42277	4.42777	4.43276
1.960	4.43782	4.44283	4.44785	4.45287	4.45789	4.46291	4.46794	4.47297	4.47800	4.48303
1.970	4.48808	4.49312	4.49816	4.50321	4.50826	4.51331	4.51836	4.52342	4.52847	4.53352
1.980	4.53860	4.54367	4.54874	4.55381	4.55889	4.56396	4.56904	4.57413	4.57921	4.58429
1.990	4.58939	4.59448	4.59958	4.60468	4.60978	4.61489	4.61999	4.62510	4.63021	4.63531
2.000	4.64044	4.64556	4.65068	4.65581	4.66093	4.66606	4.67120	4.67633	4.68147	4.68660
2.010	4.69175	4.69690	4.70205	4.70720	4.71235	4.71751	4.72267	4.72783	4.73299	4.73815
2.020	4.74333	4.74850	4.75368	4.75885	4.76403	4.76922	4.77440	4.77959	4.78478	4.78996
2.030	4.79517	4.80037	4.80557	4.81077	4.81598	4.82119	4.82640	4.83161	4.83683	4.84204
2.040	4.84727	4.85249	4.85772	4.86295	4.86818	4.87342	4.87865	4.88389	4.88914	4.89438
2.050	4.89963	4.90488	4.91014	4.91539	4.92065	4.92591	4.93117	4.93644	4.94171	4.94697
2.060	4.95226	4.95753	4.96281	4.96809	4.97338	4.97867	4.98396	4.98925	4.99454	4.99983
2.070	5.00514	5.01045	5.01575	5.02106	5.02637	5.03168	5.03700	5.04232	5.04764	5.05296
2.080	5.05829	5.06362	5.06895	5.07429	5.07962	5.08496	5.09031	5.09565	5.10100	5.10634
2.090	5.11170	5.11706	5.12242	5.12778	5.13314	5.13851	5.14387	5.14925	5.15462	5.16000

APPENDIX A

ORIGINAL PAGE IS
OF POOR QUALITY

TABLE A26.- Continued

M	0	0.001	0.002	0.003	0.004	0.005	0.006	0.007	0.008	0.009
2.100	5.16538	5.17076	5.17614	5.18153	5.18692	5.19231	5.19770	5.20310	5.20850	5.21390
2.110	5.21931	5.22472	5.23013	5.23554	5.24096	5.24637	5.25180	5.25722	5.26265	5.26807
2.120	5.27351	5.27894	5.28438	5.28981	5.29526	5.30070	5.30615	5.31160	5.31705	5.32250
2.130	5.32796	5.33342	5.33889	5.34435	5.34982	5.35529	5.36076	5.36624	5.37172	5.37720
2.140	5.38268	5.38817	5.39366	5.39915	5.40464	5.41014	5.41564	5.42114	5.42664	5.43215
2.150	5.43766	5.44317	5.44869	5.45421	5.45973	5.46525	5.47077	5.47630	5.48183	5.48737
2.160	5.49290	5.49844	5.50398	5.50953	5.51507	5.52062	5.52617	5.53173	5.53728	5.54284
2.170	5.54841	5.55397	5.55954	5.56511	5.57068	5.57625	5.58183	5.58741	5.59300	5.59858
2.180	5.60417	5.60976	5.61535	5.62095	5.62655	5.63215	5.63775	5.64336	5.64897	5.65458
2.190	5.66019	5.66581	5.67143	5.67705	5.68268	5.68830	5.69393	5.69957	5.70520	5.71084
2.200	5.71648	5.72212	5.72777	5.73342	5.73907	5.74472	5.75038	5.75604	5.76170	5.76735
2.210	5.77303	5.77870	5.78437	5.79004	5.79572	5.80140	5.80708	5.81276	5.81845	5.82414
2.220	5.82983	5.83553	5.84123	5.84693	5.85263	5.85834	5.86404	5.86976	5.87547	5.88118
2.230	5.88690	5.89262	5.89835	5.90407	5.90980	5.91554	5.92127	5.92701	5.93275	5.93849
2.240	5.94423	5.94998	5.95573	5.96148	5.96724	5.97299	5.97875	5.98452	5.99028	5.99605
2.250	6.00182	6.00760	6.01337	6.01915	6.02493	6.03071	6.03650	6.04229	6.04808	6.05388
2.260	6.05967	6.06547	6.07127	6.07708	6.08289	6.08870	6.09451	6.10032	6.10614	6.11196
2.270	6.11778	6.12361	6.12944	6.13527	6.14110	6.14694	6.15278	6.15862	6.16446	6.17031
2.280	6.17616	6.18201	6.18786	6.19372	6.19958	6.20544	6.21130	6.21717	6.22304	6.22891
2.290	6.23479	6.24066	6.24654	6.25243	6.25831	6.26420	6.27009	6.27598	6.28182	6.28773
2.300	6.29368	6.29958	6.30549	6.31140	6.31731	6.32322	6.32914	6.33506	6.34098	6.34691
2.310	6.35283	6.35876	6.36469	6.37063	6.37657	6.38251	6.38845	6.39439	6.40034	6.40629
2.320	6.41225	6.41820	6.42416	6.43012	6.43608	6.44205	6.44802	6.45399	6.45996	6.46594
2.330	6.47192	6.47790	6.48388	6.48987	6.49586	6.50185	6.50785	6.51384	6.51984	6.52585
2.340	6.53185	6.53786	6.54387	6.54988	6.55590	6.56192	6.56794	6.57396	6.57999	6.58601
2.350	6.59205	6.59808	6.60412	6.61015	6.61620	6.62224	6.62829	6.63434	6.64039	6.64644
2.360	6.65250	6.65856	6.66462	6.67069	6.67675	6.68282	6.68889	6.69497	6.70105	6.70713
2.370	6.71321	6.71930	6.72539	6.73148	6.73757	6.74367	6.74977	6.75587	6.76197	6.76808
2.380	6.77419	6.78030	6.78641	6.79253	6.79865	6.80477	6.81090	6.81702	6.82315	6.82927
2.390	6.83542	6.84156	6.84770	6.85384	6.85999	6.86613	6.87229	6.87844	6.88459	6.89075
2.400	6.89691	6.90308	6.90924	6.91541	6.92158	6.92776	6.93393	6.94011	6.94630	6.95248
2.410	6.95867	6.96486	6.97105	6.97724	6.98344	6.98964	6.99584	7.00205	7.00826	7.01447
2.420	7.02068	7.02690	7.03311	7.03934	7.04556	7.05178	7.05801	7.06424	7.07048	7.07672
2.430	7.08295	7.08920	7.09544	7.10169	7.10794	7.11419	7.12044	7.12670	7.13296	7.13922
2.440	7.14549	7.15175	7.15802	7.16430	7.17057	7.17685	7.18313	7.18941	7.19570	7.20199
2.450	7.20828	7.21457	7.22087	7.22717	7.23347	7.23977	7.24608	7.25239	7.25870	7.26501
2.460	7.27133	7.27765	7.28397	7.29030	7.29663	7.30296	7.30929	7.31562	7.32196	7.32830
2.470	7.33464	7.34099	7.34734	7.35369	7.36004	7.36640	7.37275	7.37912	7.38548	7.39185
2.480	7.39821	7.40459	7.41096	7.41734	7.42372	7.43010	7.43648	7.44287	7.44926	7.45565
2.490	7.46205	7.46844	7.47484	7.48125	7.48765	7.49406	7.50047	7.50688	7.51330	7.51972
2.500	7.52614	7.53256	7.53899	7.54541	7.55184	7.55828	7.56471	7.57115	7.57760	7.58404
2.510	7.59049	7.59694	7.60339	7.60984	7.61630	7.62276	7.62922	7.63568	7.64215	7.64862
2.520	7.65510	7.66157	7.66805	7.67453	7.68101	7.68750	7.69399	7.70048	7.70697	7.71347
2.530	7.71996	7.72647	7.73297	7.73948	7.74599	7.75250	7.75901	7.76553	7.77205	7.77857
2.540	7.78509	7.79162	7.79815	7.80468	7.81122	7.81775	7.82429	7.83084	7.83739	7.84393
2.550	7.85048	7.85703	7.86359	7.87015	7.87671	7.88327	7.88984	7.89641	7.90299	7.90955
2.560	7.91613	7.92271	7.92929	7.93587	7.94246	7.94905	7.95564	7.96223	7.96883	7.97543
2.570	7.98203	7.98864	7.99525	8.00186	8.00847	8.01508	8.02170	8.02832	8.03494	8.04157
2.580	8.04820	8.05483	8.06146	8.06810	8.07474	8.08138	8.08802	8.09467	8.10132	8.10797
2.590	8.11462	8.12128	8.12794	8.13460	8.14127	8.14793	8.15460	8.16128	8.16795	8.17463

APPENDIX A

TABLE A26.- Continued

M	C	0.001	0.002	0.003	0.004	0.005	0.006	0.007	0.008	0.009
2.600	8.18131	8.18799	8.19468	8.20136	8.20805	8.21475	8.22144	8.22814	8.23484	8.24154
2.610	8.24825	8.25496	8.26167	8.26838	8.27510	8.28182	8.28854	8.29527	8.30199	8.30871
2.620	8.31545	8.32219	8.32892	8.33566	8.34241	8.34915	8.35590	8.36265	8.36940	8.37615
2.630	8.38291	8.38968	8.39644	8.40320	8.40997	8.41674	8.42352	8.43029	8.43707	8.44384
2.640	8.45064	8.45742	8.46421	8.47100	8.47780	8.48459	8.49139	8.49819	8.50499	8.51179
2.650	8.51862	8.52543	8.53224	8.53906	8.54588	8.55270	8.55953	8.56636	8.57319	8.58002
2.660	8.58685	8.59369	8.60053	8.60738	8.61422	8.62107	8.62792	8.63478	8.64163	8.64848
2.670	8.65535	8.66222	8.66908	8.67595	8.68282	8.68970	8.69657	8.70345	8.71034	8.71721
2.680	8.72411	8.73100	8.73789	8.74479	8.75168	8.75858	8.76549	8.77239	8.77930	8.78620
2.690	8.79312	8.80004	8.80696	8.81388	8.82080	8.82773	8.83466	8.84159	8.84852	8.85545
2.700	8.86240	8.86934	8.87629	8.88323	8.89018	8.89713	8.90409	8.91105	8.91801	8.92497
2.710	8.93193	8.93890	8.94587	8.95284	8.95982	8.96680	8.97378	8.98076	8.98775	8.99473
2.720	9.00173	9.00872	9.01572	9.02271	9.02971	9.03672	9.04373	9.05075	9.05775	9.06476
2.730	9.07178	9.07880	9.08582	9.09284	9.09987	9.10690	9.11393	9.12097	9.12800	9.13503
2.740	9.14209	9.14913	9.15618	9.16323	9.17028	9.17734	9.18440	9.19146	9.19852	9.20558
2.750	9.21266	9.21973	9.22680	9.23388	9.24096	9.24804	9.25512	9.26221	9.26930	9.27638
2.760	9.28348	9.29058	9.29768	9.30478	9.31189	9.31900	9.32611	9.33322	9.34033	9.34744
2.770	9.35457	9.36169	9.36882	9.37595	9.38308	9.39021	9.39735	9.40449	9.41163	9.41877
2.780	9.42592	9.43307	9.44022	9.44737	9.45453	9.46169	9.46885	9.47601	9.48317	9.49033
2.790	9.49752	9.50470	9.51187	9.51905	9.52624	9.53342	9.54061	9.54780	9.55499	9.56218
2.800	9.56939	9.57659	9.58379	9.59099	9.59820	9.60541	9.61263	9.61984	9.62706	9.63427
2.810	9.64151	9.64873	9.65596	9.66319	9.67043	9.67767	9.68490	9.69215	9.69939	9.70663
2.820	9.71389	9.72114	9.72840	9.73565	9.74291	9.75018	9.75744	9.76471	9.77198	9.77924
2.830	9.78653	9.79381	9.80109	9.80837	9.81566	9.82294	9.83024	9.83753	9.84483	9.85212
2.840	9.85943	9.86673	9.87404	9.88135	9.88866	9.89597	9.90329	9.91061	9.91793	9.92524
2.850	9.93259	9.93991	9.94725	9.95458	9.96192	9.96926	9.97660	9.98395	9.99129	9.99863
2.860	10.00600	10.01335	10.02071	10.02807	10.03544	10.04280	10.05017	10.05754	10.06492	10.07229
2.870	10.07967	10.08705	10.09444	10.10183	10.10921	10.11661	10.12400	10.13140	10.13880	10.14619
2.880	10.15361	10.16101	10.16842	10.17584	10.18325	10.19067	10.19809	10.20551	10.21294	10.22036
2.890	10.22780	10.23523	10.24267	10.25010	10.25755	10.26499	10.27244	10.27988	10.28733	10.29477
2.900	10.30225	10.30971	10.31717	10.32463	10.33210	10.33957	10.34704	10.35452	10.36199	10.36946
2.910	10.37695	10.38444	10.39193	10.39942	10.40691	10.41441	10.42190	10.42940	10.43691	10.44441
2.920	10.45192	10.45943	10.46695	10.47446	10.48198	10.48950	10.49703	10.50455	10.51208	10.51960
2.930	10.52715	10.53468	10.54222	10.54977	10.55731	10.56486	10.57241	10.57996	10.58751	10.59506
2.940	10.60263	10.61019	10.61776	10.62533	10.63290	10.64047	10.64805	10.65562	10.66320	10.67077
2.950	10.67837	10.68596	10.69355	10.70115	10.70874	10.71634	10.72394	10.73155	10.73915	10.74676
2.960	10.75438	10.76199	10.76961	10.77723	10.78485	10.79247	10.80010	10.80773	10.81536	10.82299
2.970	10.83064	10.83828	10.84592	10.85356	10.86121	10.86886	10.87651	10.88417	10.89182	10.89947
2.980	10.90715	10.91482	10.92249	10.93016	10.93783	10.94551	10.95319	10.96087	10.96855	10.97623
2.990	10.98393	10.99162	10.99931	11.00701	11.01471	11.02241	11.03012	11.03783	11.04554	11.05325
3.000	11.06096	11.06868	11.07640	11.08413	11.09185	11.09958	11.10731	11.11504	11.12277	11.13050
3.010	11.13823	11.14596	11.15369	11.16143	11.16917	11.17690	11.18464	11.19238	11.20012	11.20786
3.020	11.21561	11.22336	11.23111	11.23886	11.24661	11.25436	11.26211	11.26986	11.27761	11.28536
3.030	11.29312	11.30087	11.30862	11.31637	11.32412	11.33187	11.33962	11.34737	11.35512	11.36287
3.040	11.37063	11.37838	11.38613	11.39388	11.40163	11.40938	11.41713	11.42488	11.43263	11.44038
3.050	11.44812	11.45587	11.46362	11.47137	11.47912	11.48687	11.49462	11.50237	11.51012	11.51787
3.060	11.52562	11.53337	11.54112	11.54887	11.55662	11.56437	11.57212	11.57987	11.58762	11.59537
3.070	11.60312	11.61087	11.61862	11.62637	11.63412	11.64187	11.64962	11.65737	11.66512	11.67287
3.080	11.68037	11.68812	11.69587	11.70362	11.71137	11.71912	11.72687	11.73462	11.74237	11.75012
3.090	11.75787	11.76562	11.77337	11.78112	11.78887	11.79662	11.80437	11.81212	11.81987	11.82762

ORIGINAL PAGE 1
OF POOR QUALITY

APPENDIX A

TABLE A16. - Continued

X	1	2	3	4	5	6	7	8	9	10
3.100	11.64553	11.65359	11.66148	11.66940	11.67745	11.68543	11.69341	11.70144	11.70941	11.71744
3.110	11.92549	11.93341	11.94141	11.94942	11.95743	11.96544	11.97345	11.98147	11.98948	11.99749
3.120	12.20554	12.21357	12.22160	12.22963	12.23767	12.24570	12.25374	12.26177	12.26980	12.27783
3.130	12.48593	12.49399	12.50204	12.51010	12.51816	12.52622	12.53428	12.54234	12.55040	12.55846
3.140	12.76591	12.77466	12.78342	12.79217	12.80093	12.80969	12.81845	12.82721	12.83597	12.84473
3.150	12.94750	12.95590	12.96431	12.97271	12.98112	12.98953	12.99794	13.00635	13.01476	13.02317
3.160	13.20966	13.21867	13.22769	13.23671	13.24573	13.25475	13.26377	13.27279	13.28181	13.29083
3.170	13.41009	13.41925	13.42841	13.43757	13.44673	13.45589	13.46505	13.47421	13.48337	13.49253
3.180	13.69178	13.69996	13.70814	13.71633	13.72451	13.73269	13.74087	13.74905	13.75723	13.76541
3.190	13.97372	13.98190	13.99008	13.99826	14.00644	14.01462	14.02280	14.03098	14.03916	14.04734
3.200	14.25592	14.26415	14.27239	14.28063	14.28887	14.29711	14.30535	14.31359	14.32183	14.33007
3.210	14.51836	14.52664	14.53492	14.54320	14.55148	14.55976	14.56804	14.57632	14.58460	14.59288
3.220	14.78110	14.78938	14.79766	14.80594	14.81422	14.82250	14.83078	14.83906	14.84734	14.85562
3.230	15.04384	15.05212	15.06040	15.06868	15.07696	15.08524	15.09352	15.10180	15.11008	15.11836
3.240	15.30658	15.31486	15.32314	15.33142	15.33970	15.34798	15.35626	15.36454	15.37282	15.38110
3.250	15.56932	15.57760	15.58588	15.59416	15.60244	15.61072	15.61900	15.62728	15.63556	15.64384
3.260	15.83206	15.84034	15.84862	15.85690	15.86518	15.87346	15.88174	15.89002	15.89830	15.90658
3.270	16.09480	16.10308	16.11136	16.11964	16.12792	16.13620	16.14448	16.15276	16.16104	16.16932
3.280	16.35754	16.36582	16.37410	16.38238	16.39066	16.39894	16.40722	16.41550	16.42378	16.43206
3.290	16.62028	16.62856	16.63684	16.64512	16.65340	16.66168	16.66996	16.67824	16.68652	16.69480
3.300	16.88302	16.89130	16.89958	16.90786	16.91614	16.92442	16.93270	16.94098	16.94926	16.95754
3.310	17.14576	17.15404	17.16232	17.17060	17.17888	17.18716	17.19544	17.20372	17.21200	17.22028
3.320	17.40850	17.41678	17.42506	17.43334	17.44162	17.44990	17.45818	17.46646	17.47474	17.48302
3.330	17.67124	17.67952	17.68780	17.69608	17.70436	17.71264	17.72092	17.72920	17.73748	17.74576
3.340	17.93398	17.94226	17.95054	17.95882	17.96710	17.97538	17.98366	17.99194	18.00022	18.00850
3.350	18.19672	18.20500	18.21328	18.22156	18.22984	18.23812	18.24640	18.25468	18.26296	18.27124
3.360	18.45946	18.46774	18.47602	18.48430	18.49258	18.50086	18.50914	18.51742	18.52570	18.53398
3.370	18.72220	18.73048	18.73876	18.74704	18.75532	18.76360	18.77188	18.78016	18.78844	18.79672
3.380	18.98494	18.99322	19.00150	19.00978	19.01806	19.02634	19.03462	19.04290	19.05118	19.05946
3.390	19.24768	19.25596	19.26424	19.27252	19.28080	19.28908	19.29736	19.30564	19.31392	19.32220
3.400	19.51042	19.51870	19.52698	19.53526	19.54354	19.55182	19.56010	19.56838	19.57666	19.58494
3.410	19.77316	19.78144	19.78972	19.79800	19.80628	19.81456	19.82284	19.83112	19.83940	19.84768
3.420	20.03590	20.04418	20.05246	20.06074	20.06902	20.07730	20.08558	20.09386	20.10214	20.11042
3.430	20.29864	20.30692	20.31520	20.32348	20.33176	20.34004	20.34832	20.35660	20.36488	20.37316
3.440	20.56138	20.56966	20.57794	20.58622	20.59450	20.60278	20.61106	20.61934	20.62762	20.63590
3.450	20.82412	20.83240	20.84068	20.84896	20.85724	20.86552	20.87380	20.88208	20.89036	20.89864
3.460	21.08686	21.09514	21.10342	21.11170	21.11998	21.12826	21.13654	21.14482	21.15310	21.16138
3.470	21.34960	21.35788	21.36616	21.37444	21.38272	21.39100	21.39928	21.40756	21.41584	21.42412
3.480	21.61234	21.62062	21.62890	21.63718	21.64546	21.65374	21.66202	21.67030	21.67858	21.68686
3.490	21.87508	21.88336	21.89164	21.89992	21.90820	21.91648	21.92476	21.93304	21.94132	21.94960
3.500	22.13782	22.14610	22.15438	22.16266	22.17094	22.17922	22.18750	22.19578	22.20406	22.21234

APPENDIX A

TABLE A.1.1 - (continued)

M	U	0.001	0.002	0.003	0.004	0.005	0.006	0.007	0.008	0.009
1.600	16.1514	16.1544	16.1574	16.1604	16.1634	16.1664	16.1694	16.1724	16.1754	16.1784
1.610	16.1814	16.1844	16.1874	16.1904	16.1934	16.1964	16.1994	16.2024	16.2054	16.2084
1.620	16.2114	16.2144	16.2174	16.2204	16.2234	16.2264	16.2294	16.2324	16.2354	16.2384
1.630	16.2414	16.2444	16.2474	16.2504	16.2534	16.2564	16.2594	16.2624	16.2654	16.2684
1.640	16.2714	16.2744	16.2774	16.2804	16.2834	16.2864	16.2894	16.2924	16.2954	16.2984
1.650	16.3014	16.3044	16.3074	16.3104	16.3134	16.3164	16.3194	16.3224	16.3254	16.3284
1.660	16.3314	16.3344	16.3374	16.3404	16.3434	16.3464	16.3494	16.3524	16.3554	16.3584
1.670	16.3614	16.3644	16.3674	16.3704	16.3734	16.3764	16.3794	16.3824	16.3854	16.3884
1.680	16.3914	16.3944	16.3974	16.4004	16.4034	16.4064	16.4094	16.4124	16.4154	16.4184
1.690	16.4214	16.4244	16.4274	16.4304	16.4334	16.4364	16.4394	16.4424	16.4454	16.4484
1.700	16.4514	16.4544	16.4574	16.4604	16.4634	16.4664	16.4694	16.4724	16.4754	16.4784
1.710	16.4814	16.4844	16.4874	16.4904	16.4934	16.4964	16.4994	16.5024	16.5054	16.5084
1.720	16.5114	16.5144	16.5174	16.5204	16.5234	16.5264	16.5294	16.5324	16.5354	16.5384
1.730	16.5414	16.5444	16.5474	16.5504	16.5534	16.5564	16.5594	16.5624	16.5654	16.5684
1.740	16.5714	16.5744	16.5774	16.5804	16.5834	16.5864	16.5894	16.5924	16.5954	16.5984
1.750	16.6014	16.6044	16.6074	16.6104	16.6134	16.6164	16.6194	16.6224	16.6254	16.6284
1.760	16.6314	16.6344	16.6374	16.6404	16.6434	16.6464	16.6494	16.6524	16.6554	16.6584
1.770	16.6614	16.6644	16.6674	16.6704	16.6734	16.6764	16.6794	16.6824	16.6854	16.6884
1.780	16.6914	16.6944	16.6974	16.7004	16.7034	16.7064	16.7094	16.7124	16.7154	16.7184
1.790	16.7214	16.7244	16.7274	16.7304	16.7334	16.7364	16.7394	16.7424	16.7454	16.7484
1.800	16.7514	16.7544	16.7574	16.7604	16.7634	16.7664	16.7694	16.7724	16.7754	16.7784
1.810	16.7814	16.7844	16.7874	16.7904	16.7934	16.7964	16.7994	16.8024	16.8054	16.8084
1.820	16.8114	16.8144	16.8174	16.8204	16.8234	16.8264	16.8294	16.8324	16.8354	16.8384
1.830	16.8414	16.8444	16.8474	16.8504	16.8534	16.8564	16.8594	16.8624	16.8654	16.8684
1.840	16.8714	16.8744	16.8774	16.8804	16.8834	16.8864	16.8894	16.8924	16.8954	16.8984
1.850	16.9014	16.9044	16.9074	16.9104	16.9134	16.9164	16.9194	16.9224	16.9254	16.9284
1.860	16.9314	16.9344	16.9374	16.9404	16.9434	16.9464	16.9494	16.9524	16.9554	16.9584
1.870	16.9614	16.9644	16.9674	16.9704	16.9734	16.9764	16.9794	16.9824	16.9854	16.9884
1.880	16.9914	16.9944	16.9974	17.0004	17.0034	17.0064	17.0094	17.0124	17.0154	17.0184
1.890	17.0214	17.0244	17.0274	17.0304	17.0334	17.0364	17.0394	17.0424	17.0454	17.0484
1.900	17.0514	17.0544	17.0574	17.0604	17.0634	17.0664	17.0694	17.0724	17.0754	17.0784
1.910	17.0814	17.0844	17.0874	17.0904	17.0934	17.0964	17.0994	17.1024	17.1054	17.1084
1.920	17.1114	17.1144	17.1174	17.1204	17.1234	17.1264	17.1294	17.1324	17.1354	17.1384
1.930	17.1414	17.1444	17.1474	17.1504	17.1534	17.1564	17.1594	17.1624	17.1654	17.1684
1.940	17.1714	17.1744	17.1774	17.1804	17.1834	17.1864	17.1894	17.1924	17.1954	17.1984
1.950	17.2014	17.2044	17.2074	17.2104	17.2134	17.2164	17.2194	17.2224	17.2254	17.2284
1.960	17.2314	17.2344	17.2374	17.2404	17.2434	17.2464	17.2494	17.2524	17.2554	17.2584
1.970	17.2614	17.2644	17.2674	17.2704	17.2734	17.2764	17.2794	17.2824	17.2854	17.2884
1.980	17.2914	17.2944	17.2974	17.3004	17.3034	17.3064	17.3094	17.3124	17.3154	17.3184
1.990	17.3214	17.3244	17.3274	17.3304	17.3334	17.3364	17.3394	17.3424	17.3454	17.3484
2.000	17.3514	17.3544	17.3574	17.3604	17.3634	17.3664	17.3694	17.3724	17.3754	17.3784
2.010	17.3814	17.3844	17.3874	17.3904	17.3934	17.3964	17.3994	17.4024	17.4054	17.4084
2.020	17.4114	17.4144	17.4174	17.4204	17.4234	17.4264	17.4294	17.4324	17.4354	17.4384
2.030	17.4414	17.4444	17.4474	17.4504	17.4534	17.4564	17.4594	17.4624	17.4654	17.4684
2.040	17.4714	17.4744	17.4774	17.4804	17.4834	17.4864	17.4894	17.4924	17.4954	17.4984
2.050	17.5014	17.5044	17.5074	17.5104	17.5134	17.5164	17.5194	17.5224	17.5254	17.5284
2.060	17.5314	17.5344	17.5374	17.5404	17.5434	17.5464	17.5494	17.5524	17.5554	17.5584
2.070	17.5614	17.5644	17.5674	17.5704	17.5734	17.5764	17.5794	17.5824	17.5854	17.5884
2.080	17.5914	17.5944	17.5974	17.6004	17.6034	17.6064	17.6094	17.6124	17.6154	17.6184
2.090	17.6214	17.6244	17.6274	17.6304	17.6334	17.6364	17.6394	17.6424	17.6454	17.6484
2.100	17.6514	17.6544	17.6574	17.6604	17.6634	17.6664	17.6694	17.6724	17.6754	17.6784
2.110	17.6814	17.6844	17.6874	17.6904	17.6934	17.6964	17.6994	17.7024	17.7054	17.7084
2.120	17.7114	17.7144	17.7174	17.7204	17.7234	17.7264	17.7294	17.7324	17.7354	17.7384
2.130	17.7414	17.7444	17.7474	17.7504	17.7534	17.7564	17.7594	17.7624	17.7654	17.7684
2.140	17.7714	17.7744	17.7774	17.7804	17.7834	17.7864	17.7894	17.7924	17.7954	17.7984
2.150	17.8014	17.8044	17.8074	17.8104	17.8134	17.8164	17.8194	17.8224	17.8254	17.8284
2.160	17.8314	17.8344	17.8374	17.8404	17.8434	17.8464	17.8494	17.8524	17.8554	17.8584
2.170	17.8614	17.8644	17.8674	17.8704	17.8734	17.8764	17.8794	17.8824	17.8854	17.8884
2.180	17.8914	17.8944	17.8974	17.9004	17.9034	17.9064	17.9094	17.9124	17.9154	17.9184
2.190	17.9214	17.9244	17.9274	17.9304	17.9334	17.9364	17.9394	17.9424	17.9454	17.9484
2.200	17.9514	17.9544	17.9574	17.9604	17.9634	17.9664	17.9694	17.9724	17.9754	17.9784
2.210	17.9814	17.9844	17.9874	17.9904	17.9934	17.9964	17.9994	18.0024	18.0054	18.0084
2.220	18.0114	18.0144	18.0174	18.0204	18.0234	18.0264	18.0294	18.0324	18.0354	18.0384
2.230	18.0414	18.0444	18.0474	18.0504	18.0534	18.0564	18.0594	18.0624	18.0654	18.0684
2.240	18.0714	18.0744	18.0774	18.0804	18.0834	18.0864	18.0894	18.0924	18.0954	18.0984
2.250	18.1014	18.1044	18.1074	18.1104	18.1134	18.1164	18.1194	18.1224	18.1254	18.1284
2.260	18.1314	18.1344	18.1374	18.1404	18.1434	18.1464	18.1494	18.1524	18.1554	18.1584
2.270	18.1614	18.1644	18.1674	18.1704	18.1734	18.1764	18.1794	18.1824	18.1854	18.1884
2.280	18.1914	18.1944	18.1974	18.2004	18.2034	18.2064	18.2094	18.2124	18.2154	18.2184
2.290	18.2214	18.2244	18.2274	18.2304	18.2334	18.2364	18.2394	18.2424	18.2454	18.2484
2.300	18.2514	18.2544	18.2574	18.2604	18.2634	18.2664	18.2694	18.2724	18.2754	18.2784
2.310	18.2814	18.2844	18.2874	18.2904	18.2934	18.2964	18.2994	18.3024	18.3054	18.3084
2.320	18.3114	18.3144	18.3174	18.3204	18.3234	18.3264	18.3294	18.3324	18.3354	18.3384
2.330	18.3414	18.3444	18.3474	18.3504	18.3534	18.3564	18.3594	18.3624	18.3654	18.3684
2.340	18.3714	18.3744	18.3774	18.3804	18.3834	18.3864	18.3894	18.3924	18.3954	18.3984
2.350	18.4014	18.4044	18.4074	18.4104	18.4134	18.4164	18.4194	18.4224	18.4254	18.4284
2.360	18.4314	18.4344	18.4374	18.4404	18.4434	18.4464	18.4494	18.4524	18.4554	18.4584
2.370	18.4614	18.4644	18.4674	18.4704	18.4734	18.4764	18.4794	18.4824	18.4854	18.4884
2.380	18.4914	18.4944	18.4974	18.5004	18.5034	18.5064	18.5094	18.5124	18.5154	18.5184
2.390	18.5214	18.5244	18.5274	18.5304	18.5334	18.5364	18.5394	18.5424	18.5454	18.5484
2.400	18.5514	18.5544	18.5574	18.5604	18.5634	18.5664	18.5694	18.5724	18.5754	18.5784
2.410	18.5814	18.5844	18.5874	18.5904	18.5934	18.5964	18.5994	18.6024	18.6054	18.6084
2.420	18.6114	18.6144	18.6174	18.6204	18.6234	18.6264	18.6294	18.6324	18.6354	18.6384
2.430	18.6414	18.6444	18.6474	18.6504	18.6534	18.6564	18.6594	18.6624	18.6654	18.6684
2.440	18.6714	18.6744	18.6774	18.6804	18.6834	18.6864	18.6894	18.6924	18.6954	18.6984
2.450	18.7014	18.7044	18.7074	18.7104	18.7134	18.7164	18.7194	18.7224	18.7254	18.7284
2.460	18.7314	18.7344	18.7374	18.7404	18.7434	18.7464	18.7494	18.7524	18.7554	18.7584
2.470	18.7614	18.7644	18.7674	18.7704	18.7734	18.7764	18.7794	18.7824	18.7854	18.7884
2.480	18.7914	18.7944	18.7974	18.8004	18.8034	18.8064	18.8094	18.8124	18.8154	18.8184
2.490	18.8214	18.8244	18.8274	18.8304	18.8334	18.8364	18.8394	18.8424	18.8454	18.8484

ORIGINAL FILED IN
OF POOR QUALITY

X	Y	0.001	0.002	0.003	0.004	0.005	0.006	0.007	0.008	0.009	0.010	0.011	0.012	0.013	0.014	0.015	0.016	0.017	0.018	0.019	0.020	0.021	0.022	0.023	0.024	0.025	0.026	0.027	0.028	0.029	0.030	0.031	0.032	0.033	0.034	0.035	0.036	0.037	0.038	0.039	0.040	0.041	0.042	0.043	0.044	0.045	0.046	0.047	0.048	0.049	0.050	0.051	0.052	0.053	0.054	0.055	0.056	0.057	0.058	0.059	0.060	0.061	0.062	0.063	0.064	0.065	0.066	0.067	0.068	0.069	0.070	0.071	0.072	0.073	0.074	0.075	0.076	0.077	0.078	0.079	0.080	0.081	0.082	0.083	0.084	0.085	0.086	0.087	0.088	0.089	0.090	0.091	0.092	0.093	0.094	0.095	0.096	0.097	0.098	0.099	0.100	0.101	0.102	0.103	0.104	0.105	0.106	0.107	0.108	0.109	0.110	0.111	0.112	0.113	0.114	0.115	0.116	0.117	0.118	0.119	0.120	0.121	0.122	0.123	0.124	0.125	0.126	0.127	0.128	0.129	0.130	0.131	0.132	0.133	0.134	0.135	0.136	0.137	0.138	0.139	0.140	0.141	0.142	0.143	0.144	0.145	0.146	0.147	0.148	0.149	0.150	0.151	0.152	0.153	0.154	0.155	0.156	0.157	0.158	0.159	0.160	0.161	0.162	0.163	0.164	0.165	0.166	0.167	0.168	0.169	0.170	0.171	0.172	0.173	0.174	0.175	0.176	0.177	0.178	0.179	0.180	0.181	0.182	0.183	0.184	0.185	0.186	0.187	0.188	0.189	0.190	0.191	0.192	0.193	0.194	0.195	0.196	0.197	0.198	0.199	0.200	0.201	0.202	0.203	0.204	0.205	0.206	0.207	0.208	0.209	0.210	0.211	0.212	0.213	0.214	0.215	0.216	0.217	0.218	0.219	0.220	0.221	0.222	0.223	0.224	0.225	0.226	0.227	0.228	0.229	0.230	0.231	0.232	0.233	0.234	0.235	0.236	0.237	0.238	0.239	0.240	0.241	0.242	0.243	0.244	0.245	0.246	0.247	0.248	0.249	0.250	0.251	0.252	0.253	0.254	0.255	0.256	0.257	0.258	0.259	0.260	0.261	0.262	0.263	0.264	0.265	0.266	0.267	0.268	0.269	0.270	0.271	0.272	0.273	0.274	0.275	0.276	0.277	0.278	0.279	0.280	0.281	0.282	0.283	0.284	0.285	0.286	0.287	0.288	0.289	0.290	0.291	0.292	0.293	0.294	0.295	0.296	0.297	0.298	0.299	0.300	0.301	0.302	0.303	0.304	0.305	0.306	0.307	0.308	0.309	0.310	0.311	0.312	0.313	0.314	0.315	0.316	0.317	0.318	0.319	0.320	0.321	0.322	0.323	0.324	0.325	0.326	0.327	0.328	0.329	0.330	0.331	0.332	0.333	0.334	0.335	0.336	0.337	0.338	0.339	0.340	0.341	0.342	0.343	0.344	0.345	0.346	0.347	0.348	0.349	0.350	0.351	0.352	0.353	0.354	0.355	0.356	0.357	0.358	0.359	0.360	0.361	0.362	0.363	0.364	0.365	0.366	0.367	0.368	0.369	0.370	0.371	0.372	0.373	0.374	0.375	0.376	0.377	0.378	0.379	0.380	0.381	0.382	0.383	0.384	0.385	0.386	0.387	0.388	0.389	0.390	0.391	0.392	0.393	0.394	0.395	0.396	0.397	0.398	0.399	0.400	0.401	0.402	0.403	0.404	0.405	0.406	0.407	0
---	---	-------	-------	-------	-------	-------	-------	-------	-------	-------	-------	-------	-------	-------	-------	-------	-------	-------	-------	-------	-------	-------	-------	-------	-------	-------	-------	-------	-------	-------	-------	-------	-------	-------	-------	-------	-------	-------	-------	-------	-------	-------	-------	-------	-------	-------	-------	-------	-------	-------	-------	-------	-------	-------	-------	-------	-------	-------	-------	-------	-------	-------	-------	-------	-------	-------	-------	-------	-------	-------	-------	-------	-------	-------	-------	-------	-------	-------	-------	-------	-------	-------	-------	-------	-------	-------	-------	-------	-------	-------	-------	-------	-------	-------	-------	-------	-------	-------	-------	-------	-------	-------	-------	-------	-------	-------	-------	-------	-------	-------	-------	-------	-------	-------	-------	-------	-------	-------	-------	-------	-------	-------	-------	-------	-------	-------	-------	-------	-------	-------	-------	-------	-------	-------	-------	-------	-------	-------	-------	-------	-------	-------	-------	-------	-------	-------	-------	-------	-------	-------	-------	-------	-------	-------	-------	-------	-------	-------	-------	-------	-------	-------	-------	-------	-------	-------	-------	-------	-------	-------	-------	-------	-------	-------	-------	-------	-------	-------	-------	-------	-------	-------	-------	-------	-------	-------	-------	-------	-------	-------	-------	-------	-------	-------	-------	-------	-------	-------	-------	-------	-------	-------	-------	-------	-------	-------	-------	-------	-------	-------	-------	-------	-------	-------	-------	-------	-------	-------	-------	-------	-------	-------	-------	-------	-------	-------	-------	-------	-------	-------	-------	-------	-------	-------	-------	-------	-------	-------	-------	-------	-------	-------	-------	-------	-------	-------	-------	-------	-------	-------	-------	-------	-------	-------	-------	-------	-------	-------	-------	-------	-------	-------	-------	-------	-------	-------	-------	-------	-------	-------	-------	-------	-------	-------	-------	-------	-------	-------	-------	-------	-------	-------	-------	-------	-------	-------	-------	-------	-------	-------	-------	-------	-------	-------	-------	-------	-------	-------	-------	-------	-------	-------	-------	-------	-------	-------	-------	-------	-------	-------	-------	-------	-------	-------	-------	-------	-------	-------	-------	-------	-------	-------	-------	-------	-------	-------	-------	-------	-------	-------	-------	-------	-------	-------	-------	-------	-------	-------	-------	-------	-------	-------	-------	-------	-------	-------	-------	-------	-------	-------	-------	-------	-------	-------	-------	-------	-------	-------	-------	-------	-------	-------	-------	-------	-------	-------	-------	-------	-------	-------	-------	-------	-------	-------	-------	-------	-------	-------	-------	-------	-------	-------	-------	-------	-------	-------	-------	-------	-------	-------	-------	-------	-------	-------	-------	-------	-------	-------	-------	-------	-------	-------	-------	-------	-------	-------	-------	-------	---

APPENDIX A

TABLE A-1. - (Continued)

M	N	1.001	1.002	1.003	1.004	1.005	1.006	1.007	1.008	1.009
4.600	26.7111	26.71194	26.71317	26.71454	26.71594	26.71734	26.71871	26.72006	26.72139	26.72270
4.61	26.72269	26.72405	26.72544	26.72687	26.72831	26.72976	26.73121	26.73266	26.73411	26.73556
4.62	26.73697	26.73847	26.73997	26.74147	26.74297	26.74447	26.74597	26.74747	26.74897	26.75047
4.63	26.75197	26.75347	26.75497	26.75647	26.75797	26.75947	26.76097	26.76247	26.76397	26.76547
4.64	26.76697	26.76847	26.76997	26.77147	26.77297	26.77447	26.77597	26.77747	26.77897	26.78047
4.65	26.78197	26.78347	26.78497	26.78647	26.78797	26.78947	26.79097	26.79247	26.79397	26.79547
4.66	26.79697	26.79847	26.79997	26.80147	26.80297	26.80447	26.80597	26.80747	26.80897	26.81047
4.67	26.81197	26.81347	26.81497	26.81647	26.81797	26.81947	26.82097	26.82247	26.82397	26.82547
4.68	26.82697	26.82847	26.82997	26.83147	26.83297	26.83447	26.83597	26.83747	26.83897	26.84047
4.69	26.84197	26.84347	26.84497	26.84647	26.84797	26.84947	26.85097	26.85247	26.85397	26.85547
4.70	26.85697	26.85847	26.85997	26.86147	26.86297	26.86447	26.86597	26.86747	26.86897	26.87047
4.71	26.87197	26.87347	26.87497	26.87647	26.87797	26.87947	26.88097	26.88247	26.88397	26.88547
4.72	26.88697	26.88847	26.88997	26.89147	26.89297	26.89447	26.89597	26.89747	26.89897	26.90047
4.73	26.90197	26.90347	26.90497	26.90647	26.90797	26.90947	26.91097	26.91247	26.91397	26.91547
4.74	26.91697	26.91847	26.91997	26.92147	26.92297	26.92447	26.92597	26.92747	26.92897	26.93047
4.75	26.93197	26.93347	26.93497	26.93647	26.93797	26.93947	26.94097	26.94247	26.94397	26.94547
4.76	26.94697	26.94847	26.94997	26.95147	26.95297	26.95447	26.95597	26.95747	26.95897	26.96047
4.77	26.96197	26.96347	26.96497	26.96647	26.96797	26.96947	26.97097	26.97247	26.97397	26.97547
4.78	26.97697	26.97847	26.97997	26.98147	26.98297	26.98447	26.98597	26.98747	26.98897	26.99047
4.79	26.99197	26.99347	26.99497	26.99647	26.99797	26.99947	27.00097	27.00247	27.00397	27.00547
4.80	27.00697	27.00847	27.00997	27.01147	27.01297	27.01447	27.01597	27.01747	27.01897	27.02047
4.81	27.02197	27.02347	27.02497	27.02647	27.02797	27.02947	27.03097	27.03247	27.03397	27.03547
4.82	27.03697	27.03847	27.03997	27.04147	27.04297	27.04447	27.04597	27.04747	27.04897	27.05047
4.83	27.05197	27.05347	27.05497	27.05647	27.05797	27.05947	27.06097	27.06247	27.06397	27.06547
4.84	27.06697	27.06847	27.06997	27.07147	27.07297	27.07447	27.07597	27.07747	27.07897	27.08047
4.85	27.08197	27.08347	27.08497	27.08647	27.08797	27.08947	27.09097	27.09247	27.09397	27.09547
4.86	27.09697	27.09847	27.09997	27.10147	27.10297	27.10447	27.10597	27.10747	27.10897	27.11047
4.87	27.11197	27.11347	27.11497	27.11647	27.11797	27.11947	27.12097	27.12247	27.12397	27.12547
4.88	27.12697	27.12847	27.12997	27.13147	27.13297	27.13447	27.13597	27.13747	27.13897	27.14047
4.89	27.14197	27.14347	27.14497	27.14647	27.14797	27.14947	27.15097	27.15247	27.15397	27.15547
4.90	27.15697	27.15847	27.15997	27.16147	27.16297	27.16447	27.16597	27.16747	27.16897	27.17047
4.91	27.17197	27.17347	27.17497	27.17647	27.17797	27.17947	27.18097	27.18247	27.18397	27.18547
4.92	27.18697	27.18847	27.18997	27.19147	27.19297	27.19447	27.19597	27.19747	27.19897	27.20047
4.93	27.20197	27.20347	27.20497	27.20647	27.20797	27.20947	27.21097	27.21247	27.21397	27.21547
4.94	27.21697	27.21847	27.21997	27.22147	27.22297	27.22447	27.22597	27.22747	27.22897	27.23047
4.95	27.23197	27.23347	27.23497	27.23647	27.23797	27.23947	27.24097	27.24247	27.24397	27.24547
4.96	27.24697	27.24847	27.24997	27.25147	27.25297	27.25447	27.25597	27.25747	27.25897	27.26047
4.97	27.26197	27.26347	27.26497	27.26647	27.26797	27.26947	27.27097	27.27247	27.27397	27.27547
4.98	27.27697	27.27847	27.27997	27.28147	27.28297	27.28447	27.28597	27.28747	27.28897	27.29047
4.99	27.29197	27.29347	27.29497	27.29647	27.29797	27.29947	27.30097	27.30247	27.30397	27.30547

APPENDIX A

ORIGINAL PAGE 1
OF FOUR QUALITY

TABLE A27. - CONVERSION FACTORS FOR VARIOUS PRESSURE UNITS

[From ref. A4]

Pressure unit value in -	millibar	mm Hg (0° C)	in. Hg (0° C)	g/cm ²	lb/in ²	lb/ft ²	cm H ₂ O (20° C)	in. H ₂ O (20° C)
1 atm	1013.250	760.000	29.9213	1033.23	14.69595	2116.22	1035.08	407.513
1 millibar	1	.75006	.029533	1.0197	.014504	2.0886	1.0215	.4018
1 mm Hg (0° C)	1.3332	1	.03937	1.3595	.019337	2.7845	1.3609	.53577
1 in. Hg (0° C)	33.864	25.400	1	34.532	.49116	70.726	34.566	13.609
1 g/cm ²00060	.73556	.028959	1	.014224	2.0482	1.0010	.39409
1 lb./in ²	68.94757	51.715	2.0360	70.307	1	144	70.376	27.707
1 lb./ft ²47880	.03613	.014149	.08824	.0069444	1	.48872	.19341
1 cm H ₂ O (20° C)07354	.73474	.028907	.00621	.014198	2.0445	1	.3937
1 in. H ₂ O (20° C)4804	1.8050	.074424	2.5355	.036066	5.1930	2.5400	1

APPENDIX A

TABLE A28.- CONVERSION FACTORS, EQUIVALENTS, AND FORMULAS FOR U.S. CUSTOMARY
UNITS AND THE INTERNATIONAL SYSTEM OF UNITS (SI)

(a) Conversion Factors

[from ref. A5]

Length

1 foot (ft)	0.3048 meter (m)
1 nautical mile	1852 meters (m)
1 statute mile	1609.3 meters (m)
1 inch (in.)	2.54 centimeters (cm)

Speed

1 ft/sec	0.3048 meter/second (m/sec)
1 ft/min	0.01678 meter/second (m/sec)
1 mile/hour (mph)	1.60934 meter/second (m/sec)
1 knot	1.852 meter/second (m/sec)

Acceleration

1 ft/sec ²	0.3048 meter/second ² (m/sec ²)
-----------------------	--

Mass

1 slug	14.5939 kilograms (kg)
1 pound (lb)	0.4535924 kilograms (kg)

Force

1 pound (lb)	4.44822 newtons (N)
--------------	---------------------

Pressure

1 lb/ft ²	47.88026 pascals (Pa) or N/m ²
1 inch of mercury (in. Hg)	3386.38 pascals (Pa) or N/m ²
1 millibar	100 pascals (Pa) or N/m ²

Density

1 slug/ft ³	515.478 kilograms/meter ³ (kg/m ³)
1 lb/ft ³	160.184 kilograms/meter ³ (kg/m ³)

Volume

1 ft ³	0.0283168 cubic meter (m ³)
1 in ³	16.3871 centimeters ³ (cm ³)

Viscosity

1 lb-sec/ft ²	47.88026 pascals-seconds (Pa-s)
1 lb-ft-sec	1.48816 pascals-seconds (Pa-s)

Temperature¹

°(°F)	$T(^{\circ}\text{C}) = (T(^{\circ}\text{F}) - 32) \times 5/9$
°(°C)	$T(^{\circ}\text{F}) = T(^{\circ}\text{C}) \times 9/5 + 32$

Magnetic flux density

1 tesla	10,000 gauss
---------	--------------

¹T(°C) = 273.15 + 459.67 (°F - 32) = 273.15 + 5/9 (°F - 32)

APPENDIX A

ORIGINAL PAGE
OF POOR QUALITY

TABLE A28.- Continued

(b) Equivalents (primary constants and atmospheric properties)

Quantity	U.S. Customary Units	SI Units
P_0	2116.22 lb/ft ² 29.9213 in. Hg	101 325 Pa
\bar{P}_0	0.076474 lb/ft ³	
ρ_0	0.0023769 slug/ft ³	1.2250 kg/m ³
t_0	59.0° F	15.0° C
T_0	518.67° R	288.15° K
μ_0	$1.2024 \cdot 10^{-5}$ lb-ft-sec $3.7372 \cdot 10^{-7}$ lb-sec/ft ²	$1.7894 \cdot 10^{-4}$ Pa-sec
q_0	32.1741 ft/sec ²	9.80665 m/sec ²
a_0	1116.45 ft/sec 761.22 mph 661.48 knots	343.294 m/sec 1225.0 km/hr
$\alpha_{w,0}$	28.9644 (dimensionless)	28.9644 (dimensionless)
R^*	1545.31 ft-lb/(lb mol) °R	$8.31447 \cdot 10^3$ J/(kg-mol)
\bar{R}	53.352 ft-lb/(lb mol) °R	
R	1716.5 ft-lb/slug-°R	$287.05 \cdot 10^3$ J/(kg-mol)

^aFor altitudes up to 290 000 ft, $\alpha_{w,0} = \alpha_{w,0}$.

TABLE A28.- Concluded

(c) Formulas

Formulas for -	U.S. Customary Units ^a	SI Units
\bar{J}	g	
\bar{R}	$R^*/W_{m,o}$	
R	$R^*g/W_{m,o}$	$R^*/W_{m,o}$
N (newton)		m-kg/sec ²
Pa (pascal)		N/m ² = kg/m-sec ²
J (joule)		N-m = m ² -kg/sec ²

^aThe formulas for the gas constants \bar{R} and R in U.S. Customary Units also apply to the metric (mks) system, i.e., for $R^* = 847.819 \text{ m-kg/}^\circ\text{K-kmol}$, $\bar{R} = 29.271 \text{ m-kg/}^\circ\text{K-kmol}$, and $R = 287.05 \text{ m}^2\text{-kg/}^\circ\text{K-kmol-sec}^2$.

APPENDIX B

ORIGINAL PAGE IS
OF POOR QUALITY

SAMPLE CALCULATIONS

Part I - Static-Pressure Errors and Flight Quantities

In this section, sample calculations are presented for the determination of (1) the position error Δp by two of the flight calibration methods described in chapter IX, (2) values of calibrated airspeed V_C , pressure altitude H , and Mach number M from the indicated values of these quantities and a given value of Δp , (3) the lift coefficient C_L from given values of Δp , the measured impact pressure q_C' , and the measured static pressure p' , and (4) true airspeed V from given values of calibrated airspeed V_C , pressure altitude H , and ambient temperature t .

Determination of Position Error Δp

Two calibration procedures, the pacer-aircraft method and the ground-camera method, are used to illustrate the determination of Δp (i.e., $p' - p$). With the pacer-aircraft method, the value of p is derived from the calibrated installation on the pacer aircraft, while with the ground-camera method, the value of p at the flight level is calculated from measurements of p and T at the ground and the assumption of a standard temperature gradient up to the flight level.

Pacer-aircraft method. - For the calculation of Δp by this method, it is assumed that the altimeter indication in the test aircraft is 29 600 ft and that the corrected altimeter indication in the pacer aircraft is 30 000 ft. From table A2 of appendix A, the static pressure p' at 29 600 ft is 639.962 lb/ft², and the static pressure p at 30 000 ft is 628.433 lb/ft². The position error of the test aircraft is then

$$\begin{aligned}\Delta p &= p' - p \\ &= 639.962 - 628.433 = 11.529 \text{ lb/ft}^2\end{aligned}\quad (2.2)$$

For altitude increments no greater than about 1000 ft, the value of Δp can also be derived from equation (3.6), here expressed as

$$\Delta p = -\frac{\gamma_0}{g} \bar{\rho}_m \Delta H \quad (3.1)$$

where $\Delta H = H' - H = 29\,600 - 30\,000 = -400$ ft and $\bar{\rho}_m$ is the density at the midpoint between H' and H . From table A8 of appendix A, the value of $\bar{\rho}_m$ for an altitude increment of 400 ft is essentially 1.0. From table A3, the density at the midpoint (29 800 ft) is 0.028823 lb/ft³. From equation (3.1), the value of Δp is then

$$\Delta p = (-0.028823)(-400) = 11.529 \text{ lb/ft}^2$$

APPENDIX B

Ground-camera method.— For the calculation of Δp by this method, it is assumed that (1) the pressure p' of the aircraft installation is measured by an absolute-pressure recorder (in contrast to the statoscope used in the test described in chapter IX), and (2) that for the elevations in figure 9.10, $E_C = E_R$ and $h_C = h_R$.

It is further assumed that h_C is 1000 ft, that the height of the air ΔZ above h_C is 400 ft, and that the pressure measured by the absolute-pressure recorder at the flight level is 1973 lb/ft². The pressure p and temperature T at the ground (at h_C) are 2000 lb/ft² and 500° R. From table A2 of appendix A, the standard pressure p_s at 1000 ft is 2040.85 lb/ft²; from table A4, the standard temperature T_s at 1000 ft is 515.104° R; and from table A3, the standard density $\bar{\rho}_s$ at 1000 ft is 0.074261 lb/ft³ and the standard density $\bar{\rho}_s$ at 1200 ft is 0.073825 lb/ft³. From equation (3.1), density $\bar{\rho}$ at h_C is

$$\begin{aligned}\bar{\rho} &= \bar{\rho}_s \frac{p T_s}{p_s T} \\ &= 0.074261 \left(\frac{2000}{2040.85} \right) \left(\frac{515.104}{500} \right) = 0.074973 \text{ lb/ft}^3\end{aligned}$$

From equation (9.29), the density $\bar{\rho}_m$ at the midpoint (1200 ft) is

$$\begin{aligned}\bar{\rho}_m &= \bar{\rho} - (\bar{\rho}_s - \bar{\rho}_{s,m}) \\ &= 0.074973 - (0.074261 - 0.073825) = 0.074537 \text{ lb/ft}^3\end{aligned}$$

From equation (9.28), the pressure increment Δp_C corresponding to a height increment ΔZ is

$$\begin{aligned}\Delta p_C &= -\bar{\rho}_m \Delta Z \\ &= (-0.074537)(400) = -29.8 \text{ lb/ft}^2\end{aligned}$$

From this pressure increment and the existing pressure (2000 lb/ft²) at the ground (h_C), the value of p at $Z = 1400$ ft is

$$\begin{aligned}p &= p_{h_C} - \Delta p_C \\ &= 2000 - 29.8 = 1970.2 \text{ lb/ft}^2\end{aligned}$$

For the value of p' of this example, the position error Δp of the aircraft installation is then

$$\begin{aligned}\Delta p &= p' - p \\ &= 1973 - 1970.2 = 2.8 \text{ lb/ft}^2\end{aligned}$$

APPENDIX B

Calculation of V_c and ΔV_c , H and ΔH , and M and ΔM

For these calculations, the indicated airspeed V_i , indicated altitude H' , and indicated Mach number M' measured by the cockpit instruments are corrected for the position error Δp of the aircraft installation to yield values of V_c , H , and M . The values of the errors, ΔV_c , ΔH , and ΔM corresponding to the value of Δp are also calculated.

It is assumed that V_i is 300 knots, H' is 30 000 ft, M' is 0.79, and Δp is 8 lb/ft². From table A12 of appendix A, the impact pressure q_c' at 300 knots is 320.694 lb/ft²; and from table A2, the static pressure p' at 30 000 ft is 628.433 lb/ft².

Calculation of V_c and ΔV_c .— From equation (9.20),

$$\begin{aligned} q_c &= q_c' + \Delta p \\ &= 320.694 + 8 = 328.694 \text{ lb/ft}^2 \end{aligned} \tag{9.20}$$

ORIGINAL PAGE 1.
OF POOR QUALITY

From table A12 of appendix A, the calibrated airspeed V_c corresponding to this value of q_c is 303.5 knots. From equation (5.9), the airspeed error is

$$\begin{aligned} \Delta V_c &= V_i - V_c \\ &= 300 - 303.5 = -3.5 \text{ knots} \end{aligned} \tag{5.9}$$

Calculation of H and ΔH .— From equation (2.2),

$$\begin{aligned} p &= p' - \Delta p \\ &= 628.433 - 8 = 620.433 \text{ lb/ft}^2 \end{aligned} \tag{B4}$$

From table A2 of appendix A, the altitude H corresponding to this value of p is 30 281 ft. From equation (5.8), the altitude error is

$$\begin{aligned} \Delta H &= H' - H \\ &= 30\,000 - 30\,281 = -281 \text{ ft} \end{aligned} \tag{5.8}$$

Calculation of M and ΔM .— In chapter III, it was shown that M is a function of q_c/p . For values of q_c' and p' , therefore, M is a function of $q_c' + \Delta p$ (eq. (9.20)) and $p' - \Delta p$ (eq. (B4)). Thus,

$$\frac{q_c}{p} = \frac{320.694 + 8}{628.433 - 8} = 0.5298$$

APPENDIX B

From table A26 of appendix A, the value of M corresponding to this q_c/p is 0.804. From equation (5.10), the Mach number error is

$$\begin{aligned}\Delta M &= M' - M \\ &= 0.79 - 0.804 = -0.014\end{aligned}$$

In the preceding examples, the signs of ΔV_c , ΔH , and ΔM are all negative, when the sign of Δp is positive. It is also true that when Δp is negative, ΔV_c , ΔH , and ΔM are positive.

In the preceding calculations, the values of ΔV_c , ΔH , and ΔM have been expressed in terms of errors in the measured quantities. In many aircraft manuals, however, these errors are expressed in terms of corrections with signs opposite to those of the errors. An example of a flight-manual correction for the airspeed and altitude errors of an airplane installation is presented in figure B1.

Calculation of C_L

As stated by equation (5.2), the lift coefficient C_L is expressed in terms of the dynamic pressure q , the aircraft weight W , and the wing area by the following equation:

$$C_L = \frac{W}{qS}$$

From equation (5.3), the dynamic pressure q is determined from values of ρ and M as follows:

$$q = 0.7\rho M^2$$

For the following computation of C_L , it is assumed that $V_i = 260$ knots, $H' = 25,000$ ft, $\Delta p = 6$ lb/ft², $W = 172,000$ lb, and $S = 2400$ ft². From table A12 of appendix A, the value of q_c' at 260 knots is 237.841 lb/ft². From equation (9.20), the value of q_c is

$$\begin{aligned}q_c &= q_c' + \Delta p \\ &= 237.841 + 6 = 243.841 \text{ lb/ft}^2\end{aligned}$$

From table A1, the value of p' at 25,000 ft is 785.308 lb/ft². Thus, the value of p is

$$\begin{aligned}p &= p' - \Delta p \\ &= 785.308 - 6 = 779.308 \text{ lb/ft}^2\end{aligned}$$

APPENDIX B

The value of q_c/p is then $\frac{243.84}{779.308} = 0.3129$. From table A26, the value of M for this q_c/p value is 0.636, so that the value of M^2 is 0.4045. From equation (B5), the value of q is

$$q = (0.7)(779.308)(0.4045) = 220.7 \text{ lb/ft}^2$$

From equation (5.2), the value of C_L is then

$$C_L = \frac{172\ 000}{(220.7)(2400)} = 0.325$$

ORIGINAL PAGE IS
OF POOR QUALITY

Calculation of V

In this example, the true airspeed V is calculated for a calibrated airspeed V_c of 300 knots, a pressure altitude H of 35 000 ft, and an ambient temperature of -60°F . From table A12 the value of q_c for 300 knots is 320.694 lb/ft^2 . From table A2 the value of p at 35 000 ft is 497.956 lb/ft^2 . The value of q_c/p is then $\frac{320.694}{497.956} = 0.64402$. From table A26 the value of M corresponding to $q_c/p = 0.64402$ is 0.87357. From equation (3.27), the speed of sound a in knots is

$$a = 29.045 \sqrt{T} \quad (2.27)$$

where the unit of T is $^\circ \text{R}$. From table A28, the value of T for $t = -60^\circ \text{F}$ is

$$T = -60 + 459.67 = 399.67^\circ \text{R}$$

The value of a is then

$$a = 29.045 \sqrt{399.67} = (29.045)(19.992) = 580.67 \text{ knots}$$

From equation (3.21),

$$V = Ma \quad (3.21)$$

The value of V is then

$$V = (0.87357)(580.67) = 507.2 \text{ knots}$$

APPENDIX B

Part II - Pressure Increments in the International System of Units

In this section, equations (3.3) and (3.4) are applied to determine static pressure increments in SI Units. With both equations, the pressure increment Δp for a height increment ΔZ of 400 m is computed and compared with values in table A15. Note that for 0 to 400 meters the values of g, ρ, μ, T in terms of Z are the same as those in terms of H .

Equation (3.3) is

$$\Delta p = -g \rho \Delta Z$$

From table A16, the value of ρ at 200 m is 1.2017 kg/m³. From table II of reference A1 of appendix A, the value of g at 200 m is 9.8060 m/sec². Then, for $\Delta Z = 400$ m,

$$\Delta p = (-9.8060)(1.2017)(400) = -4714 \text{ kg/m-sec}^2 \text{ (Pa)}$$

From table A15, the value of Δp as derived from the differential form of equation (3.3) is the same, i.e., 96 611 - 101 325 = -4714 Pa.

Equation (3.4) can be written as

$$\Delta p = -g \frac{\rho}{RT} \Delta Z$$

From table II of reference A1 of appendix A, the value of g at 200 m is 9.8060 m/sec². From table A15, the value of p at 200 m is 98 945.3 Pa (kg/m-sec²). From table A28, the value of R is 0.28705 $\times 10^3$ J/°K-kmol. From table A17, the value of t at 200 m is 13.70° C. From table A28, the value of T is 13.70 + 273.15 = 286.85° K. Then, for $\Delta Z = 400$ m,

$$\Delta p = (-9.8060) \frac{98\,945.3}{(287.05)(286.85)} (400) = -4713 \text{ kg/m-sec}^2 \text{ (Pa)}$$

From table A15, the value of Δp is essentially the same, that is, 96 611 - 101 325 = -4714 Pa.

The other form of equation (3.4) can be written as

$$\Delta p = - \frac{p}{RT} \Delta Z$$

APPENDIX B

The values of p , t , and T remain the same. From table A28, the value of \bar{R} is 29.271 m-kg/^oK-kmol. Then, for $\Delta Z = 400$ m,

$$\Delta p = \frac{-98\,945.3}{(29.271)(286.85)}(400) = -4714 \text{ kg/m-sec}^2 \text{ (Pa)}$$

As in the previous cases, the value of Δp from table A15 is -4714 Pa.

Part III - Pressure-System Lag and Leaks

In this section, sample calculations are presented for the determination of (1) the airspeed and altitude errors due to the pressure lag of a static-pressure system and (2) the altitude error resulting from a leak in that system.

Calculation of Airspeed and Altitude Errors Due to Pressure Lag

In this example, the airspeed and altitude errors of a static-pressure system are determined for an indicated airspeed of 300 knots in a climb of 12 000 ft/min at an altitude of 30 000 ft. The system consists of four cockpit instruments (having a combined volume of 100 in³) connected to a 50-ft length of tubing 3/16 in. (0.188 in.) in inside diameter (I.D.). From equation (10.3), the lag constant λ is

$$\lambda = \frac{128\mu LC}{\pi d^4 p} \quad (10.3)$$

ORIGINAL PAGE IS
OF POOR QUALITY

From table A6 of appendix A, the value of μ at 30 000 ft is 3.106×10^{-7} lb-sec/ft². From table A2, the value of p at 30 000 ft is 628.433 lb/ft². The value of C in cubic feet is 0.05787, the value of d in feet is 0.01567, and the value of L is 50 ft. From equation (10.3), the lag constant λ at 30 000 ft is then

$$\lambda = \frac{128(3.106 \times 10^{-7})(50)(0.05787)}{3.1416(0.01567)^4(628.433)} = 1.0 \text{ sec}$$

From equation (10.2), the pressure drop Δp is

$$\Delta p = \lambda \frac{dp}{dt} \quad (10.2)$$

From table A2 of appendix A, a 100-ft increment at 30 000 ft corresponds to a pressure increment of 2.86 lb/ft². Since the rate of climb is 12 000 ft/min

APPENDIX B

(or 200 ft/sec), dp/dt is $(2)(2.86)$ or 5.72 (lb/ft²)/sec. From the value of λ of 1.0 sec, the value of Δp is

$$\Delta p = (1.0)(5.72) = 5.72 \text{ lb/ft}^2$$

From table A2 of appendix A, the altitude increment at 30 000 ft corresponding to a pressure increment of 5.72 lb/ft^2 is 200 ft. Thus, the altitude error for a rate of climb of 12 000 ft/min at 30 000 ft is 200 ft. From table A12 of appendix A, the airspeed increment at 300 knots corresponding to a pressure increment of 5.72 lb/ft^2 is 2.5 knots. Thus, the airspeed error for a rate of climb of 12 000 ft/min at 30 000 ft is 2.5 knots.

To determine whether the conditions of this example meet the requirement for laminar flow as stated by equation (10.6), the pressure drop per foot must be determined. Since the pressure drop Δp is 5.72 lb/ft^2 and the length of tubing is 50 ft, the pressure drop per foot is $0.1 \text{ (lb/ft}^2\text{)/ft}$. From table 10.1, the limiting value of $\Delta p/L$ for laminar flow in 0.188-in. I.D. tubing at 30 000 ft is $2.3 \text{ (lb/ft}^2\text{)/ft}$. Thus, since the $\Delta p/L$ value of this example is only 5 percent of the limiting value, the flow can be considered laminar.

Calculation of Altitude Error Due to a Leak

For this example, it is assumed that the instrument system is the same as that used in the lag calculations (namely, four cockpit instruments connected to a 50-ft length of 3/16-in. I.D. tubing). It is also assumed (1) that in a ground test of the system at a test pressure corresponding to an altitude of 40 000 ft, the system was determined to have a leak rate equivalent to a rate of change of altitude of 100 ft/min and (2) that the leak is located in the cockpit.

To determine the altitude error that would be caused by this leak, it is assumed that the aircraft is at an altitude of 30 000 ft and that the cabin pressure corresponds to an altitude of 5000 ft. The pressures for this flight condition and the pressures involved in the ground test of the system are shown in the diagrams in figure B2.

From equation (10.7), the lag constant λ_l of the leak is

$$\lambda_l = \left(\frac{P_{T,o} - P_{T,a}}{dp/dt} \right) \left(\frac{P_{T,o} + P_{T,a}}{P_c + P_a} \right) \quad (10.7)$$

From table A1 of appendix A,

$P_{T,o}$ at sea level is 2116.22 lb/ft^2

$P_{T,a}$ at 40 000 ft is 391.683 lb/ft^2

APPENDIX B

P_a at 30 000 ft is 628.433 lb/ft²

P_c at 5000 ft is 1760.79 lb/ft²

Also from table A2, the pressure increment corresponding to an altitude increment of 100 ft at 40 000 ft is 1.88 lb/ft². The pressure rate dp/dt corresponding to a leak rate of 100 ft/min is thus 1.88 (lb/ft²)/min or 0.0314 (lb/ft²)/sec. The lag constant of the leak is then

$$\lambda_l = \left(\frac{2116.22 - 391.683}{0.0314} \right) \left(\frac{2116.22 + 391.683}{1760.79 + 628.433} \right) = 57\,650 \text{ sec}$$

From equation (10.8), the pressure error Δp_l due to the leak is

$$\Delta p_l = \frac{\lambda}{\lambda_l + \lambda} (P_c - P_a) \quad (10.8)$$

For a system lag λ of 1.0 sec at 30 000 ft, the value of Δp_l is

$$\Delta p_l = \left(\frac{1.0}{57\,650 + 1.0} \right) (1760.79 - 628.433) = 0.02 \text{ lb/ft}^2$$

From table A2 of appendix A, the pressure increment corresponding to a 1-ft increment at 30 000 ft is 0.028 lb/ft². Thus the altitude error corresponding to a Δp_l of 0.02 lb/ft² is less than 1 ft.

APPENDIX B

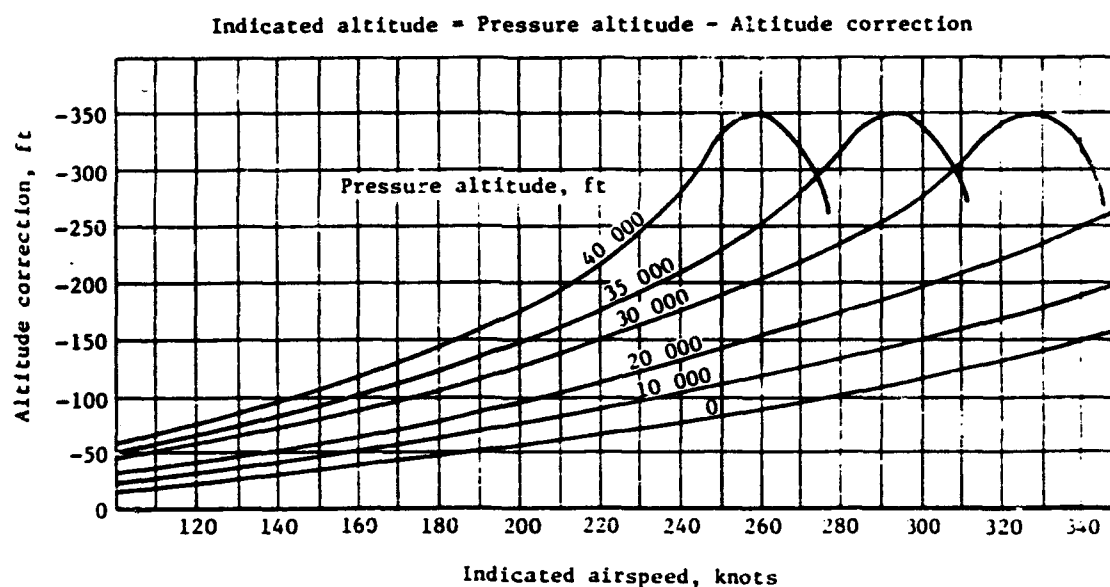
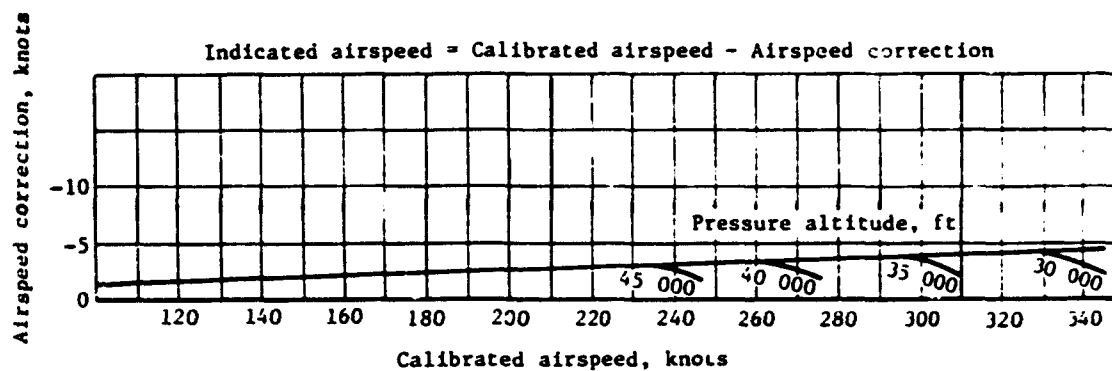
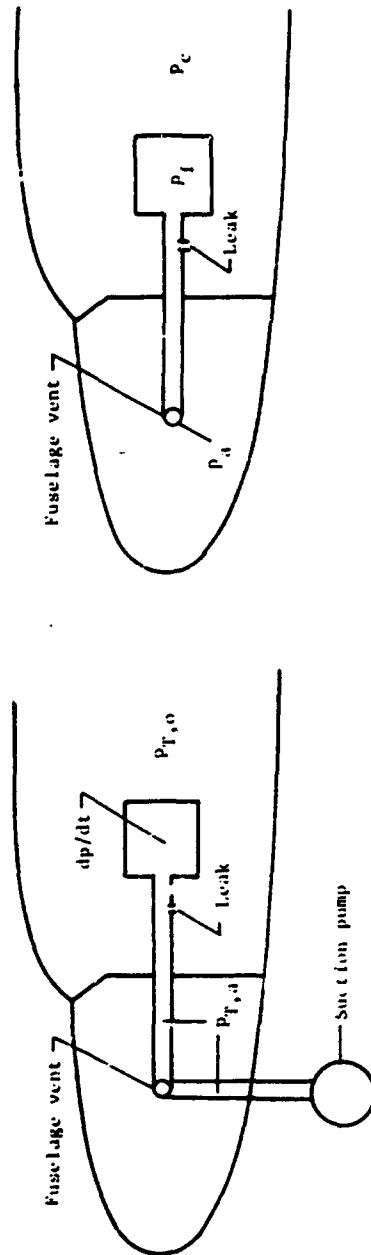


Figure B1.- Flight-manual correction charts for the airspeed and altitude errors of the static-pressure installation of an airplane. These correction charts are used to determine the indicated airspeed and indicated altitude at which the airplane should fly to achieve a desired calibrated airspeed and pressure altitude.

APPENDIX B



Ground test		Flight (30 000 feet)	
$P_{T,a}$	ambient pressure - 2116.22 lb/ft ² (sea level)	P_a	pressure at fuselage vent - 628.433 lb/ft ² (30 000 ft)
$P_{T,a}$	test pressure in system - 391.683 lb/ft ² (40 000 ft)	P_c	cabin pressure - 1760.79 lb/ft ² (5 000 ft)
dp/dt	rate of pressure change due to leak (0.0314(lb/ft ²)/sec based on rate of altitude change of 100 ft/min)	P_i	pressure inside instrument
		dp_i	pressure error due to leak, $P_i - P_a$

Figure B2.- Pressures used in example of computation of pressure error due to leak.

INDEX

- Acceleration due to gravity, 12, 219
 - tables, 237, 253
- Accelerometer method, 131
- Adiabatic temperature rise, 18
- Aerodynamic compensation, 109
 - installations, 110
 - tubes, 110
- Aftereffect, 172, 187
- Air
 - density, 11, 12
 - gas constant, 12
 - mean molecular weight, 12
 - pressure, 1, 11, 12
 - ratio of specific heats, 14, 15
 - speed of sound, 14, 18
 - temperature, 12, 13, 18, 19
 - viscosity, 166
- Air data computer, 175, 176
- Airspeed
 - calibrated, 15, 50
 - corrections, 282, 288
 - equations, 14, 15
 - equivalent, 16
 - errors, 50, 57, 281
 - indicated, 16, 50, 137
 - tables, 238-244, 254-262
 - true, 1, 14, 16-18
- Airspeed indicator, 4, 173
 - calibration, 173
 - tolerances, 182
- Altimeter, 4, 172
 - calibration, 172
 - settings (barometric scale), 199
 - tolerances, 180
 - types, 172, 176
- Altitude
 - corrections, 282, 288
 - equations, 12
 - errors, 50, 57, 58, 281
 - geopotential, 12
 - indicated, 50
 - pressure, 1, 12, 199
 - tables, 225, 227, 247, 248
- Angle of attack, 27
- Angle of sideslip, 79
- Angle of yaw, 27
- Atmosphere, standard, 11
 - equations, 12
 - properties, 13

- Barometers, 177
- Barometric scale, altimeter, 172, 199
 - QFE setting, 201
 - QNE setting, 199
 - QNH setting, 200
- Bellows, 3, 176, 196
- Bernoulli's equations
 - compressible flow, 14
 - incompressible flow, 47
- Blocking effect, 59, 60, 75, 79

- Calibrated airspeed, 15
 - equations, 15
 - tables, 238-244, 254-262
- Calibrations
 - instrument, 172-174
 - static-pressure installations, 75-80, 121-143
 - static-pressure tubes, 59-62
 - total-pressure installations, 121
 - total-pressure tubes, 25-29
- Capacitance altimeter, 217
- Capsules
 - aneroid, 3, 8
 - differential-pressure, 3, 8
- Collar, static-pressure tubes, 59, 60
- Compensated static-pressure tubes, 109
- Compressibility, 14
 - factor, 16
- Computer, air data, 175
- Conversion factors
 - pressure units, 275
 - U.S. Customary and International Systems, 276
- Corrections, airspeed and altitude, 282
- Cosmic ray altimeter, 219

- Density
 - altimeter, 218
 - equations, 11
 - tables, 229, 249
- Diaphragms, 3, 177, 197
- Drift, 172, 173, 187
- Dynamic pressure, 14
 - equations, 14, 49

Equivalent airspeed, 16

Errors

- airspeed, 50, 57, 281
- altitude, 50, 57, 58
- instrument, 5, 6, 171-177, 204
- instrument system, 6, 203
- Mach number, 50, 58
- position, 49, 75
- static pressure, 5, 49
- temperature, 5
- total pressure, 4

Field

- flow, 47, 48, 52
- induced velocity, 136, 156
- pressure, 47, 48, 52

Flight calibration methods, 121-139

Flight technical error, 202, 213

Flow

- compressible, 14, 48
- field, 47, 48, 52
- incompressible, 14, 47

Free-stream

- static pressure, 4, 48
- temperature, 4, 18
- total pressure, 4, 14, 47, 52

Fuselage vent

- configuration, 79
- errors, 100-102
- installation, 79

Gas constant

- air, 12, 277
- universal, 12, 277

Geometric height, 12, 199

Geopotential altitude, 12

Gravity meter, 219

Ground camera method, 129, 139

Height, geometric, 12, 199

Hysometer, 218

Hysteresis, 172, 187

- Impact pressure, 5, 14
 - equations, 5, 15
 - tables, 238-244, 254-262
- Indicated airspeed, 16
 - equation, 137
 - tables, 238-244, 254-262
- Installation error, 49, 75
 - effect of lift coefficient, 76, 77, 80
 - effect of Mach number, 76, 78-80
- Installation, static-pressure, 75
 - design considerations, 82
 - fuselage nose, 75
 - fuselage vent, 79
 - vertical fin, 78
 - wing tip, 77
- Instruments, 4, 171-177
 - mechanical, 3, 171
 - servoed, 175
 - transducer, 176
- Instrument errors, 5, 6, 171-177
- Instrument scale error, 5, 171, 172, 187, 188
- Instrument system error, 6, 203, 204
- International System (SI) of Units
 - conversion factors and equivalents, 276
 - tables, 247-264

Kiel total-pressure tube, 27, 33

Lag

- acoustic, 165
- constant, 166
- due to leak, 168, 286
- equations, 165, 166
- pressure, 165, 285

Laser altimeter, 217
Leaks, pressure system, 168, 286
Lift coefficient, 49, 282
Limited-range pressure altimeter, 218
Local static pressure, 47, 52, 54
Local velocity, 47, 52

Machmeter, 4, 174

- calibration, 174
- tolerances, 184

Mach number, 1

- error, 50, 281
- equations, 17
- indicated, 50
- tables, 265

Magnetometer, 220
Manometer, 177
Mean molecular weight, 12, 277
Microprocessor, 175, 176

Orifice, static-pressure
 axial location, 59
 radial configurations, 61
 size and shape, 48, 62, 74
Overall altitude error, 203

Pacer aircraft method, 125
Phototheodolite, 128
Pitot-static tubes, 3, 7, 48, 53
Pitot tubes, 3, 7, 25, 31
 shielded, 27, 33, 35, 36
 swiveling, 27, 33, 121
Position error, 49, 75
 effect of lift coefficient, 76, 77, 80
 effect of Mach number, 76, 78-80
Prandtl pitot-static tube, 26, 60, 66
Pressure
 altimeter, 172
 altitude, 1, 199
 conversion factors, 275
 dynamic, 14, 49
 field, 47, 48, 52
 free-stream, 4
 impact, 5, 14, 15
 static, 1, 5, 12
 total, 1, 4, 14, 47

QFE barometric setting, 199, 201
QNE barometric setting, 199
QNH barometric setting, 199, 200

Radar
 altimeter, 215
 phototheodolite, 128, 138
 tracking, 128, 142
Radio altimeter, 215
Range of insensitivity
 static-pressure tubes, 61
 total-pressure tubes, 26
Rate-of-climb indicator, 4, 174
 calibration, 174
 tolerances, 185

- Ratio of specific heats, 14, 15
- Recording thermometer method, 133
- Recovery, 172, 187
- Recovery factor, 18
- Reynolds number, 69, 166

- Scale error 5, 171
- Servoed instruments, 175
- Shock wave, 48
 - effect on static-pressure measurement, 76, 78
 - effect on total-pressure measurement, 25
 - total-pressure loss through, 26
- Sonic altimeter, 217
- Sonic speed method, 137
- Speed course method, 137
- Speed of sound
 - equations, 14, 18
 - tables, 236, 252
- Standard atmosphere, 11
 - equations, 12
 - properties, 13
- Standard deviation, 142, 143, 303
- Static pressure
 - error, 5, 48, 49, 59, 75
 - free-stream, 5, 48
 - installations, 75
 - local, 47, 52, 54
 - measurement, 47
 - tables, 225-227, 247, 248
 - tubes, 59-62
- Static-pressure installations, 75
 - calibration procedures, 121, 143
 - design considerations, 82
 - effect of lift coefficient, 76, 77, 80
 - effect of Mach number, 76, 78-80
- Static-pressure tubes, 3, 7, 48, 59
 - compensated, 109
 - design considerations, 60
 - effect of angle of attack, 61, 62
 - effect of Mach number, 59, 60
- Statoscope, 140, 157
- Strut, static-pressure tube, 48, 53, 59, 60

Tables

- acceleration due to gravity, 237, 253
- airspeed, 238-244, 254-262
- altitude, 225-227, 247, 248
- coefficient of viscosity, 235, 251
- conversion factors, 275, 276

- density, 229, 249
- impact pressure, 238-244, 254-262
- Mach number, 265
- speed of sound, 236, 252
- static pressure, 225-227, 247, 248
- temperature, 231, 233, 250
- true airspeed, 246, 264
- Temperature
 - adiabatic rise, 19
 - error, 5
 - equations, 5, 19, 133, 138
 - free-stream, 4
 - gradient, 13
 - probe, 4, 9, 23, 190
 - tables, 231, 233, 250
 - total, 19, 133, 138
- Theodolite, 129
- Tolerances
 - instrument, 171, 180, 182-185
 - installation, 81
 - leak, 168
- Total pressure
 - error, 4
 - equations, 1, 14, 47
 - free-stream, 4, 47
 - loss through normal shock wave, 26
 - measurement, 25
- Total pressure installations
 - calibration procedures, 121
 - design considerations, 25
- Total pressure tubes, 3, 7, 25, 31
 - design considerations, 29
 - effect of angle of attack, 26-29
 - effect of Mach number, 25
 - shielded, 27, 33, 35, 36
 - swiveling, 27, 121
- Total temperature, 19
 - equations, 19, 133, 138
- Total-temperature method, 138
- Tower method, 127
- Tracking-radar method, 128, 139
- Tracking-radar/pressure-altimeter method, 130
- Trailing-anemometer method, 134
- Trailing-bomb method, 124
- Trailing-cone method, 125
- Transducer, 176, 177, 196, 197
- Transducer, pressure, 176
 - analog, 177, 197
 - digital, 176, 196

True airspeed, 1
 equations, 14, 16-18
 tables, 246, 264
True airspeed indicator, 1, 4, 173
 calibration, 173
 tolerances, 183
Tubes
 compensated static-pressure, 109
 pitot, 3, 7, 25, 31
 shielded total-pressure, 27, 33, 35, 36
 static-pressure, 3, 7, 48, 59
 swiveling, 27, 33, 121
 total-pressure, 3, 7, 25, 31

U.S. Customary System of units
 conversion factors and equivalents, 276
 tables, 247-264

Velocity
 free-stream, 47, 52
 induced, 136, 156
 local, 47, 52
Vent, fuselage
 configuration, 48, 79
 errors, 100-102
 installations, 79
Vertical speed indicator, 4, 174
Viscosity, 166
 tables, 235-251

1 Report No. NASA RP-1046	2 Government Accession No.	3 Recipient's Catalog No.
4 Title and Subtitle MEASUREMENT OF AIRCRAFT SPEED AND ALTITUDE	5 Report Date May 1980	6 Performing Organization Code
7 Author(s) William Gracy	8 Performing Organization Report No. L-10610	10 Work Unit No. 505-41-13-01
9 Performing Organization Name and Address NASA Langley Research Center Hampton, VA 23065	11 Contract or Grant No.	13 Type of Report and Period Covered Reference Publication
12 Sponsoring Agency Name and Address National Aeronautics and Space Administration Washington, DC 20546	14 Sponsoring Agency Code	
15 Supplementary Notes Because scales of instruments described in this text and all data derived from their calibration and use are in U.S. Customary Units, the requirement that the International System of Units (SI) be used has been waived. NASA RP-1046 is a forthcoming publication of John Wiley & Sons, Inc. and is scheduled for release in late 1980.		
16 Abstract This text examines problems involved in measuring speed and altitude with pressure-actuated instruments (altimeter, airspeed indicator, true-airspeed indicator, Machmeter, and vertical-speed indicator). Equations relating total pressure and static pressure to the five flight quantities are presented, and criteria for the design of total- and static-pressure tubes are given. Calibrations of typical static-pressure installations (fuselage nose, wing tip, vertical fin, and fuselage vent) are presented. Various methods for flight calibration of these installations are described, and the calibration of a particular installation by two of the methods is described in detail. Equations are given for estimating the effects of pressure lag and leaks. Test procedures for the laboratory calibration of the five instruments are described, and accuracies of mechanical and electrical instruments are presented. Operational use of the altimeter for terrain clearance and vertical separation of aircraft is discussed, along with flight technical errors and overall altitude errors of aircraft in cruise operations. Altitude-measuring techniques based on a variety of properties of the Earth and the atmosphere are included. Two appendices present airspeed and altitude tables and sample calculations for determining the various flight parameters from measured total and static pressures.		
17 Key Words (Suggested by Author(s)) Airspeed Altitude Static pressure Total pressure Aircraft instruments Pressure measurements	18 Distribution Statement Unclassified - Unlimited Subject Category 15	
19 Security Class. of this report Unclassified	20 Security Class. of this page Unclassified	21 No. of Pages 308 22 Price* \$11.75

* For sale by the National Technical Information Service, Springfield, Virginia 22161

NASA-Langley, 1980